Deep Foundations Institute in collaboration with
Indian Institute of Technology Gandhinagar and Indian
Geotechnical Society Ahmedabad Chapter present:

DFI-India 2018: November 15-17, 2018 8th Conference on Deep Foundation Technologies for Infrastructure Development in India

IIT Gandhinagar, Gujarat,India

IGS Ahmedabad Chapter







APPLICATIONS OF ROCK PENETRATION H PILE FOR DEEP EXCAVATION RETAINING SYSTEM

Nagarajan. D, Senior Design Engineer, Geotechnical- CMPC, EDRC, Heavy Civil Infra, Larsen & Toubro, Chennai, India, nagarajan-d@lntecc.com.
Raja Rajan. K, Assistant Engineering Manager, Geotechnical-CMPC, EDRC, Larsen & Toubro, Chennai, India, k-raja@lntecc.com.
Vijaykumar. T, Head, EDRC-CMPC, Heavy Civil Infra, Larsen & Toubro, Chennai, India, tvk@lntecc.com.

ABSTRACT

Mumbai Metro Line 3 (MML3) Project of 33.5km underground metro, proposed from Colaba to SEEPZ at Mumbai in India. Underground Package UGC-07 is one of the 7 packages of MML3 project. Deep excavations for underground metro station construction carried out by conventional secant pile wall as earth retaining system. Secant pile walls formed by overlapping reinforced concrete piles with un-reinforced piles. In SEEPZ station at launching shaft location, construction of secant pile for entire length of station not possible due to delay in land acquisition. To make the excavation within available land, Rock penetration H pile proposed 30m away from the existing Head Secant pile wall across the launching shaft layout. In Rock penetration H pile, Structural beam used as reinforcement. Considering quick installation and the dismantling scheme, Rock Penetration H Piles proposed as retaining system across launching shaft. This paper describes the modelling of Rock Penetration H pile along with installing and dismantling scheme as retaining system in lieu of reinforced secant pile.

Keywords: Deep excavation, finite element Analysis, Ground Anchor, H-pile, PLAXIS, Retaining system, rock penetration, Secant Pile Underground Metro.

INTRODUCTION

For underground metro stations, deep excavations in urban areas impose specific challenges, especially to the safety and impact on adjacent structures. Effective risk management in the construction of deep excavations includes the design of excavation support, ground water control system and the implementation of monitoring systems. Deep excavations for underground construction carried out by secant pile wall as retaining system**.** Instead of providing reinforcement inside the pile, structural beam been introduced and socketed into rock as Rock Penetration H pile (RPH). Primary reason for providing Rock Penetration H (RPH) pile is quick installation and dismantle. Moreover, embedded structural beam shall be taken and re-used in other structures after dismantling. Rock penetration H-pile modelled and analyzed in 2D finite element analysis for various excavation stages in order to obtain the wall moments.

PROJECT SITE DETAILS

To make the excavation within available land for lowering TBM, Rock penetration H pile (RPHP) proposed 30m away from the Existing Head Secant pile wall across the launching shaft layout. Proposed RPH pile across the ramp shall be dismantled while constructing the ramp portion after acquiring the remaining land.

Rock Penetration H pile modelled along with ground anchor and rock bolts for different excavation stages in PLAXIS to obtain anchor and rock bolt forces. Ground anchor and rock bolts design not provided in this paper, however properties considered for anchor and rock bolts provided for better understating. Plan view of the Launching Shaft SEEPZ station shown in Fig.1 and Site photo showing the proposed RPH pile wall shown in Fig -2.

© 2018 Deep Foundations Institute

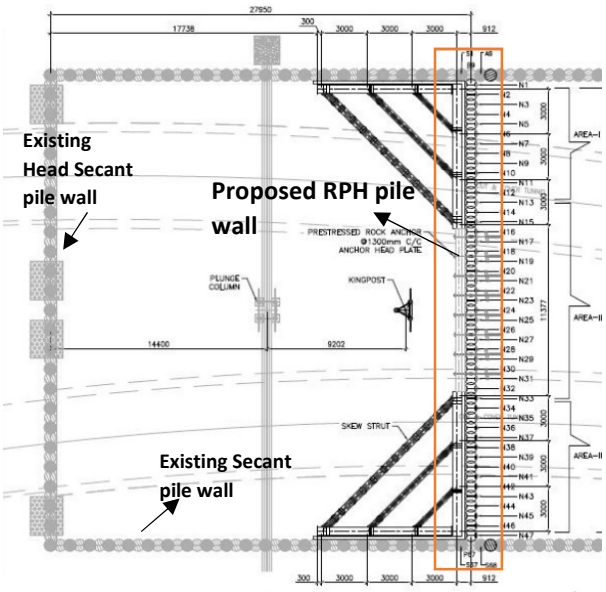


Fig. 1. Plan view of launching shaft area showing proposed temporary secant pile



Fig. 2. Site Photo of launching shaft area showing proposed temporary secant pile

ROCK PENETRATION H-PILE WALL

RPH pile for deep excavation developed based on ground, ground water and site constraints. RPH pile with embedded beam (NPB600) considered as shoring system in lieu of reinforced Secant pile. RPH pile with Structural beam proposed across the ramp for easy in construction and dismantling while constructing the remaining ramp portion. Only steel beam inside the pile shall take the moment, axial and shear force exerted by earth, water and surcharge loads. Since each pile has embedded beam inside the pile, the influence width of each pile taken as 0.65m (shown in Fig: 3). The adopted RPH pile schematic drawing in plan shown in Fig. 3.

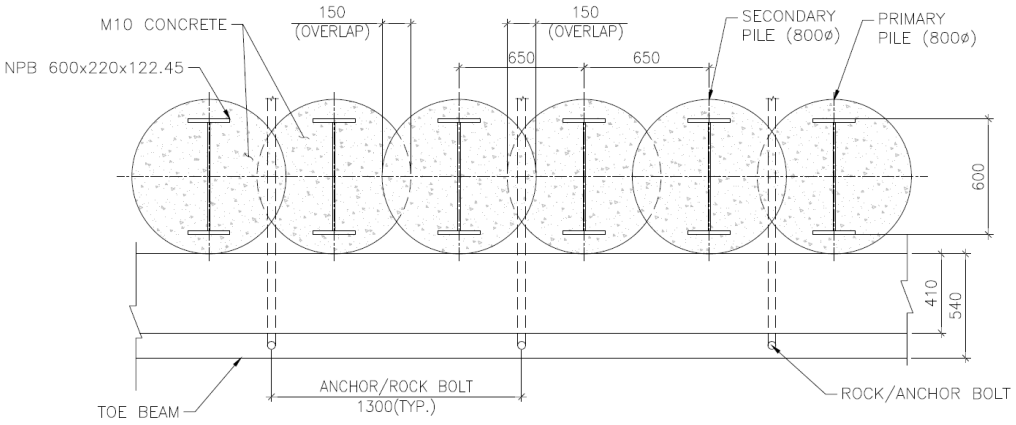


Fig. 3. Schematic drawing- Secant bored pile wall (H Pile)

GEOLOGICAL PROFILE

Subsurface profile in the Launching Shaft area generally consists of fill overlying residual soils underlain by completely weathered rock and then Basalt/Breccia bedrock.

Fill consisting mostly of sandy gravel with boulders encountered directly at the ground surface. Residual soils, consisting of brown clayey sand, encountered below fill layer. Based on Standard Penetration Tests (SPT), relative density of this layer ranged between medium dense to dense.

Completely weathered bedrock encountered at depths between 0.5 and 4.5m below ground surface. This layer formed by the complete disintegration of parent bedrock material, but remains the original rock mass structure. Core Recoveries in this layer was less than 30 percent, while Rock Quality Designations (RQDs) was nil.

Highly weathered, grey Basalt bedrock encountered at depths between 3.0m and 7.5m below ground surface. Core Recoveries in the bedrock ranged between 30 and 69 percent, while RQDs were 0 to 66 percent. Slightly weathered to Fresh Grey Basalt bedrock typically encountered at depths between 3.0m and 12.5m below ground surface. Core Recoveries in the bedrock ranged between 77 and 100 percent, while RQDs ranged between 7 and 100 percent. Subsurface profile encountered for Launching shaft location as shown in Fig.4 below.

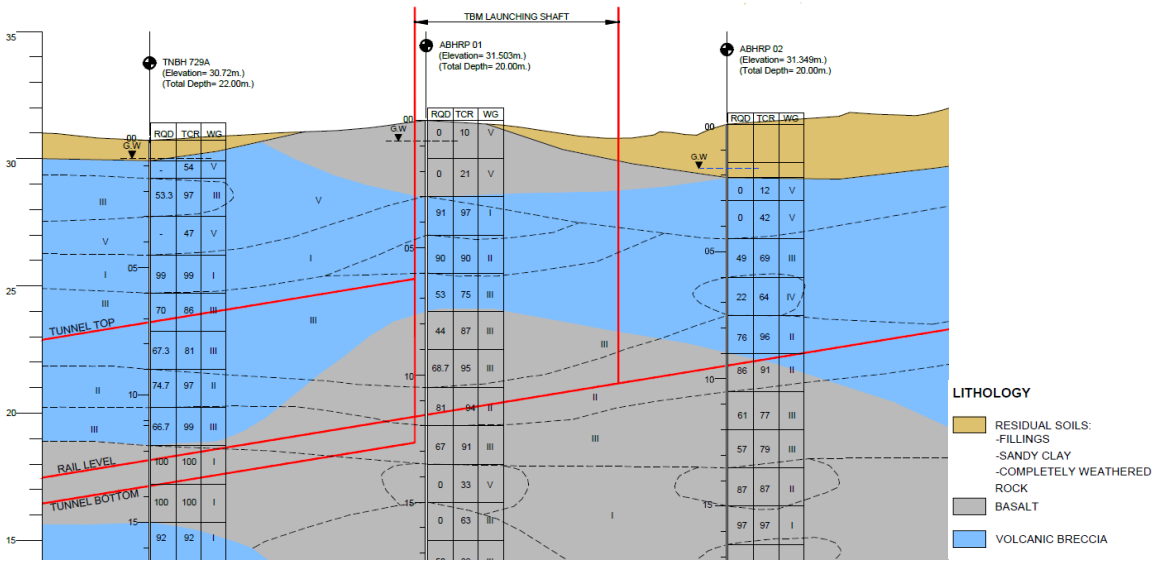


Fig. 4. Subsurface Profile- Launching shaft Location

Table 1: Generalized subsurface profile – Ramp Area

Layer No.	Subsoil Profile	Symbol	Depth (m)	
			From	To
1	Fill (Top Layer)	--	0.0	1.50
2	Residual Soil	SC	3.0	4.5
3	Completely weathered Basalt	RG V	4.50	7.50
4	Highly to Moderately weathered Breccia	RG IV-III	7.50	12..5
5	Fresh to Slightly weathered Breccia	RG I-II	Below 12.5	

NUMERICAL MODELLING –PLAXIS

Finite Element Method (FEM) used to model the interaction between soil/rock and RPH Pile Earth retaining system. Analysis done for every stage of excavation works to study the effect of the Excavation to the surrounding ground as well as to obtain the structural member forces in the temporary walls and support elements. The analysis had been carried out by using finite element based software PLAXIS 2D to determine the structural forces, deformation, stability, and groundwater flow in temporary earth retaining system. Both quadratic 6-node and fourth order 15-node triangular elements are available to model stresses and deformations in soil/rock

Material Properties considered same as provided in approved geotechnical Interpretive Report which was a part of project document. Properties of soil/rock as per geological profile tabulated in table 2.

Table 2: Material Properties –Soil/Rock Model

Parameter	Name	Unit	Fill	Residual soil	Breccia GIV	Breccia GIII
General						
Material model	Model	-	MC	HS	HS	HB
Type of material behavior	Type	-	Drained	Drained	Drained	Non-porous
Dry Unit Weight	Y_{unsat}	kN/m³	18	19	23.5	23.5
Saturated Unit Weight	Y_{sat}	kN/m³	18	21	23.5	23.5
Initial void ratio	e_{init}	-	0.5	0.5	0.5	0.5
Parameter						
Loading stiffness	$E_{50}ref$	kN/m²	-	$20x10^3$	$230x10^3$	-
Unloading / reloading stiffness	$E_{ur}ref$	kN/m²	-	$60x10^3$	$690x10^3$	-
Young's Modulus	E	kN/m²	$20 \cdot 10^3$	-	-	$590x10^3$
Poisson's ratio	v_{ur}		0.3	0.3	0.25	0.25
Uniaxial compressive strength	σci	kN/m²	-	-	-	$25x10^3$
Geological strength index	GSI	-	-	-	-	36
Cohesion	c_{ref}	kN/m²	0	10	46	159
Friction angle	φ	-	30	28	33	55

Pile properties- Plaxis

The secant pile wall modelled as plate element. The interfaces around the plates used in order to model ground-structure interaction effects. Due to numerical reasons, the interfaces extended 1m below the wall. The interface strength between secant pile wall and embankment, soil and soft rock (GIV, GV) set to R_{inter} = 0.5 and R_{inter} = 1 for hard rock (GIII). Each pile embedded with structural beam and gap filled with M10 concrete. The overlapping between piles considered as 0.15m. For modelling the wall, properties of structural member only considered. The moment of inertia calculated for the influence width of 0.65m (C/C spacing refer Fig-3), in order to account each beam in each pile. Table 3 shows the material properties considered for modelling the Pile in PLAXIS.

Table 3: Material Properties –Pile Model

Description	Unit	Value
Diameter, D (Pile)	m	0.8
Moment of inertia, I (Beam)	m^4	9.28 E -4
Moment of inertia per m (Beam)	m^4	14.166E-4
Young's Modulus, E (Beam)	kPa	2E8
Axial stiffness EA per m (Beam)	kN/m	4.8E+06
Flexural rigidity EI per m (Beam)	kNm^2/m	2.83E+05

Strut Properties

Struts modelled as fixed-end anchor in order to support the secant pile wall. Diagonal struts provided from adjacent sidewall. The Parameters considered for fixed-end anchor elements tabulated in table 4.

Table 4: Parameters for fixed-end anchor elements for Piles

Description	Unit	Value
Type of behaviour		Elastic
Young's Modulus	kN/m^2	2.0E+08
Cross section area	m^2	0.0434
Axial stiffness	kN	8.68E+06
Spacing out of plane	m	3.0

Ground Anchor Properties

Ground (cable) anchors modelled as a combination of node-to-node anchor and ~~a~~ geogrid. The geogrid simulates the grout body whereas the node-to-node anchor simulates the anchor rod. Table 5 shows the parameters considered to model the ground anchor in PLAXIS.

Table 5: Parameters for node-to-node elements

Description	Unit	Value
Type of behaviour	-	Elastic
Young's Modulus, E	kN/m^2	2.0E+08
Cross section area	m^2	0.0010
Axial stiffness	kN	2.0E+05
Spacing out of plane	m	1.29

Rock bolt Properties

With respect to the rock bolts, elastic properties are considered. Bolt length is 4 m and bolt diameter is 25 mm. Parameters considered to model the rock anchor in PLAXIS is tabulated in the below Table -6.

Table 6: Parameters for Rock bolts elements

Description	Unit	Value
Bolt diameter	mm	25
Bolt area,	m^2	4.91E-04
Yield strength, fy	MPa	500
Yield load	kN	245

All the above parameters considered for modelling the pile, strut, ground anchor and rock bolts for different excavation stages as mentioned in the construction stages.

DESIGN LOADS

Self-weight of 25 kN/m^3 for reinforced concrete (piles) apart from structural beam weight used for calculation. No seismic load considered for temporary secant pile wall structures. For Live loads, a uniform surcharge load of 50 kPa considered as building surcharge with a distance of 5m from the pile wall. Uniform surcharge load of 25 kPa considered as vehicular and pedestrian loads.

Groundwater Loads due to water pressure shall be full hydrostatic pressure and calculated with density of 10 kN/m^3 for water. Furthermore, it considered that groundwater table within the launching shaft area reduced gradually to the pit bottom during excavation by dewatering techniques. No gantry loads/ crane loads considered for temporary RPHP wall design.

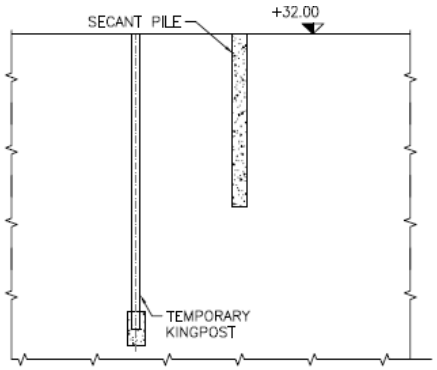
CONSTRUCTION STAGES

Modelling of construction sequences done using PLAXIS in stage wise. These stages include excavation sequence, installation of support systems and checking of global stability. Following are the stages included in PLAXIS. The modelling of the construction stages shall correspond to the construction process. The construction stages used in the model summarized in Table 7.

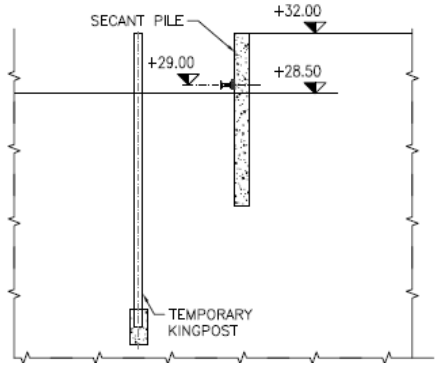
Table 7: Construction stages considered in PLAXIS

Stage	Description
0	Initial stresses (groundwater table at ground level)
1	Reset displacements previously; activation of surcharge load of 25/ 50kPa
2	Reset displacements previously; Construction of bored pile wall up to 10.0m bgl
3	Reset displacements previously; Excavation down to 3.5m bgl (First Excavation)
4	Installation of struts at 3.0m bgl (Strut Install)
5	Excavation down to 7.0m bgl (Second Excavation)
6	Installation of cable anchor at 6.5m bgl); pre-stressing. (Anchor Installation)
7	Excavation down to 9.0m bgl (Third Excavation)
8	Installation of rock bolts in every secondary pile (1.3m spacing) (Rock bolt)
9	Excavation down to 11.5m bgl; Installation of shotcrete and rock bolts around the remaining rock base (GIII) (Fourth Excavation)
10	Excavation down to14.0m bgl; Installation of shotcrete and rock bolts around the remaining rock base (GIII). (Fifth Excavation)

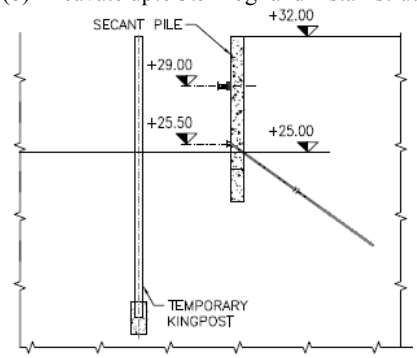
Real advantages of Rock Penetration H piles is quick installation and dismantling as stated earlier. Main Construction stages for H piles with staged excavation shown in Fig. 5. Staged Excavation followed by installation of first level strut and second level anchor in RPH pile system. After the excavation for launching shaft completed, tunnel-boring machine lowered for tunneling operation. After availability of land, remaining ramp portion will be excavated by dismantling the existing Rock penetration H piles as shown in Fig.6.



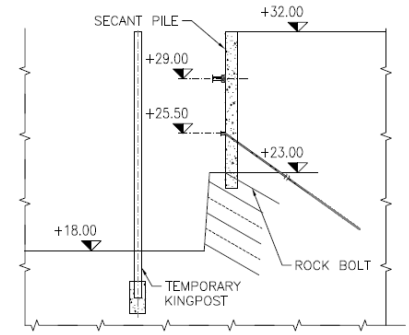
(a) Install soldier Pile



(b) Excavate upto 3.5m bgl and install strut at 3m bgl

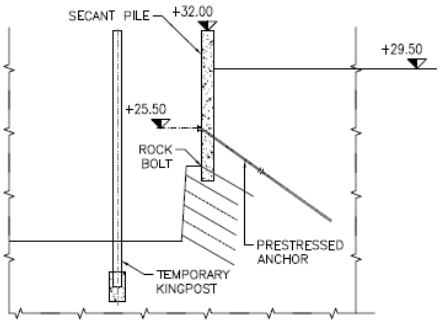


(c) Excavate upto 7m bgl and install anchor

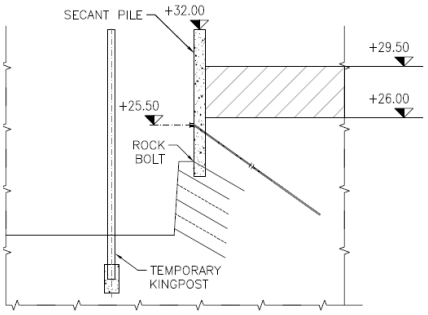


(d) Excavate upto14.0m bgl & Install of shotcrete & rock bolts

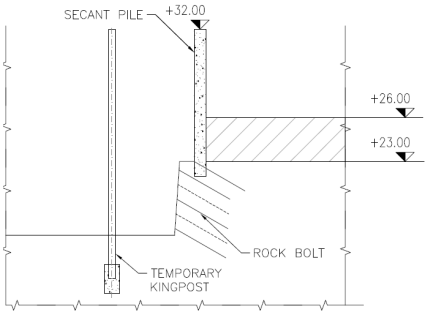
Fig.5. Main Construction Sequence



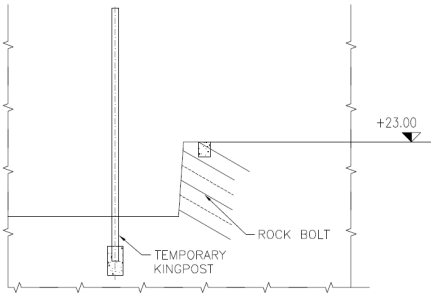
(a) Excavate behind the wall



(b) Deactivate waller and further excavation



(c) Deactivate anchor & excavate up to pile toe



(d) Dismantling the secant pile

Fig.6. Dismantling Sequence

RESULTS

RPH piles been designed by extracting the peak bending and shear forces from the PLAXIS model. Peak ULS forces checked against the requirements of Indian standards/contractual specifications. Bending Moment and shear forces for each stages of excavations shown in Fig.7 and Fig.8. Anchor forces and rock bolts were designed based on the maximum forces extracted from PLAXIS analysis.

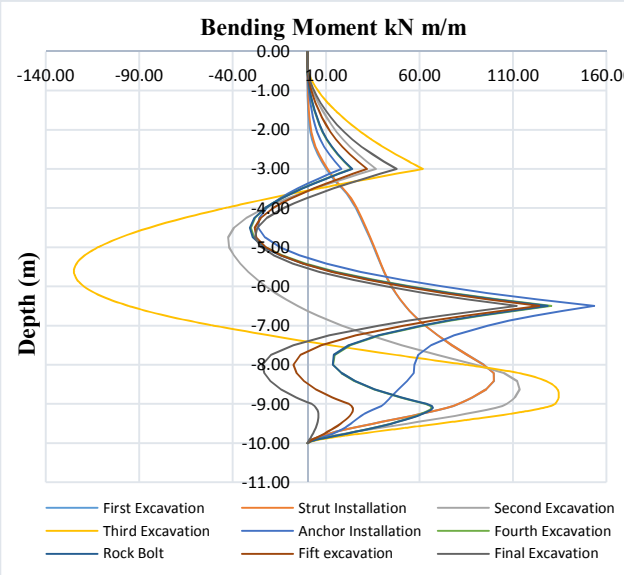


Fig.7. Wall Bending moments

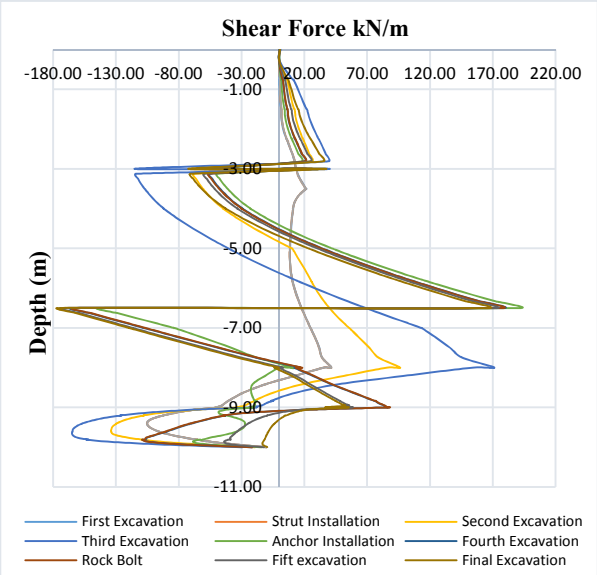


Fig.8. Shear forces of the wall

Pile Displacement at Final Excavation Level

Theoretical displacement estimated in PLAXIS found to be 9.5mm for critical case. Permissible displacement of pile at pile head was 0.15% of excavation depth as per contractual requirement, which accounts to allowed deflection of 15mm. Inclinometers installed nearby RPH piles and monitored at regular intervals. Lateral displacement and vertical displacement of the wall at the final excavation were shown in Fig 9 and Fig.10 below.

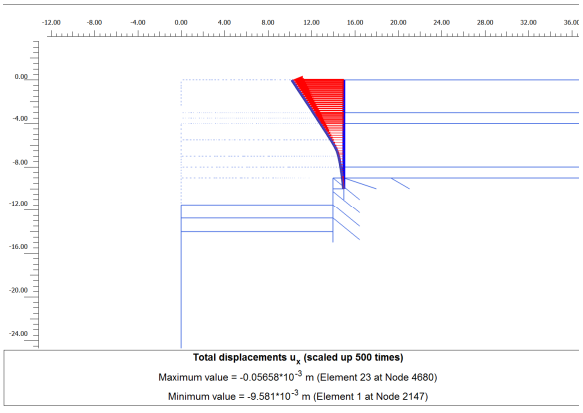


Fig. 9 Lateral Displacement at final excavation

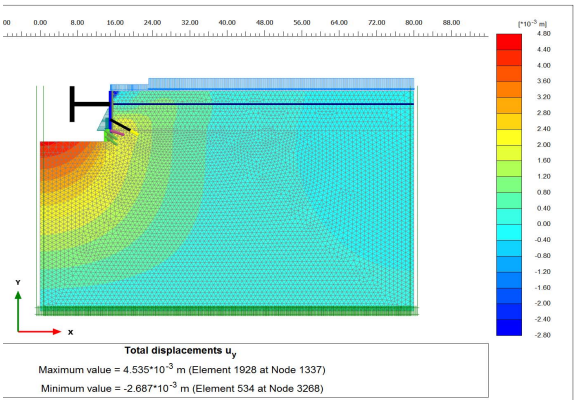


Fig. 10. Vertical Displacement at final excavation

CONSTRUCTION PROGRESS

RPH pile wall as per design been constructed in stipulated time for quick launch of TBM inside launching shaft in SEEPZ Station. Steel beam only used instead of reinforcement in RPH pile wall as per design. Total length of temporary RPH piles were bifurcated as Area I, II & III with respect to pile depth based on encounter of rock strata. RPH Piles of varying depth of 6.0, 8.0 and 10.0m below ground level constructed with minimum depth of socketing as 1.0m in Grade III rock. Rock socketing calculated for vertical load in line with Indian Standards. Diagonal strut placed on area I & area III pile locations. One level of anchor provided in area II and area III at a depth of 3.0m and 6.5m below ground level respectively. Level of anchors and struts along the RPH pile wall system shown in Fig.11. Excavation progress photo showing anchor and strut shown in Fig.12 and Fig.13.

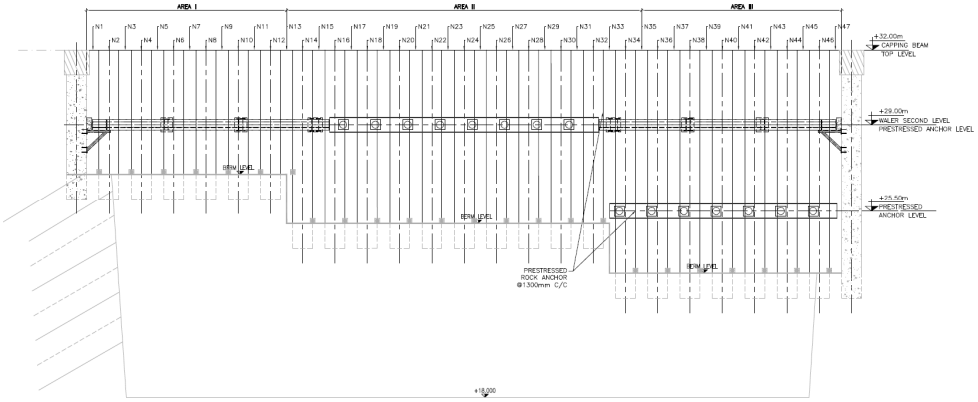


Fig. 11. Elevation of secant pile wall of Area I, Area II & Area III



Fig. 12. Site Photo showing the anchor and strut along the secant pile wall



Fig.13. Site Photo showing Excavation in progress in Launching Shaft Location

APPLICATIONS AND ADVANTAGES

Some of the Applications of Rock penetration H pile in deep excavation are listed below.

- RPH piles shall be used as temporary earth retaining system.
- RPH piles predominantly used where land acquisition has partly completed. Excavations started within the land availability by RPH piles as temporary retaining system.
- RPH piles had been used adjacent to existing utility in underground metro station. Excavated earth other than utility covered by retaining panel welded to RPH piles

RPH piles has many advantages compared to conventional secant pile system and a few are listed below.

- RPH pile system allows quick installation and dismantle
- In conventional secant pile system, dismantling shall be difficult as reinforcement hinders the dismantling process, whereas in RPH pile system, filled concrete can be chipped off and structural beam shall be removed by gas cutting
- No requirement of higher strength of concrete for RPH piles. Only M10 concrete required to cater the seepage pressure as the pile moments taken only by the structural beam
- Time cycle for RPH piles shall be drastically reduced when compared to the conventional secant pile. Excavation to be started after concrete achieve its strength whereas in RPH piles, excavation can be started immediately after the RPH pile installation.
- Verticality of pile shall be well maintained in RPH pile when compared to conventional secant pile system.
- Walers shall be directly welded to structural beam of RPH piles unlike the requirement of special bracket in conventional secant pile system.
- Structural beam inside the RPH piles can be re-used which is very advantage to the contractor.

CONCLUSION

The RPH pile system for excavation were developed and executed successfully based on ground and site constraints for the excavation. Rock penetration H piles had been used in most of the locations where utility lines encountered in line of reinforced secant pile. Smart and simple use of steel beams led to economy in the project and ease to construction.

The overall behavior of rock penetration H piles in retention system was effective, reduces significant time in project, and reduces the investment of contractor in retaining system. This paper is a case study useful for numerical modelling of secant pile wall system in PLAXIS 2D.

ACKNOWLEDGEMENT

The author is thankful to the management of L&T Construction for granting permission for this paper to be published. The author extends gratitude to Project site Team and Colleagues in extending their support to the paper in their own way. Thanks to the Mumbai Metro line 3 Package 7.

REFERENCES

Bureau of Indian Standards IS 456 (2000), Code of Practice for Plain and Reinforced Concrete. New Delhi.
Mumbai Metro Line 3, ‘Geotechnical Interpretation Report, Launching shaft and ramp’.
Tomlinson, M.J., (1977), Pile design and construction practice, A viewpoint publication, London.
PLAXIS 2D, (2017), Reference Manual and Help Manuals.

BEHAVIOR OF PILE IN COHESIVE SOIL SUBJECTED TO COMBINED VERTICAL AND LATERAL LOAD CONSIDERING P-Δ EFFECT

Tanumaya Mitra, Research Scholar, Civil Engineering, IIEST Shibpur, WB, INDIA, +91 9674333976, tanumayamitra@gmail.com
Kalyan Kumar Chattopadhyay, Professor of Civil Engineering, IIEST Shibpur, WB, INDIA, +91 9433090560, kkc@civil.iiests.ac.in
Ambarish Ghosh, Professor of Civil Engineering, IIEST Shibpur, WB, INDIA, +91 9831286527, ambarish@civil.iiests.ac.in

ABSTRACT

In this study, Beam on Nonlinear Winkler Foundation (BNWF) approach has been used to assess the behaviour of pile embedded in homogeneous clay bed, under combined vertical and lateral load. Non-linearity of soil and P-Δ effect have been taken into account. The result shows that if P-Δ effect is considered, the effect of vertical load will reduce the lateral load carrying capacity and increases the pile head deflection by inducing additional moment at pile head. The effects of variation of soil cohesion, slenderness ratios (L/D) and pile stiffness factors (Ep/Es) have also been investigated in this study. With the increase in pile stiffness factor, pile head deflection increases whereas increase in L/D ratios and cohesion lead to decrease the depth of fixity and lateral displacement of pile, under a fixed lateral load. For lower L/D ratios ($L/D < 20$), pile behaves like a rigid pile; for $L/D \geq 30$, pile behaviour changes from rigid to flexible.

Keywords: Combined load, Winkler model, P- Δ effect, FEM, BNWF

INTRODUCTION

Behaviour of pile under combined vertical and lateral load is much more complicated than pile under pure vertical load or pure lateral load. Pile foundation supporting structures subjected to seismic shaking, pile under bridge abutment, offshore piles etc. are subjected to combined loading. In conventional design methods, the vertical and lateral responses of piles are often evaluated separately neglecting their possible interaction (Hazzar et al., 2017). Different methods are available to study the behaviour of pile e.g., continuum based modeling, subgrade reaction approach etc. In this study, an analytical approach based on subgrade modulus concept (Hetenyi, 1946) has been used. To incorporate the effect of soil nonlinearity, depth dependent load-displacement curves, known as *p-y* curves have been used. Previous researches have revealed that axial load on pile may influence the lateral behaviour of pile in both sandy and clayey soil. Anagnostopoulos and Georgiadis (1993) have shown experimentally that the effect of axial load on lateral response of pile embedded in soft clay bed is negligible. Karthigeyan et al. (2006, 2007) has conducted experimental study and shown that with the increase in vertical load, lateral load carrying capacity of pile increases in sand. Kershaw and Luna (2013) conducted a field test on full scale micropiles embedded in stiff clay and concluded that axial load has a minimal effect on the lateral behaviour of micropiles installed in stiff clay. Jegatheeswaran and Muthukkumaran (2016) reported a similar result using numerical study, that the lateral load carrying capacity of piles embedded in sand increases. Babu et al. (2016) numerically investigated the lateral response of monopile in dense sand and stiff clay, subjected to vertical load and demonstrated that vertical load has a favorable effect on the lateral load response of piles in dense sand, but in stiff clay, decrease in lateral load carrying capacity was observed. Hazzar et al. (2017) carried out a continuum model based numerical study for piles in both sand and clay and reported similar response for piles in sand, whereas for piles

© 2018 Deep Foundations Institute

embedded in clay, lateral capacity reduces with the application of vertical load. Hence, it can be seen from the previous research work that no clear-cut guideline is available for piles under combined vertical and lateral load, particularly for piles installed in clay. For sand, most of the researchers have agreed that the presence of vertical load on pile head increases the lateral load carrying capacity of pile, but in clay the behaviour is still not fully understood as some researchers have mentioned limited effect on lateral behavior of pile whereas the others have mentioned reduction in lateral load carrying capacity. So, it is necessary to develop a simple methodology to study the behaviour of pile under combined axial and lateral load. In this study, the effect of vertical load on lateral response of pile in homogeneous clay layer has been investigated.

METHODOLOGY

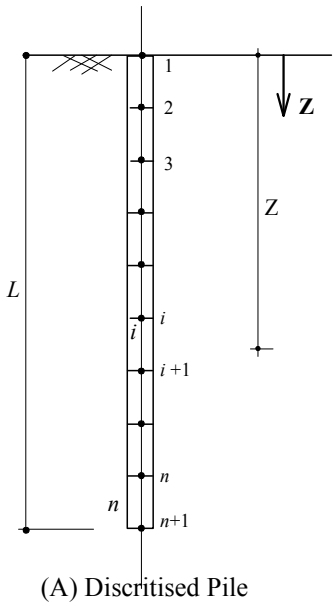
The governing differential equation for deformation of pile at any depth z (Fig. 1), under combined axial compressive load and lateral load is expressed as,

$$EI\frac{d^4y}{dz^4} + P\frac{d^2y}{dz^2} + ky = 0 \qquad (1)$$

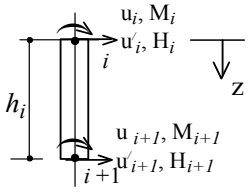
Where, P is the applied axial load at pile head, EI is the flexural rigidity of the pile, *y* is the deflection of pile at depth z and k is the lateral stiffness of soil, which can be determined using *p-y* curves.

NUMERICAL SOLUTION

In the present study, a finite element based approach has been used for the numerical solution of the governing differential equation. The embedded pile is assumed to be made of n number of elements as shown in Fig. 1.



(A) Discritised Pile



(B) Typical Element Showing Nodal Forces and Displacements

For an element i, the lateral displacement at depth z, is expressed as,

$$u(z) = C_1 cos\alpha\frac{z}{h}cosh\beta\frac{z}{h} + C_2 cos\alpha\frac{z}{h}sinh\beta\frac{z}{h} + C_3 sin\alpha\frac{z}{h}cosh\beta\frac{z}{h} + C_4 sin\alpha\frac{z}{h}sinh\beta\frac{z}{h} \qquad (2)$$

Where, $\alpha = \sqrt{\sqrt{\frac{k}{4EI}} + \frac{P}{4EI}}$ (3.a), $\beta = \sqrt{\sqrt{\frac{k}{4EI}} - \frac{P}{4EI}}$ (3.b)

C_1, C_2, C_3 *and* C_4 are the integrating constants, which can be determined by using suitable boundary conditions applied at the nodes of the i[th] element as shown in Fig. 1. (b).

The boundary conditions applied are as follows,

Boundary Condition 1: $u(0) = 1, u'(0) = 0, u(h) = 0, u'(h) = 0$ (4.a)

Boundary Condition 2: $u(0) = 0, u'(0) = 1, u(h) = 0, u'(h) = 0$ (4.b)

Boundary Condition 3: $u(0) = 0, u'(0) = 0, u(h) = 1, u'(h) = 0$ (4.c)

Boundary Condition 4: $u(0) = 0, u'(0) = 0, u(h) = 0, u'(h) = 1$ (4.d)

The nodal force displacement relationship for the i[th] element expressed as,

$$\begin{Bmatrix} H_i \\ M_i \\ H_{i+1} \\ M_{i+1} \end{Bmatrix} = [k] \begin{Bmatrix} u_i \\ u'_i \\ u_{i+1} \\ u'_{i+1} \end{Bmatrix} \quad (5)$$

Where, $[k]$ is the element stiffness matrix, can be expressed as;

$$\begin{bmatrix} k11 & -k12 & k13 & -k14 \\ k21 & -k22 & k23 & -k24 \\ -k31 & k32 & -k33 & k34 \\ -k41 & k42 & -k43 & k44 \end{bmatrix} = \frac{EI}{h^2} \begin{bmatrix} E11 & E12 & E13 & E14 \\ E21 & E22 & E23 & E24 \\ E31 & E32 & E33 & E34 \\ E41 & E42 & E43 & E44 \end{bmatrix} \times \begin{bmatrix} c_{11} & c_{12} & c_{13} & c_{14} \\ c_{21} & c_{22} & c_{23} & c_{24} \\ c_{31} & c_{32} & c_{33} & c_{34} \\ c_{41} & c_{42} & c_{43} & c_{44} \end{bmatrix} \quad (6)$$

where,

$\mathrm{E11} = 0, \mathrm{E12} = \frac{1}{\mathrm{h}}(\beta^3 - 3\alpha^2\beta), \mathrm{E13} = \frac{1}{\mathrm{h}}(3\alpha\beta^2 - \alpha^3), \mathrm{E14} = 0, \mathrm{E21} = (\beta^2 - \alpha^2), \mathrm{E22} = 0, \mathrm{E23} = 0, \mathrm{E24} = 2\alpha\beta$

$\mathrm{E31} = \frac{1}{\mathrm{h}}[(\beta^3 - 3\alpha^2\beta)\sinh\beta\cos\alpha + (\alpha^3 - 3\alpha\beta^2)\cosh\beta\sin\alpha]$

$\mathrm{E32} = \frac{1}{\mathrm{h}}[(\beta^3 - 3\alpha^2\beta)\cosh\beta\cos\alpha + (\alpha^3 - 3\alpha\beta^2)\sinh\beta\sin\alpha]$

$\mathrm{E33} = \frac{1}{\mathrm{h}}[(\beta^3 - 3\alpha^2\beta)\sinh\beta\sin\alpha - (\alpha^3 - 3\alpha\beta^2)\cosh\beta\cos\alpha]$

$\mathrm{E34} = \frac{1}{\mathrm{h}}[(\beta^3 - 3\alpha^2\beta)\cosh\beta\sin\alpha - (\alpha^3 - 3\alpha\beta^2)\sinh\beta\cos\alpha]$

$\mathrm{E41} = [(\beta^2 - \alpha^2)\cosh\beta\cos\alpha - (2\alpha\beta)\sinh\beta\sin\alpha], \mathrm{E42} = [(\beta^2 - \alpha^2)\sinh\beta\cos\alpha - (2\alpha\beta)\cosh\beta\sin\alpha]$

$\mathrm{E43} = [(\beta^2 - \alpha^2)\cosh\beta\sin\alpha + (2\alpha\beta)\sinh\beta\cos\alpha], \mathrm{E44} = [(\beta^2 - \alpha^2)\sinh\beta\sin\alpha + (2\alpha\beta)\cosh\beta\cos\alpha]$

$$\begin{bmatrix} c_{11} & c_{12} & c_{13} & c_{14} \\ c_{21} & c_{22} & c_{23} & c_{24} \\ c_{31} & c_{32} & c_{33} & c_{34} \\ c_{41} & c_{42} & c_{43} & c_{44} \end{bmatrix} =$$

$$\begin{bmatrix} 1 & 0 & 0 & 0 \\ 0 & \frac{\beta}{h} & \frac{\alpha}{h} & 0 \\ \cosh\beta.\cos\alpha & \sinh\beta.\cos\alpha & \cosh\beta.\sin\alpha & \sinh\beta.\sin\alpha \\ \frac{\beta}{h}\sinh\beta.\cos\alpha - \frac{\alpha}{h}\cosh\beta.\sin\alpha & \frac{\beta}{h}\cosh\beta.\cos\alpha - \frac{\alpha}{h}\sinh\beta.\sin\alpha & \frac{\beta}{h}\sinh\beta.\sin\alpha + \frac{\alpha}{h}\cosh\beta.\cos\alpha & \frac{\beta}{h}\cosh\beta.\sin\alpha + \frac{\alpha}{h}\sinh\beta.\cos\alpha \end{bmatrix}^{-1} \quad (7)$$

The nodal forces {F} and displacement {Δ} of the embedded pile are related as,

$\{F\} = [K]\{\Delta\}$,

Where, the global stiffness matrix $[K]$ for the embedded soil-pile system is assembled from the stiffness matrix $[k]$ of individual element. A computer code in MATLAB has been developed to assess the behaviour of single pile under combined lateral and vertical load.

SOIL NONLINEARITY

Different researchers have suggested various methods for generation of *p-y* curves. Matlock (1970) and Georgiadis et al. (1992) developed *p-y* relationship for soft clay. Dewaikar and Patil (2006) proposed a hyperbolic model to develop *p-y* curves for clay; Reese et al. (1975) have proposed *p-y* curves for stiff clay. Reese et al. (1974) has developed *p-y* relationship for sand. Guidelines to develop *p-y* curves are available in API (2000). Nonlinear *p-y* curves proposed by Georgiadis et al. (1992) have been used in this study to determine the stiffness of soil. Iterative procedure has been used to modify the stiffness of soil considering secant modulus approach.

A hyperbolic relationship for developing *p-y* curve proposed by Georgiadis et al. (1992) is

$$p = \frac{y}{\frac{1}{k}+\frac{y}{p_u}} \tag{8}$$

Where, k is the modulus of subgrade reaction expressed as, $k = 0.65 \sqrt[12]{\frac{E_s d^4}{EI}} \frac{E_s}{1-\mu^2}$ (Vesic, 1961); E_s is the Young's modulus of soil, μ is the Poisson's ratio of soil and d is the diameter of pile.

P-Δ Effect

When a structure deflects under applied loading, the deflection gives rise to additional secondary moment. This secondary effect can be approximated by the use of P-Δ analysis. In this present study, this effect has been included. For a pile under combined vertical and lateral load, the vertical load present at pile head induces additional moment due to the lateral deformation of the pile. Under the influence of this additional induced moment, pile further deflects leading to a reduction in lateral load carrying capacity of pile.

SENSITIVITY STUDY

Before carrying out a parametric study, it is essential to know the optimum number of elements (N) and number of iterations required to study the convergence of the result. With the increase in number of elements and number of iterations, pile deformation, bending moment and shear force will gradually change and become constant after a certain number of elements and number of iterations. Fig. 2 shows a typical convergence study for a pile of slenderness ratio 20, under a lateral load of 300 kN. It was observed that the analysis converges at 7th iteration for twenty numbers of elements. Hence, 7th iteration and element aspect ratio of one have been considered for all the analysis in this study.

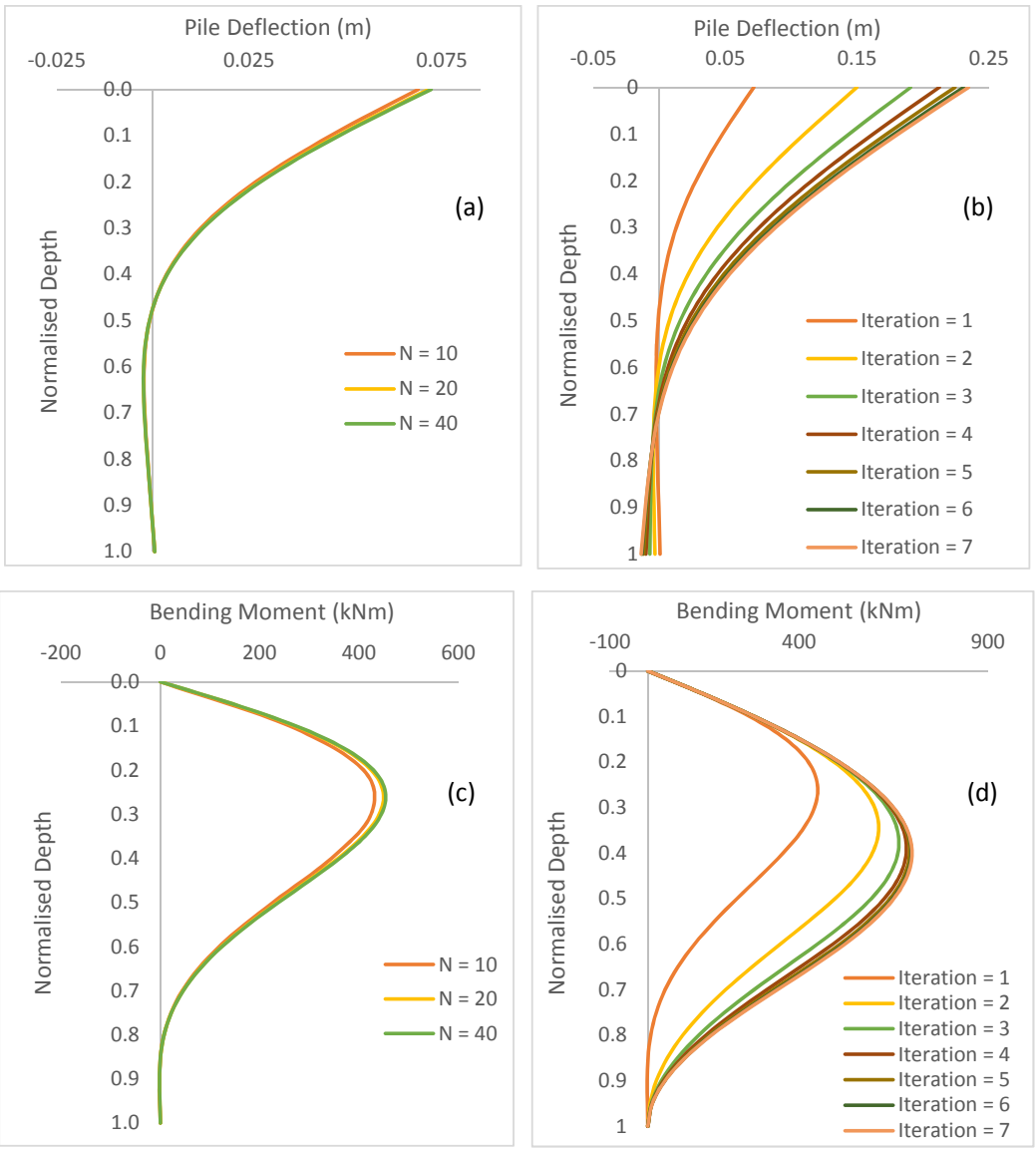


Fig. 2 Typical Sensitivity Analysis for Pile (a) Convergence of pile deflection with number of elements, (b) Convergence of pile deflection with number of iterations, (c) Convergence of bending moment of pile with number of elements and (d) Convergence of bending moment of pile with number of iterations (L/D = 20, H = 300 kN)

VALIDATION OF THE ANALYSIS

Lateral load vs deflection result obtained from present study has been compared with the field test result reported by Comodromos (2003) as illustrated in Fig. 3. A good agreement between the results obtained from present study and the reported result has been found.

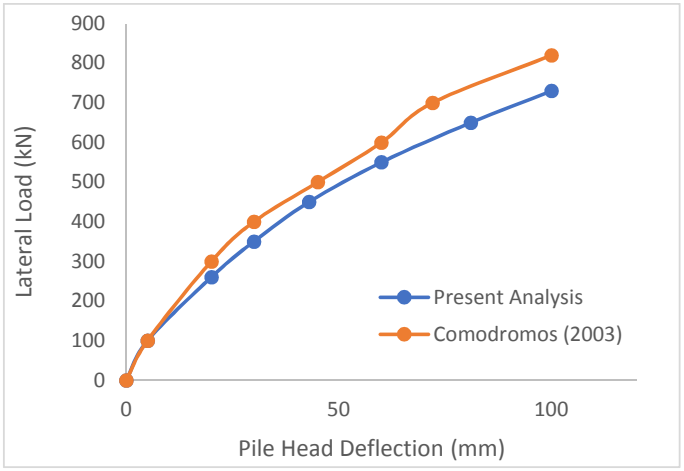


Fig. 3. Comparison of the result obtained by present analysis with the field test data obtained by Comodromos (2003)

PARAMETRIC STUDY

An investigation on the response of pile has been made to examine the effect of various pile-soil parameters on the lateral response of pile under combined vertical and lateral load. The effect of vertical load on load-deformation characteristics of piles with different slenderness ratios (L/D = 10, 20 and 30) with and without P-Δ effect has been illustrated in Fig. 4. Ultimate compressive load carrying capacity of pile (Vu) has been determined and used to study the influence of vertical load on lateral response of pile. In non-linear analysis without P-Δ effect, the effect of vertical compressive load on lateral capacity of pile was found to be insignificant, for L/D < 20. However, when the effect of P-Δ is accounted in the analysis, a reduction in lateral load capacity of pile under same vertical load is observed. For piles with L/D ≥ 20, reduction in lateral capacity of pile under axial compressive load was found more pronounced considering P-Δ effect. Figure 5 presents the influence of vertical load on deformation of pile shaft for slenderness ratios (L/D) of 10, 20 and 30 under a lateral load intensity corresponding to lateral deformation of 10 % pile diameter. Change in deformation of pile shaft considering P-Δ effect was found to be significant up to a nomalized depth of 0.4 for L/D < 20 and 0.1 for L/D ≥ 20. Fig. 6 depicts the influence of shear parameter of soil (cohesion = 30 kPa, 45 kPa and 60 kPa) and vertical load on lateral load-deflection behaviour of pile. It is found, the lateral load carrying capacity of pile increases with the increase in soil cohesion and decreases with the increase in vertical load irrespective of L/D ratio. Effect of slenderness ratio of pile on pile deflection behaviour has been portrayed in Fig. 7. With the increase in L/D ratios, pile deflection reduces under constant lateral load applied at pile head and pile behavior changes from rigid to flexible. For L/D < 20, pile behaves as a rigid pile for all the pile stiffness factors (Ep/Es) (Fig. 8), whereas for L/D > 30, pile behaves as flexible pile. For $20 \leq L/D < 30$, pile behaves as an intermediate pile. For L/D ≥ 20, pile head deflection is found to be constant, i.e., further increase in L/D ratio will no longer influence the pile head deflection. Influence of pile stiffness factors (Ep/Es) on deflection of pile shaft has been presented in Fig. 8. With the increase in Ep/Es ratio, pile deflection increases for all the L/D ratios (10, 20 and 30) considered. Figure 8 also indicates that the pile head deflection increases with the increasing pile stiffness factor irrespective of slenderness ratios. In case of short pile (Fig. 8.(a,b)), points of rotation was observed at a depth ≈ 0.7 L for all Ep/Es values. For long piles (Fig. 8. (e)), it is found that depth of fixity increases with the increase in pile stiffness factor.

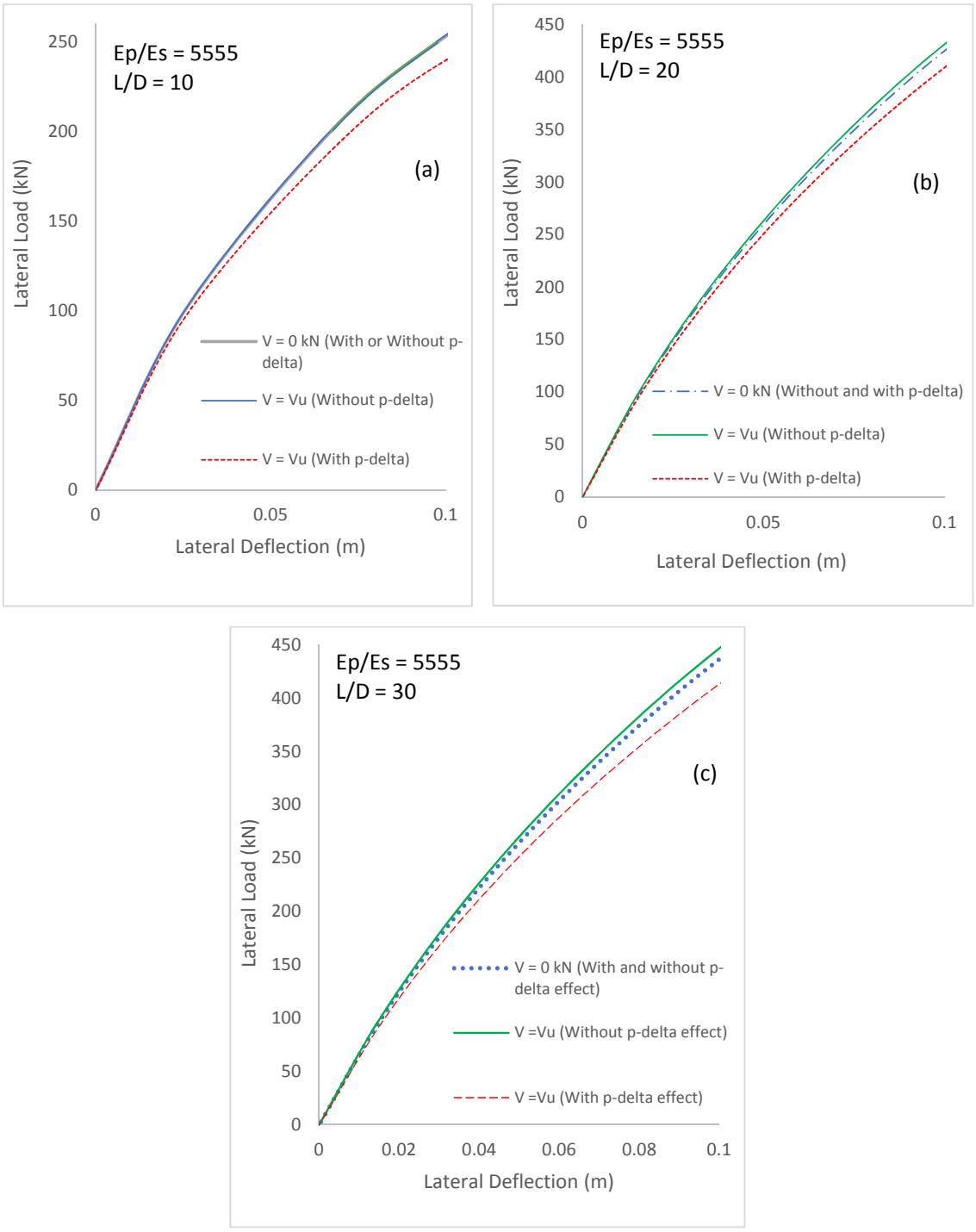


Fig. 4. Effect of Vertical load on Lateral Load – Deflection Behavior of pile for (a) L/D = 10, (b) L/D = 20 and (c) L/D = 30 for a constant pile stiffness factor

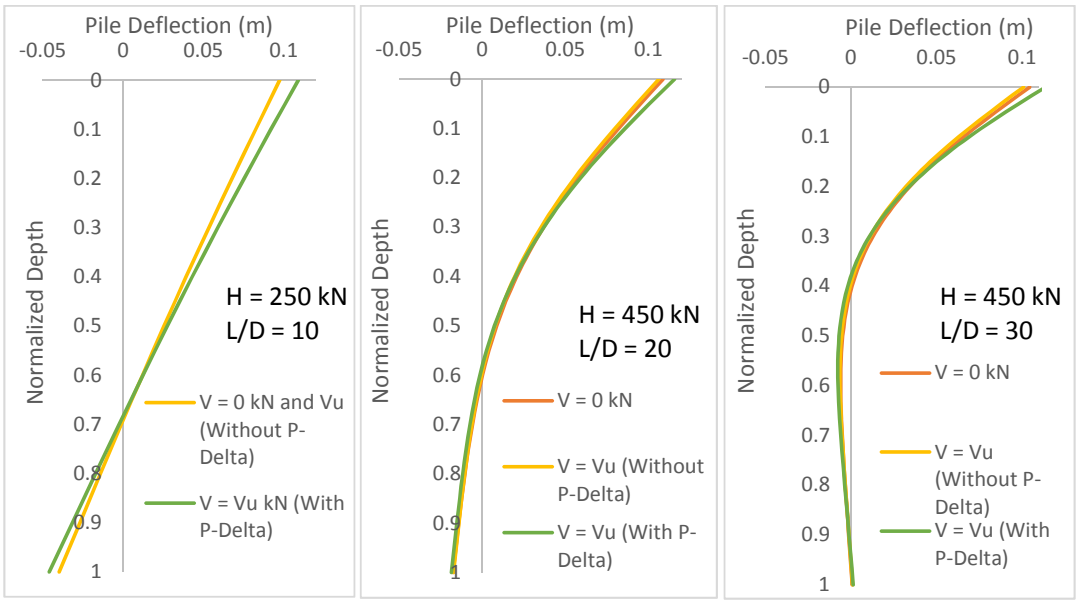


Fig. 5 Effect of Vertical load on Deflection Behavior of pile for (a) L/D = 10, (b) L/D = 20 and (c) L/D = 30

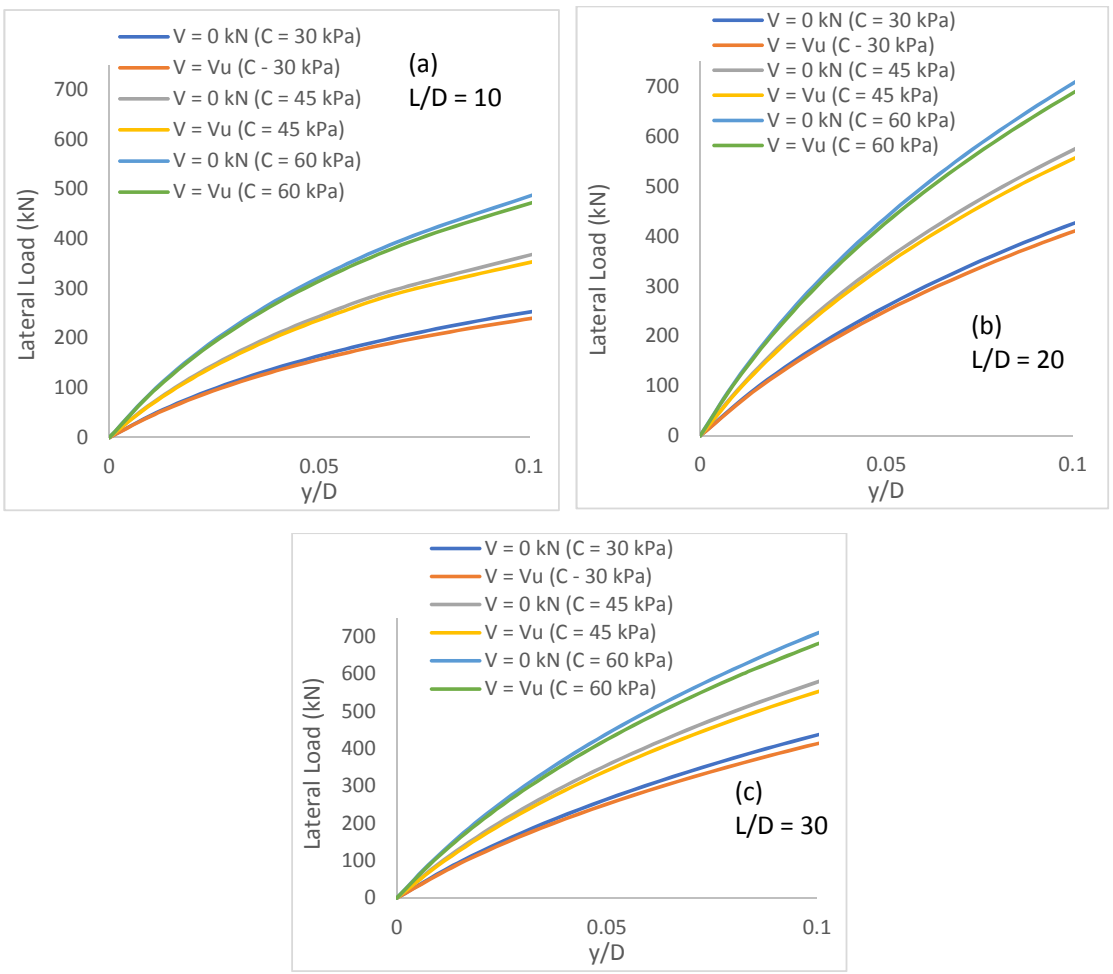


Fig. 6 Influence of Soil Cohesion and Vertical Load on Lateral Load- Deformation characteristics of pile for (a) L/D = 10, (b) L/D = 20 and (c) L/D = 30

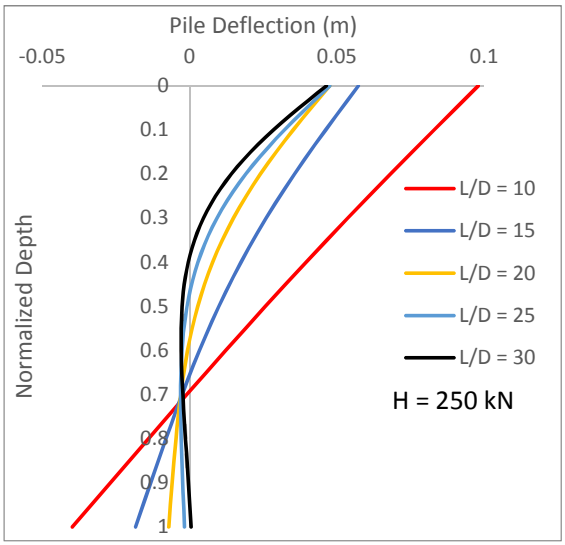
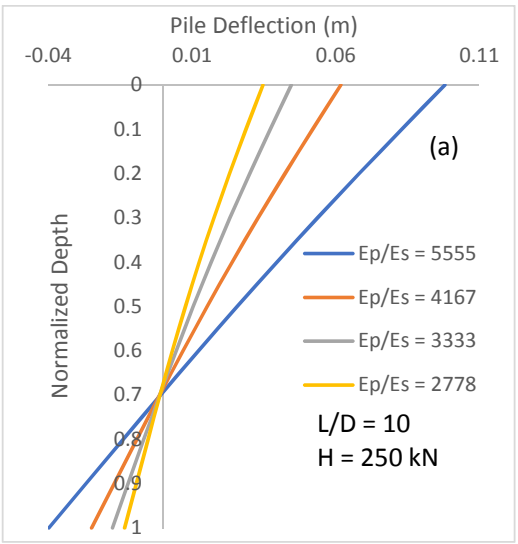
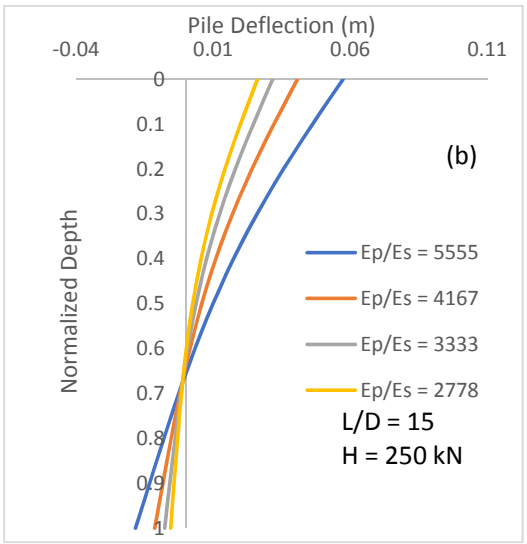
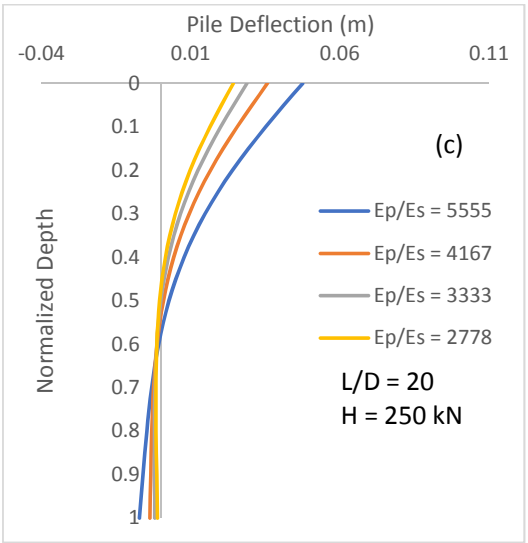


Fig. 7. Effect of Slenderness Ratio on Pile Deflection







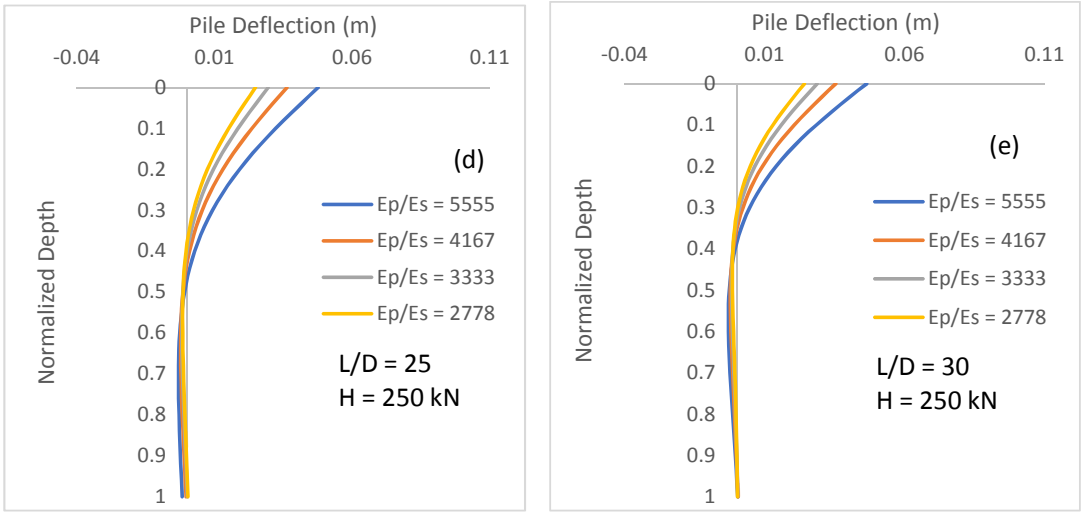


Fig. 8. Comparison of Pile Deflection profile with different Ep/Es ratio for (a) L/D = 10, (b) L/D = 15, (c) L/D = 20, (d) L/D = 25 and (e) L/D = 30

SUMMARY AND CONCLUSIONS

In this study, the effect of vertical load on lateral deflection of pile under combined axial and lateral load has been studied by solving the fourth order differential equation of pile deflection. P-Δ effect and soil nonlinearity have been incorporated in the solution. The influence of pile stiffness factor (Ep/Es), slenderness ratio (L/D) and cohesion of soil on deflection behavior of pile shaft under combined loading have also been studied. The summary of conclusions in present study may be drawn as follows.

- The agreement between the results of proposed theoretical analysis with the reported field test results is found to be quite satisfactory.
- Presence of vertical load increases the lateral deflection of pile embedded in clay, under combined axial and lateral load, irrespective of any other pile-soil parameters.
- Lateral load carrying capacity increases with the strength of soil.
- With the increase in pile slenderness ratio, pile head deflection reduces and behaviour of pile changes from rigid to flexible.
- For L/D < 20, pile behaves as a rigid pile for all the pile stiffness factors, whereas for L/D $\geq$ 30, pile behaves as flexible pile. For $20 \leq L/D < 30$, pile behaves as an intermediate pile.
- For rigid pile (L/D<20), point of rotation exists at a normalized depth of 0.7, irrespective of pile stiffness factors.
- For flexible pile (L/D≥30), depth of fixity increases with the increase in pile stiffness factor.
- These findings may find potential application for assessing the response of piles passing through clayey deposit in the field.

REFERENCES

Anagnostopoulos, C., and Georgiadis, M., 1993. Interaction of axial and lateral pile responses. Journal of Geotechnical Engineering, 119(4), 793-798.

Babu, K. V., Viswanadham, B. V. S., and Vaibhav, V. N., 2016. Numerical Studies on Lateral Load Response of Monopiles Subjected to Vertical Loading, Advances in Civil, Environmental, and Materials Research (ACEM16).

Comodromos, E. M., 2003. Response prediction for horizontally loaded pile groups, Journal of the Southeast Asian Geotechnical Society 2003; 34(2):123-33.

Dewaikar, D. M., & Patil, P. A., 2006. A new hyperbolic p-y curve model for laterally loaded piles in soft clay. In Foundation Analysis and Design: Innovative Methods (pp. 152-158).

Georgiadis, M., Anagnostopoulos, C., & Saflekou, S., 1992. Cyclic lateral loading of piles in soft clay. Geotechnical engineering, 23(1).

Hazzar, L., Hussien, M. N., & Karray, M., 2017. Vertical load effects on the lateral response of piles in layered media. International Journal of Geomechanics, 17(9), 04017078.

Hetényi, M., 1971. Beams on elastic foundation: theory with applications in the fields of civil and mechanical engineering. University of Michigan.

Jegatheeswaran, B., & Muthukkumaran, K., 2016. Behavior of pile due to combined loading with lateral soil movement. International Journal of Geo-Engineering, 7(1), 8.

Karthigeyan, S., Ramakrishna, V. V. G. S. T., and Rajagopal, K., 2006. Influence of vertical load on the lateral response of piles in sand. Computers and Geotechnics, 33(2), 121-131.

Karthigeyan, S., Ramakrishna, V. V. G. S. T., and Rajagopal, K., 2007. Numerical investigation of the effect of vertical load on the lateral response of piles. Journal of Geotechnical and Geoenvironmental Engineering, 133(5), 512-521.

Kershaw, K. A., and Luna, R., 2013. Full-scale field testing of micropiles in stiff clay subjected to combined axial and lateral loads. Journal of Geotechnical and Geoenvironmental Engineering, 140(1), 255-261.

Matlock, H. (1970). Correlations for design of laterally loaded piles in soft clay. Offshore Technology in Civil Engineering's Hall of Fame Papers from the Early Years, 77-94.

Reese, L. C., Cox, W. R., & Koop, F. D., 1974. Analysis of laterally loaded piles in sand. Offshore Technology in Civil Engineering Hall of Fame Papers from the Early Years, 95-105.

Reese, L. C., Cox, W. R., & Koop, F. D., 1975. Field testing and analysis of laterally loaded piles in stiff clay. In Offshore Technology Conference. Offshore Technology Conference.

RP2A-WSD, A. P. I., 2000. Recommended practice for planning, designing and constructing fixed offshore platforms–working stress design.

Vesic, A. B., 1961. Beams on elastic subgrade and the Winkler's hypothesis. In Proceedings, 5th International Conference on Soil Mechanics and Foundation Engineering (Vol. 1, pp. 845-850).

BI-DIRECTIONAL STATIC LOAD PILE TEST – CASE STUDIES

Justin St George, Strainstall Singapore Pte Ltd., 1 Bukit Batok Crescent, 04-33 WCEGA Plaza, 658064, Singapore, +65-6561-4628, justin@strainstall.com.sg
Ravi Sundaram, Cengrs Geotechnica Pvt. Ltd., A-100 Sector 63, Noida, Uttar Pradesh, India 9810538095 ravi@cengrs.com
Sorabh Gupta, Cengrs Geotechnica Pvt. Ltd., A-100 Sector 63, Noida, Uttar Pradesh, India 9910861118 sorabh@cengrs.com

ABSTRACT

Bi-Directional Static Load Pile Tests (BDSLT) was performed on a barrette pile of dimensions 1.2 m x 2.8 m extending to 21.278 m below the cut-off level. The test load applied was 10,800 tonnes which can usually not be applied by a traditional static load test. The test results indicated that the pile mobilized an ultimate unit skin friction value of 188.4 T/m^2 and an end bearing result of 734.5 T/m^2. Equivalent load-settlement curve indicates settlement of 4.6 mm at 100% the proposed working load, and 7.8 mm for 150% of the working load.

Keywords: Ultimate Load Test, Working Load Test, Bi-Directional Static Load Test, Skin Friction, End Bearing, Kentledge Test

INTRODUCTION

Bi-Directional Static Load Pile Tests (BDSLT) as per ASTM Standard D8169/D8169M-18, 2018 are becoming an increasing trend within the civil construction industry since its inception in 1989 (Leung et al, 2003) due to pile designs becoming larger in both diameter and length to withstand larger test load capacities. This paper presents a case study where the BDSLT method was used to conduct an ultimate load test. It includes the test results obtained and highlight lessons learned.

BI-DIRECTIONAL STATIC LOAD TEST METHODOLOGY

A Bi-Directional Static Load Test (BDSLT) differs from its conventional counterpart (Kentledge Static Load Test) predominantly from the application method of the applied test load (Schmertmann et al, 1998). Instead of the test load being applied from above the test pile by means of a hydraulic jack and counter weight, a BDSLT pile is broken into segments with hydraulic jacks cast within the concrete and uses the geotechnical soil resistance of the test pile as the test load reaction; namely the unit skin friction and unit end bearing.

The BDSLT method results in the applied load profile along the pile length differing from that of a conventional test; as shown in the two plots in Figure 1. A conventional test pile applies the load to the pile head, resulting in the applied load being transferred from the pile head to the pile toe. A BDSLT applies the load from within the test pile; typically positioned around approximately two thirds of the pile length from the pile cut-off level (dependent on actual soil conditions), transferring the applied load equally in the upward and downward directions from the hydraulic jack level. This enables the load to be applied directly to the layers of interest within the test pile, offering a solution for mobilizing stiffer layers within test piles, i.e. test pile socketed into rock, where a de-bonded casing would be required for the equivalent conventional test.

© 2018 Deep Foundations Institute

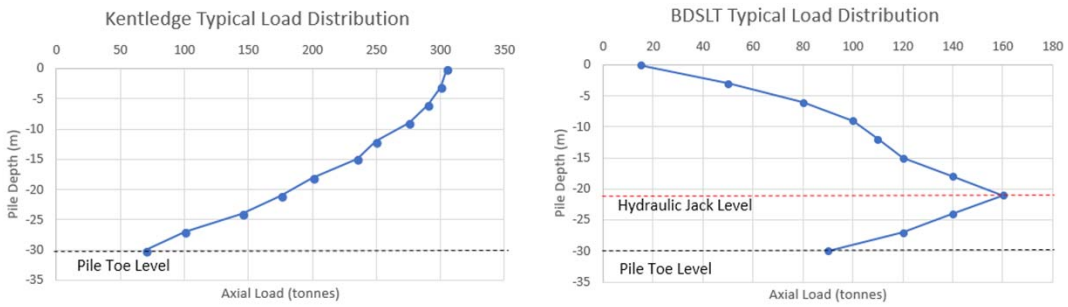


Figure 1: Load Distribution comparison between a conventional kentledge test and a BDSLT

A combination of sacrificial hydraulic jacks are individually calibrated and positioned within the test pile to apply an equal and opposite combined load in both the upward and downward directions, using the skin friction of the segment above the hydraulic jacks as the reaction for the bottom segment, and the combined skin friction and end bearing of the segment below the hydraulic jacks as the reaction for the upper segment. A schematic of a typical BDSLT can be seen in Figure 2.

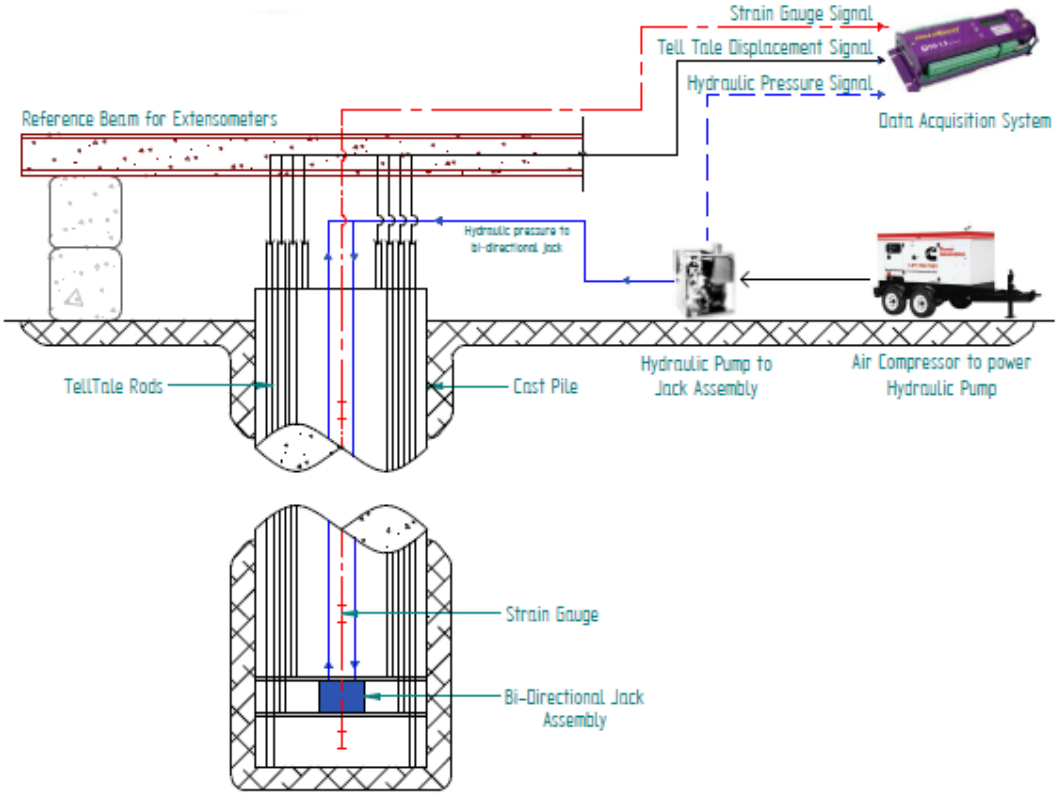


Figure 2: Side View Schematic of a BDSLT (Strainstall scheme)

PROJECT DETAILS

Great World Station was proposed to be developed in Singapore, consisting of the main train station, with attached shopping mall, plus all the connecting tunnels for the underground train lines. The development required excavation to a depth of 31.5m below ground level, resulting in the top 31.5m meters of soil not being of interest to the consultants.

The project consultant was particularly interested in determining the ultimate capacity of the G(III) rock layer; found at 49 m below ground level, based on the nearest borehole which is presented pictorially in Appendix B for reference. The test pile was a barrette pile, with dimension of 1.2m x 2.8m, designed with a length of 21.278 m from cut-off level to pile toe and required an applied test load of 10,800 tonnes. A schematic of the test pile has been included in Appendix A.

Due to the large test load and requirement to fully mobilize the stiffer G(III) layer to determine ultimate geotechnical capacity, a conventional test posed many risks and was deemed unsafe. The BDSLT method was therefore proposed to safely test the pile to required test loads in a safe and controlled manner.

A combination of six no. 900 tonne jacks were positioned at 2.60m above the pile toe, providing a test load of 5,400 tonnes in both the upward and downward direction, resulting in a combined test load of 10,800 tonnes. The test pile was loaded from 0 tonnes to 10,800 tonnes in 5% increments; following the ASTM-D1143 loading schedule, to obtain test results in a higher resolution.

Thirteen levels of concrete embedded strain gauges were installed to the reinforcement bar cage along the pile length prior to casting. Strain gauge results were used to determine the load transfer between each level of strain gauges, which could then be used to determine the ultimate soil/rock resistance to a known applied load.

TEST RESULTS

Obtained results achieved an ultimate mobilized unit skin friction value of 188.4 T/m^2 for the G(III) rock layer, with an end bearing result of 734.5 T/m^2. An Equivalent top load-pile head settlement curve was constructed to include additional elastic compression of concrete, which provided values of 4.6mm equivalent pile head settlement at 100% of the proposed working load, and 7.8mm for 150% of the working load. Both settlement values falling below the allowable settlement criteria of 7mm and 14mm for 100% and 150% of the working load respectively.

Table 1 below summarizes the ultimate test results achieved. Fig. 3 and 4 present the load Vs Displacement plots for both loading cycles (Cycle 1 from 0-300% of the working load, and Cycle 2 from 300–390% of the working load). Fig. 5 presents the equivalent top loaded settlement curve, including the additional elastic compression of the concrete, while Fig. 6 presents the calculation table for the equivalent top loaded settlement curve calculation.

Table 1. Maximum Design Parameters Obtained During Testing

Load Transfer Zone	Depth (m below GL)	Soil Type	Average SPT-N	Mobilized Unit Shaft Friction (tonnes/m^2)		
				%WL	Skin Friction (tonnes/m^2)	Ks Value
LEVEL 1 to 2	-19.222 to -2.222	SILT G(VI)	5 - 6	390	2.6	N/A
LEVEL 2 to 3	-12.222 to -4.222	SILT G(VI)	10 - 39	325	5.5	1.4
LEVEL 3 to 4	-4.222 to 0.678	SILT G(V)	26 – 48	275	6.3	1.3
LEVEL 4 to 5	0.678 to 2.678	SILT G(V)	46 – 100	390	10.1	1.1
LEVEL 5 to 6	2.678 to 5.678	SILT G(V)	100	390	14.9	1.5
LEVEL 6 to 7	5.678 to 8.678	SILT G(V)	100	390	20.6	2.1
LEVEL 7 to 8	8.678 to 11.678	G(V)	100	325	22.9	2.3
LEVEL 8 to 9	11.678 to 13.678	G(IV)	100	390	30.0	3.0

Load Transfer Zone	Depth (m below GL)	Soil Type	Average SPT-N	Mobilized Unit Shaft Friction (tonnes/m^2)		
				%WL	Skin Friction (tonnes/m^2)	Ks Value
LEVEL 9 to 10	13.678 to 15.678	G(IV)	100	390	39.4	3.9
LEVEL 10 to 11	15.678 to 17.678	G(IV)	100	390	61.1	6.1
LEVEL 11 to J1	17.678 to 18.678	G(III)	100	390	74.7	7.4
LEVEL J1 to 13	18.678 to 20.428	G(III)	100	390	188.4	18.9
Mobilised Unit End Bearing (tones/m^2)				**%WL**	**End Bearing (tonnes/m^2)**	**kPa**
TOE				390	734.5	7345

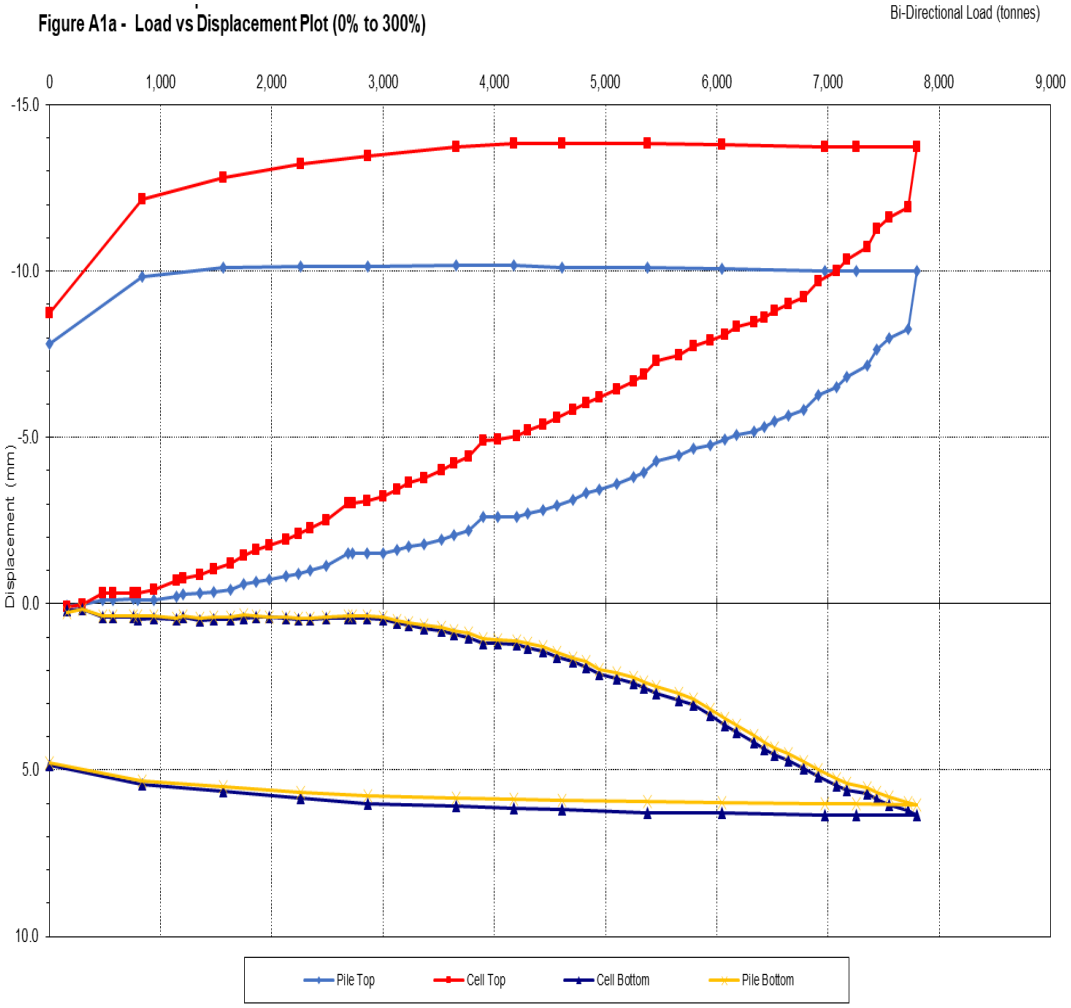


Figure 3. Recorded Settlement of Test Pile Between 0% to 300% of the Test Load.

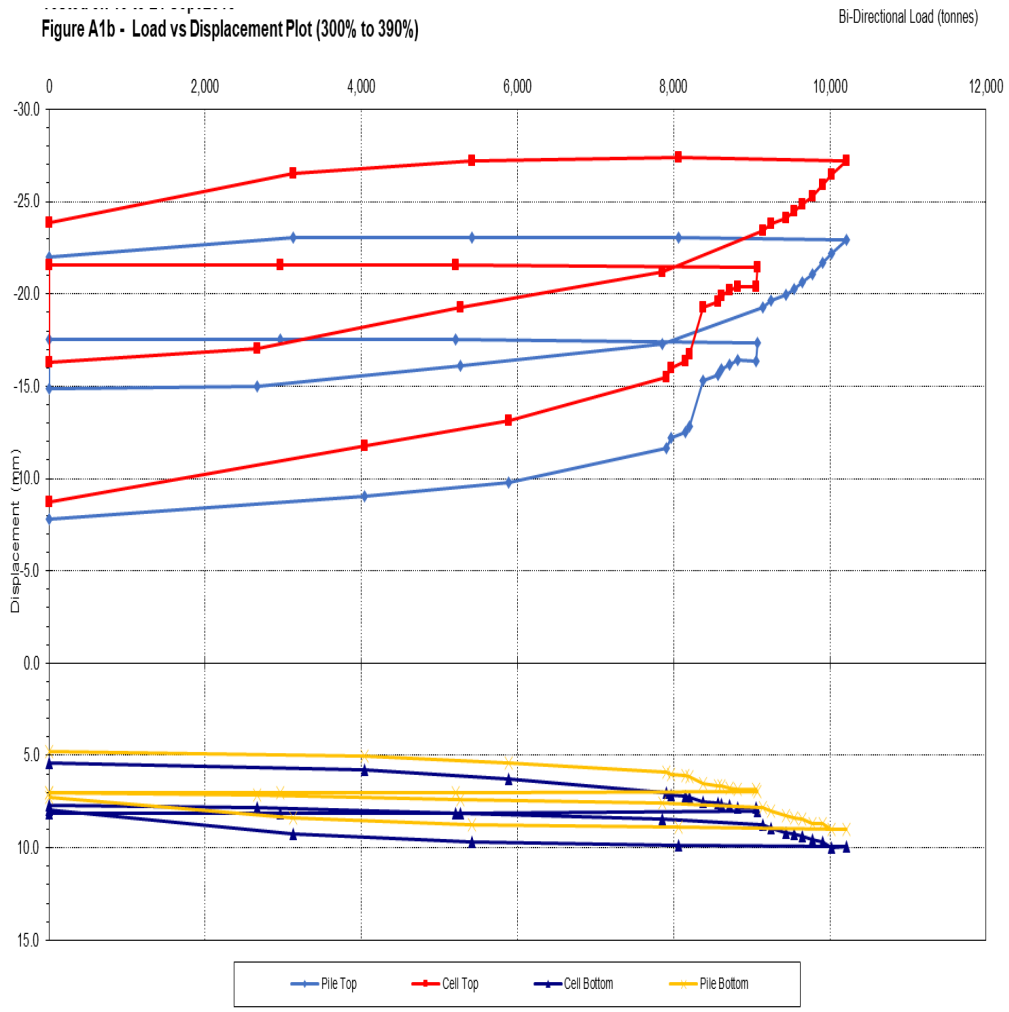


Figure 4. Recorded Settlement of Test Pile between 300% to 390% of the Test Load.

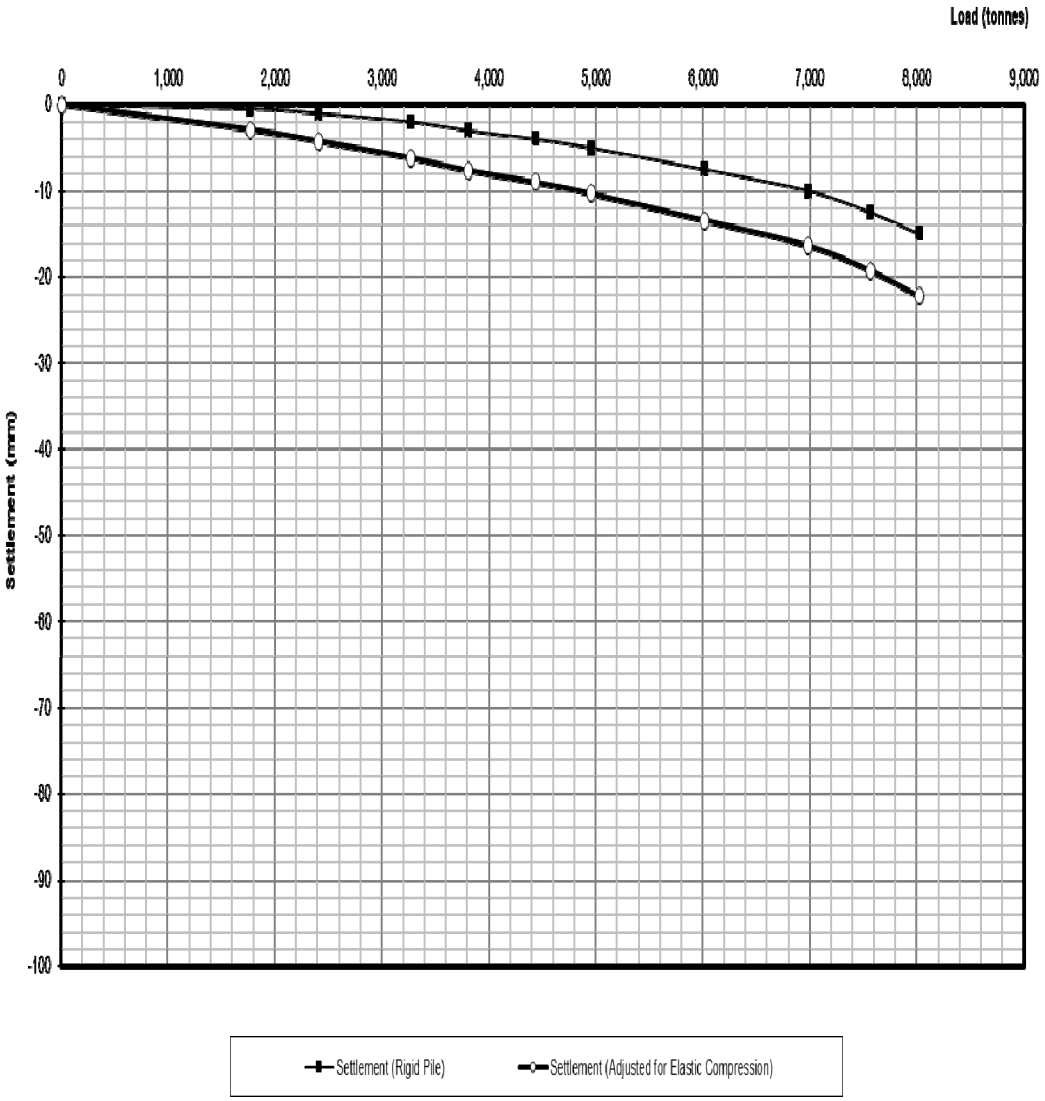


Figure 5. Equivalent Top Loaded Settlement Curve

Pile diameter	2800 x 1200	mm
Friction Centroid Factor (C_1)	0.50	
Length above GL, ℓ_0	0	mm
Length above Jack A below COL, ℓ (ℓ_1 + ℓ_2)	18,678	mm
Length above water level	18,678	mm
Height of water level above Jack A	0	mm
Cross Sectional Area of Pile (A)	3.36E+06	mm^2
Elastic Modulus of Concrete (E)	1.72	$tonnes/mm^2$
Density Concrete (ρ)	2.45	$tonnes/m^3$
Weight of Concrete above Jack A (W' ℓ_0 + ℓ)	154	tonnes
Pile Length Above Jack A (ℓ_0 + ℓ)	18,678	mm

ΔBDSLT (mm)	Q↓A (tonnes)	Q↓A' (tonnes)	Q↑A (tonnes)	Q↑A' (tonnes)	Equivalent Load (P single) (tonnes)	δ↓ ℓ0 (mm)	δ↓ ℓ1+ ℓ2 (mm)	δTLT (mm)	δBDSLT (mm)	Δδ (mm)	ΔBDSLT + Δδ (mm)
0.00	0	0	0	0	0	0.0	0.0	0.0	0.0	0.0	0.0
-0.50	1345	1345	420	420	1765	0.0	2.8	2.8	0.4	2.4	-2.9
-1.00	1820	1820	585	585	2405	0.0	3.7	3.7	0.5	3.2	-4.2
-2.00	2355	2355	910	910	3265	0.0	5.0	5.0	0.8	4.2	-6.2
-3.00	2615	2615	1190	1190	3805	0.0	5.7	5.7	1.1	4.6	-7.6
-4.00	2825	2825	1610	1610	4435	0.0	6.4	6.4	1.4	5.0	-9.0
-5.00	3000	3000	1950	1950	4950	0.0	7.0	7.0	1.7	5.3	-10.3
-7.50	3335	3335	2675	2675	6010	0.0	8.3	8.3	2.4	5.9	-13.4
-10.00	3600	3600	3385	3385	6985	0.0	9.4	9.4	3.0	6.4	-16.4
-12.50	3820	3820	3745	3745	7565	0.0	10.1	10.1	3.3	6.8	-19.3
-15.00	4100	4100	3925	3925	8025	0.0	10.7	10.7	3.5	7.3	-22.3

Figure 6. Equivalent Top Loaded Settlement Curve Calculation

Applying the test load from within the test pile and positioning the hydraulic jacks directly within the G(III) layer allowed successful mobilisation of the lower regions of the test pile. This enabled the test results to confirm the consultants design parameter for the skin friction capacity of the G(III) rock layer; initially proposed at 90 tonnes/m^2 ultimate capacity. This result provided the consultants with the information required to further optimize the pile design to reduce the pile length for the working test piles.

Bi-Directional Static Load Tests can be beneficial in obtaining test results in difficult soil conditions where large test loads are required. BDSLT's can be tailored to obtain the parameters of most interest to the consultants, where the hydraulic jack level can be adjusted to fully mobilize the regions of interest, obtaining ultimate capacities of the soil strata to optimize the pile design.

Careful consideration must be taken when designing the proposed level of the hydraulic jack within the test pile to ensure the upper and lower segment capacities of the test pile are evenly matched approximately 50% each, achieving this is also heavily dependent on the initial geotechnical design parameters provided by the consultants.

A BDSLT test should be precisely planned to ensure that the construction and casting of the test pile is of satisfactory standard to ensure a successful test.

CONCLUDING REMARKS

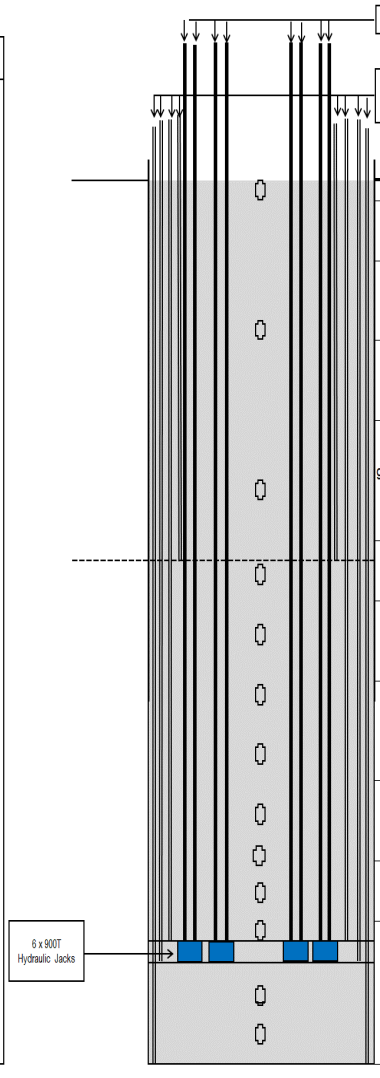
Bi-Directional Static Load Testing (BDSLT) can be used as an accepted alternative to its conventional counterpart (Kentledge Static Load Test), especially where large test loads are required to mobilize deep foundations. Applying the test load from within the test pile, as well as directly to the stiffer layers found in the lower portion of deep foundations, can result in fully mobilizing the lower layers for the test pile to obtain ultimate soil parameters to verify and optimize the pile design.

The position of the hydraulic jack assembly is crucial in the design of a BDSLT to ensure the capacity of the upper and lower segments of the test pile are balanced approximately 50/50.

APPENDIX – A: SCHEMATIC OF TEST PILE

Pile No. BULT2 - BRP5

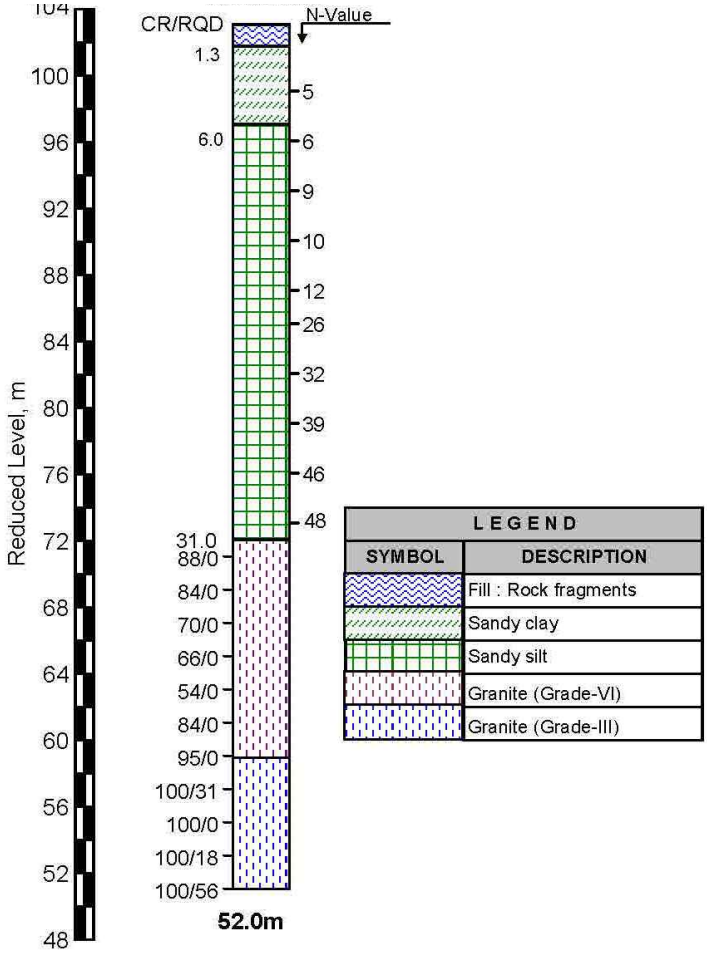
LEVEL REFERENCE	LEVEL DESCRIPTION	DEPTH-RL (m)	DEPTH (m)
TOG	Top Of Guidewall	103.200	31.522
GL	Ground level	102.900	31.222
SG1	Strain Gauges (4 nos)	90.900	19.222
SG2	Strain Gauges (4 nos)	83.900	12.222
SG3	Strain Gauges (4 nos)	75.900	4.222
COL	Cut-off Level	71.678	0.000
SG4	Strain Gauges (4 nos)	71.000	-0.678
SG5	Strain Gauges (4 nos)	69.000	-2.678
SG6	Strain Gauges (4 nos)	66.000	-5.678
SG7	Strain Gauges (4 nos)	63.000	-8.678
SG8	Strain Gauges (4 nos)	60.000	-11.678
SG9	Strain Gauges (4 nos)	58.000	-13.678
SG10	Strain Gauges (4 nos)	56.000	-15.678
SG11	Strain Gauges (4 nos)	54.000	-17.678
J1	Hydraulic Jack assembly (to bottom plate)	53.000	-18.678
SG12	Strain Gauges (4 nos)	52.000	-19.678
SG13	Strain Gauges (4 nos)	51.250	-20.428
PT	Pile Toe	50.400	-21.278



SPT No.	DEPTH-RL (m)		
0	102.90	to	101.60
5	101.60	to	96.90
6	96.90	to	90.90
10 - 12	90.90	to	84.90
26 - 39	84.90	to	75.90
46 - 48	75.90	to	72.90
G(V)	72.90	to	67.90
G(V)	67.90	to	59.90
G(IV)	59.90	to	57.90
G(IV)	57.90	to	53.90
G(III)	53.90	to	50.400

Fill
Firm, light grey, slightly sandy CLAY (Kallang Formation)
Firm, yellowish brown mottled reddish brown, sightly sandy SILT, G(IV)
Stiff, light grey, slightly sandy SILT, residual soil G(VI)
Very stiff, light grey mottled dark grey, sandy SILT, original rock texture preserved, completely weathered, G(V)
Hard, light grey mottled dark grey, sandy SILT, completely weathered G(V)
Weak to moderately weak, light grey spotted white and dark grey, GRANITE, completely weathered G(V) with highly weathered G(IV)
Weak to moderately weak, light greenish grey, light grey, GRANITE, copletely weathered G(V) with highly weathered G(IV)
Light greenish grey/ dark grey, highly weathered G(IV)
Moderately strong, light greenish grey to dark grey, moderately weatheed G(IV)
Moderately strong, light grey to dark grey, GRANITE, moderately weatheed G(III)

APPENDIX – B: BORELOG



REFERENCES

ASTM Standard D8169/D8169M – 18, (2018) Standard Test Methods for Deep Foundations Under Bi-Directional static Axial Compressive Load, ASTM International, West Conshohocken, PA. pp. 1.

Leung, C. F., Shen, R. F., (2003) Comparison of Conventional and Osterberg Cell Pile Load Tests, *Proceedings: Sixth International Symposium,* Oslo, Norway. pp. 1.

Schmertmann, J. H., Hayes, J. A., Molnit, T. & Osterberg, J. O., (1998) O-cell Testing Case Histories Demonstrate the Importance of Bored Pile (Drilled Shaft) Construction Technique, *Proceedings: Fourth International Conference on Case Histories in Geotechnical Engineering*, St. Louis, MO. pp.1103 - 1115.

CONTACT FREE SENSOR TO MONITOR PRESTRESSING ANCHORS IN GEOTECHNICAL STRUCTURES

Lucian Bogdan, DYWIDAG Systems International, Long Beach, CA, USA, 1-562-295-3907, lucian.bogdan@dsiamerica.com

Rajiv Pandey, DSI-Bridgecon, New Delhi, Delhi, India, 011+91 99 714 32223, RAJIV.PANDEY@dsi-bridgecon.com

Shahid Islam, DYWIDAG Systems International, Bolingbrook, IL, USA, 1-630-972-4028, shahid.islam@dsiamerica.com

ABSTRACT

There is a rapid expansion of world's infrastructure and simultaneously existing infrastructure is aging. The maintenance of infrastructures has been of particular concern to the engineering community. Monitoring and evaluating the structures have become more significant than ever. Ground anchor is an important part of the structure where it is installed. Unfortunately there are limited testing methods available to assess the force in the pre-stressing steel. High cost, complicated equipment and limitation of space often prevent these methods from being implemented. DYNA Force sensors have been developed to measure the force in the pre-stressing steel during construction and at any time during the lifetime of the structure. These sensors make use of the magneto-elastic properties of ferrous materials. A readout unit is designed to magnetically energize the steel through the sensor and measure the response of the steel to the process. The readout unit then converts the response into a direct force reading. They can be used for bare, epoxy-coated, galvanized and greased-sheathed steel in the bonded, un-bonded, grouted or un-grouted length of the tendon. It measures the force of the steel element at the location where it is installed and can be recorded manually, automatically, or remotely. The sensor is robust, requires no maintenance and it is expected to have a similar service life to that of the surrounding structure. Sensors have received attention in terms of accuracy, performance, ease in installation, durability, and cost effectiveness. This paper describes its application in tie-back and tie-down anchors and force monitoring of retaining walls, bridge abutment and concrete dams where the data were collected manually, automated and remotely.

Keywords: post-tensioning, force monitor, sensor, tie-back, retaining wall, dam

INTRODUCTION

Some structures are expensive to maintain and there is a large demand for implementing health monitoring of structures. Many retaining walls, dams and other geotechnical structures are post-tensioned or retrofit using post-tensioning tiebacks or tiedowns system. On many occasions during construction and service life of the structure, it is useful to know the existing force of these the post-tensioning anchors. Although there are many methods to measure the tendon force, most of them are cumbersome, expensive, and the accuracy varies depending of the method used.

The elasto-magnetic (EM) technology is a novel approach to monitor forces in steel elements. The DYNA Force sensor is built based on EM technology (See Fig. 1). It is composed of a primary coil and a secondary coil (sensing coil). By passing current through the primary coil, ferromagnetic material is magnetized. The sensing coil picks up induced electromotive force that is proportional to change rate of applied magnetic flux (Faraday's law) and relative permeability. As permeability of core changes, output voltage changes. The output voltage is calibrated to measure the force. A readout unit is designed to magnetically energize

© 2018 Deep Foundations Institute

the steel through the sensor and measure the response of the steel to the process. The readout unit then converts the response into a direct force reading. The sensor has an embedded thermistor which allows for temperature compensation. Due to the diversity of the magnetic property of steel, calibration is done for each type of steel allowing the sensors to perform at their highest accuracy.

$$\varepsilon = -\frac{d}{dt}(\phi_B)$$ Where, $\varepsilon =$ electromotive force $\phi_B =$ magnetic flux

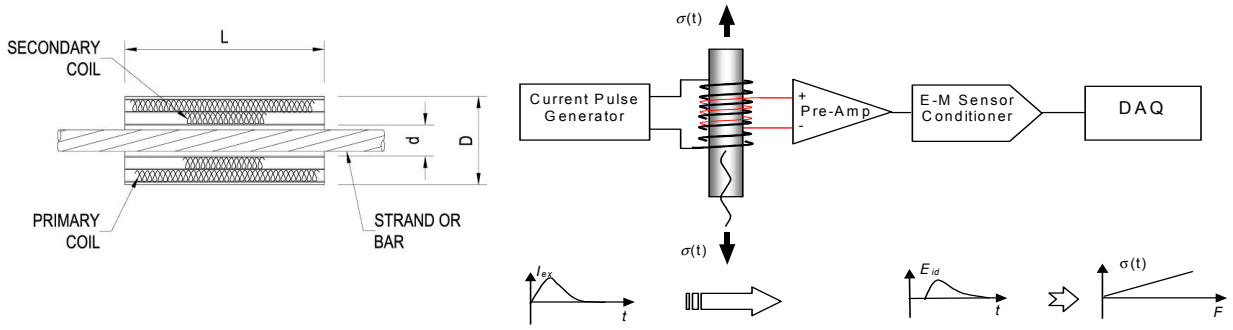


Fig. 1. Elasto magnetic sensor coils and indicative working chart showing final force

Sensors are cylindrical in shape and are installed over steel elements prior to stressing (fig.2). The sensor is robust, requires no maintenance, has no moving parts and is not subject to any load. It is expected to have a similar service life to that of the surrounding structure. They can be used for bare, epoxy-coated, galvanized and greased-sheathed steel in bonded, un-bonded, grouted or un-grouted length of the tendon. The accuracy of the force measurement for the sensor is equal or better than the conventional load cells.



Fig. 2. Sensor installed on uncoated threadbar (left) and on steel uncoated and HDPE coated strand

SENSOR SYSTEM

The Sensor System consists of sensor, readout unit and multiplexer (fig. 3). Additonal items are included inside a permanent storage box (fig.4). Sensor dimensions are shown in Table 1. Additional cable connections, multiplexers, modem & controller are required for continuous and remote reading. In the Manual option, each sensor is individually connected to the readout unit and the force in the strand or bar can be obtained in a few seconds.

In the remote and automated reading option, all sensors are connected to the readout unit using extension cables, multiplexers and main cables. The readout unit is programmed to record the temperature and force readings of all sensors at a specified time interval. It can record up to a maximum of 2,400 sets of data. The

recorded data may be downloaded to a laptop computer using a RS232 port attached to the Unit. The data is in Txt or ASCII format and can be imported to other programs and analyzed.

Extension cables and main cables are guided to a water proof NEMA type box. Insise the box, for the remote, automatic reading, a modem and a controller are also attached to the readout unit. A cellular SIM card with a data plan or ethernet terminal server is installed to communicate from a remote computer with a static IP address. Software is provided to collect data from the readout unit through a RS232 port. It can either take readings from a remote computer as needed or can get data stored at specified intervals in the readout unit positioned at the point of use. The output from the readout unit may be incorporated into other data acquisition systems as well. Data is in Txt or ASCII format and can be imported to other programs and analyzed.



Fig. 3 Sensor **Readout unit** **Multiplexer**



Fig. 4 Solar panels and NEMA box with readout unit, modem, controller

Table 1. Sensor dimensions DYWIDAG Threadbar and strand

Strand Size	Strand Grade	Sensor Dimensions (in)		
[in]	[ksi]	I.D.	O.D.	Length
0.5-0.62	270	0.79	1.42	5.2
Bar Size	Bar Grade	Sensor Dimensions (in)		
[in]	[ksi]	I.D.	O.D.	Length
#7-#11	75-100	1.69	3.15	7.09
#14	80-100	2.09	3.90	7.87
#18/#20	80-100	2.87	5.71	12.20
#24	75-100	3.35	6.10	12.99
1”-1-3/8”	150	1.69	3.15	7.09
1-3/4”	150	2.09	3.90	7.87
2-1/2”	150	2.87	5.71	12.20
3”	150	3.35	6.10	12.99

SENSOR APPLICATIONS

Sensors have been successfully used in more than eighthy projects such as cable-stay bridges, new and repair post-tensioning tendons in bridge and building structures, air traffic control and wind energy towers, or as tieback and tiedown anchors for slope stabilization, retaining walls and concrete dams. Some of the sensor applications in geotechnical structures in USA are presented below.

Crib Wall Retrofit with Permanent Strand Tiebacks. DSI supplied 345 permanent tieback anchors with 9-0.6 inch diameter strands to retrofit the 1700-ft long crib wall of up to 50-ft tall of the Patton Creek shopping center in Birmingham, Alabama that showed sign of slow moving. Tieback was fabricated with a double corrosion protection system. Anchors were proof or performance tested to 80% of strand ultimate strength and locked at less than 70% Fu. Partial view of wall with precast units and stressing of anchors are shown in fig. 5. One sensor was installed in each of 4 anchors and the forces in these anchors were measured after lock-off, after 28 days and after 6 years in service and the results are shown in Fig. 6. The latest data shows the forces in three anchors have increased as compared to 28 days readings. The increase in load in the anchors may be a result of newly opened bridge road adjacent to the anchor wall.



Fig. 5. Precast units applied over crib wall and anchor stressing for Patton Creek mall, Alabama

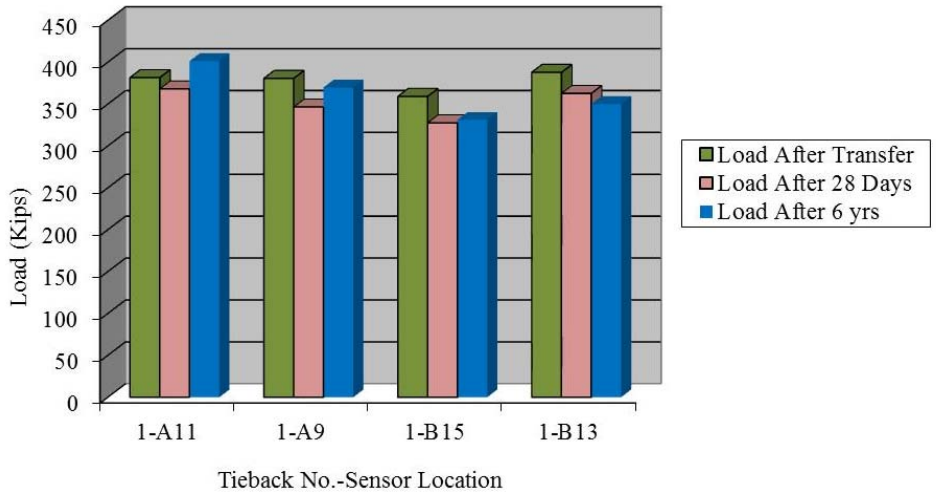


Fig. 6. Anchor force monitoring for slope stability of Patton Creek mall, Alabama

Tiedown Rock Anchors Stabilize Concrete Dam. Twenty-eight 59-0.6" strand anchors were used for the stability and safety of the dam at the Willow Island Hydroelectric project in West Virginia. Rock mass was excavated to allow for installation of a power generator. In order to monitor the forces in the anchors during excavation of rocks, three sensors were installed in each anchor. A total of 84 sensors were installed in these permanent rock anchors. All sensors were connected to a multiplexer using extension cables and all multiplexers were connected to the readout unit via main cable. Modem, controller and Cell SIM card were installed so the data could be accessed from a remote location. Battery and solar panels were used to power the readout unit. Figure 7 shows general view of dam the anchor force at various loading stages. It is apparent that sensor readings were close to the jack readings as compared to the load cell readings. Valuable data from all of the sensors were being taken remotely every 3 hours, analyzed and reported to the owner.

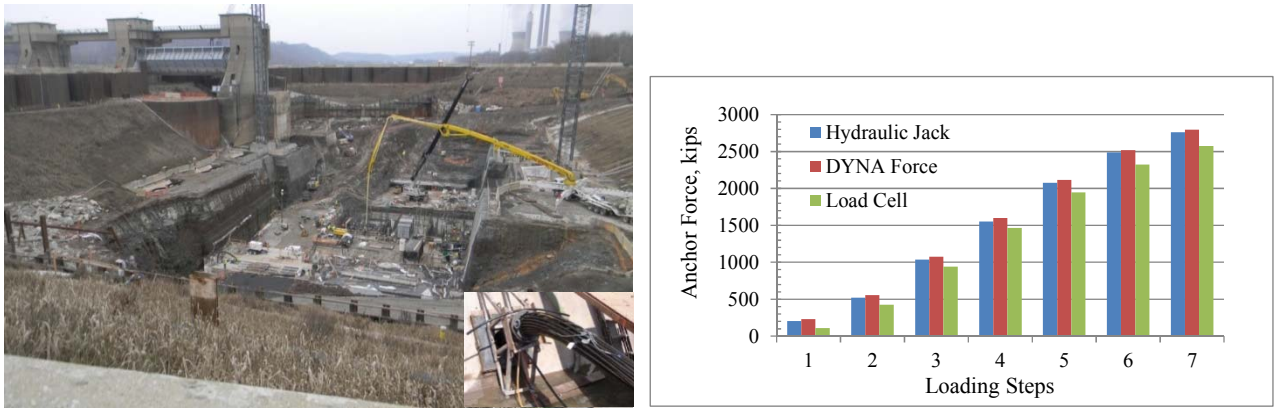


Fig. 7. Sensors for Willow Island Hydroelectric Project, West Virginia

Slope Stability at Bridge Abutment. DSI supplied 56 strand sensors for both permanent and test ground anchors for Sellwood Bridge in Oregon, USA (fig. 8). The main purpose was to monitor the slope stability in front of the bridge abutment. For the test anchors six sensors were installed in the bonded length and one in the free length. For the permanent anchors two sensors were installed in each of the anchors with number of strands varying from 8 to 24. Fifteen automated readout units were installed to record the force readings

of the sensors at every 4 hours. Software was provided so that the engineer could transfer the recorded data to a laptop. Sensors provided valuable information for both test and permanent anchors.



Fig. 8. Preacast panel with tieback at bridge abutment, Sellwood bridge, Portland, Oregon

Two Permanent Retaining Walls with Strand Tiebacks along the Freeway. 470 anchors with 4 thru 8-0.6" strand permanent tiebacks stabilized two retaining walls built to widen the highest congested freeway in the country, freeway 405 in Los Angeles, CA, as shown in Fig. 9. Forty-eight sensors were installed on tieback anchors to monitor the performance of the retaining wall. Automated readout units were installed to record the force at every 4 hrs (fig. 10). Sensors are providing very consistent and valuable information to the owner.



Fig. 9. Two permanent retaining walls with strands tiebacks, Fwy 405, Los Angeles, California



Fig. 10. Retaing wall, strand anchorage with sensor cable and automated reading assembly box

Landslide Stabilization with Precast Panels and Tiebacks. In order to prevent landslide of a major highway in North Dakota, USA, tieback anchors were installed. Sensors were installed in the bonded zone to monitor the forces along the length of the pre-production anchor. Sensor DF13 was at 40 ft into the bonded length, Sensor DF14 was at 20 ft into bonded length and sensor DF15 was at 5 ft into the bonded length. The sensor readings were recorded at various stages of loadings. Stressing procedure and force readings are plotted on a graph as shown in Fig. 11. Sensor located at 40 ft and 20 ft into bond length showed little or no force meaning full bond between the strand and soil through grout. Sensor located at 5 ft into bond length showed almost half of the jacking force indicating de-bonding at this location. The engineer reported the force transfer was as expected. The sensor readings provided valuable information to the engineer so that they can move with design and avoid any risk of anchor failure.

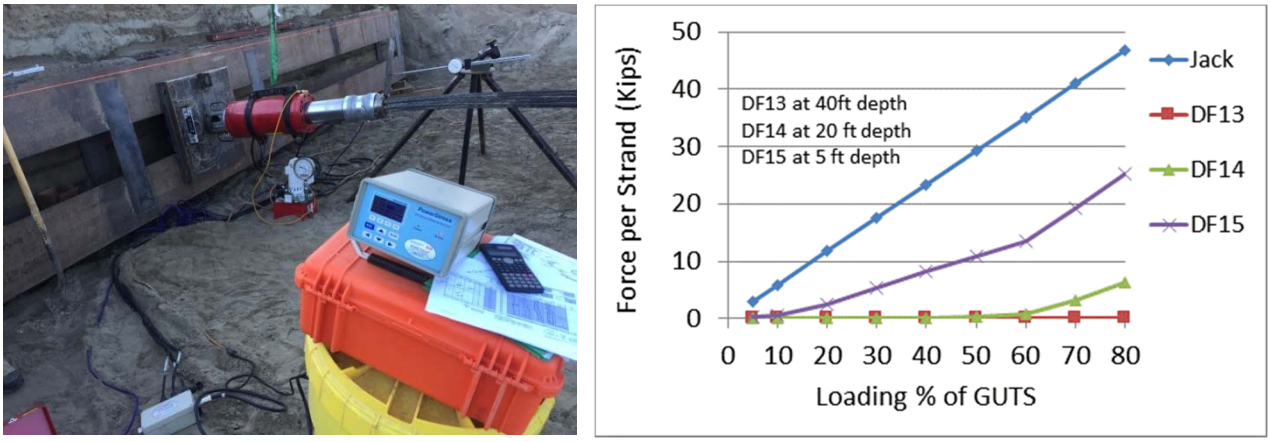


Fig. 11. Stressing procedure and monitoring of load transfer in anchor bonded length

Landslide Stabilization with Precast Panels and Tiebacks. Road adjacent to Pacific Ocen at White Point Reserve, Los Angeles was falling down due to slope slope movement (fig,12). Contractor proposed slope stabilization with very long strand anchors installed through large precast panels. Two,

6-0.6“ strands pre-production anchors were installed with three sensors in the bonded length (DF5, DF6, DF7, DF13, DF14, DF15) and other four sensors along the unbonded length. They were proof stressed and readings taken (fig 13, 14). Bonded length sensors had zero load or almost zero readings and unbonded length had readings close to the jack preassure gauge. They were continue taken readings even after all permanent anchors were installed and lock-off.

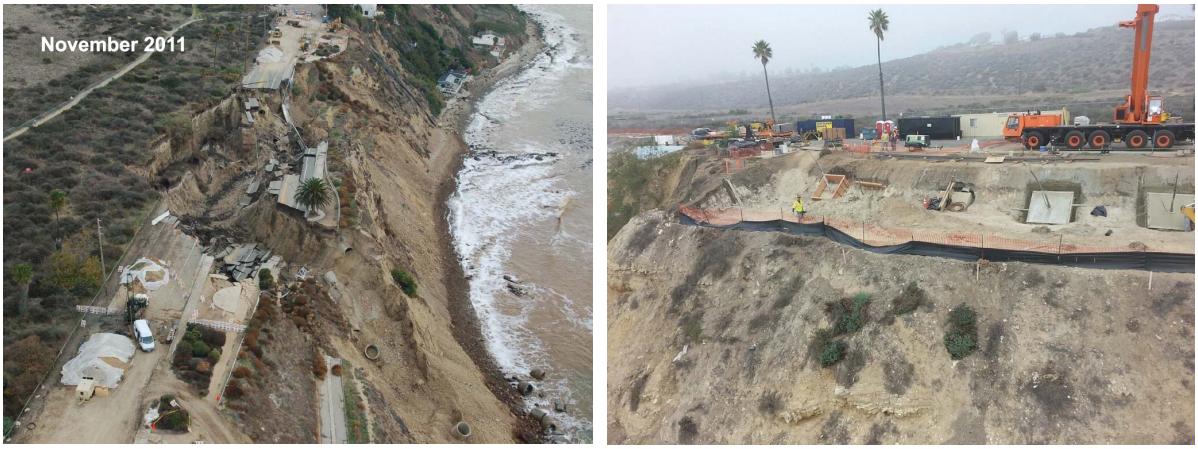


Fig. 12. Slope and road damaged and installation of precast panels with strand tiebacks

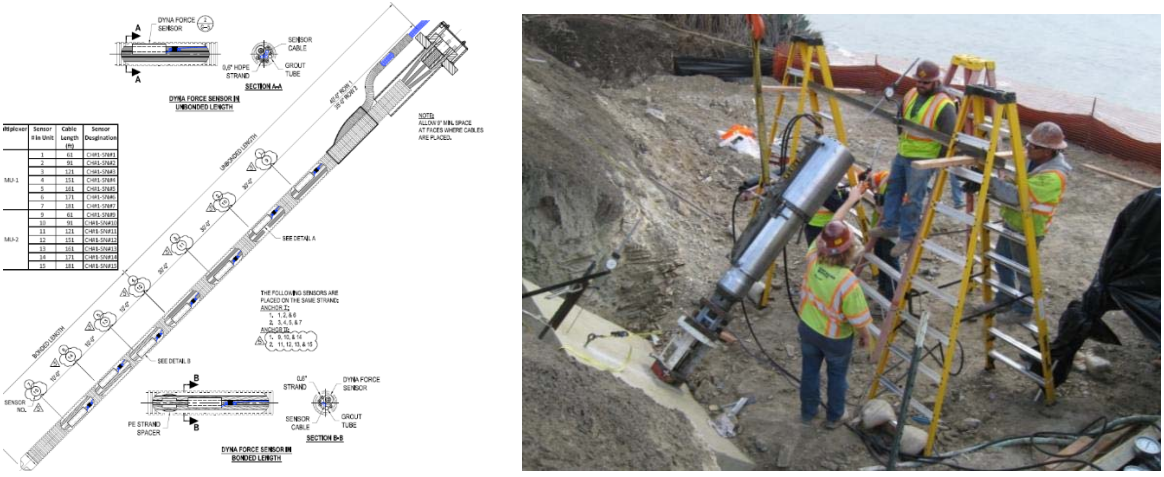


Fig. 13. Details of sensors placement along the anchor length and stressing procedure

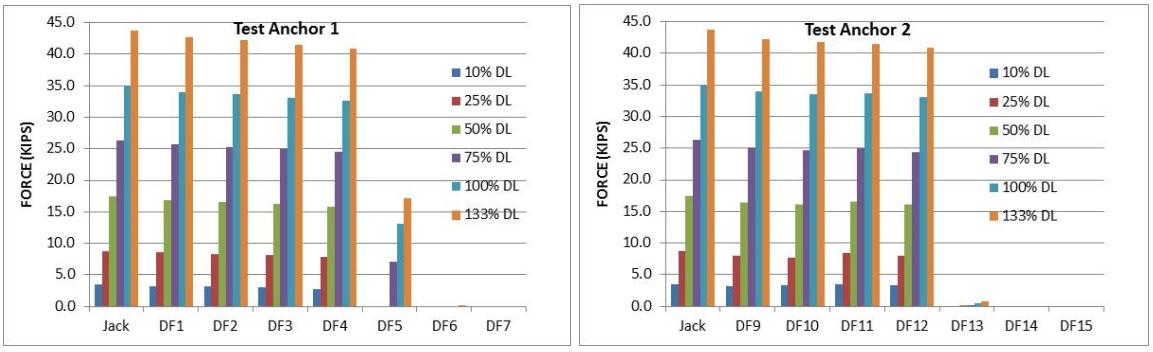


Fig. 14. Load monitoring during testing

Permanent Strand Tieback Retaining Wall Along Highway. 75 tiebacks with 10-0.6“ strands per anchor were installed along highway 101 in Northern California to stabilized slope behind highway that was moving (fig. 15). Ten anchors had installed 2 sensors in the unbonded length behind the anchorage. Solar panels provided energy to battery pack so they were continuasly automatic load monitoring to see any sign of load movement (fig. 16).



Fig. 15. Up to 4 concrete tiers of tiebacks were installed against soldier pile retaining wall



Fig. 16. Testing procedure with DYWIDAG jack and automatic load monitoring assembly

CONCLUSIONS

DYNA Force system has been used in over eighty projects and proven to be the preferred technique to monitor forces in steel elements in terms of accuracy, its performance, ease in installation, durability, and cost effectiveness. The sensors are very easy to install and being inside the hole, do not require massive anchorage and thick concrete wall as other methods. Sensors can be used for bare, epoxy-coated, galvanized and greased-sheathed steel in bonded, unbonded, grouted or ungrouted length of the tendon or anchor.

The owner can regularly monitor forces in pre-stressing steel manually, continuously and even from a remote access. There is high accuracy of the force measurement. The sensor is robust, requires no maintenance, has no moving parts and is not subject to any load. It is expected to have a similar service life to that of the surrounding structure.

ACKNOWLEDGMENTS

The authors wish to acknowledge the support of Dr. Yang Zhao. The authors would like to thank all members of the DFI Technical Committee for their support and contribution.

REFERENCES

Bogdan, L., 2017. New Technology of Force Monitoring for Post Tensioning Ground Anchors. Southeastern Transportation Geotechnical Engineering Conference, Savannah, GA, USA

Islam, S., and Purinton, K. 2015. Long-term force monitoring of prestressed anchors used on dam rehabilitation projects. Dam Safety 2015 Conference, New Orleans, LA, USA

Islam, S., and Purinton, K. 2015. Long-term force monitoring of prestressed anchors used on dam rehabilitation projects. Dam Safety 2015 Conference, New Orleans, LA, USA.

Islam, S., 2014. Force monitoring of post-tensioned steel elements in bridge and building structures. Proc. the fourth international fib Congress (pp. 733-737), Mumbai, India.

Bogdan, L., 2011. DYNA Force-An Elasto-Magnetic Sensor for Force Measuring of Post Tensioning Ground Anchors, Southwest Geotechnical Conference, Reno, NV, USA.

Bogdan, L. 2011. New Method of Force Measuring of Post Tensioning Ground Anchors. Geo3-T2 Conference, Raleigh, NC

Islam, S., 2008. Long term force monitoring of post-tensioning tendons and cable stays in concrete segmental bridges, ASBI international symposium on future technology for concrete segmental bridges, San Francisco, California, USA.

Wang, M. L., Koontz, S., and Jarosevic, A., 1998. Monitoring of cable forces using magneto-elastic sensors, 2nd U.S.-China symposium workshop on recent developments and future trends of computational mechanics in structural engineering (pp. 337-349), Dalian, PRC.

CONTINUOUS FLIGHT AUGER PILES – A TECHNOLOGY INITIATIVE FOR FASTER PILING IN INDIA

Sunil.S. Basarkar[1]*, KS Ramakrishna[2], I.V. Anirudhan[3] and K. Pitchumani [4]
[1]M/s AFCONS Infra. Ltd., Mumbai; [2] DFI of India, Chennai; [3]M/s Geotechnical Solutions, Chennai; [4]M/s AECOM, Chennai

* Corresponding Author: sunil.basarkar@afcons.com

ABSTRACT
Concept of Bored Cast-in-Situ (BCIS) piling was introduced in India during early 1950s and since then are used widely. BCIS piles, despite being widely used today, require skilled supervision, and may not offer faster and quality guaranteed solution under certain sub-surface conditions. There is an urgent need to introduce latest piling technology to ensure higher productivity with high quality standards, addressing safety requirements during execution. Such foundation technology is expected to be an economical answer to accelerate country's growing infrastructural needs.
Realizing this technology gap, DFI of India along with DFI (USA) set ahead an ambitious technology initiative for introduction of Continuous Flight Auger (CFA) piles in India. Looking at the piling practices in USA and Europe, it is well accepted that CFA piles would take less time for installation compared to BCIS piles for a certain range of loads and sub-soil conditions; and therefore, would play a pivotal role to address India's fast track piling requirements during its immediate future.
This paper presents details of the plans and actions on the DFI of India's CFA technology initiative which is expected to provide useful information on the philosophies of design and execution to be adopted, critical areas and considerations that are currently being addressed for its successful implementation. In fact, there are wide possibilities of CFA piles in assisting fast track projects and is expected to set up a positive ambience for gainful acceptance in India, which otherwise, had been viewed sceptically in the past.

1. CFA PILE TECHNOLOGY – NEED OF THE HOUR

Construction Industry in India is poised for a major contribution to the rapid development of various sectors of India's economy. Commencing from early 2000s, the country has witnessed rapid stride in development of many infrastructure projects with several mega plans on anvil in near future.

Foundation engineering practice in our country is still in a nascent stage in sharp contrast to the foundation technologies, equipment, materials and construction methods practiced and adopted in USA and Europe. While our knowledge and research in the geotechnical engineering may be comparable with those in the advanced countries, the same cannot be said about the foundation engineering and construction practices. A lot needs to be done on priority to ensure that the foundation works in every project keeps abreast with the progress requirements and quality construction in India.

It is of utmost importance to realize that quality and speed are essential in the case of foundation works because of the simple fact that in most of the foundation works we do not see what we construct. Technologies are available to address these issues, where the quality and speed of foundations can bring significant savings to the project.

© 2018 Deep Foundations Institute

In Indian context, principle clients taking the wholehearted lead in implementing value-based initiatives are very likely to trigger speedier response from whole industry in adapting new technology initiatives. Thanks to key client organizations, who made it mandatory to employ hydraulic rotary bored piling rigs in their projects, past two decades have witnessed rise in the number of hydraulic rotary pilings in our India from zero to around 900 numbers. This number needs to be at least three to four times if all clients and consultants impose hydraulic piling rigs for bored piling works in their projects. It should be acknowledged here that the role being played by the representatives of equipment manufacturers and piling subcontractors is praiseworthy even though they do not match with what our country needs in the short and long terms.

DFI of India (DFII), as one of its missionary objectives, has been putting consistent efforts to highlight current gaps in deep foundation industry and remedies to address the same by bringing global expertise to the doorstep of India.

Looking at above mentioned technology gulf in piling practices in India, DFII proposed CFA technology implementation initiative with following defined objective statement:

To demonstrate installation of CFA piles under Indian scenario, testing for compression, uplift and lateral loading and to prepare a comprehensive guideline manual for design, installation and testing of CFA piles for its confident implementation in India.

DFI USA approved the CFA initiative proposal during April 2017 and later, CFA committee was formed comprising members from public sector enterprises, contractors, consultants, equipment manufacturers, academia and experts from DFI USA, to plan, design and implement this project. The CFA initiative is estimated to cost around Rs 50 lakhs (USD 70,000), out of which DFI USA sanctioned a grant of Rs. 20 lakhs (USD 30,000). This joint initiative has provided invaluable stimulus for this technology initiative ball to roll with Nuclear Power Corporation of India Limited (NPCIL) chipping in by being a host and providing site and other support for its implementation.

It is well established that CFA piles require lesser installation time compared to Bored piles of same diameter. With minor modification with existing hydraulic rigs, there would be significant increase in piling progress per day. Additionally, construction CFA piles is without significant vibration or excessive noise being produced and, no temporary casing or bore stability methods are required, thus providing a high degree of reliability and quality assurance.

With above background, this paper presents status and developments so far in this ambitious CFA initiative, with immediate plans to disseminate the knowledge and experiences, and at the same time invite discussions and deliberations so that CFA piles in India establishes its firm roots in Indian Industry.

2. DFII's CFA PILING TECHNOLOGY TRIAL PROJECT

DFII intends to introduce and establish CFA system of piling to the deep foundation industry in India by conducting a field trial as a technology demonstration for the benefit of all its stakeholders. This deep foundation system is well-proven abroad and being practiced internationally. The main object of this field trial in India is to design and construct the piles according to India codes and standards. A design and construction manual based on this trial is planned and expected to provide necessary inputs to a design-execution team to evaluate the use of CFA piles in the Indian market.

The trial is also expected to outline specific requirements in the design and use of concrete or grout and reinforcement. The importance of maximizing safety and quality assurance through continuous monitoring at every stage of the construction of CFA piles and the importance of the competency of the key project personnel are expected to be highlighted by the trials. NPCIL agreed to extend their support to conduct the CFA trials at their upcoming plant site at state of Haryana, India.

2.1. Site Details for Trials and Geographic Location

The plot proposed for trials comprise 40m x 34 m land with some free space around in the NPCIL project site at Gorakpur in Fatebad District of Haryana, India. This site is roughly 210 km west of New Delhi, the capital of India.

The site is part of the alluvial Ghaggar-Yamuna plain of central India located in a plain ground at about 214.8m above mean sea level. It experiences somewhat extreme cold and hot climates with temperature as low as 3ºC (34ºF) in January and a high of 46ºC (115ºF) during May-June. The average rain fall during a year is about 490 mm, the maximum rains occur during the months of July and August. Gorakpur river flows west of the site and the river is known to carry water during most of the year.

The trial plot location is shown in Figure 1. The site has access from the East gate of NPCIL which is on the Hissar side. The peripheral road after the security gate leads to the main entrance of the plant. The trial location has two lattice towers mounted 1 KV high tension lines. The trial pile locations are at about 32m clear distance from the nearest high-tension line. The clear head room below the line is roughly 7.0m.

2.2. Trial CFA Piles – Concept and Layout Plan

The trial pile locations and the exploratory borehole locations are marked in Figure 2. Taking into considerations the movement of machinery, planned sequence of construction is also indicated in Figure 2.

It is planned to have six CFA piles at this site, 600mm diameter and about 18m depth. These piles shall be executed as per carefully and well deliberated methodology suitable under Indian conditions, with witnessing process involving key players and stakeholders in piling industry including project owners, Bureau of Indian Standards (BIS) representatives, experts from India and abroad, consultants, academicians, equipment agencies etc.

Two axial compression, two axial tension and two lateral load tests are planned and summarized in Table 1. These load tests shall be performed as per Indian code, IS: 2911 (Part 4) and capacities determined as per standard design practice. While, Low strain dynamic testing, shall be performed on each pile before carrying out static load tests.

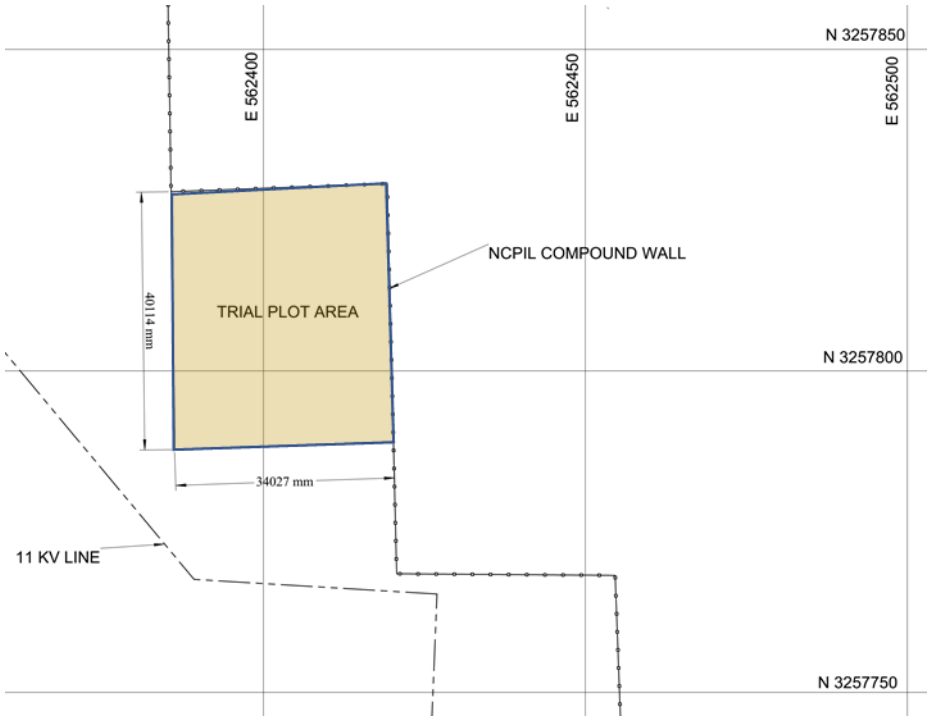


Figure 1: Trial plot area in the NPCIL land

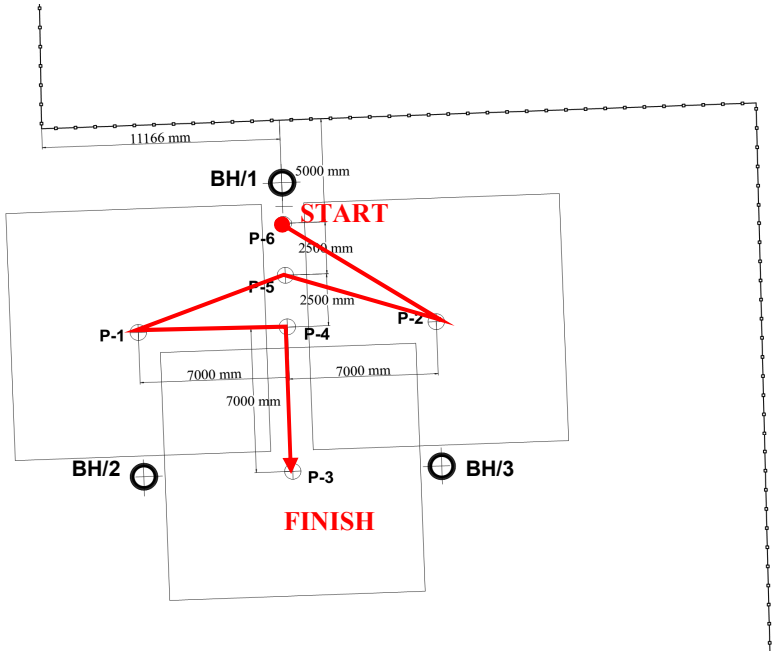


Figure 2: Trial pile layout plan, exploratory boreholes; piling sequence

Table 1: Summary of Testing program

Sl. No	Test Sequence	Test Pile Numbers	Remarks
1	Lateral Load Test 1 LLT1	P6	Reaction load shall be drawn from the soil
2	Lateral Load Test 1 LLT1	P4	
3	Compression load test 1 CLT 1	One out of P1, P2 & P3	The reaction platform shall be away from other piles
4	Compression load test 1 CLT 2	One out of P1, P2 & P3	
5	Pull out load test PLT 1	P5	The reaction from Piles P4 & P6
6	Pull out load test PLT 2	Remaining of P1, P2 & P3	The reaction from RC footings

2.3. Sub-Surface Features of the Site

Geotechnical investigations comprising three exploratory boreholes were carried out in the trial locations during November-December 2017. The sub-surface profile as captured by these boreholes are summarized in Figure 3. As observed, the subsoil comprises sandy silt layers occasionally interlaced with silty sand layers and thin sand layers. In general, the soil is fine sandy silt with negligible amount of clay with D_{50} in the range of 0.02mm to 0.10mm. The plasticity is reported to be *Nil*. Borehole BH3 recorded medium plasticity clayey sandy silt after 25m depth.

The shear strength in terms of SPT N is gradually improving towards depth except for relatively denser layer between 3.0m and 6.0m depth. The top 3.50m sandy silt is relatively weak. Water Table is observed at about 3.2m below ground at the time of investigations.

3. CFA PILE DESIGN BACKGROUND

In USA, standard design procedure applicable for drilled shafts is applied to CFA piles also. The accepted procedure after review of several field load test data is very close to the procedure suggested by Reese et. al (2006) and AASHTO (2006). These procedures consider the ultimate base resistance to be mobilized at a tip displacement equal to 5% of the pile base diameter. The design procedure recommended in IS 2911 Part 1/ Sec 2 considers the ultimate base resistance realizing at a pile head displacement equivalent to 10% of the pile base diameter. The IS 2911 follows a bearing capacity estimation approach for estimating the base resistance and effective stress approach for estimating the side friction. This is different from the empirical approach recommended by Reese et. al (2006) and AASHTO (2006). In the current initiative, design proposal for CFA piles gives prominence to IS 2911 so that the CFA technology using the national code of practice finds gainful acceptance in India.

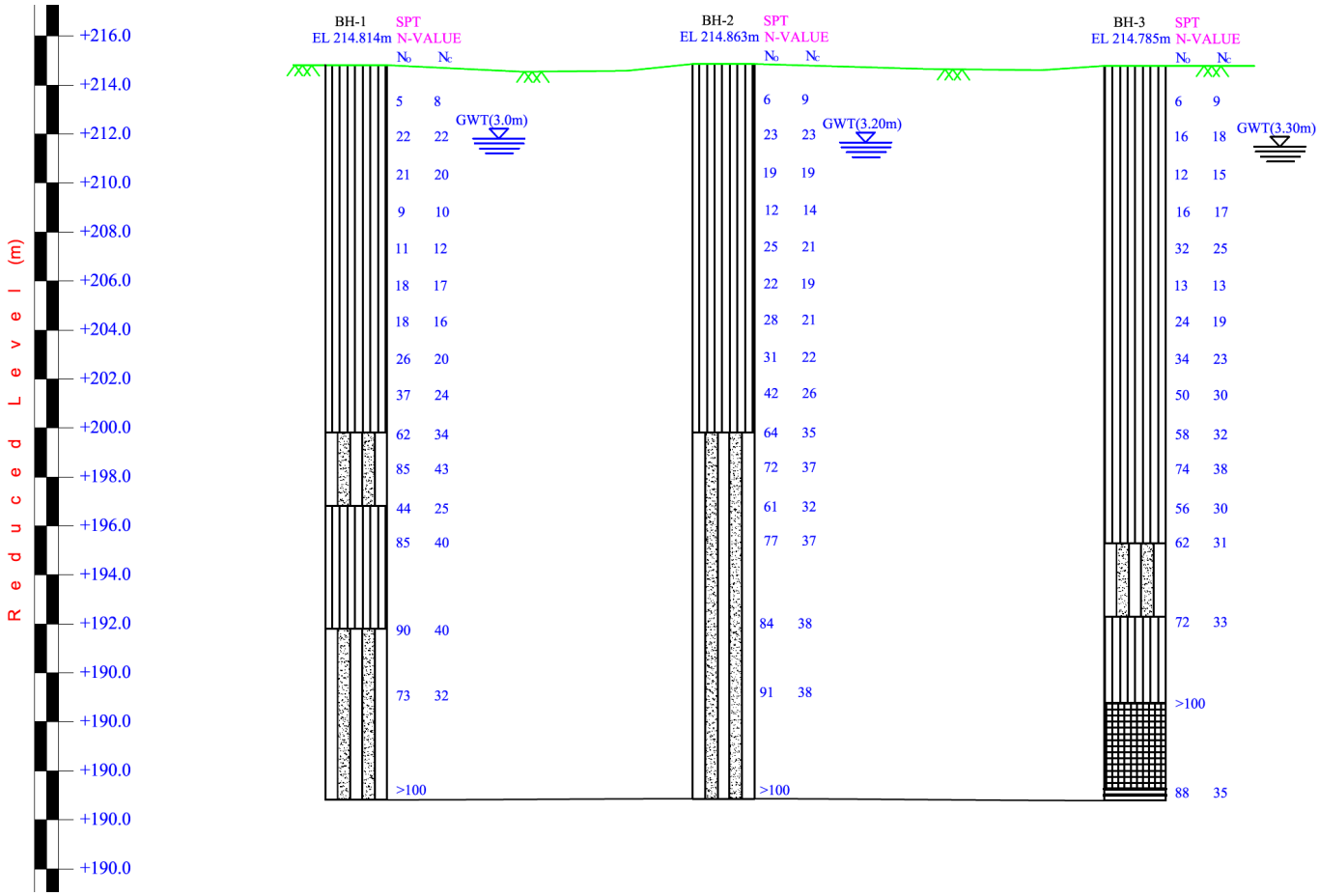


Figure 3: Sub-surface Soil Profile

3.1. Design Parameters & Philosophies, Test loads

Taking findings of geotechnical investigation further to design, the shear strength of fine sandy silt with no plasticity as prevalent at the site, has been characterized by angle of shearing resistance, ϕ, and the compressibility in terms of soil modulus, E_s, both estimated from the corrected SPT N values. Two corrections are applied to the SPT N values considering the SPT N values are close to N_{60}. Initially the correction for the standard overburden pressure is applied, followed by submergence correction. The standard correlations between the relative density and the corrected SPT N values in such deposits are used to arrive at value of, ϕ. The classification suggested by Peck (1953), suitably modified by the proposal by R.K. Hough (1957) to account for the influence of particle size distribution is used to estimate, ϕ. Relatively lower range of ϕ, is estimated for sandy silt deposits. The soil modulus, E_s, is determined from Schultz and Muhs (1966) curve but applying a reduction factor 0.90 for the fine sandy silt soil at this site.

The subgrade soil modulus variation coefficient η_h based on the recommendations from Terzaghi (1955) and Garassino et. al (1976) (on saturated deposits) are estimated from the relative density. Both these ranges are significantly varying, and many researchers report that the Reese estimations are more realistic. IS 2911 Part1/Section 2 for the design and construction of bored cast-in-situ piles is recommending the η_h values suggested by Terzaghi.

It is not intended to go through complete analytical details of the pile design, since they are expected to be a part of a detailed CFA pile manual. However, with above background, summary of the axial compression and axial tension capacities for pile 18m below GL are presented in Tables 2 and 3 respectively.

Table 2: Ultimate Compression Capacities for piles up to 18.0m below GL with Cut-off-Level (CoL) 0.80m below GL

Procedure	Side friction (kN)	End bearing (kN)	Total (kN)
IS 2911 Part1/ Sec 2 (procedure 1)	1839	1292	3131
IS 2911 Part1/ Sec 2 (procedure 2)	1079	905	1984
IS 2911 Part1/ Sec2 (limiting K and N_q)	1338	668	2006
O' Neill & Reese for sett=5% of D	1484	569	2053
Recommended	1500	600	2100

The resistance of soil against pullout is normally close to the side friction under compression loading. However, the design practice is to consider 75% to 80% of the positive skin friction as the ultimate axial tension capacity. The submerged weight of the pile is added to this value.

Table 3: Ultimate Axial Tension Capacities kN for piles at 18.0m below GL with CoL 0.80m below GL

Pile length	IS 2911 (1) (kN)	IS 2911 (2) (kN)	IS 2911 (3) (kN)	Reese (kN)	Recommended (kN)
18.0m long pile	1447	1147	1338	1255	1255

The subgrade modulus, η_h, recommended by Terzaghi (1955) and Garassino et. al (1976) are used in separate analyses to determine lateral load capacity of CFA piles. The results are presented in Figure 4.

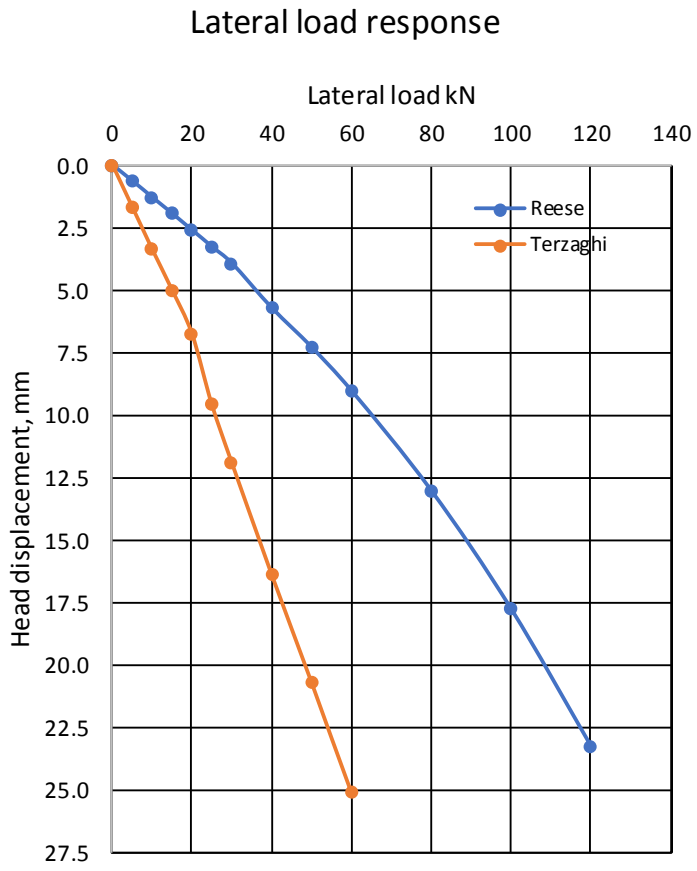


Figure 4: Response of 600mm diameter CFA piles under lateral loading

With above analytical background, planned test loads would correspond to recommended ultimate pile capacities shown in Table 4.

Table 4: Ultimate capacities of CFA Trial piles

Pile size	Compression (kN)	Lateral (kN)	Axial Tension (kN)	Remarks
600mm dia	2500.0	120.0	1400.0	Max bending moment under the lateral load is 160 kNm

4. PILE CONCRETE/GROUT AND REINFORCEMENT

Proposition for using either controlled concrete or grout for the CFA piles is a matter under serious discussions and research. Major requirement in the case of CFA piles is more workability that would allow pumping of the concrete without bleeding or segregation. The concrete placed through annular hole within the flight auger shall be workable enough to introduce the rebar cage within entire pile length without or with a nominal vibration. All solids should remain in suspension without excessive bleeding throughout the transit and pumping of concrete. The slump at the time of pouring should be 200mm to 220mm.

One of the major requirements for the concrete in CFA piles is the minimum resistance to the reinforcement cage while lowering into the green concrete. In this context, the coarse aggregate size shall preferably smaller than 9.5mm. High workability is achieved by right selection of the aggregate sizes and proportion, additives such as water reducers, set retarders and fly ash.

Above mix design requirements are for a transit period of about 120 minutes (from a likely batching plant location of about 45 km) and applicable for summer temperatures of 45 ºC. The placement shall be done using a concrete pump with approximate 20 bar pumping pressure capacity.

The maximum compression load on the pile is 2500 kN, which is roughly 8840 kN/m^2 (8.9 MPa). Concrete/ grout with compressive strength 35 MPa is proposed for the piles. Rebar cage shall be designed to carry a maximum tension of 1400 kN and bending moment 160 kNm.

5. CFA PILES – EXECUTION METHODOLOGY AND CRITICAL CONCERNS

CFA piling methodology can be broadly summarized through Figure 5, which comprise boring a hole with a single length auger during its downward travel and concreting the bore during simultaneous upward withdrawal of the flight auger. Reinforcement cage pushing into green concrete is the final operation.

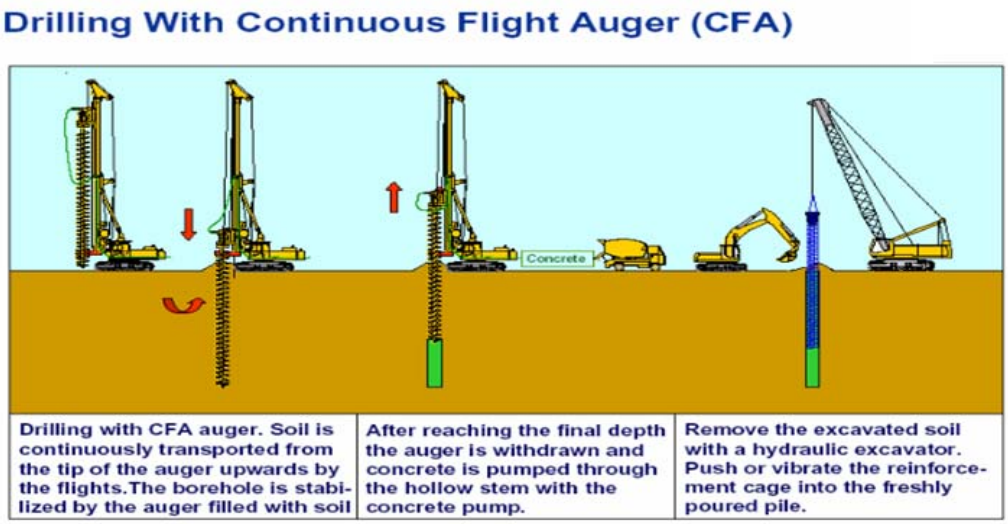


Figure 5: CFA Piling Methodology

While above steps define standard field methodology for CFA piling, following three critical issues are currently being under serious discussions to arrive at a viable and dependable execution at site. Smooth and efficient CFA operations would depend on how successfully these issues are implemented in field.

Concrete/ Grout quality: Success of CFA will depend on how effectively the concrete or the grout will be able to maintain its fluidity to allow the cage to be pushed into entire length of pile. The concrete mix design, the aggregate size, therefore, would require careful considerations.

Equipment Adaptability: A dominant factor for economic execution of CFA piles in India would require conventional hydraulic rigs to be modified to fit the CFA kit. In this connection, intense discussions are in progress with the experts and equipment suppliers to have continuous flight auger fitted to conventional hydraulic rig to give an economical edge not just during the trials, but also during long term of CFA piling under the event that this technology finds gainful acceptance from all stakeholders.

Rigidity of Reinforcement cage: Rebar cage will have to be pushed into green concrete/grout, and therefore, shall possess sufficient rigidity, which the structural design should cater to. Important factor would be the readiness to push cage through entire pile depth, preferably without vibratory arrangements.

6. CFA PILE TECHNOLOGY INITIATIVE - ROAD SO FAR AND TASKS AHEAD

Chronologically, the journey so far is enumerated below:

(i) DFII reached understanding with NPCIL during July-August 2017 for executing CFA test pile project at their site at Haryana, near Delhi.

(ii) A full-fledged CFA committee was formed in July 2017 for a structured approach, smooth coordination and implementation of plans for successful implementation of this initiative.

(iii) As of this date, following activities have been completed:

   a. Soil Investigation completed during November 2017 after NPCIL confirmed the site availability during October 2017.
   b. Initial Draft manual for pile design, pile installation/testing have been prepared by DFII and the commented documents have been received from DFI USA on May 2018 after being reviewed by experts.
   c. The final document is expected to be compiled by July'18 which will form the basis for execution of CFA test pile project.

(iv) Brochure for CFA test pile has been finalized with joint efforts of DFI and DFII highlighting benefits this technology can offer to Indian Deep Foundation Industry including on-going efforts on implementation of test pile project.

(v) DFII team had meeting with M/s ITD Cementation, Mumbai during March 2018, followed subsequently by a tele-conference meeting during May 2018 to seek their support and assistance during field execution through their available establishments and resources. for pile installation and testing.

(vi) Plans are in advanced stage for identifying equipment manufacturer with piling rig fitted with CFA kit. With the field trials planned during mid November 2018, execution and testing of piles are expected to be completed by end of 2018.

Post field exercises would include steps to disseminate the knowledge and experience gained from trials so that CFA piles gains a rightful place in Indian deep foundation industry to implement in different infrastructure projects across India. It will be endeavour of DFII to share inputs of this new technology with owners, their engineers, major contractors, concrete suppliers as all of them need to work together for its implementation in new projects. Knowledge and experience dissemination will be done through various seminars/workshops/conferences organized by DFII and by having one on one meeting with respective stakeholders. Comprehensive CFA manual would be finalized which shall contain guidelines for design,

execution and implementation of CFA piles exclusively suiting Indian conditions. Further, required efforts will be put to have IS Code draft for a favourable approval through BIS.

ACKNOWLEDGEMENTS

DFII gratefully acknowledges continuous thrust and support from DFI USA during all phases of this CFA project journey. Very realization of the possibility of implementation of this venture owes a lot to NPCIL, thanks for their decision to provide land and wholehearted encouragements to carry out the piling works; and for their assistance both from Head Office and Site during every phase of developments so far. DFII expresses their immense thanks to M/s ITD Cementation for gracefully accepting to render all possible assistance with their site establishments for piling, load testing and site activities. Support from the Equipment manufacturers is encouraging us to take future steps and look ahead confidently. DFII extends their sincere thanks to all having assisted in past and to those assuring us for all assistance during coming days to ensure that the CFA piling technology successfully finds acceptance in India.

REFERENCES

i. AASHTO (2006). LFRD Bridge Design Specifications, 4th Edition, American Association of State Highway and Transportation Officials, Washington DC.
ii. Garassino et. al (1976). Soil Modulus for Laterally loaded piles in sands and NC clays, Proceedings of the 6th European Conference, ISSMFE, Vienna, Vol 1, No:2, pp 429-434.
iii. Hough, B.K. (1957). Basic Soils Engineering, The Ronald Press Company, New York.
iv. IS 2911 (Part 1/ Section 2) (2010). Design and Construction of Pile Foundations — Code of Practice, Part 1 Concrete Piles, Section 2 Bored Cast In-situ Concrete Piles.
v. IS 2911(Part4) (2013). Design and Construction of Pile Foundations — Code of Practice, Part 4 Load Test on Piles.
vi. Peck, Hanson & Thornburn (1953). Foundation Engineering, John Wiley and Sons, New York
vii. Reese, L.C., Isenhower, W.M. and Wang, T.N. (2006). Analysis and Design of Shallow and Deep Foundations, section 11.6.3, Wiley, 2006
viii. Schultz, E. & Muhs, H. (1966). Bodenuntersuchungen for Ingenier – bauten (in German), Springer Verlag, Berlin.
ix. Terzaghi, K. (1955), Evaluation of Coefficient of Subgrade Reaction, Geotechnique, Vol. 5, p 297.

DESIGN OF COFFERDAM FOR WELL FOUNDATION CONSTRUCTION - A CASE STUDY

Vinoj Kumar M., Asst. Engineering Manager, L&T Construction, Mumbai, mvinoj@lntecc.com

Sandeep S Nikam, Asst. Engineering Manager, L&T Construction, Mumbai, sandeepnikam@lntecc.com

Rajib Mandal, Engineering Manager, L&T Construction, Mumbai, rajibmandal@lntecc.com

Vipul Dobhada, Chief Engineering Manager, L&T Construction, Mumbai, vipuldobhada@lntecc.com

ABSTRACT:

This paper deals with the special technique adopted for well foundation construction in maritime environment by creating an island using steel liner and sheet pile cofferdam. By adopting this technique, conventional method of constructing well foundation using steel caissons was eliminated. This technique of well foundation construction provided quantum reduction in steel quantities as well as construction time. This paper gives an insight to design and construction technique adopted for well foundation construction of long span steel bridge Package CTP 15B across river Narmada, Gujarat using sheet pile and steel liner cofferdam.

Key words: Sheet pile cofferdam, Steel liner cofferdam, Well foundation, Numerical modelling.

INTRODUCTION

The execution of foundations in maritime environments often involves important temporary works in order to provide a safer workplace complying with environmental and quality requirements. General construction methodology adopted for the construction of well foundation in maritime environment where depth of water is more than six to seven meters involves use of well caissons, which is more robust, and time proven method. However, this requires construction of huge steel caissons, which are completely non-retrievable and lead to higher costs due to its fabrication and erection/sinking efforts in the maritime environment. If by some method a Dry Island is created at the foundation location, the well foundation can then be constructed vis-à-vis like in land mode.

OVERVIEW OF THE PROJECT

Indian Railways is developing dedicated freight corridor for movement of freight trains through M/s. Dedicated Freight Corridor Corporation of India Ltd (DFCCIL). The 2nd Phase of the Western Dedicated Freight Corridor (WDFC) consists of 555km of double line electrified track from JNPT (Jawaharlal Nehru Port) to Vadodara (422km) and Rewari to Dadri (128km) along the existing Indian Railway Tracks. The track is capable of operating at a maximum train speed of 100kmph with an initial axle load of 25tonnes axle load. The 2nd Phase is divided into various packages.

The consortium of L&T Construction and IHI Infrastructure has received an EPC (Engineering, Procurement and construction) order from DFCCIL for the construction of special steel bridges over JNPT -Vadodara and Rewari-Dadri sections of the WDFC. Construction of these special steel bridges is divided into three packages.

- Package CTP 15 A consist of 8 steel bridges, 3 minor bridges and 2 RUBs (Road Under Bridge)
- Package CTP 15 B consist of a major long span steel bridge across river Narmada and a RUB
- Package CTP 15 C consist of two major bridges across Yamuna and Hindon and a RFO (Rail Fly Over)

© 2018 Deep Foundations Institute

This paper provides insight to special technique adopted for construction of well foundation. Package CTP-15B involves construction of: (1) Special Steel Bridge across Narmada river near Bharuch including bridge approaches of 200m length from abutments on both sides of the bridge, one (1) Road under bridge (RUB) located near the northern abutment of this bridge, guide bunds and protection works. The total length of the bridge is approximately 1400m. This bridge is located in Sachin to Vadodara section of Phase 2 (JNPT to Vadodara and Rewari to Dadri) of the western Dedicated Freight Corridor and is planned on the detour alignment away from the existing IR (Indian Railways) network.

GENERAL LAYOUT OF THE BRIDGE

The general layout of the bridge has 29 spans of 48.15m length supported by 30 well foundations of 11m diameter and each 40m depth. Out of 30 well foundations, 17 are in land mode and 13 are in water mode. The substructure has wall type pier of about 12m height and the superstructure consists of two underslung trusses in each span weighing about 150MT. Well foundations for A1 to P11 and P25 to A2 are constructed as land mode. Well foundations for P12 to P24 are constructed as water mode with the help of cofferdams.

GEOLOGICAL CONDITIONS

The project area is transected by the Narmada River. The Narmada, which debouches into the Gulf of Cambay, follows the trend of a major Geo-fracture known as the Narmada-Son fault. This causes the river to flow westwards, opposite to the regional slope. The Narmada River originates at Amarkantak. The Narmada flows through a basalt dominated terrain. Associated with these Late Cretaceous basalts (Deccan Traps) are outcrops of Cretaceous Bagh sandstones and Proterozoic quartzite. Narmada alluvium is also encountered in this area. The Narmada alluvial fan is one of the largest in the world. The geotechnical investigation was carried out along the proposed alignment at each pier and abutment location to indicate the sub soil and rock stratification. As the part of investigation, the geotechnical investigation report was obtained and studied.

The stratigraphy at the river crossing may be divided into six (6) generalized strata as described below**:**

Stratum – I (sandy silt / clayey silt): Firm to stiff clayey silt / silty clay and medium dense sandy silt is met to about RL 5 to -3 m. Field SPT values in this stratum range from 4-18. In general, this surficial layer is not met in the river water portion area.

Stratum – II (silty fine sand / fine sand): Below Stratum-I, a loose to medium dense silty fine sand / fine sand is encountered to about RL -7.4 to -16.2 m. SPT values in this stratum range from 4-26.

Stratum –III (hard clayey silt / silty clay): Below Stratum-II, hard clayey silt / silty clay is met to about RL -19 to -26.0 m. Field SPT values in this stratum range from 36-80.

Stratum – IV (silty fine sand / fine sand): Below Stratum-III, very dense fine sand / silty fine sand is encountered to about RL -33 to -41 m. In this stratum refusal (N > 100) is met.

Stratum –V (clayey silt / silty clay): Stratum-V consists of very stiff to hard clayey silt / silty clay to about RL -52 to -58 m. However, at P24 and P28 locations, the clayey silt/ silty clay stratum extends to about RL -72.2 m. SPT values in this stratum range from 42 to 90 to about RL-48 m. Below this, refusal (N >100) is encountered.

Stratum – VI (silty fine sand / fine sand with gravel): Below Stratum-V, very dense fine sand / silty fine sand with gravel is encountered to about RL -60 to -63 m. In this stratum, refusal (N > 100) is met.

The river water was met in these borehole locations at RL -0.8 m to RL 4.4 m.

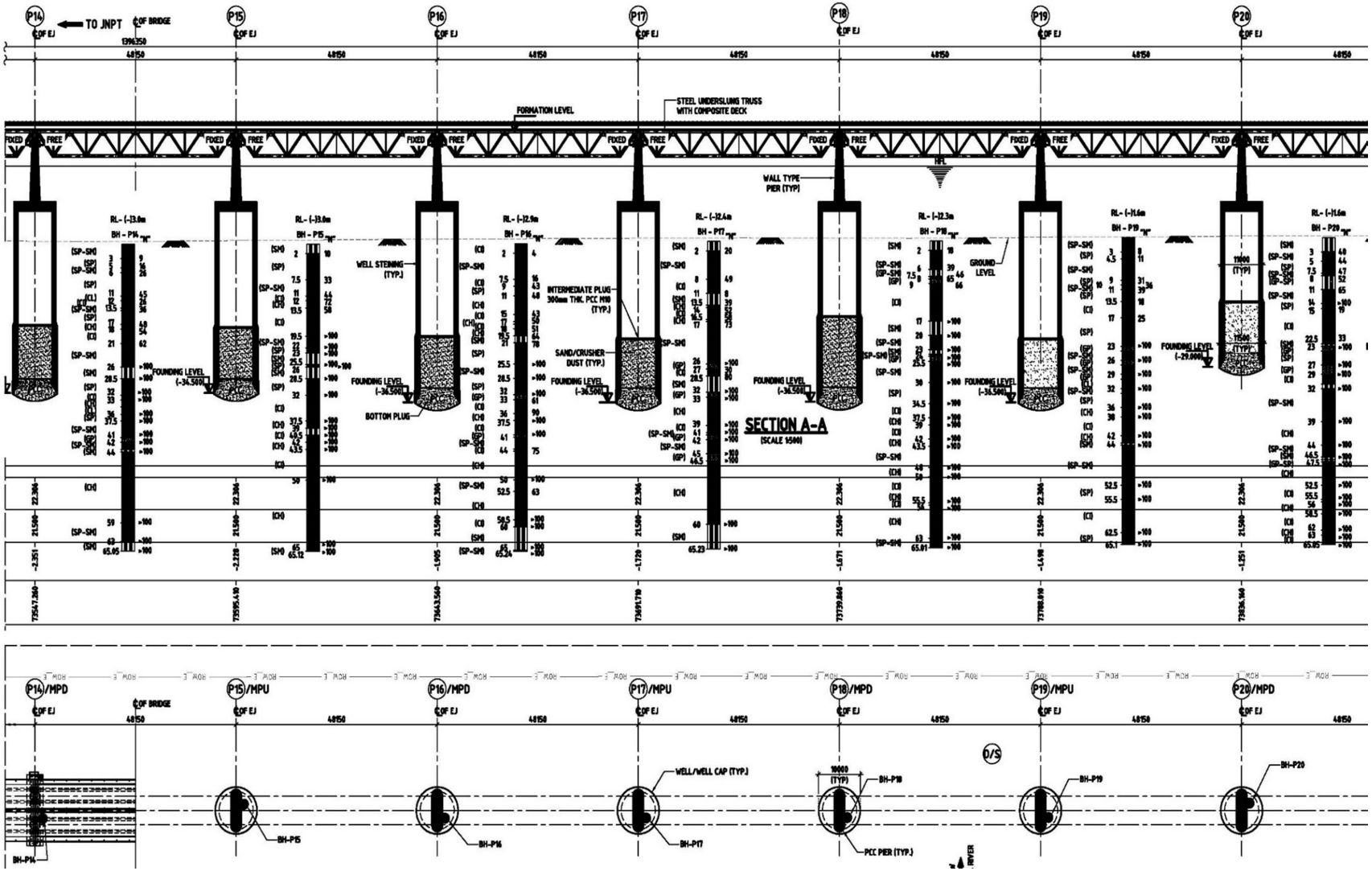
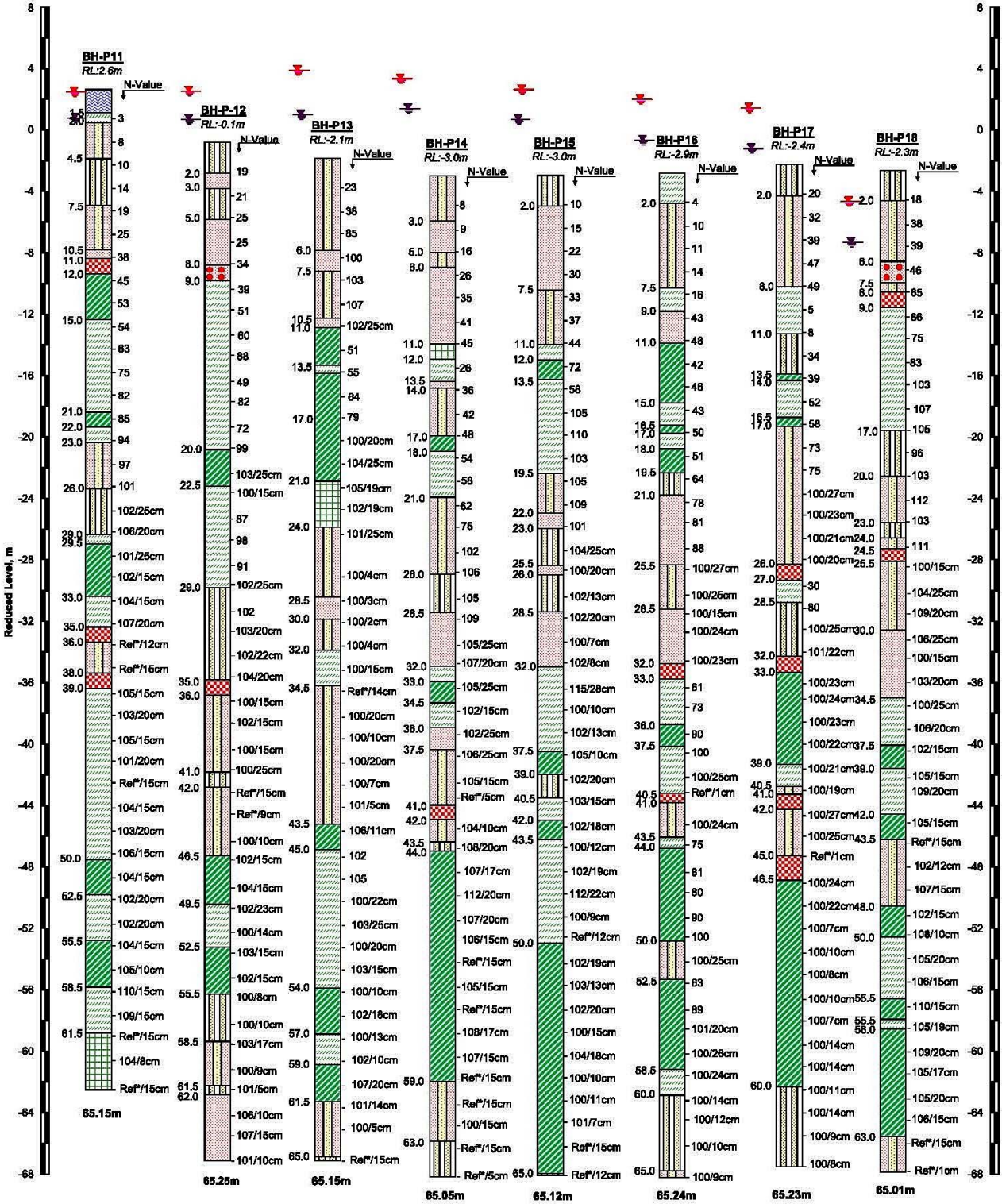


Fig. 1. General Layout of Bridge (P14 to P20)



LEGEND			
SYMBOL	DESCRIPTION	SYMBOL	DESCRIPTION
	Silty sand (SM)		Sand with gravel (SP-GP)
	Sandy silt (CL)		Low tide water level
	Fine sand (SP-SM)		High tide water level
	Clayey silt (CI)		
	Silty clay (CH)		
	Coares sand (SP)		
	Cobbles & Pebbles		
	Water table		

Fig.2. Typical subsurface profile of area

From investigation report, the sub soil at this bridge location can generally be stratified as alluvial deposits of Silty sand / Silty gravel / Silty clay/Clayey silt/ Fine sand. The subsoil is having thick continuous layers of alternate sand/silt and clay layers with intermittent clay or sand bands. The longitudinal soil profile has been presented as Fig. 2. It is observed that field SPT N values were greater than 100 (refusal strata) from (-) 20 m, RL onwards.

The site is severely affected with daily tidal variation of minimum 3 m to occasional 4.5 m. Since well cutting edge and well curb required dry area for construction, an effective retention system was proposed.

Liner pile cofferdam system

- Steel Liner piles of varying diameters can be used as per the design requirements for cofferdam construction.
- Different combinations of the liner connections are possible (Fig.3.). Some commonly adopted connections are as follows-

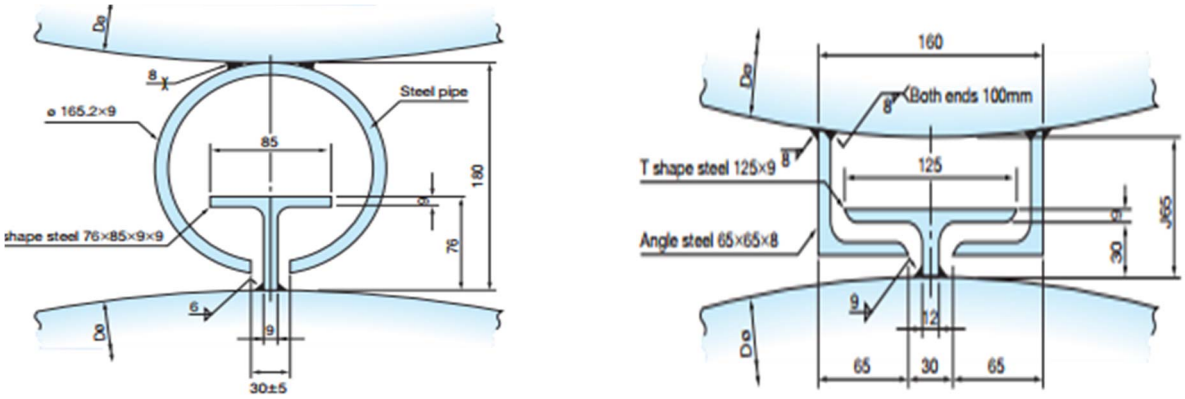


Fig. 3. Typical liner connections

DESIGN OF COFFERDAM

The basic functional requirement of the cofferdam and its construction scheme is to prevent water from infiltrating into the work area for the construction of well foundation. The cofferdam had to be designed such that it remained stable during installation, backfilling and during construction of well foundation.

Each well foundation being circular in shape, its cofferdam was also kept circular with diameter 16.2m in plan, consisting of circular liner piles of 1500 mm diameter with thickness 10 mm and single sheet pile (AU-25) sections for the walls. The liner/sheet pile levels maintained for P12 to P24 location were as shown in Table 1.

Table 1. Cofferdam Elevations

Well Location	P12	P13	P14	P15	P16	P17	P18	P19	P20	P21	P22	P23	P24
Cofferdam Top Level	+5.50	+5.50	+5.50	+5.50	+5.50	+5.50	+5.50	+5.50	+5.50	+5.50	+5.50	+5.50	+5.50
River Bed Level	-1.90	-3.00	-4.00	-4.00	-4.00	-4.00	-4.00	-4.00	-1.16	-1.00	-1.01	-0.65	-0.64
Cofferdam Toe Level	-9.28	-18.35	-18.35	-18.35	-18.35	-18.35	-18.35	-18.35	-12.00	-12.00	-12.00	-12.00	-16.00

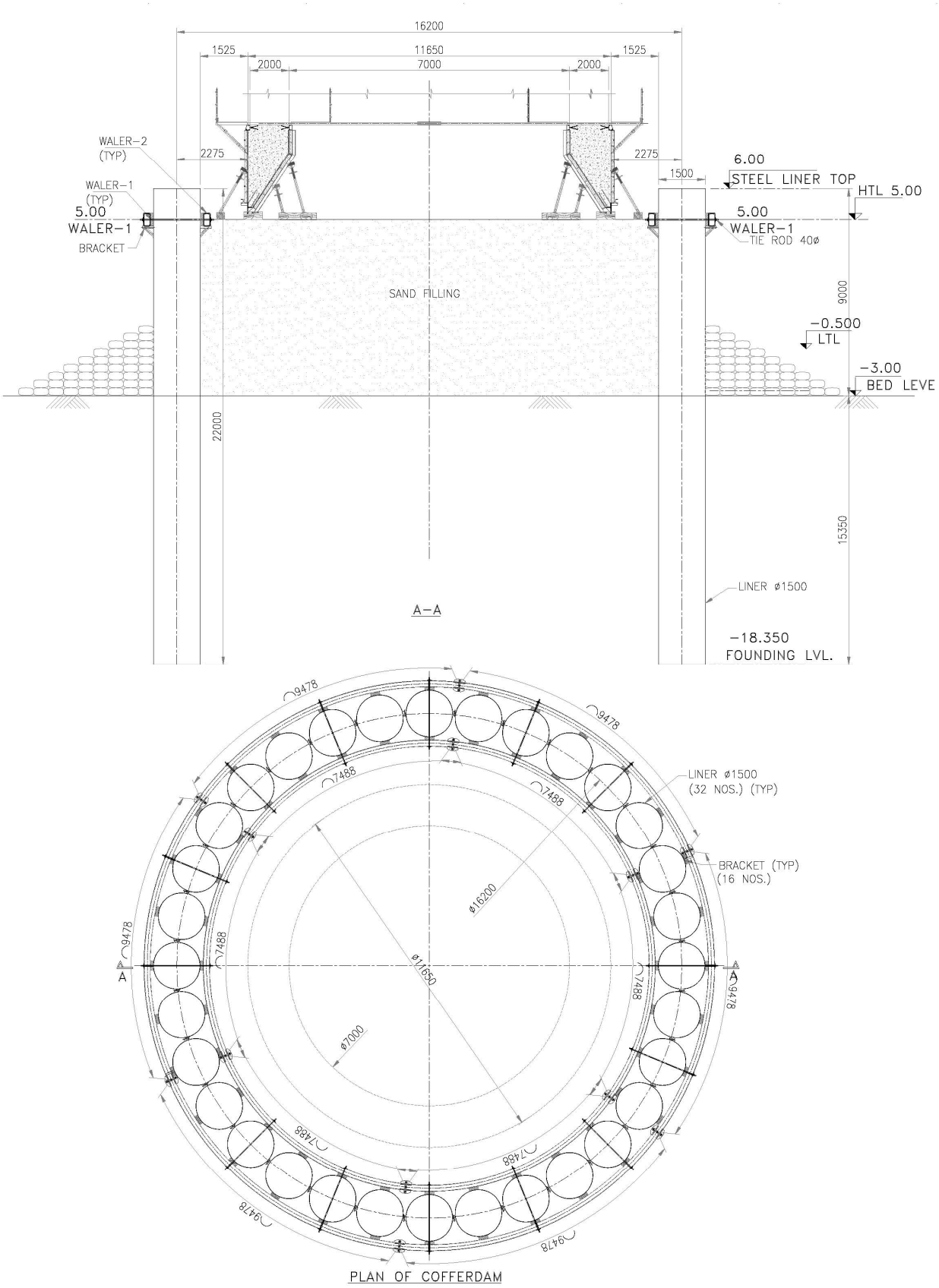


Fig. 4a. Typical elevation and plan of liner pile coffer dam

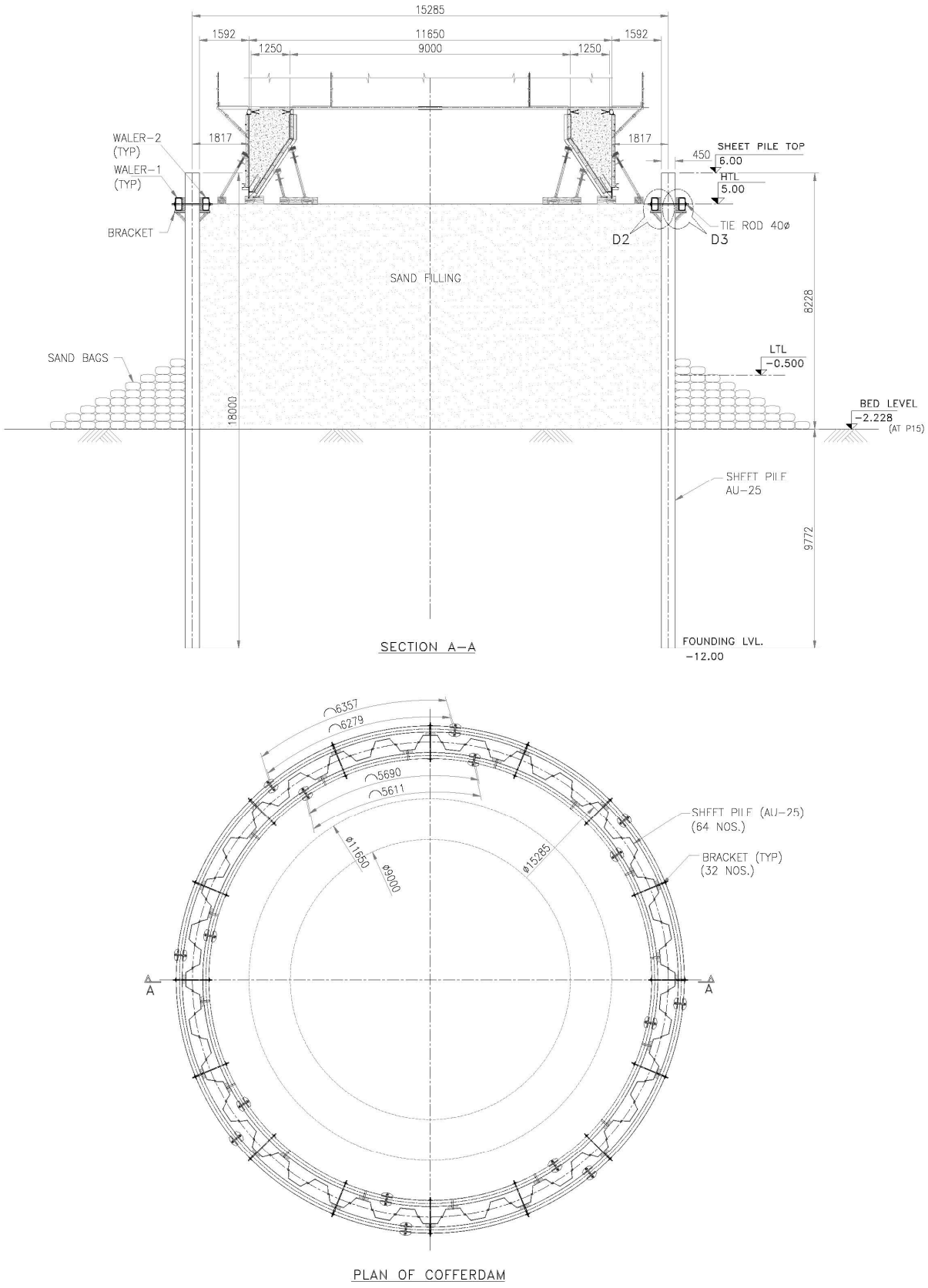


Fig. 4b. Typical elevation and plan of sheet pile coffer dam

WALLAP software was used to analyse the liner/ sheet pile for load cases generated during construction process. As soil type is cohesionless, drained analysis was performed. Liner/ sheet pile wall model was subjected to following soil parameters (for P-20 location).

Table 2. Soil Parameters assumed for analysis

Reduced Level, m		Soil Classification	Bulk Density, kN/m^3	Young's Modulus of soil E, kN/m2	ϕ, degrees	Active limit, K_a	Passive limit, K_p	Wall Stiffness EI, kN.m2/m
From	To							
5.5	-1.16	Sand Fill	17	1000 kN/m^2/m	30	0.333	3	1461600 (Liner 1500mm Dia)
-1.16	-4.57	Dense silty sand (SM)	19	12500	32	0.307	3.255	
-4.57	-16.57	Dense fine sand(SP-SM)	20	19500	34	0.283	3.537	

Stage wise analysis was done to simulate site conditions, to evaluate the generated forces, deformation pattern and strut forces. The soil and water pressures profile applied to the wall were the actual pressures expected in the system at each stage. The model below (Fig. 5.) indicates the typical final loading stage with surcharge of well curb.

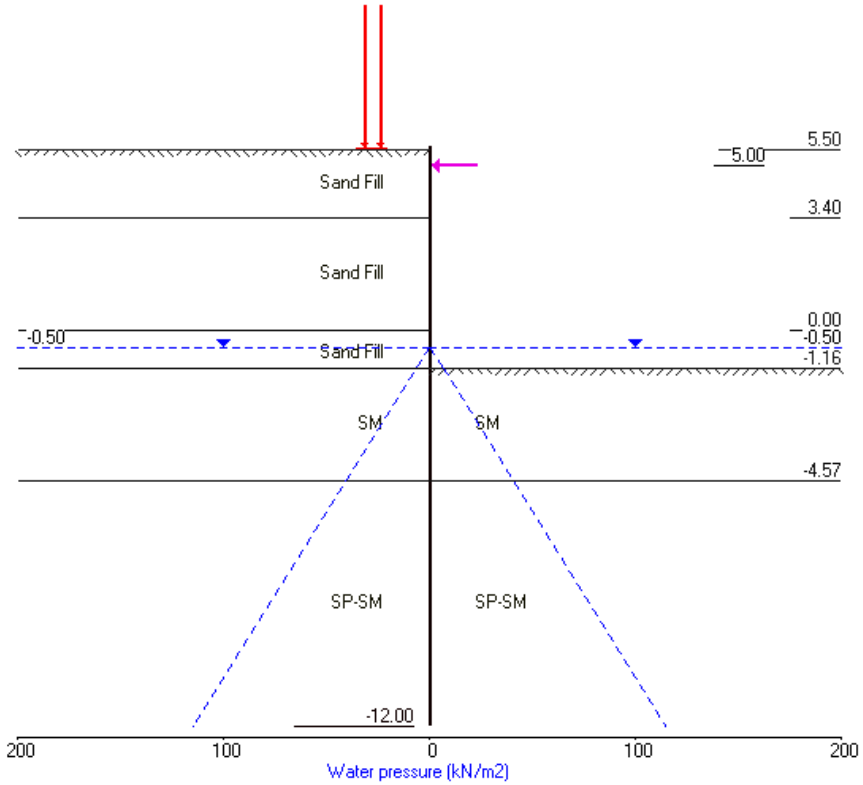


Fig. 5. WALLAP model (For P20 location)

WALLAP model for each location was analysed for respective soil parameters as per geotechnical report. The wall stiffness was adopted as per the section seen in Figs. 4a and 4b.

Construction stages of defined in WALLAP

1. Fill to elevation 0.00 on ACTIVE side with soil “Sand Fill”
2. Install strut or anchor no.1 at elevation 5.00
3. Fill to elevation 3.40 on ACTIVE side with soil “Sand Fill”
4. Fill to elevation 5.50 on ACTIVE side with soil “Sand Fill”
5. Apply surcharge no.1 at elevation 5.50. (Surcharge due to well curb and steining)

The cofferdam system was modelled in WALLAP and designed for the results obtained. Fig.5. shows final loading stage with strut level and Fig.6. shows maximum bending moment (black colour line) and maximum shear force (red colour line) respectively. The structural strength of both the steel liner and sheet pile sections were checked for the maximum design forces obtained from the WALLAP analysis.

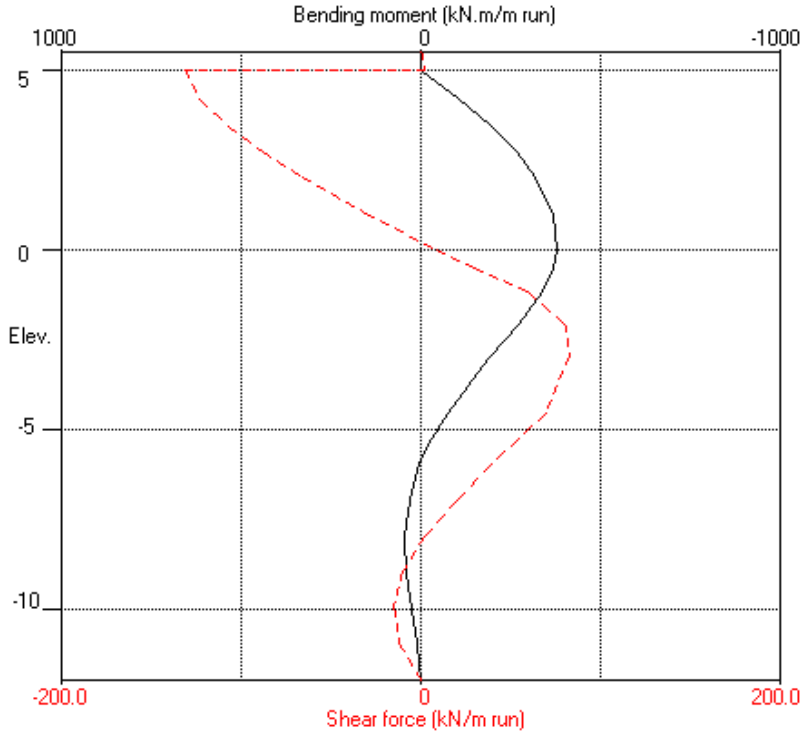


Fig. 6. Max SFD and BMD

CONSTRUCTION OF COFFERDAM

Material and crane barges were used for the construction of cofferdam for well foundation.

Basic steps followed in the well foundation construction were as follows:

1. Surveying, positioning of barge
2. Liner/ Sheetpile driving with Vibro hammer
3. Placing strut/waler system
4. Sand filling inside cofferdam
5. Placing formwork for well foundation
6. Concreting for well foundation

The below Figures.7a, 7b, 7c and 7d show the steps involved in the construction of cofferdam.



Fig.7a. Construction of Cofferdam



Fig.7b. Sand filling inside cofferdam in progress



Fig.7c. Completed cofferdam with well curb formwork placed on it

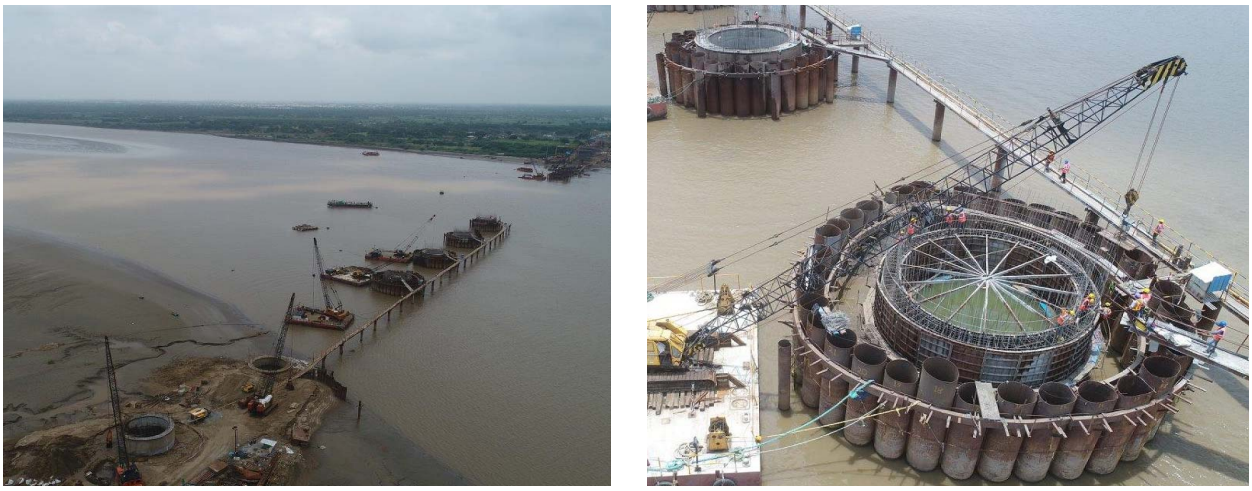


Fig.7d. Construction of well foundation and well sinking in progress

CONCLUSION

The cofferdam system for the project was designed based on geotechnical and hydrological requirement. It was evident that overall reliability of the structural performance in such cases is very sensitive to the soil stiffness parameters.

Adopting cofferdam system for construction of well foundation in this project resulted in quantum reduction in enabling steel quantities. Rate of progress of the foundation is also significantly higher compared to conventional system of caisson, because the foundation could be taken up in land mode. The cofferdam system can be erected in advance before taking up the well foundation in that location.

Among many parameters for consideration of this method for construction of the well foundation, one is judicious decision with regards to founding level for cofferdam sheet piles and liners. In this regard, effect of scour for that location has also to be accounted.

ACKNOWLEDGEMENTS

The author(s) are thankful to the management of L&T Construction for granting permission for this paper to be published. The author(s) extends gratitude to the Project site team and colleagues in extending their support to the paper. Special thanks to Mr. T Vijayakumar (Head CMPC) and Mr. Tushar M Urankar (Project Manager) for their guidance and valuable inputs.

REFERENCES

CIRIA SP 95: The design and construction of sheet-piled cofferdams.

Rameez Gahlot, Prof. Roshni John and Roshan Zemse, 2014, Cofferdams- Forces Analysis and Design Criteria, International Journal of Scientific & Engineering Research, Volume 5, Issue 12,

BORIN, D.L. WALLAP anchored and cantilevered retaining wall analysis program: User's manual (Version 5), Geosolve, London, 2007.

EXPERIMENTAL STUDY ON PULLOUT CAPACITY OF VERTICAL SHALLOW MULTI-PLATE HELICAL PILES IN SAND

[1]Swapnali S. Pawar, [2]Dinesh Bishnoi, [3]Upendra M., [4]Venkateswarlu P., [5]Jignesh B. Patel

[1,2,3,4] Post Graduate student, Applied mechanics department, SVNIT, Surat, Gujarat, India,
Phone Number: [1]+91 7666469660, [2]+91 8780093039, [3]+91 8178518767, [4]+91 9904849487,
email: [1]swapnali9660@rediffmail.com, [2]dineshbishnoi664@gmail.com, [3]upendarjntuk@gmail.com,
[4]pvenkateswarlu95@gmail.com, [5]jig8107@gmail.com.

ABSTRACT

Helical piles are structural elements which are not only capable of resisting compressive and tensile loads but which can also counterbalance the overturning moments. Current uses of helical piles range from shallow to deep foundation types. Present investigation has been carried out on use of helical multi plate piles as shallow foundation piles and their pullout resistance in dense sands. The pile models cylindrical multi plate helical pile (CMHP) and tapered multi plate helical piles (TMHP) were used to investigate the effect of varying plate geometry of TMHP from the CMHP on pullout load for different embedment depths. Both model piles TMHP and CMHP exhibited increased pullout load capacities with increasing embedment depths. It was observed that the TMHP show improvement in pullout capacity as compared to the CMHP only after a certain embedment depth was reached. For embedment ratio more than 2.5, TMHP shows marginal improvement over CMHP while for embedment ratio less than 2.5 CMHP shows better results than TMHP. Experimental results of pullout load capacity are in good agreement with theoretical model results given by Mitsch and Clemence.

Keywords: Multi plate helical pile, Embedment ratio, Breakout factor

INTRODUCTION

With the demand for growth of Infrastructure in India construction industries are seeking new, reliable and low cost foundations which cause minimum damage to environment. At present, heavy structure constructions demand large foundation sizes which warrant use of special equipments thus increasing project costs as well as surrounding disturbances. Helical piles provide potentially low cost and environment friendly solution wherein high capacity piles can be easily installed using smaller installation machines, therefore removing some major issues of equipment transportation. Single plate helical piles can be made of prefabricated steel helical plate welded to a steel shaft. Likewise a multiple plate helical pile would consist of a number of steel helical plates welded onto the shaft with suitable spacing in between them. Helical pile is installed in ground by applying turning moment (torque) to shaft causing the helical plates to penetrate soil deposit. A constant seating axial compressive load applied to the pile ensures its consistent advancing in soil such that depth of penetration is equal to a single pitch for every revolution. Helical piles are structural elements which are not only capable of resisting compressive and tensile loads but which can also counterbalance the overturning moments. There are also some other advantages of using helical piles, other than the ones discussed earlier. They can be loaded effective immediately after installation, have rapid speed of installation and their suitability for construction in very limited access conditions. Also they are easy to remove once they reach their service life. Since helical plates of the pile are installed in soil by torque application, there is reduction in noise and vibration caused due to installation and also minimum disturbance to the surrounding environment is observed. Helical piles have high vertical bearing and also large pulling resistance. Current uses for helical foundations include foundation for commercial and residential structures, failed foundation restorations,

© 2018 Deep Foundations Institute

pipeline and pumping equipment support, bridge abutments, transmission tower foundations, floating structures for deep water oil and gas projects etc.

LITERATURE REVIEW

Several three dimensional analysis have been performed on single plate piles to develop empirical theories which can be used to estimate their pullout resistance in soil. These studies have related anchor shape effect to uplift of the piles (Merifield et al. 2006, 2003; Wang 2009). However these theories cannot be applied to estimate pullout capacity of multi-helical plate piles as an issue of interaction between adjacent helical plates could arise. The ultimate capacity and failure mode could get affected as the stress zones above individual plates would get overlapped (Merifield and Smith 2010).

Mitsch and Clemence (1985), analyzed cylindrical shear method for helical piles in cohesionless soils, the stress strain relationship developed was observed to depend on pile geometry, number of helical plates, pitch provided for each of the plates and inter-helical spacing. Their field and laboratory studies on triple helical plate piles demonstrated development of cylindrical failure surface below the top helical plate above which failure surface was dependent on installation depth, installation method and relative density. But the failure mechanism consisted of general bearing capacity failure and the limit equilibrium approach used was based on a significant number of assumptions.

Meyerhoff and Adams (1968) established after observing failure in sand that helical piles could be approximated as shallow and deep depending on relative density (R_d), angle of internal friction of soil (φ) and embedment ratio (H/D). They observed that in the lab tests on sand with R_d from 47% to 90% a helical pile behaves as shallow anchor with H/D<5 (H is the embedment depth up to first helical plate and D is diameter of the plate) They generalized the angles as $\varphi/4 < \Theta < \varphi/2$ and proposed separate analyses for deep and shallow piles. They concluded that the geometry of failure surface is distinct but its variation of shape and extent with varying H/D ratio was seen.

Tshua et al. (2013) considered the ultimate capacity (Q_u) for tests as the load producing a relative displacement of 10% of the average helix diameter. It was observed that gain in uplift capacity for tapered triple helical plate pile model was about 8%. They concluded that the efficiency of lower helical plates in sand decreases with the increase in relative density and top helical plate diameter.

The best method for making a comparison with predicted results is evidently 5% failure criterion in comparison to 10% failure criterion as displacement levels of 10% for helix diameters could exceed the settlement tolerance levels (Sakr 2009, 2011). However, for helical plates of smaller diameters, 10% failure criterion is considered adequate and more appropriate than 5% failure criterion (Mohajerani 2016) Spacing ratio of a helical pile is the ratio of spacing between the two consecutive helical plates to the helical diameter (average of helical plate diameters in case of tapered helical piles)(Sakr 2009; Narasimha Rao et al. 1993). The spacing ratio forms the basis of distinction of failure mechanisms, individual or cylindrical.

From the aforementioned review it is clear that there has been extensive study on use of helical piles as deep foundation piles. But little investigation has been carried out on use of helical multi plate piles as shallow foundation piles and their pullout resistance in dense sands.

Model helical piles categorized as shallow on the basis of embedment ratio were tested for different conditions in this experimental study. The findings are expected to help in better understanding of helical pile designs with different embedment depths.

SCOPE OF THE INVESTIGATION

The present investigation reports the results of experimental tests and comparison of the same with the theoretical models proposed in the previous studies on the multi-plate helical piles. The comparison of pullout resistance of two types of multi-plate helical piles were done, they are cylindrical and tapered multi-plate helical pile. Total 6 tests were carried out for three different embedment depths on the two pile models. The specific objectives of the investigation were (1) Estimate pullout capacity of shallow multi-plate helical piles in sand of high relative density; (2) Study variation of pullout load resistance with change in the embedment ratio; (3) Compute pull-out capacity of the modeled pile based on theoretical model proposed by Mitsch and Clemence (4) To compare, validate and study the possible cause of errors in pullout load computation.

LABORATORY MODEL TESTS

Properties of sand

Poorly graded sand with properties as mentioned in Table 1 was used for the experiments conducted. Relative density of 60% was maintained throughout the tests. Relative density experiment was conducted on sand and the angle of internal friction for 60% relative density was found to be 37.17 degrees and the unit weight as 16.54 kN/m^3.

Table 1. Physical properties of sand

Property of Sand	Value
Specific Gravity (G)	2.611
Effective size of particle (D10), mm	0.21
Mean size of particle (D50), mm	0.7
Coefficient of uniformity (Cu)	4.76
Coefficient of curvature (Cc)	0.76
USCS Classification	SP
Minimum unit weight, kN/m^3	14.87
Maximum unit weight, kN/m^3	17.87
Angle of Internal friction at loose state, degrees	28.44
Angle of Internal friction at dense state, degrees	38.29

Model helical piles

The proposed helical multi-plate pile models were made of mild steel with square shaft of 30mm diagonal length. The thickness of shaft steel was 2mm and that of the blades welded on it were 1mm. The models were designed so that the effect of the shape of the helix on the pile performance in pullout could be studied. The cylindrical multi-plate helical piles (CMHP) and tapered multi-plate helical piles (TMHP) consisted of two helical plates having a pitch of 20mm welded over the shaft with an appropriate spacing such that the spacing ratio is maintained in both the models. Due to fabrication difficulties in achieving the exact dimensions best effort was made to achieve the approximate same value of spacing ratio (SR) for both the models.

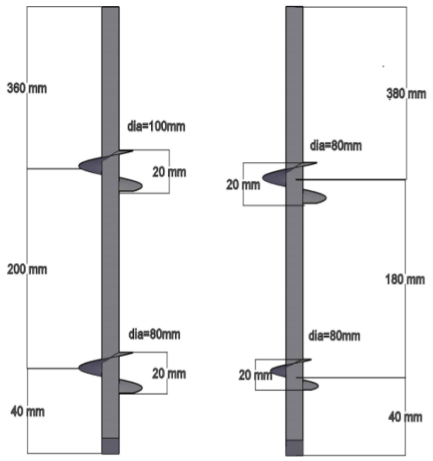


Fig. 1. Typical model of CMHP and TMHP



Fig. 2. Fabricated model of CMHP and TMHP

Table 2. Details of multi-plate helical piles fabricated

Sr. No.	Helical pile type	Embeddment depth (H)	Helical pile designation	Diameter of helical plate (upper)	Diameter of helical plate (lower)	Pitch of helical blades	Spacing between helical plates	Distance between soil surface and top helical plate	Distance from bottom of shaft to the lower plate	Total embedded length of pile	Spacing Ratio (SR)
1	P	180	P1	80	80	20	180	180	40	400	2.25
2	P	200	P2	80	80	20	180	200	40	420	2.25
3	P	240	P3	80	80	20	180	240	40	460	2.25
4	T	180	T1	100	80	20	200	180	40	420	2.22
5	T	200	T2	100	80	20	200	200	40	440	2.22
6	T	240	T3	100	80	20	200	240	40	480	2.22

The CMHP have been designated as P and TMHP as T in the Table 2 mentioned above. For facilitating better understanding of the geometry of the model piles has been illustrated in figure 1 and figure 2. Further depending on the embedment depth they have been designated as P1,P2,P3 and T1,T2,T3 for embedment depths 180mm ,200mm ,240mm each respectively. Provision of through and through holes at top of the shaft was made to introduce tie rod during installation and to facilitate attachment of a load cell during pullout.

Model Tank

The tests were carried out in a metal tank fabricated with four panels of metal sheets (thickness 1.02mm) at bottom and sides and a transparent acrylic glass panel (thickness 6mm) in the front. The internal tank dimensions were 0.6 x 0.6 x 0.6 meter. The dimensions of the testing tank were chosen to be sufficient to accommodate the failure mechanism of the helical piles without allowing any boundary effects. This choice was based on the maximum expected size of the failure surface in view of the values reported in the literature for helical piles. The figure 3 below shows the general experimental setup used.



Fig. 3. Experimental setup showing pullout arrangements

METHODOLOGY

The uplift performance of helical piles was examined in dense sand deposit. A sand-placing technique was developed and used in the testing program to achieve the predetermined relative density of sand. By means of rainfall technique, the fall of sand height was 360mm for achieving density of sand as 60%. When the sand was placed from this height it was observed that the required density was accurately achieved as compared to the traditional volume weight method.

After the completion of the sand-placing process, the surface was smoothed carefully and the anchor was installed by applying torque to the top of the anchor's shaft .This was done by means of a tie rod passing though the holes in shaft. No axial load was applied to the anchor's shaft during the installation process. However, special attention was given to the anchor's rate of penetration in the sand so that rotation in place was not permitted. The anchor's shaft was maintained vertical throughout the installation depth in the sand by using a guide frame mounted on the top of the testing tank.

TESTING PROGRAM

Loading tests were done to evaluate pullout load on 6 configurations of helical piles. With three embedment depths evaluating peak pullout load capacity for the TMHP and CMHP models. After the installation of the pile in the model tank, the pile was instrumented with load cell of capacity 1 tonne and

a linear variable displacement transducer (LVDT) with an accuracy of 0.1 mm (figure 3). The pull out load applied to the pile at a strain rate of 0.5 mm/min. Loads were recorded at an interval of 0.2 mm displacement. The maximum vertical upward displacement of 10 mm was recorded in all the model tests. This is the 10% of the helical pile maximum diameter considered in the study.

RESULTS AND DISCUSSIONS

The pullout resistance of helical pile configuration depends on embedment depth of the pile and also on the shape of the plates. This can be observed from the results shown in the Table 3. The figure 4 illustrates the comparisons of pullout load capacities of TMHP and CMHP at the respective embedment ratios.

Table 3. Measured ultimate pullout load capacities

Helical pile designation	Embedment depth H (mm)	Embedment ratio H/D	Displacement δ (mm)	Pullout load Qu (kg)
P1	180	2.25	9.8	51.7
T1	180	2.25	7.6	45.4
P2	200	2.5	9.4	57.2
T2	200	2.5	7.4	60.4
P3	240	3	9.2	66.8
T3	240	3	8.2	73.8

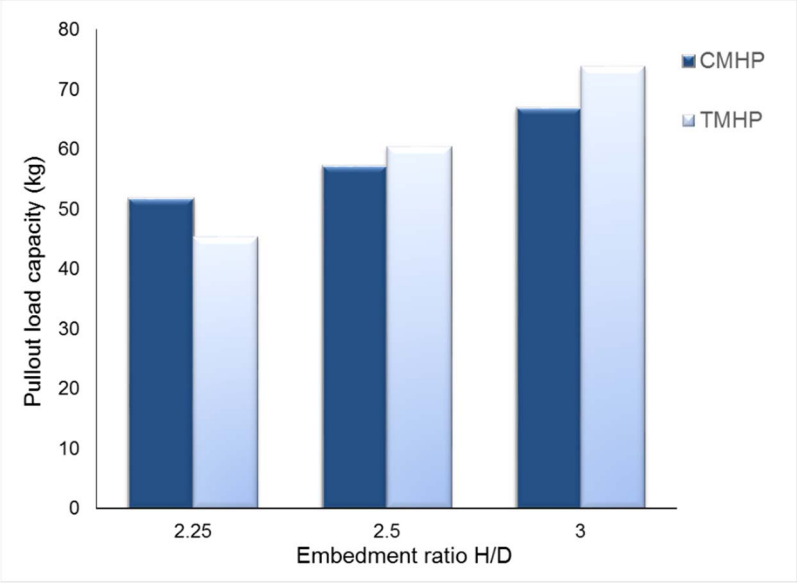


Fig. 4. Pullout load capacity v/s embedment ratio for CMHP and TMHP

According to the 10% failure criterion, 8mm for CMHP and 10mm for TMHP was decided to be the approximate value of displacement around which the peak pullout load capacity could be observed. The results obtained corroborate with the values and accordingly the maximum/mobilized displacement is established at the maximum pullout load capacity.

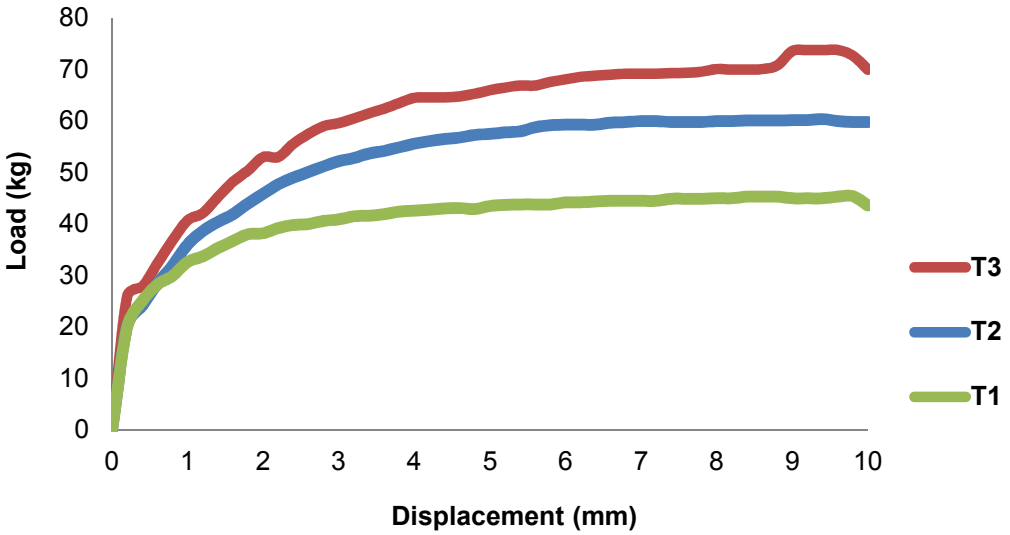


Fig. 5. Pullout load capacity v/s displacement for TMHP

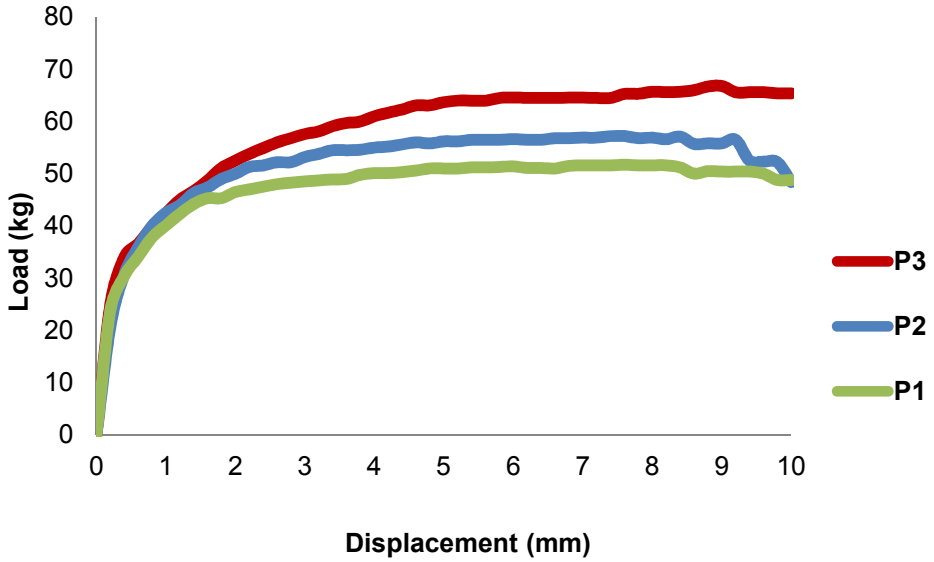


Fig. 6. Pullout load capacity v/s displacement for CMHP

The peak pullout load increases at a higher rate with increased depth of embedment for TMHP configurations (figure 5) as compared to CMHP configurations as seen from the figure 6. The pull out loads for TMHP at 200mm and 240mm embedment depths were observed to be more than CMHP. However at 180mm embedment depth apparent reversal in this trend was seen.

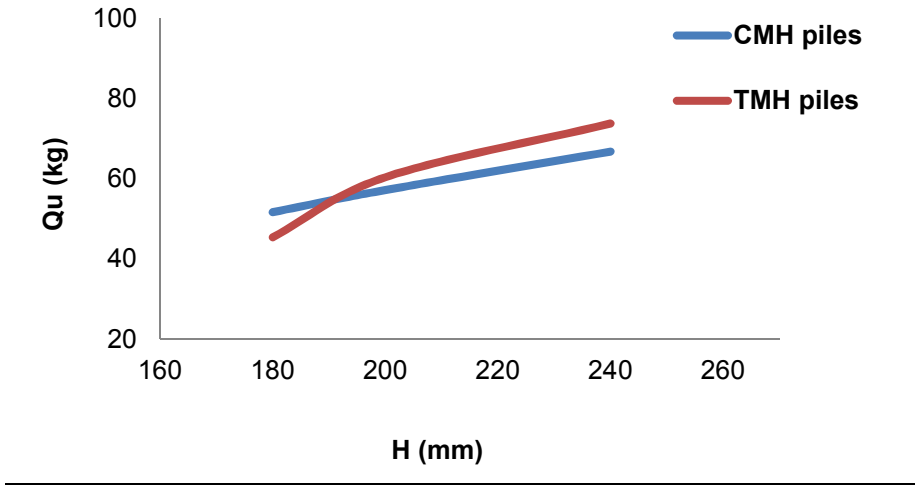


Fig. 7. Pullout load capacity v/s installation depth

In Figure 8, TMHP show reducing trend in displacement as embedment ratio increases. CMHP on the other hand when compared at same embedment ratios as that of TMHP show increasing trend in displacement with increasing embedment ratios.

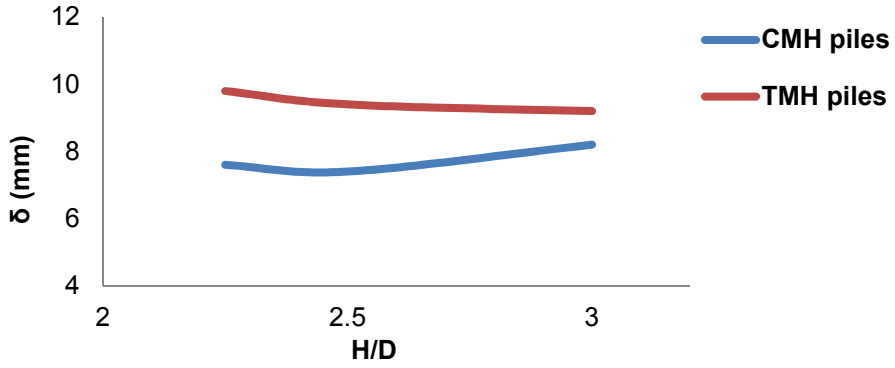


Fig. 8. Displacement v/s Embedment ratio

For further investigations the comparison of the experimental values was done with the values obtained from the theoretical model proposed by Mitsch and Clemence (1985). The model has limitations and they are as mentioned below

- Sand is homogenous and behaves as rigid perfectly elastic material.
- Helical plate is assumed to be thin, rigid, in full contact with surrounding sand and friction between sand and blade surfaces are ignored.
- Weight of the pile is negligible.

The dimensionless breakout factor (N_q) for helical plates in dense sand can be used to directly relate the performance of piles to their embedment ratios. This would further help to evaluate the capacity of helical

piles irrespective of their relative magnitudes of installation depth, diameter of plates and density of sands (Ilampurthi et al. 2002). It can be defined as follows

$$N_q = \frac{Q}{\gamma AH} \qquad \text{- (1)}$$

Where, A is plan area of helical plate, γ is the effective unit weight of the sand bed.

The Table 4 demonstrates the validity of theoretical values (Mitsch and Clemence model) and experimental values using breakout factor (N_q).

Table 4. Theoretical and experimental breakout factors

Helical pile designation	Embedment depth H (mm)	Embedment ratio H/D	(Nf)e Experimental	(Nf)t theoretical	[(Nf)e] / [(Nf)t]
P1	180	2.25	33.47	38.99	0.859
T1	180	2.25	36.98	40.74	0.908
P2	200	2.5	34.40	35.46	0.970
T2	200	2.5	36.32	40.71	0.892
P3	240	3	34.54	34.08	1.014
T3	240	3	30.33	36.41	0.833

CONCLUSION

1. The improvement in the pull out load capacity of TMHP is observed to be significant after a certain embedment ratio and thus the embedment ratio and the shape of plates used in helical pile play important role in determining the improved strength of TMHP over CMHP.
2. It was observed the TMHP configurations showed reduced displacements at peak loads as compared to CMHP configurations whose displacements were seen to increase with the increasing embedment ratios.
3. The theoretical comparison of peak pullout load capacity with experimental values based on Mitsch and Clemence model gave a ratio of their breakout factors in the range of .86 to 1. Though the values were seen to be quite close to each other and given the assumptions the errors could be attributed to small scale modeling.
4. For further studies, investigation analyzing the increased diameter of helical plate for a given embedment depth and the effect it has on the pullout load capacity can be carried out. Also the role density of soil would play in such cases can be studied.

ACKNOWLEDGMENTS

The technical support from the Sardar Vallabhbhai National Institute of Technology (SVNIT) laboratory is gratefully acknowledged.

REFRENCES

Adams, J.I., and Hayes, D.C., 1967. The uplift capacity of shallow foundations. Ontario Hydro Research Quarterly, 19(1): 1-15.
Das B.M. and Shukla S.K., 2013. Earth Anchors. J. Ross publishing, Inc., U.S.A.

Demir, A. and Ok, B., 2015. Uplift response of multi-plate helical anchors in cohesive soil. Geomechanics and Engineering, Vol. 8, No. 4, 615-630.

Ilamparuthi, K., Dickin, E.A. and Muthukrisnaiah, K., 2002. Experimental investigation of the uplift behavior of circular plate anchors embedded in Sand. Canadian Geotechnical Journal 39:648–664.

Lutenegger, A.J., 2009. Cylindrical Shear or Plate Bearing? – Uplift Behavior of Multi-Helix Screw Anchors in Clay. Contemporary Issues in Deep Foundations, ASCE: 456-463.

Lutenegger, A.J., 2011. Behavior of Grouted Shaft Helical Anchors in Clay, DFI Journal - The Journal of the Deep Foundations Institute, 5:1, 58-67.

Meyerhof, G.G., and Adams, J.I., 1968. The ultimate uplift capacity of foundations. Canadian Geotechnical Journal, 5: 225–244.

Mitsch, M.P., and Clemence, S.P., 1985. The uplift capacity of helix anchors in sand. In Uplift Behaviour of Anchor Foundations in Soil, Proceedings of ASCE, New York, pp. 26–47.

Merifield, R.S., 2011. Ultimate uplift capacity of multiplate helical type anchors in clay. Journal of geotechnical and geoenviromental engineering © ASCE, 704-716.

Mohajerani , A., Bosnjak, D. and Bromwich D., 2016. Analysis and design methods of screw piles: A review. Soils and Foudations © The Japanese Geotechnical Society, 56(1):115-128

Nasr, M., 2009. Performance based design for helical piles. International Foundation Congress and Equipment Expo 496-503.

Pack, J.S. Design of helical piles for heavily loaded structures, New Technological and Design Developments in Deep Foundations © ASCE, 353-367.

Rawat, S. and Gupta A.K., 2017. Numerical modeling of pullout of helical soil nail. Journal of Rock Mechanics and Geotechnical Engineering 9, 648-658.

Rao, S.N. and Prasad, Y.V.S.N., 1993. Estimation of Uplift capacity of helical anchors in clays. Journal of Geotechnical Engineering, Vol. 119, No. 2, 352-357.

Sakr, M., 2009. Performance of helical piles in oil sand. Canadian Geotechnical Journal 46: 1046–1061.

Sakr, M., 2011. Installation and performance characteristics of high capacity helical piles in cohesionless soils, DFI Journal - The Journal of the Deep Foundations Institute, 5-1, 39-57.

Terzaghi, K., 1943. Theoretical soil mechanics. John Wiley & Sons, New York.

Tsuha C.H.C., Santos T.C., Rault G., Thorel L. and Garnier J., 2013. Influence of multiple helix configuration on the uplift capacity of helical anchors. International Conference on Soil Mechanics and Geotechnical Engineering, 18, Paris, 2893-2896.

EXTENT OF FAILURE ZONE IN SOIL AT THE CUTTING EDGE OF OPEN CAISSON: FE EVALUATION AND REGRESSION ANALYSIS

Jitesh T. Chavda, Research Scholar, Indian Institute of Technology Madras, Chennai, India, Email: jiteshchavda03@yahoo.in

G. R. Dodagoudar, Professor, Indian Institute of Technology Madras, Chennai, India, Email: goudar@iitm.ac.in

ABSTRACT

Open caissons are deep foundations sunk into the ground by removal of soil within the caisson shaft. A cutting edge with a tapered inner face is used at the bottom of the caisson to allow the bearing failure of the soil which is in contact with the cutting edge. The soil is removed within the shaft of the caisson during sinking which results in bearing failure of the soil due to self-weight of the caisson. The formation of influence zone in the soil at the cutting edge is termed as failure zone. In this study, the finite element (FE) analysis is carried out to evaluate the extent of failure zone in the c-ϕ soil at the cutting edge of the open caisson. The cutting edge is penetrated into the soil and the extent of the failure zone is evaluated. The effect of variation of tapered angles of the cutting edge, the radii ratio of the open caisson, unit weight, friction angle and cohesion of the soil, and magnitude of the surcharge on the extent of the failure zone is investigated. From the FE results, the multivariate linear and nonlinear regression analyses are performed and easy to use predictive equations are developed to estimate the extent of failure zone in the soil beneath the cutting edge. These equations help in quick estimation of the extent of failure zone based on the configuration of the open caisson adopted at the construction site.

Keywords: open caisson, cutting edge, finite element analysis, failure mechanism, c-ϕ soil, regression analysis

INTRODUCTION

Open caissons are massive hollow structures classified as deep foundations. The components of open caisson are the cutting edge with a tapered inner face, steinning which is constructed in parts, and top cap to support the superstructure. The open caissons are sunk into the ground by removal of the soil within the shaft i.e. through the circular opening of the steinning. The caissons are used to support bridges over roadways and railways, onshore structures like coastal protection wall, jetties, ports, etc., launching shaft for the tunnel boring machines, and isolated structures like silos, chimneys, wind turbines, transmission line towers, etc. They can be sunk through various types of soils like sandy strata, non-stiff clays, boulder soils, and to a limited extent in the rocky strata. In India, open caissons are known as well foundations. Major bridges in India are supported on well foundation. Old Kali bridge, Karwar, Deopani bridge, Bogibeel bridge, Indravati bridge near Jagdalpur, Narmada bridge at Khalghat, Lohit bridge near Brahmakund, Passighat bridge, Teesta bridge, Toong bridge, Bakacha Chu, Bascule part of Pamban bridge, etc. are supported on well foundations (Jain et al. 2008; Kumar et al. 2017; Bhide and Sastry 2017; Kumar and Dhiman 2017). The Taj Mahal, Agra is supported on well foundation. The Mehtab Burj in Mehtab garden at the back side of the Taj Mahal, St. Andrew's Church in Chennai (Kurian 2005), Larsen and Toubro headquarter in Chennai, and many other structures are supported on well foundations.

The control sinking of caisson is one of the important aspects in the successful completion of a project wherein a number of caissons are involved. The method of excavation of soil within the caisson and at the cutting edge level ensures the high capacity and reliable control in the vertical sinking of the caisson. The practicing engineers have faced many problems during the execution of the open caisson, such as tilting,

© 2018 Deep Foundations Institute

misalignment, sudden drop, freezing i.e. no further sinking of caisson, etc. are reported in the literature (Salamov et al. 1965; Ter-Galustov et al. 1966; Belous 1968; Opershtein 1969; Bolyachevskii and Chumakov 1975; Baitsur and Zakharov 1975; Maslik et al. 1978; Nonveiller 1987; Chandler et al. 1984; Chatterjee and Dharap 1999; Saha 2007; Panda 2015). The detailed site investigation, engineering judgment, instrumentation, skilled labor, informed decisions, etc. are necessary to avoid such problems. The experimental investigations have been carried out and reported to evaluate the contact pressure distribution at the base and sides of the caisson, load settlement and deflection behaviour, earth pressure mobilization in caissons embedded in soft clay, and the formation of failure zone in sand during penetration of the cutting edge of the caisson (Katti and Dewaikar 1977; Alampalli and Peddibotla 1997; Kumar and Rao 2010; Royston et al. 2016). It is observed from the above literature that many difficulties have been faced during the execution of the open caisson.

The tapered angle of the cutting edge is one of the important factors which governs the sinking response of the caisson. The tapered angle of the cutting edge is selected based on the soil type. IS: 9527, Part 1 (1981) and IS: 3955, (1965) recommend the inclination of the inner face of the cutting edge with respect to the vertical between 30° and 45° depending on the type of strata. In the case of stiff clays, an angle of 30° and in the case of sands or soft clays, an angle of 45° is recommended. Tomlinson (2001) recommends flatter tapered angles for sand and steeper tapered angles for clay. Some studies were carried out to evaluate the bearing capacity factor N_γ using limit equilibrium theory for various configuration of the cutting edge (Berezantsev 1952; Solov'ev 2008; Yan et al. 2011). It can be stated that the sinking response of the open caisson depends on the configuration of the cutting edge adopted.

The soil which is in contact with the cutting edge fails in bearing when the cutting edge is loaded with the dead weight of the steinning. The bearing failure leads to a formation of influence zone termed as failure zone. This bearing failure is important to permit the controlled sinking of the open caisson. The estimation of the vertical and radial extent of the failure zone will help in planning proper excavation strategies to achieve the controlled sinking. In the present study, the failure zone in the c-ϕ soil at the cutting edge of the open caisson is evaluated using finite element analysis (FEA). The extent of the failure zone corresponding to the various parameters is determined. The parameters considered are radii ratio, tapered angle of the cutting edge, unit weight, friction angle, and cohesion of the soil, and the depth of sinking. The radii ratio of the open caisson is the ratio of the inner radius to outer radius of the open caisson. The radial and vertical extent of the failure zone obtained from the FEA is normalized by dividing the obtained extent with the width of the cutting edge which is termed as normalized zone of failure. Linear and nonlinear multivariate regression analyses are carried out and the corresponding predictive equations are developed to provide preliminary estimation of the extent of the failure zone. The results of the present study have significance in the field application of the sinking process of the open caisson by providing a clear picture of the extent of the failure zone around the cutting edge. This information will help in planning of the proper excavation strategies so that the controlled sinking can be achieved in the field.

SINKING MECHANICS OF OPEN CAISSON

The first step of the construction sequence of the open caisson is the construction of the cutting edge on the ground (see Fig. 1). The cutting edge has tapered side on the inner face of the steinning to allow the bearing failure of the soil and the movement of soil towards the central axis of the caisson. The steinning of caisson is constructed in lifts i.e. in segments/parts. The self-weight of the cutting edge and first lift of the steinning increase the contact pressure and initiate the bearing failure of the soil, which results in sinking of the caisson. The reaction offered by the soil at the cutting edge reaches a new state of equilibrium and sinking stops. Then, the soil within the caisson is removed up to the tip level of the cutting edge which increases the contact pressure and again initiates the bearing failure beneath the

cutting edge causing the further sinking of the caisson. As the caisson sinks, the surrounding soil in contact with the steinning offers the skin friction. This skin friction is reduced by providing a slit (or gap) between the outer surface of the caisson and the surrounding soil, which is filled with the bentonite slurry. The second lift of the steinning is constructed and the entire process is continued until the caisson is reached up to the required depth.

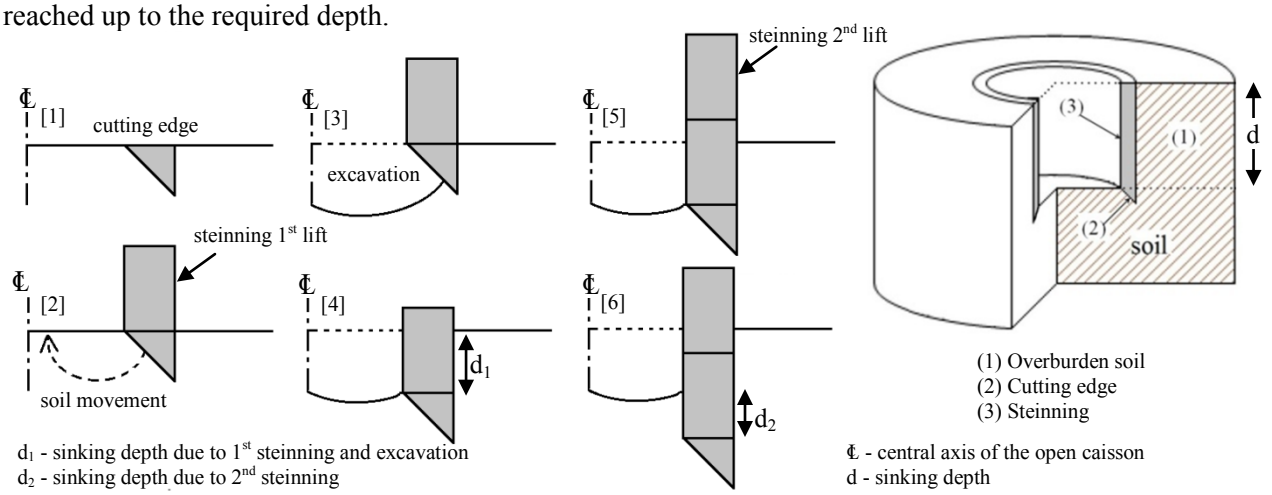


Fig. 1. Schematic of sinking phenomenon of open caisson with cutting edge

In general, the sinking of caisson is affected by: (i) the tapered angle of the cutting edge (ii) the radii ratio of the caisson (iii) the steinning thickness (iv) the lift height of the steinning i.e. the weight of steinning which initiates the bearing failure of soil at the cutting edge (v) the soil type and strength parameters (vi) the reduction in friction between the soil and outer surface of the caisson (vii) the sinking depth, and (viii) ground water conditions.

PROBLEM DEFINITION

Finite Element Analysis: *FE model*

The advantage of the symmetry is taken and circular open caisson is model as an axisymmetric problem using PLAXIS-2D program. Figure 2 shows the FE model of the open caisson showing the mesh discretization, boundary conditions, element type, FE mesh dimensions, and the radial and vertical extent of the failure zone. The cutting edge is modeled as linear elastic having a radius ratio, $r_i/r_o = 0.8$, width of cutting edge, $B = 1$ m, and tapered angle, $\beta = 45°$. The soil is assumed as elastic perfectly plastic with Mohr-Coulomb failure criterion. The material properties assigned to the cutting edge and soil are given in Table 1. The non-associative flow rule is used (i.e. $\psi = 0°$). The interface with $R_{int} = 0.5$ is assigned between the outer vertical face of the cutting edge and soil in order to simulate the realistic behavior. The open caisson problem consists of simulation of surcharge when the caisson sinks to a certain depth, d (see Fig. 2). The surcharge is simulated by assigning a line load of $q = \gamma d$, acting radially outward over the top boundaries of the FE mesh from the outer face of the cutting edge. The FE mesh selected is the fine mesh in the PLAXIS program. The overall FE mesh dimensions are 30 m in radial direction and 15 m in vertical direction. These dimensions are arrived based on the formation of the plastic regions well within the boundaries.

Normalized failure zone, X/B and Y/B

The penetration of the cutting edge within the soil is simulated by assigning the prescribed displacements of 0.5 m over the nodes representing the top boundaries of the cutting edge. The basic FE model consist of $r_i/r_o = 0.8$, $B = 1$ m, $\beta = 45°$, $\gamma = 20$ kN/m^3, $c = 10$ kPa, $\phi = 20°$, $\psi = 0°$, $E = 200$ MPa, and $\nu = 0.35$.

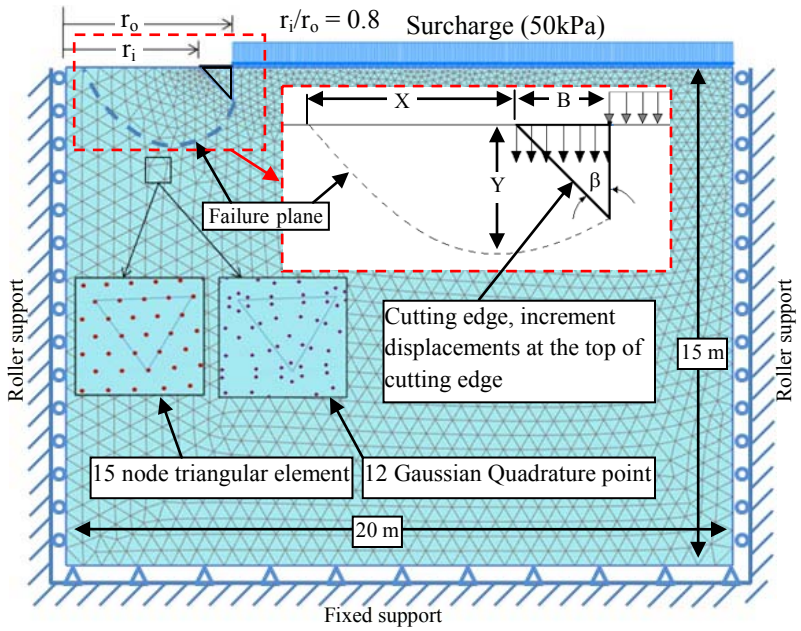


Fig. 2. FE model of open caisson with cutting edge

Table 1. Input parameters used in the finite element analysis

	Parameter	Value	Unit	Range	Increment
Soil	r_i/r_o	0.8	-	0.5 - 0.9	0.1
	β	45	degree	30 - 90	15
	γ	20	kN/m^3	14 - 22	2
	c	10	kPa	0 - 30	10
	ϕ	20	degree	5 - 30	5
	q	50	kPa	0 - 150	50
	E	200	MPa	-	-
	ν	0.35	-	-	-
Cutting edge	γ	20	kN/m^3	-	-
	E	300	GPa	-	-
	ν	0.15	-	-	-

MC - Mohr-Coulomb model for soil; LE - Linear elastic model for cutting edge, dilation angle, $\psi = 0°$, E - Young's modulus, ν - Poisson's ratio of the soil.

In the basic model, the effect of radii ratio on the extent of the failure zone is determined by varying only the radii ratio of the cutting edge and the other parameters mentioned above are kept constant. The incremental displacements are plotted and the radial distance at which the magnitude of the incremental displacement = 0 in contact with the top boundary towards the central axis is measured as X (see Fig. 2). The maximum vertical distance in the vertical direction from the top boundary of the FE model to the line representing the zero incremental displacement is measured as Y. The radial and vertical extent of the failure zone obtained from the FEA is normalized by dividing the X and Y with the width of the cutting edge. Similarly, the effect of tapered angle is determined by varying only the tapered angle of the cutting edge and the other parameters are kept constant in the analysis. The X/B and Y/B are obtained corresponding to the variation of each of the geometric parameters of the cutting edge (r_i/r_o and β), soil parameters (γ, c, and ϕ), and the surcharge (q) representing the sinking depth (d).

Regression Analysis

Based on the results of the parametric analysis, linear and nonlinear trends have been seen between the X/B and Y/B with some of the parameters. The linear trend is observed for γ, ϕ, and q; whereas the nonlinear trend is observed for r_i/r_o, β, and c. The multivariate linear and nonlinear regression analyses are carried out using MATLAB program. The step-by-step procedure mentioned in Brown (2009) is used for linear regression and *Multivariate Polynomial Regression* program developed by Cecen (2013), available free online, is used for nonlinear regression. The multivariate polynomial regression is of 2nd order. The predictive equations are developed to estimate the extent of the failure zone for a given range of the parameters and units as given in Table 1. The equations to estimate the X/B and Y/B values are given as

Multivariate linear regression

$$X/B = -0.9817 + 5.6522(r_i/r_o) - 0.0276(\beta) + 0.0374(c) + 0.0325(\phi) + 0.0028(q) - 0.0307(\gamma) \qquad R^2 = 0.82 \qquad [1]$$

$$Y/B = 1.0596 + 1.5214(r_i/r_o) - 0.0167(\beta) + 0.0120(c) + 0.0101(\phi) + 0.0013(q) - 0.0093(\gamma) \qquad R^2 = 0.80 \qquad [2]$$

Multivariate nonlinear regression: Polynomial of power 2

$$X/B = 0.1201(q) - 0.0128(\phi)(q) + 0.002(c)(q) - 0.0006(\beta)(\gamma) - 0.0081(\beta)(q) + 0.015(\beta)(\phi) + 0.6046(r_i/r_o)(q) - 17.9066(r_i/r_o)^2 + 0.0007(\beta)^2 - 0.0019(c)^2 \qquad R^2 = 0.94 \qquad [3]$$

$$Y/B = 0.0986(q) - 0.0070(\phi)(q) + 0.0007(c)(q) - 0.00015(\beta)(\gamma) - 0.0043(\beta)(q) + 0.0081(\beta)(\phi) + 0.2894(r_i/r_o)(q) - 9.4378(r_i/r_o)^2 + 0.0003(\beta)^2 - 0.0008(c)^2 \qquad R^2 = 0.97 \qquad [4]$$

These equations are used to evaluate the X/B and Y/B values and are compared with the FE results. The 'R-square' known as the coefficient of determination is a statistical measure of how close the data are to the fitted regression. The coefficients of determination for the developed equations [Eqs. (1) - (4)] are 0.82, 0.80, 0.94, and 0.97 respectively.

RESULTS AND DISCUSSION

The extent of the failure zone depends on the geometric configuration of the cutting edge, the soil properties, and the depth of sinking. The parametric variations adopted for the above parameters as given in Table 1 are chosen from the practical considerations which are usually encountered in the field. The normalized failure zone, X/B and Y/B, is obtained from the FE analysis. Figure 3 depicts the extent of failure zone for the specific case of tapered angle of the cutting edge = 45°. The radial and vertical extent of the failure zones can be obtained from the incremental displacement plot. The width of the cutting edge is taken as 1 m in the FE analysis.

Geometry of the cutting edge

The effect of the geometry of the cutting edge on the extent of the failure zone is investigated by varying the radii ratio and tapered angle of the open caisson. The radius ratio is varied from 0.5 to 0.9 with an increment of 0.1. Figure 4(a) depicts the effect of variation of radii ratio of the open caisson on the extent

of the failure zone in the radial and vertical directions. The size of the failure zone increases with increase in the radii ratio of the open caisson. The tapered angle is varied from 30° to 90° with an increment of 15°. Similarly, Fig. 4(b) depicts the effect of variation of tapered angle of the open caisson on the extent of the failure zone in the radial and vertical directions. The size of the failure zone reduces with increase in the tapered angle of the open caisson. The predictions made by Eqs. [(3) - (4)] match well with the FE results for the variation of the radii ratio and tapered angle of the caisson.

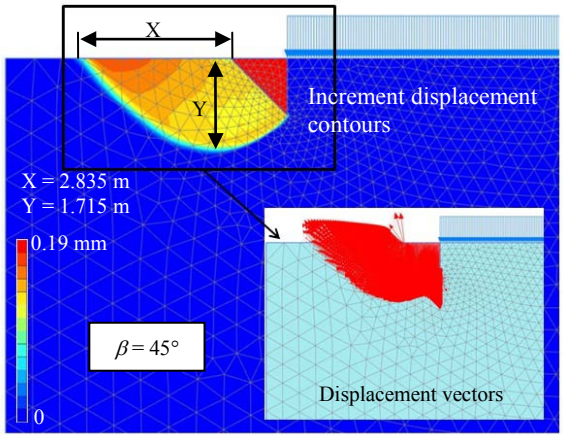


Fig. 3. Radial and vertical extent of failure zone with tapered angle of the cutting edge, β = 45°

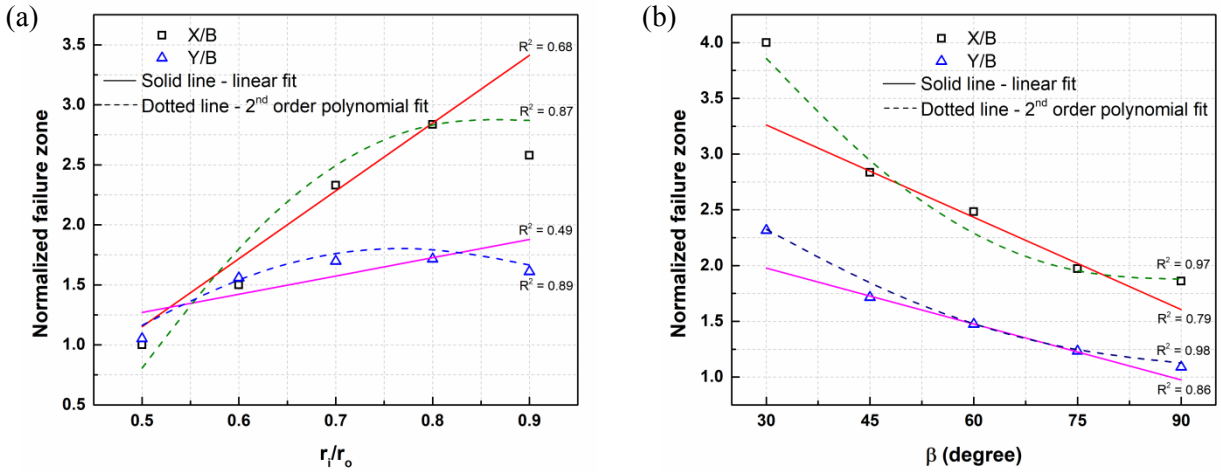


Fig. 4. Radial and vertical extent of failure zone with varying: (a) radii ratio (b) tapered angles of the cutting edge

Soil properties

The effect of soil properties on the extent of the failure zone is investigated by varying the unit weight, cohesion, and friction angle of the soil. The unit weight of soil is varied from 14 to 22 kN/m^3 with an increment of 2 kN/m^3. Figure 5(a) depicts the effect of variation of the unit weight of the soil on the extent of the failure zone in the radial and vertical directions. The size of the failure zone reduces with increase in the unit weight of the soil. The cohesion is varied from 0 to 30 kPa with an increment of 10 kPa. The effect of variation of cohesion on the extent of the failure zone in the radial and vertical directions is shown in Fig. 5(b). The size of the failure zone increase with increase in the cohesion. The friction angle of the soil is varied from 0 to 30° with an increment of 5°. Similarly, Fig. 5(c) depicts the effect of variation of friction angle of the soil on the extent of the failure zone in the radial and vertical directions. The size of the failure zone increases with increase in the friction angle of the soil. The

predictions made by Eqs. [(3) - (4)] match well with the FE results for the variation of the cohesion and Eqs. [(1) and (2)] provide comparable results for the variation of the unit weight and friction angle of the soil.

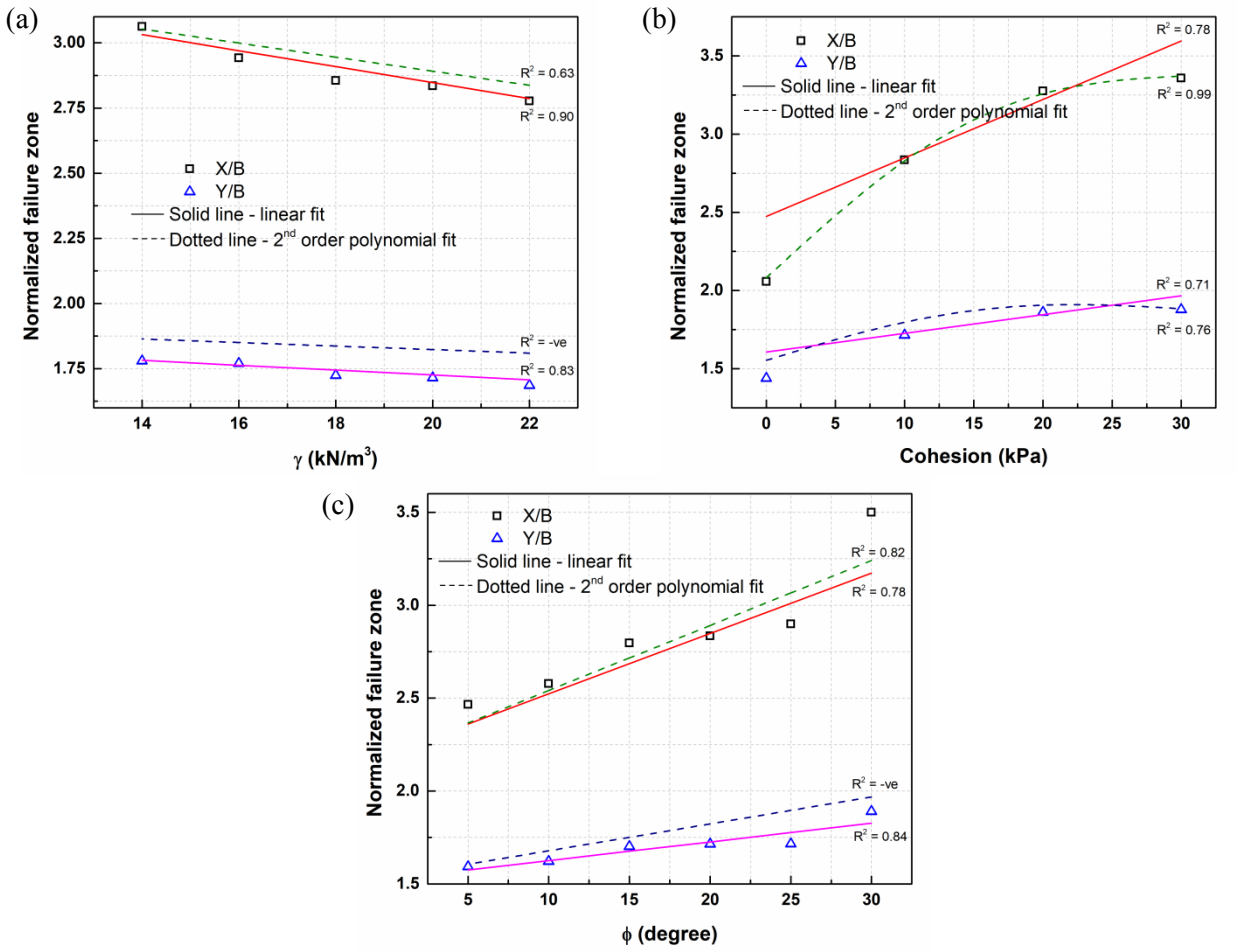


Fig. 5. Radial and vertical extent of failure zone with varying: (a) unit weight (b) cohesion (c) friction angle of the soil

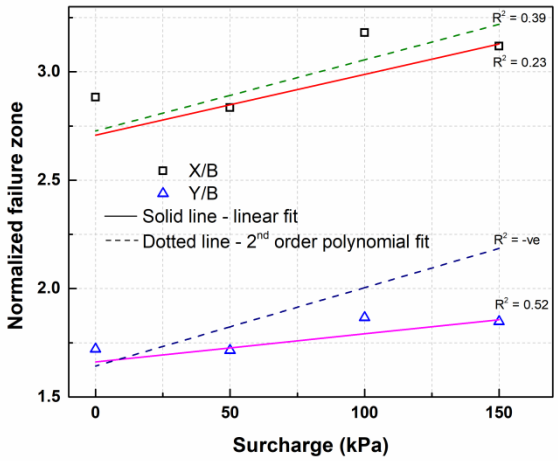


Fig. 6. Radial and vertical extent of failure zone with varying surcharge at the level of cutting edge

Sinking depth

When caisson sinks; with respect to the position of the cutting edge, the overburden increases outside the cutting edge of the caisson. The depth of soil (d) from the ground level to the top of the cutting edge acts as a surcharge at the top level of the cutting edge. This surcharge can be represented by the line load of magnitude $q = \gamma d$ in the analysis. The effect of depth of sinking of the caisson on the size of the failure zone is investigated by varying the magnitude of the surcharge. The surcharge is varied from 0 to 150 kPa with an increment of 50 kPa. Figure 6 depicts the effect of variation of surcharge on the extent of the failure zone in the radial and vertical directions. It is seen from the figure that the size of the failure zone increases with increase in the magnitude of the surcharge. In this case, Eqs. [(1) and (2)] provide the reliable predictions for the size of the failure zone (X/B and Y/B).

CONCLUSIONS

In the present study, the finite element analyses have been carried out to investigate the effect of variation of geometry of the cutting edge, soil properties, and the depth of sinking of the caisson on the extent of the failure zone in the soil at the cutting edge of the open caisson. The radius ratio and tapered angle of the cutting edge are considered for geometric variation, unit weight, cohesion, and angle of internal friction of the soil are considered for soil properties variation, and the magnitude of surcharge is considered for the depth of sinking variation. The multivariate linear and nonlinear regression analyses are performed using FE results to obtain the predictive equations to evaluate the extent of the failure zone. These equations can be used in the preliminary estimation of the extent of the failure zone in the radial and vertical directions for the selected configuration of the open caisson. Based on the results of the present study, the following conclusions are arrived at:

1. The size of the failure zone is affected by the geometric configuration of the cutting edge, the strength parameters of the soil, and the depth of sinking. The extent of the failure zone in the radial and vertical directions increases with increase in the radii ratio of the cutting edge, friction angle and cohesion of the soil, and the depth of sinking. The extent of the failure zone in the radial and vertical directions reduces with increase in the tapered angle of the cutting edge and the unit weight of the soil.
2. The easy to use predictive equations have been developed to estimate the radial and vertical extent of the failure zone in the soil at the cutting edge of the open caisson using multivariate linear and nonlinear regression analyses. The predictions made by the multivariate linear regression match well for the parametric variation in the radii ratio, tapered angle of the cutting edge, and cohesion of the soil. The predictions made by the multivariate nonlinear regression match well for the parametric variation in the unit weight, friction angle of the soil, and the depth of sinking. It is noted that the predictive equations developed using multivariate nonlinear regression analysis evaluate the extent of the failure zone with higher accuracy as compared to the equations developed using multivariate linear regression analysis.

REFERENCES

Alampalli, S. and Peddibotla, V. 1997. Laboratory investigation on Caissons-deformations and vertical load distributions. Soils and Foundations, 37(2) 61-69.

Baitsur, A.I. and Zakharov, I.B. 1975. Experimental investigations of anchoring of open caissons by means of radial piles (for purposes of discussion). Soil Mechanics and Foundation Engineering, 12(5) 296-299.

Belous, N.P. 1968. Deformation of soils and settlement of reference points at the zone where a caisson is sunk. Soil Mechanics and Foundation Engineering, 5(5) 359-361.

Bhide, D. A. and Sastry, P.N.S.S. 2017. Development of concept and general arrangement for 2nd bridge across river Kali on NH 66 (old NH 17), near Karwar in Karnataka State, India. Indian Highways, 45(9) 19-25.

Bolyachevskii, B.I. and Chumakov, I.S. 1975. Construction of precast open caissons with forced regulation of their sinking. Soil Mechanics and Foundation Engineering, 12(6) 362-365.

Brown, S.H. 2009. Multiple linear regression analysis: a matrix approach with MATLAB. Arabian Journal of Mathematics, 34 1-3.

Cecen, A. 2013. Multivariate Polynomial Regression. http://ahmetcecen.github.io/MultiPolyRegress-MatlabCentral/.

Chandler, J.A., Hinch, L.W., Fair, R.I., Hughes, D.A., Peraino, P. and Rowe, P.W. 1984. Jamuna River 230 kV crossing, Bangladesh. Part 2: Construction. IEE Proceedings C - Generation, Transmission and Distribution, 131(7) 319-332.

Chatterjee, A.K. and Dharap, V.M. 1999. Problems of construction of caisson foundations of the Second Hooghly Bridge (Vidyasagar Setu) at Calcutta and their solutions. presented at Foundations for major bridges, IABSE Colloquium, New Delhi, India.

IS: 9527, Part 1, 1981. Code of practice for design and construction of Port and Harbour structures, Part 1 Concrete Monoliths. Bureau of Indian Standards, New Delhi.

IS: 3955, 1965. Code of practice for design and construction of well foundations. Bureau of Indian Standards, New Delhi.

Jain, P.K., Kumar, R., Selot, A. and Mittal, S.K. 2008. Typical bridge foundations - selected cases. The 12th International Conference of International Association for Computer Methods and Advances in Geomechanics (IACMAG), 4771-4777.

Katti, R.K. and Dewaikar, D.M. 1977. Studies on circular well foundations in Clay media. Proceeding of 5th Southeast Asian Conference on Soil Engineering, Bangkok, Thailand, 2-4 July 1977, pp 41-54.

Kumar, M.K., Bhattacharyya, D. and Shrivastava, S.K. 2017. Deopani bridge - gateway to Dibang valley in Arunachal Pradesh. Journal of the Indian Road Congress, 78(1) 37-44.

Kumar, N.D. and Rao, S.N. 2010. Earth pressures on caissons in marine clay under lateral loads - a laboratory study. Applied Ocean Research, 32(1) 58-70.

Kumar, V. and Dhiman, R.K. 2017. Segmental construction for bridges in hilly areas: an overview. Indian Highways, 45(11), 19-27.

Kurian, N.P. 2005. Design of Foundation Systems - Principles and Practices. Narosa Publishing House, New Delhi, India.

Maslik, V.P., Kiselev, V.I and Chizhov, I.I. 1978. New method of sinking open caissons in a double thixotropic jacket. Soil Mechanics and Foundation Engineering, 15(2) 98-99.

Nonveiller, E. 1987. Open caissons for deep foundations. Journal of Geotechnical Engineering, ASCE, 113(5) 424-439.

Opershtein, V.L. 1969. Waterproofing of the walls of open caissons. Soil Mechanics and Foundation Engineering, 6(2) 115118.

Panda, J. 2015. Correction of tilt in well No. 5 of railway bridge across river Luna in Odisha: A case study. Indian Highways, 43(2) 19-27.

Royston, R., Phillips, B.M., Sheil, B.B. and Byrne, B.W. 2016. Bearing capacity beneath tapered edges of open dug caissons in sand. Proceedings of Civil Engineering Research in Ireland, Galway, Ireland.

Saha, G.P. 2007. The sinking of well foundations in difficult situations. Journal of Indian Road Congress, 68(2) 123-131.

Salamov, K.P., Bernar, D.N. and Korsunskii, E.V. 1965. Construction of the underground rooms of continuous steel casting units by the open caisson method (from the seminar on foundation engineering at the exhibition of achievements of the national economy). Soil Mechanics and Foundation Engineering, 2(3) 167-171.

Solov'ev, N.B. 2008. Use of limiting-equilibrium theory to determine the bearing capacity of soil beneath the edges of caissons. Soil Mechanics and Foundation Engineering, 45(2) 39-45.

Ter-Galustov, S.A., Ponomarenko, A.I., Opershtein, V.L. and Ivanov, V.D. 1966. Experience in sinking an open caisson in a thixotropic lining. Soil Mechanics and Foundation Engineering, 3(2) 128-131.

Tomlinson, M.J. 2001. Foundation Design and Construction. 7th ed., Prentice Hall, Harlow, England.

Yan, F.Y., Guo, Y.C. and Liu, S.Q. 2011. The bearing capacity analyses of soil beneath the edge of circular cassion. Advanced Materials Research, 250 1794-1797.

INSTABILITY ANALYSIS OF MONO PILE IN FLEXURAL AND BUCKLING MODES DUE TO LIQUEFACTION INDUCED LATERAL SPREADING

P Ravi Prakash[1] and Amit Prashant[2]

[1] Graduate Student, Civil Engineering, Indian Institute of Technology Gandhinagar, India,
e-mail: patnayakuni.prakash@iitgn.ac.in, Tel.: +the 91-9725434777
[2]Professor, Civil Engineering, Indian Institute of Technology Gandhinagar, India,
e-mail: ap@iitgn.ac.in, Tel.: +91-8511360509; Fax: +91-7923972324

ABSTRACT

A simplified framework has been developed for quantification of critical axial load on mono pile subjected to liquefaction-induced instability. Several case studies are reported in the literature, where severe damage has been observed in pile foundations due to liquefaction even though designed with a good factor of safety. Consideration of incorrect failure mechanism in the design of pile foundation is the probable reason for these failures. Previous studies idealize pile as a column and a buckling mode of failure is considered as the failure mechanism. Scenarios like the liquefaction-induced lateral spreading of soil results in large lateral loads on the pile and in turn it may result into a different failure mode. This limitation is alleviated in the present study by a beam-column idealization of the pile and its failure analysis is performed against combined buckling and flexural instabilities. A case study is presented to demonstrate the critical axial load on a given pile-soil system subjected to liquefaction-induced lateral spreading. Parameters like critical lateral spreading and critical failure axial load are studied intricately. Furthermore, the effect of lateral spreading on the critical axial load on the pile, in turn on the mode of failure is quantified. It was evident from the results that increase in lateral spreading will increase the susceptibility towards flexural failure.

Key words: Mono pile, Liquefaction, Lateral spreading, Instability, and Displacement based modeling.

INTRODUCTION

Earthquakes represent one of the severe natural hazards to which the infrastructure utilities may be subjected in their design life period. In the context of pile foundation subjected to seismic loading, the liquefaction and its associated lateral spreading constitute important design considerations as they may result in the collapse of the entire structural system. Design of pile foundations in liquefiable soils has become important due to several failures observed in the past especially due earthquake-induced liquefaction (NRC, 1985 Youd et al. 2001), and several design procedures have been developed over the past decades. Liquefaction represents a physical phenomenon due to earthquakes, which results in loss of shear strength of saturated soils. In a typical pile-soil system, the loss of shear strength of surrounding soil during liquefaction results in loss of shaft resistance. In view of the above mentioned physical phenomena, the mechanical behavior of pile is usually idealized as a column and several design methodologies have been proposed (Bhattacharya, 2003). The effective lengths for these columns can be evaluated utilizing the procedure given by Fleming et al. (1992). In terms of failure mechanisms, buckling failure and

© 2018 Deep Foundations Institute

flexural failure are the most predominantly postulated failure mechanisms. For instance, Granholm (1929) postulated the buckling instability of piles of certain critical length as a function of relative pile-soil stiffness. Bhattacharya (2003) postulated a buckling mode of failure hypothesis for pile foundations susceptible to liquefaction. According to his hypothesis, pile fails in buckling due to the loss of confinement offered by the adjacent soil at the verge of liquefaction. However, in scenarios like liquefaction-induced lateral spreading which is due to down slope displacement of soil adjoining pile, severe damage in pile foundations have been observed. Ishihara (1993) postulated that flexural mode of failure as the principal reason for such phenomena. Also, it is to be noted that flexural instability in pile foundation is augmented by the presence of non-liquefied crust which drags the pile during lateral spreading.

In the context of the design of pile foundations in liquefiable soils, the provisions of building codes are prescriptive in nature. For instance, the Japanese code of practice (JRC, 1996) assumes a flexural mode of failure in its design guidelines on pile foundations against liquefaction. Eurocode 8 Part 5 (2004) asserts that pile sections should remain elastic during liquefaction. However, critical physical parameters like soil-structure interaction, support conditions, and vertical settlement are ignored in the building codes and they suggest performance based design approach in situations with even moderate departures from the conditions assumed by the codes. Also, several empirical methods are available in the literature for instability analysis of pile foundations susceptible to liquefaction. Notable empirical design methodologies include the instability analysis methodology proposed by Bhattacharya (2003) and the pseudo-static analysis methodology proposed by Liyanapathirana and Poulos (2005). Furthermore, several numerical models have been developed for seismic analysis of the pile-soil system subjected to liquefaction (e.g. Choudhury et al. 2009, Meera et al. 2007 and Phanikanth et al. 2013). Complex soil-structure interaction in such analysis is often incorporated in a simplified manner utilizing the Winkler's springs. However, the above mentioned numerical frameworks do not consider combined buckling and bending instability which is addressed in the current study.

In the present study, incorporating the effects of lateral spreading, the pile-soil system is analyzed using a displacement-based approach. The soil in the pile-soil system is modeled as a linear elastic Winkler spring element which is characterized from the SPT data. In case of liquefied crust, the same elastic spring elements are considered with stiffness degradation factor of 0.01, as suggested by Tokimatsu (1999). For a given pile-soil system, instability analysis is performed for buckling and flexural instabilities. It is to be noted that, flexural instability is accounted by quantifying the axial load on the *P-M* interaction envelope at the interface of liquefied and non-liquefied crust. The effect of lateral displacement on the critical axial load on pile and in turn on the mode of failure is quantified at various depths of non-liquefied crust. Furthermore, parameters like critical lateral displacement and critical axial load are studied in detail.

MODELING OF PILE FOUNDATION IN LIQUEFIABLE STRATA

This section illustrates the procedure adopted for modeling a pile foundation in liquefiable soil. For a given pile of length *L* which is embedded in a saturated soil consisting of three layers with top non-liquefied crust *(L1)*, middle liquefied crust *(L2)*, and bottom non-liquefied crust *(L3)*. It is to be noted that the water table for the given scenario is located at the interface of *L1* and *L2*. Figure 1 demonstrates the schematic representation of the above mentioned field conditions. An axial load *P* and free field ground displacement *Xg* is applied to the given pile-soil system as shown in Fig.1. In the present study, the critical axial load on mono pile is parametrically investigated with due consideration to depth of water table and lateral displacement.

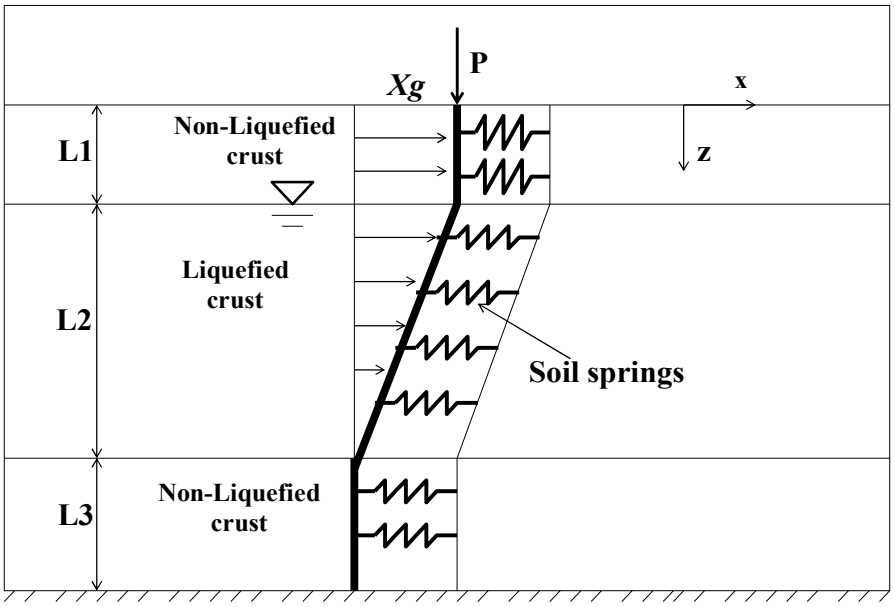


Fig.1. Displacement-based model for pile foundation during liquefaction.

As discussed previously, the soil is modeled as an elasto-plastic Winkler's springs in both liquefied as well as non-liquefied crust. According to this approach, the linear mapping between lateral soil pressure p and lateral deflection x is given by the following relation

$$p = k_{hn}.x, \tag{1}$$

where, k_{hn} is the modulus of subgrade reaction (MN/m^3) and is calculated using the empirical equation proposed by Architecture Institute of Japan (2001) and Japan Road Association (1980), which is given by

$$k_{hn} = 56N.D^{-0.75}, \tag{2}$$

where, N represents SPT blow count and D is diameter of the pile (cm). Same procedure is applied for quantifying k_{hn} in case of liquefied crust, however with a stiffness reduction factor of 0.01. For a given pile of flexural rigidity $E_P I_P$, axial load P, diameter D, lateral soil pressure p and lateral deflection x, the governing mathematical model for lateral deflection along pile is taken from the work of Hetenyi (1946) on beams on elastic foundations as

$$E_P I_P \frac{d^4x}{dz^4} + \frac{d}{dz}\left[P.\frac{dx}{dz} \right] = -p.D. \tag{3}$$

Utilizing the direct stiffness method, above mentioned mathematical model is solved with p-Δ effects along with boundary conditions as specified in (O Rourke et al. 1994).

VALIDATION STUDY

The model validation is established by comparing the predictions obtained from considered mathematical model against the field observations of a pile in Niigata Family Courthouse (NFCH) building in Niigata as reported by O'Rourke et al. (1994). The field observations are taken post liquefaction. To be mentioned, Meera et al. (2007) performed a numerical investigation on the pile-soil system under consideration utilizing nonlinear *p-y* springs. Figure.2 gives the schematic of site conditions of the considered pile-soil. The average SPT value for the aforementioned soil strata was observed to be 9 and the detailed SPT profile can be seen in O Rourke et al. (1994). The diameter of the pile is 350 mm; the modulus of elasticity of pile is 2.74×10^7 KN/m. Figure.3 shows the comparisons lateral displacements and moments along the depth of the pile obtained using the developed framework (linear model) against field results as well as numerical results of Meera et al. (2009).

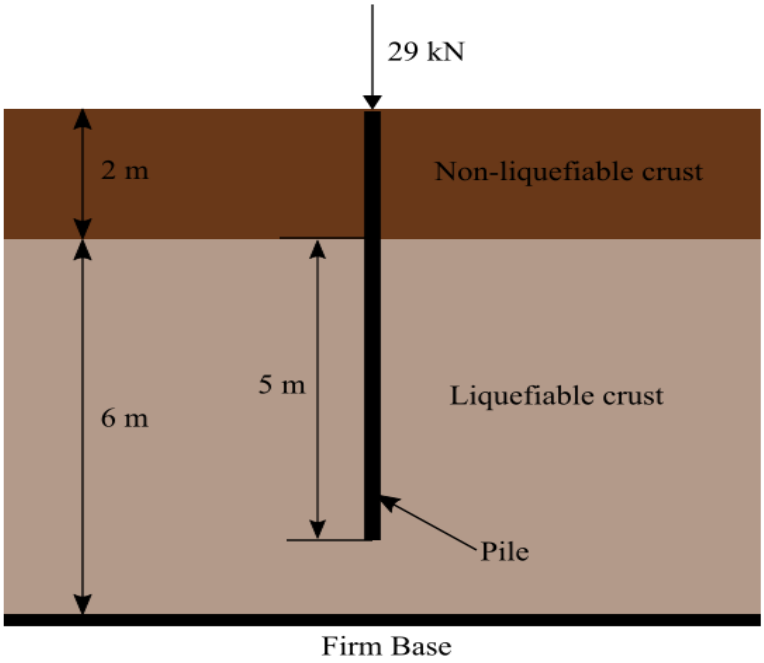


Fig.2. Soil condition at NFCH building (O Rourke et al. 1994)

The results indicate that predictions of developed framework are in good agreement with reference to field observations and also with results of Meera et al. (2007). From the field observations, yielding of the pile is observed at the liquefied-nonliquefied crust interface. It is to be noted that numerical results also indicate a similar phenomenon at the interface and strongly strengthen the argument of considering both buckling as well as flexural instabilities in the design methodology.

PROCEDURE FOR CRITICAL FAILURE LOAD QUANTIFICATION

This section illustrates the methodology for quantifying the critical failure load on mono pile. For a given pile-soil system, the field ground displacement on the top of pile foundation is quantified utilizing the empirical method proposed by Tokimatsu (1999). Utilizing this free field ground

displacement, the critical axial load on mono pile is quantified considering both buckling and flexural instabilities. For a given pile foundation, the critical Eulerian buckling load is given by

$$P_{cr} = (\pi^2 E_P I_P) / L_{eff}^{\ 2}, \tag{4}$$

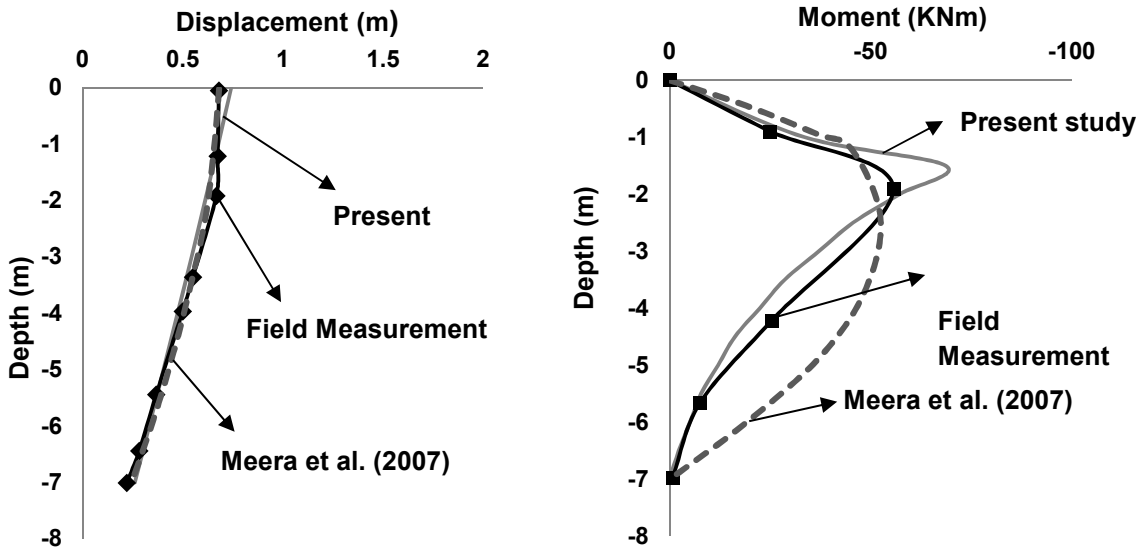


Fig.3. Computed vs Field results of (NFCH) Pile.

where, P_{cr} represents the critical buckling load on pile, L_{eff} is the effective length of pile adapted from Fleming et al. (1992), and $E_P I_P$ represents the flexural rigidity of the pile. The lateral resistance offered by a soil spring is given by

$$F_i = k_{nh}.S.D.x_i \tag{5}$$

where, F_i represents the force in ith spring, S is the spacing of springs, k_{nh} is the modulus of subgrade reaction, D is diameter of pile and x_i is the lateral displacement of the pile corresponding to the ith spring. The moment at the interface of the liquefied layer and non-liquefied crust is computed as

$$M_n = \sum_{i=1}^{i=n} F_i.z_i + P.Xd \tag{6}$$

where, M_n is the moment at the interface, z_i represents the distance of soil spring from the bottom of non-liquefied-crust, Xd is the pile tip lateral displacement. It is to be noted that for a beam-column members like pile, the critical axial load is governed by the *P-M* interaction envelope. For a given yield moment M_y and yield axial load P_y, the *P-M* interaction envelope at the liquefied-non-liquefied crust interface is given by

$$\left(\frac{P}{P_y}\right)^{\frac{3}{2}}+\left(\frac{M_n}{M_y}\right)=1. \qquad (7)$$

INSTABILITY ANALYSIS

The developed framework assumes the principle of linear superposition of lateral and axial loads on the pile. The critical axial load is quantified from the instability curves by accounting for the buckling load as well as the *P-M* interaction envelope of the pile section. Figure.4 demonstrates instability envelopes in *P-M* space for slender and non-slender piles. In case of slender piles, the critical buckling load (P_{cr}) dominates the axial crushing load (P_y). This phenomenon is incorporated and the instability curve (*A-B-C*) is subsequently developed in *P-M* space as shown in Fig.4a. In case of non-slender piles, the original *P-M* space is considered as shown in Fig.4.b as an instability curve (*D-B-C*). As shown in Fig.4, for a given lateral displacement, moment at the liquefied-non-liquefied-crust is evaluated and subsequently, the critical axial load is backtracked using eq.(7) . This is schematicaaly demonstrated through arrows as shown in Fig.4, which trace the critical axial load for a given instability curve.

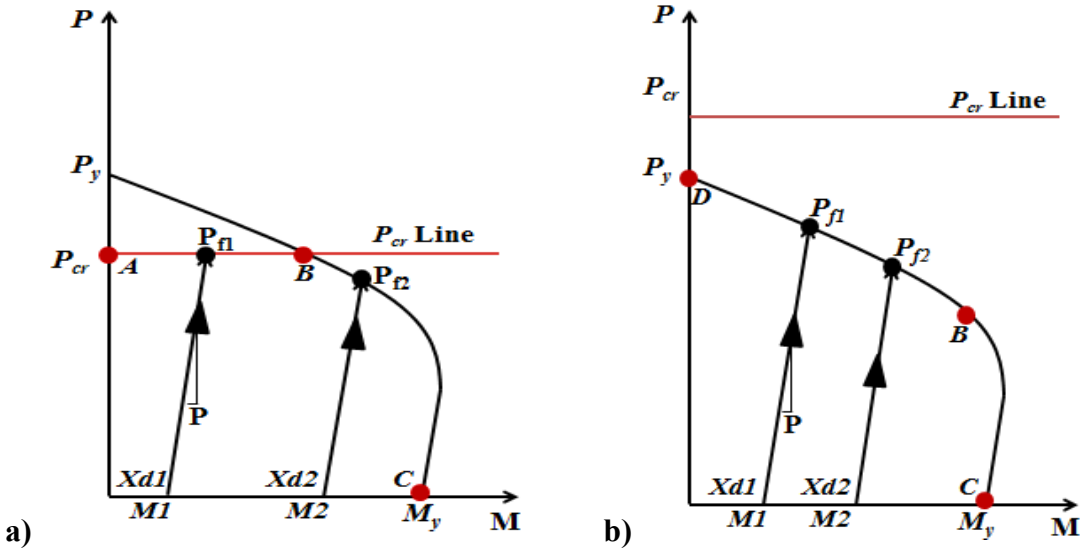


Fig.4. Instability curves for mono pile (a) Slender piles, (b) Non-slender piles.

Further a critical axial load factor p_f is introduced which is a normalized critical failure axial load with reference to buckling load. Subsequently, permissible axial load factor p_d, on mono pile is evaluated as

$$p_f=\frac{P_F}{P_{cr}},$$
$$p_d=\begin{cases} p_f, & p_f<1 \\ 1, & p_f\geq 1 \end{cases}. \qquad (8)$$

CASE STUDY: PILE INSTABILITY RESPONSE OF MONO PILE WITH VARYING STRATA

This case study presents the effect of lateral displacements and depth of water table on the instability response of mono pile in liquefiable strata. A concrete mono pile of specifications (L=8m; E=2.74×10^7 KN/m^2; f_{ck}=30MPa; diameter 350mm; 10 evenly spaced 16mm sized reinforcement, M_Y=151KNm; P_Y=2160KN) is considered. The site conditions for the pile-soil system are same as that of shown in Fig.2.

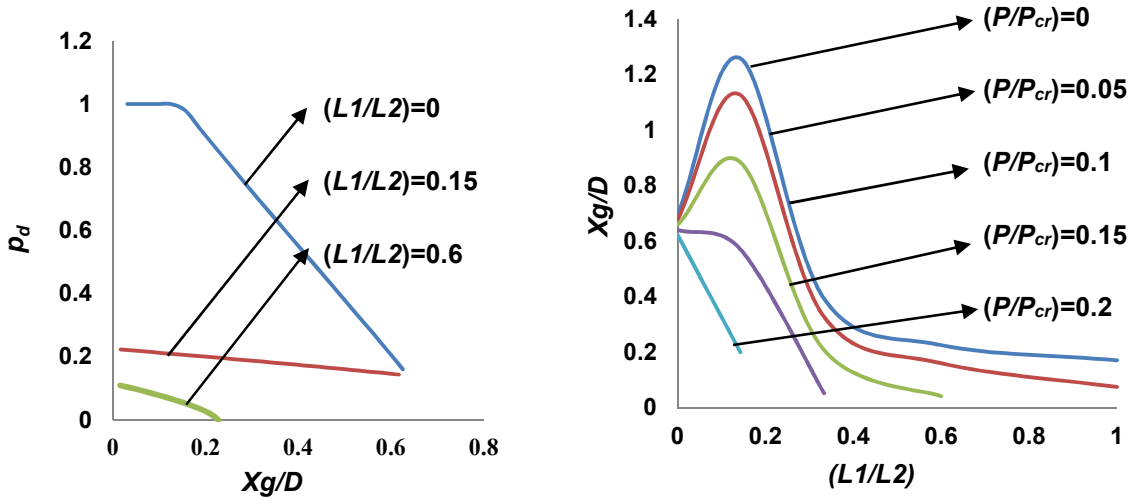


Fig.5. a) Effect of non-liquefied crust on the critical axial load at various lateral spreading b) Effect of non-liquefied crust on the critical lateral spreading at various axial loads.

Yield moment and corresponding axial load for the aforementioned pile is computed from SAP-2000. Figure.5a demonstrates the parametric studies on permissible axial load factor with varying ($L1/L2$) ratio (non-liquefied/liquefied crust depth ratios) at various levels of lateral spreading. It can be observed that for completely submerged boundary condition, up to a displacement factor (Xg/D) of 0.1, buckling mode of failure is observed in pile followed by a flexural failure. Whereas in presence of significant non-liquefied crust, flexural failure dominates over buckling failure in the entire displacement range. Also, it can be observed that the increase of depth of non-liquefied crust resulted in reduction of the axial load contribution towards instability. Eventually, the pile is susceptible to failure with merely lateral spreading without application of axial load. The principal reason for this phenomenon is severe drag force exerted by the non-liquefied crust on the pile associated with the change of boundary conditions.

Parametric studies on critical lateral spreading as shown in Fig.5b indicate initial increase in the critical lateral spreading followed by a decrease in case of piles with (P/P_{cr}) ratio up to 0.1. This is mainly due to augmentation of the stiffness of the pile-soil system with the increase in ($L1/L2$)

ratio, which leads to an initial increase in the critical lateral spreading. However, further increase in (*L1/L2*) ratio reduces the critical lateral spreading due to increase in the drag force exerted on the pile. Moreover, in case of piles with significant (P/P_{cr}) ratios, critical lateral spreading decreases with increase in (L1/L2) ratio. This is due to the predominant contribution of axial load towards the instability. Furthermore, the simplified framework proposed in the present study does not account for nonlinear behavior of soil, which may be addressed in further research.

CONCLUSIONS

A simplified framework for quantifying the permissible axial load on mono pile has been presented in this paper. It accounts for both flexural and bucking instabilities in a displacement based approach setting. A case study has been presented to demonstrate the instability analysis of mono pile in liquefiable-non-liquefiable soil strata. It has been observed that, along with mechanical properties, boundary conditions also play key role in postulating the failure mechanism during liquefaction. For fully submerged boundary condition, buckling mode of failure has been observed at lower levels of lateral spreading. A decrease in the critical axial load on pile has been observed with the increase in lateral spreading and it even vanished in case of piles subjected to lateral spreading of significant non-liquefied crust depth. Also, presence of non-liquefied crust resulted in flexural mode of failure due to the severe drag force exerted by it on the pile foundation. Given the simplified nature of the developed framework with due consideration to buckling and flexural instabilities, the developed framework can be utilized for performance based design of mono piles under liquefiable soils.

ACKNOWLEDGMENTS

The authors would like thank Indian Institute of Technology Gandhinagar for their support.

REFERENCES

Architectural Institute of Japan (2001). Recommendations for Design of Building Foundations (in Japanese).

Bhattacharya S 2003. Pile instability during earthquake liquefaction. Ph.D. thesis. University of Cambridge, UK.

Choudhury, D., Phanikanth, V. S., and Reddy, G. R. 2009. Recent advances in analysis and design of pile foundations in liquefiable soils during earthquake: A review. Proc. Natl. Acad. Sci. India, 79(A), 141–152.

EN 1998-5 2004. Eurocode 8: Design of structures for earthquake resistance, Part 5: Foundations, retaining structures and geotechnical aspects. CEN European Committee for Standardization.

Fleming, W.G.K., Weltman, A.J., Randolph, M. F., and Elson, W.K 1992, Piling Engineering. Surrey University Press, John Wiley and Sons, New York.

Granholm, H 1929. On the elastic stability of piles surrounded by a supporting medium. Proceedings of the Royal Swedish Institute for Engineering Research, pp 1-56.

Hetenyi M 1946. Beams on elastic foundations. University of Michigan Press, Ann Arbor, Michigan.

Ishihara, K 1993. Rankine Lecture: Liquefaction and flow failure during earthquakes. Geotechnique 43, No-3, pp 351-415.

JRA 1980. Japanese Road Association, Specification for Highway Bridges. Part V, Seismic Design.

Liyanapathirana, D. S., and Poulos, H. G. 2005. Pseudo-static approach for seismic analysis of piles in liquefying soil. J. Geotech. Geoenviron. Eng., 131(12), 1480–1487.

Meera, R. S., Shanker, K., and Basudhar, P. K. 2007. Flexural response of piles under liquefied soil conditions. Geotech. Geol. Eng., 25(4), 409–422.

Nikolaou, S., Mylonakis 1985. Liquefaction of Soils during Earthquakes. NRC, Report No. CETS-EE-001, Committee on Earthquake Engineering, National Academy Press, Washington, D.C.

O'Rourke TD, Myerson WD, Shaba Y, Chaudhary D 1994. Evaluation of pile response to liquefaction induced lateral spread. Technical Report NCEER-94– 0026, NCEER, Buffalo, NY, 457–479.

Phanikanth, V., Choudhury, D., and Reddy, G. 2013. Behavior of Single Pile in Liquefied Deposits during Earthquakes. Int. J. Geomech., 13(4), 454–462.

Tokimatsu K 1999. Performance of pile foundations in laterally spreading soils. Pros 2nd international conf. on Earthquake Geotechnical Engineering, Lisbon, Portugal, 957–964.

Youd, T. Leslie, and Izzat M. Idriss. "Liquefaction resistance of soils: summary report from the 1996 NCEER and 1998 NCEER/NSF workshops on evaluation of liquefaction resistance of soils." Journal of geotechnical and geoenvironmental engineering 127.4 (2001): 297-313.

MICROPILES – A STORY OF SUCCESS

Dipl.-Ing, Andreas Brandner, IB-Brandner, Karl-Schoenherr-Strasse 8, A-6020 Innsbruck – Austria,
Phone +43 512 563 3320, Fax +43 512 563 3324, Email office@ib-brandner.com

ABSTRACT

Micropiles are not new, but they are not well known. They have been used already for a very long period as foundation elements – driven piles more than a thousand years – and several European cities are built on thousands of piles. Micropiles in the present meaning are defined in the European Standard EN 14199 as either bored piles with a diameter not exceeding 300 mm or displacement piles with a diameter not exceeding 150 mm. Bored piles can be done with or without casing depending on soil conditions.

Micropiles as mentioned above were used in the middle of the past century as so called "pali radici" in Italy, and then later in Germany and the whole of Europe.

In the paper the exact definition, and differences in design principles between Europe and other parts of the world will be covered as well as design and execution rules.

Examples of the design and erection process show how micropiles can be used not only as foundation elements, but also for slope stabilization projects, soil reinforcement, or solving anchoring problems.

GENERAL TECHNICAL PRINCIPLES

In Europe design of micropiles follows Eurocode 7 – Geotechnical design – Part 1: General rules EN 1997-1 and its National annexes, which contain the basics of geotechnical design, geotechnical data, execution supervision, control and maintenance, pile foundations, anchors, supporting structures, and global stability. Execution and quality control are covered in additional European standards. Execution is covered in Eurocode 7 in the aspect of necessity for keeping the technical requirements of design. Earthquake design rules are covered in the Eurocode 8 EN 1998. All these standards are based on the semi probabilistic principle using partial safety factors.

Necessary conditions are the gathering of geotechnical bases and data by qualified personnel, design by qualified and experienced designers, adequate supervision of execution and quality control measures on site, execution by trained and experienced staff, use of building materials according to micropile approvals, maintenance of the structure in an adequate extent and duration to provide safety and durability and use of the structure according to design.

HISTORY – A SHORT LOOK BACK

The earliest used micropiles were wooden displacement piles used as foundation elements in soft soil, as foundations near or at the seashore, and for building housings, and port facilities or bridge foundations. At the beginning of the fifties of the past century, "pali radici" (or injection piles) came into general use, first as casing bored piles like GEWI piles or other root piles followed by the hollow bar injection piles by DSI, or the TITAN system by Ischebeck.

© 2018 Deep Foundations Institute

The real breakthrough of drilled micropiles started nearly 40 years later with the development of small but strong flexible drilling and injection units. Micropiles were then used not only for foundation and underpinning works but also for other purposes under difficult access conditions, and in steep terrain, such as strengthening of existing structures, settlement reduction, underpinning, anchoring, soil reinforcement, buoyancy protection and slope stabilization.

DESIGN

General technical specifics

Micropiles can either be end bearing piles – more common in the US and Canada – or friction piles – more common in Europe. Design must consider the differences in bearing type – end bearing or friction piles.

As micropiles are rather slender components, there some specific concerns must be considered with the design of a micropile project.

Keep micropiles free of bending moments – due to their slenderness micropiles can take only small bending moments.

Keep micropiles free of horizontal loads – horizontal loads cause bending moments in micropiles. As micropiles have a diameter less than 300 mm lateral bedding in layered soil cannot be considered.

Buckling of micropiles - especially in soft soils buckling of micropiles, when used as end bearing piles, is an issue not to be neglected as the linearity of a micropile is not as accurate as shown in a drawing. Boulders and other obstacles might cause deviation from a straight line increasing the danger of buckling.

Depending on the type of Micropile – hollow bar or ribbed steel bar – corrosion protection is an item either done by hot dip galvanizing, DUPLEX-protection or additional cross-section area for rusting e.g. shown in “Recommendations of the Committee for Waterfront Structures, Harbours, and Waterways” (EAU – Empfehlungen des Arbeitsausschußes Ufereinfassungen der Hafenbautechnischen Gesellschaft e.V. und der Deutschen Gesellschaft für Erd- und Grundbau).

Design procedure

Based on soil data and necessary partial safety factors foundation design can be done for the single pile and/or a combined system like a pile raft foundation, where the loads are taken by the piles as well as by the foundation raft. With this kind of foundation settlement can be reduced easily, even if no end bearing piles are used.

Depending on the type of project or structure to be supported it may be advisable to choose the layout in a way, such that no or minimum bending moments occur in the micropiles – e.g. battered piles in different directions. In case alternating loads occur – e.g. foundations of wind turbine towers, powerline towers or ropeway towers – micropiles can be used, but friction must be reduced.

When used as foundation elements in permafrost soil one must be aware, that friction can be taken only in soil and not in ice, and the most important item is not to induce heat into the soil causing melting.

When used for slope stabilization shear forces in the pile are an issue, but deformation and deflection do not matter as before.

As an anchoring measure, micropiles can be used for buoyancy protection as well as tie rods for different purposes. Preferably in karst anchoring with micropiles may prevent cracking and destroying the structure of the karst.

In soil, micropiles used as tie rods show some deflection of the head, as frictional resistance must be activated by slight movements. This must be considered in combination with the superstructure.

In Europe, depending on soil conditions, foundations with micropiles are mostly designed as friction piles and not end bearing piles, which often leads to shorter pile lengths in design.

Most mistakes and failures come from the fact, that bending moments are neglected or underestimated, which can easily be avoided by a sophisticated layout of battered piles causing mainly tension and compression in the piles.

EXECUTION

The following is some advice on the execution of micropiles.

With hollow bar systems, – not depending on the supplier - injection is the main item to keep eye on it, especially in a hot climate. Depending on available cement grade combined with compact soil or porous rock, it might be tricky to get them grouted properly. It might cause problems also under cold conditions – temperatures below freezing, where the use of heated water and injection grout may be considered.

Depending on soil conditions different methods of casting the drill cuttings may be used for hollow bars systems, - e.g. air, water – but the best outcome can be achieved by flushing with cement grout and continuous injection during drilling.

To improve bearing capacity by increasing friction it might help to use a special injection head and higher pressure, so that the diameter of the injection body may be increased.

With cased, bored micropiles it is easier to provide the correct diameter but depending on soil type – e.g. clay or silt - casing may limit side friction. Handling the casing might be difficult under extreme site conditions – e.g. steep terrain –and is time consuming and increases cost.

To improve side friction in clay or silt it might help to postgrout through a system of additional injection pipes. This works well also in cracked or porous rock.

If cracks are wide or in karst the use of “stockings” prevents loss of injection grout.

During drilling and injection inn permafrost soil the induction of heat must be limited and on the other hand freezing of injection grout must be prevented. This can be achieved by use of specific mixtures and antifreeze agents.

Depending on site conditions and accessibility drill rigs can be mounted on different carriers as shown in the following pictures.



Fig. 1 – excavator mounted rig



Fig. 2 – crawler type vehicle mounted rig



Fig. 3 – drilling rig on sledge unit



Fig. 4 – drilling rig on lightweight crawler

Fig. 1 and 2 show drilling rigs used with hollow bar system micropiles, Fig. 3 and 4 show the cased boring system for GEWI piles.

EXAMPLES – CASE STUDIES

1. Road securing project in Queensland Australia

In Queensland, Australia a coastal road was affected by a landslide and the road shoulder had to be secured and the landslide stabilized. Access with drilling rigs for big diameter bored piles as planned in the original layout was not possible due to danger of destabilization of the slope. An alternative project using micropiles solved the problem and made it possible to keep the road open for traffic on one lane. As this kind of use was not common in Australia at that time, discussions with the client took 3 weeks for assurances that the proposed solution would work. This solution was used for many years in Austria to reinforce road shoulders on alpine roads after settlement problems and shallow landslides.

In this project hollow bars supplied by Ischebeck were used. Due to an aggressive environment the DUPLEX-protection system was applied to provide durability against corrosion. Drilling could be done with an excavator mounted drilling rig from the road.



Fig. 5 – drilling works



Fig. 6 – drilling works

2. Foundation of reinforced soil construction in Alps

In a big Austrian ski resort an access road as well as room for a ski slope was needed. This access road crossed a creeping slope, where wet silty clay with boulders overlaid the weak rock beneath.

To stabilize the slope and to get a solid foundation for the up to 30 m high embankment formed by reinforced soil, a battered micropile foundation was designed and executed during a short summer period.

More than 3500 m of micropiles were drilled in a steep environment under difficult access conditions and formed together with a pile grill to provide the foundation for the reinforced soil.



Fig. 7 – excavator mounted rig



Fig. 8 – injection while drilling

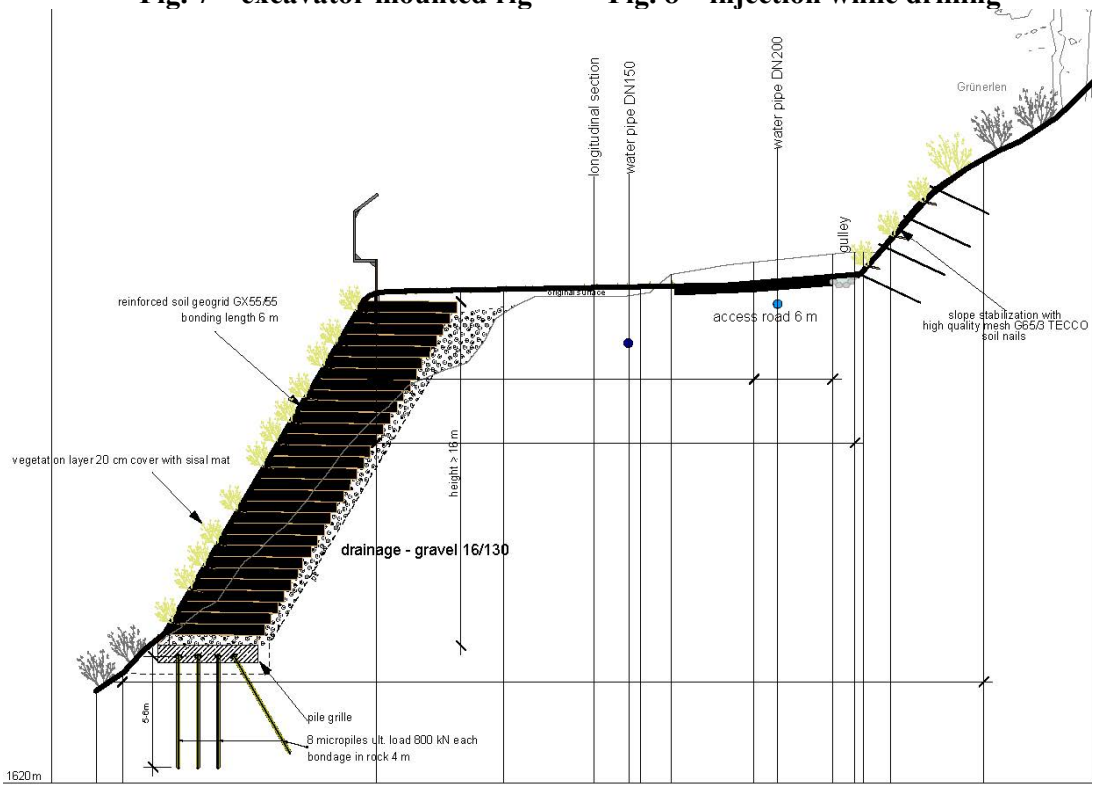


Fig. 9 – regular section of reinforced soil embankment

3. Slope stabilization

After a severe flooding in late August a creek in a big Austrian Ski Resort eroded the riverbank causing a landslide. To secure the station of a ropeway the slope had to be stabilized.
Depending on varying soil layer thickness two different ways of safety analyses were carried out – sliding circles and sliding plane according to layers.

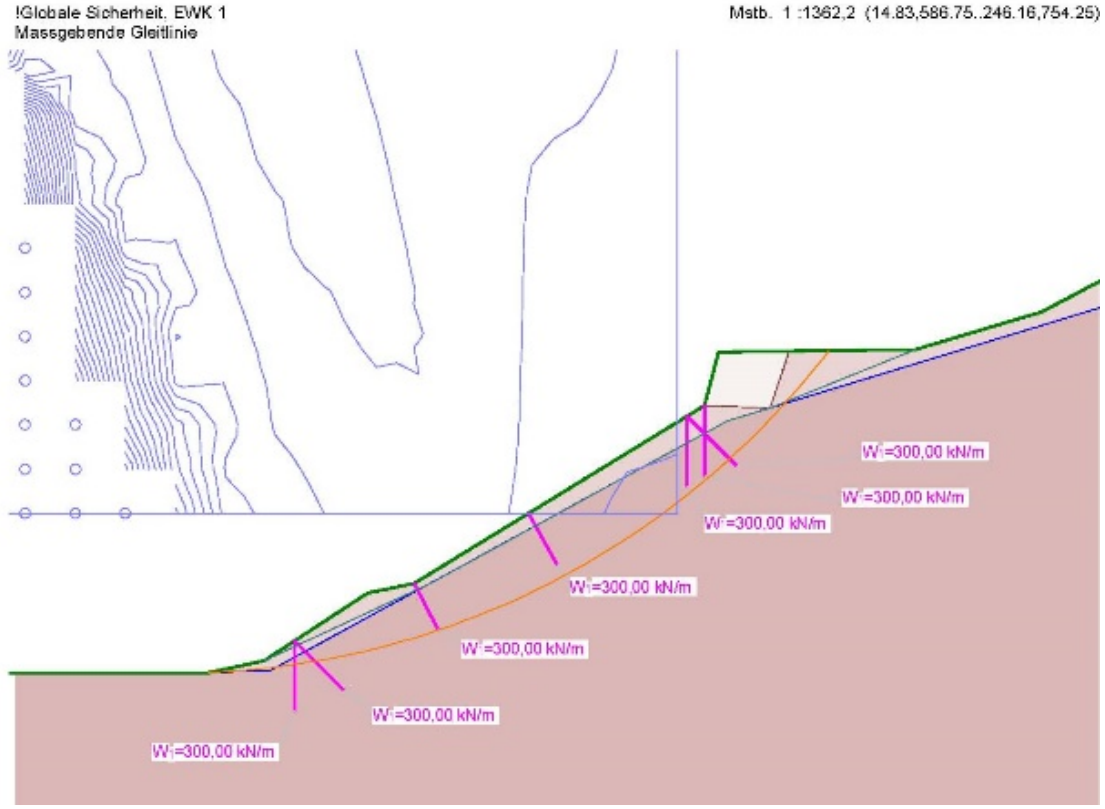


Fig. 10 – sliding circle V1

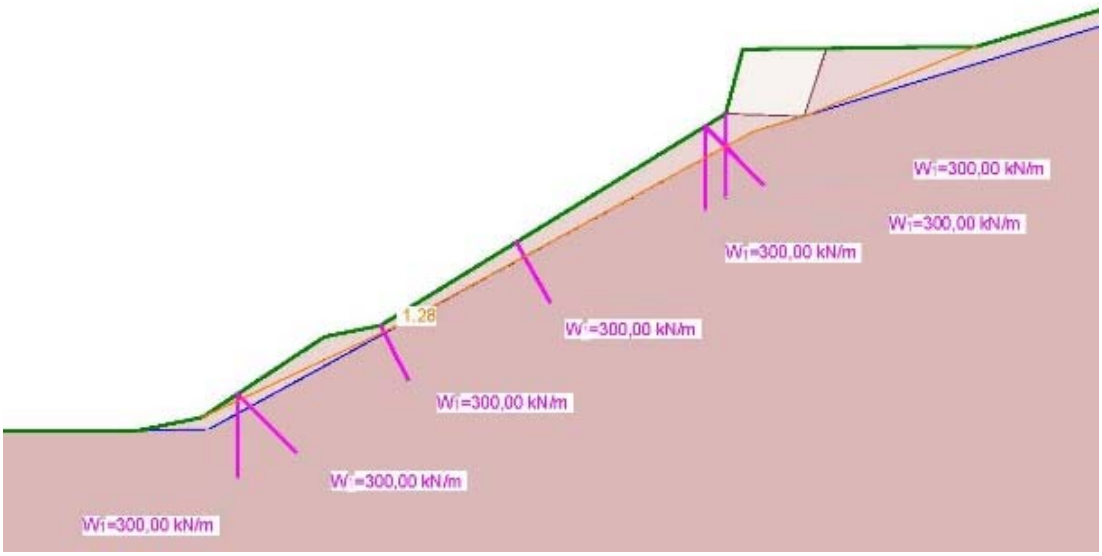


Fig. 11 -sliding plane V2

First, stability analyses were carried out – based on different theories and sliding circles versus planes - the layout of the number of dowels was fixed. Drilling works started in autumn and were finished in mid of November under severe weather conditions, – Winter brought low temperatures and snow to the site.
In the following summer the planned works – drainage, slope stabilization with high quality mesh and nails, and riverbank securing works with boulders and recultivation were carried out and left a stable and green slope.



Fig. 12 – drilling works in late autumn



Fig. 13 – secured and stabilized slope after 2 years

4. Tower foundation – e.g. high ropeway towers

Another successful use of micropiles is the foundation of high towers. For a ropeway project in Germany towers with heights up to 60 meters had to be built. Due to restricted foundation space within a huge exhibition centre, lots of electric and hydraulic lines and filled ground it was difficult to find space for a secure tower foundation. Based on experience with the use of micropiles for such projects a solution with a three-legged tower on micropile footings was proposed and accepted by the client. Without any damage to the existing lines and without any

settlement of the foundation the towers were erected within the intended time and the ropeway was opened in time for the opening of the EXPO 2000.



Fig. 14 – EXPO ropeway in Hannover

5. Extreme pit lining

In an Austrian village a parking garage had to be built adjacent to a slope at the border of the village. Excavation heights were up to 25 meters, and an additional problem was, that the owner of the neighbouring property behind the road did not allow anchors to be installed in his ground. Therefore, a pit lining system using a combination of micropiles and soil nails was worked out, which used no more than the space available.

Due to nearby housing and other buildings a continuous geodetic survey of possible movements was carried out, which proved the correctness of the design. During two short periods of work - April to June, and September to November -, the pit lining was carried out despite difficult soil conditions – boulders up to 20 m³ embedded in silty clayey gravel (moraine). Big boulders reaching into the profile of excavation were bedded in shot concrete and subsequently ablated with care to avoid big cavities in the pit lining and disrupt the system.

Cased, bored micropiles with 150 mm diameter type GEWI 63,5 were used as main support; nails were hollow bar type IBO R32-280. With this system – A-frame of micropiles, nails and shotcrete lining - a kind of gravity dam was erected, which supported the excavation pit permanently. Despite of the challenging soil conditions the alignment of the micropiles was accurate, which was checked permanently during drilling.

As corrosion protection the system of additional cross-section area as rust allowance was chosen – for the GEWI piles as well as for the soil nails hollow bar type.

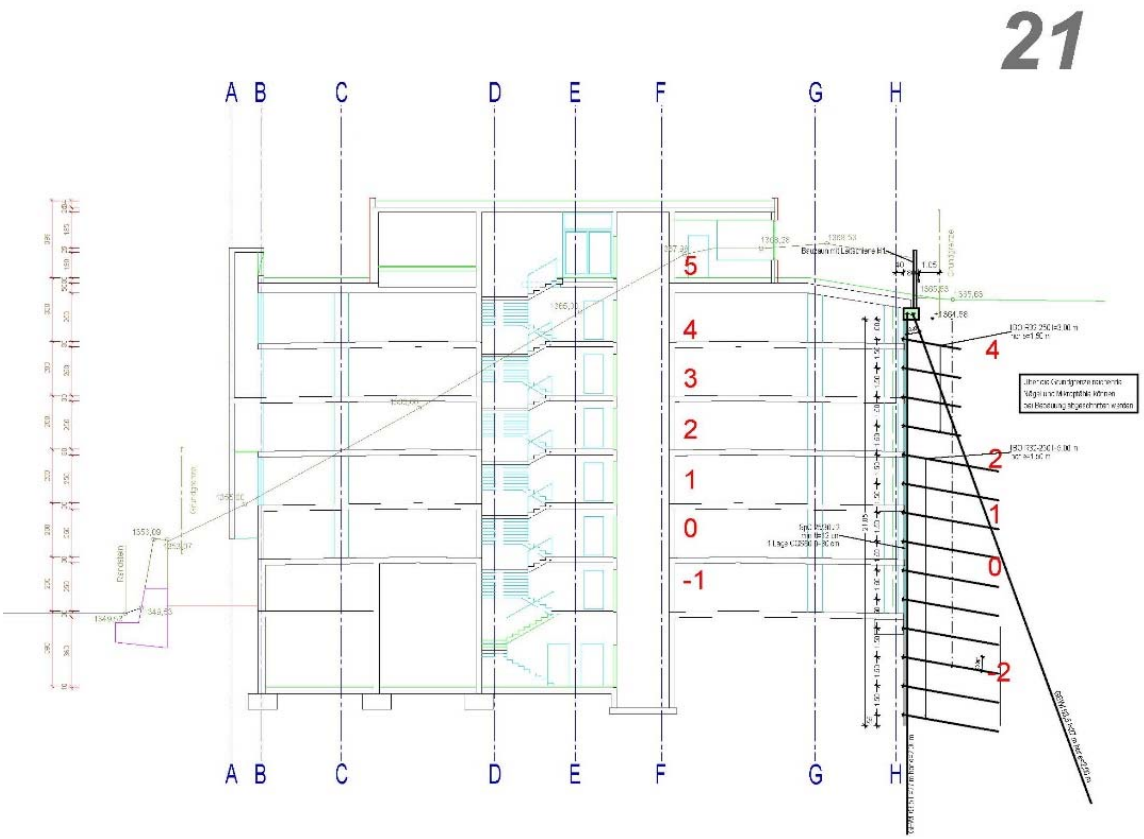


Fig. 15 – section of pit lining



Fig. 16 – general view of pit lining

During pit lining works, the maximum deflection – resulting from horizontal and vertical movements - of the pit lining was 60 mm at a height of 25 meters, causing no damage to the buildings close by.

CONCLUSIONS

Micropiles are a flexible building component, which can be used under various conditions purposes and environment.

Installation of micropiles is simple and lightweight and can be done even in extreme and difficult access with narrow working space.

The design of micropiles is not so easy, as a lot of factors must be considered – slenderness, limited bending moments, and horizontal stiffness. But if these items are considered, the design and layout can be a success.

References:

EN 1990 Eurocode – *Basis of structural design*
EN 1991-1 *Eurocode 1: Actions on structures*
EN 1993-1 *Eurocode 3 — Design of steel structures*
EN 1997-1 *Eurocode 7: Geotechnical design — Part 1: General rules (consolidated version)*
EN 14199 *Execution of special geotechnical works — Micropiles*
LARIX 5+7 – geotechnical software by Cubus AG., Zurich
Grundbau Taschenbuch Teil 1, 2, 3 – Ernst&Sohn 2009 and 2018
DYWIDAG DSI – Approval documents GEWI+ and Hollow Bar IBO
ISCHEBECK – Approval documents hollow bar TITAN
EAU 2012 – Empfehlungen des Arbeitsausschusses Ufereinfassungen, Ernst&Sohn, 11-2012, ISBN: 978-3-433-01848-4
EA-Pfähle 2012 – Empfehlungen des Arbeitskreises „Pfähle“, Ernst&Sohn 01-2012, ISBN: 978-3-433-03005-9

NEED FOR UPGRADATION OF FOUNDATION CODE FOR HIGHWAY TRANSPORTATION INFRASTRUCTURE (IRC:78-2014)

Alok Bhowmick
Managing Director, B&S Engineering Consultants Pvt. Ltd., Noida, U.P., India, Mb. +91 9811175255,
E-mail: bsec.ab@gmail.com

ABSTRACT: In this paper, an attempt is made to highlight the shortcomings of the current provisions of the code on Foundation and Substructure published by Indian Roads Congress (i,e. IRC:78-2014)[6]. Possible solution is also suggested. Inconsistencies between this code and other published codes of IRC brought out. Some of the contentious provisions in the code, which quite often creates confusion to structural and geotechnical engineers in the design of bridge foundations are also highlighted. Indian Roads Congress (IRC) is working for more than 15 years now to harmonize the IRC codes pertaining to highway bridge design to limit state philosophy. Significant progress has already been made in this regard. Codes on concrete, steel as well as composite structures have been revised with limit state philosophy. The code on Foundation and Substructure (IRC:78-2014) is however still outdated in many respects, including the fact that it is maintaining the working stress philosophy of design and yet to fall in line with the rest of the suite of codes.

Keywords: Foundation, Allowable Settlement, Liquefaction, Geotechnical Investigation

HISTORICAL BACKGROUND OF THE CODE IRC:78

The Indian Roads Congress (IRC) Standard Specifications and Code of Practice for Road Bridges in India was first published in the year 1937. Successive revisions over the years reflected incremental improvements but unfortunately the IRC codes have not kept up pace with the worldwide explosion of knowledge and advances in new technology. The gaps between national and international codes are getting wider and wider as technology advances even more rapidly. IRC codes therefore needs to be updated on a regular basis, on a fast track, for durable, safe and sustainable design of structures. However, mere updating of the code doesn't mark the end of the process but marks the beginning of a far more substantial task of ensuring compliance to code by the users. Once a code is substantially revised, it invariably heralds a trying period of the unfortunate people who have to practice with such new regulations. All their worksheets, software's, training notes, presentations and detailing practices would require updating. This applies to practicing engineers and manufacturers who have to comply with the new code in their designs& manufacture, academicians who have to teach students with the information on latest codes and standards and clients, who have to administer such regulations in the industry.

IRC:78 was first published in July 1980 as Part 1 – General Features of Design(covering upto clause 706 of the current code). It was decided to bring out the Part-II of the code subsequently covering the design and construction of foundation (covering clause 707 onwards of the current code). The first revision to the code was published subsequently in December 1983, as a unified code incorporating Part-II. The second revision of the code was published in November 2000. Major amendments were brought into this code in 2003 with regard to seismic provisions. Third revision of this code was published in 2014.

IRC is working for more than 15 years now to harmonize the suite of codes pertaining to bridges and converting them from working stress (WS) to limit state (LS) philosophy. Significant progress has already been made in this regard. Codes on concrete, steel as well as composite structures have been revised with limit state philosophy. The code on Foundation and Substructure (IRC:78-2014) is however still maintaining the WS philosophy. The upgradation is presently on the anvil and it is expected that this code will also be in sync with the rest of the codes soon. Till such time, the bridge engineers have to deal with the contradictions and conflicts that exists between IRC 78 and rest of the bridge design codes.

Carrying out the changes in the code from WS philosophy to LS philosophy, particularly for foundation design, is not an easy task. This change in design philosophy would be a significant departure from the prevailing practice and it would require a herculean effort from code makers to cross over the usual resistance for change from practicing engineers, for fear of unknown.

© 2018 Deep Foundations Institute

In this paper, a critical appraisal of the provisions of IRC:78-2014 is made in its present form. Inconsistencies between this code and other published codes of IRC, highlighted. Some of the contentious provisions in the code, which quite often creates confusion to structural and geotechnical engineers in the design of foundation are highlighted. The paper also assesses the implications of introducing limit state philosophy for geotechnical design in IRC codes.

SCOPE & COVERAGE OF THE CODE

This code (IRC:78) deals with the design and construction of foundations and substructure for road bridges. The term 'road bridges', is a generic term, used in IRC codes for all types of highway structures.

Type of structures covered in IRC code is spelt out in IRC:5-2015[5]. Clause 102.1 of IRC:5 classifies the bridges on the basis of function, as follows:

a) River Bridge / Bridge over stream
b) Viaduct
c) Flyover
d) Grade Separator
e) Road Over Bridge (ROB)
f) Road Under Bridge (RUB)
g) Foot Over Bridge (FOB)
h) Underpasses
i) Subways
j) Overpasses

Foundation for all these types of structures should ideally form a part of IRC:78. However, the codal clauses at present covers only structures under items a) to f) and j). There is no provision in the code regarding design of Underpasses, Subways, FOBs, though such types of structures are prevalent all over the country. Underground (UG) structures have features that makes their behavior distinct from above-surface structures. Construction of UG structures may involve deep excavations, with sheet piles / diaphragm walls / soil anchors / braced excavations. It is important to include design provisions for all the components of buried structures, either in IRC:78 or else separate guidelines be prepared by IRC to cover these structural elements. The coverage shall include the following:

a) Diaphragm Walls
b) Anchored Walls
c) Soil Nailing
d) Buried Wide Box Structures
e) Prestressed Rock Anchors / Soil Anchors

In order for IRC:78 to be consistent with current structural design practice, the scope and coverage of this code would require complete change by introduction of LS philosophy with partial load factors and material safety factors. Provisions of Euro Code (EC7) on Geotechnical Design is an excellent reference standard and should be considered by IRC code committee for emulation in this regard.

CONTENTIOUS PROVISIONS IN THE CODE

Geotechnical Issues

Clause 701.4.4 : Definition of 'Safe Bearing Capacity'
'Safe bearing capacity' is defined in this clause as 'net safe bearing capacity' plus 'original overburden pressure'. The term 'original overburden pressure' is not clearly defined in the code, which often leads to confusion and misinterpretation by practicing geotechnical / structural engineers. For scouring river bridges, the bed level is not permanent and during floods there will be scour. The confusion is therefore whether the 'original' overburden pressure should be calculated with respect to :

a) Original bed level at the time of boring for investigation or
b) Maximum scour level (i.e. $2d_{sm}$ below HFL) or.
c) Average scour level (i.e. d_{sm} below HFL)

Fig. 1 attached shows the various interpretation of the term 'Original Overburden Pressure'.

'Overburden pressure' is an important and sensitive design parameter for SBC. It has direct impact on gross SBC calculations and indirect impact on the net safe bearing capacity, since this term is used for estimation of allowable settlement also. There can be significant difference in the results depending upon which of the above three assumption is made by the geotechnical engineer. Therefore greater clarity in the definition of SBC should be there in the code.

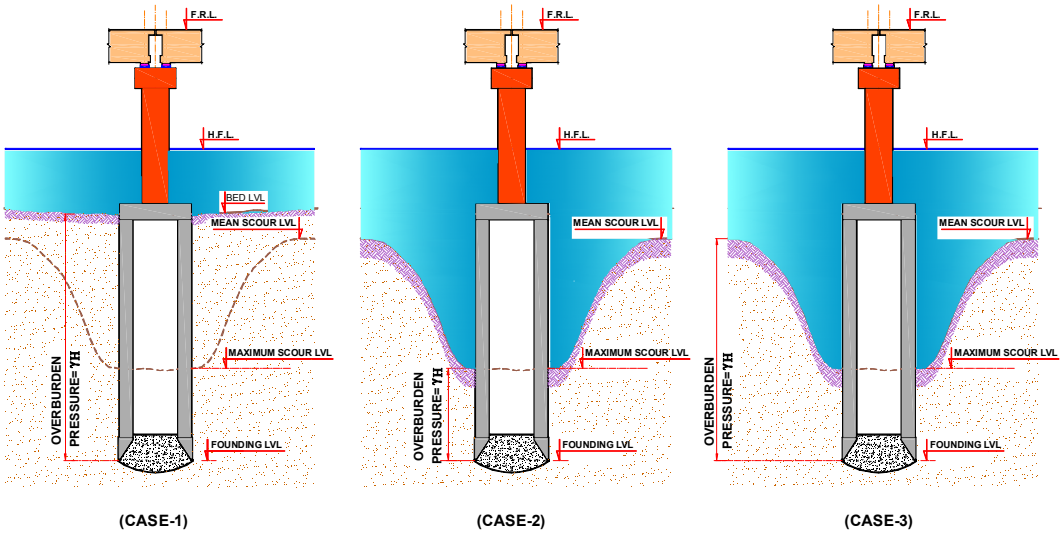


Fig. 1 : Various interpretations of 'Original Overburden Pressure' for SBC calculations

Allowable Settlement for SBC Calculations

- What should be the allowable settlement for bridge foundation?
- Which loads are to be considered for calculation of allowable settlement of foundations?

These are questions often asked by practicing engineers. These issues are not adequately addressed in IRC:78. Clause 706.3.2.1 of the code mentions about the allowable differential settlement between the two adjacent foundations (i,e. 1 in 400), from consideration of serviceability of the bridge structure. Clause 706.3.2.2 states that for structures sensitive to differential settlement, the tolerable limit has to be fixed for each case separately.

It is well recognized that the stability and safety of a bridge depends more upon the distortion of the structure as a result of differential movements of the foundations, rather than upon the absolute magnitude of the overall settlement of the foundation. Experience has shown that bridges can accommodate more movement and/or rotation than traditionally allowed or anticipated in design. Geotechnical Engineers responsible for prediction of SBC for bridges rarely take cognizance of this important clause. Mostly SBC is derived assuming a fixed allowable settlement for the foundation (which ranges from 25mm to 100mm), without giving importance to the span length, statical system of the bridge, type of structure and its sensitivity to settlement. This leads to a very conservative and un-economical design.

In case of bridges, a large fraction of the total load in foundation is dead load and imposed dead load (i,e. to the tune of 80% to 90%). Most of the dead loads are going to act during the construction stage itself, when the superstructure is yet to be cast/erected. Instantaneous settlements caused by such loads have no consequence in the serviceability of the bridge structure. Therefore depending upon the span length, the statical system of superstructure, the allowable settlement should be decided at the end of the construction period. Only post construction settlement need be considered for geotechnical purpose. Larger total settlement may be allowed.

Clause 704 : Sub-Surface Exploration

Quality Geotechnical investigation is a pre-requisite for safe and economical design of foundations. Globally, over the years substantial progress has been made in particular, in the developed world with regard to quality, adequacy and appropriateness of the geotechnical investigations. On the other hand, most of the investigations in India are lagging behind for a variety of reasons. The practice in India varies very widely. In terms of field investigations, the most primitive equipment to fairly sophisticated equipment are in use at present. Unfortunately in majority of the cases the practice is nearer to the primitive one. As an example, single tube core barrels are conventionally used as drilling tools, whereas triple tube core barrel is the norm in developed countries, which ensures high quality of cores. Also the type of drilling rig used are of primitive type which do not ensure correct sampling. Similarly in the laboratory testing also the practices widely vary. There is very little standardization and there are no requirement of accreditation of Investigation Agencies.

Dr N V Nayak, one of the leading geotechnical expert in India highlighted in one of his recent technical paper[1] several shortcomings in geotechnical investigations and analyses being practiced in India today. He opines that this state of affairs is partly from lack of adequate knowledge, partly due to acceptance of lowest bid and partly owing to very low importance given to geotechnical investigation by stakeholders. He highlighted some of the steps to improve the quality of geotechnical investigation and analysis. These are reproduced below :

- For collecting UDS from clay soils, only "Seamless Tubes" and not welded tubes should be used.
- 'Area ratio' of the sampling tubes should preferably be 10to 12% but in any case not more than 20% and samplers should have sharp cutting edges.
- UDS should be collected only in case of cohesive soils and not for cohesion less soils. Even in cohesive soils, UDS should be collected mainly from the strata with N values of SPT equal to $4 \leq N \leq 20$. No UDS should be collected from clay strata with N value of SPT >30.
- UDS in sampling tube should be properly sealed after cleaning, stored at site under shade under wet hessian cloth, and transported to the laboratory in the wooden boxes. In testing laboratory, UDS samplers should be stored in humidity chamber till they are tested.
- For testing, sample from testing tube shall be extracted in the same direction as it enters during the collection.
- All laboratories should have desiccators and it should be placed next to the oven.

The author is of the view that the foundation code needs to address all the above cited issues. Detailed procedure for ground investigation and testing should be covered in the code. In addition, there is a need to put emphasis for accreditation of GI firms, which should be made compulsory for bridges. Grading of GI firms depending on the capacity, size / turnover/ resources may be done, so as to relate the quality needs as per size and importance of the project.

Clause 708.4.2 : Procedure For Calculation of Side Earth Resistance of Well Foundation

Clause 708.4.2.1 of the code deals with the side earth resistance for well foundation passing through and resting on sandy or clayey soils. The clause states that "*The side earth resistance may be calculated as per guidelines given in Appendix-3. The use of provisions IRC:45 may be used for pier well foundation in cohesion less soil*".

The above clause is quite confusing and its interpretation quite often leads to difference of opinion between the designer and proof checker causing inordinate delays in design finalization. One interpretation of this clause is that the side earth resistance can be calculated as per formulas given in Appendix-3. For pier well foundations passing through and resting on cohesion less soil, IRC:45 may also be used. This means that for pier wells on cohesion-less soil, the designer has choice to adopt either Appendix-3 or IRC:45-1972. Alternative interpretation is that for pier wells in cohesion less soil, only IRC:45-1972 is permitted in the code. Third interpretation is that for pier wells in cohesion less soils, both the methods are to be followed and design shall satisfy worst of these requirements. The confusion is further compounded in Appendix-3 of the code, wherein the factor of safety over ultimate pressure is given for Pier Wells in 'cohesive soils' only, giving the impression that for cohesion less soil, provisions of IRC:78 are not applicable.

Author is of the view that code should avoid prescribing two methods for side resistance calculations. IRC:45-1972 is an outdated code which has not been revised ever since its first publication. It would be prudent to withdraw this code and delete reference of this code in IRC:78.

Clause 709.3.1 : Design Approach for Piles Socketed in Intermediate Geo Material and Rock
This clause specifies two methods for socketed piles and stated in Appendix-5 of the code. Method-I is applied when cores of rock sample can be taken and Core recovery as well as RQD data can be established and also UCS can be established by laboratory tests. Method-II is applicable where strata is highly fragmented with cores and/or core testing results are not available. In this method shear strength values used for calculation are related to extrapolated SPT values.

There appears some fallacy in the formulation of the pile capacity. For Method-I, the ultimate shear strength of rock along socket length, 'C_{us}' is given as '$0.225\sqrt{qc}$' subject to a limit of 3 Mpa. For Method-II, the shear strength is related to average 'N' value of socket portion. In many practical situations, author faced a situation where method-II gives a higher capacity as compared to Method-I, since the value of 'C_{us}' in case of method-II is not restricted to '$0.225\sqrt{qc}$'.

Abbreviations above are as follows :

- C_{us} = Ultimate shear strength of rock along socket length;
- q_c = Average unconfined compressive strength of rock core below base of pile for the length twice the diameter/least lateral dimension of pile in Mpa
- N = SPT value

Liquefaction of Soil
Liquefaction susceptibility of soil is not addressed in IRC:78, IRC:SP:114-2018, Appendix A-5 gives an illustration of liquefaction potential of soil, which is in line with provisions of IS:1893 (Part-1) - 2016. The provisions are grossly inadequate and raises more questions than it answers. Some of the issues of concern are :

a. Inappropriate correction factor for SPT, as given in IS:1893 (Part-1), which is also reproduced in IRC:SP:114.
b. Lateral Spreading in sloping ground – Which is not covered at present in BIS / IRC codes
c. Design Water Table level to be considered for liquefaction assessment – There is hardly any clarity. IRC:SP:114 considers the water table to be at the ground surface, which is too onerous and not in line with the international practice.

There is a need to address this important consideration holistically by all the codemakers. Following aspects in this regard needs to be included in the code :

a. Setting up of a simplified design procedure for evaluation of liquefaction potential of the soil at bridge locations.
b. Preparation of a detailed guideline on design of bridge foundations in liquefiable soils. This may include recommendations on :
    - Guideline on various Ground improvement techniques,
    - considerations for liquefaction induced lateral spreading on sloping ground and its impact
    - Consideration on what return period shall be considered for liquefaction analysis?
    - Considerations on what water table should be considered for liquefaction potential analysis?
    - neglecting skin friction in liquefiable portion of soil in case of pile foundation, considering negative skin friction in the zone of liquefiable soil, design for lateral loading in the liquefiable zone.
    - Effect of buckling on pile foundation due to liquefaction.
    - Impact of plastic hinge formation in piles during liquefaction

Issues on Loads, Load Combination and Structural design / detailing provisions

Loads & Load Combinations :
Clause 706.1.1 of the code gives the loads, forces and their combinations. The clause is ambiguous and in conflict with the corresponding provisions of IRC:6. As per this clause, the load combination given in

IRC:78 is to be followed for structural design of foundation as well as for the stability checks on foundation. Clause 706.1.2 gives increase in permissible stresses in various members under seismic/wind combinations.

Footnote number 9) below Table B.4 of IRC:6 on the contrary states that the structural design of foundation shall be based on limit state philosophy with load combination as given in Table B.4. Load combination given in IRC:78shall be followed only for checking base pressure under foundation till such time when IRC:78 changes its philosophy from working stress design approach to limit state approach.

Clause 202.3 and Table 1 of IRC:6adds further confusion to the whole issue. As per this clause, Table 1 load combination shall be adopted for working out stresses in the members. Since there is no provision / scope for working stress design in any of the material codes (IRC 112, IRC 24, IRC 22), this table has become redundant. Principle difference between the two set of load combination is as shown in Table 1 below :

Table 1: Contradiction in Load Combinations Between IRC:78& IRC:6

Load Combination as per IRC:78	Load Combination as per Table 1 of IRC:6
1. 100% Live Load considered under Seismic load combination.	1. 20% Live Load in Load Comb. with Seismic considered. 50% Live load considered under load comb. with temperature gradient.
2. Snow Load & Live Load not combined in any load comb.	2. Snow Load & Live Load combined
3. SV Loading and Congestion Factor loadings not included in Load Comb.	3. SV Loading and Congestion Factor loadings not included in Load Comb.
4. Vehicle Collision Load, Temperature, Deformation Effects and Grade Effects not considered	4. Vehicle Collision Load , Temperature, Deformation Effects and Grade Effects considered
5. Hydraulic loads and Buoyancy considered with accidental load comb.	5. Hydraulic loads and Buoyancy not considered in load comb. with accidental loads.

The author is of the view that Table 1 load combination should be shifted to IRC:78, which can be followed for base pressure checks in the interim period till IRC:78 is upgraded to limit state status. Present load combination available in IRC:78 is outdated and should be replaced.

Stability Checks :
Clause 706.3.4 of the code provides factor of safety against sliding and overturning for open foundations. Factor of safety against uplift is not specified in this clause. There are situations when foundations may be subjected to uplift. For underpass structures, check against floatation is necessary. Hence uplift shall also be covered.

Structural Design & Detailing Provisions :
IRC 78 has many provisions pertaining to structural design and detailing, which is in conflict with the current provisions of relevant IRC codes. Structural design of substructure and foundation elements is strictly not within the purview of this code and ideally these provisions are supposed to be transferred to respective loading code or material based codes (such as IRC:112 (concrete), IRC:24 (steel), IRC:40 (Masonry) & IRC:6 (Loads & Load Combination)). Details of these clauses are given in Para 4 below. IRC has already taken steps in this direction and it is hoped that these amendments will be reflected in the code soon.

Issues on Hydrology, Hydraulics Including Scour

Determination of general scour during a flood (in the absence of any bridge) is a difficult task due to the fact that a large numbers of geometric, flow and sediment parameters e.g. flood peak, duration of flood, bed and plan forms of river, sediment transport, human activities etc. govern general scour.

Estimation of local scour in the vicinity of piers and abutments poses another added challenging problem to hydraulic engineers. Whereas any under estimation of scour will result in bridge collapse, overestimation of scour leads to escalation of cost. The best way of assessing the depth of scour in a river is to observe the same during the passage of highest flood.

Real time scour has been measured at bridge sites by USGS by deploying instruments like fathometer/ADCP and other electronic devices. The observed scour has been verified with predicted scour for proving mathematical model e.g.HEC-18. Unfortunately, with very little field data, regarding bridge scour together with corresponding flow and geometric parameters governing scour, available in India, it has not been possible to prove the various mathematical models used for estimation of scour. Design engineer, therefore, generally relies on the use of empirical formulae for calculation of scour depth.

Provisions for estimation of general and local scour in IRC:78 is oversimplification of the complexity involved. IRC method of estimation of scour is based on Lacey's regime theory, which was developed by Lacey (1930) and Inglis (1944), based on observations made on canals in India and Pakistan with regime flow condition. There are several limitations in Lacey's method for application in bridge scour calculation. It ignores many parameters which governs the scour around bridge piers. Lacey did not consider the sediment transport and threshold condition of bed motion [2],[3],[4].

Using lacey's formula for all types of strata, including clayey and bouldary strata is an abuse of the lacey's regime theory. Clause 703.2.2.2 refers to Appendix-1 for calculation of mean scour depth, in absence of any data on scour for such materials, but Appendix-1 covers only formulas for clayey material and not for bouldary strata.

Author is of the firm view that a single comprehensive state of the art document dealing with Hydrology and Hydraulics of river bridges, covering all possible aspects, should be published, for the benefit of bridge engineers. Code should also cover the need for field measurement of scour at existing major bridge sites, which can help the authorities to predict scour more accurately for future bridges on the stream.

Depth of Foundation for Bridges in Near Vicinity of Existing Bridges

Clause 705.1 of the code states that "In case of bridges where the mean scour depth 'd_{sm}' is calculated with Clause 703.2, the depth of foundation shall not be less than those of existing structures in the vicinity". This clause has been misused and abused by many bridge engineers in recent past. The question that remains unanswered in this clause is 'what should be considered as 'in the vicinity'?

In one of the recent major river bridge project over river Ganga, the Authority's Engineer has demanded that founding level of the bridge foundation shall have to be kept same as that of the next bridge on the stream, located 25 Km downstream. The matter could be amicably resolved through persuasion and the Authority's Engineer had to withdraw this unjust demand. But the clause is confusing and generates controversies in many projects. It is important for the code makers to clarify the basic intent of this clause and modify this clause to avoid blatant misuse.

Author is of the opinion that this clause is applicable for those foundations which are so close to each other that there 'pressure bulbs' interfere with each other within the influence zone (say within 1.5 times the width of foundation below the founding level). In case these foundations are wide apart and the pressure bulbs do not interfere, there is no impact of one foundation over the other and in such cases, the founding level of new bridge need not be kept the same as the old bridge. **Fig.2** shows the two possible scenarios for better clarity. In case-1, there is influence of existing foundation to the new foundation, while in case-2, there is no influence of existing foundation to the new foundation.

Check for Ovalisation of Well Foundation (Clause 708.3.4)

It is stated in this clause that "*The horizontal annular section of well steining shall also be checked for ovalisation moments by any rational method taking account of side earth pressures evaluated as per Clause 708.4*" The procedure for ovalisation check of well foundation is neither given in any text book and nor in the code. Absence of any guideline / literature on this subject makes it difficult for most of the structural designers to carry out this check. Very rarely this check is performed by Consultants. It is strongly recommended that an Appendix be added for ovalisation check of well foundation.

Load Testing and Acceptance Criteria for Pile Foundation (Clause 709)

For pile load testing and acceptance criteria, reference is made to IS:2911 (Part 4), with minor modification in one of the criteria. As per IRC:78, the acceptance criteria for pile foundation is as under :

1) Two-thirds of the final load at which the total displacement attains a value of18 mm or maximum of 2 percent pile diameter whichever is less unless otherwise required in a given case on the basis of nature and type of structure in which case, the safe load should be corresponding to the stated total displacement permissible;

2) 40 percent of the final load at which the total displacement equal to 10 percent of the pile diameter in case of uniform diameter piles and 7.5 percent of bulb diameter in case of under-reamed piles.

The first criteria relates to serviceability requirement while the second criteria relates to strength requirement (ultimate limit state).

The serviceability criteria given in the code were fixed in IS:2911 (Part-4) – 1985, based on experience of 400mm to 600mm diameter piles in the country. With time, the pile diameter has increased and there is also an increase in load carrying capacity of pile. In light of these changes, this criteria should have been re-visited by the code makers. For large diameter piles with high load carrying capacity, elastic shortening of the pile itself will be quite significant. The upper limit of 18mm in settlement criteria means that for pile diameter greater than 900mm, the allowable settlement is independent of the diameter of pile. This leads to very conservative estimate of pile load carrying capacity. It is very common in bridges to have diameter ranging from 1000mm to 2500mm. The 18mm limit therefore should be waived. Allowable settlement shall be kept as 2% of pile diameter.

INCONSISTENCIES BETWEEN IRC:78 AND OTHER PUBLISHED CODES

There are several provisions in IRC:78 which is at present in conflict with the provisions of other IRC codes. Some of these clauses (as identified by the B-3 committee of IRC) are highlighted below :

a. Structural Design and reinforcement Detailing provisions for open foundation, pier walls, well foundations …etc. are in conflict with the provisions of IRC:112. Relevant clauses which needs to be shifted to IRC 112 are : Clause 707.2, 708.3.3, 708.3.4, 708.3.6, 709.4, 709.5, 710.1, 710.2.9, 710.3, 710.7, 710.8.7, 710.9, 710.10.3 & 710.10.4

b. Some of the clauses pertains to loading, which should be in the domain of "Loads & Load Combination" and should be shifted to IRC:6 to avoid conflict. Relevant clauses are : Clause 710.2.9, 710.4.2 to 710.4.5 & 710.4.7.

c. Some of the clauses pertains to brick masonry, which should be in the domain of IRC:40.Relevant clauses are : Clause 708.3.2, 708.3.5, Fig. 3 of Appendix-3.

PROVISIONS OF EUROCODE EC7 WHICH CAN BE EMULATED BY IRC

The foundation code should be a framed in a manner so that it becomes a tool to help all the Indian geotechnical engineers to speak in the same language. The code should also be a necessary tool for effective dialogue between geotechnical engineers and structural engineers, when it comes to soil-structure interaction. It should be framed in a manner which promotes research and has provision for accommodating future changes.

Provisions of Euro Code on Geotechnical Design (EC7) covers all these aspects beautifully and is an excellent reference standard which should be considered by IRC code committee for emulation in this regard. Euro code EC7 is in two parts, namely: "Part 1 : General Rules" and "Part 2 : Ground Investigation & Testing".

Part 1 of EC7 has 12 sections, which are as under :

- Section 1 : General
- Section 2 : Basis of Geotechnical Design
- Section 3 : Geotechnical Data

- Section 4 : Supervision of construction, monitoring and maintenance
- Section 5 : Fill, Dewatering, ground improvement & reinforcement
- Section 6 : Spread Foundations
- Section 7 : Pile Foundations
- Section 8 : Anchorages
- Section 9 : Retaining Structures
- Section 10 : Hydraulic Failures
- Section 11 : Site Stability
- Section 12 : Embankments

Part 2 of the code has 6 sections, which are as under :
- Section 1 : General
- Section 2 : Planning and reporting of ground investigations
- Section 3 : Drilling, Sampling and GW measurements
- Section 4 : Field tests in soil and rocks
- Section 5 : Laboratory tests in soil and rocks
- Section 6 : Ground investigation report

In addition, there are number of informative Annexes in EC-7 to supplement. It is a well-structured and comprehensive code with wide coverage of all aspects of foundation design, including the soil-structure interaction. Admittedly, the conversion of present code to limit state mode is a huge challenge. However this is a bitter pill to be swallowed by the B-3 committee of IRC for harmonization of this code with other codes.

CONCLUSION

It is imperative that national Standards are continually improved and updated to reflect the changes happening in international scenario based on global research and best practices.

There is no need to re-invent the wheels always. IRC is following this philosophy and made a good (though somewhat delayed) progress in this direction. New Generation codes with rational limit state design philosophy, which is based on concepts of reliability, safety, serviceability, durability, and economy, are being developed.

It is only the foundation code which needs to be transformed to limit state version. This however is not an easy task. Challenges are much more daunting for transformation of foundation code, which involves interaction between the structure and soil, combining elementary as well as very advanced construction methods in varying degrees.

It should be considered that knowledge of the ground conditions depends on the extent and quality of the geotechnical investigations. Such knowledge and the control of workmanship are usually more significant to fulfilling the fundamental requirements than is precision in the calculation models and partial factors. Therefore codification on geotechnical investigation needs urgent attention.

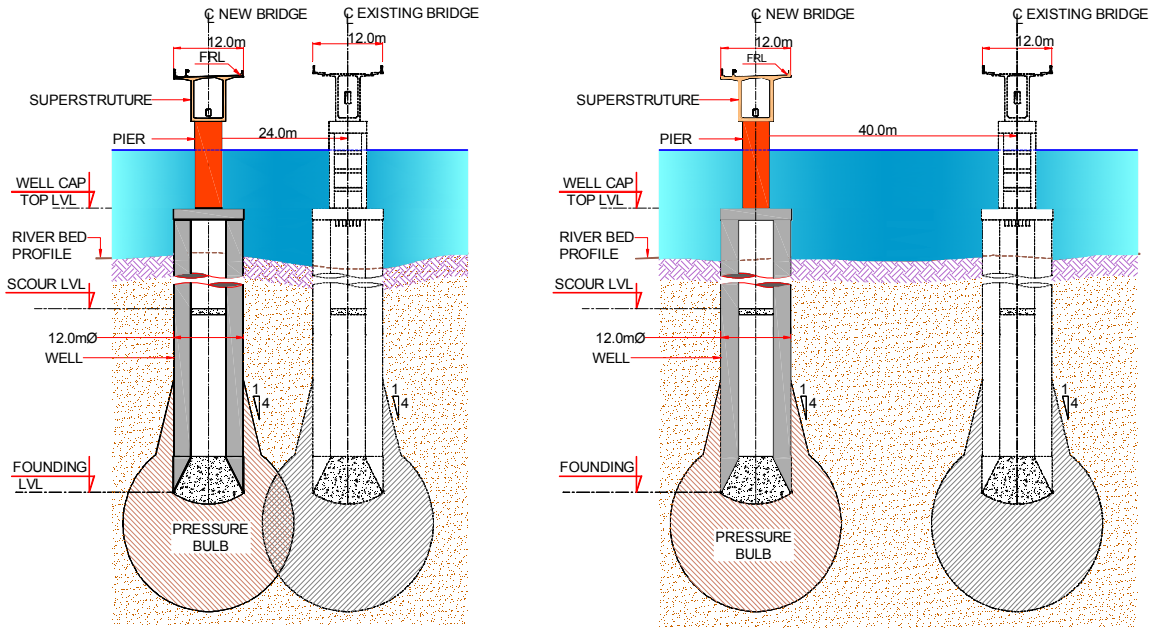


Fig. 2 : Foundations of Bridges in near Vicinity of an Existing Bridge

REFERENCES

1. Nayak N V: Guidelines for Quality Geotechnical investigation and analysis, published in IGS Newsletter, Volume 49, Oct-Dec 2017.

2. Kothiyari Umesh C: Indian practice on estimation of scour around bridge piers – A comment, published in Sadhana, Vol. 32, Part 3, June 2007, pp187-197

3. Mazumder S K: Estimation of scour in bridge piers on alluvial non-cohesive soil by different methods, published in Indian Highways.

4. Garde R J and Kothiyari U C: Scour around Bridge Piers, PINSA 64, A, No. 4, July 1998, pp 569-580

5. IRC:5-2015 Standard Specifications & Code of Practice for Road Bridges – Section I – General Features of Design - (Eighth Revision)Design).

6. IRC:78-2014 Standard Specifications & Code of Practice for Road Bridges – Section VII – Foundation & Substructure (Revised Edition)

NEW TECHNOLOGIES FOR FUTURE IN DEEP FOUNDATION INDUSTRY IN INDIA

Manish Kumar, Senior Vice President**,** ITD Cementation India Ltd., Mumbai, Maharashtra, India
Mob: +91-9820698739, Email: manish.kumar@itdcem.co.in
Sachin Kamat, Assistant General Manager**,** ITD Cementation India Ltd., Mumbai, Maharashtra, India
Mob: +91-9920838286, Email: sachin.kamat@itdcem.co.in

ABSTRACT

Government of India has taken initiative to augment infrastructure in the country in an expeditious manner. Accordingly, they have planned major investments in roads, water supply, railways, MRTS systems, tunnels, ports etc. Almost 8% of our Gross Domestic Product (GDP) is utilized for new construction in infrastructure and other fields. While the investment is assured and the projects are coming, the need of the hour is to accelerate the pace of construction. This has induced opportunities for introducing new technologies for fast track construction to reduce the cost and time of construction. In the geotechnical arena, we need to seriously look at newer technologies for faster construction of piles and their applications. In this paper, the utilization of Barrette Piles, Continuous Flight Auger (CFA) piles and Spun Concrete Piles have been discussed. Also, discussed is a special application of bored piles, namely Secant Piles which has gained popularity in recent times because of requirement of very deep excavations in thickly populated urban areas for construction of underground stations for MRTS systems.

Keywords: Barrette Pile, CFA Piles, Spun Pile, Secant Pile

INTRODUCTION

Infrastructure sector is a major sector propelling growth of Indian economy. Government of India has taken initiative to augment infrastructure in the country in an expeditious manner. Accordingly, they have planned major investments in roads, water supply, railways, MRTS systems, tunnels, ports etc. Almost 8% of our GDP is utilized for new construction in infrastructure and other fields.

As India moves ahead on the economy front, demands for fast track projects are gaining momentum. The size of project has increased while the project duration is shrinking. This necessitates a serious look at newer technologies for faster construction of piles and broadens the horizon of their applications.

In following sections, utilization and constructional aspects of Barrette Piles, Continuous Flight Auger (CFA) piles, Spun Concrete Piles and Secant Piles have been discussed.

Although, there have been some reservations, there should be no doubt that these techniques can be successfully executed/adopted in India as well if ground conditions are suitable.

BARRETTE PILES

Barrette Piles are load-bearing elements that have a similar construction method as that of a diaphragm wall. Barrettes provide resistance to horizontal loads and to bending moments better than circular piles of the same section area. One single pile is usually sufficient under one column as the increased cross sectional area is also able to support very large vertical loads. Sophisticated machines with self-guided,, cable-operated or Kelly-guided grabs are used to ensure excavation efficiency and acceptable verticality. Barrette piles are typically constructed in lengths of up to 6m depending upon the soil conditions and stability of the trench (Foundation Design and Construction Manual 2006).

© 2018 Deep Foundations Institute

Conventional piles often become impractical and uneconomical when very heavy column loads are to be transmitted to a very deep bearing stratum. Barrettes are used to carry heavy loads and therefore a single barrette can replace a few conventional piles, resulting in savings in construction time, quantity of concrete, steel and size of pile caps, etc. .

In some cases, the designer would need foundation elements to resist lateral loads and bending moments in a preferential direction in addition to vertical loads. It would be more advantageous in such cases to use rectangular shapes instead of circular sections. By adopting barrettes, the designer would be able to increase the moment of inertia and bending moment resistance in the required direction without having to increase the concrete area by properly orientating the barrette (Ramaswamy S.D. et al.1986)

Merits and Demerits of Barrette piles
Merits:

- A single barrette can replace a group of bored piles or driven piles and thus can result in a more compact and reliable foundation system with advantages of savings in time and cost.

Demerits

- Difficulties involved in load test of barrette piles makes designers apprehensive while selecting barrette as a foundation element.

Construction of barrettes
Steps involved in construction of Barrette piles can be broadly listed as below.

- Guide wall of about 1 metre depth from ground level along the perimeter of the barrette is built before commencing the excavation.
- Barrette trench is excavated using crane supported grabs or hydraulic grabs. The barrettes are commonly excavated with one bite of grab. During the trenching for the barrette, bentonite/ polymer slurry is continuously fed into the trench as it proceeds and the slurry level is maintained at the guide wall bottom level.
- After trenching up to desired depth, barrette tip is cleaned by flushing fresh bentonite/ polymer slurry.
- Rigid reinforcement cage is then lowered into the trench and Concreting is done using tremie method.

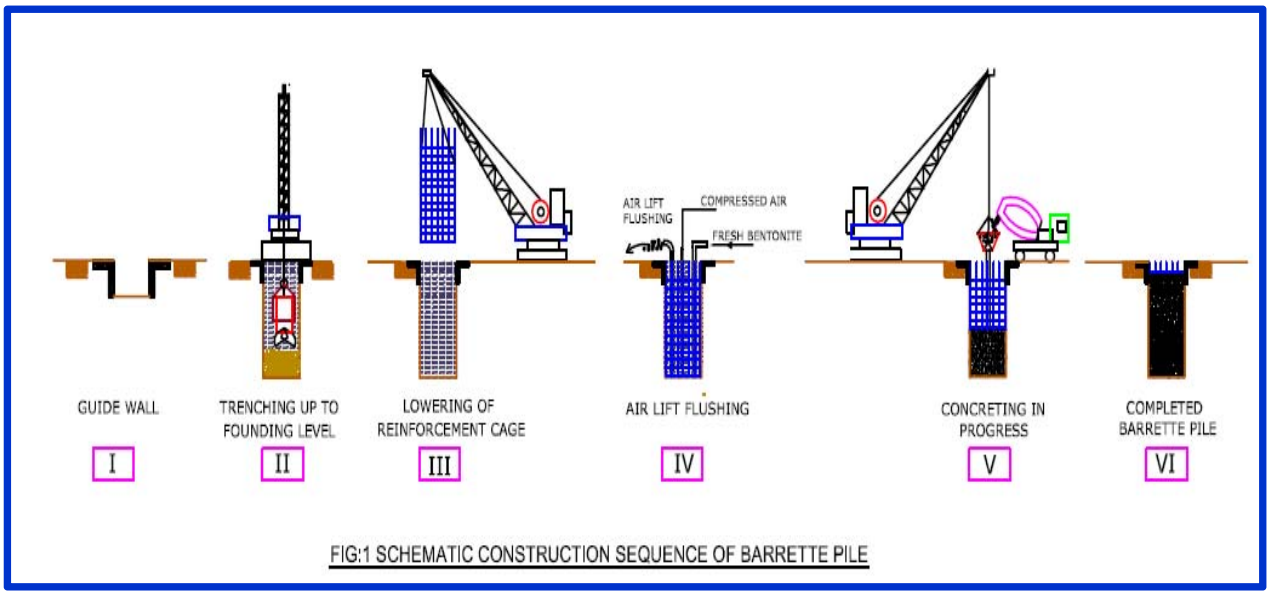


FIG:1 SCHEMATIC CONSTRUCTION SEQUENCE OF BARRETTE PILE

Case History – Barrette Piles for a 54 Storied Residential Complex in Mumbai

Barrette Piles were recently installed for four number, 54 story residential Towers with four level basements in Mumbai. The basement was constructed using permanent, load bearing diaphragm walls with three levels of inclined ground anchors. The subsurface conditions at site indicated presence of marine clay up to 6 to 8m followed by weathered and jointed Basaltic rock up to 12m to 13m depth. Moderately weathered basalt was encountered at 13m to 15m below ground level. L, T and rectangular shaped barrettes were installed up to 14 to 15m depth below ground level. The barrette piles installed were 3m to 6m long and had widths of 600mm and 800mm. Barrettes were socketed in moderately weathered basalt for 3to5 times the thickness of the barrettes. The socketing in the rock was done by first drilling some pilot holes followed by chiseling with cranes. Thereafter, grab trenching could be resorted to.

CONTINUOUS FLIGHT AUGER (CFA) PILES

Continuous Flight Auger (CFA) piles are cast in-situ piles that are formed by drilling with a hollow, continuous flight auger through which a high slump grout mix/ concrete is pumped and the auger is slowly withdrawn. The walls of the boreholes are continuously supported by the spiral flight and the cuttings within them. The reinforcement is often confined to the upper 10 to 15 m of the pile for ease of installation and also due to the fact that in many cases, relatively low bending stresses are transferred below these depths. CFA piles are typically installed with diameters ranging from 0.3 to 0.9 m and lengths of up to 30 m. CFA piles are cost effective and quick construction alternatives to other deep foundation systems (Geotechnical Engineering Circular No.8 2007).

Construction of CFA piles
The construction sequence of CFA Pile is as follows (Ref.figure.2)

- The pile is drilled to the design depth in one continuous process using a continuous flight auger. While the auger is drilled into the ground, the flights of the auger are filled with soil, providing lateral support and maintaining the stability of the hole.
- After reaching the required depth, the auger is lifted for about 150 to 300 mm and grout is pumped under pressure to expel the plug at the base of the internal pipe and commence the flow. The auger is then screwed back down to the original pile tip level to establish a small head of grout or concrete on the auger and to achieve a good bearing contact at the pile tip.
- The grout is pumped continuously under pressure up to 2 MPa measured at the top of the auger while the auger is lifted smoothly in one continuous operation.
- Simultaneously, as the auger is lifted, the soil is removed from the flights at the ground surface.
- After the grouting / concreting procedure is completed, the top of the pile is cleared of debris.
- Reinforcement cage is lowered into the hole filled with fluid concrete / grout to the required depth immediately after withdrawal of the auger. A minimum cover of 75 mm is commonly adopted for most applications.

Merits and Demerits of CFA piles
Merits
- Unlike bored piles, the use of casing or slurry to temporarily support the hole is avoided.
- Drilling the hole in one continuous process is faster than drilling operation that requires lowering the boring tools multiple times to complete the boring.
- CFA piles generally work well in soil conditions such as medium to very stiff clay soils, cemented sands or weak limestone, residual soils having a small amount of cohesion, medium dense to dense silty sands if the groundwater table is deeper than the pile length, rock overlain by stiff deposits.

Demerits

- The torque requirement to install the continuous auger pile is high compared with a bored pile of similar diameter; therefore, the diameter and length of CFA piles are generally less than bored pile.
- Placement of reinforcement can be more difficult in a CFA pile than in a conventional drilled shaft or slurry wall, in which the reinforcement is placed ahead of the concrete.

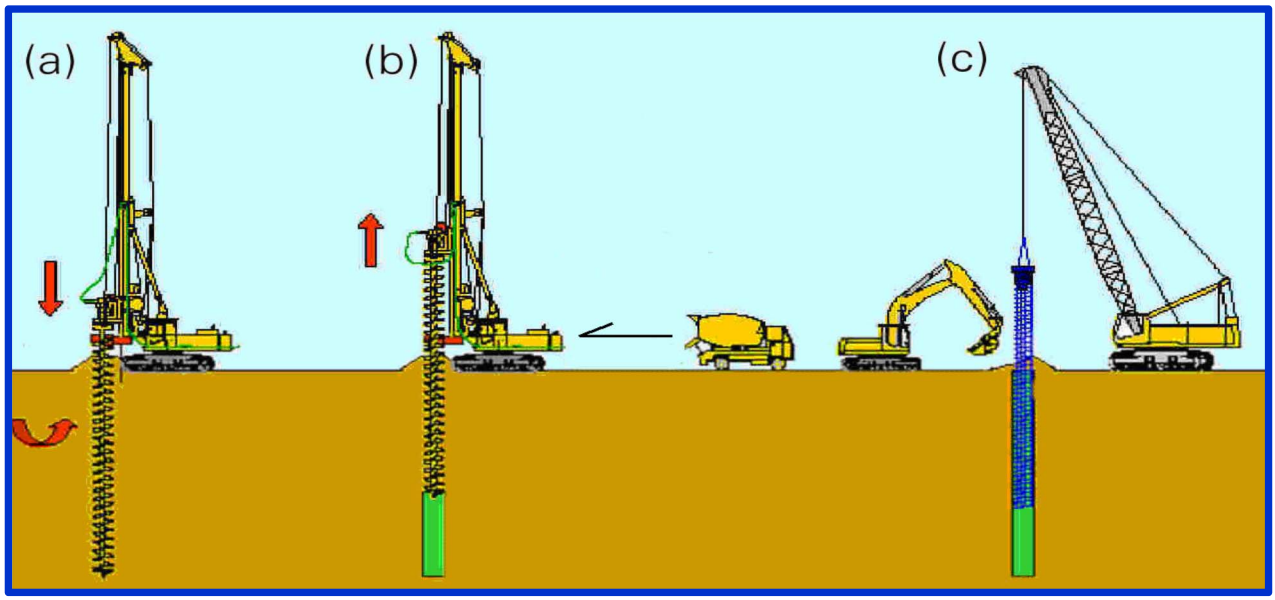


Fig. 2 Construction Sequence of CFA Piles (Ref. Geotechnical Engineering Circular No.8 2007)

SPUN CONCRETE PILES:

Spun concrete piles are tubular precast pre stressed piles manufactured usually up to 600mm in diameter by centrifugal compaction process. Centrifugal spinning process along with the use of the high strength concrete (M50 grade or more) gives much higher density of concrete which is more durable with high corrosion resistance. Pretension wires (7mm diameter) are generally used as reinforcement. Steel plates are provided at both ends which are used for pre tensioning and splicing. The casting length of spun pile is typically 12m and it is steam cured. Continuous welding is done along the end plates to achieve longer lengths of piles. Spun concrete piles are driven into grounds by hydraulic hammers. Spun piles are less permeable than reinforced concrete piles. Thus, it has a good performance in a marine environment as well (Foundation Design and Construction Manual 2006).

Advantages:

- Spun piles give consistent and superior quality compared to cast in situ piles. Spinning process makes hollow tubes and reduces the weight of concrete at least 45-55% compared to normal vibrated concrete.
- Much higher density of concrete is achieved by centrifugal spinning process at 1500-1600RPM which is more durable and highly corrosion resistant.

Disadvantages:

- While driving, there is a possibility to get spalling, cracking and breaking of piles (Foundation Design and Construction Manual 2006).
- Transportation cost will be more if manufacturing unit is far away from the construction site.
- Wastages are more in variable ground conditions.
- It is difficult to drive the piles in bouldary strata.

Case History- Installation of Precast Driving of Precast Spun Piles works at BOP for Ethane Receipt and Storage Terminal at Dahej

The subsurface conditions at site indicated presence of loose silty sand up to 6 to 11m followed by stiff to very stiff clay up to 12m to 13m depth. Dense to very dense sand was encountered at 25 m to 30m below ground level. Ground water table was observed from 2m to 3m depth below ground level. The SPT values ranged between 8 and 34 along the pile shaft. Total 1684 numbers of segmented spun piles were installed in this project (figures 3 to 6). The lengths of spun piles were originally planned to be 24m. They were installed in two segments of 12m each. The piles were installed using a 9 T, Hydraulic Hammer with drop height ranging from 300mm to 1000mm. On an average, installation time for each pile was about three hours. With 5 numbers of rigs at site, about 20 to 30 numbers of piles could be driven per day. Subsequent to initial piles, total pile length was restricted to 22m. These later piles were driven in two segments of 12m and 10m, respectively.

Initial vertical load tests were conducted on two number of test piles. Maximum test load of 252.0T was applied considering safe load of 100.0T. These tests would have confirmed a higher load carrying capacity for Spun pile, but the applied load was restricted due to the limited reaction frame arrangement for the test.



Fig.3 Spun Pile Driving with Hydraulic Hammer



Fig.4 Pre-stressed Spun Piles

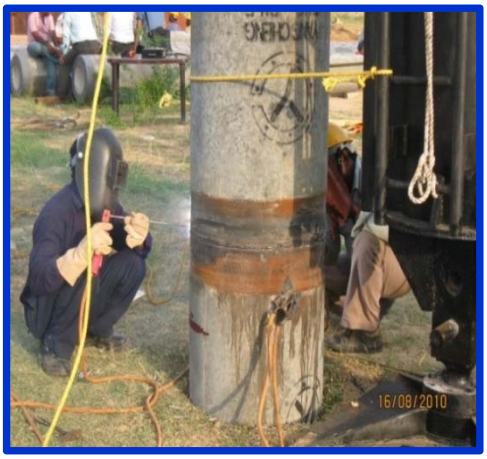


Fig.5 Welding of Joints in Progress



Fig. 6 Driven Spun Concrete Piles with connecting Rebars

SECANT PILE

Secant piles are defined as a series of primary (Unreinforced) and secondary (Reinforced) piles that are installed in a configuration such that they intersect one another. This method consists of boring and concreting of primary piles at center's slightly smaller than twice the nominal pile diameter followed by boring and concreting of secondary piles. Secondary piles are bored through primary piles before the concrete in primary pile have achieved its full strength (Deep Excavation: a practical manual 2003).

For deep excavations, where subsoil consists of permeable, granular soils with high ground water table conditions, Secant piles can be utilized as an economical and effective soil and water retaining structure. In such cases, secant piles can be used as a solution for side protection of deep excavations.

For secant pile construction, the sequencing of pile installation, cycle time of one pile, setting time and initial strength characteristics of the concrete are some critical parameters.

Types of secant pile
Hard – soft secant piling:
When greater wall flexibility is desired and for providing effective water seal at the pile overlap joints, , the primaries may be built using weaker grades of concrete of around 1 to 3 Mpa at 28 days and the secondary piles are then constructed with normal reinforced concrete. Alternate soft piles without any reinforcement are first constructed which is then followed by construction of intermediate secondary piles which actually cut into the pre-installed adjacent primary piles. The process is repeated to result in the formation of a continuous wall of alternating hard and soft piles. This method is commonly known as the "hard - soft" secant piling.

Low early strengths of primary piles requires better controls in concrete preparation and this is usually achieved by using concrete mixes with cement and bentonite.

Hard – Firm Secant Piling:
The sequencing, spacing and reinforcement of piles is similar to the Hard - Soft pile scheme however, the primary, Firm piles in this case are constructed using concrete with characteristic strength between 10 to 20 MPa at 56 days and retardation is used to allow easier cutting of the primary piles. This method is commonly known as the "hard - Firm" secant piling.

Hard – Hard Method:
Unlike the above two Secant pile schemes which basically cater for normal loading conditions, for cases where loads are very heavy, each pile of the system needs to be reinforced. , Large number of reinforcing bars in secondary pile alone will create congestion and might hinder the free flow of concrete. In such cases, primary piles can also be reinforced.

Construction aspects
Secant piles are constructed by boring alternate primary piles first followed by intermediate secondary piles. The general sequence of construction is as follows

- A guide wall as shown in Fig.7 is built along the wall alignment before commencing any activity. Guide wall helps in maintaining alignment, location and verticality of secant pile.
- A series of primary piles are installed first using hydraulically operated piling Rig.
- For construction of Primary pile, temporary casing with cutting teeth along the periphery is positioned and advanced into the ground, The inside of the casing is then augured out. The sequence continues till the required depth is reached..
- Once the pile bore has been drilled and properly cleaned out, concrete is then poured in to the pile bore using tremie method.
- Immediately after concreting, the temporary casing is extracted gradually with a rotational action.

- Secondary pile is then drilled in between two adjacent primaries so as to intersect these primary piles and to cut into their shafts.
- Before drilling secondary piles, the strength of the primary pile concrete should be high enough to prevent it from slumping or cracking, but it should be low enough to offer minimum resistance to the action of the cutting crown.
- While drilling secondary piles, special attention must be paid to maintaining verticality in order to ensure that the minimum designed amount of intersection is achieved throughout the length of the shaft particularly at greater depths.
- Casing for the secondary pile is generally installed using powerful hydraulic drilling rigs.
- After reaching final depth, pile tip is cleaned and reinforcement cage is placed in the pile bore.
- Concrete is then poured in to the pile bore and casing is gradually pulled out.

Advantages

The following are some of the advantages inherent in the use of the secant piles.

- Secant pile walls can be successfully installed in most ground conditions.
- Secant pile walls are ideal for urban construction projects, as they can be installed in relatively tighter spaces and are more flexible in shape than diaphragm walls.
- Secant piles can be designed as load-bearing structures and incorporated to form an integral part of the main structure.
- Secant piles require much lighter construction equipment than that for construction of a Diaphragm wall.

Disadvantages

Like all other techniques, secant piling method has its disadvantages in certain situations:

- Secant pile wall produces more joints than the diaphragm wall method. In water-bearing ground therefore more cares needs to be taken to ensure good quality hence it's quality and performance is extremely construction sensitive..
- Generally, the circular section of bored pile requires heavier reinforcement to produce a moment of resistance equivalent to that of the constant section of the diaphragm wall.

CASE HISTORY - SECANT PILE WALL CONSTRUCTION AT MUMBAI METRO LINE -3

Secant piles have been successfully installed in Mumbai Metro Line 3 project. The secant piled walls were constructed for station buildings at Sidhivinayak, Dadar, Shitladevi and launching shaft at St. Xaviers, Mahim. Vertical shaft at St. Xaviers formed launching area for tunnel boring machine which facilitates construction of rail tunnels. Table 1 reports the details of secant pile wall constructed at St. Xaviers launching shaft. . The subsurface conditions at site indicated presence of residual soil up to 9 to 10 m followed by highly weathered Breccia up to 13m to 15m depth. Moderately to slightly weathered breccia/ basalt was encountered at 13m to 15m below ground level. The ground water was observed at about 2m below ground level. All the piles were installed using hydraulically operated rotary rigs of 18 to 22 Tm Torque capacities. Double walled temporary casings were used to stabilize the sides of pile bore. The centre to centre distance between alternate piles was maintained as 1410 mm. The grade of concrete used for primary and secondary pile was M10 and M40, respectively. Capping beam was provided above these piles to take care of differential changes in earth pressures in adjacent piles.

It may be noted that the pile depths were restricted to about 16 metres only due to presence of very hard rock beyond this depth. A horizontal ledge was provided at around 14 metre depth and further excavation was taken up providing vertical cut in the competent rock. At some locations, shotcreting was used to control ground water seepage through joints in the rock formation. Ring beams were provided at two levels. Fig.8 shows final view of secant piles along launching shaft at St. Xaviers Launching Shaft Location.

Table1: Details of Secant Piles at St. Xavier Launching Shaft

Sr. No.	Construction Details	Primary Piles	Secondary Piles
1	Excavation depth below Ground level	23.4 m	
2	Pile Diameter	880 / 800 mm	880 / 800 mm
3	Grade of Concrete	M10	M40
4	Spacing between alternate piles	1460 mm	1460 mm
5	Total Length of Pile	15.5 to 16.5 m	15.5 to 16.5 m
6	Total Length of Pile in Rock	6 to 7 m	6 to 7 m
7	Type of Rock	Grade III and IV Breccia/Basalt	Grade III and IV Breccia/Basalt



Fig. 7 Guide Wall and Installation of Casing



Fig. 8 Secant Pile Wall at St. Xavier's Launching Shaft

CONCLUDING REMARKS

While basic methodologies of deep foundations shall continue to be used with necessary improvements, new technologies needs to be adopted for achieving progress at a faster rate

Technologies like Continuous flight auger piles are cost effective options for bigger projects. Barrette piles and spun piles have been rarely adopted in the past and yet to find acceptance in India. Load tests performed on spun piles proved that they can be used safely. Nonetheless, Secant piles have also been successfully carried out in many projects in India.

Finally, utilisation of such modernised technologies of deep foundations in construction projects will lead to tremendous savings in time and cost of projects.

AKNOWLEDGEMENT

The authors express their gratitude to management and staff of ITD Cementation India Limited, Mumbai, for encouragement and support in research and innovative endeavors. Thanks are also extended to DFI, India for providing august platform for sharing their experiences.

REFERENCES

Deep Excavation: a practical manual, 2003. Second Edition, Thomas Telford Publishers, London, E14 4JD, 571 p.

Foundation Design and Construction, 2006. Geo publication No.1, The Government of Hong Kong Special administrative Region.

Geotechnical Engineering Circular (Gec) No. 8, 2007. Design and Construction of Continuous Flight Auger Piles. Federal Highway Administration, Washington D.C., 293 P.

Ramaswamy, S. D., and Pertusier, E. M., 1986. Construction of Barrettes for High-Rise Foundations. American Society of Civil Engineers, Journal of Construction Engineering Manage., 112(4):455-462.

PERFORMANCE OF LARGE-DIAMETER BORED PILE WITH SHORT SOCKETED LENGTH IN IGNEOUS ROCK IN THAILAND

Zaw Zaw Aye, Seafco PCL, Bangkok, Thailand, +66859091029; zaw@seafco.co.th
Thayanan Boonyarak, PhD, Seafco PCL, Bangkok, Thailand, +66805818799; thayanan@seafco.co.th
Sereyroath Chea, Seafco PCL, Bangkok, Thailand, +66935503967; sereyroath_eng@seafco.co.th
Nutthapon Thasnanipan, Seafco PCL, Bangkok, Thailand, +66846660555; nutthapon@seafco.co.th

ABSTRACT

Large-diameter bored piles have been utilized extensively in soft soil for more than four decades in Thailand, whereas there are only limited numbers of rock-socketed bored pile constructed. To date, load transfer and settlement behavior of piling in rock in Thailand is still not fully understood, especially when the socketed-length is less than one time the pile diameter. The objectives of this paper are to analyze load distribution and to investigate load-settlement relationship of bored pile in rock. Collected data in this study was from pile load test results of more than 90 large-diameter bored piles, socketed in igneous rock such as granite and andesite. Bored piles were constructed using rotary drilling method, having socketed length varying from 0.3 to more than 3 times the pile diameter. Factors that influenced pile settlement behavior, consisting of socketed length and construction method were analyzed. The effects of socketed length on load-settlement relationship and ultimate load bearing capacity were investigated. Load-settlement behavior, unit shaft resistance and unit end bearing is presented and discussed. Also, guidelines of estimation of pile settlement in rock is proposed. According to measured and calculated data, settlement of pile was mainly due to elastic shortening. This is because shaft friction in granite was the major component for pile resistance. For piles with socketed length per diameter ratio (S/D) of greater equal one, the mobilized shaft friction and end bearing are significantly larger than those with S/D of less than one. This is because socketed length is sufficient in rock to provide fully mobilized end bearing, resulting in relatively large stiffness at pile base.

KEYWORDS:

Load transfer mechanism, Socketed length, Design parameters, Igneous rock

INTRODUCTION

In Thailand, major deep foundation projects are located in Bangkok area where soft ground such as soft marine clay and alluvial soils are encountered (Boonyarak et al., 2016). Due to demand in urbanization of the country, deep foundation in rock gradually increase as the construction projects extent to other cities where rock depth is relatively shallow. Minimum socketed length in rock adopted from some codes of practice, for example Building Department of Hong Kong SAR, specifies 0.5 m in fresh or slightly weathered igneous rock (BD, 2009). However, due to lack of experience and suitable rock drilling tools, the ability to excavate in rock of many piling contractors in Thailand is about 0.3 m only in moderately weathered granite. Thus, behavior of bored pile in igneous rock, especially when socketed-length per diameter ratio (S/D) is less than one, is not fully understood. Thus, further research is still required to minimize variation and to obtain guideline in design of piling in igneous rock in Thailand.

This paper presents interpretation of load testing results of more than 90 piles, socketed in granite and andesite. Analysis results of load-settlement, pile settlement estimation, factor for calculating shaft friction and end bearing are reported. A case study of pile behavior where the S/D is less than one with possibilities of large and differential settlement is described. Discussion and explanation of pile behavior in igneous rock are provided.

© 2018 Deep Foundations Institute

BORED PILE CONSTRUCTION IN ROCK

Geology

Figure 1 shows Geological map of Thailand (Department of Mineral Resources, 1999). Major urban development has taken place in Greater Bangkok area, where soil conditions consist of soft marine deposit at the top 10-20 m follow by alternating layers of sand and clay. Igneous rocks are mainly located in the North, East and South. The most common rock encountered during bored pile construction in these regions is granite. Typical unconfined compressive strength of granite from several projects the authors have collected is ranging from 40-150 MPa.

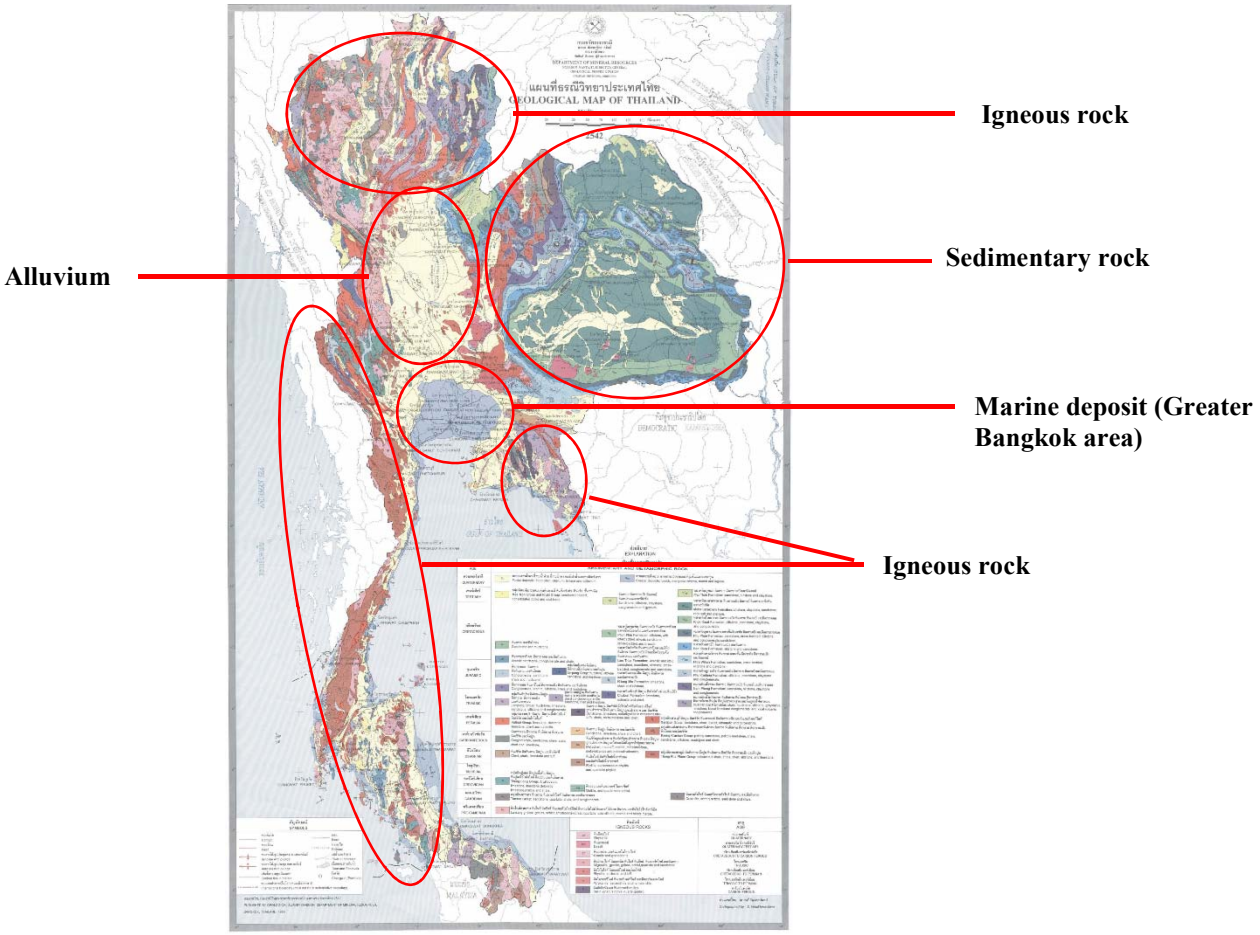


Fig. 1 Geological map of Thailand (Department of Mineral Resources, 1999)

Bored pile construction sequences and quality control

Typical construction sequences of bored pile in rock are shown in Figure 2. The sequences are as follows: (a) First, pre-boring of hard soil at the surface is carried out. (b) Temporary steel casing is driven using vibro hammer to protect borehole collapse in soft soil layers (i.e., loose sand and soft clay). (c) Excavation is carried out using flight auger inside the casing or in hard clay layer. (d) Prior to encounter unstable soil layer beneath the depth of the casing, bentonite slurry is poured into the borehole for stabilization. Drilling bucket is used for excavation under the slurry until reaching rock layer. Slurry circulation using pump and

desander is used for cleaning of slurry in the borehole. (e) Reinforcement cages are lowered into the borehole one after another. Afterwards, concrete is placed through a tremie pipe to replace the drilling fluid until reach the pile cut-off level. (f) Finally, the temporary casing is extracted before the concrete sets.

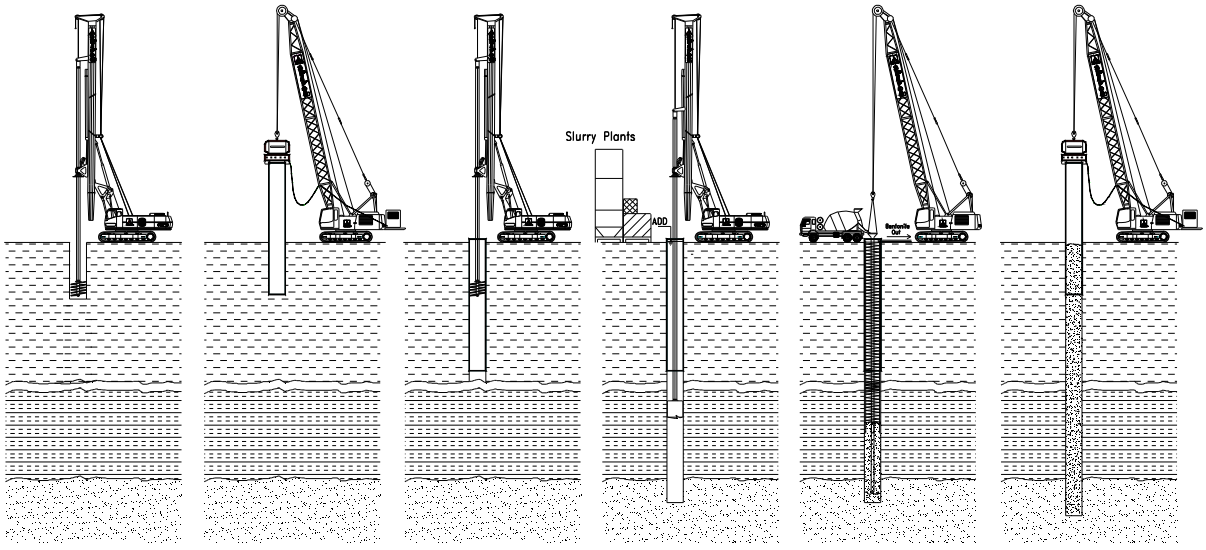


Fig. 2 Typical construction sequences for bored pile

Drilling in rock

To drill in completely and highly decomposed granite, bullet teeth installed on an auger is adopted (as shown in Fig. 3a). The samples taken using rock auger is shown in Figure 4a. However, in slightly weathered to fresh rock, auger with bullet teeth cannot be efficiently drilled into these layers. Maximum socketed length in hard layer using rock auger is from 0.3 to 0.5 m for moderately weathered granite. To penetrate further into slightly weathered granite, core barrel with bullet teeth is used as shown in Fig. 3b. In order to penetrate into the slightly weathered or fresh granite to depth more than 1 m, roller bit installed on core barrel as shown in Fig. 3c is adopted. By using roller bit installed core barrel, rock sample can be collected as a piece as shown in Fig. 4b.



Fig. 3 Tools for excavation in rock (a) rock auger with bullet teeth; (b) core barrel with bullet teeth; (c) core barrel with roller bits



(a) (b)

Fig. 4 Rock material excavated by (a) rock auger with bullet teeth; (b) core barrel with roller bits

Quality control in construction

Deviation and inclination of the borehole are controlled to be within 75 mm at ground level and 1:100, respectively. The methods for controlling deviation and inclination of borehole are conventional survey technique, visual inspection of verticality of kelly bar and drilling monitor apparatus (if specified in the project). To ensure the quality of the drilling fluid, routine testing is carried out prior to excavation and concreting (FHWA, 2010). Prior to reinforcement cage lowering, rock samples at the pile base are identified and sediment measurement using sounding method by measuring tape is carried out. Concrete slump and setting time for wet-process bored pile are 150-200 mm and 4-6 hours, respectively. For Tremie concrete, apart from flow ability, stability to prevent bleeding and channeling is also required (EFFC/DFI, 2018).

LOAD TESTING AND DATA ANALYSIS

To validate load bearing capacity of the constructed pile, pile load test is carried out. For most of infrastructure projects, static pile load test is performed. Apart from static load test, high strain dynamic load test is carried out to verify the integrity and capacity of piles to save cost and time of testing.

Static pile load test

Axial compression static load tests according to ASTM D1143 standard are carried out on working piles of the project. If friction is adequate, four anchor piles for each test pile are used as a reaction system. In a case that friction is not adequate for anchor piles, dead load on kentledge is adopted as the reaction system. Maintained loading procedures up to 2.0 or 2.5 times the design working load are adopted. Table 1 summarizes details of test piles using static load test method to determine load-settlement curve and verify the capacity of each pile in this paper.

Dynamic pile load test

Apart from pile testing with static load method, which is time consuming and required costly preparation, high strain dynamic load test (ASTM 4945) can be adopted as supplementary tests. In many projects, static load tests are carried out on 2-3 pilot piles and dynamic load tests are carried out on working pile to randomly investigate the integrity and load bearing capacity of piles in each project. In this paper, results from 80 test piles using high strain dynamic load test were analyzed (details are not shown in table for brevity of paper).

Table 1. Details of test piles using static load test method

Province, Region	Pile ID	Pile diameter (m)	Socket length (m)	S/D*	Pile tip (m)	Max. test load (kN)	Rock type
Chonburi, East	SLT1	1.5	2.8	1.9	20.3	20,250	Granite
Chonburi, East	SLT2	0.8	3.0	3.8	18.0	4,400	Granite
Chonburi, East	SLT3	0.8	2.0	2.5	15.5	4,400	Granite
Chonburi, East	SLT4	0.8	1.0	1.3	14.0	4,400	Granite
Chonburi, East	P46	1.0	3.0	3.0	24.0	13,750	Andesite
Rayong, East	T1	0.8	1.7	2.1	13.7	4,400	Granite
Rayong, East	T2	1.5	3.0	2.0	15.7	18,000	Granite
Rayong, East	T3	1.8	3.0	1.7	14.4	26,000	Granite
Saraburi, Northeast	T120	1.2	18.0	15.0	26.0	16,500	Andesite
Saraburi, Northeast	T150	1.5	18.0	12.0	26.0	18,000	Andesite
Saraburi, Northeast	T180	1.8	18.0	10.0	26.0	26,000	Andesite
Songkla, South	TP	1.5	0.5	0.3	17.4	20,000	Granite
Phuket, South	BP43	0.6	0.3	0.5	19.7	2,700	Granite
Phuket, South	DP29	0.6	0.3	0.5	8.6	2,700	Granite
Phuket, South	KP18	0.6	0.3	0.5	11.4	2,700	Granite
Phuket, South	IP14	0.6	0.3	0.5	9.6	2,700	Granite

Note: * S/D is socketed length per diameter ratio

INTERPRETATION OF RESULTS

Load-settlement relationship

Figure 5 shows normalized load-settlement relationships of bored pile socketed in rock. To compare results from piles with different depths, diameters and applied loads, the applied load and settlement are normalized with section area and pile diameter, respectively. Load-settlement data was divided into two groups, socketed-length per diameter (S/D) ratio of less than one and greater equal one. In most tests, there are two cycles of loading, first cycle testing is up to the safe working load (SWL) following by unloading and second cycle loading to two times the SWL and rebound. In some tests, maximum test load can be up to 2.5 or 3 times the SWL.

For the piles with S/D greater equal one, normalized pile settlement at SWL is less than 0.5%, which is significantly less than fully mobilized friction condition proposed by Boonyarak et al. (2016). At two or more times the SWL, normalized pile settlement of the group of S/D greater equal one is relatively smaller than 2%, suggesting that friction is not fully mobilized and so is the end bearing. This is because of sufficient socketing in rock that provided high stiffness at the pile base and contributed to large capacity for bored pile.

On the contrary, for piles with S/D less than one, large variation of normalized settlements at SWL from 0.3% to 1.9% were observed. It suggests that, differential settlement may occur if these piles are supporting the same structure. At two times the SWL, the variation in settlement became larger, the maximum settlement was close to 5% which is the ultimate capacity suggested by Boonyarak et al. (2016). For short-socketed pile, when load transfer to toe, large pile settlement occurs. This can be also affected by the workmanship problem of inappropriate pile base cleaning. The piles with large settlement are in only one project in Phuket (summarized in Table 1). These piles required modification of foundation design and rectification measure to minimize differential settlement in each building. This measure is discussed in the Section "Rectification measure to minimize differential settlement".

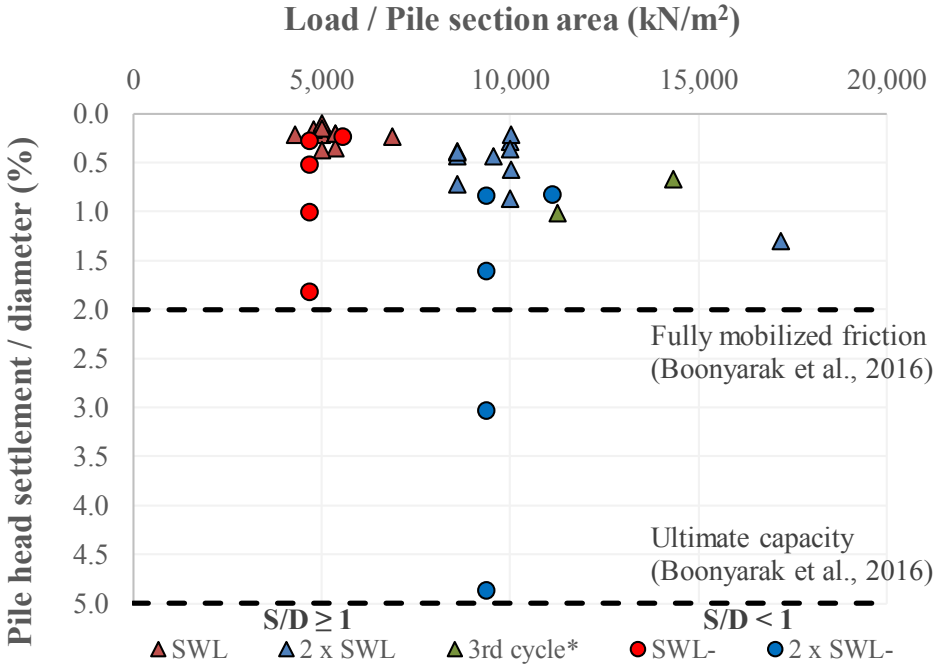


Fig. 5 Load-settlement curves of test piles

Estimation of pile settlement

Figure 6 shows comparison between measured and computed pile settlement at the maximum load of each test for pile with S/D greater equal one. Pile settlement can be estimated using Equation 1 proposed by Tomlinson (1995) as shown below.

$$\delta = \frac{(W_s+2W_b)L}{2A_sE_p} + \frac{\pi W_b B(1-\nu^2)I_p}{4A_bE_s} \quad [1]$$

The first and second terms in this equation refer to elastic shortening of the pile and settlement of soil at pile base, respectively. Symbols in Equation 1; δ, W_s, W_b, L, B, A_s, A_b, ν, I_p and E_s denote settlement at pile head, load carry by shaft, load carry by base, pile length, pile width (diameter), shaft area, base area, Poisson's ratio, friction distribution factor and Young's Modulus of soil at pile base, respectively. The modulus of elasticity of rock adopted is 50 times unconfined compressive strength (UCS). The modulus of elasticity of reinforced concrete of each pile (E_p) is assumed to be 34 GPa.

From the comparison, calculated settlement reasonably agrees with the measured results. However, for some piles embedded in granite, substantial difference between measured and calculated results is observed at measured settlement of 10-12 mm. A possible reason for this discrepancy is variation in degree of

weathering that was not considered in the estimation causing inaccuracy of estimation of elastic modulus of rock at pile base.

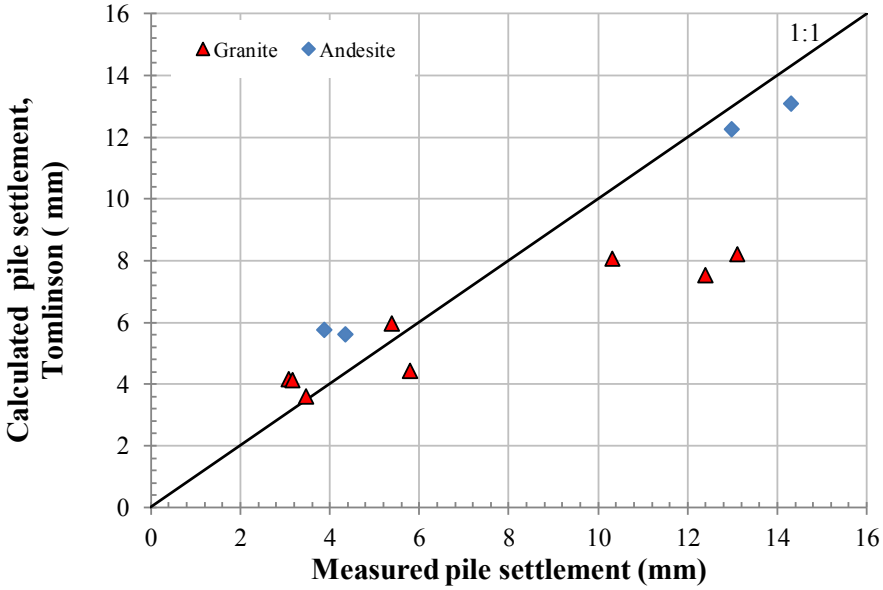


Fig. 6 Comparison between measured and calculated pile head settlement

BACK ANALYSIS OF PILE RESISTANCE

Results from high strain dynamic load test are able to estimate total shaft friction and end bearing of each pile. This estimation was obtained from input and output signal matching. Note that the maximum load activated on each test pile may not be the maximum load bearing capacity as the test load was designed to be slightly larger than the specified test load. Thus, the maximum resistance of pile is expected to be larger than those shown in this paper.

Mobilized shaft friction

Figure 7a shows mobilized average shaft friction of pile with different S/Ds. The estimation of shaft friction reported in this paper is obtained for the entire pile length in soil and rock. For the piles with S/D less than one, average mobilized shaft friction was ranging from 20 to 60 kN/m^2. This is because of the end bearing in rock cannot be fully developed and pile settlement was relatively large (refer to Fig. 5). The large pile settlement caused smaller pile stiffness as stiffness of soil reduced with increasing shear strain.

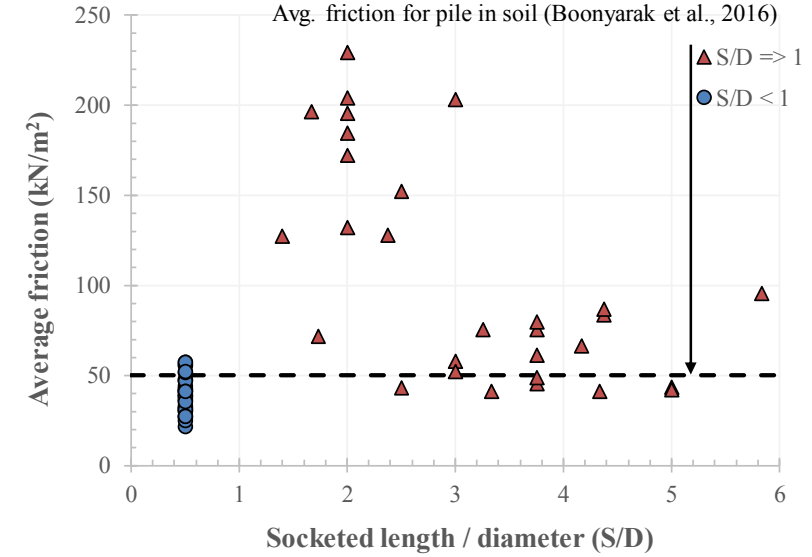
For mobilized friction for piles with S/D ranging from 1 to 3, average friction was the largest (120 – 230 kN/m^2). This is because the pile is socketed in slightly weathered granite and the pile base stiffness was the largest. It results in largest friction developed along the pile shaft. The pile with S/D more than 3 has the mobilized friction between 40 – 100 kN/m^2. These range of friction was larger than those in soil reported by Boonyarak et al. (2016). It should be noted that, the average shaft friction does not increase proportionally with S/D. This maybe because for weaker rock or higher degree of weathering, the socketed length is required to be larger in order to support the design load.

Mobilized unit end bearing in rock

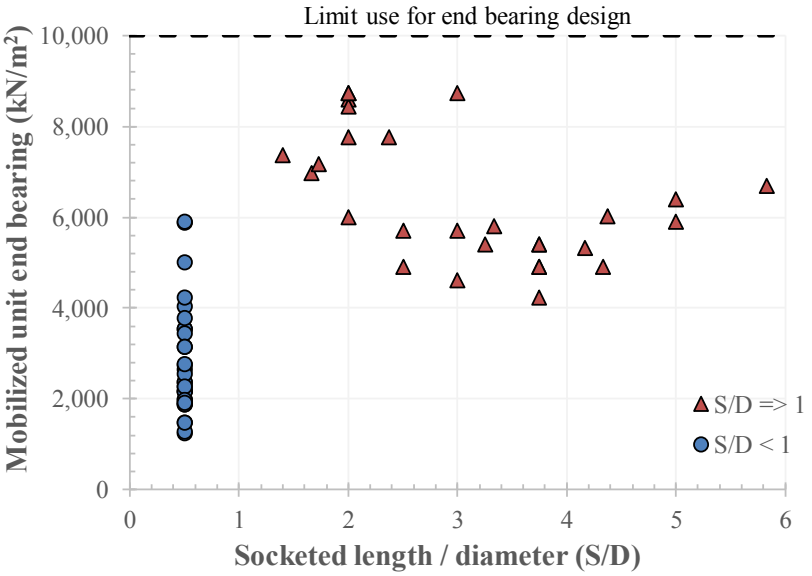
In Fig. 7b, mobilized unit end bearing with different S/Ds is illustrated. Large variation and low end bearing was observed for pile with S/D of 0.5. This observation may be caused by poor rock material at pile base or

poor base cleaning of pile. In addition, the socketed length was not sufficient to develop firm base behavior in rock resulting in large pile settlement (refer to Fig. 5). The mobilized unit end bearing for pile with S/D of 0.5 is ranging from 1,500 to 6,000 kN/m^2. This end bearing is only slightly larger than those pile constructed in soil where unit end bearing can be developed from 2,000 to 3,000 kN/m^2.

For piles with S/D more than one, the unit end bearings were between 4,500 and 9,000 kN/m^2. There is no clear trend between S/D and unit end bearing. It suggests that minimum S/D of one may be adequate to develop sufficient end bearing. Note that the mobilized unit end bearing does not reach 10,000 kN/m^2 which is the limit of commonly design value. This is because load activated by high strain dynamic load test was not large enough to fully mobilize the end bearing in rock.



(a)



(b)

Fig. 7 Pile resistance provided by (a) friction; (b) end bearing

RECTIFYING MEASURE FOR MINIMIZING DIFFERENTIAL SETTLEMENT

As stated earlier that pile settlement in one project with S/D of 0.5 has large variation in pile settlement (refer to Fig. 5), rectifying measures for reducing differential settlement was carried out. There are total 10 five-story buildings in this project and each building is supported by about 50 to 60 piles. The pile diameter is 600 mm and it was specified that only 300 mm is socketed in slightly weathered granite. However, according to test results, settlement in some piles were larger than 30 mm (5% of pile diameter) at two times the safe working load. To minimize the possibilities of differential displacement, spring stiffness of each pile group was evaluated based on load testing results. Unlike other project that spring stiffness for each pile diameter is a constant, the spring stiffness of pile group in this project vary area by area even the pile diameter is the same.

Pile re-striking with drop hammer to reduce settlement

After determination of pile spring stiffness was completed, piles with significantly low spring stiffness were selected. The head of these piles were prepared to be flat and smooth. Figure 8 shows the eight ton drop hammer for re-striking of bored pile with relatively low spring stiffness. Drop height, pile driving formula and factor of safety adopted were 0.6 m, Danish formula and 3, respectively. Settlements per blow in each pile were recorded and checked against the driving criteria given to achieved the working load of 1,350 kN per pile.

Monitoring of building settlement during construction

During construction of each building, four settlement markers were installed on the column of all four corners of the building. The record of building settlement was taken every month. According to the record, the maximum building settlement is ranging from 2 to 4 mm and differential settlement was within 1:1000, which is within the acceptance criteria.



Fig. 8 Drop hammer for re-striking of bored pile

SUMMARY AND CONCLUSIONS

Interpreted results from static and dynamic pile load tests are reported in this paper. Bored piles were constructed using rotary drilling and socketed into granite and andesite in Thailand. Load-settlement behavior and pile resistance were analyzed and discussed. A case study where socketed length per pile diameter ratio (S/D) of less than one was described and explained. According to the interpretation of data, following conclusions may be drawn:

- Settlement of pile with S/D greater equal one is less than 0.5% the pile diameter (D) at safe working load and less than 2%D at test load up to three times the safe working load. It suggests that, main component of pile settlement is contributed by shaft shortening.
- Calculation of pile settlement using analytical equation such as Tomlinson's provide a reasonable estimation. Young's modulus of rock at pile base is estimated to be 50 times the unconfined compressive strength of the rock sample.
- For piles with S/D of about 0.5, mobilized skin friction and end bearing behavior was only slightly larger than the pile constructed in soil. This is because pile base stiffness was not sufficient, resulting in relatively low pile resistance. For pile with S/D greater equal one, mobilized skin friction and end bearing are relatively high as the pile base is firm. There is still no clear sign of increasing in end bearing with increasing S/D. This is because S/D of greater equal one is sufficient to fully mobilize the end bearing in rock.
- To minimize the possibilities of differential settlement, some measures can be effectively adopted. These measures consist of determine spring stiffness of pile in each zone or re-striking of pile (if required) to minimize settlement at pile base.

ACKNOWLEDGEMENTS

The Authors would like to thank executives and staffs of Seafco Public Company Limited, Thailand for providing data for the analysis of this paper.

REFERENCES

ASTM D 1143. 1994. Standard test method for piles under static axial compressive load, West Conshohoken, P.A., USA

ASTM D 4945. 2012. - Standard Test Method for High-Strain Dynamic Testing of Piles, West Conshohoken, P.A., USA

Boonyarak, T., Aye, Z. Z., Thasnanipan, N., Supawo, S. and Chea, S. 2016. Settlement prediction of large-diameter bored pile in Bangkok soils. Proceeding of the Sixth International Conference on Geotechnique, Construction Materials and Environment (GEOMATE 2016), 14-16 November 2016, Bangkok, Thailand.

Building Department. 2009. Practice Note for Authorized Persons APP-24. Technical notes for guidance in assessing the effects of civil engineering construction / building development on railway structures and operations. Building department of the government of HKSAR.

Department of Mineral Resources. 1999. Geological map of Thailand Scale 1:2,500,000. Ministry of Natural Resources and the Environment. Online http://www.mapofthailand.org/geography-map/geological-map-of-thailand/

EFFC/DFI. 2018. Guide to tremie concrete for deep foundations, the joint EFFC/DFI Concrete Task Group. Online http://www.effc.org/content/uploads/2018/05/EFFC_DFI_Tremie_Concrete_Guide_2nd-Edition_2018_ Final.pdf

FHWA (U.S. Department of Transportation Federal Highway Administration). 2010. Drilled Shafts: Construction Procedures and LRFD Design Methods. National Highway Institute

Tomlinson M.J.,1995. Pile foundation, The carrying capacity of piles and pile groups, Foundation design & Construction 6th edition, pp. 265-316.

RECOGNIZED CORROSION PROTECTION METHODS FOR PERMANENT GROUND ANCHORS

Chris Irvin, Dywidag-Systems International Ltd., Warwickshire, UK
Devon Mothersille, Geoserve Global Ltd., London, UK
Rajiv Pandey, DSI Bridgecon, Delhi, India

Abstract

Ground anchors are widely used in civil engineering for retaining wall tieback and uplift restraint in deep basements as well as a range of other applications where traditional construction methods are either unsuitable or uneconomic. The ability to provide active restraint using a stressed tendon offers significant benefits in reducing the size and weight of the structure.

Recent projects in India include the Sivok-Rangpo Tunnel and the Middle Bhotekoshi Hydro-Electric Project in Nepal, utilized permanent anchors with double corrosion protection to fulfill the required lifespans of the structures.

For permanent ground anchors with lifespans up to 120 years, durability in the form of corrosion protection is critical, as failure through insufficient corrosion protection is unacceptable. Applying the correct corrosion protection is one of the most misunderstood principles in ground anchoring practice. This paper seeks to highlight the pitfalls of incorrect corrosion protection methods, as well as outlining and updating recognized corrosion protection principles in accordance with internationally recognized ground anchor standards.

Introduction

The most common methods considered for corrosion protection are: Double Corrosion Protection, Single Corrosion Protection (with in-situ testing), Epoxy Coating, Galvanizing, Sacrificial Corrosion Allowance and Borehole Grout. A number of these are not suitable for permanent anchors and one has practical limitations during site handling.

Further confusion as to which method to apply, has arisen due to the following misconceptions:

a) The claim that hand applied epoxy paint is a corrosion protection method for protecting anchor tendons.
b) The belief that a lower level of corrosion protection applicable to different installations (i.e. mini piles or soil nails) may be suitable for ground anchors.
c) Incorrect reclassification of the anchor as a tension pile, in order that a lower level of protection may be applied.

© 2018 Deep Foundations Institute

d) The desire to utilise a self-drilling hollow bar where ground conditions are variable or where cased installation is problematical.

The importance of corrosion protection for permanent anchors is illustrated below in figures 1 and 2, where the durability of the anchor is relied upon as a dependable element of the permanent works.



Figure 1 Aviva Stadium Dublin



Figure 2 Bhotekoshi Hydroelectric, Nepal

Classification of Installation Type (Ground Anchor, Mini Pile, Soil Nail)

In order that the appropriate level of corrosion protection may be selected, the installation should be classified according to load, mode of loading (active or passive, tension or compression), consequences of failure and required design life. Table 1 summarises typical installations together with their requisite levels of protection.

Table 1

Installation / Component	**Load Classification** (indicative)	**Mode of Loading**	**Consequence of Failure due to Corrosion**	**Corrosion Protection, Technical Standard**
Ground Anchors (soil anchors, rock anchors)	Often heavily loaded 500-20,000 kN	*Active* (debonded, prestressed free length)	Risk of overload to adjacent anchors	Double corrosion protection to BS8081 or Single barrier protection, Tube-a- Manchette / sheathing combinations to EN1537
Mini Piles / Micro Piles (Tension)	Up to 3,500 kN (single bar reinforcement)	Passive (Fully Bonded)	Risk dependent on loading and application	Double corrosion protection (BS8081) or lower level of protection depending on risk or aggressivity levels (EN14199)

Mini Piles / Micro Piles, Compression	Up to 2,000 kN (single bar reinforcement)	Passive (Fully Bonded)	Settlement (Lower corrosion risk due to compression loading)	Sacrificial corrosion allowance, galvanizing, grout cover (EN14199)
Soil Nails	Lightly loaded 30-150 kN	Passive (Fully Bonded)	Low risk (built-in system redundancy)	Sacrificial corrosion allowance or galvanizing (CIRIA 637, EN14490)
Rock Bolts / Rock Dowels (*external*)	Lightly loaded 30-100 kN	Passive (Fully Bonded)	Low risk (built-in system redundancy)	Sacrificial corrosion allowance, galvanizing or stainless steel

Common Corrosion Protection Methods

The most commonly considered methods for corrosion protection, together with their constraints for use on permanent anchorages, are outlined below.

Double Corrosion Protection

Double corrosion protection (i.e. double barrier protection) is the provision of two impermeable barriers between the tendon and the external environment, such that the outer barrier ensures the integrity of the inner barrier should the potential for damage arise during handling or installation.

Protection measures that constitute acceptable barriers in accordance with BS8081:1989/2015 and EN1537:2013 are often misrepresented, leading to confusion. Borehole grout, galvanizing or sacrificial corrosion allowance are all not accepted by the above standards. Acceptable barriers must ensure:

a) durability over the lifespan of the anchorage (often up to 120 years),
b) integrity, i.e. an impermeable barrier over the full length of the tendon,
c) remain intact during handling, installation and stressing.

Double corrosion protection for bar anchors and strand anchors are summarised below.

Bar Anchors

Permanent bar anchors comprise a threadbar, of either high yield or prestressing steel, surrounded by an internal cement grout encapsulated within a corrugated plastic duct (see figure 3). The internal grout should be applied under factory conditions and is not to be confused with borehole grout, which does not constitute a fully protective barrier (see separate section, borehole grout).

The internal grout of bar anchors may be considered as an acceptable barrier to corrosion on the basis that crack widths generated under load at each threadform, can be limited to less than 0.1mm. Each crack width is uniform in thickness, due to the regularity of the thread pitch in conjunction with the linear extension of the bar. Crack width control is reliant upon the confinement from the corrugated plastic duct in order that the cracks propagate at each threadform as opposed to intermittently (see figure 4).

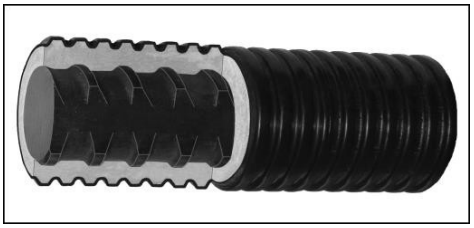


Figure 3. Section of permanent bar anchorage, showing duct encapsulation of pregrouted bar



Figure 4. Crack width control on pregrouted section

Strand Anchor
Corrosion protection for strand anchors is provided by two plastic sheaths as the internal grout is unable to act as a protective barrier. Crack width control of the grout on strand anchors is not possible due to:

a) the lack of ribs or threads on the strand,
b) the increased strain of the strand (strand is worked much harder than bar).

Triple Corrosion Protection
This is somewhat of a misnomer and usually arises from either, the aspiration to add a further protective layer on the assumption that it is a simple process, or the misinterpretation of borehole grout or galvanizing as a protective barrier. Neither is credible. Double corrosion protection remains one of the most practical methods of protecting permanent anchors and provides the highest level of protection in comparison to other systems.

Corrugated Plastic Ducting - Wall Thicknesses
The corrugated plastic duct is an integral part of corrosion protection systems for both bar and strand anchorages.

For double corrosion protection, current developments are incorporating increased wall thicknesses of 1.0-1.5mm for the corrugated ducts (previously 0.8mm taking account of manufacturing tolerances), on the basis that there are two barriers.

For single barrier protection, guidelines laid down by EN1537:2013 (Clause 6.5.1.4) have incorporated even greater wall thicknesses for the single corrugated duct (see table 2). Both systems now provide better abrasion resistance, should the potential for damage arise during handling or placement of the anchor.

Table 2

External Corrugated Duct (i.d.)	Wall Thickness
≤ 80 mm	1.0 mm
> 80 mm but ≤ 120 mm	1.25 mm
> 120 mm	1.5 mm

For high capacity strand anchors used in dam stabilization, even larger corrugated ducts of diameters up to 254mm with a 3mm wall, are now being used.

Epoxy Coatings

Epoxy Coated Strand
The epoxy coating of strand is acknowledged as a popular process in the USA, Japan and elsewhere for stay cable or structural concrete applications, but its application for ground anchors is not common and has potential limitations in the bonded section, where potential for long term creep needs careful evaluation, as the hardness of epoxy coatings is often overestimated.

Where epoxy coating is employed as a protection barrier, its application needs to be carefully controlled, under factory conditions. The recognized process for reliable application is fusion bonding followed by baking.

Site applications, utilizing hand applied epoxy paint by local labour, followed by hand sanding to achieve bonding between layers, is fraught with inconsistencies and unlikely to provide a barrier to corrosion, even where three layers are applied. Furthermore, hand painting does not incorporate the baking process, therefore the hardness / durability of the coating is compromised. *It is the area of least cover that defines the level of corrosion protection.*

Where epoxy coating is considered, the main areas where attention is required are:

a) Creep under load of the bonded strand within the grout. Creep values need quantifying.
b) Adhesion of the epoxy to the strand. Adhesion is heavily dependent on the strand preparation process (i.e. shot blasting or pickling in acid).
c) Abrasion damage during handling. Sand added to the epoxy coating to enhance its bond in the grout is extremely abrasive, requiring special care on multi-strand anchorages.
d) Coating thickness and uniformity. Both require careful checking.
e) Grip of the wedges. Long teeth are required to bite through the epoxy coating, in order that the steel can be gripped.

Epoxy Coated Bars
Epoxy coatings are occasionally applied to rock bolts or anchors in hard rock tunnelling applications, where slenderness of the borehole is a key cost requirement. The coating has the added benefit in that its application process or chemical composition is not detrimental to prestressing grade steel threadbars, which are sometimes used in areas of high loading in tunnels.

Damage during handling remains the limiting factor for epoxy coated threadbars. The baked coating is brittle, with the highpoint of each thread particularly susceptible to nicks or chipping during transportation and handling. Each bar requires wrapping individually in a disposable protective sleeve, which is removed prior to installation. On site repairs can be time consuming as multiple nicks or chips all require repairing (see figure 5).



Figure 5 Repairs to chipped epoxy coatings.



Figure 6 Damage to Duplex coated hollow bar, caused by hydraulic jaws used for rod release.

Duplex Coatings - Self-Drilled Hollow Bar

Duplex coating is a term used to describe two protective coatings, typically comprising a galvanized coating overlaid with a layer of epoxy or polyester. Its application has led to confusion as it does not offer double corrosion protection. It is rarely used on solid bars and has real limitations when used on self-drilled systems as the coating becomes compromised through:

a) Abrasion damage from rotary installation.
b) Perforation of the coating by hydraulic jaws or stilsons, used to grip the bar for release from the drill head (see figure 6). Soft jaws have been trialed, but have proved ineffective.

Limitations of Borehole Grout as a Protective Barrier

Borehole grout (i.e. grout injected during installation or subsequently) is often misquoted as a barrier for protection. Whilst it will provide a degree of protection, its cover and integrity cannot be verified in-situ, hence its use for permanent anchors is not recognised by either BS8081:2015 or EN1537:2013.

Where borehole grout is used with self-drilled hollow bar systems, installed using the simultaneous drill and grout technique, its effectiveness as a protective barrier is problematical due to:

a) Reduced grout cover at coupler locations or at points along the full length of the drilled bar, which often takes the form of a lazy spiral. Spacers are disruptive, restricting grout circulation / flush and causing disturbance to the borehole wall.
b) Crack width control of the grout body, irrespective of threadform, is inconsistent at coupler locations or in areas of poor confinement.
c) Grout placement is workmanship sensitive. Simultaneous drill and grout can produce grout bulbing through the assistance of reaming, but it is irregular over the full length of the tendon. Exhumed tendons have shown wide variations in grout cover.
d) Contamination of the grout from the drill spoil or ground water.

BS8081:2015 Clause 13.2.3 summarises the limitations of borehole grout as "*grout injected in situ to bond the tendon to the ground does not constitute a part of a protective system because the grout quality and integrity cannot be assured*".

In recent years, self-drilled systems have become popular for soil nailing, as the concept of a self-drilled system in loose overburden has attractive cost benefits over conventional drilled and cased systems. However, their use as permanent anchors is universally not accepted.

Sacrificial Corrosion Allowance

This method has evolved from sheet piling and buried corrugated steel structures. It is now also regularly applied to soil nails and rock bolts (both passive installations), as these are generally classified as low risk installations, on the basis of an element of redundancy. This is not routinely the case for ground anchors.

In addition, the application of sacrificial corrosion allowance to anchor tendons is not acceptable as corrosion rates are rarely uniform and not predictable, tending to extend more rapidly at localized pits or surface irregularities.

Both BS8081:1989/2015 and EN1537:2013 preclude the use of sacrificial corrosion allowance for the permanent protection of anchors, with EN1537:2013 (Clause 6.3.1.1) stating "*There is no certain way of identifying corrosive circumstances with sufficient precision to predict corrosion rates of steel in the ground. All steel components which are stressed shall be protected against corrosion for their design life"*.

Galvanizing

Galvanizing is universally recognized as a method of protecting exposed steel surfaces. Its use on low risk installations such as rock bolts (figure 7) or soil nails (figure 8) is popular as it provides a robust coating, but its use as a protective coating for anchor tendons is not accepted.

The use of galvanizing as a means of increasing lifespans for buried installations, should be considered on the following basis:

a) Lifespans are variable and are dependent upon the aggressivity levels of the environment, typically 5-15 years for buried installations.
b) Coating thicknesses vary according to the application process. Hot Dipped Galvanizing (in accordance with EN1461:1999) provides a minimum zinc cover of 85 µm (microns), Electro Plated Galvanizing only offers 5-12 µm.
c) It is not suitable for prestressing grade threadbars as the preparation process (pickling in acid) can induce the potential for hydrogen embrittlement.
d) Both BS8081:2015 and EN1537:2013 preclude the use of galvanizing as permanent protection, on the basis that it is a sacrificial coating.

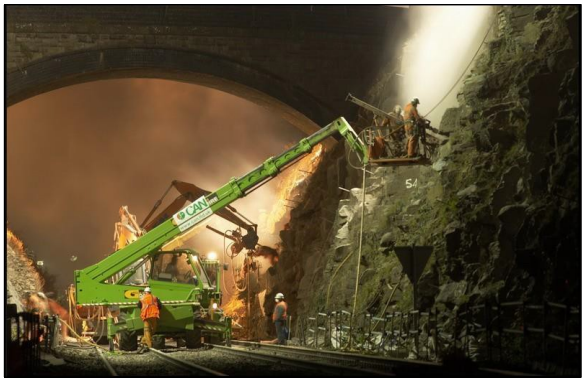


Figure 7. Galvanized Rock Bolts



Figure 8.Galvanized Soil Nails

Alternative Protection for Permanent Anchors

EN1537:2013, The European Standard for Ground Anchors, includes a range of protection options:

a) Double Corrosion Protection, as detailed above
b) Tube-a-Manchette and Compression Tube Anchorages. Each system features different mechanisms for load transfer in the bond length, but both anchorages include for two impermeable barriers as corrosion protection.
c) Electrically Isolated Anchorages, as detailed below.

Electrically Isolated Anchorages
These anchorages feature a single protective barrier (typically a corrugated plastic duct), which is subjected to an electrical resistance test. The principle of the system is based upon proving the integrity of the protective barrier by measuring the resistance between the anchorage and the surrounding soil. The concept is attractive to designers, as it enables the integrity of the protective barrier to be checked, following installation and stressing.

There are however two considerations where a detailed understanding of the system is required:

a) Contractual implications of the system are quite complicated, as the integrity of the plastic sheathing should be tested at the time of delivery to site, where ownership of the anchor is transferred to the installer. Conductivity tests prior to installation require a water bath.
b) Moisture is a problem, as resistivity readings can be unreliable and difficult to interpret.

Other Corrosion Protection Options

Stainless Steel and Cathodic Protection are occasionally considered for corrosion protection of permanent anchorages. The use of stainless steel is rare on permanent anchorage applications and there is little guidance on its use without protective barriers in either BS8081:2015 or EN1537:2013. Its application for external rock bolting or dowelling is more common. Durability of stainless steel is dependent on the grade, also the cost of higher grades can be prohibitive.

Cathodic Protection, whilst popular in other applications, has practical limitations for ground anchorages in the following respects:

a) the determination of the correct electrical current sufficient to provide protection,
b) the need for continual monitoring and maintenance of an impressed current system.

Ground Anchor or Tension Pile?

The key distinction between ground anchors and tension piles, is that ground anchors are *active* installations (featuring a prestressed free length), as opposed to tension piles which are *passive* installations (fully bonded, initially unstressed). A debonded tension pile requiring stressing is a misnomer and should be classified as a ground anchor.

The extension characteristics of tension piles (figure 9) under service loadings differ from those of ground anchors (figure 10). Tension piles will extend under load as restraint is progressively mobilised in the ground, whereas ground anchors do not, as they feature a free length which enables the extension to be stressed out at the time of installation.

For temporary works the increased extension of a tension pile is often not critical, but for permanent works the increased extension often requires careful consideration in the context of the overall structure, where additional movement could lead to cracking in the concrete faces. Typically a design incorporating tension piles will have to allow for movement on a global basis.

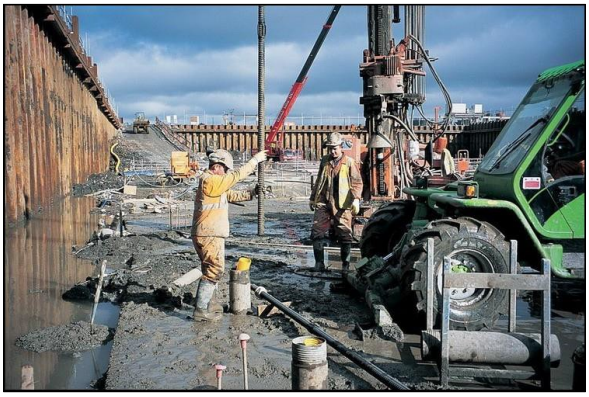


Figure 9 Tension piles for uplift resistance



Figure 10 Ground Anchors for structure tieback

Critical Areas of Anchors Requiring Protection

The location at the underside of the bearing plate is typically the area of highest risk. At this point both oxygen and moisture are present, which when combined will promote corrosion if the tendon is unprotected. Access to this area for inspection, even with the use of an endoscope, is notoriously difficult (see figure 11). Repairs are usually only possible by de-stressing the anchorage and removing the full head assembly.
Protective end caps, used on the face of the bearing plate to enclose the anchor head, do not contribute to protection below the plate. It is the section of anchorage directly below the bearing plate which requires comprehensive protection.



Figure 11. A typical application for anchors. Access to the underside of the bearing plate is notoriously difficult.

Practical Issues on Site

Wash-back of Grout at the Anchor Head
Flushing out of the grout (wash-back) over the top 1.0m of the anchor tendon is required in order to avoid any strut effect during stressing and also to facilitate the placement of the sealing tube (at the underside of the bearing plate) over the anchor tendon, see figure 12.

This is of particular importance for bar anchors, where the grease filled sealing tube is an integral part of the bearing plate. Failure to flush out can lead to the sealing tube not being properly placed around the anchor tendon, resulting in the potential for corrosion.

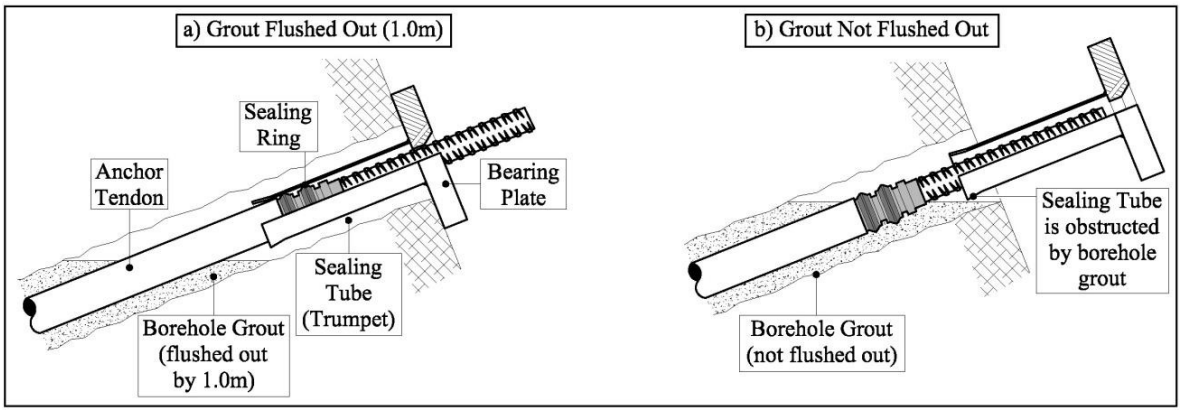


Figure 12. The importance of flushing out, for placement of the sealing tube.

Prevention of Ingress of Ground Water in Anchor Heads
In areas of high ground water pressure, additional sealing measures may be required. This is a complicated detail that needs to be carefully thought through, as practical limitations during installation require a specific order of assembly.

The use of hydrophilic strips at the underside of the bearing plate or additional sealing components, gaskets as well as the injection of specialist resins should be considered where high water pressures are anticipated.

Conclusion

Ground anchors remain a popular choice with engineers for a range of applications. Their durability in permanent works is of utmost importance, requiring careful attention in respect of corrosion protection. The re-classification of the installation in order that a lower level of protection may be applied, or the application of unsuitable barriers, is to ignore the fundamental issues of durability. It is the area of least protection that defines the effectiveness of all corrosion protection measures.

In practice, the corrosion protection principles outlined in both BS8081:1989/2015 and EN1537:2013 tend to complement each other, in that either double corrosion protection or single barrier protection (coupled with an in-situ integrity test) will ensure permanent protection for the anchor.

Acknowledgements:
The use of photographs from the following contractors are acknowledged: Ritchies, CAN, Systems Geotechnique and Cementation.

References:
1. British Standards Institute. BS 8081:1989 British Standard Code of Practice for Ground Anchorages.
2. British Standards Institute. BS 8081:2015 British Standard Code of Practice for Ground Anchorages.
3. European Standard. EN 1537:2013 Execution of Special Geotechnical Work - Ground Anchors.
4. European Standard. EN 14199:2005 Execution of Special Geotechnical Work - Micropiles.
5. European Standard. EN 14490: (2004) Execution of Special Geotechnical Work - Soil Nails.
6. CIRIA. C637 Soil Nailing. Best practice guidance.
7. British Standards Institute. BS EN ISO 1461:1999 Hot dip galvanized coatings on fabricated iron and steel articles - Specifications and test methods.
8. EN1997-1:2004+A1 Chapter 8. Anchors.

RISK ANALYSIS, RISK ASSESSMENT AND DESIGN OF A NEW DEVELOPED SLOPE STABILIZATION

Professor Dr.-Ing. Rolf Katzenbach, Technische Universität Darmstadt, Robert-Bosch-Str. 9, 64293 Darmstadt, Germany, katzenbach@geotechnik.tu-darmstadt.de
Dipl.-Ing. Christiane Bergmann, Ingenieursozietät Professor Dr.-Ing. Katzenbach GmbH, Robert-Bosch-Str. 9, 64293 Darmstadt, Germany, c.bergmann@katzenbach-ingenieure.de

ABSTRACT

In a river valley with extremely steep slopes a 160 m high and about 1.7 km long Motorway bridge is to be built. By the use of the observational method, relevant downhill orientated slope displacements have been detected with inclinometers. To secure the overall stability of the bridge piers and of the slope challenging stabilization measures become necessary. Due to the extremely complicated local conditions a new technical method for slope stabilization has been developed. Therefore about 45 m deep shafts with a diameter of 6.6 m are constructed. For the load transfer the shafts are connected with a 4.2 m x 6.3 m thick and 32 m long strongly reinforced head board and tied back with up to 55 m long permanent anchors. This new developed slope stabilization construction will be used in combination with permanent groundwater lowering. To analyse the applicability of the construction, a nonlinear 3D-Finite-Element-Model of the steep slope with the anchored shafts was developed and a parameter study has been conducted.

In this paper the risk analysis, the risk assessment and the new developed slope stabilization scheme using the anchored shafts as well as the 3D-FE-Analysis will be described in detail.

Keywords: Natural Hazards, Slope Stability, Observational Method, Landslides

INTRODUCTION

According to national laws and regulations the responsibilities for the planning, construction and materials used at any kind of construction project are different around the world. Never the less it is necessary to have a safety concept for risk minimisation in all planning and construction phases and for the quality of the construction material. In geotechnical engineering the soil represents the construction material. In any case the soil risk is connected to the chosen construction process and the type of construction. The soil risk and the system risk are strongly related to each other.

The so-called system risk explains that the chosen construction technique, construction material, construction process is not applicable to the soil and groundwater conditions.

Soil is used as an active or passive construction material. If soil is used for the load transfer of a superstructure over a foundation system into the underground, it is used as a passive construction material. Soil is used as an active construction material if it is used e.g. for fillings and dams.

The difficulty of soil as a construction material is that even by an extensive soil and groundwater investigation program less than 0.1 ‰ of the soil that is influenced by the building can be determined, as shown in Fig. 1.

© 2018 Deep Foundations Institute

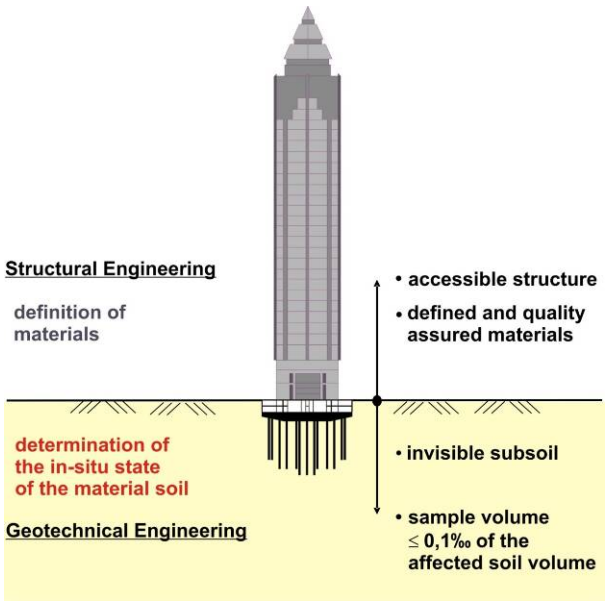


Fig. 1. Differences between structural and geotechnical engineering.

Due to the random character of the soil investigation an element of risk remains. This risk means that the real soil conditions probably cannot be determined in detail. The soil risk remains as unavoidable risk. Damages or time delays may occur even though an extensive soil investigation was made. Fig. 2 shows the process to the decision if soil risk is fulfilled.

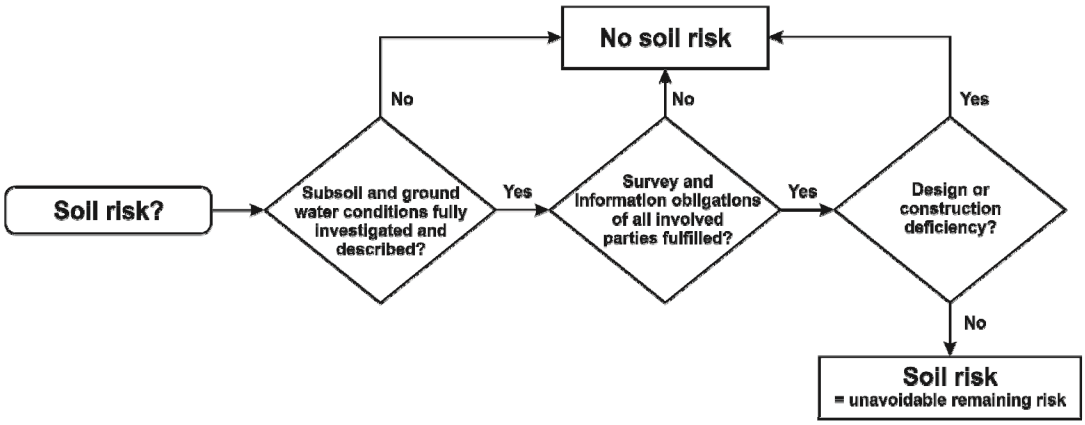


Fig. 2. Definition process of soil risk.

It is no soil risk in the following cases:

- lack of geotechnical investigations
- wrong interpretation of the results of geotechnical investigations
- wrong investigation techniques
- mistakes in the design
- incompletion of the design
- differences between the design and the construction work
- etc.

The system risk is similar. The system risk includes the construction process and the type of construction. Most forensic geotechnical tasks deal with the handling of the soil risk resp. system risk.

In forensic engineering it is necessary to investigate the problem characterisation, the development of failure hypotheses and to analyse the failure by back analysis, with in-situ observations and by using monitoring systems (Lacasse 2016).

CONCEPT FOR SAFETY AND QUALITY CONTROL

For minimisation of the soil risk a concept for safety and quality control is necessary. This concept consists mainly of:

- qualified experts for planning, design and construction
- extensive soil investigation
- independent peer review during planning, design and construction (4-Eye-Principle)
- observational method

The last two aspects will be explained in detail.

IINDEPENDENT PEER REVIEW

The process for an independent peer review is shown in Fig. 3. It mainly consists of 3 parts. The investor, the experts for planning and analysing and the construction company belong to the first party. Planning and design is done according to the requirements of the investor and all relevant documents to obtain the building permission are prepared. The building authorities constitute the second part and are responsible for the building permission which is given to the investor. The third part consists of the publicly certified experts. They are appointed by the building authorities but work as independent experts. They are responsible for the technical supervision of the planning, analysing process and the construction.

To achieve the licence as a publicly certified expert for geotechnical engineering by the building authorities the following requirements should be given:

- intensive studies of geotechnical engineering at university
- large experiences in geotechnical engineering with special knowledge about the soil-structure-interaction

examination by a group of publicly certified experts

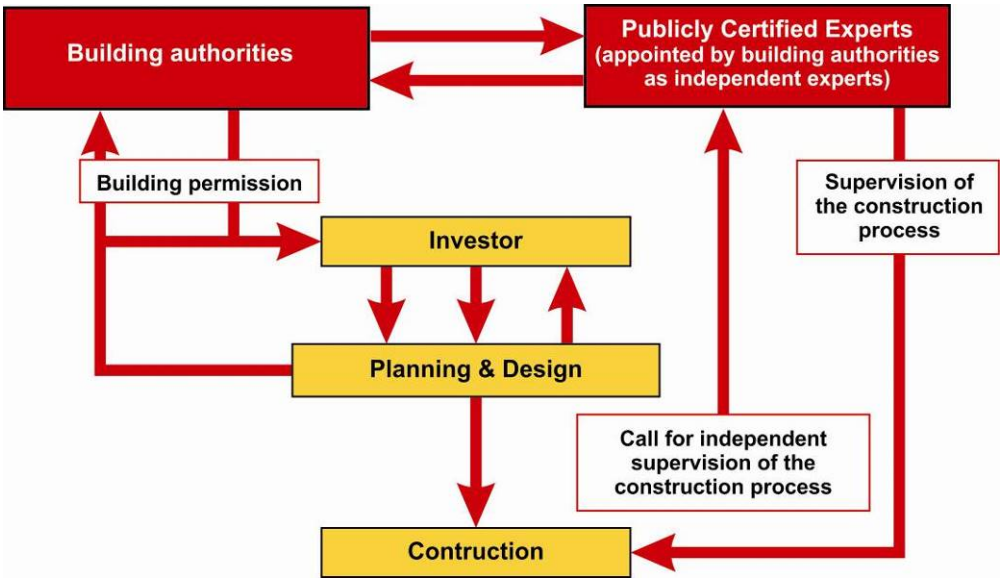


Fig. 3. Independent peer review process.

The independent peer review by publicly certified experts for geotechnical engineering makes sure that all information including the results of the soil investigation including the laboratory and field tests and the boundary conditions defined for the geotechnical design are complete and correct.

In the case of damage, the publicly certified expert for geotechnical engineering can be involved as an independent expert to find out the reasons for the damage and to develop a concept for the reconstruction.

OBSERVATIONAL METHOD

If the identification of the mechanical behaviour of soil is difficult, it is necessary to apply the observational method to review the design during the construction time and (if necessary) during service time. For example, in the European Standard Eurocode 7 (EC 7) the effect and the boundary conditions of the observational method are defined.

The application of the observational method is recommended for the following types of construction projects (Katzenbach et al. 2013):

- very complicated/complex projects,
- projects with a distinctive soil-structure interaction, e.g. mixed shallow and deep foundations, retaining walls for deep excavations, Combined Pile-Raft-Foundations (CPRFs),
- projects with a high and variable water pressure,
- complex interaction situations consisting of ground, excavation and neighbouring buildings and structures,
- projects with pore-water pressures reducing the stability,
- projects on slopes.

The observational method is always a combination of the common geotechnical investigations before and during construction together with the theoretical modelling and a plan of contingency actions (Fig. 4). Only monitoring to ensure the stability and the serviceability of the structure is not sufficient and, according to the standardization, not permitted for this purpose.

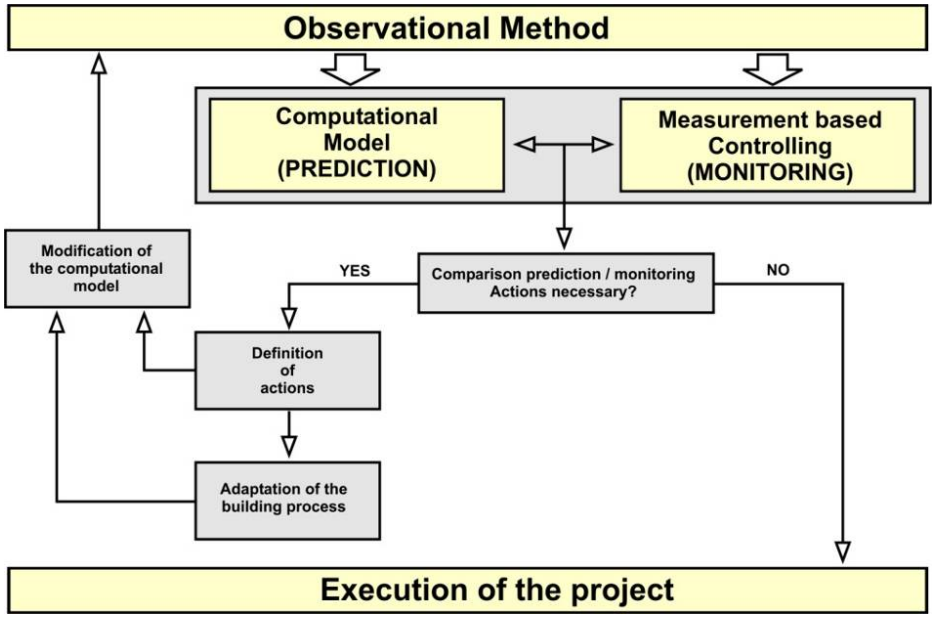


Fig. 4. Principle of the observational method.

Overall the observational method is an institutionalised controlling instrument to verify the soil and rock mechanical modelling (Abel 2003, Blume, Glötzl 2003, Brandl 1999, Herten 2010, Katzenbach et al. 1999, Nagel et al. 2012, Rodatz et al. 1999).

The identification of all potential failure mechanisms is essential for defining the measure concept. The concept has to be designed like that, so that all these mechanisms can be observed. The measurements need to be reliable and should be done in a direct and defined way. The measurement devices need to be of an adequate accuracy to allow the identification of critical tendencies. The required accuracy as well as the boundary values need to be identified within the design phase of the observational method.

Contingency actions need to be planned in the design phase of the observational method. The construction method or design method depends on the ductility of the system. It is essential that contingency action can be applied. The observational method must not be seen as a potential alternative for a comprehensive soil investigation campaign. A comprehensive soil investigation campaign is in any case of essential importance.

To establish the above mentioned boundary values before the construction has started is a challenging task and requires powerful calculation tools which reply on suitable constitutive laws for the soil.

As a secondary effect the observational method is a tool of quality assurance and allows the verification of the parameters and calculations applied in the design phase. The observational method helps to accomplish an economic and safe construction.

RISK ANALYSIS AND RISK ASSESSMENT OF A STEEP SLOPE

In a river valley with extremely steep slopes a 160 m high and about 1.7 km long Motorway bridge is built (see Fig. 5). By the use of the observational method according to the Eurocode 7 (EC7) relevant downhill orientated slope displacements have been detected with inclinometers.



Fig. 5. Visualization of the 160 m high and 1.7 km long Motorway bridge

In the depth of about 22 m a sliding zone of the steep slope has been detected during the consequent use of the observational method according to the Eurocode EC 7 with inclinometers. Since May 2000 to September 2016 a head deformation of 2.5 cm has been measured by the exemplary inclinometer shown in Figure 3. The shear band is between the axis 2 and 3 of the bridge at a steep slope with an inclination of about $\beta = 25°$ (see Fig. 6)

The shear band is overlaid with deposits/hillside loam and exterior weathering argillaceous schist. Below the shear zone the soil consists of decomposed argillaceous schist till a depth of about 80 m. With the depth of 80 m argillaceous schist as a rock was determined. The groundwater level is illustrated in Figure 6.

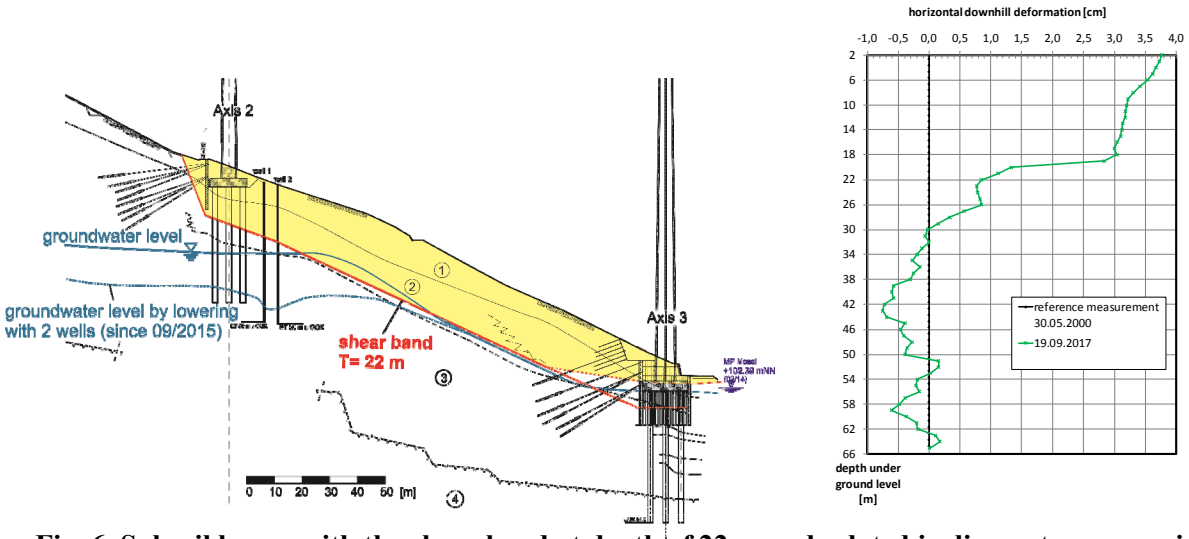


Fig. 6. Subsoil layers with the shear band at depth of 22 m and related inclinometer measuring.

The soil parameters of the different layers illustrated in Fig. 6 are given in Table 1.

Table 1. Soil Parameters

No.	Layer	γ/γ_r [kN/m³]	φ' [°]	c' [kN/m²]
1	deposits/hillside loam	22/11	30.0	15.0
2	exterior weathering argillaceous schist	22/11	30.0	15.0
	shear band	-	22.0	7.0
3	decomposed argillaceous schist	22/11	30.0	33.0
4	argillaceous schist	26/16	≥ 40.0	0.0

Due to the risk analysis and risk assessment it was clear to secure the overall stability of the bridge piers and of the slope. Therefore, challenging stabilization constructions are necessary.

DETECTION OF THE NECESSARY STABILIZATION FORCE

For the dimension of the slope stabilization the necessary stabilization force had to be calculated. Due to the fact that the piers will be fixed points, it has to be assumed for the worst-case scenario when the slope will fail that the force of the moving body of the landslide will be transferred by side friction to the soil body between the piers. The principle is shown in Fig. 7.

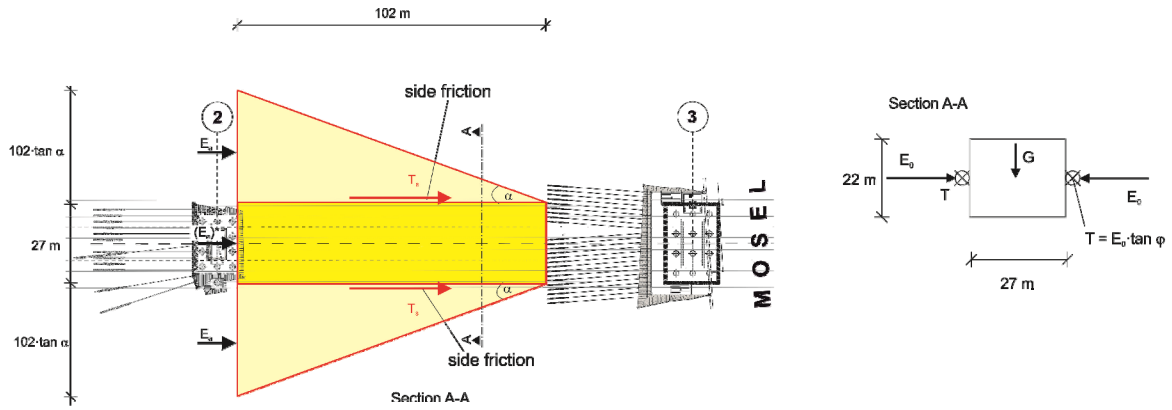


Fig. 7. Model to dimension the side force.

The calculation of the side friction was conducted by the approach of the maximum of the transferable force with the earth pressure at rest as follows for each side:

$K_{0g} = 1 - \sin\varphi = 1 - \sin 30° = 0.500$ [1]

$E_0 = ½ \cdot h^2 \cdot l \cdot \gamma \cdot K_{0g} = ½ \cdot (22m)^2 \cdot 102m \cdot 22\ kN/m^3 \cdot 0.500$ [2]

$E_0 = 271{,}524\ kN = 271.5\ MN$ [3]

$C = h \cdot l \cdot c = 22m \cdot 102m \cdot 0.015\ MN/m^2 = 33.7\ MN$ [4]

$T_\varphi = E_0 \cdot \tan\varphi = E_0 \cdot \tan 30° = 157{,}7\ MN\ (c = 0)$ [5]

$T_{(\varphi+c)} = T_\varphi + C = 156.7\ MN + 33.7MN = 190{,}4\ MN$ [6]

To reach a stable and according to the Eurocode 7 (EC 7), section 11, proved overall stability of the slope with the additional load of the side friction, a slope stabilization construction had to be dimensioned to a force of about 540 MN. A special challenge thereby was the restriction to build the construction with small machines due to the steep slope and the risk that big load introduction could initiate the slope failure.

SLOPE STABILIZATION CONSTRUCTION

For the slope stabilization to guarantee the Overall Stability according to the Eurocode 7 (EC 7), section 11, a new construction has been developed.

Therefor overall 6 shafts will be constructed with a diameter of 6.6 m and a depth of 45 m. The shafts will be protected with a 30 cm thick shotcrete lining during the construction. The reinforced concrete ring of the shaft will be about 1.0 m thick (see Fig. 8).

The shafts will be spread into two rows with 3 shafts between the pier 2 and pier 3. Each row will be connected with a 4.2 m x 6.3 m thick and 32 m long strongly reinforced head board for the load transfer. The head boards are going to be tied back with up to 55 m long permanent anchors. These anchors have to carry a design load of 3.0 MN. Additionally, a groundwater lowering is necessary to prove the Overall Stability according to the Eurocode 7 (EC 7). By reason of groundwater lowering one shaft will be built as a drainage shaft. On this drainage shaft 10 horizontal drainages in two layers with 5 horizontal drainages with a length up to 50 m are connected (see Fig. 8).

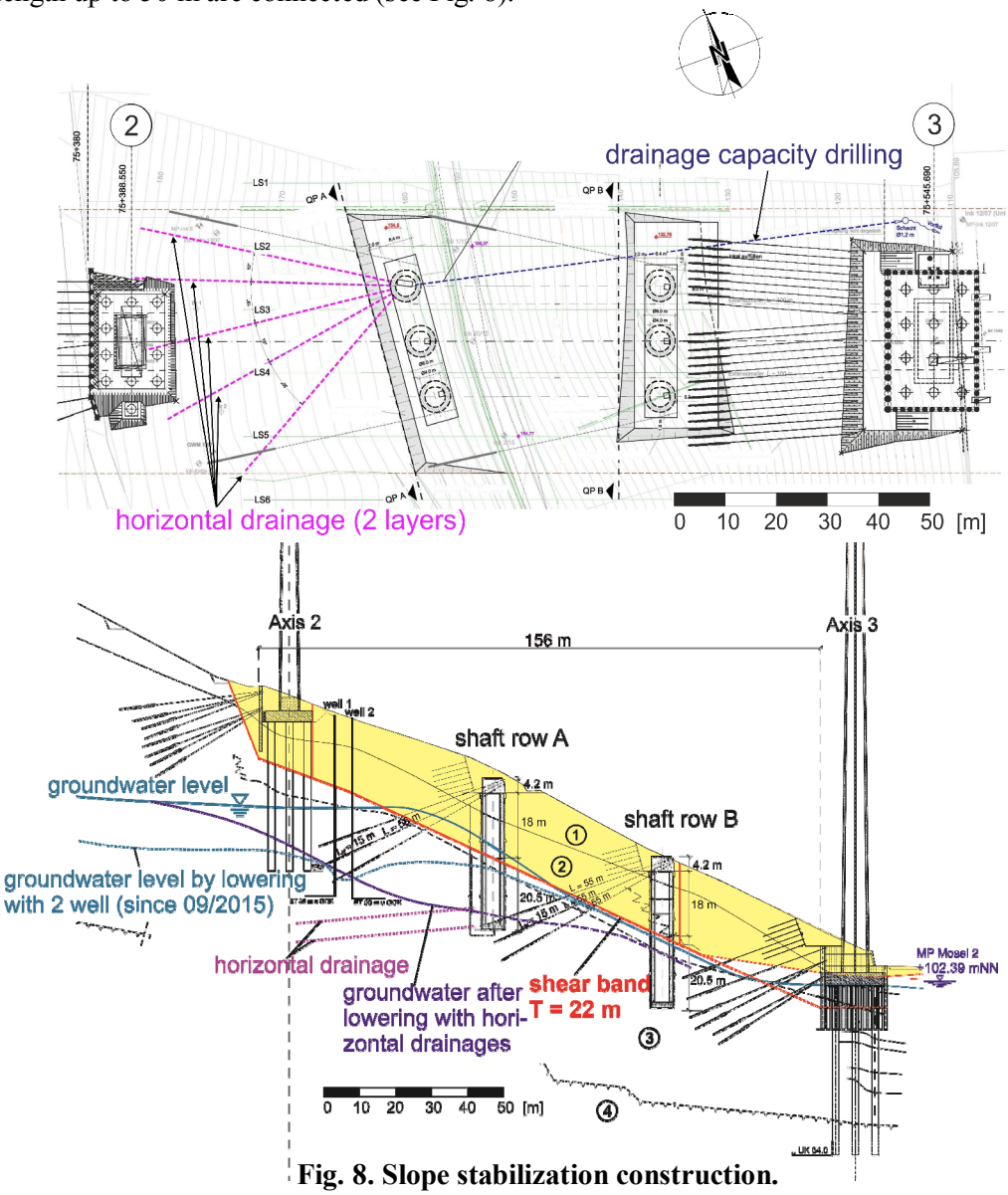


Fig. 8. Slope stabilization construction.

3-D-FINITE-ELEMENT MODEL OF THE SLOPE STABILIZATION CONSTRUCTION

To prove the approach of the transferable force and the function of the slope stabilization construction a 3D-Finite-Element-Analysis has been conducted. The 3D-Finite-Element-Model has a width of 200 m and a length of 320 m. The ground surface of the steep slope has been modelled with an average inclination of $\beta = 25°$ according to the true conditions at the slope.

The material behaviour of the layers has been modelled with linear elastic - ideal plastic material law. As the friction condition according to the Mohr-Coulomb friction condition, which is described with the shear parameters φ' and c', was conducted. The soil parameters can be obtained in Table 1.

The modelling of the shafts and the head board have been carried out in Plaxis 3D with plate elements. The interaction between the soil and the shafts was modelled with Interface-Elements. For the reproduction of the anchors beam elements has been used. The grout body was built with Embedded Piles (see Fig. 9).

The shafts were modelled linear elastic with a modulus of elasticity of 30,000 MN/m² and a Poission's ration of 0.2. The anchors were also modelled linear elastic, the maximum surface friction of the grout body was defined with $q_{s,k} = 250$ kN/m². For the numerical calculation the incremental sequences of the calculation steps were elected to be able to analyse the changes from the actual situation with activated sliding joint to the situation after the installation of the shafts.

With the help of the 3D-Finite-Element-Modell it was possible to prove and confirm the necessary stabilization load that has been calculated by a simple model with the transferable force. Further it could be verified, that the planned slope stabilization construction is able to absorb the load, which will occur by the slope failure. Therefor it could be proven that the bedding of the piers will be conserved.

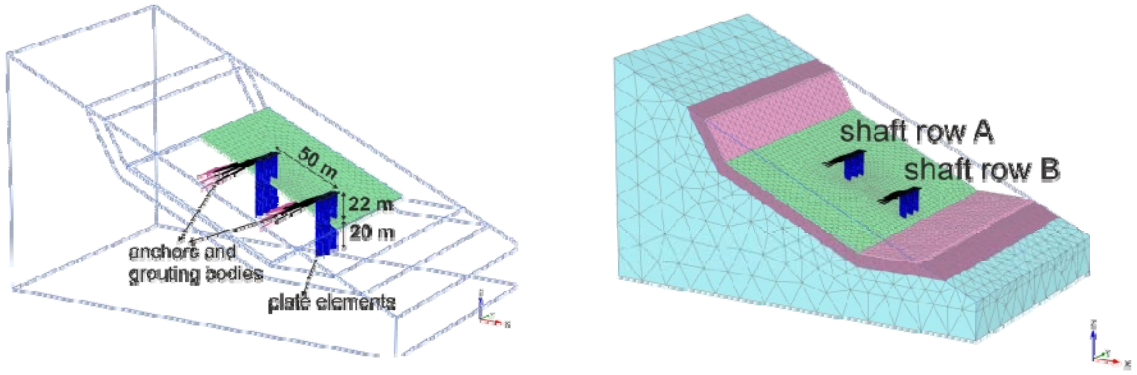


Fig. 9. 3D-Finite Element Model.

Further it was possible to prove with the 3D-Finite-Element Modell that the forces will spread equally over the anchors of each shaft row. Due to the high account of anchors and the distribution all over the panel a sliding between the shafts will be prevented.

CONCLUSION

With the help of the 3D-Finite-Element Model it was possible to show that the developed slope stabilization construction with six anchored shafts will work to absorb the occurring forces of the worst case scenario and the proof of Overall Stability according to the Eurocode 7 (EC 7), section 11 is given.

REFERENCES

CEN European Committee of Standardisation (2008). Eurocode 7: Geotechnical design – Part 1: General rules.

Abel, F. (2003). Einsatz der Beobachtungsmethode zur Optimierung von Tunneldränagesystemen. Dissertation, Ruhr-Universität Bochum.

Blume, K.-H., Glötzl, B. (2003). Anwendung der Beobachtungsmethode am Beispiel der BAB A26. Erd- und Grundbautagung 2003 in Stade

Brandl, H. (1999). Risk analyses, quality assurance, and regulations in landfill engineering and environmental protection. 3rd International Congress on Environmental Geotechnics, Lisabon. Proceedings A.A. Balkema, 1299-1328

Herten, M. (2010). Anwendung der Beobachtungsmethode. BAW-Kolloquium Tiefe Baugruben an Bundeswasserstraßen am 22. Juni 2010 in der BAW Karlsruhe, 83-90

Katzenbach, R., Schmitt, A., Turek, J. (1999). Co-operation between the geotechnical and structural engineers – experiences from projects in Frankfurt. COST Action C7, Soil-Structure-Interaction in urban civil engineering, 1.-2.10.1999, Thessaloniki, Greece, 53-65.

Katzenbach, R., Leppla, S., Weidle, A., Choudhury, D. (2013). Aspects regarding management of soil risk. Fourth International Seminar on forensic geotechnical engineering, 10.-12.01.2013, Bengaluru, India, 83-94

Lacasse, S. (2016). Forensic Geotechnical Engineering – Theory and Practice. Forensic Geotechnical Engineering, Developments in Geotechnical Engineering, Springer India

Nagel, F., Spohr, I., Speier, L. (2012). Beobachtungsmethode in der Geotechnik – Verknüpfung von Messung und Simulation. Tunnel 3/2012, 40-47

Rodatz, W., Gattermann, J., Bergs. T. (1999). Results of five monitoring networks to measure loads and deformations at different quay wall constructions in the port of Hamburg. 5th International Symposium on Field Measurements in Geomechanics, 1.-3.12.1999, Singapore, 4 p.

SECANT PILE WALL FOR CUT OFF AT SUNDILLA BARRAGE

Dr Ir Chandramohan P.V., President (technical), Navayuga Engineering Company Ltd, Hyderabad, Telengana, India, Phone:91 98490 11789, pvcmohan@gmail.com

Chandrasekhara Reddy M, Manager (designs), Navayuga Engineering Company Ltd, Hyderabad, Telengana, India, Phone:91 94416 99516, chandu_iitkgp@yahoo.com

ABSTRACT

Secant pile walls are being widely employed as retaining structures mostly in the basements. These are generally classified as bulkheads. They are tied back at the top or at a couple of levels depending on the height of retention. Rock anchors are employed for tie backs at the lower levels. This wall is a substitute for diaphragm walls, which requires mobilization of heavy equipment. But secant pile wall was contemplated in a new role at Sundilla. Cut off for the barrage was made in the form of a secant wall. The paper describes the construction details.

Key words: Secant pile, cut off wall, barrage, hydraulic gradient, plain concrete pile

INTRODUCTION

The paper describes the construction details of a secant pile wall at Sundilla barrage. The secant pile structure was selected for the purpose and designed by the owners. Secant pile walls can be categorized as a bulk head like sheet piles or diaphragm walls. They are utilized as earth retaining structures. They are common in the construction of basements for buildings. In rare cases, they could be free standing from the ground acting like a cantilever. If the retention height is more, they are tied back at the top with the help of a waling beam. For still higher retention, multi tie backs are employed at different levels. This type of structure is not common in India. They are widely employed in the middle-east. This is perhaps prompted by the presence of lime stone layer at shallow depths there. Simplicity of this type of structure is earmarked by the fact that this can be installed by a simple piling rig unlike in the case of heavy mobilization for diaphragm walls. Previous case of a secant wall being used in a dam is at Arapuni dam in Newzealand. But the purpose there was to close out the seepages in the foundation. Secant wall was done when the dam was in service and after the leakage was noticed. Since there was no structural function involved, all piles were of plain concrete with a diameter of 400mm @ 350mm c/c.

INSTALLATION

The wall consists of a series of piles. The piles are installed in a particular sequence. As is seen in Fig. 1, the piles overlap into each other.

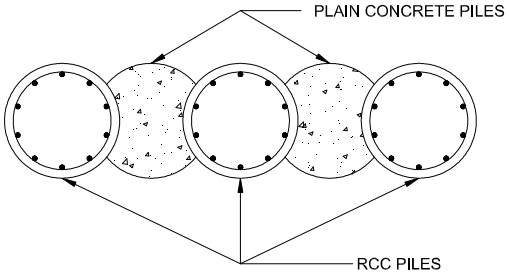


Fig. 1. Typical Cross section of secant pile wall

The overlap is as per requirement of the function. General criterion is 150mm to 250mm. Alternate piles are of plain concrete. They are also called soft piles. Other piles are reinforced. In the case of a retaining structure, the force will be resisted by the reinforced concrete pile. Earth pressure on this pile will be more than that of the width of that pile. The plain concrete pile (dummy) piles will

© 2018 Deep Foundations Institute

transfer the earth pressure on them to the reinforced piles. This is done by these piles horizontally spanning between reinforced piles. Force from the lateral earth pressure will be solely resisted by the reinforced piles. Plain concrete piles (alternate) are installed first. Boring is then made partly through the soil and partly through the adjacent plain concrete piles for installation of the reinforced piles. Since plain concrete piles do not resist main bending, and since boring has to be made partly through them, they are sometimes made of concrete of a lower strength. It is preferable to attempt boring when the concrete has not attained high strength. At the same time, concrete in the pile should not be green. An age of 24 to 48 hours is preferable. Once the boring is ready, reinforcement cage is lowered into the bore and the bore hole is concreted. The top of the wall is tied back to either a dead man or by a rock anchor. Sometimes, the secant wall will become part of the permanent structure. In that case, a concrete waling beam is cast at the top. If it is for temporary use, the waling beam is made of steel sections. Similar to diaphragm walls, guide walls are used for correct alignment and verticality. Fig. 2 shows the guide wall template used at Sundilla. Guide wall after the removal of the template is shown in Fig. 3.



Fig. 2. Photo. Guide wall template for Sundilla



Fig. 3. Photo. Guide wall ready for piling

Boring for the plain concrete piles is shown in Fig. 4. Exposed secant piles after concreting are shown Fig. 5.



Fig. 4. Photo. Boring for plain concrete piles at Sundilla



Fig. 5. Photo. Exposed secant wall at Sundilla

COMPONENTS OF A SECANT PILE WALL

Major components of a secant wall acting as a retaining structure, apart from the piles, are the waling beam, tie back arrangements including ties going in as rock anchor or tie and a deadman. A typical diagram of the components is shown in Figs. 6 and 7. A photo of the secant wall used as a retaining structure is given in Fig. 8.

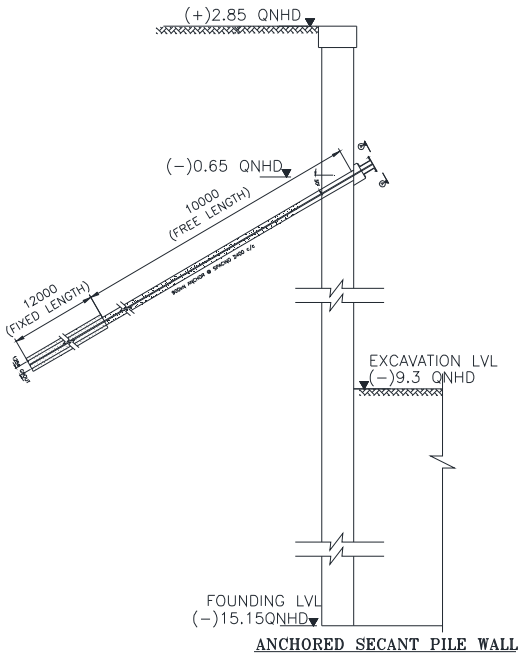


Fig. 6. Section of secant wall

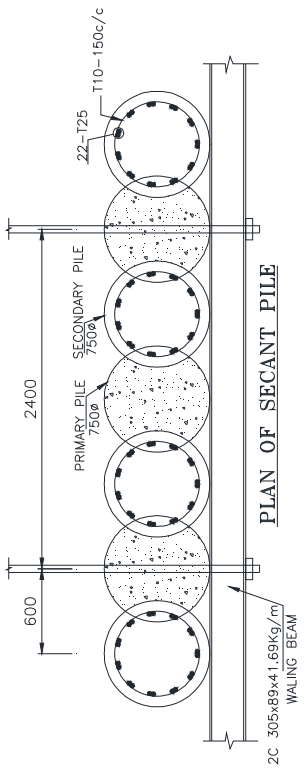


Fig. 7. Waling beam arrangement



Fig. 8. Photo. View of a secant retaining wall after excavation

CUT OFF AT SUNDILA BARRAGE

The function of the secant wall at Sundila barrage is totally different. In dams and barrages, water is retained to a finite height on the upstream side. Considerable hydrostatic head acts on the structure on one hand. On the other hand, this hydrostatic head acts on the upstream bed as well. Downstream of the barrage, the tail water level is low. This differential hydraulic head will give rise to percolation of water from the upstream of the barrage to the downstream through the base soil. This slow flow could develop into a phenomenon called piping. If unchecked, this flow could carry soil particles from the base also towards the downstream. This will endanger the stability of the structure in the long run. It is important to reduce the hydraulic gradient to reduce percolation. This is done by increasing the length of percolation. Horizontal length could be increased by putting up aprons on the upstream and downstream sides. But vertical cut off is more effective than the horizontal length. As per the present data vertical percolation will offer three times resistance than horizontal. So, multiple cut off walls are provided under the structure. Usually, sheet pile walls or plastic diaphragm walls are provided as impervious curtains. But at Sundilla barrage in Peddapally district of Telangana, a novel structure was tried out.

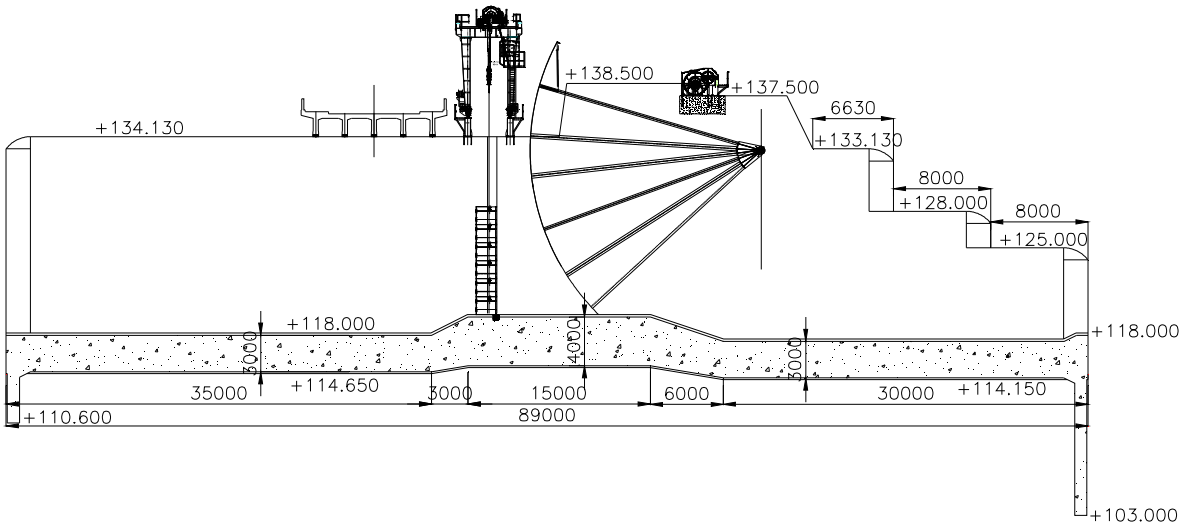


Fig. 9. Section of barrage with cut off

Length of the barrage is 1344m. Crest level is at +118.5. High Flood Level is +132.13. This means that there will be 13.63m of water above the crest at HFL. The barrage facilitates a discharge of 57000 cumecs. The scour depth was computed to be 19.43m. Level of scoured bed at the upstream side is +112.67. On the downstream side, this level is +107.813. At the level of +114.65, the base pressure exerted by the superstructure of the barrage is computed to be 300kPa. For section of the barrage, please see Fig. 9. Photo of the barrage piers and gate fixtures are given in Fig. 10 and Fig. 11. At Sundilla, Reinforced piles are of M30 concrete while plain concrete piles are of M20 grade.



Fig. 10. Photo. View of the barrage piers



Fig. 11. Photo. Gate fixtures on the pier

CREEP LENGTH CONSIDERATION

Total width of the barrage is 89m. This is the length of the horizontal percolation path. Please see Fig. 12. Two cutoff walls – one at the upstream end and the other at the downstream end are provided.

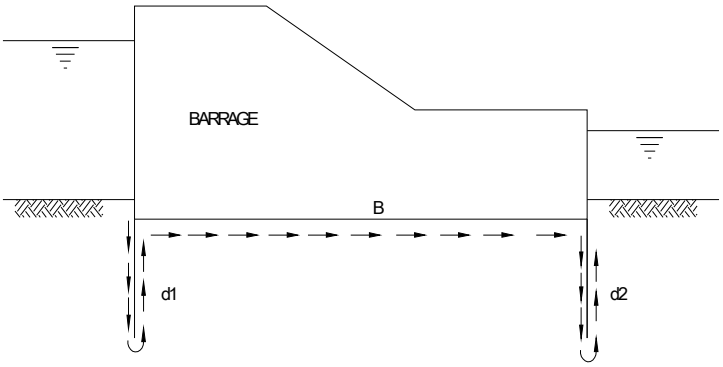


Fig. 12. Percolation path

The percolation path goes down and up vertically by the two cut offs, also moves horizontally under the base of the structure. The creep length is computed as

$$= \frac{B}{3} + (2d_1 + 2d_2) \quad \ldots [1]$$

CONCLUSION

This is unique case of a secant pile wall being used for cut off. This has been done for a barrage at Sundilla. Selection of the secant pile wall for the cut off and its design were carried out by the owners. The paper describes the construction aspects of the structure. At Sundilla, construction of the wall has been completed and superstructure of the barrage work is in progress.

REFERENCE

Central Bureau of irrigation and power, 1985. Publication No 179, Volume 1: 'Manual on barrages and weirs on permeable foundations'.

SIMPLIFIED ONE-DIMENSIONAL MODELS FOR PILE–SOIL-PILE INTERACTIONS OF A DUO-PILE SYSTEM

Kolli Mohan Krishna, PhD Scholar, Indian Institute of Technology Gandhinagar, Gujarat, India, 8500441687, mohan.kolli@iitgn.ac.in
Dhiman Basu, Assistant Professor, Indian Institute of Technology Gandhinagar, Gujarat, India, 9925433861, dbasu@iitgn.ac.in
Amit Prashant, Professor, Indian Institute of Technology Gandhinagar, Gujarat, India. 8511360509, ap@iitgn.ac.in

ABSTRACT

The design of Duo-pile foundation system for elevated railways and highways is very critical with respect to lateral deflection which can affect serviceability and the stability of superstructure. In duo-pile system, interaction between piles, i.e., pile-soil-pile interaction plays a major role in final response of the system. Four types of pile-soil-pile interaction take place in duo-pile system: 1) Edge effect due to lateral load in transverse direction; 2) Shadow effect due to lateral load in longitudinal direction; 3) Couple effect due to moment transfer in the longitudinal direction and 4) Interaction due to vertical load. Objective of this study is to arrive at the appropriate spring constants for pile such that incorporating these interactions into an equivalent one-dimensional (1-D) model will approximately simulate the target displacement from the associated three-dimensional (3-D) model. Firstly, 3-D models comprising of only two piles are explained. For each interaction, appropriate 1-D models are presented and corresponding spring constant factors are proposed.

Key words: Duo-pile, Pile-Soil-Pile Interactions, Spring Constant Factors, Couple Effect, Simplified 1-D Model.

INTRODUCTION

Monopile and Group piles are the most commonly used deep foundation systems for the urban transportation facilities like flyovers and elevated railways. These facilities appear to be the simple structural systems but involve in-depth study, forethoughts and conceptualization. These structures under serviceability have relatively stringent limits on the tip deflection of piers to check against misalignment with superstructure affecting its stability. It requires precise estimation of lateral response of bent systems under the action various types of forces like vertical (Dead load and Live load), Longitudinal loads (Braking, Tractive effort, Wind load, Temperature effect and Seismic forces) and Transverse loads (Live load, Wind load, Temperature effect and Seismic forces).

Monopile has been trending as substructures for metro-rails instead of group piles (Smith and Hendy, 2009). Total deflection at ground level in a monopile is contributed from the combined effects of lateral load and overturning moment. Instead, group-piles can be used to transfer the moments better so that lateral deflections can be minimized. Although group-piles are extensively used in practice, construction of closely spaced piles with a common pile-cap and pier(s) erecting from it can be altogether a cumbersome and costly system. The combine advantage of moment transfer and ease in construction can be obtained by using two piles with a beam at pile cut-off and take the advantage of frame action (duo-pile system). Duo-pile system offers a good alternative to the monopile and group-piles systems. Duo-pile foundation with the pile capping beam (See Fig. 1) constructed monlithically with the piles enable moment transfer. The transfer mechanism of moment in duo-pile occurs through a force-couple (Frame Action) which results in vertical displacement of piles but reducing the overall lateral deflection.

© 2018 Deep Foundations Institute

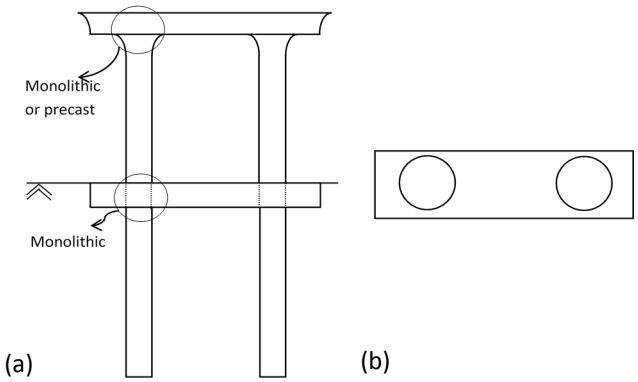


Fig. 1 Two-pier bent system with duo-pile as foundation a) Transverse section b) Plan view

Before characterizing the response of duo-pile system, the behavior of two individual piles needs to be understood and characterized under various type of interactions involved in the system. In duo-pile system, the type of pile-soil-pile interactions are similar to group piles. But it was observed in literature that interaction that occurs due to moment transfer has not been observed by the community. The moment transfer mechanism by means force couple has to be studied carefully. These interaction mechanisms can be studied numerically by Finite Element method (3-D and / or 1-D modelling). For all practical purposes, 1-D model is easy to practise provided the response is approximated reasonably well. 3-D model may simulate real scenario relatively better but at high computational expense. Winkler (1867) theory of beams resting on elastic foundation was extended in analysis of pile. It is observed in the literature clearly that subgrade reaction model with several recommendations on spring constants Terzaghi 1955; Muskhelishvili 1963; Matlock 1970; Poulos 1971; Scott 1980; Mylonakis 2001; Rani and Prashant 2014 are available in the past for approximating the response of single pile. Another type of spring called p-y spring models (Matlock 1970; Reese and koop 1974; Reese and welch 1975) and closed form solutions (Hetenyi 1946) are also available. Laterally loaded pile groups have been analyzed initially using elastic continuum approach (Poulos & Davis 1980) and group equivalent pile procedure (Ooi 2004). To incorporate pile-soil-pile interaction, large numbers of studies have been done on p-multipliers to incorporate interaction effects in the p-y curves (US Army 1993; Reese et al. in 1996; AASHTO 2000; Reese and Van Impe in 2001; Budiman and Ahn 2005; Rollins 2006; Chandrasekaran 2010). The approach to incorporate pile-soil-pile interaction by modifying subgrade reaction to be used as spring constant in linear 1-D analysis is studied very minimal. The Canadian Foundation Engineering Manual (1978) and The Japan Road Association (1976) proposed such reduction factors which are generally conservative in nature. But there are limited studies on the reduction of spring constant to be considered in the case of linear spring constants as most of the studies concentrated on p-multipliers for nonlinear springs. The unique moment transfer (couple) pile-soil-pile interaction has been not studied previously, which can be addressed in terms of linear interaction springs. The primary objective of this study is to develop simplified models of two piles to approximate the displacement of piles approximately the 3-D model response that can accommodate pile-soil-pile interactions in its spring constants.

In this study spring constant as a relationship between spring stiffness (k_s) and Young's modulus of soil (E_s) to be used for pile under the interaction of another pile is found by minimizing the difference between the 3-D response of pile in a group and 1-D of single pile response by iteratively finding spring constant factor. For this purpose both 3-D and 1-D models are created in OPENSEES2.5.0 (Open System for Engineering Earthquake Simulations) with GiD12 as a pre- and post-processors. A new type of interaction spring has been introduced to take care of pile-soil-pile interaction that is happening due to force-couple in piles. Finally, simplified 1-D models are proposed by taking into account the effects of pile-

soil-pile interaction for both transverse and longitudinal response of two piles in compliance with the results from 3-D model.

PILE-SOIL-PILE INTERACTIONS IN A DUO-PILE SYSTEM

The behavior of duo-pile is much different from the behaviour of single pile or symmetric group of piles. The response in its longitudinal direction is unique and different compared to transverse direction. In transverse direction of duo-pile, the deformation mode is cantilever mode which is similar to single pile. In longitudinal direction, there will be vertical relative movement of piles which is due to transfer of moment by beam as force-couple to piles and is also due to the end conditions of piles (not restrained).

Similar to group piles, due to overlap of influence zones over which same stiffness of soil is shared by multiple piles, there exists pile-soil-pile interactions in the system in both transverse (edge effect) and longitudinal (shadow effect) directions. The pile-soil-pile interaction due to transverse loading is due to overlap of edges of influence or strain zones of two piles, hence, called as edge effect. In longitudinal loading of two piles, the leading pile will be in the shadow of influence zone of trailing pile and hence, this pile-soil-pile interaction is called as shadow effect. Under vertical loads the vertical interaction may also prevail in this system. In duo-pile system under longitudinal loading, beam transfers moment as vertical load in to the piles as in the form that both piles have equal and opposite vertical loads (like a couple force). Under this couple loading also the influence zones of piles coincides and have effect on the final response of system.

DESCRIPTION OF MODEL

Fig. 2 schematically describes the model of only two piles with piers of a duo-pile system without beam considered in this study. The geometry and material properties of the piles and piers are provided in the Table 1. The center to center spacing between piles is varied in the range of *3d* to *8d*, where, 'd' is diameter of pile. Soil is assumed to be homogeneous and a range of values are considered to cover most of the possible scenarios. The piles are not designed for particular case but their sizing is considered in normal range as the soil's young modulus is varied for parametric study.

Table 1 Details of two pile model

Structural element	Young's modulus (MPa)	Poison's ratio	Length (m)	Cross-sectional dimensions
Piles	29.58×10^3	0.3	15	1m diameter
Piers	29.58×10^3	0.3	8	1m diameter

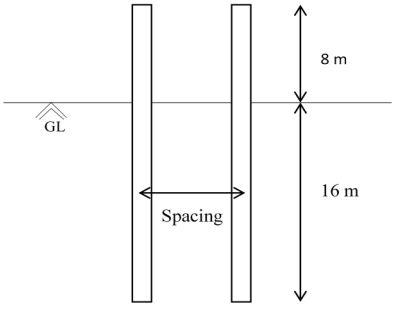


Fig. 2 Details of two pile system

To study pile-soil-pile interaction due to lateral load both in transverse and longitudinal direction and for vertical force couple, 3-D models of two piles for different spacing's is created. Numerical study is carried out throughout in this study using OPENSEES2.5.0 with GiD12 as a pre- and post-processors. Soil, piles and piers are modelled using the 8 node Iso-parametric brick elements and their behaviour is restricted to the linear elastic. The interface of pile-soil is assumed to be perfectly bonded or glued. All degrees of freedom of the nodes at the base of soil domain are restrained. All the nodes on lateral boundary are restrained against lateral translation. The response of pile-soil system is usually influenced by the size of the domain, which is addressed by performing domain convergence study. An optimum size of *15d* laterally from pile center and *5d* from bottom of pile tip is selected and utilized through out of this study. Mesh convergence is also carried out which leads to a mesh size of 0.3x0.3x0.5m for pile and soil elements and it remains the same upto bottom of soil domain. Further, the soil element size is increased laterally from near the pile to lateral end of domain while the vertical size is kept constant. Pier element size is also kept at 0.3x0.3x0.5m. The final domain is shown in Fig. 3 which is used for further investigations. In case of loading of force couple, the model domain below the pile is extended up to 15*d*.

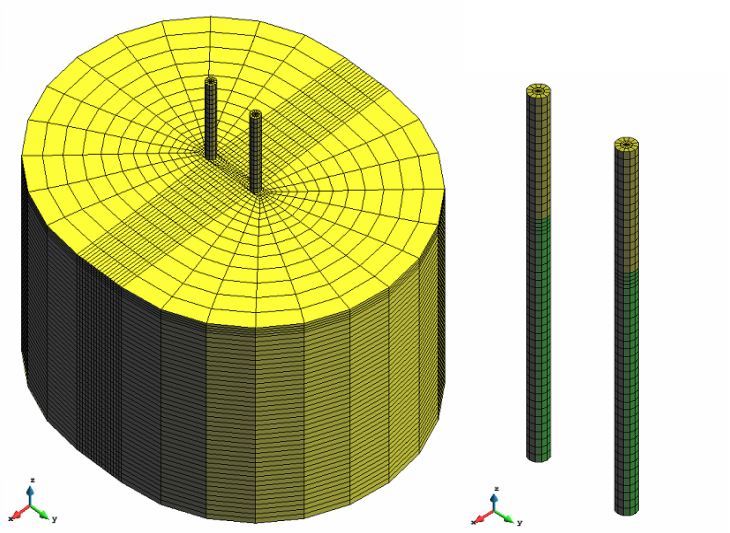


Fig. 3 3-D Model of two piles

Two piles having large spacing between them, when loaded on one pile should give the same response as that of the response of single pile. So, verification of only two pile 3-D model is done by comparing the only two-pile model 3-D FE ground level displacements of pile (only one pile is loaded) with 3-D FE model ground level displacements of single pile. The difference in computed displacement from two models was less than 2%. The single pile 3-D model is verified by comparing with Randolph (1981) solution and error was less than 3%.

CAPTURING EDGE EFFECT AND SHADOW EFFECT IN 1-D MODEL

The whole idea behind this study is to capture the pile-soil-pile interactions in the form of spring constants that can be used in 1-D models. To capture the edge effect, both piers are loaded by 1000 kN in the transverse direction on the top of each pier in 3-D model. The 3-D response of one pile out of two as ground level displacement for different spacing of piles is shown in Fig. 4a. It is used as target displacement to be matched by 1-D model displacements for each spacing of piles. In 1-D model pile-pier is idealized as beam column elements with discrete lateral translational springs subjected to lateral load of 1000 kN similar to mono-pile as shown in Fig. 5. The mesh size selected is 0.25m in laterally loaded pile and spring constant

is taken equal to the soil young's modulus. The interface between pile and soil is assumed to be perfectly bonded. 1-D response of single pile for lateral load as ground level displacement is plotted in Fig. 5b. The spring constant factor is determined for every Young's modulus of soil considered for different spacing of piles by minimizing the difference between the deflections from 1-D and 3-D linear models (Rani and Prashant 2014). The lateral spring factor in transverse direction (f_{ppt}) was found out to be function of soil's Young's modulus for different spacing of piles and is given by plotted in Fig. 6a. The lateral spring constant factor in transverse direction (f_{ppt}) can be estimated by using eq. (1) which have root mean square error of about 0.1 to 0.15 for different spacing and diameter of piles.

$$f_{ppt} = 9 * (1 - \left(\frac{d}{s}\right))^{0.4} * \left(\frac{E_s}{E_p}\right)^{0.2} \quad (1)$$

To capture the pile-soil-pile interaction due to lateral load in longitudinal direction, both piers are loaded in the longitudinal direction on the top of each pier in 3-D model. The response of one pile out of two as ground level displacement for different spacing of piles is shown in Fig. 4b and is used as target displacement to be matched by 1-D model (Fig. 7a) displacements for each spacing. The spring constant factor is determined for every Young's modulus of soil for different spacing of piles by minimizing the difference between the deflections from 1-D and 3-D linear models. The lateral spring constant factor in longitudinal direction (f_{ppl}) was found to be function of soil's Young's modulus as shown in Fig. 6b and this relationship can be approximated by eq. (2) which have root mean square error of about 0.1 to 0.15 for different spacing and diameter of piles.

$$f_{ppl} = 9 * (1 - \left(\frac{d}{s}\right))^{0.5} * \left(\frac{E_s}{E_p}\right)^{0.2} \quad (2)$$

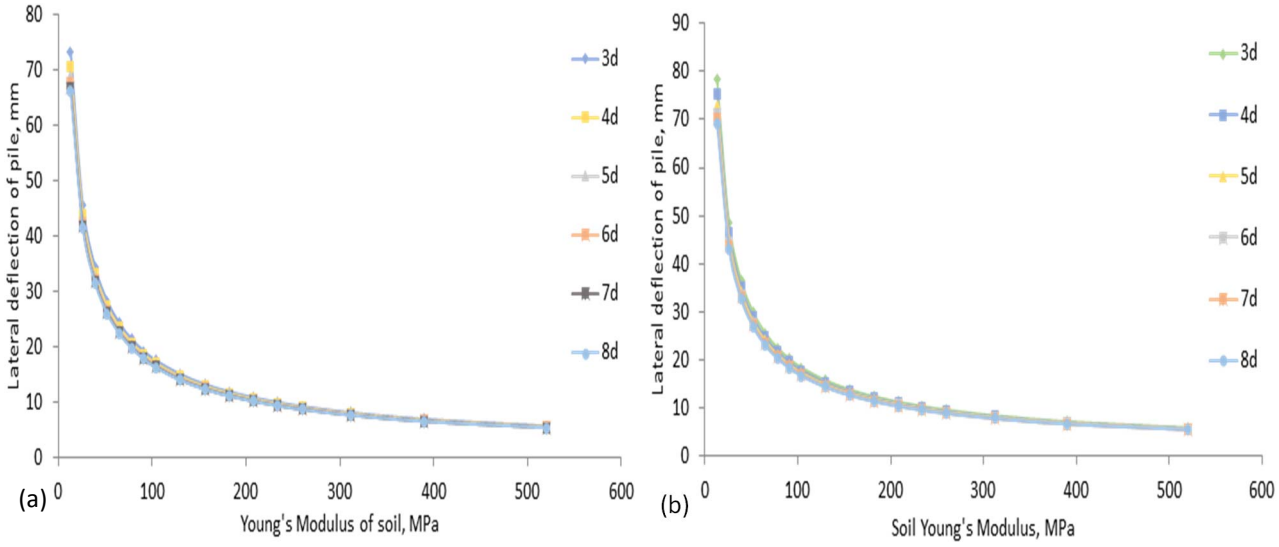


Fig. 4 3-D response of two piles subjected to load at top of pier in a) Transverse direction b) Longitudinal direction

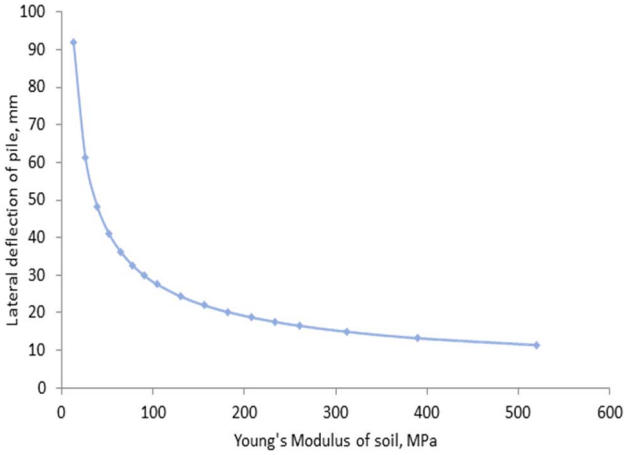


Fig. 5 1-D response of single piles subjected to a lateral load at top of pier

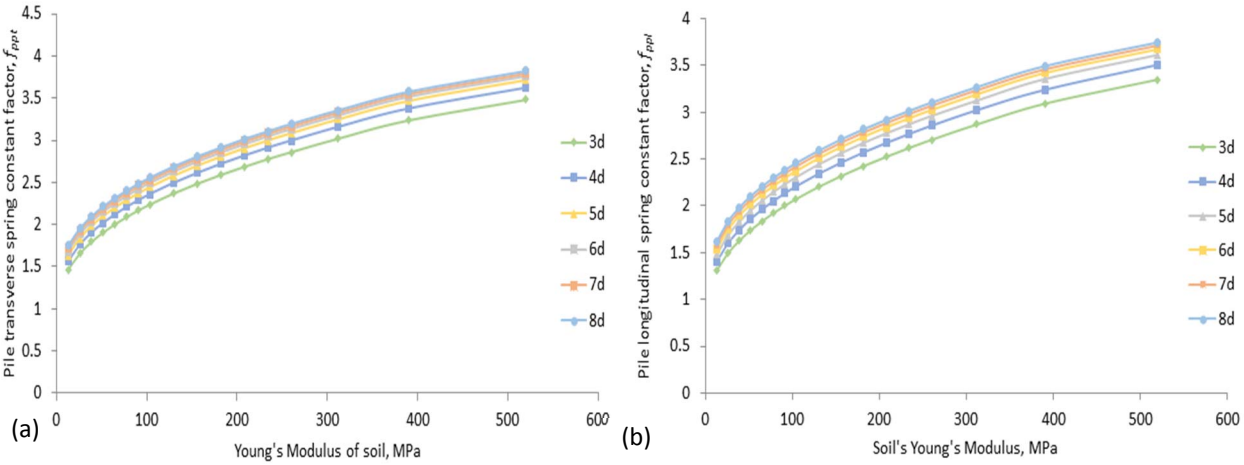


Fig. 6 Spring constant factors of pile for a) Edge effect b) Shadow effect

CAPTURING VERTICAL INTERACTION EFFECT IN 1-D MODEL

To capture the pile-soil-pile interaction due to vertical load, both piers are loaded by 8000 kN in the vertically downward direction on the top of each pier in 3-D model. The response of one pile out of two, as ground level displacement for different spacing of piles, is shown in Fig. 9a and is used as target displacement to be matched by 1-D model displacements for all spacing's of piles. 1-D model of pile-pier is idealized in which beam with discrete vertical translational springs subjected to a vertical load of 8000 kN as shown in Fig. 7b. The mesh size selected is 1m in this model. Base resistance of pile is neglected in this model as most of the piles are bored piles. 1-D response of pile subjected to vertical load as ground level displacement is plotted in Fig. 8a. The spring constant factor is determined for every Young's modulus of soil for different spacing of piles by minimizing the difference between the deflections from 1-D and 3-D linear models. The vertical spring factor (f_{ppv}) (Fig. 8b) was found out to be less dependent on soil Young's modulus for different spacing of piles and hence equation is proposed independent of soil modulus as given by eq. (3) which have root mean square error of about 0.02 for different spacing and diameter of piles.

$$f_{ppv} = 0.7 * (1 - \left(\frac{d}{s}\right))^{0.7} \quad (3)$$

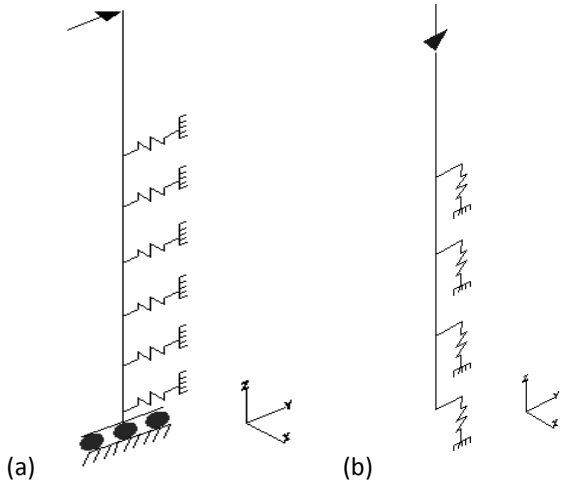


Fig. 7 1-D Model of single pile with pier subjected to a) lateral load b) vertical load

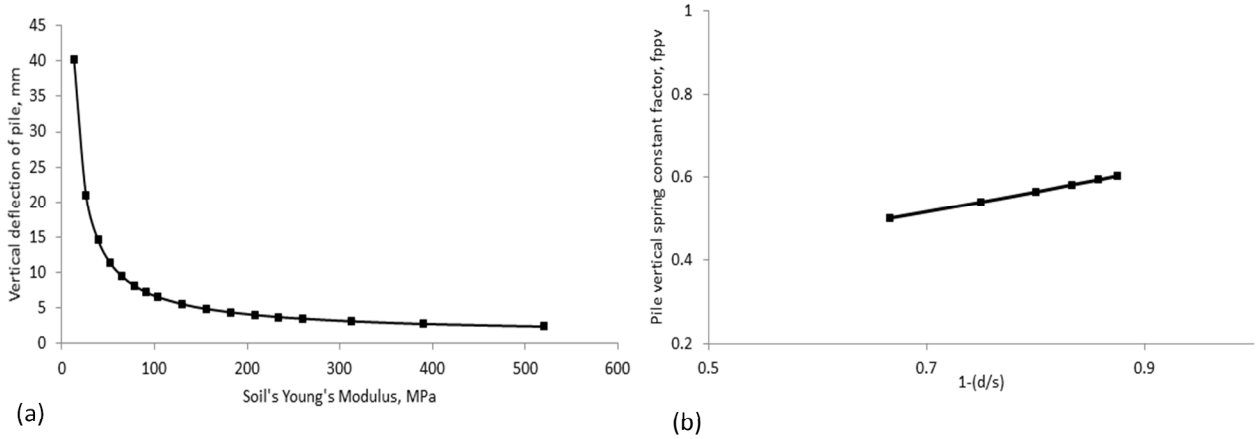


Fig. 8 a) 1-D response of single pile subjected to vertical load b) Corresponding vertical pile spring constant factor

CAPTURING COUPLE EFFECT IN 1-D MODEL

In order to capture the couple effect, one pile is loaded vertically upwards while the other pile is loaded vertically downward but with the same magnitude of 8000 kN load in 3-D model. The response of one of the pile out of two as ground level displacement for different spacing of piles is shown in Fig. 9b.

To capture the interaction due to force couple in 1-D model a new type of two piles model with couple interaction springs is considered as shown in Fig. 10a. In this model, the pile nodes parallel to each other are connected to a zero length vertical springs. These interaction springs are given equal degree of freedom to pile nodes, these springs will come into picture only when there is relative movement of pile nodes. The mesh size for the pile in this case is selected to be 0.25m.

The spring constant factor is determined for every Young's modulus of soil for different spacing of piles by minimizing the difference between the deflections from 1-D and 3-D linear models by iterating

the interaction spring constant factor while the vertical spring constants of pile are kept as calculated from eq. (3). The couple interaction spring factor (f_{cppv}) (Fig. 10b) due to couple effect is noted to be independent of Young's modulus of soil and is given by eq. (4) which have root mean square error of about 0.01 for different spacing's and diameters..

$$f_{cppv} = 1.5 * \left(\frac{d}{s}\right) \quad (4)$$

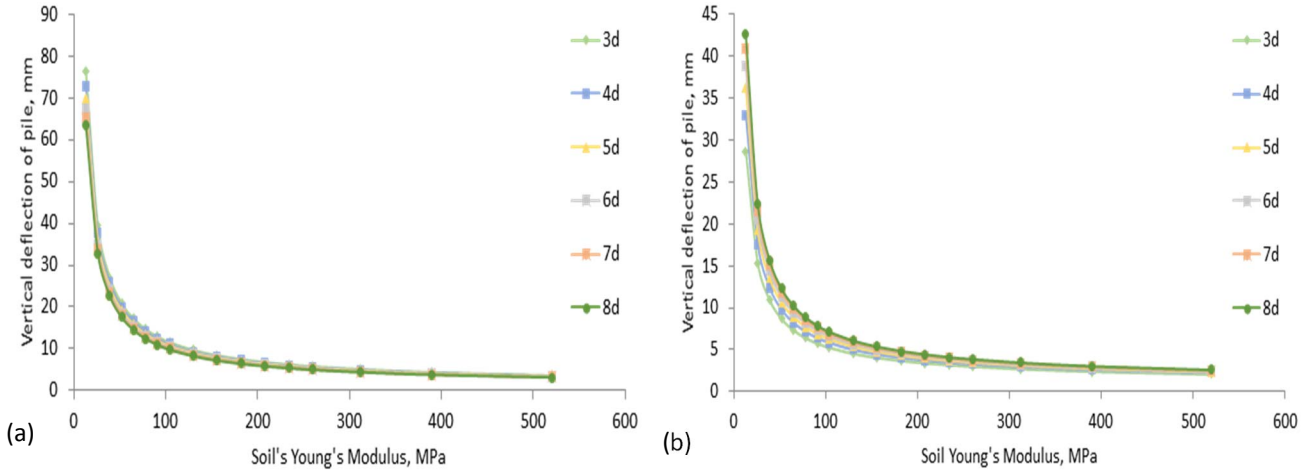


Fig. 9 3-D response of two piles subjected load at top of pier as a) Vertical load b) Couple force

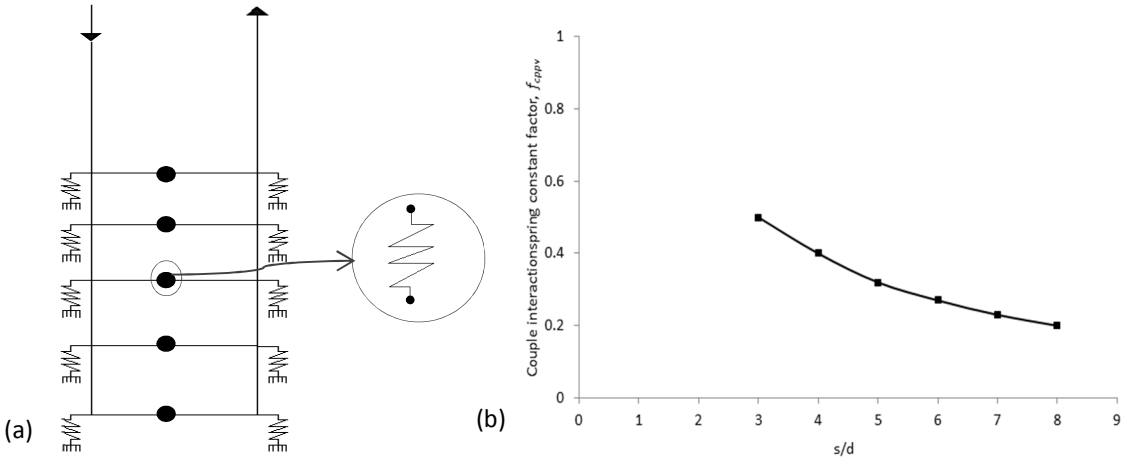


Fig. 10 a) 1-D Model of two piles subjected to a force couple with couple interaction springs b) Corresponding couple interaction spring constant factor

SUMMARY

Pile-soil-pile interaction plays a key role in the final response of duo-pile system. In this study an attempt was made to capture them in the form of spring constant factors to be used in 1-D model. For each interaction, appropriate 1-D models are presented and the corresponding spring constant factors are proposed. A new type of interaction between piles called couple interaction that will even prevail in the group piles is identified and explained. A 1-D model for capturing couple effect is proposed which can be extended to simplify modelling of group piles with appropriate spring constant factors. These spring constants further can be used in full 1-D model of a duo-pile or a pile group.

REFERENCES

AASHTO. (2000). Bridge design specifications, Washington, DC.

Allahverdizadeh, P. (2015). “Group effects on piles behavior under lateral loading.” In IFCEE 2015 (pp. 1142-1151).

Ashour, M., Pilling, P., & Norris, G. (2004). “Lateral behavior of pile groups in layered soils.” Journal of Geotechnical and Geoenvironmental Engineering, 130(6), 580-592.

Budiman, J., & Ahn, K. (2005). “Effects of pile cap in single pile and lateral capacity of pile group.” In Advances in Deep Foundations (pp. 1-16).

Canadian Geotechnical Society. Foundations Committee. (1978). “Canadian foundation engineering manual.” Canadian geotechnical society.

Chandrasekaran, S. S., Boominathan, A., & Dodagoudar, G. R. (2010). “Experimental investigations on the behaviour of pile groups in clay under lateral cyclic loading.” Geotechnical and Geological Engineering, 28(5), 603-617.

Daloglu, A. T., & Vallabhan, C. G. (2000). “Values of k for Slab on Winkler Foundation. Journal of Geotechnical and Geoenvironmental Engineering,” 126(5), 463-471.

Hetényi, M. (1946). “Beams on Elastic Foundation: Theory with Applications in the Fields of Civil and Mechanical Engineery.” University of Michigan press.

Japan Road Association. (1980). “Specifications for road bridges.” Vol. IV (in Japanese).

Joseph, E. Bowels. (1982), “Foundation Analysis and Design.” Singapore. Mc.

Matlock, H. (1970). "Correlations for design of laterally loaded piles in soft clay." Proceeding 2nd Offshore Technology Conference, Houston, Texas, 1, 577-594.

Matlok, H, M. and Reese, C. L. (1960). "Generalized solution for Laterally Loaded Piles." Journal of the Soil Mechanics and Foundation Divisions, Proceedings of the American Society of Civil Engineers.

Mylonakis, G. (2001). “Winkler modulus for axially loaded piles.” Geotechnique, 51(5), 455-462.

Ooi, P. S., Chang, B. K., & Wang, S. (2004). “Simplified lateral load analyses of fixed-head piles and pile groups.” Journal of Geotechnical and Geoenvironmental Engineering, 130(11), 1140-1151.

Poulos, H. G., & Davis, E. H. (1980). “Pile foundation analysis and design”

Poulos, H. G. (1971a). "Behavior of laterally loaded piles: I – single piles." Journal of Soil Mechanics, ASCE, 97(SM5), 711-731.

Randolph, M. F. (1981). "The response of flexible piles to lateral loading." Geotechnique, 31(2), pp 247-259.

Rani, S. (2013). "Estimation of linear spring constant of laterally loaded pile embedded in nonlinear soil." M.Tech Thesis, Indian Institute of Technology Gandhinagar, India.

Rani, S., & Prashant, A. (2014). “Estimation of the linear spring constant for a laterally loaded monopile embedded in nonlinear soil.” International Journal of Geomechanics, 15(6), 04014090.

Rani, S., & Prashant, A. (2014). “Difficulties in 1D Modelling and Analysis of Monopile subjected to Lateral Force.” In Tunneling and Underground Construction (pp. 385-395).

Reese, L. C., Cox, W. R. & Koop, F. D. (1974). "Analysis of laterally loaded piles in sand." Proceedings 6th Offshore Technology Conference, Houston, Texas, 2, 473-483.

Reese, L. C. & Welch, R. C. (1975) "Lateral loading of deep foundations in stiff clay," Journal of Geotechnical Engineering, ASCE, Vol: 101, No. GT7, pp 633-649.

Reese, L. C. (2001). Van Impe. WF, Single Piles and Pile Groups under Lateral Loading, AA Balkema, Rotterdam.

Rollins, K. M., Olsen, K. G., Jensen, D. H., Garrett, B. H., Olsen, R. J., & Egbert, J. J. (2006). “Pile spacing effects on lateral pile group behavior: Analysis.” Journal of geotechnical and geoenvironmental engineering, 132(10), 1272-1283.

Scott, R. F. (1981). "Foundation Analysis." Prentice-Hall, Inc., Englewood Cliffs, NJ 07632.

Terzaghi, K. (1955). "Evaluation of Subgrade Reaction." Geotechnique, England, 5(4), 279-326.

U.S. Army Corps of Engineers (USACE). (1993). “Design of pile foundations.” Technical engineering and design guides No. 1, Washington, DC.

Winkler, E. (1867). "Die Lehre von der Elasticitaet und Festigkeit." Prag, Dominicus.

Yang, Z., Lu, J., and Elgamal, A., (2008) "OpenSees Soil Models and Solid-fluid Fully Coupled Elements: User's Manual, Version 1," University of California, San Diego.

A REVIEW ON T SHAPED DEEP MIXING TECHNOLOGY IN ENGINEERING PROJECTS

Rashmi Patel, Research Scholar, SVKM's NMIMS MPSTME, Mumbai, Maharashtra, India, swtrashmi@gmail.com
Jigisha Vashi, Assistant Professor, SVKM's NMIMS MPSTME, Mumbai, Maharashtra, India, vashi.jigisha@gmail.com

Abstract:

Deep mixing (DM) method is commonly used for supporting embankments on soft grounds for highway and railway engineering. This method is replete with issues of insufficient mixing, grout spilling, and column strength decreasing with depth. These problems can be resolved by the new technology of T-Shaped Deep Mixing column, which improves the quality of soft soil, which in turn further improves the embankment stability. TDM column have an enlarged cap and therefore it can take more applied load in comparison to the conventional column which further results in less stress in soil further resulting in decreased soil settlement and differential settlement of the ground, and an increase in consolidation rate. The parameters studied here for field embankment loading conditions were, stress concentration ratio, excess pore water pressures generated in the soft clays, total monitored settlement, and lateral soil displacement. From the literature it is observed that TDM columns has significant advantages over conventional DM columns because of mitigation of settlement and improved performance of the embankments while decreasing construction costs. It is also found that material used in TDM column is less compared to conventional DM column which decreases the construction cost of the project. The results indicate that TDM method is a more economic and efficient solution for soft ground improvement under embankments. Earlier works by numerous researchers on T- shaped deep mixing column including laboratory work, full-scale field tests, analytical and numerical analyses related to improvement of soft soil is reviewed in this paper. Results are discussed with the help of figures depicting charts, failure modes and it has been found that T- shaped deep mixing method provides an enhanced alternative to the existing methods of improving soft clay with regard to soil bearing capacity and settlement criterion.

Introduction

T shaped deep mixing methodology is a new method for construction of TDM column to support highway and railway embankment. The column shape relates to letter 'T', where the diameter of the column is larger at the shallow depth and lesser at the deeper depth. This technique can reduce the amount of cement and overall construction cost of the project which leads to more economical solution in comparison to conventional DM column. Liu., et. al 2012, from the research evaluated that maximum soil lateral displacement of TDM column supported ground is 44% and 47% at site A and B at Husuzhe Highway in Jiangsu Province, China., that of conventional DM supported ground at site C at the same location, which indicated that the TDM column had better performance than DM column in inducing lesser settlement in both vertical and lateral directions under embankment loading; the field study indicated that TDM columns provide a economical and a technologically sound solution for soft ground improvement in comparison to DM column. Yi., et. al 2009 also performed experiment which found that the maximum lateral displacement in TDM column was much less in comparison to DM column which showed that TDM column was more economical.

© 2018 Deep Foundations Institute

Research on T-shaped Deep Mixing Method.

Laboratory and Field Research

Liu., et. al 2012 carried out field tests on highway embankment on soft clayey soil supported by both TDM and conventional DM columns. Column installation, in situ plate loading tests, and monitoring results under embankment loading, including stress concentration ratio, column efficacy, excess pore water pressure, ground total settlement, and lateral soil displacement at the embankment toe were evaluated for three different sites A, B, and C at Husuzhe Highway in Jiangsu Province, China. Site A and B were installed with TDM columns and site C was installed with conventional DM column. It was found from the research that at site A and B there was cement saving of 15 and 7% by weight and construction time saving of 28 and 19% in comparison to conventional DM columns. Ultimate bearing capacities of TDM columns supported ground was more than twice of those of conventional DM supported ground. It was further found that the stress concentration ratio of TDM column supported was lower than the ground supported by DM columns. It was also observed that the post construction settlement of TDM column-supported ground is 72% and 47 % at site A and B, respectively that of conventional DM column supported ground at site C. Yi., et.al 2017 studied 1-g laboratory and full-scale field loading tests to investigate the vertical bearing capacity behavior of single T-shaped column on soft ground. The results indicated that the ultimate bearing capacity of a T-shaped column was considerably higher than that of the corresponding conventional column, and it generally increased with the diameter and length of column cap. Since the section area of the column cap was remarkably higher than that of the deep-depth column, the stress concentration occurred in the deep-depth column just under the cap, leading to column failure there.

Yi., et. al 2009 found for similar embankment height, the maximal lateral displacement in TDM column composite foundation was 20.84 mm while in conventional DM column composite foundation was 55.57 mm. it was observed that ground surface settlement and maximal lateral displacement in TDM composite foundation are much less than in conventional DM column composite foundation while cost less cement. The lateral displacement for both the column can be compared from the figure.1. a & 1.b

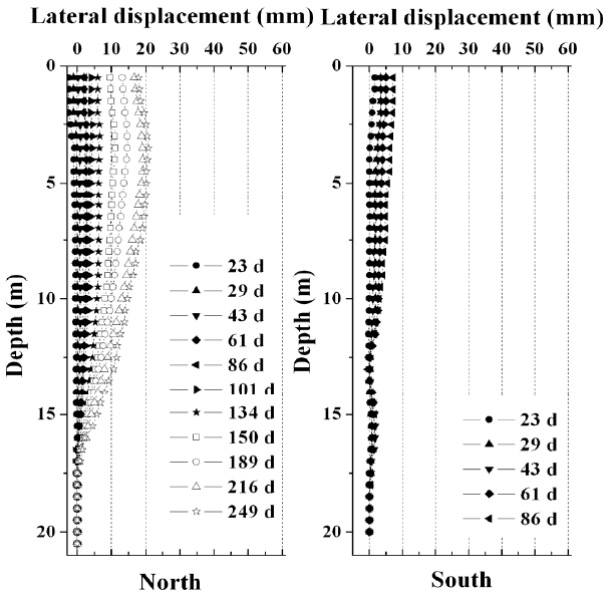


Fig. a. TDM column composite column

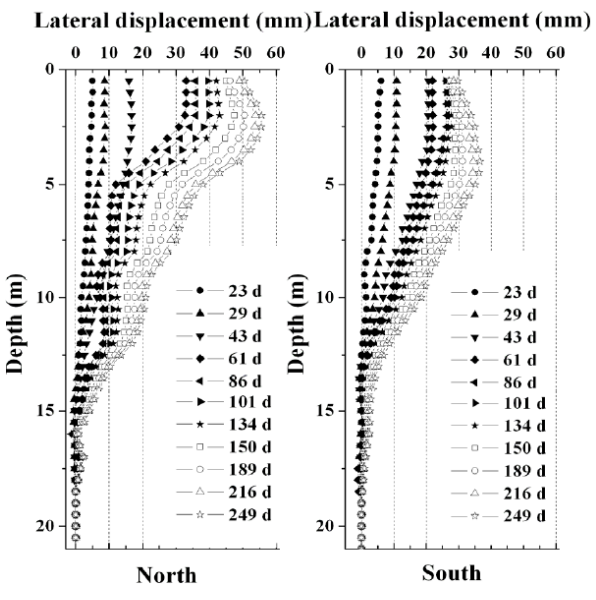


Fig. b. conventional DM column composite column

Fig 1. Variation of lateral displacement during embankment filling

Yi., et.al 2012 considered two similar field test sites at Husuzhe Highway in Jiangsu Province, China, and observed that the TDM column installation resulted in 6.5% reduction in cement use and 19% reduction of construction time when compared with the conventional DM column installation. The total settlement and the maximum lateral movement of the TDM column treated ground were only 67% and 31% that of the conventional DM column treated ground, indicating the performance of the former was superior to that of the latter. Liu., et.al 2009 observed that double slurry mixing method can significantly improve the mixing uniformity of columns than the single slurry mixing method. Yi., et.al 2016 performed laboratory test and observed that the T-shaped column had an enlarged cap, more applied load was taken by the T-shaped column than by the conventional column, resulting in less stress on the soil. This effect reduced the soil settlement and differential settlement of the ground and increased its consolidation rate.

Numerical Research

Yi., et.al. 2010 investigated the performance of the three layered soft ground improved by cross shaped DM columns and comparing it with conventional DM columns. The analysis was carried out in FLAC 3D and it was found that the maximum surface settlement improved by 37.1% for cross shaped DM column over conventional DM column. Xi., et.al. 2014 studied the load transfer mechanism based on the fast Lagrangian finite difference method for T shaped DM columns at different load levels and it was found that the axial force increased with the load level increasing and the axial force decay velocity of expanding head was much faster than the lower part. Bolton., et.al., 2015 investigated the effect of soil cement column diameter and spacing on overall settlement beneath a road embankment situated on normally consolidated estuarine deposits in the South East Queensland region. PLAXIS 2D was used for the modelling and it evaluated that there was considerable decrease in settlement at equivalent Area Replacement Ratios when using smaller diameter columns at closer center to center spacings when compared to larger diameter columns at higher spacings. The study also shows that the use of soil cement columns results in overall settlements of below 20% of the actual measured embankment settlement. The resulting reduction in settlement could result in a significantly reduced delay in the construction sequence.

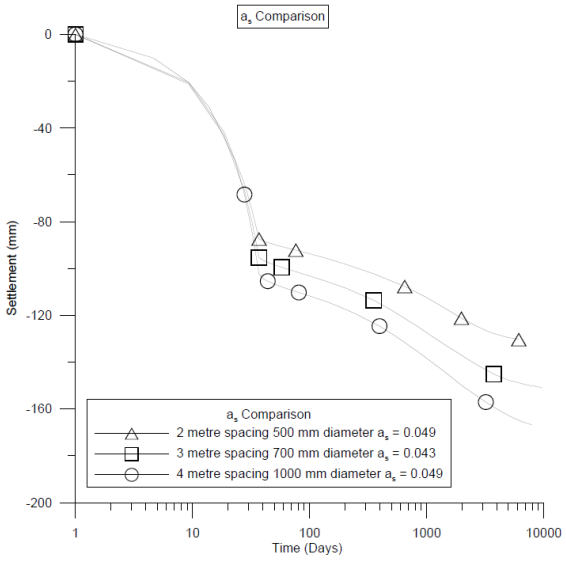


Fig.2.a Settlement comparison of similar area replacement ratio

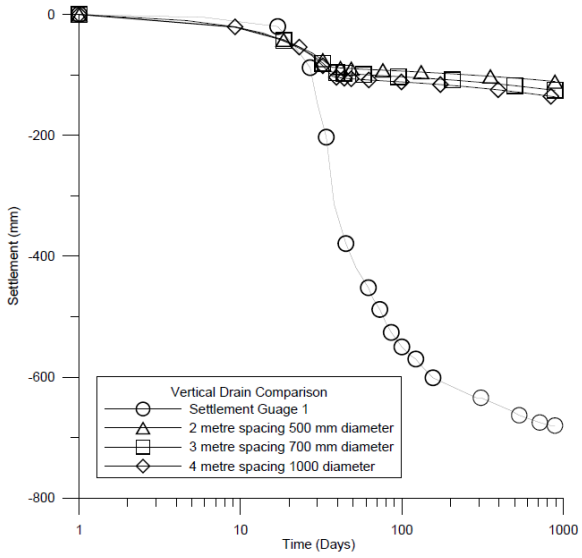


Fig. 2.b Settlement comparison of SG-1 with model results at a_s = 0.49

Bolton., et.al., 2015 showed that there is a considerable reduction in settlement, as would be expected, when comparing the actual embankment settlement to the modelled data which can be observed from figure 2.a & 2.b.

Conclusion

From the above literature review, it is obvious that the T shaped deep mixing method provides a better alternative to the existing method of conventional Deep Mixing for improving soft clay ground and is suitable for use on any type of soil property.

TDM columns was selected as the ideal alternative to mitigate a potentially weak foundation. The results of this study have shown the beneficial effects of deep soil mixing. Therefore, On the basis of literature survey carried out following concluding remarks are made:

- With respect to conventional DM column supported ground, TDM column supported ground offers reduced total settlement and postconstruction settlement
- High strengths can be achieved in the final soil cement product.
- Lateral settlement of columns is less in TDM column compared to conventional DM column
- Ultimate Bearing Capacity of ground is more in TDM column compared to conventional DM column
- Stress concentration ratio is also less in TDM columns compared to DM columns

References

Bolton M., Noonan J., and Erwin O., 2016. Effect of soil cement column spacing and Area replacement ratio on Embankment Bearing Capacity: A Queenland case study. International Journal of GEOMATE, Oct., 2016, Vol. 11, Issue 26, pp. 2589-2594

Chen L and Liu S.Y.,2008. Consolidation Calculation of Soft Ground Improved by T-shaped Deep Mixing Columns. GeoCongress 2008, 620-627.

Liu S.Y., Zhang D., and Zhu Z., 2009. On the Uniformity of Deep Mixed Soil-Cement Columns with ElectricalResistivity Method . Advances in Ground Improvement. Pp. 140-149

Liu S.Y., Du Y.J., Yi Y.L., and Puppala A.J., 2012. Field Investigations on Performance of T-Shaped Deep Mixed Soil Cement Column–Supported Embankments over Soft Ground. Journal of Geotechnical and Geoenvironmental Engineering- ASCE , Vol-138, No.6, pp. 718-727.

Muntohar A.S., 2010. A Laboratory test on the strength and load settlement characteristics of improved soft soil sing lime column. Dinamika TEKNIK SIPIL/Vol. 10/No.3/September 2010: pp. 202-207

Rashid A.S., Bunawan A.R., and Said K.N., 2017. STATE-OF-THE-ART REVIEW-The Deep Mixing Method: Bearing Capacity Studies. Geotechnical Geological Engineering (Springer) Vol 35, Issue 4, pp 1271-1298

Xi P., Zhang X., Liu B., 2014. Numerical simulation of load transfer mechanism of T-shaped soil-cement deep mixing column. Applied Mechanics and Materials Vols. 580-583 (2014) pp 118-122.

Yao K., Yao Z., Song X., Zhang X., Huc J.,and Pan X., 2016. Settlement evaluation of soft ground reinforced by deep mixed columns. International Journal of Pavement Research and Technology 9 (2016) pp. 460–465

Yi, Y.L. and Liu, S.Y., 2008. Bearing behavior of single T-shaped cement-soil deep mixing column. Proceeding of International Symposium on Lowland Technology, 261-265.

Yi Y., Liu S.Y., Zhang D., and Zhu Z., 2009. Experimental Study on T-shaped Soil-cement Deep Mixing Column Composite Foundation. GeoHunan International Conference 2009, pp1-7

Yi Y., Liu S.Y., Du Y., Jing F., and Gong N., 2010. Comparison of performance between cross shaped and conventional deep mixed columns for three layered soft ground improvement under embankment load. Geo-Shanghai 2010 International Conference- PP 65 -70.

Yi Y', Liu S.Y., Du Y., Zhu Z., and Du G., 2012. The T-Shaped Deep Mixed Column Application in Soft Ground Improvement. Proceedings of the Fourth International Conference on Grouting and Deep Mixing, pp. 389-399

Yi Y., Liu S., Puppala AJ., 2016. Laboratory modelling of T-shaped soil–cement column for soft ground treatment under embankment. Geotechnique 66(1): pp.85–89

Yi Y., Liu S.Y., Puppala A.J., Xi P.,2017. Vertical bearing capacity behaviour of single T-shaped soil–cement column in soft ground: laboratory modelling, field test, and calculation. Acta Geotechnica-Springer-Verlag Berlin Heidelberg

ASSESSING DEPTH OF WELL FOUNDATION – CASE STUDY

Ravi Sundaram, Cengrs Geotechnica Pvt. Ltd., A-100 Sector 63, Noida, Uttar Pradesh, India 9810538095
ravi@cengrs.com
Sanjay Gupta, Cengrs Geotechnica Pvt. Ltd., A-100 Sector 63, Noida, Uttar Pradesh, India 9810138095
sanjay@cengrs.com
Sorabh Gupta, Cengrs Geotechnica Pvt. Ltd., A-100 Sector 63, Noida, Uttar Pradesh, India 9910861118
sorabh@cengrs.com

ABSTRACT

Parallel seismic test and sonic pulse echo response test are effective non-destructive methods to determine the depth of an existing foundation. The paper presents a case where depth of well foundation installed for a bridge across a drain was questioned by the owner. While the contractor insisted that the well depth was 12.2 m below the well cap as per the drawings, the owner doubted it. The results conclusively proved that the well depth was about 11 m below the well cap. The tests provided a scientific basis for confirming the as-constructed depth of the foundation.

Keywords: foundation depth assessment, NDT Testing, Parallel seismic test, sonic echo response test, well foundations

INTRODUCTION

Well foundations had been provided for a bridge under construction across a drain in Faridabad (Haryana), Due to a debate with the contractor, the owner wanted a confirmation on the depth of the wells. As per the drawings, the well depth was 12.2 m below the well cap but the customer doubted whether the well had actually been extended to the required depth.

To resolve the issue and preferably avoid litigation, it was decided to go in for non-destructive testing. The non-destructive determination of depth of unknown foundation (Olson et al. 1996) used for this study is as follows:

- Sonic Echo / Impulse Response test.
- Borehole Parallel Seismic method, and

The authors have used a combination of these techniques to assess unknown depth of piles (Sanjay Gupta et al, 2015). The paper presents a case study demonstrating application of NDT methods to assess the depth of well foundations installed for the bridge and confirms reliability of the technique for such application .

While the tests are usually carried out to assess unknown depth of piles, this case study presents application for well foundation. The analysis for well foundation presents a challenge because the concrete well has filled with sand and water.

PROJECT DETAILS

A four lane dual carriageway bridge was under construction across a drain in Faridabad (Haryana). Six well foundations, four wells for the abutment (two at each abutment) and two wells for the piers had been provided.

© 2018 Deep Foundations Institute

As per the project specifications, the well foundation dimensions are as follows:

Outer Diameter of well	:	6.0 m
Thickness of well lining	:	650 mm
Depth of well below bed of drain	:	9.5 m
Depth of well below well cap	:	12.2 m

A view of the partly completed bridge is presented on Fig. 1. The further construction had been stopped by the owner to resolve the issue regarding well depth.



Fig. 1. View of the well cap and deck of bridge under construction

Fig. 2 presents a schematic section of the bridge at the well location showing the well details at the abutment location.

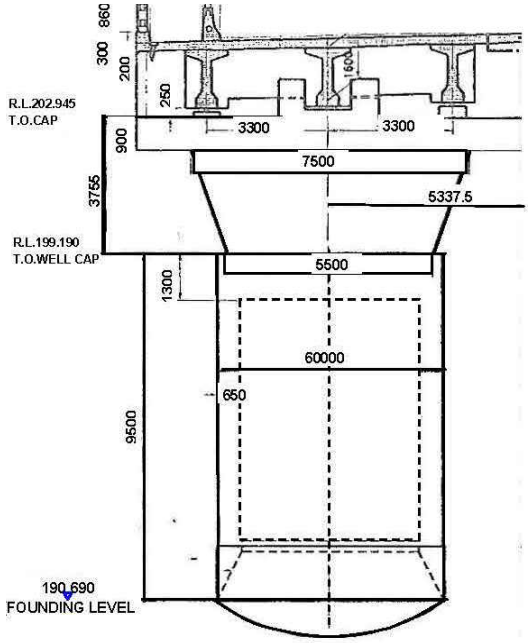


Fig. 2. Section of bridge at abutment well location

PULSE ECHO RESPONSE TEST

Low-strain pulse echo response test was carried out at the project site using a hand held hammer (Rausche et al, 1988). A photograph of the test equipment is presented on Fig. 3. The equipment, primarily used for low strain pile integrity testing, has been used to evaluate the well depth.



Fig. 3. Pulse Echo Response Equipment

A small portion of the well cap was leveled and the accelerometer was placed on it. The hammer was impacted on the edge of the well cap. The response obtained is presented on Fig, 3.

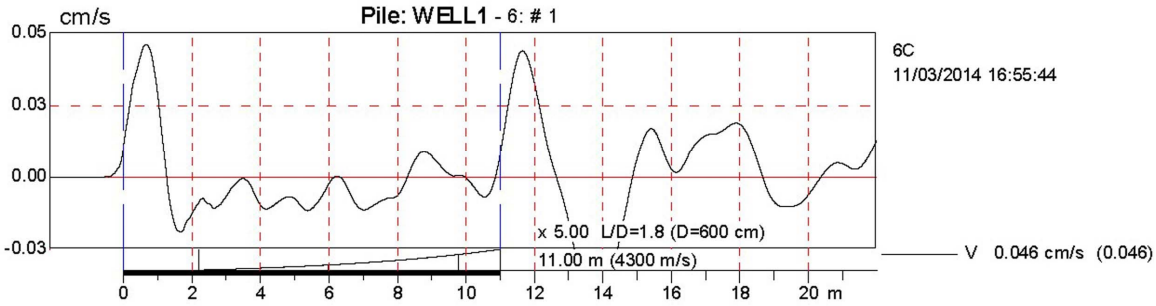


Fig. 4. Sonic echo response data (time domain)

For the purpose of analysis, the velocity of the wave was taken as 4300 m/s. A strong reflection at 11 m depth suggested that the well depth below the well cap is about 11 m.

For a better assessment, a profile analysis was done (Rausche and Likins, 2000). The results of the analysis are presented in Fig. 5. Reviewing the well profile interpreted from the test, the interpreted well depth is 11 m.

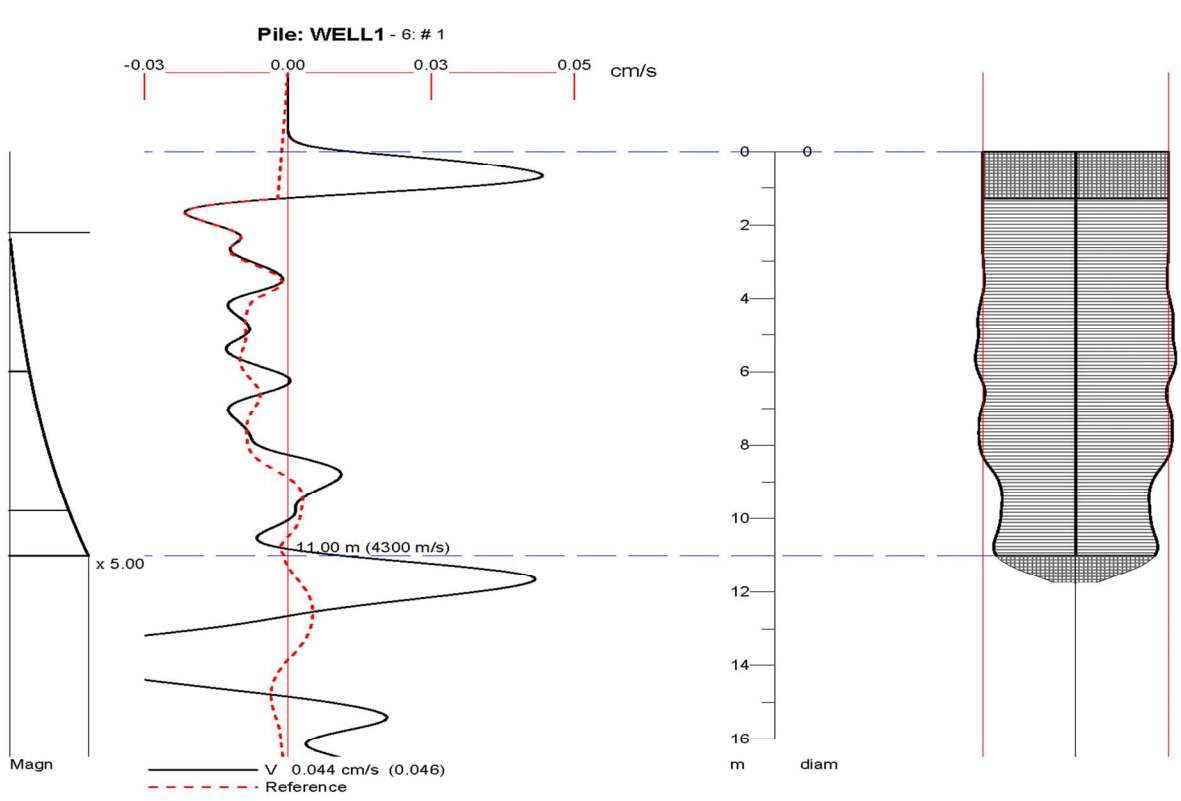


Fig. 5. Sonic echo response Well Profile Analysis

The well profile analysis from the pulse-echo test suggested that the bottom of the well was probably at about 11 m depth. It also indicated possible reduction in diameter of the well below 9 m depth.

PARALLEL SEISMIC TEST

To assess the depth of the well foundation, parallel seismic test was performed on one abutment. The test can give reasonable assessment of depth of unknown foundation (Stain, 1982). The basic concept is that if there is a change in the trend of wave-arrival time and the velocity when reflection is obtained from the concrete foundation and that obtained from soil medium. For good results, a borehole is drilled as close to the existing foundation as possible and geophone is placed in the hole to obtain the response as a hammer impacts the top of the foundation.

For conducting the test, a borehole was drilled about 0.9 m distance from the RCC false steining of the well foundation at an abutment location. The borehole diameter was 150 mm. A 75 mm diameter PVC pipe was placed in the hole and the annular space between the pipe and the hole was grouted using cement-bentonite slurry. The grout was allowed to set for about a week before performing the test.

A 5 kg hand-held hammer with a teflon tip was used to impact the bridge structure. The point for hammer impact was selected carefully on the edge of the well cap so as to ensure that the wave travels through concrete.

Two down-hole triaxial geophones at 1.0 m spacing were used to receive the compression and shear waves traveling down the foundation. Measurements were taken for every 1.0 m depth interval up to the final borehole depth of 18.5 m. A schematic of the test setup is presented on Fig. 6.

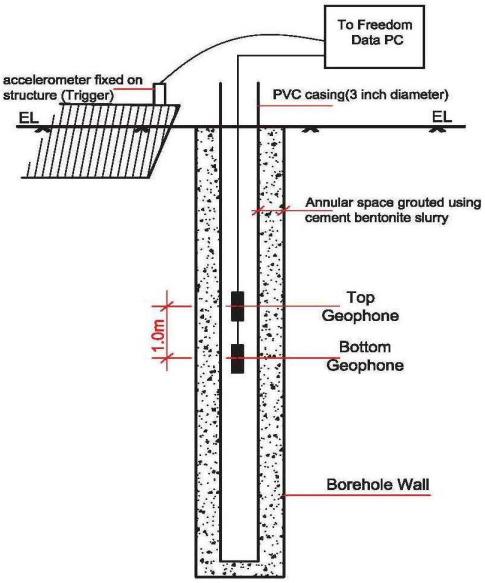


Fig. 6. Schematic of Test Arrangement

The data acquired is the time of arrival of the P-wave. The arrival times from both geophones (spaced 1 m apart) are recorded and plotted versus depth. A clear change in the slope of the time of arrival of P-wave versus depth (See Fig. 7) helped identify the well depth.

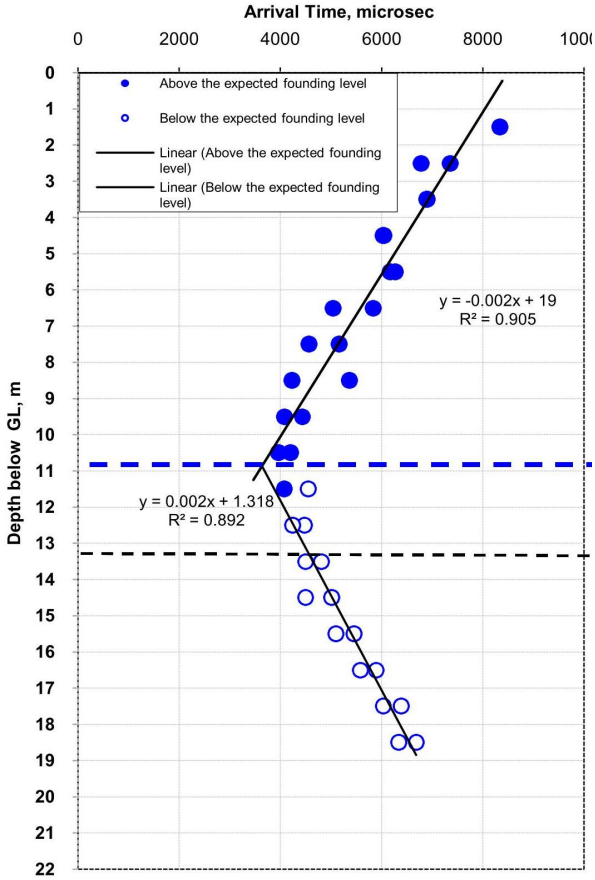


Fig. 7 Parallel seismic test results – Arrival time versus depth

To estimate the trend of wave velocity, it was plotted against the hypotenuse distance between the geophone and the top of the well. A clear break is seen and the change is observed at 11.2 m depth.

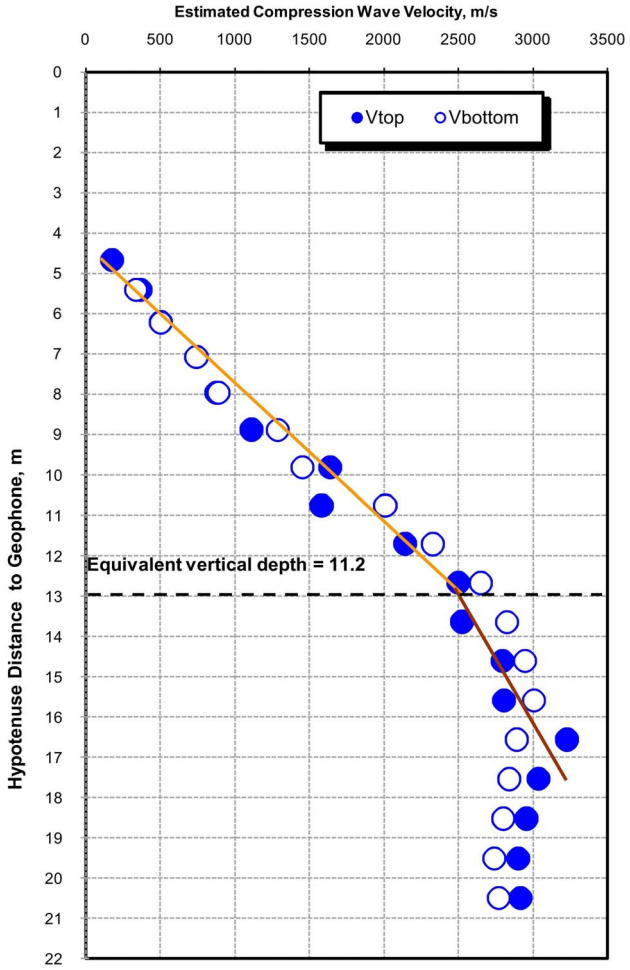


Fig. 8 Parallel seismic test results – P-wave velocity versus hypotenuse depth

The results of the parallel seismic test indicated well depth of 11.2 m whereas the pulse-echo test indicated well depth of 11 m.

INTERPRETED WELL DEPTH

The interpretation is based on the analysis of the wave arrival time. The tests confirmed that the well extended to 11.2 m depth below the well cap, falling marginally short of the required depth of 12.2 m. The test provided a basis for taking a decision on the issue to conclude the debate in a scientific manner. It helped the owner and the contractor resolve the issue.

CONCLUDING REMARKS

Parallel seismic test is a proven method of assessing unknown depth of an existing foundation. It is commonly used to assess pile depth. Coupled with pulse-echo response test, usually used to assess integrity of piles, a very good and reliable assessment of foundation depth can be made.

The present case study demonstrates successful assessment of well foundation depth using these two tests. The tests provide a reliable option for forensic evaluation to resolve disputes on the depth of deep foundations.

REFERENCES

Sanjay Gupta, Ravi Sundaram, Sorabh Gupta (2015). NDT techniques for determining depth of foundations, Proceedings, *Indian Geotechnical Conference, IGC-2015*, Pune.

Olson, L. D., Ming Liu and Marwan F. Aouad, Borehole NDT techniques for unknown subsurface bridge foundation testing, *Proc. SPIE 2946, Nondestructive Evaluation of Bridges and Highways, 10 (November 13, 1996)*; doi: 10.1117 / 12. 259133.

Stain, R.T. (1982), Integrity Testing, *Civil Engineering*, New York, NY, April, pp.53-73.

Rausche, F., Likins, G. E., Hussein, M.H. (1988), Pile Integrity By Low And High Strain Impacts, *Third International Conference on the Application of Stress-Wave Theory to Piles*, Ottawa, Canada; 44-55.

Rausche, F., Likins, G. E. (2000), Recent Advance and proper use of PDI low strain pile integrity testing, *Application of Stress-Wave Theory to Piles*, Balkema, Rotterdam; 211-218.

DESIGN AND CONSTRUCTION OF PILE FOUNDATIONS IN THE CONGESTED PART OF OLD DHAKA CITY OF BANGLADESH - CASE STUDY ON MAYOR MOHAMMAD HANIF FLYOVER

- Avik Kumar Mandal, Chief General Manager, LEA Associates South Asia Pvt. Ltd., New Delhi, India, +91-9650806816, avik@lasaindia.com, m_avik74@yahoo.co.uk
- S. Sailesh, Associate General Manager, LEA Associates South Asia Pvt. Ltd., New Delhi, India, sailesh@lasaindia.com
- Pradyot Biswas, Associate Director, LEA Associates South Asia Pvt. Ltd., New Delhi, India, +91-9818010183, pradyotbiswas@lasaindia.com
- J. P. Das, Sr. Consultant (Bridges), LEA Associates South Asia Pvt. Ltd., New Delhi, India, jpdas@lasaindia.com
- Dinakar Mandal, Chief General Manager, LEA Associates South Asia Pvt. Ltd., New Delhi, India, dinakar@lasaindia.com

ABSTRACT

Presently Mayor Mohammad Hanif Flyover is the longest Elevated corridor in Bangladesh. This flyover was built in the congested part of the Old Dhaka City namely Sonir Akhra - Jatrabari - Gulistan - Polashi Area of Bangladesh connecting with the main highway bound to Chittagaong Port. The total length of the flyover was 10.6 km including 11 numbers of UP/Down ramps and related infrastructure. The entire flyover including all the ramps are supported by cast-in-situ RCC Bored Pile foundation of 1.20 m diameter and of varying length from 16.25 m to 37.25 m. The alignment of the flyover passes through the old Dhaka city having numbers of different types of underground utilities namely water pipe line, electric cable line, sewerage pipe lines, gas pipe lines and T&T lines. It was a great challenge to finalize the details of pile group and its cap for the foundation of entire flyover by keeping most of the major different utilities in its own position without relocating the same. As a result, separate design for all the 315 numbers of pile group of different regular and irregular shapes comprising of total 2366 numbers of pile shaft was done for the entire flyover. The LRFD method of AASHTO 4th Edition 2007 was adopted for the design of pile foundation of the flyover. Hydraulic Drilling Rig was used for pile boring and plant made ready mix concrete (RMC) through "Tremie" was used to do the pile concerting. This paper presents the detailed design philosophy and construction methodology of pile foundations of the flyover.

KEYWORDS

Flyover, Ramp, Geotechnical Investigation, Pile Foundation, Underground Utilities, Pile Load Tests

INTRODUCION

Dhaka, the capital and largest city of Bangladesh, is about 400 years' traditionally old city. Dhaka is one of the most traffic congested cities in the world and smooth traffic mobility in Dhaka City is one of the major problems of the city that the city dwellers are facing in their everyday life. The Jatrabari - Gulistan road was over saturated with unbearable traffic congestion, slowing speeds, increased road accidents, fuel wastage, environment pollution and excessively high vehicle operating cost. In a World Bank report of 2005 it has been stated that 16,320 Million Taka (i.e. ~190 Million USD) wasted in 20 years due to traffic Jam at Jatraabari - Gulistan Road alone. The overwhelming problem of decreased mobility on the road between Jatrabari to Gulistan had intensified with the increased traffic demands.

© 2018 Deep Foundations Institute

Since at-grade intersections represent primary capacity constraints, grade separation provides one of the best means of handling capacity problems. Despite huge cost involvement, the implementing authority had to go for construction of elevated corridor i.e. flyover as there was no scope to horizontally expand the road because of existence of huge built up commercial structures on either side and there was no other alternate route for development. There was no alternative but to implement such huge projects through "Public Private Partnership (PPP)" as the government alone cannot implement this with its own resources.



Photograph 1: Traffic condition of Jatrbari-Gulistan road before flyover construction

The project started from the place called Sonir Akhra beyond Jatrabari and ended at Polashi near Gulistan with at-grade corridor / intersection improvement.

The flyover was named as "Mayor Mohammad Hanif Flyover", in the name of the first Mayor of "Dhaka City Corporation". By virtue of the project location the responsibility of project execution was with "Dhaka South City Corporation (DSCC)" and the concessionaire company was "Orion Infrastructure Limited, Dhaka, Bangladesh".



Photograph 2: Heavily built up area along alignment of Flyover

Our Company, LEA Associates South Asia Pvt. Ltd. India was the design as well as project management consultant on behalf of the concessionaire. The company namely "Consulting Engineering Services Pvt. Ltd, India" was the design review and supervision consultant of the project client DSCC. The overall project contractor was Simplex Infrastructure Ltd., India.

ALIGNMENT OF FLYOVER

The detailed layout plan of the "Mayor Mohammad Hanif Flyover" covering main flyover and all the ramps is shown in **Figure 1** below:

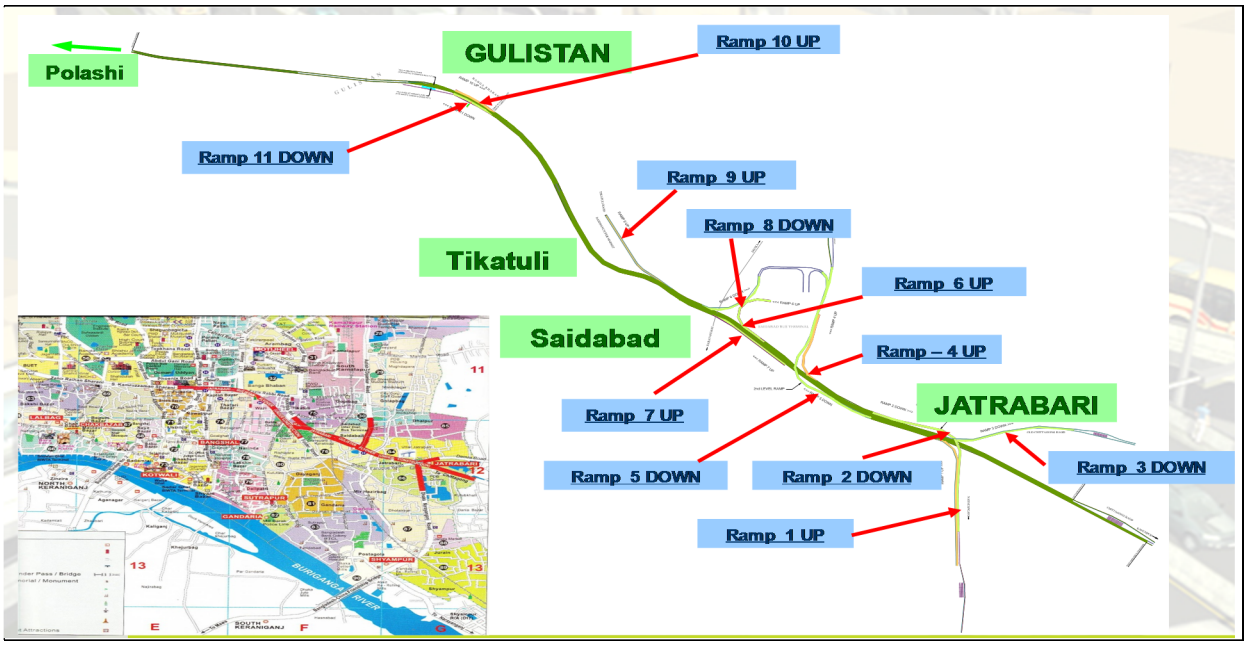


Figure 1: Sketch showing Layout plan of "Mayor Mohammad Hanif Flyover"

STRUCTURAL COMPONENTS OF FLYOVER

The entire flyover comprises of total 4.8 Km long main flyover and 11 numbers of up and down ramps having total length of 5.8 Km. Out of total 4.8 Km long main flyover, 3.6 Km is 4-lane divided carriageway width and remaining 1.2 km is 2-lane carriageway width. The 150 m long merging/ demerging lane for safe driving with least disruption to traffic flow of through vehicles has also been provided in every junction of ramps with main flyover. Considering the at grade road as first tier, the flyover arrangement is in total three tiers. The main flyover and 9 numbers of ramps are in second tier. In the third tier there are 2 numbers of ramps namely "Ramp 2" and "Ramp 5". The typical cross-sectional view of 4-lane main flyover as designed is given below in **Figure 2**.

Superstructures

Continuous PSC box girder with span configuration of 4 x 38 m, 3x 38 m, 24 m + 2 x 38 m + 24 m, 5 x 38 m with precast segmental section span-by-span construction methodology is adopted for the superstructure of main flyover. The types of super structures for the ramps are same as main flyover. However, cast-in-situ PSC box girder is adopted for portion having sharp curvature. The superstructure in the entire viaduct approaches of the main flyover and ramps are precast pre-tensioned PSC I-Girder.

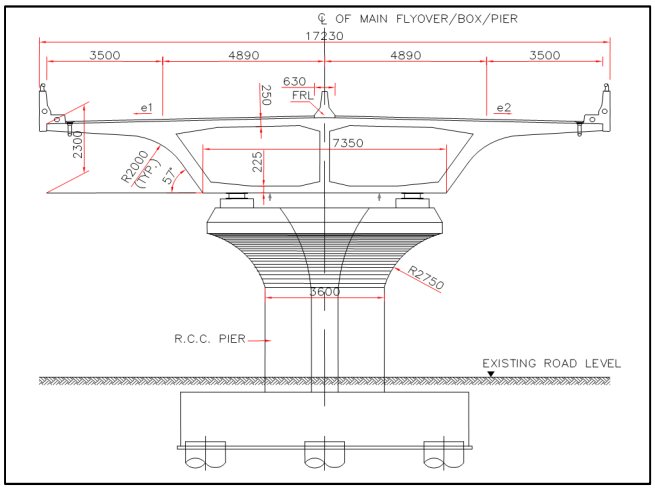


Figure 2: Typical Cross-section of 4-lane Flyover

Substructures

RCC Rectangular sections with RCC Cap are adopted for the substructures (Pier and Abutments) along Main Flyover and all the Ramps.

Foundations

RCC Bored Cast-in-situ Pile Foundations of mostly 1.2 m and sometimes 1.0 m and 0.800 m diameter without or with permanent liner of varying length have been adopted for the main flyover and ramps.

GEOTECHNICAL INVESTIGATION AND FOUNDAION SOIL PROFILE

For the engineering assessment of foundation of structures, a detailed "Geotechnical Investigation Work" comprising of both field and laboratory tests was undertaken at substructure locations along the main flyover and also along the ramps of the project. Total 102 numbers of boreholes of 35 - 40 m depth were explored all along the alignment of flyover in two phases. Some of the exploratory boreholes were obstructed initially by the various underground utilities and later those boreholes points were shifted in nearest position.

The field investigation program was consisted of minimum 150 mm diameter boring/drilling up to the desired depth and the recording of subsurface profile along with all related field tests and also the collection of different types of foundation soil samples following the related AASHTO and ASTM guidelines.

The detailed laboratory investigations namely soil classification tests (Grain Size Analysis, Atterberg Limits i.e. LL, PL, PI and SL), natural moisture contents (NMC), in-situ density, specific gravity, shear strength tests (cohesion and angle of shearing resistance), settlement parameters (compression index,

recompression index, void ratio and co-efficient of consolidation) of the collected soil samples and chemical tests of subsoil and ground water were conducted as per the ASTM guidelines.

The water table was found at 3.00 to 5.00 m depth below the original ground level as observed through the exploratory boring, which had also been verified from the record of different Government Authorities namely Dhaka WASA and Bangladesh Water Development Board. Following **Table 1** gives the broad range of the foundation soil stratifications below the existing pavement as found through investigations.

Table 1: Broad Range of Foundation Soil Stratification along Flyover below Existing Pavement

Description of Foundation Soil Layers	Range of Cumulative Thickness of Layers (m)	Range of Field Recorded SPT (N) value (Blows/300 mm)
Soft / Medium Stiff to Stiff / Very Stiff / Hard Silty Clay / Clayey Silt with some or no trace of Sand	4.00 – 15.00	4 - 46
Loose / Medium Dense to Dense / Very Dense Sandy Silt / Silty Sand with or without mica	Minimum 25.00 – 30.00	5 - 100

TYPES OF FOUNDATIONS

The RCC Bored Cast-in-situ Pile Foundations of 1.2 m diameter with varying length from 16.25 m to 37.25 m generally have been adopted depending upon the foundation soil strata and maximum load requirements. In special circumstances under some substructures in main flyover, the 1.00 m diameter pile has also been provided because of the constrained space available between the existing underground utilities. Similarly in few locations along ramps of the flyovers, the 1.00 m as well as 0.800 m diameter pile foundations have also been adopted based on space available after keeping the existing various underground utilities in its original position.

DESIGN STANDARDS FOR FOUNDATIONS

The design of foundations for the flyover in general was based on the provisions of the guidelines namely "AASHTO LRFD Bridge Design Specification, SI Units, 4th Edition, 2007". The chapter on "Foundations" and other related chapters were used for the design finalization of the flyover. Wherever, the said AASHTO code was silent, reference was made to other International codes, standards and reputed text books. The following codes were also used as supplemented codes for the design and construction of foundations of flyover.

1. Design and Construction of Driven Pile Foundation No. FHWA HI 97-013, VOL 1, 1998
2. ACI Specifications and Codes of practices
3. Bangladesh National Building Code (BNBC)

TYPES OF EXISTING UNDERGROUND UTILITIES

The different types of underground utilities which were present in huge numbers all along the alignment of the flyovers and its ramps in the old Dhaka city are given below.

- Water pipe lines of diameters ranging from 50 mm to 1200 mm.
- Sewerage pipe lines of diameter ranging from 450 mm to 1800 mm.
- Electric cables for 11 KVA, 33 KVA and 132 KVA
- Gas pipe lines of diameter ranging from 50 mm to 450 mm and
- Bunches (2 to 7 numbers) of optical fiber T & T i.e. Telephone lines

In addition, no record was available with the respective government agencies about the location of the above mentioned underground utilities. So it was required to identify manually the actual position of all underground utilities at each of the substructure locations. Following photographs (**Photograph 3**) give the glimpses of the type of underground utilities encountered along the flyover and its ramps.



Photograph 3: Types of Major Underground Utilities along the Flyover and its Ramps

GEOTECHNICAL DESIGN OF PILE FOUNDATIONS AND ITS IMPEDIMENTS

Methodology for estimation of load carrying capacity of pile

The geotechnical design of pile foundation consisted of estimating the "Vertical and Lateral Load Carrying Capacity of Pile Shaft". The design was made as per the AASHTO LRFD Bridge Design Specifications (SI Units, 4th Edition 2007). The geotechnical engineering data required for the design estimation such as foundation soil layering and variable soil shear strength namely cohesion and angle of shearing resistance and other input soil parameters were taken from the relevant subsoil investigation report.

Vertical Load Carrying Capacity of Pile

The "Safe Vertical Load Carrying Capacity of Pile" was defined as "Factored Shaft Resistance" based on the AASHTO guidelines of "Strength Limit State Design Method". The total "Factored Shaft Resistance" of pile consisted of "Factored Shaft Tip i.e. Base Resistance" and "Factored Shaft Side Resistance". The "Factored Shaft Tip Resistance" was obtained from the "Nominal i.e. Ultimate Shaft Tip Resistance" and multiplying that with the relevant "Resistance Factor for Tip Resistance" which were considered as 0.40 and 0.45 respectively in clayey and sandy foundation strata following the guidelines. Similarly, the "Factored Shaft Side Resistance" is obtained from the "Nominal i.e. Ultimate Shaft Side Resistance" and multiplying that with the relevant "Resistance Factor for Shaft Side Resistance" which were considered as 0.45 and 0.55 respectively in clayey and sandy strata based on the guidelines. The "Safe Vertical Load Carrying Capacity of Pile" i.e. the "Factored Shaft Resistance" of single pile in the group was less than the individual resistance of pile due to the overlap of shear zones in the surrounding soil between adjacent shafts and also due to the loosening of soil during construction. Since the pile spacing in the pile group was mostly maintained as 3 times of diameter of pile and even sometimes closer than that, so the pile group efficiency factor under vertical loading was taken as less than 1.00 for estimating the safe capacity of single pile shaft in the group in the flyover project.

Ground water table was considered at ground level so that vertical capacity of pile foundation was derived as the minimum safe available even if worst fluctuation of water table takes place. The "Down-drag i.e. Negative Skin Friction Forces", if any, were considered for abutment piles i.e. for pier piles where additional fill were envisaged on very soft to soft cohesive soil.

Sometimes the permanent casing i.e. liner of minimum adequate thickness was used along the pile shaft within the collapsible zone of surrounding foundation soil or in any other conditions due to the close proximity of underground utilities to the pile shaft. In case of any use permanent casing, the reduction factor to the pile shaft side resistance was used as 0.50 both in cohesive and cohesionless foundation strata as per the guidelines.

The "Resistance Factors for Shaft Side Resistance in Uplift" was considered as 0.35 and 0.45 respectively for clayey and sandy foundation soil as per the AASHTO guidelines.

The piles in the project were partly frictional and partly end bearing in nature, resting on dense to very dense silty sand / sand layer.

Lateral Load Carrying Capacity of Pile

The "BROM's Method of Analysis" as per the FHWA HI 97-013, VOL 1 had been used to determine the "Safe Lateral Load Carrying Capacity" of pile shaft.

Pile had been designed as "Long Pile" so that the length of pile was well extended beyond the point of fixity. The lateral load was determined based on shear failure condition of surrounding soil (up to 5 to 6D, D = pile diameter) as well as for the conditions corresponding to the horizontal deflection of 1% of pile diameter (i.e. 1% of 1200 mm = 12 mm). The "Safe Lateral Load" of pile had been recommended as the minimum of these two estimated loads. The "Safe Lateral Load" of the pile in the group was less than the individual resistance of pile due to the overlap of shear zones in the surrounding soil between adjacent shafts and also due to the loosening of soil during construction. Since the pile spacing in the pile group was mostly maintained as 3 times of diameter of pile and some cases closer than that, so the pile group efficiency factor under horizontal load was taken as less than 1.00 for estimating the safe capacity of single pile shaft in the group in the flyover project.

The working pile under the cap represented the pile with fixed headed condition. So the safe lateral load corresponding to the free headed condition of working pile had also been estimated. The safe or service lateral / horizontal load corresponding to the "free-headed condition" of pile was established in site through horizontal load test. The corresponding / equivalent safe lateral load of actual working pile in "fixed headed condition" was automatically established.

The **Table 2** below gives the typical range of design recommendations of pile geometry and its capacities in summarized form along the main flyover, merged portion and ramps of flyover.

Table 2: Summary of Design Recommendation on Pile Geometry and its Capacities of Flyover

Portion of Flyover	**Main Flyover**		**Merged Portion**		**Ramps**	
Type of Piers & Abutments	Free and Expansion	Fixed	Free and Expansion	Fixed	Free and Expansion	Fixed
Dimeter of Pile (mm)	1000 - 1200	1200	1000 - 1200	1000 - 1200	800 - 1200	1000 - 1200
Spacing of Piles in Group (D)	2.50 - 3.00	2.50 - 3.00	2.50 - 3.00	2.50 - 3.00	2.43 - 4.00	2.50 - 3.00
Length of Pile from Pile Cut-off Level (m)	21.25 - 36.53	18.25 - 27.25	22.25 - 35.25	21.25 - 34.25	16.25 - 37.25	20.25 - 35.25
End Bearing Stratum with SPT (N) Range	Dense to Very Dense NP Sandy Silt to Silty Sand / Sand (N : 34 - 100)					
Safe Vertical Axial Load Carrying Capacity of Single Pile considering Group Efficiency (ton)	140 - 385	200 - 300	200 - 330	220 - 275	110 - 430	170 - 350
Safe Vertical Axial Load Carrying Capacity of Single Pile (ton)	290 -500	280 - 375	300 - 470	330 - 410	150 - 550	250 - 470
Safe Axial Uplift Load Carrying Capacity of Single Pile considering Group Efficiency (ton)	140 - 260	110 - 185	130 - 220	140 - 220	85 - 280	105 - 225
Top Foundation Soil Strata up to Critical Depth (5D to 6D) with SPT (N) Range	Very Soft / Soft to Medium Stiff / Stiff / Very Stiff Silty Clay / Clayey Silt with little Sand (N: 1 - 21)					
Safe Service Load / Working Load of Single Pile in Fixed Headed Condition in the Pile Group (ton)	7 - 38	15 - 38	14 - 37	22 - 37	6 - 38	16 - 33
Safe Service Load / Working Load of Single Pile in Free Headed Condition (ton)	5 - 22	7.5 – 21.0	7 - 24	11 - 24	6 - 23	8 - 17

The test loads were considered as 250% and 150% of the safe or service load of the individual pile respectively in "Initial Load Test over Test Pile" and "Routine Load Test over Working Pile". All these

load tests were conducted both in vertical and horizontal direction for establishing the estimated pile capacities of single shaft.

Design Finalization of Foundation with all existing underground utilities in their original positions

As per the concession agreement, the project client DSCC was supposed to complete the relocation of utilities within 180 days (i.e., Latest on December 31, 2010). However, since the water pipe line and 132KVA electric line was imported items, its replacement would cause time overrun of the project and due to various other reasons the Authority could not relocate major utilities and the concessionaire had to commence and continue the design and construction of the flyover with underground utilities of all hues in position.

Considering the criticality of foundation design arising out of existence of huge underground utilities, the design consultant had to adopt an integrated and iterative approach for design of pile foundation of the flyover to meet the given objective. The final foundation design of each substructure could be issued after passing through three stages of iterative process as stated below with actual site photographs.

- **Stage I**: A preliminary design was prepared and advance drawing showing tentative positions of piles with shape and size of the pile cap was issued to contractor for each pier/abutment to identifying utility locations. Based on this drawing, Scissor type "Cross Trench" (refer **Photograph 4**) of 0.8 m to 1.0 m wide and 2.5 m deep encompassing the entire influence zone of each pile cap was dug at each pier location and information was passed to the design cell.



Photograph 4

- **Stage II**: Based on information about utility location from cross trenching, detail design with modified positioning of piles within the spaces available between adjacent utilities was prepared and advance drawing issued. The 1.5 m to 1.7 m diameter manual pit cutting to 2.5 m depth was done based on this advance drawing at each pile location (refer **Photograph 5**) and confirmation is passed on to the design cell with changes required, if any.



Photograph 5

- **Stage III**: In case, any utility encountered in pit cutting, further adjustment was done in pile location & pile cap and subsequently verification was taken up again to confirm the utility freeness. Once confirmed, the "Hydraulic Rig" started pile boring (refer **Photograph 6**). In some cases, utility had been found even up to 9 m below road level during driving, requiring further revision in design and drawing.



Photograph 6

Though the method was quite conventional, time consuming and involve more efforts, this iterative method was found successful and there had been no major accident or damage to underground utilities in driving 2366 number of piles tantalizingly close to underground utilities of all hues. Following, adjustments in design had to be made:

- Separate design for all the 315 numbers of foundations of substructures
- Use of different diameter of piles in same foundation group
- Different spacing between the piles
- Different shape and thickness of pile caps
- Consideration of huge eccentricity between center lines of pier and pile cap
- Change in span configuration
- Change in alignment geometry

The following **Figure 3** shows the typical details of pile group and its cap in association with the existing underground utilities.

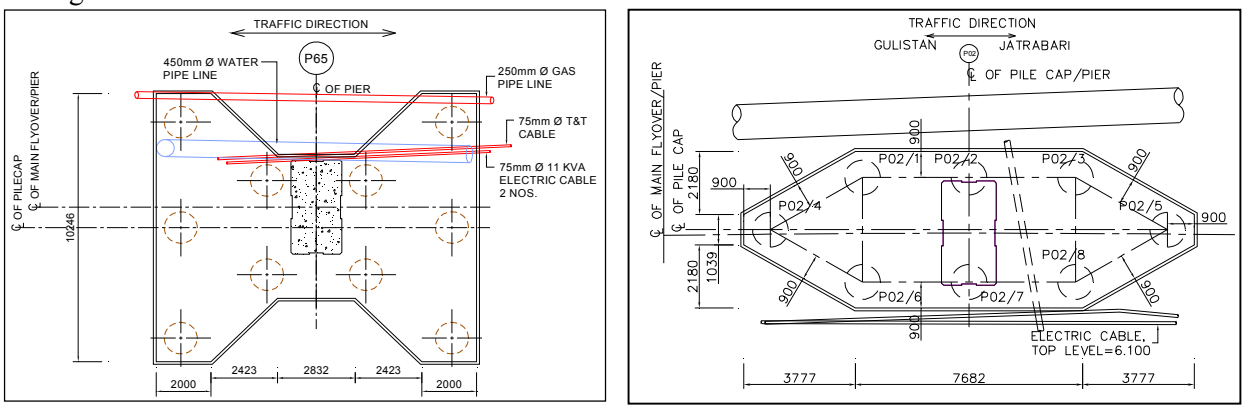


Figure 3: Typical Details of Pile Group and its Cap in association with Existing Underground Utilities

The Situation was more challenging to the design team as their mobilization was done 3 months after contractor's mobilization and they had to supply design details for 3 hydraulic rigs at a time, each of them capable of driving two piles per day. In spite of such adverse situation and complexity, issue of GFC drawings of foundations was made in time, so that single minute idling of rigs for want of drawings did not occur. The final recommended design and drawing, construction method have been reviewed and approved by the "Independent Consultant" on behalf of project client.

Effects of working with in-place various underground utilities

- Pile cap level had to be raised above road level at many places resulting permanent loss of precious land and compromise to at-grade landscaping below flyover. Raised pile cap and bigger size pile cap to accommodate underground utilities resulted to the permanent constriction in at-grade road facilities and traffic movement. The actual site photographs of raised and irregular pile cap are shown below.



Photograph 7 : Raised and Irregular Pile Caps along the Flyover

- Working with exiting underground utilities made delay in construction schedule for multi-stage verification and design & drawing revisions. It was required to adopt special construction methodology and also to do the mobilization of additional resources to maintain the scheduled completion target.
- Many utilities had to be buried leading to a situation difficult for future maintenance of existing utilities. These details are shown in **Figure 4** and actual construction photograph (**Photograph 8**) here.

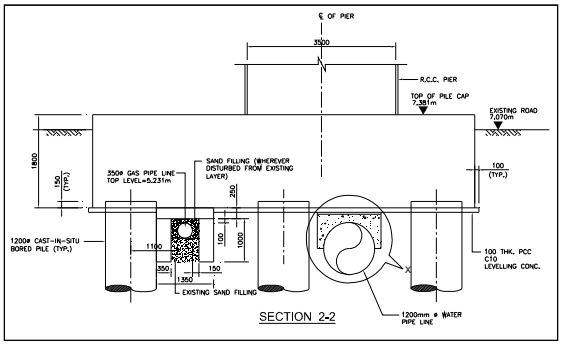


Figure 4: Utilities buried under Pile Cap



Photograph 8

- Concessionaire had to bear huge additional costs in overall.
- As consequence of working with exiting underground utilities, the movement of different construction machineries was quite restricted and there was significant constraint in the working space for the construction also.
- Less Space for traffic diversion was available.
- There was enormous risk of accidental damage to the life and assets along the route of flyover.

CONSTRUCTION OF PILE FOUNDATIONS INCLUDING ITS QUALITY CONTROL

Considering limited availability of work front due to various site reasons three numbers of computerized hydraulic Rig IMT- INDUSTRIA MECCANICA TRIVELLE - HYDRAULIC DRILLING RIGS Model AF 220 of Italy was deployed. The plant made ready mix concrete i.e. RMC of C30 grade was used for concreting of pile and pile cap. Total numbers of piles installed in the said project was 2366. The output and construction quality was quite satisfactory. On an average 5 number of piles of length 35 m was constructed per day in spite of very cautious driving required for initial 10 m because the foundation work had to be carried out without causing damage to existing underground utilities running in close proximity of piles. All the checklists related to the different phases of piling work namely the fixing of pile position, casing driving and pile boring, pile history sheet, pile reinforcement and cage lowering, pile concreting including the "Tremie Chart" and "Piling Pour Card" were regularly maintained under quality control program. The safety measures for all the engineers and construction workers were taken care. There were some cases of less consumption of concrete observed during pile foundation construction. The remedial measures were undertaken in various ways namely by introduction of high plastic bentonite, doing construction time management and maintaining the viscosity of pile boring fluid, providing increased diameter of cutting tools etc. Due to presence of filled up / loose strata of top soil, some of the piles were constructed with permanent liner up to depth of 9 to 10 m. Bottom sampler was also used to confirm the proper cleaning of pile bore bottom after adequate & profuse flushing and before start of pile concreting.

FIELD TESTING OF PILE FOUNDATIONS

To establish the estimated safe pile capacities of the single shaft, the load tests were conducted over the "Test Pile" as well as over the "Working or Service Pile" both in vertical and horizontal direction. Total 8 numbers of "Initial Load Test over Test Pile" were conducted for the entire flyover and ramps. The different locations of "Test Piles" were selected based on the variation in foundation soil profiles spreading all along the layout of structure. The typical photographs of conducting vertical pile load test are shown under **Photograph 9** and the vertical load vs pile head deflection curve of "Test Pile" is shown below in **Figure 5**. The pile load corresponding to the gross settlement of 12 mm was recorded in between 750 ton and 1070 ton as per the load-deflection behavior of "Test Pile". The numbers of routine load tests were also



Photograph 9

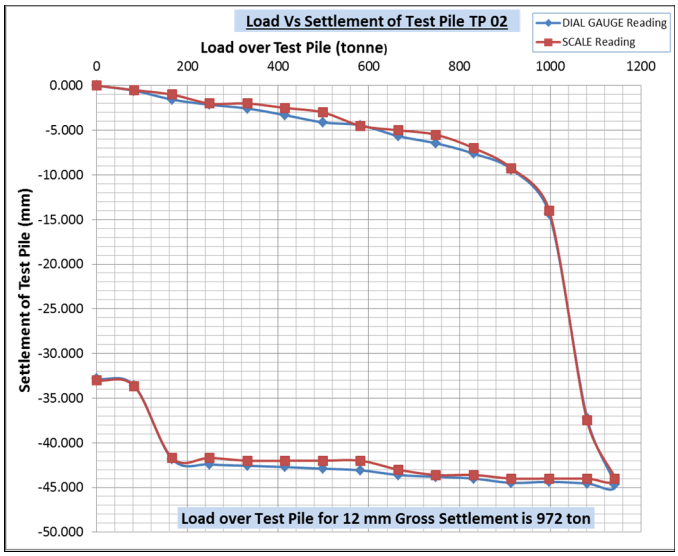


Figure 5: Vertical Load Deflection Curve of 1200 mm Pile

conducted over the working pile both in static and dynamic manner to confirm the pile capacities before pile cap construction. The "High Strain Dynamic Pile Load Test (HSDL)" was conducted during routine test after establishing the correlation with the conventional static load test as per the ASTM guidelines.

The horizontal load corresponding to total deflection of 5 mm and 12 mm were recorded from the load-deflection behavior of horizontal i.e. lateral pile load test. The typical lateral load deflection curve (refer **Figure 6**) of "Test Pile" including the photograph (refer **Photograph 10**) of conducting horizontal pile load tests are shown here.



Photograph 10

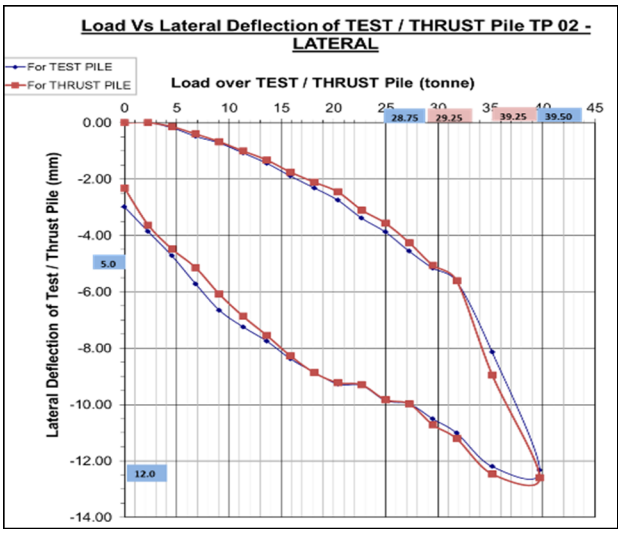


Figure 6: Lateral Load Deflection Curve of 1200 mm Pile

To check the continuity and integrity of the pile shaft, numbers of "Low Strain Dynamic Pile Integrity Tests (PIT)" were conducted over the working piles along the flyover and its ramps. The results of all the different types of pile load tests were interpreted following the AASHTO and other standard guidelines.

CONCLUSIONS

This paper describes the detailed design philosophy and construction methodology of foundation of the longest flyover in Bangladesh in the most congested part of old DHAKA city. It was quite challenging situation for installing the pile foundations by keeping with lots of various underground utilities all along the flyovers and its ramps. By constructing the flyover the additional overhead road space was created and the acquisition of built-up lands on either side was minimized, which was quite costly and time-consuming, besides causing great hardship to those affected. It also helped to achieve significant enhancement in traffic flow and thereby reduction in vehicle operating cost. The travel time has reduced substantially to a mere five minutes. It has segregated long distance traffic from local traffic. The **Photograph 11** shown here is the completed flyover which was finally inaugurated by Hon'ble Prime Minister of Bangladesh, Sheikh Hasina on 11th October 2013 and opened for public use.



Photograph 11

REFERENCES

- AASHTO LRFD Bridge Design Specification, SI Units, 4th Edition, 2007, American Association of State Highways and Transportation Officials, Washington, DC 20001, pp. 10-123 to 10-145.
- Design and Construction of Driven Pile Foundation, Workshop Manual - Volume I, U.S. Department of Transportation, FHWA, Publication No. FHWA HI 97-013, Revised November 1998, 830 p
- Bowles, J. E., 1997. Fifth Edition, Foundation Analysis and Design, The McGraw-Hill Companies Inc., pp 867 - 1054
- Poulos, H. G. and Davis, E. H., The University of Sydney, 1980. Pile Foundation Analysis and Design, Rainbow-Bridge Book Co., 410 p
- Tomlinson, M. J., 1994. Fourth Edition, Pile Design and Construction Practice, E & FN Spon, 2–6 Boundary Row, London, 587 p.

EFFECT OF GEOTECHNICAL PARAMETERS IN DESIGN AND CONSTRUCTION OF METRO TUNNEL BELOW THE RIVER GANGES IN KOLKATA, INDIA

Biswanath Dewanjee
Chief Engineer,
Kolkata Metro Rail Corporation Limited
City- Kolkata, Country-India, biswanath_dewanjee@hotmail.com

ABSTRACT

The Ganges is one of the most prominent rivers in India and historically major cities like Kolkata are developed along the banks. There was a rapid upsurge in population in the Kolkata metropolitan area during the last 50 years and consequently it is necessary to develop a modern mass transportation facility in this region. Kolkata East-West Metro is a crucial mass transit corridor project connecting Kolkata and its twin city Howrah on other side of river. Twin bored tunnels were built below the river Ganges to connect the cities. The tunnel is 16m to 19m below the river bed. The 5.55 meter (m) internal diameter tunnels are constructed with concrete RCC segmental liners. The 520 m river crossing was accomplished using earth pressure balancing tunnel boring machines (TBM). This is the first transportation tunnel project in India under such a large and revered river. This ambitious initiative involved meticulous planning and investigation of the Ganga- Brahmaputra deltaic region juvenile alluvial sub-soil. This paper covers geotechnical investigation, hydrological data collection, selection criteria for alignment design, type of construction, and selection of the tunnel boring machine.

Key Words: Kolkata, Geotechnical investigation, Tunneling, Underwater, Face Pressure

1. INTRODUCTION

Tunnels and underground caverns often provide an effective transportation solution in densely populated built up cities with minimal impact to natural and social environment.

The major uncertainty with tunnel projects is the nature and character of the ground through which the tunnel is constructed. Tunneling below open water is even a greater challenge. The success of an open water tunnel project is dependent on following fundamental principles:

- Consideration of the character of the ground and it's behavior in the selection of the tunnel alignment and the excavation technique.
- Optimization of the alignment to pass through impermeable ground to minimize difficulties from groundwater and potentially flowing ground.
- Planning to minimize difficult and infrequent access to the TBM cutter head.

Tunnels under open water bodies have connected cities and countries in many parts of the world starting from the famous tunnel under River Thames in year 1843. Such precedence is not available in India. Planning and execution of the Metro twin tunnel under river Ganges in Kolkata required sustained efforts, technical expertise, and demanded a high degree of precaution and care.

© 2018 Deep Foundations Institute

2. GEOTECHNICAL INVESTIGATION

The sedimentation in the Bengal Basin occurred at different stages after the outpouring of Rajmahal trap in the Cretaceous period. The southern riverine delta developed through alluviation where river sediments built-up and pushed out the sea front forming a shallow offshore zone. The river gradient subsequently decreased to the south forming numerous oxbow lakes and acute meander loops.

Kolkata is located in the lower deltaic plain of the Ganga-Brahmaputra river system at elevations ranging between 1.5 m and 9.0 m above sea level. The city is spread along the banks of the river Ganges from north to south. The topography of the ground surface slopes slightly away from the river to the east and south east towards the saline lakes or East Kolkata wetlands (Sengupta, 2009).

The geotechnical investigation for the Kolkata East-West Metro Project river was carried out by marine cable percussion method using floating rafts/boats. Investigations were performed in the planning stage and during project execution. The construction was delivered through a design-build contract. Because of the impervious capping layer of clayey subsoil in the upper strata of sub-soil, it was necessary to plug the boreholes to avoid river water infiltration in lower strata which could be detrimental for tunneling. Cement slurry was tremied during casing withdrawal.

Extensive laboratory tests were conducted on soil samples collected. The SPT data obtained in boreholes advanced along the tunnel sections were corrected to $N_{60,}$ normalized values for SPT, corrected for overburden and field procedures. Drained and undrained shear strength tests were undertaken on U100 samples. Strength and deformation parameters summarized from laboratory testing is shown in Table 1.

Table 1: Principles adopted for determination of strength and deformation parameters

Parameter	Alternatives for determination	Reference		Remarks
Undrained shear strength [c_u]	$c_u = 6N_{60}$	Established relationship by Stroud (1989)	Rationalization of alternatives	Varies with depth for Unit 3
	Laboratory triaxial unconsolidated undrained (UU) and unconfined compression (UC) tests			
	$c_u / \sigma v_o' = 0.11+0.0037IP$ [IP = Plasticity Index]	Skempton (1957)		
	$c_u /pa = 1.7\ e^{(-4.6*IL)}$ [IL=Liquidity index]	Wood (1983)		
Drained Shear Strength	Laboratory test results			
Undrained Youngs Modulus	$E_u=300c_u$ for Unit 2 & $E_u=350c_u$ for Unit 3. Over consolidation ratio (OCR) for Unit 2 and Unit 3 was determined from the Oedometer test results which indicates Unit 2 to be normally consolidated to slightly over consolidated near surface. Unit 3 is also normally consolidated to slightly over consolidated.	Correlation of E_U/c_u suggested by Jamiolkowski (1979)		Varies with depth for Unit 3
Drained Young's Modulus	$E' = 0.8E_u$ for Unit 2 and Unit 3			

Engineering characteristics of sub-soil in tunneling horizon is shown in Table 2:

Table 2: Engineering Characteristics of Sub-Soil

Soil Strata & Nature	Depth	Tunnel Section	Unit Weight (y)	N Value	Poisson's Ratio (ν)	Angle of Friction (φ')	Cohesion (c')	Undrained Shear Strength (Cu)	Drained Young's Modulus (E')	Undrained Young's Modulus (Eu)
			kN/m³			Deg	kPa	kPa	MPa	MPa
Unit 1 Made Ground	5.5m MSL to 4.5m MSL	All	19		0.3	28°	0	n/a	12	n/a
Unit 2 Organic Clay	4.5m MSL to -10m MSL	All	17.5	Westside: 4-18 East side: 2-7	0.25	25°	5	25	6	8
Unit 3a Firm to stiff clay Silt	-10m MSL to -40m MSL	West Side of river	19	12-40	0.2	30° 32° (below – 24m MSL)	0	(z+7.2222) -0.1111	(z+4.706) -0.353	1.25x E'
		River Section		25-31				(z+7.8814) -0.0847	(z+6.875) -0.3125	
		East Side of River		12-27				(z+7.549) -0.098	(z+1.4286) -0.4286	
Unit 3b Sandy Silt / Silty Sand		West Side of river	19		0.2	30° 32° (below – 24m MSL)	0	n/a	(z+4.706) -0.353	n/a
		River Section		10-42					(z+6.875) -0.3125	
		East Side of river		16-57					(z+1.4286) -0.4286	

z = Depth in meter from MSL

3. SELECTION OF TUNNEL ALIGNMENT BELOW RIVER

3.1 Horizontal Alignment of Tunnel Below River Ganges

The horizontal alignment for river crossing was selected considering the following:

a) Tunneling below the river will occur mostly in Unit 3a which is firm to stiff clayey silt with N Values from 25 to 30 and angle of internal friction [φ'] of 32^0. This layer was selected considering favorable permeability of $1x10^{-9}$ meter/sec and coefficient of earth pressure at rest [$K_{0]}$ of 0.56. However, the sub-soil at the tunnel face required proper "conditioning" (detailed in section 6).

b) Historical Land Uses - The river Ganges in Kolkata was used for riverine transport for centuries. It was necessary to ensure that the alignment does not infringe any existing or abandoned jetty structures or shoreline development to avoid any underground obstruction. A Kolkata Port Trust report indicates the bottom of jetty piles and shoreline structures extends up to -20.3 m MSL. Therefore, the crown of the tunnel must be below that level.

c) Existing Land Uses – The availability of land is always a challenge, especially for urban underground projects in a brownfield situation like Kolkata metropolis. The acquisition of land and constructability of Howrah Station on the west bank and the ventilation shaft on the east bank were major factors for the final alignment. Comparatively vacant areas were selected along both banks and the alignment of the tunnel was guided accordingly.

d) Protection of Howrah Bridge - The proposed tunnels are at about 320 m away from existing Howrah Bridge which is a major entrance to the city. Analysis showed that tunneling work at such a distance would have no direct effect on the Howrah Bridge.

e) No Horizontal Curve: TBMs perform much more efficiently in the absence of a horizontal curve.

3.2 Vertical Alignment of Tunnel Below River

Ganges Hydrological data:

Hydrological data suggests that this is a tidal river with progressive type of tidal range of 3 m to 4 m. Bore tides also occur in this part of the river near an estuary which is characterized by a standing wave about 1.75m high and makes its first appearance about 30 km downstream of Kolkata. Kolkata Port Authority reports the highest scour at the location of the tunnel during year 1988 to 2003 was approximately 4.5 m and the highest silting deposit was about 6.5 m. The maximum water velocity was approximately 2.5 m/second.

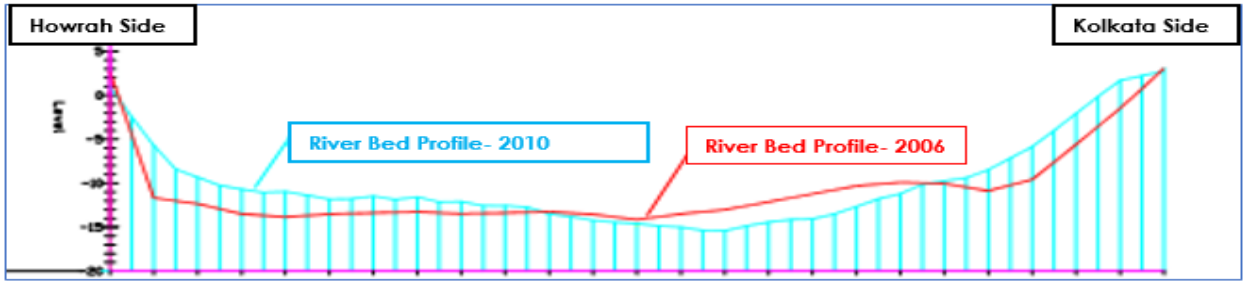


Figure 1: River Bed of Hooghly – Bathymetric Survey

A February 2004 survey observed a maximum water depth of 17 m, approximately 90 m from the Howrah side. The gradient of the river is nearly very flat. The deepest scoured river bed above the alignment of the tunnel reported as -23.865m below MSL [Kolkata Port Trust 2004].

The Japan External Trade Organization [JETRO] prepared an initial feasibility study for this river tunneling suggesting a lowest rail level of –28.74 m below MSL. This preliminary work was followed by a detailed project report [DPR].

Further bathymetric survey was conducted in the DPR stage in 2006, and after award of the construction contract in 2010. Some changes in the river bed profile were observed as shown in Figure 1. Notably, there is tendency of silting in the right bank and the deep channel is shifting towards left bank [Kolkata Side] with a maximum depth 14.4 m about 280 m from the left bank.

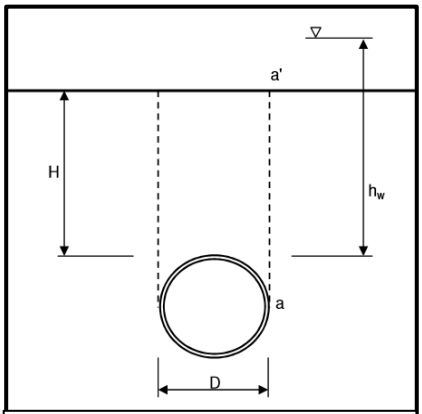


Figure 2: Schematic Diagram for Floatation Check

Checking Against Flotation & Heaving

Flotation and uplift [U] due to differential water pressure should be checked relative to restraining forces [R]. The recommended overall safety factor is $R / U \geq 1.2$ where: R is restraining force calculated by weight and shear resistance of soil and U is net uplift force considering weight of the tunnel. Factors of safety for different soil covers along the alignment are calculated and shown in Table 3.

The tunnel vertical alignment was finalized with a 3% vertical grade [permissible limit] on the basis of bathymetrical survey done in 2010 and critical soil cushion thickness. Soil cushion is the sum of cover minus scour thickness of 11.355 m [15.855 m cover - 4.5 m scour = 11.355 m cushion]. As noted earlier the maximum scour of 4.5 m was reported by Kolkata Port Trust. This cushion provides an adequate factor of safety [see Figure 3]. The cushion must also be checked against blow out criteria during application of TBM face pressure during tunneling (detailed in Section 6).

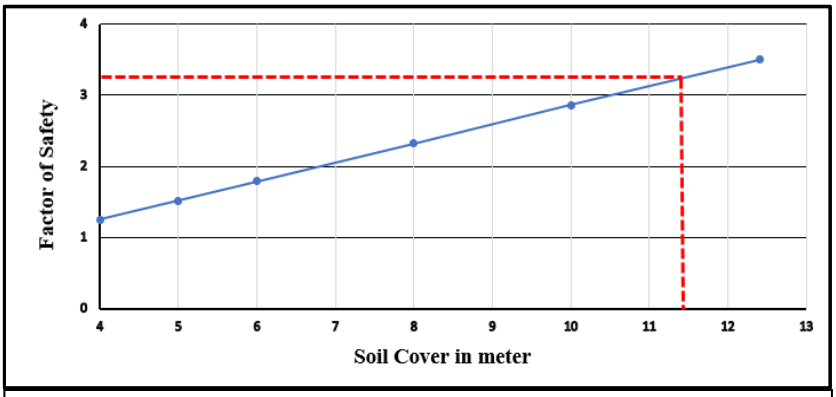


Figure 3: Factor of Safety vs Soil Cover

Another consideration in navigational a waterway is penetration of ship's anchors through the soft sub-soil condition like Kolkata. Fortunately, the riverine port of Kolkata is located furthers towards the sea from the tunnel alignment. There is no ship route in tunneling zone. However, there is inland transportation in the river for both ferry passenger and cargo using motor launches, steamers and barges. The Port Authority ensured that there will be no effect due to anchor penetration. The details of tunnel alignment below river vis-à- vis geotechnical profile is shown in Figure 4.

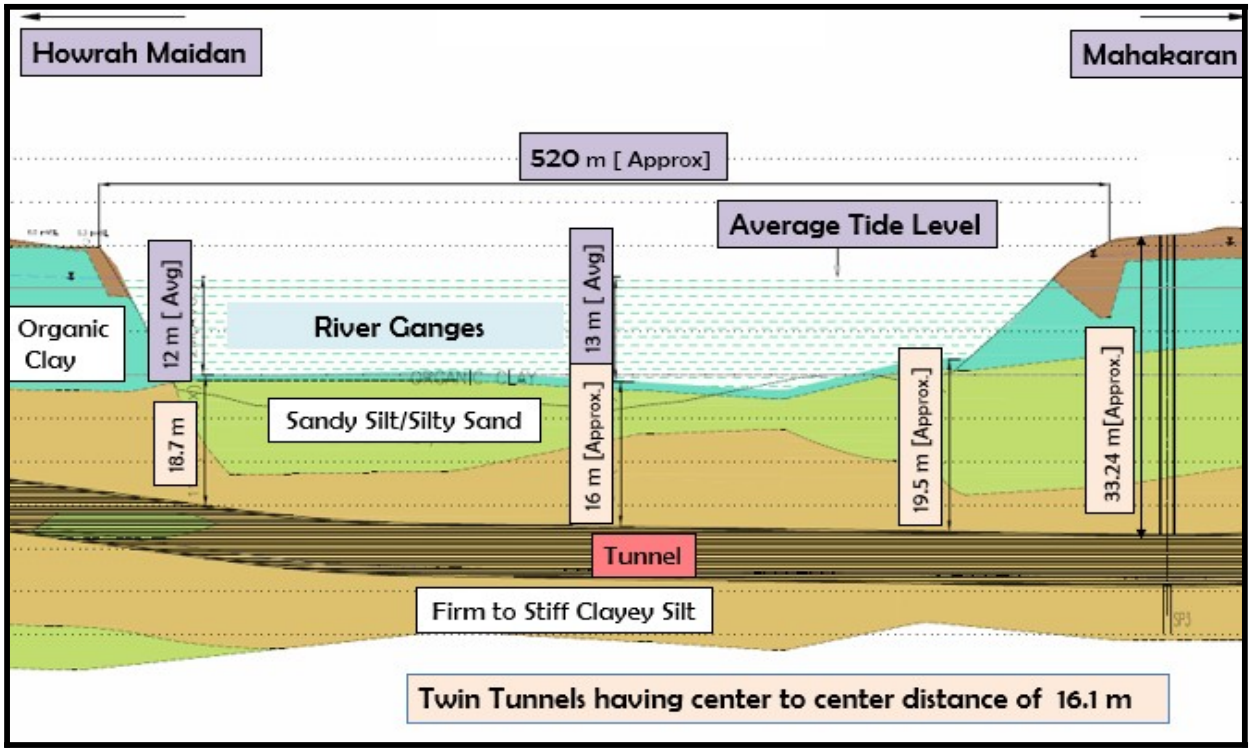


Figure 4: Tunnel alignment below river vis-à-vis geotechnical profile

4. SELECTION OF TUNNEL BORING MACHINE [TBM]

Tunneling for Phase-II of Kolkata East West Metro is a 3.8 km continuous drive from Howrah Maidan to Esplanade out of which the river crossing is a stretch of 520 m. So, the selection of tunnel boring machines is based on the technical requirements of entire tunneling length. The soil profile encountered in the tunneling horizon for entire tunneling route is shown in Figure 5 revealing that the tunnel passes through unit 3a [Firm to stiff clayey silt] in 50% of total route length. Soft ground tunnel boring machines are effective for this work.

In soft ground tunneling below open water, closed face TBMs are usually required because:

- They are effectively sealed from ground and hydrostatic pressures.
- The ability to control ground movement particularly at the face of the excavation.
- Effective at minimizing ground loss.
- Reduction of risk of development of connection to the overlying water body.
- Provide positive support to the ground and minimize the risk for problematic ground water inflows into the tunnel excavation.

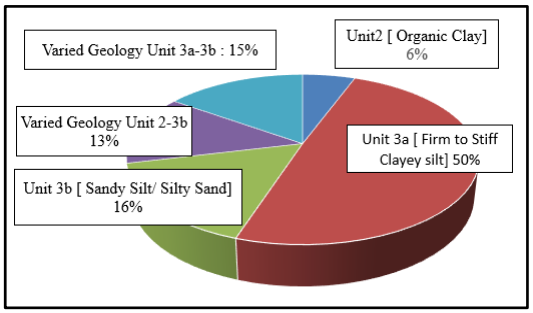


Figure 5: Soil distribution in Tunnel Face

Comparative suitability of slurry and Earth Pressure Balancing [EPB] type TBMs based on soil grain size distribution in tunneling zones are represented in generic graphs by many authors. Laboratory test results for particle size distribution [mean values] in the tunneling horizon is superimposed over a reference guideline graph (Langmaack, 2001) as shown in Figure 6. This indicates that earth pressure balancing tunnel boring machine with soil conditioning is suitable for Kolkata East West Metro project. The final selection depends on additional factors such as the presence of gas, presence of boulders, hydrostatic pressures, area available for a mining site, spoil disposal and power requirements, intervention facility etc. Face pressure requirements of about 3 bar below the river was considered in selecting the capacity of the machine. Finally, EPB tunnel boring machines of appropriate capacity were selected for this project.

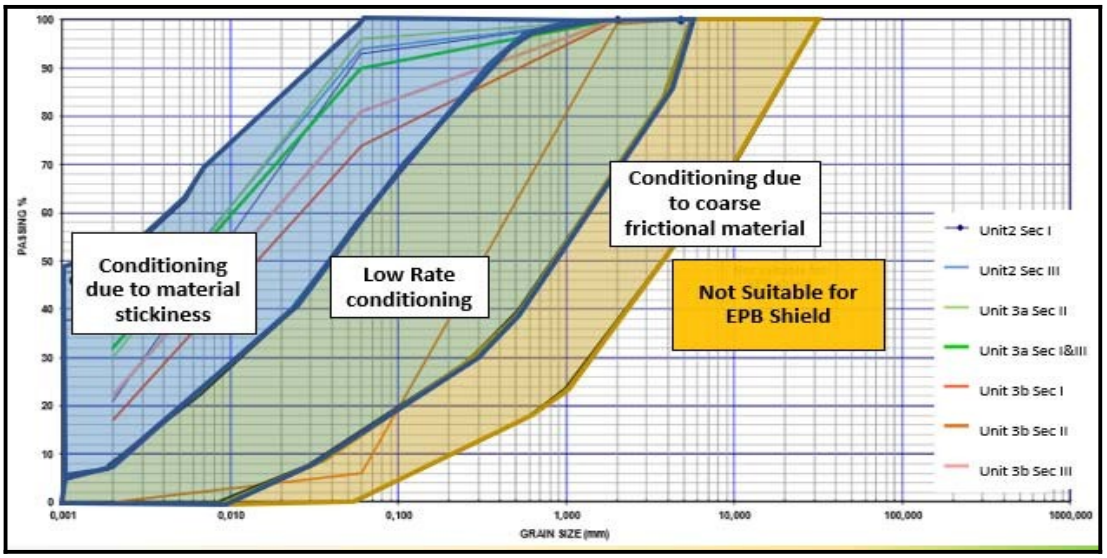


Figure 6: Superimposition of Grain Size Curves on reference curves for selection of TBM

5. GEOTECHNICAL DESIGN BASICS FOR TUNNEL LINING

Geotechnical parameters were used for the design of RCC precast segmental lining. Full bond between the lining and the subsoil is assumed. Average effective unit weight of soil is used in calculations considering the prevailing sub-soil layers and groundwater table. The effect of differential hydrostatic pressure along the circumference of the tunnel is considered in the analysis. General plane frame analysis is carried out for varying soil stiffness and differential hydrostatic load. Numerical analysis using PLAXIS 9 with followed this sequence:

1. Initialize stress condition and water pressure
2. Apply surcharge
3. Excavate tunnel and install lining for first tunnel
4. Excavate tunnel and install lining for second tunnel
5. Consolidation after construction completion
6. Change the properties of the lining to long term modulus
7. Apply seismic acceleration
8. Consolidation after seismic acceleration

Relaxation of ground stress is assumed before installation of lining. Based on the outputs, the design bending moments are compared in Figure 7 in different tunnel sections and it is found that design of RCC segmental liners is most critical in river sections and the shallowest section.

Internal diameter of the tunnels is 5.55 m and 275 mm thick segmental precast reinforced concrete liners of M50 grade were erected in position using the Tunnel boring machine itself. The complete circular tunnel is built with 6 precast segments including one keysegment.

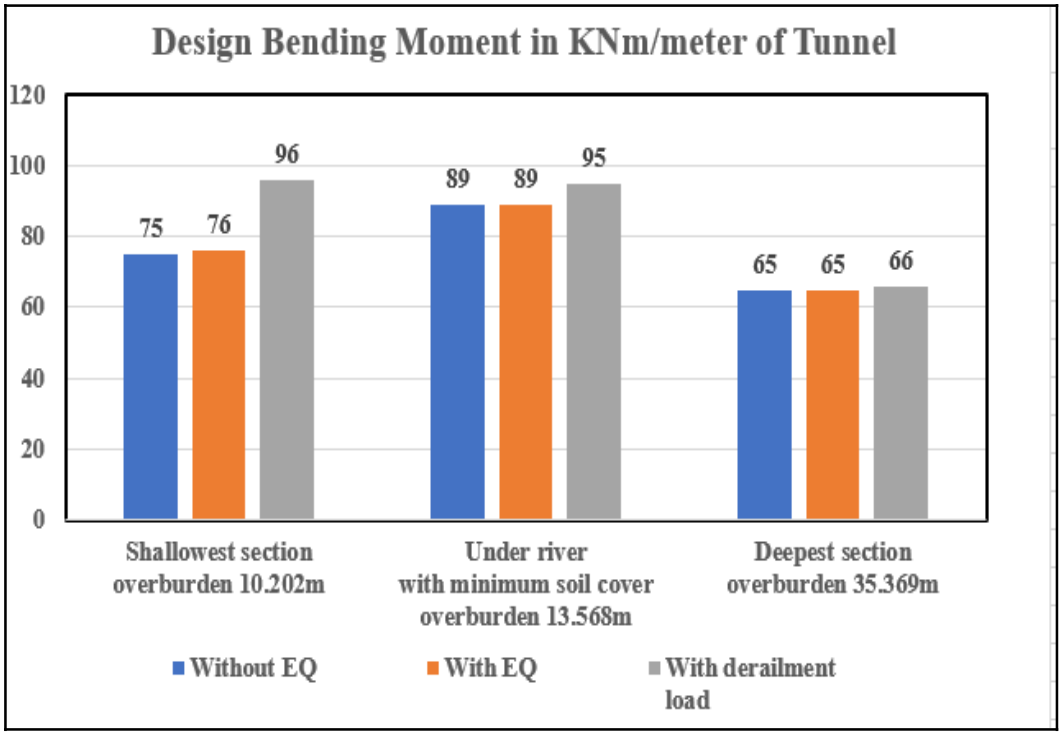


Figure 7: Design Bending Moment for tunnel liners in different tunnelstretches

6. FACE PRESSURE & GROUTING CONTROL

Effective computation of the tunnel face pressure during advancement and stoppage are critical. Control and face pressure parameter monitoring during tunneling is equally important in open water stretches as maintenance of machines below the river are expensive and involves higher risk.

Face pressures are computed using overburden and ground water parameters along the tunnel alignment using following principles:

- Face Pressure during advancement - Mean values determined at 20 m interval along the alignment by COB Method [Dutch Center Ondergroun Bowen Method]
- Face Pressure during stoppages - Mean of values determined at 20 m interval along the alignment by Maximum Ground Water Load plus 20 kPa

The mean values are further stepped in 40 m intervals, mean value graphs are generated with an upper limit of face pressure of 0.2 bar and lower limit of 0.2 bar less. Though stoppages during river crossing are not recommended, they may be required for repairs, weekend or holiday breaks, or after successive shifts. The TBM front chamber may be kept pressed by injecting Bentonite. The face pressure plot for advancement along the entire tunnel alignment is shown in Figure- 8.

The density of soil mass in the front chamber should be kept as high as possible. The value of the density of the material in chamber should never be lower than 12.0 KN/m^3 . It is desirable to keep a value of 14 KN/m^3 or higher to maintain a close pressure gradient between the soil at the front and the conditioned material in the chamber.

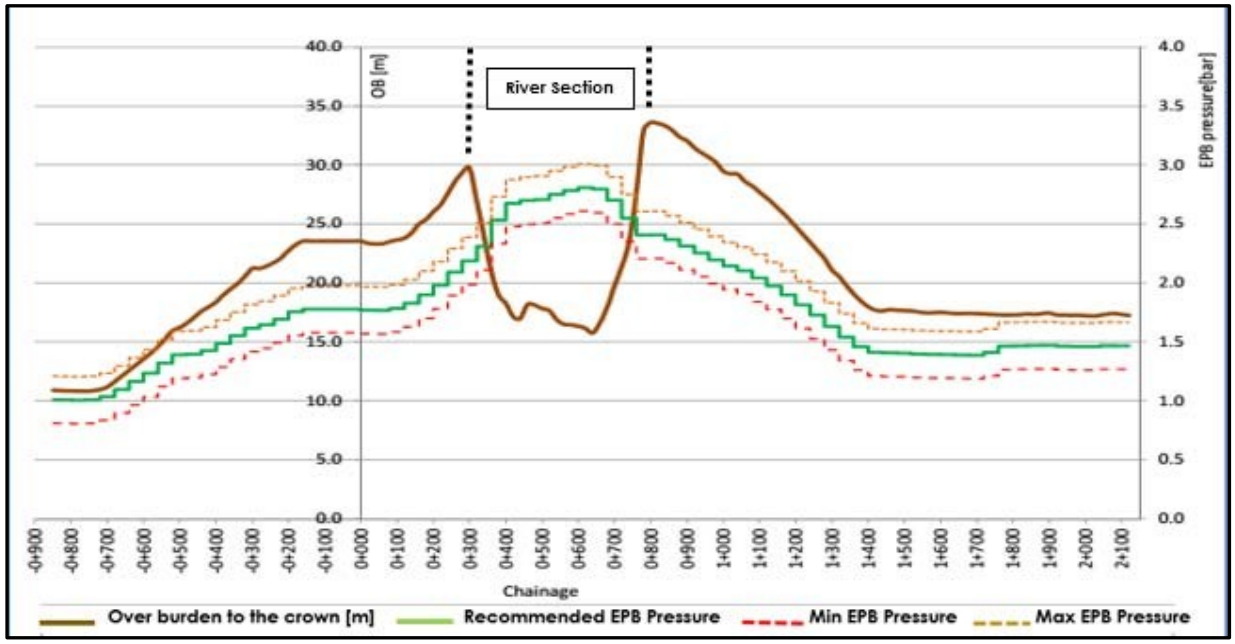


Figure 8: Typical face pressure plot for Phase-II of Kolkata East West Metro

6.1 Blow Out Verification

The riverine portion of the tunnel is vulnerable against fracturing or "blow out" phenomenon, depicted in Figure 9. The resisting force R in Figure 9 should have an adequate factor of safety against uplift blow out pressure U provided by application of tunnel face pressure. This aspect was appropriately

verified before finalization of the tunneling scheme. The maximum pressure against blow out is represented by following equation:

$$p_{max} = C \cdot \left[\gamma + \frac{2c + C \cdot k_h \cdot \gamma' \cdot \tan\phi}{D} \right]$$

Where '*C*' is soil cover up to tunnel crown in meters, *'c'* is soil cohesion in kPa, 'K_h' is horizontal earth pressure coefficient, 'γ' & 'γ'' are unit weight and effective unit weight of soil in kN/m^3 and 'Φ' is angle of shear resistance of soil in degree. The maximum pressure against blow out is plotted against face pressure in Figure 10. Note that the soil cushion provided is justified although the tunnel is most critical against blow out in the river section.

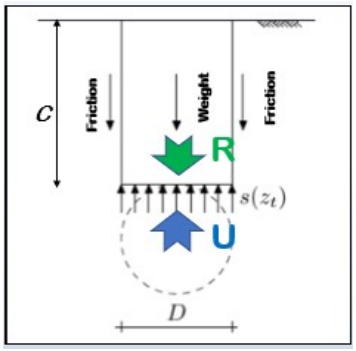


Figure 9: Schematic Diagram for Blow

7. SOIL CONDITIONING DURING EXCAVATION

In operation of an EPB tunnel shield in closed mode (i.e. with pressurized soil inside the excavation chamber), the material in the excavation chamber should behave like a homogenous and plastic mass with pulpy to soft consistency, low inner friction and low water permeability. To obtain such a suitable muck to enhance tunneling performance, additives like foam are added to the face of excavated material. Foam Expansion Ratio [FEM] is defined as the (volume of foam at working pressure)/(volume of foaming solution) expressed as a percentage and foam Injection Ratio [FIR] is defined as (volume of foam at working pressure)/(volume of in situ soil to be excavated) expressed as a percentage are the controlling parameters for use of such additives.

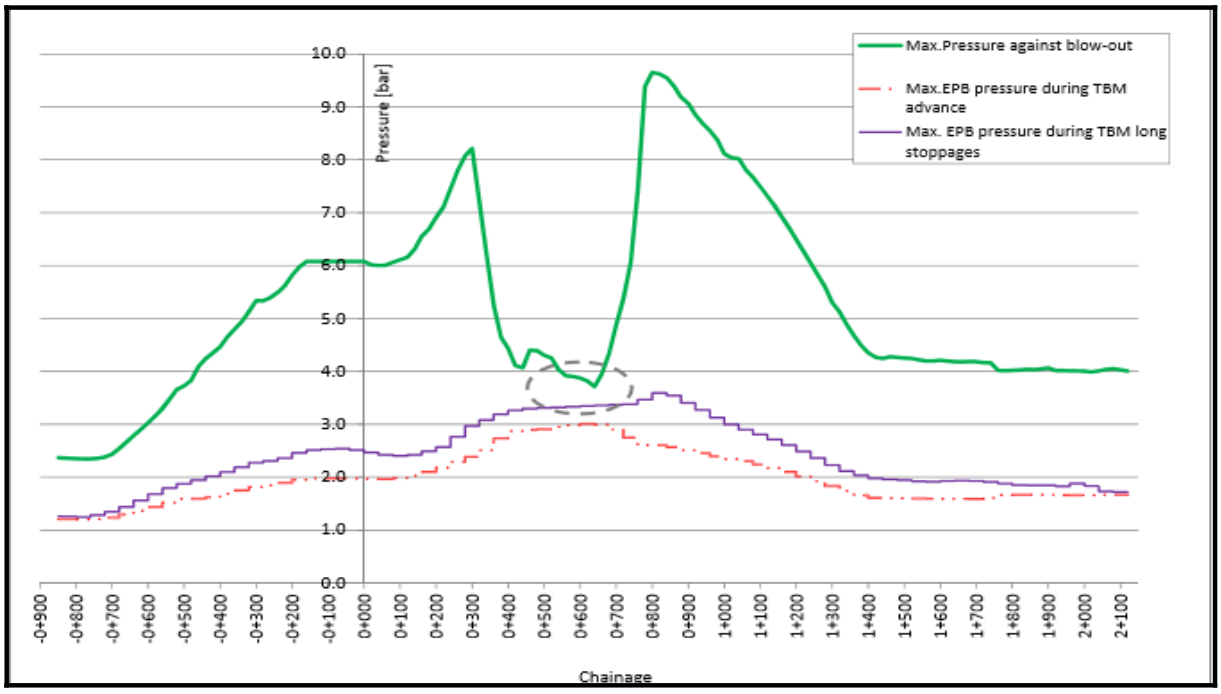


Figure 10: Pressure against Blow Out vs Tunnel Face Pressure

Base line foam parameters following EFNARC guidelines and project experience in EPB tunneling are shown against revised foam parameters developed during tunneling progress are shown in Table 3 along with average physical characteristics (moisture content and Atterberg's limits) of the soil units.

Table 3: Sub-Soil parameters in Tunnel Excavation vis-à-vis Soil conditioning parameters

			Atterberg Limit			Baseline foam parameters	Field parameters for foam
		Moisture Content [%]	LL [%]	PL [%]	PI [%]	FIR [%]: 50 [40-60] FEM [:1]: 8	Unit 2 & 3a FIR: 60-70 FER: 5-6
West Section	Unit2	36.3	54.0	25.0	29.0		
	Unit 3a	26.6	53.0	23.0	29.0		
	Unit 3b	23.7	48.0	24.0	25.0		
River Section	Unit2						Unit 3b FIR: 30-40 FER: 10-12
	Unit 3a	26.8	55.0	23.0	32.0		
	Unit 3b						
East Section	Unit2	33.5	55.0	23.0	32.0		
	Unit 3a	27.6	58.0	23.0	35.0		
	Unit 3b	28.1	50	22	28.0		

To obtain a softer and more plastic mass, it is necessary that conditioned material in the excavation chamber should have moisture content 5% higher than the average plastic limit PL. [i.e. about 28% for units 3a and 3b.]

8. CONCLUSION

Tunneling in urban project environment demands meticulous planning, investigation and design considering all the factors in the tunneling horizon. In this article a study of detailed geotechnical investigation and hydrology has assisted in collecting necessary data for the planning and design of a tunnel below river Ganges. Strict adherence to tunneling parameters and maintenance of flawless emergency protocol is mandatory for success. The success of this first transportation tunnel below such a magnificent and large river in India definitely lead the way for similar achievements in the country in coming years.

REFERENCES

Chugh,**R.S**. "Tides in Hooghly river" 1961- Published in International Association of Scientific Hydrology. Bulletin, Dec 2009

Duddeck, H.; Erdmann, J., Structural design models for tunnels in soft soil, Underground Space; United States); Journal Volume: 9:5-6, 1985

EFNARC: Specification and Guidelines for the use of specialist products for Mechanised Tunnelling (TBM) in Soft Ground and Hard Rock, April 2005

Jamiolkowski, M., et al., Design Parameters for Soft Clays, Proceedings of the 7th European Conference on Soil Mechanics and Foundation Engineering, Brighton,5,21-27, 1979

Kumar S & Dewanjee B: "Metro Twin Tunnelling Below River Hooghly at Kolkata" – Tunneling Association of India Journal, Vol 6 No 2, July 2017

Langmaack, L., 'Europe and Asia: Application of new TBM Conditioning Additives,' BAUMA 2001.

Mukhopadhyay, **Dr S.K**. " The Hooghly Estuarine System, NE Coast of Bay of Bengal, India "- Workshop on Indian Estuaries, NIO, Goa June 25, 2007.

Pennington Thomas W, Professional Associate Finalist, William Barclay Parsons Fellowship Program , April 2011

Sengupta, P.K. " Hydrogeology of Kolkata" http://jcses.blogspot.com/2009/01/hydrogeology-of kolkata.html. 2009

Skempton, A.W., and Bjerrum, L., A contribution to the analysis of settlement analysis of foundations on clay. Geotechnique, 7:168-178.(1957).

Stroud, M.A. "The Standard Penetration Test – Its Application and Interpretation, ICE Conference on Penetration Testing, 29-49. (1989)

KINEMATIC AND INERTIAL FORCES OF SINGLE PILE UNDER DYNAMIC LOADING USING NUMERCIAL APPROACH

Alireza Saeedi Azizkandi, Iran university of science and technology, Tehran, Iran, asaeedia@iust.ac.ir
Sara Hashemi, Iran university of science and technology, Tehran, Iran, sara_hashemi@civileng.iust.ac.ir
Ali Abolhasnpoor, Iran university of science and technology, Tehran, Iran, a.abolhasanpoor@yahoo.com

ABSTRACT

The importance of the structural piles has been determined on the seismic response of the site based on the analytical, numerical and laboratory studies. Due to the lack of laboratory or the numerical studies with the support of laboratory studies, the results are limited to the specific conditions, and problems with the simple geometry and elastic behaviors of the materials against the shear waves in frequency domain. Many studies have been done on the effect of kinematic and inertial interactions on the seismic responses of the soil-pile system by numerical methods. However, most numerical studies based on the results of the analytical methods, and the numerical studies have had less laboratory support. Therefore, this study investigates the effects of the kinematic and inertial interaction of the pile-soil on the dynamic response of a single pile, using physical modeling of a pile in the dry sandy soil with shaking table along with the numerical modeling verified by the laboratory results in ABAQUS FEM software simulation. Moreover, using the numerical models the effect of soil characteristics such as: the modulus of elasticity, how it is distributed in soil, pile capping etc. has been studied. It can be deduced that fix pile head with cap and soil specification, such as the modulus of elasticity, have a great impact on the distribution and the maximum amount of bending moment along the pile.

Keywords: single pile, kinematic and inertial forces, numerical modeling, bending moment

INTRODUCTION

The investigation on the soil-pile-structure interaction has been performed since the 1970s. In order to determine the deformation and the bending moment at the top of the pile or at the intersection of the layers due to the kinematic and inertia interactions, simple methods and terms have been pileosed by different scientists. Dobry and O'Rourke presented a simple formula to calculate the bending moment at the intersection of two very different layers under harmonic stimulation of the bedrock [1]. Gazetas performed a numerical study on the dynamic response of end-loaded piles in some soil profiles taking into

© 2018 Deep Foundations Institute

account the kinematic and inertia interactions [2]. Later, Kavvadas and Gazetas cleared the importance of the kinematic interaction in the seismic stimulation between the soil and the free end of the pile [3]. Sadek and Shahrour used a 3D finite element model to investigate the effect of the condition of the loading of the piles on their seismic response [4]. Dezi et al. studied the effect of kinematic interaction on the bending moment on singular and floating piles during an earthquake[5]. Boulanger et al. pileosed a method to analyze the seismic interaction of soil-pile-structure and validated it by comparing its results with a set of dynamic centrifuge model experiments [6].

Because of the importance of determination of the moment of the pile under seismic loading, the following study comprises of three steps:

1. Application of the shaking table physical model;
2. Application of the three-dimensional ABAQUS software and verification using the first step;
3. Parametric study of the problem to determine the effect of the soil layer characteristics on the singular pile response.

PHYSICAL MODEL USING THE SHAKING TABLE

A set of experiments performed on a 1g shaking table with the aim to investigate the effect of kinematic interaction on the seismic response of the singular pile have been presented. In the present study, the scaling law for shaking table tests, proposed by Iai [8] was used. Considering the space constraints of the model container, an appropriate distance of pile from the side-walls and other capabilities of the available experimental facility explained above, geometric scaling factor was chosen to be 1:10. Physical modeling of the experiments has been performed on a 1 DOF[1] shaking table. The box used in the experiments is made of Plexiglass sheets inside steel frames. This box has inner dimensions of 1.8m(length)×0.8m(width)×1.2m(height).

The details of the prototype used in the experiments can be seen in Fig. 1. The pile is 7.5m long, with other diameter of 0.5m and a 0.015m thickness made of reinforced concrete and is embedded in dense sand. In the lab model an aluminum pipe has been used. the characteristics of the soil (Firoozkuh sand, Type 161) by Eghbali and Fakharian has been presented in Table 1 [7].

[1] Degree of freedom

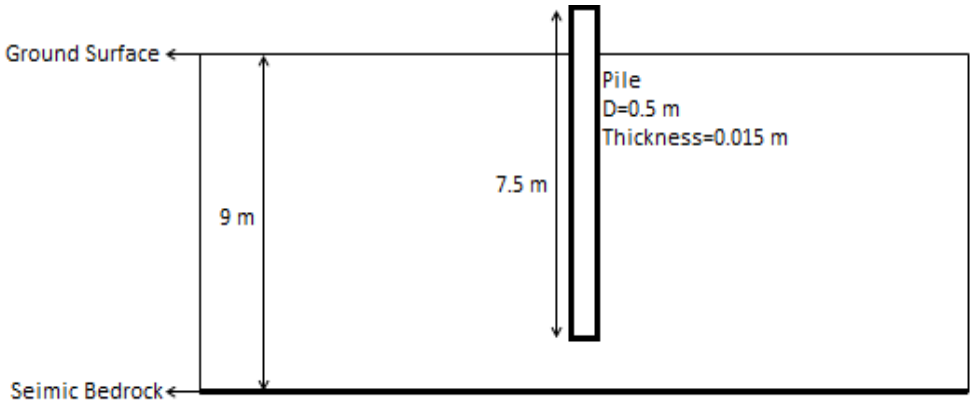


Fig. 1. Free-head single pile prototype model

Table 1. Physical properties of Firoozkuh sand, Type 161

USCS name	G_s	D_r (%)	e_{max}	e_{min}	D50 (mm)	C_u	C_c
SP	2.65	60	0.86	0.58	0.26	1.9	0.88

In order to construct the soil profile, pluvial deposition method has been used and in order to get a uniform compaction throughout the soil, (due to the relative density of 60% assumed in this study) using pluvial deposition method. After reaching the instrumentation level, all essential devices have been implemented and then other layers have been added.

INSTRUMENTATION

According to Fig. 2, accelerometers (ACC.), Linear variable differential transformers (LVDT) and strain gauges (ST.) have been used in order to record the acceleration, the displacements and the bending in different locations, respectively.

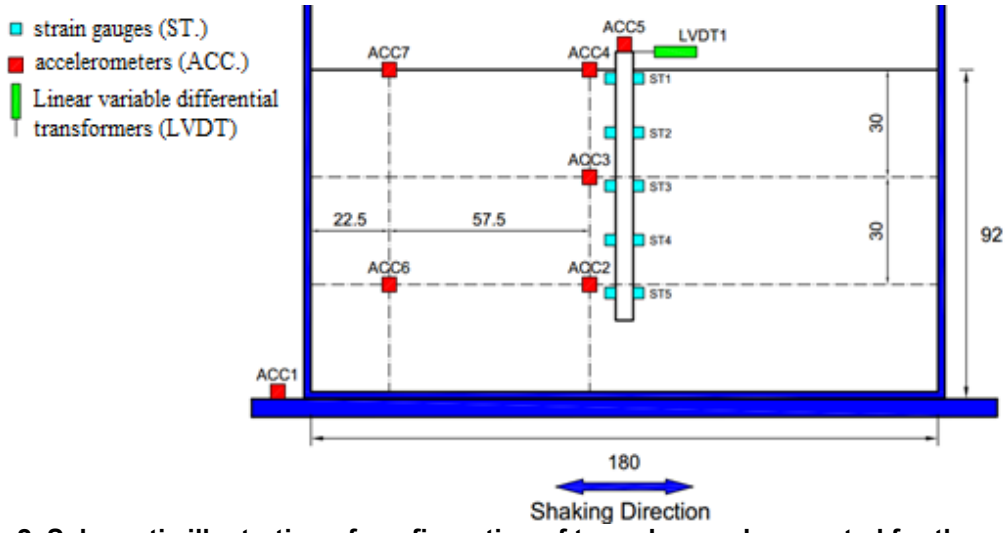


Fig. 2. Schematic illustration of configuration of transducers demarcated for the model (values in cm).

INPUT MOTIONS

Input motions has been applied using the shaking table according to Fig. 3 that shows the input in the form of a time history. Fig. 4 shows the Fourier spectra of acceleration time history. The input acceleration has been recorded using ACC1. Fig. 2

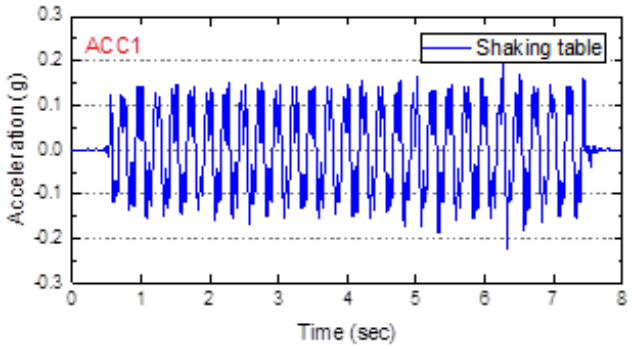


Fig. 3. Recorded time history of the input motion in model scale

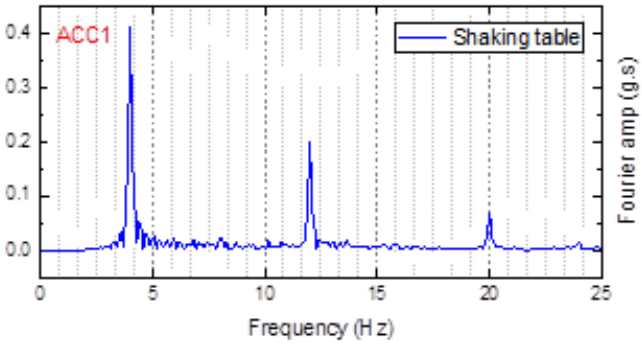


Fig. 4. Fourier spectra of acceleration time histories

NUMERICAL SIMULATION

In order to continue with the parametric studies, numerical models have been used. This has been done using three-dimensional finite element ABAQUS software. In the numerical simulations, the mesh size should be fine enough to ensure that the wave will propagate properly through a medium. This means that the mesh size is limited to 0.3 m. Because of the geometrical limitations in the numerical model such as the pile structure and the accelerometer location and also to improve the accuracy of the analysis two types of elements with the maximum mesh size of 0.05 m were adopted. The soil mass was and the box mass meshed using three-dimensional 8-node hexahedral solid elements (C3D8R) with mesh size of 0.05 m that get smaller as they closer to the pile. The pile mass was discretized with three-dimensional 4-node quadrilateral shell elements (S4R) with mesh size of 0.0125 m.

It is to be noted that using the symmetry of the problem, only half of the geometry has been simulated in the software, decreasing the computing time. The meshing can be seen in Fig. 5.

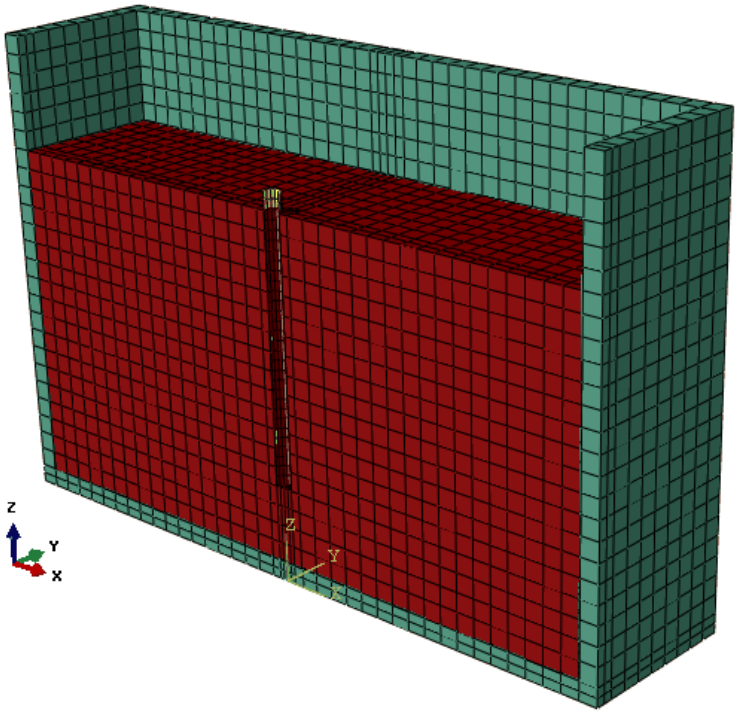


Fig .5. Isometric view of the 3D finite element mesh of a half the model

In order to validate the numerical results with those of the shaking table, it is necessary to correctly adjust the boundary condition in both cases. In this study, the bottom of box is considered a rigid body and the acceleration recorded by ACC1 has been considered as the input acceleration and dynamic loading to the bottom of the numerical model. The details of the materials used in the numerical model is given in Table 3.

Table 3. Properties of materials in scale model

Part	Material	Behaviour	Elastic modulus (MPa)	Poisson's ratio	Density (kg/m^3)	Cohesion (KPa)	Internal friction angle (°)	Dilation angle (°)
Soil	Dens sand	Mohr coulomb	40	0.3	1800	4	35	5
Pile	Aluminium	Elastic	55000	0.33	2700	-	-	-
Box	plexiglass	Elastic	3300	0.35	1190	-	-	-

Furthermore, Rayleigh damping has been used as a method to take into account the damping effect of the materials in the time domain. In this study, Rayleigh damping coefficients have been used as $\alpha = 2.91$ and $\beta = 0.0021$.

A finite sliding surface-to-surface hard contact algorithm was employed for the soil-box and the soil-pile skin contact pairs, whereas a small sliding node-to-surface hard contact algorithm was implemented for the soil-pile tip contact pair. The tangential behavior on the border of soil-box and soil-pile was simulated using the frictional penalty formulation with friction coefficients of $\mu = 0.45$ and 0.35 and for the normal contact behavior. Separation between surfaces after the contact was not permitted for contact pairs.

VERIFICATION

Fig. 6 shows the time history of the bending moment of different locations of the pile from the experiments and the comparison with the results of the numerical simulation. Also, the maximum bending moment along the pile in the experiment and the numerical model has been presented in Fig 7. As can be seen, there is good agreement between these two results.

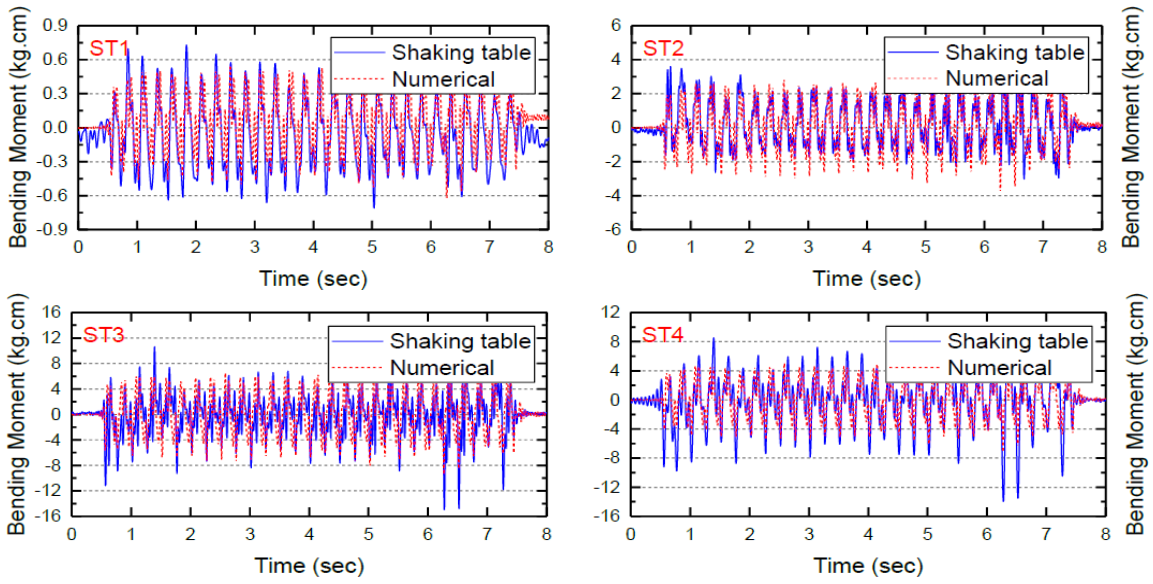


Fig .6. Comparison of recorded and calculated bending moment time histories.

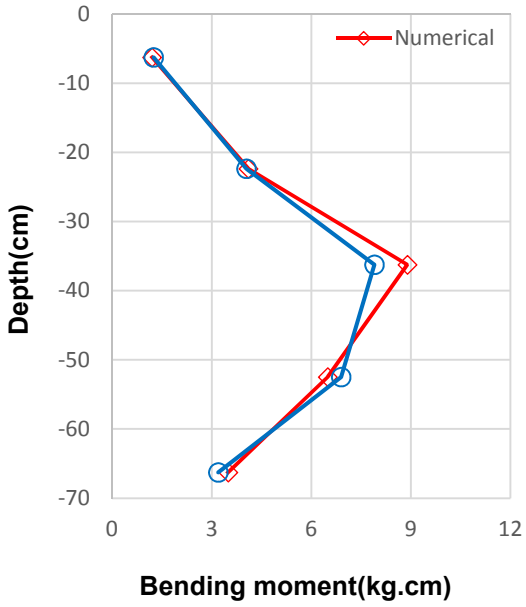


Fig. 7. Comparison of recorded and calculated maximum pile bending moment

PARAMETRIC STUDIES

Using the numerical simulations, the effect of the soil elasticity modulus distribution and the state of the tip of the pile on the singular pile seismic response. In order to perform parametric studies, a sinusoidal loading has been used that it's characteristics is given in Table 4.

Table 4. Input motion characteristics in parametric study

Input motion No.	Type	Frequency (Hz)	Amplitude (g)	Duration (s)
1	Sinusoidal	5	0.1	8

THE EFFECT OF THE SOIL ELASTIC MODULUS DISTRIBIUTION

In addition to the uniform distribution of the elasticity modulus, another type of soil has been considered in the parametric studies of the problem in which the elasticity modulus is linearly increasing with the depth. According to Fig. 8 for the type A, the distribution of the elasticity modulus is uniform and equal to 40 MPa and for type B, the linear elasticity modulus distribution is applied, from zero on the surface to 80 MPa at the bottom.

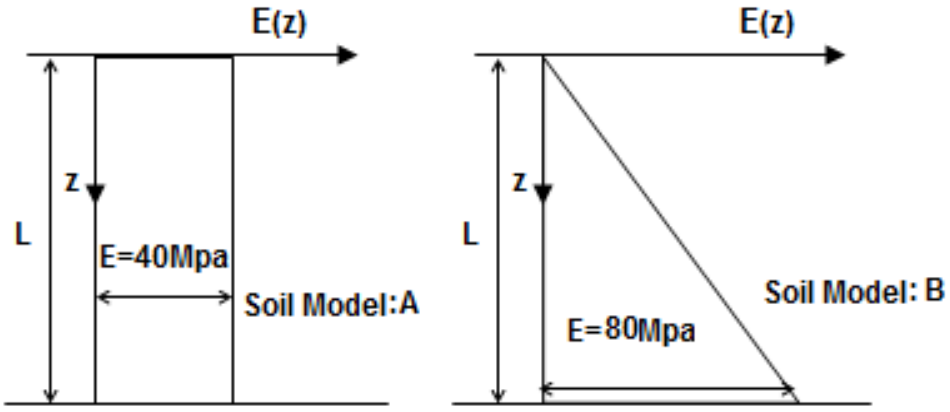


Fig. 8. Sketch of the two soil profiles studied

Fig. 9 shows the maximum bending moment versus the depth for two soil elasticity types A and B. in the case of model A, the bending moment curve has a convex shape which has its peak occurred at the middle of the pile along its depth, a zero value at the ground surface, and a non-zero value at the pile tip. As one can see the changes in the soil profile from A to B, not only affects the bending moment distribution but also it leads to a considerable reduction in the maximum bending moment and also its location rises near to the tip of the pile.

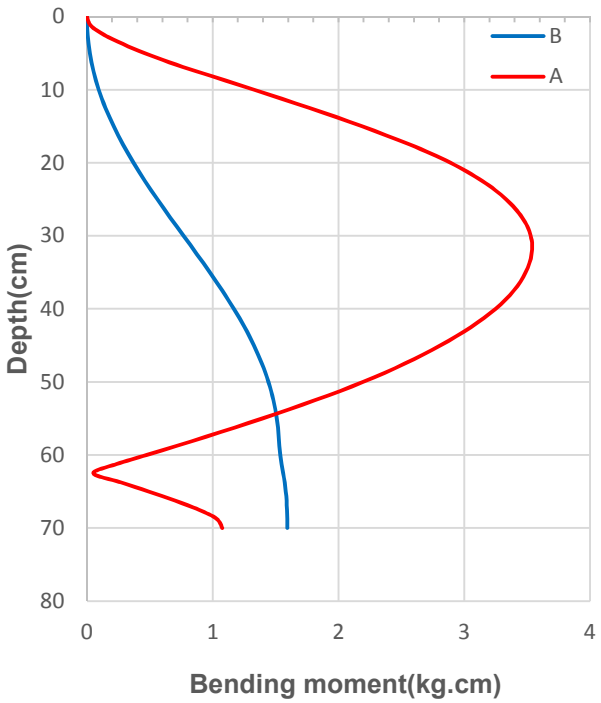


Fig. 9. Comparison of maximum pile bending moment

THE EFFECT OF THE CAP

In order to investigate the cap and its effect on the bending moment, a concrete cap has been modeled and for two cases, namely cap with weight and weightless, have been compared. In order to apply a suitable joint to the connection of the pile and the cap, the Tie contact option has been used, for both conditions, the elasticity is set to be 40 MPa. The characteristics of the concrete cap is presented in Table 5.

Table 5. Properties of cap

Part	Material	Elastic modulus (MPa)	Poisson's ratio	Density (kg/m^3)
Cap	Concrete	20000	0.25	2400

In Fig. 10 the values of the maximum bending moments versus depth has been plotted for three conditions: 1. pile, 2. Pile and cap with weight and 3. Pile with weightless cap. It can be seen that the presence of cap and considering its weight affects the bending moment significantly and generally changes the moment distribution, so that there are two point in the curve that . Using the weightless cap only affects the bending moment at the tip of the pile but does not lead to any changes in the moment at the depth, just like the pile without a cap.

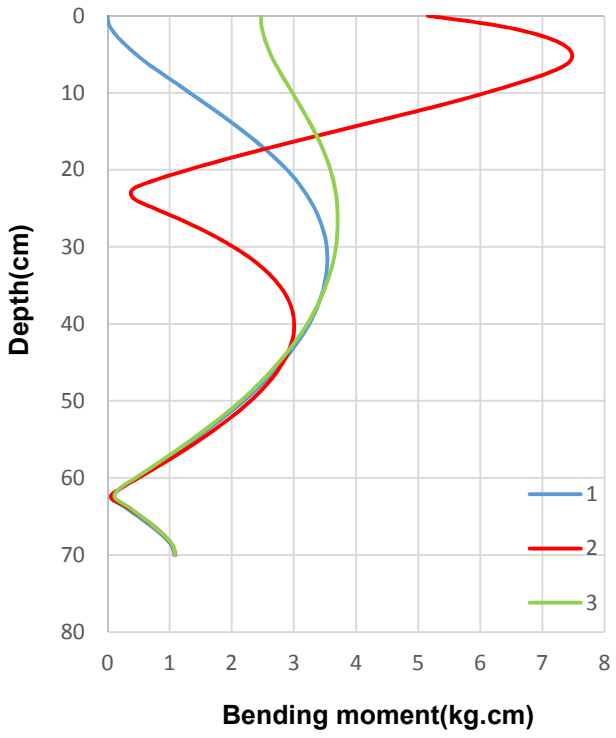


Fig. 10. Comparison of maximum pile bending moment

CONCLUSION

In the present study, using the shaking table physical modeling and the 3D ABAQUS software validated using the experimental data, the effect of elasticity modulus distribution and the joint of the head of the pile has been investigated on the seismic response of the pile. Important findings from the numerical investigation are emerged as follows:

- The maximum bending moments and its distribution depends on the soil soil inhomogeneity. In the case of soil model B (a soil of linearly increasing modulus with depth), the maximum of the bending moment decreases significantly and also its location rises near to the tip of the pile.
- By applying the boundary condition at the top of the pile, the moment distribution varies along the pile. This is beside the fact that by eliminating the inertia effect, the moment distribution is similar to that of a pile without a cap and it only affects the bending moment values.

REFERENCES

[1] Dobry R, O'Rourke MJ. Discussion on "Seismic response of end-bearing piles." by Flores Berrones R. and Whitman R.V. Journal of the Geotechnical Engineering Division—ASCE 1983;109(5):778–81.

[2] Gazetas G. "Seismic response of end-bearing single piles." Soil Dynamics and Earthquake Engineering 1984;3:82–93.

[3] Kavvadas M, Gazetas G. "Kinematic seismic response and bending of free-head piles in layered soil." Geotechnique 1993;43:207–22.

[4] Sadek, M. and Shahrour, I.,(2006). "Influence of the head and tip connection on the seismic performance of micropiles". Soil Dynamics and Earthquake Engineering, 26(5), pp.461-468.

[5] Dezi, F., Carbonari, S. and Leoni, G.,(2010). "Static equivalent method for the kinematic interaction analysis of single piles". Soil Dynamics and Earthquake Engineering, 30(8), pp.679-690

[6] Boulanger RW, Curras CJ, Kutter BL, Wilson DW, Abghari A. "Seismic soil–pile–structure interaction experiments and analyses." Journal of Geotechnical and Geoenvironmental Engineering 1999;125:750–9.

[7] Eghbali AH, Fakharian K. "Effect of principal stress rotation in cement-treated sands using triaxial and simple shear tests." Int J Civ Eng, Trans B: Geotech Eng 2014;12(1).

[8] S. Iai, "Similitude for shaking table tests on soil-structure-fluid model in 1g gravitational field." Soils and Foundations, 29 (1989) 105-118.

NUMERICAL ANALYSIS OF THE SOIL-PILE-STRUCTURE INTERACTION ON STRUCTURE'S BASE SHEAR

Alireza Saeedi Azizkandi, Iran university of science and technology, Tehran, Iran, asaeedia@iust.ac.ir

Esmaeel Hamrang Taqidizaj,Iran university of science and technology,Tehran, Iran,

hamrang_esmaeel@civileng.iust.ac.ir

Pedram Ghaderi, Iran university of science and technology, Tehran, Iran,p_ghaderi@iust.ac.ir

ABSTRACT

For the calculation of the structure's base shear value ($V = \frac{A.B.I}{R} * W$), A indicates the design reference acceleration, showing (PGA) in each area, B is the soil reflection coefficient. The product of these two parameters is spectral acceleration ($Sa = A.B$) which in fact shows the effect of the soil type on the design reference acceleration magnitude. As it can be observed, there is no coefficient which can indicate the effects of the foundation and existence of piles as increasing or diminishing factor in the design reference acceleration magnitude. Therefore, we studied this subject by using numerical modeling in ABAQUS and seismic test validations. The results show that the existence of piles have a significant effect on the design reference acceleration magnitude .Hence, the effect of the number of piles and the input frequency on acceleration magnification was investigated in this paper.

Keyword: soil-pile-structure, interaction, base shear, magnitude, PGA

1. Introduction

Overall, the earthquake occurs because of the sudden movement of the earth's crust and the acceleration which enters the soil influences the objects on the surface which is the result of the acceleration of the rocky motion. But the most important event is that the amount of the acceleration generated deep in the earth is not the same as the amount of the acceleration applied to the surface of the earth, and the amount of acceleration of the bedding undergoes changes during its movement until it reaches the surface of the earth.

In accordance with most codes, the acceleration of the bedrock is increased due to the passage of alluvial lands, as an example, Fig1 illustrates the design spectrum diagram for the various site conditions as published by the European Code. Another factor affecting the magnification level is the topography of the area which has not been paid attention in most codes. However, in the past, some researches were conducted on this subject which has been mentioned in the ASCE code.

Another point that we pay attention to is the effect of the foundation type and especially the pile group on the magnification of the acceleration and structure's base shear which has not been reviewed in any codes.

The analysis of the soil-pile-foundation system's seismic response is complicated due to the kinematic interaction between the foundation, piles, soil, and also the nonlinear behavior of the soil. In these conditions, if we consider the interaction between the built structure and the system, the complexities will increase even more. Many studies have been conducted on pile-soil interaction, while there are limited researches regarding the pile-foundation-structure systems and this is due to the complexities of the load transfer in the interaction between structure, pile, foundation, and nearby soil. The analysis of the most recent studies shows that there are no comprehensive analytical methods for the prediction of the structure's behavior and uncertainties in loading.

In this study, in order to investigate the interaction of the Pile-Soil-Structural System and its effects on the magnitude of acceleration and structure's base shear in a large scale, firstly we attempt to record the accelerometers by performing a shaking table test on a pile-soil-structure system, afterwards the validity of the numerically modeling assumptions are investigated by the numerically modeling of the same system and comparing results. In the parametric study, we investigate the effects of the number of piles on the pile group and the effects of the load frequency on the acceleration magnification and subsequently on the structure's base shear.

© 2018 Deep Foundations Institute

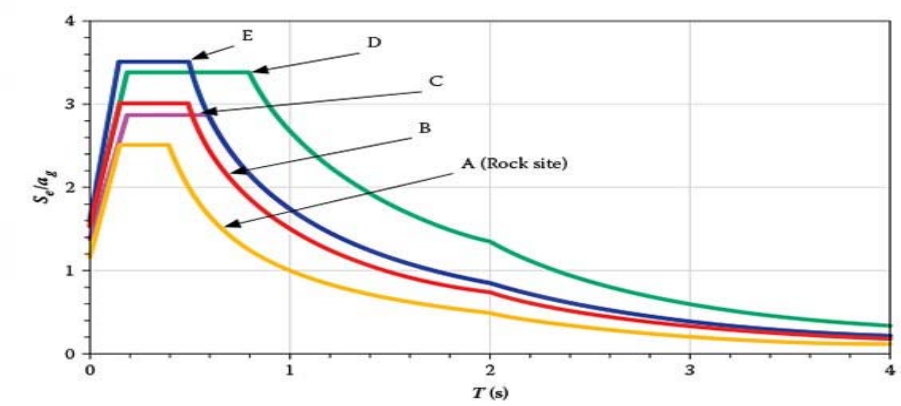


Fig 1. EC 8 2004 design spectra for different site condition for a damping ratio of 5%

A: Hard rock (V_S >1500 m/s), B: Rock (760< V_S<1500 m/s), C: Soft rock/very dense soil (360< V_S<760 m/s), D: stiff soil (180< V_S<360 m/s), E: Soft soil (V_S<180 m/s).

2. Shaking Table Experimental Tests

The experimental tests were conducted using shaking table facility of the Physical Modelling and Centrifuge Laboratory at University of Tehran (UT). This shaking table is a 1DOF(Degree Of Freedom) facility capable of inducing frequencies between 0.01 to 15 Hz using a hydraulic servo actuator. The box of shaking table for physical models had inner dimensions of 1.8 m length, 0.8 m width and 1.2 m height. A box as a soil container is not only required to hold the soil in place during shaking table tests, but also the ideal soil container should simulate free filed soil response by minimizing boundary effects and reflection of the outward propagating waves. The mentioned box at University of Tehran, has two layers of foam in internal sides to simulate the free field conditions. Gohl and Finn(1987) and Valsangkar et al. (1991) reported that absorbing layers of polystyrene foam, like those installed on UT's shaking table, represent viscous boundaries in the free field condition. The used polystyrene foam in this shaking table is commercially available EPS (Expanded Polystyrene) material, means Type I according to the ASTM classification system (2006) with a density of 16 kg/m3, poisson's ratio of 0.09 and yield strength of 30.4 (MPa). This foam has average initial tangent elastic modulus of 5 MPa according to Bathurst et al. (2002).
In this study scaling factors as suggested by Iai et al. (2005) for 1-g shaking test were employed having in mind the properties of prototype soil and dimensions of the box and the model. Table 1 summarizes the adopted scaling factors in this study and resultant dimensions of the model and prototype are presented in Table 2. It should be considered that in this study for the problem with lateral loading, bending stiffness of piles (EI) is critical. The prototype pile was considered to be a concrete pile with steel casing (with EI equal to 150742.38 (kN.m4)) and the model piles bending stiffness was chosen considering scaling rule and factors of Iai et al. (2005) as shown in Table2.

Table 1. Scaling Factors for 1-g Shaking Table Tests

Parameter	Scaling factor proposed by Iai et al. (2005) prototype/model	Adopted scaling factor
Length	Λ	10
density	λ_ρ	1
Strain	$\lambda_\varepsilon = \lambda 0.5$	3.16
Time	$(\lambda_\varepsilon \lambda)^{0.5}$	3.16
Frequency	$\lambda -0.75$	0.1778
Acceleration	1	1
Displacement	$\lambda 1.5$	31.62
Stress	Λ	10
EI of piles	$\lambda 4.5$	31622.7

Table 2. Scaled Parameters using Adopted Scaling Method of Iai et al. (2005)

Parameter	Scaling factor	Prototype	Model
Pile length (m)	10	7	0.7
Pile Diameter (m)	10	0.5	0.05
EI of Pile (kN.m^2)	31662.7	150742.3876	4.7
Raft length (m)	10	5	0.5
Raft Thickness (m)	10	1	0.1

2.1 Test set-up and result:

Dry Firoozkuh siliceous sand no.161 having a relative density of about 60% was used as a model ground. A summary of adopted material properties for Firoozkuh sand is available in Table 3.The final soil model was 90 cm in height, 80 cm in width and 170 cm length.

The piled raft model was an aluminum square raft rigidly connected to four hollow pipe aluminum piles. Material properties and dimensions of the model are presented in Table 4. It should be noted that the total length of the piles were 75 cm where upper 5 cm was embedded and screwed in the raft to ensure a rigid connection. Center-to-center piles' spacing, S, also was 20 cm, 4 times the pile diameter (S/D = 4). Regarded as a cast-in place foundation, the foundations were set by the help of clamps and it was continued to fill the box to the desired level to ensure the contact of foundation and soil.

The schematic illustration of tested models along with the boundary conditions, location of piles, linear voltage differential transducer (LVDT) sensors and strain gages are presented in Fig. 2.

Ten electrical resistance type strain gages were installed on each pile to measure the fiber strains and the consequent bending moments along the piles. In this study, the input accelerations were all with the almost same peak value of 0.3 g and frequency of 7 Hz. Fig. 3 shows a typical input acceleration employed in tests.

Table 3. Material Properties of the 161-Firoozkuh Sand

Item	Value
Density (Kg/m^3)	1550
Frictional angle (degree)	33
Dilation angle (degree)	7.8
Young Modulus (MN/m^2)	40
Poison Ratio	0.24

Table 4. Material Properties and Dimensions of Elastic Elements

Part Name	Material	Dimensions (m)	Mass Density (Kg/m^3)	Weight (kg)	Young Modulus (MN/m^2)	Poison Ratio
Cap	Aluminum	0.1×0.5×0.5	2580	64.5	69000	0.3
Pile	Aluminum	D_a = 0.05, L_b = 0.7	2580	0.4	69000	0.3
Superstructure Beam	Steel	D_a = 0.05, L_b = 0.5	6490	6.62	200000	0.3
Superstructure Head	Steel	0.1×0.2×0.2	6490	27.3	200000	0.3

[a]D: Diameter (m)
[b]L: Length (m)

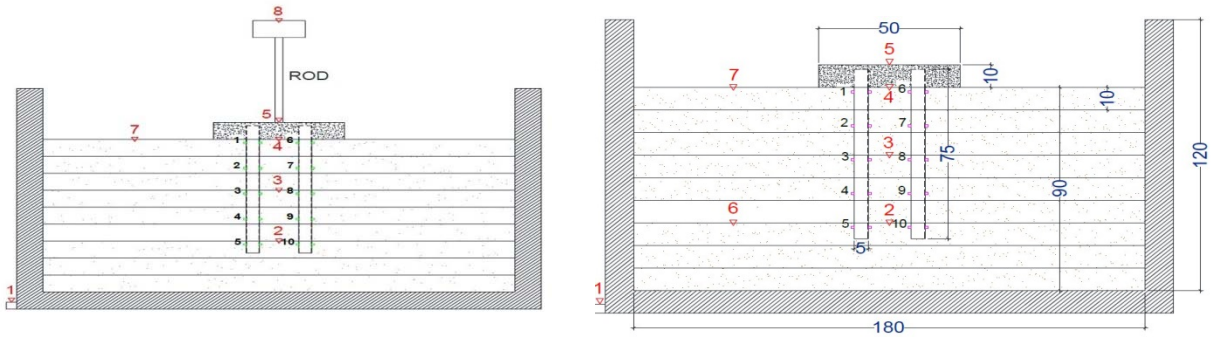


Fig. 2.(The schematic illustration of tested models)

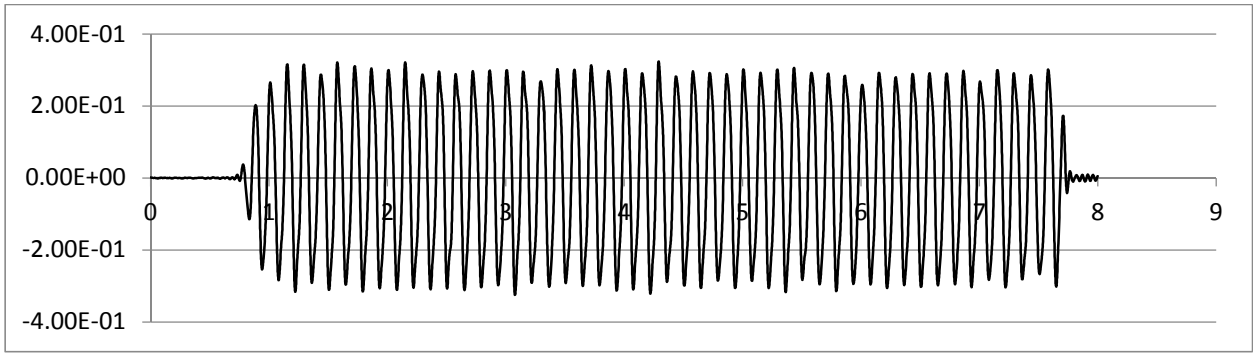


Fig. 3(input acceleration employed in tests)

Measured acceleration through accelerometer (Number 5) installed on the cap is depicted in Fig 4.

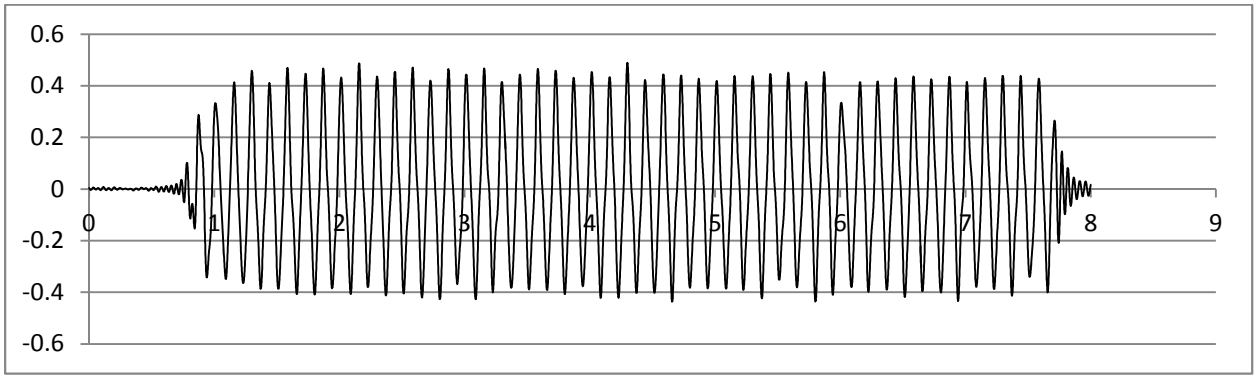


Fig. 4 (measured cap acceleration)

3. Three Dimensional Numerical Analyses and Verification

Fig.5 is plotted as a reference and shows the adopting of three dimensional finite element meshes, whose dimensions are 5 cm, and model with superstructure in ABAQUS software. The shaking table model's dimensions were adopted in numerical modelling. Soil, box, rod and superstructure were modelled with eight-node hexahedral with reduced integration brick elements (C3D8R) and the piles were modelled as eight-node hexahedral (C3D8) elements. Tangential behavior for interactions between pile-raft and soil was considered to be governed with penalty interaction having the angle of friction equal to 2/3 of the internal frictional angle of the soil. Normal behavior was

defined by a hard contact pressure over- closure relationship. Regarding the mesh size, as suggested by Helwany (2007), mesh dimension in the vicinity of pile and stress zone is as fine as 1/10D where D is the pile diameter and it is extended more than 30D for minimizing boundary effects on the solution. As a reference, meshed connected Piled Raft Foundation (CPR) with superstructure, consisted of 17142 elements, including 11220 C3D8R elements and 5922 C3D8. For dry Firoozkuh sand, considering the properties in Table 3, an elastic perfectly plastic model using Mohr-Coulomb failure criterion was adopted in this study with a non-associated flow rule. The model pile and raft were assumed to be linear elastic aluminum as mentioned in Table 4.The analyses were carried out in three steps. In the first two steps the gravity load and foundation- soil interactions were introduced using static general analysis procedure. In the third step implicit dynamic analysis procedure in time domain was employed with the maximum time increment equal to $\Delta t = 0.05$ (s) which was the same to increments of the acceleration time history in the lab. The Coulomb friction law was adopted to model the interfaces in which the interface friction coefficient and limiting displacement are required as input parameters.

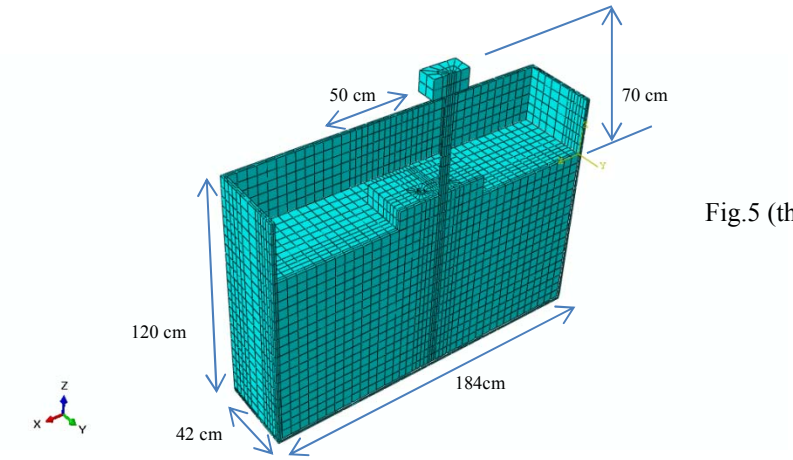


Fig.5 (three dimensional finite element mesh and model)

After completing the numerical analysis and taking the required outputs, it is essential to compare the results with the experimental results; Fig. 6 contains two diagrams, one of them is laboratory test and the other is the result of numerical analysis.

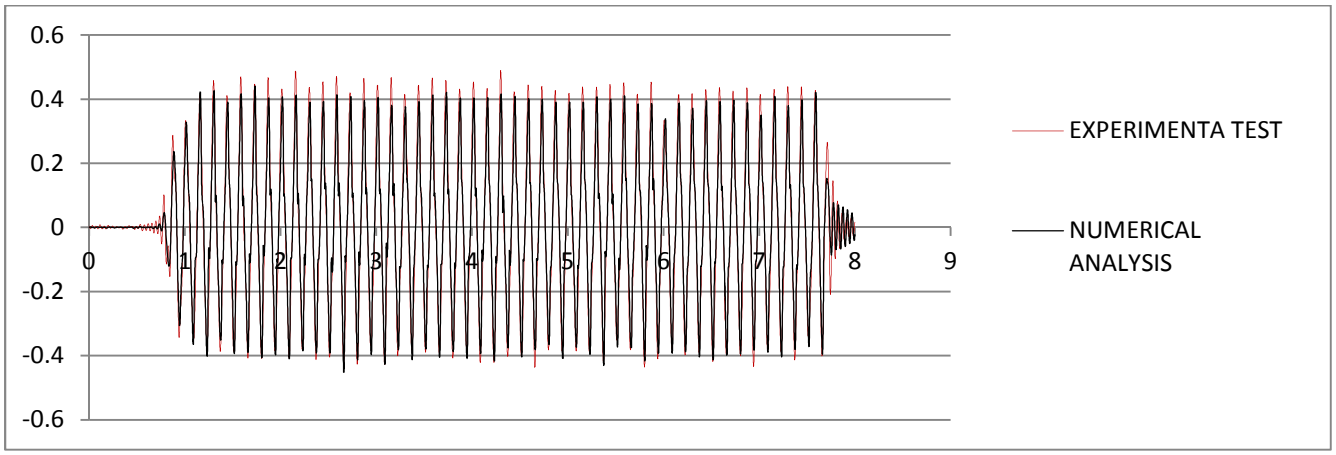


Fig.6 (experimental test and numerical analysis result)

As it is seen, in addition to the trend conformity in the graphs, the mentioned graphs are also consistent with the accuracy of the results, in terms of the magnitude of acceleration which allows us to begin our parametric study.

4- Parametric study

After the verification and assurance of numerical modeling with constant consideration of material properties, behavioral model, boundary conditions and the type of the friction between the elements and the modeling of the mesh, and the change in the model geometry, along with the dynamic load frequency input parametric study were conducted.

The parametric study consists of four different models:

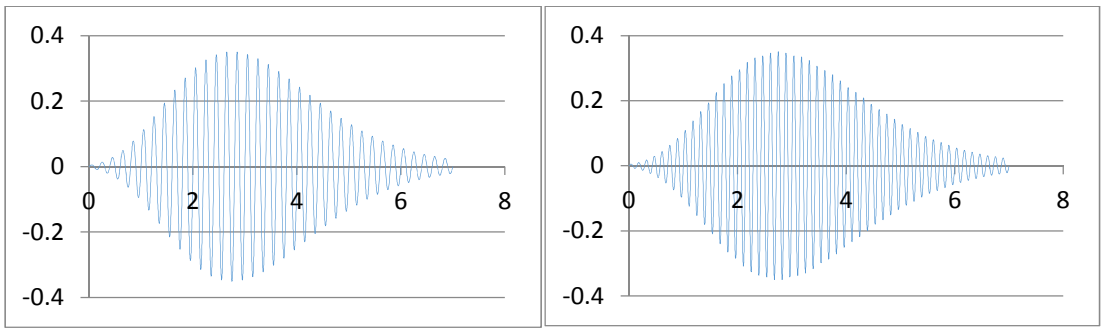
1. Cap without a pile along with a superstructure
2. Cap with single-pile and superstructure.
3- Cap with four piles and superstructure
4- Cap with nine piles and superstructure

It should be noted that again, due to the geometric symmetry of the models and the symmetry of loading along X, we performed the modeling in half, which reduces the time of the analysis.
Regarding the natural frequency of the system, we have considered seven different frequency types for the dynamic load input: 5Hz,7Hz,10Hz,13Hz,15Hz,17Hz,20Hz
In order to prevent sudden acceleration with large amplitudes , which causes an impact and error in the acceleration register, in the first moments of loading into a model, we used the formula 1 instead of applying a direct sinusoidal load, then we generated 7 dynamic loadings with different frequencies according to the fig 7(a to g). Furthermore, we cannot use actual earthquake acceleration records since we need the frequency and maximum acceleration to be various in this paramedic study In this type of loading, the acceleration range starts from small values and gradually reaches a maximum value of 0.35 g and the load time is 7 seconds.

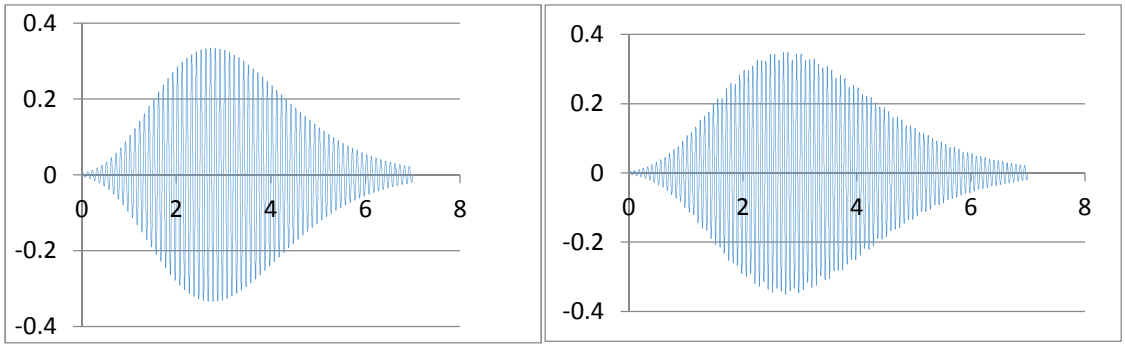
Dynamic loading formula: $\ddot{u}(t) = \sqrt{\beta . e^{-\alpha t} . t^{\xi}} Sin(2\pi . f . t)$

Formula.1 (Hatami,k.and Bathurst,R.J.200)

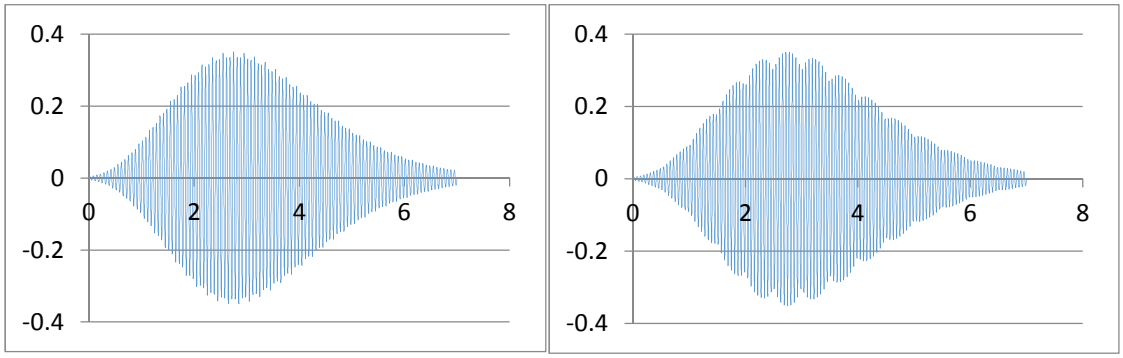
Where $\ddot{u}(t)$ is acceleration, (t) is the time of dynamic analyses and (f) is the loading frequency;
α,β,ξ are constant coefficients to produce a specified peak amplitude with trial and error method.



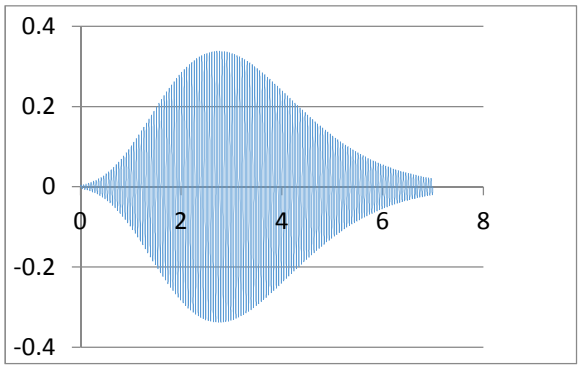
(a) (b)



(c) (d)



(e) (f)



(g)

Fig 7. (a) 5Hz,(b) 7Hz,(c) 10Hz,(d) 13Hz,(e) 15Hz,(f) 17Hz,(g) 20Hz dynamic loading

5-Conclusion:

After doing 7 analyses for each of the four models, we have a total of 28 complete analyses, for all of which the output of the acceleration-time is obtained.

Considering the maximum input acceleration amplitude, 0.35 g, by obtaining the maximum acceleration amplitude for each of the analysis, we can calculate the magnitude of acceleration for each one. Our aim is to compare the magnitude of the acceleration of the cap in the presence of a pile with the state of the absence of the pile in the 7 different input frequencies, for this purpose we obtain the magnification of the cap for the 21 analyses in which the piles are located and by dividing it by the magnification of the acceleration of a pile-free cap, a new parameter of (PMRMR), Pile-raft Magnification Raft Magnification Ratio, is defined. Not to mention, the comparison of both magnifications for an input frequency is the same.

In order to simultaneously show the effect of the incoming dynamic load frequency and the number of piles on the acceleration of the Cap, we show the results by plotting the three-dimensional diagram Fig 8, where the axes represent the input frequencies, the number of piles and the parameter RMPMR.

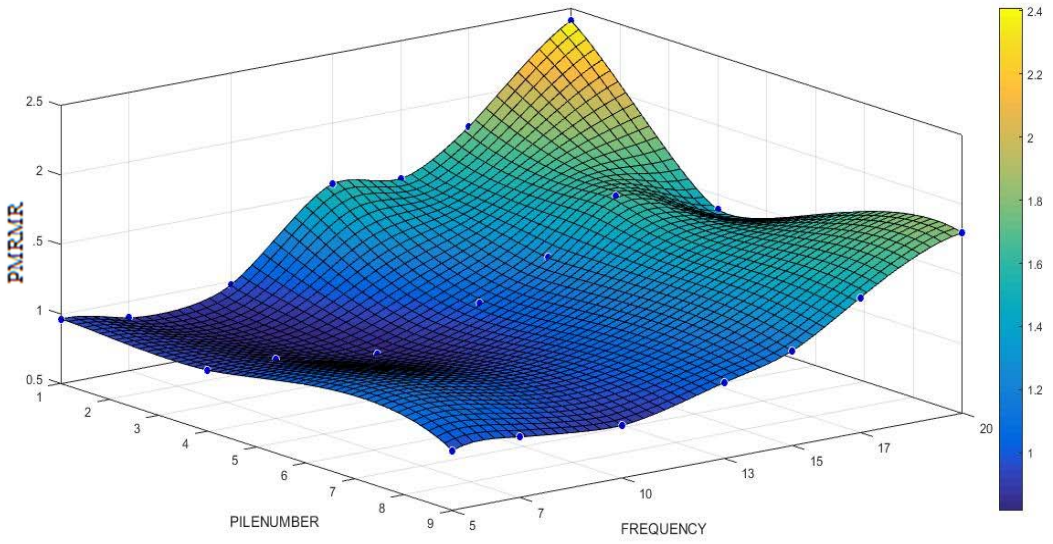


Fig (8).parametric study result

As it is seen in the results, the change in the number of piles at different input frequencies has a great influence on the magnification ratio of the pile group to the cap without pile.

The presence of more piles cannot always reduce the magnification of the acceleration and structure's base shear.

In a fixed number of piles, the magnitude of the acceleration and structure's base shear do not always increase with increasing loading frequency and they have a nonlinear relationship.

References

American Concrete Institute (ACI) (1969). "ACI standard-Building code requirements for reinforced concrete" ACI 318-19, Detroit.

Amini, F. and Ghaderi, P. (2013). "Seismic motion control of structures: A developed adaptive back stepping approach." Computers and Structures, Vols. 114-115, pp. 18-25, DOI: 10.1016/j.compstruc. 2012.09.011.

Areias, P., Rabczuk, T., and Msekh, M. A. (2016). "Phase-field analysis of finite-strain plates and shells including element subdivision."

Computer Methods in Applied Mechanics and Engineering, Vol. 312, pp. 322-350, DOI: 10.1016/j.cma.2016.01.020.

Areias, Pedro and Rabczuk, T. (2013). "Finite strain fracture of plates and shells with configurational forces and edge rotations." International

Journal for Numerical Methods in Engineering, Vol. 94, No. 12, pp. 1099-1122, DOI: 10.1002/nme.4477.

Bathurst, Richard J., Saman Zarnani, and Andrew Gaskin. (2007). "Shaking table testing of geofoam seismic buffers." Soil Dynamics and Earthquake Engineering, Vol. 27, No. 4, pp. 324-332, DOI: 10.1016/j.soildyn.2006.08.003.

Bhowmik, D., Baidya, D. K., and Dasgupta, S. P. (2013). "A numerical and experimental study of hollow steel pile in layered soil subjected to lateral dynamic loading." Soil Dynamics and Earthquake Engineering, Vol. 53, pp. 119-129, DOI: 10.1016/j.soildyn.2013.06.011.

Bowles, J. E. (1988). Foundation analysis and design, McGraw-Hill, 5th edition, 1996, pp. 650-700.

British standards Institute (BSI) (1986). Foundations, BS 8004, London.

Cao, X. D., Wong, I. H., and Chang, M. F. (2004). "Behavior of model rafts resting on pile-reinforced sand." Journal of Geotechnical and Geoenvironmental Engineering, Vol. 130, No. 2, pp. 129-138, DOI: 10.1061/(ASCE)1090-0241(2004)130:2(129).

Cooke, R. W. (1986). "Piled raft foundations on stiff clays—a contribution to design philosophy." Geotechnique, Vol. 36, No. 2, pp. 169-203, DOI: 10.1680/geot.1986.36.2.169 Fioravante, V. and Giretti, D. (2010). "Contact versus noncontact piled raft foundations." Canadian Geotechnical Journal, Vol. 47, No. 11,pp. 1271-1287, DOI: 10.1139/T10-021.

Gohl, W. B. and Finn, W. D. L. (1987). "Seismic response of single piles in shaking table studies." In: Fifth Canadian Conference Earthquake Engineering, pp. 435-444.

Hamada, J., Tsuchiya, T., Tanikawa, T., and Yamashita, K. (2012). "Lateralloading model tests on piled rafts and their evaluation with simplified theoretical equations." In Proceedings of the 9th International Conference on Testing and Design Methods for Deep Foundations (ISKanazawa 2012), Vol. 1, pp. 467-476.

Hecht, T. and Dürwang, R. (2001). "Optimierung der Gründung der Reichenbachtalbrükemit der Kominierten Pfahl-Plattengrüdung." Pfahl-Symposium, 2001, pp. 21-34.

Helwany, Sam (2007). Applied soil mechanics with ABAQUS applications,John Wiley & Sons.

Horikoshi, K., Matsumoto, T., Hashizume, Y., and Watanabe, T. (2003)."Performance of piled raft foundations subjected to dynamic loading." International Journal of Physical Modelling in Geotechnics, Vol. 3, No. 2, pp. 51-62, DOI: 10.1680/ijpmg.2003.030204.

Iai, S., Tobita, T., and Nakahara, T. (2005). "Generalized scaling relations for dynamic centrifuge tests." Géotechnique, Vol. 55, No. 5, pp. 355- 362.

Kramer, Steven L. (1996). Geotechnical earthquake engineering, Pearson Education India.

Ladd, R. S. (1978). "Preparing test specimens using undercompaction." Geotechnical Testing Journal, Vol. 1, No. 1, pp. 16-23, DOI:10.1520/GTJ10364J.

Lam, S. Y., Ng, C. W. W., Leung, C. F., and Chan, S. H. (2009). "Centrifuge and numerical modeling of axial load effects on piles in consolidatingground." Can Geotech J., Vol. 46, pp. 10-24, DOI: 10.1139/T08-095.

Lee, C. J. and Ng, C. W. W. (2004). "Development of downdrag on pilesand pile groups in consolidating soil." J. Geotech Geoenviron Eng.,Vol. 130, No. 2, pp. 905-914, DOI: 10.1061/(ASCE)1090 0241 (2004)130:9(905).

Lee, J., Kim, Y., and Jeong, S. (2010). "Three-dimensional analysis of bearing behavior of piled raft on soft clay." Computers andGeotechnics, Vol. 37, No. 1, pp. 103-114, DOI: 10.1016/j.compgeo. 2009.07.009.

Maheshwari, B. K., Truman, K. Z., El Naggar, M. H., and Gould, P. L. (2004). "Three-dimensional nonlinear analysis for seismic soil–pilestructure interaction." Soil Dynamics and Earthquake Engineering, Vol. 24, No. 4, pp. 343-356, DOI: 10.1016/j.soildyn.2004.01.001.

Matsumoto, T. (2013). "Implications for design of piled raft foundations subjected lateral loading." In Proc. Int. Symp. on Advances in Foundation Engineering, Singapore, pp. 113-136.

Matsumoto, T., Fukumura, K., Horikoshi, K., and Oki, A. (2004). "Shaking table tests on model piled rafts in sand considering influence of superstructures." International Journal of Physical Modelling in Geotechnics, Vol. 4, No. 3, pp. 21-38, DOI: 10.1680/ijpmg.2004. 040302.

Nguyen-Thanh, N., Valizadeh, N., Nguyen, M. N., Nguyen-Xuan, H., Zhuang, X., Areias, P., Zi, G., Bazilevs, Y., De Lorenzis, L., and Rabczuk, T. (2015). "An extended isogeometric thin shell analysis based on Kirchhoff–Love theory." Computer Methods in Applied Mechanics and Engineering, Vol. 284, pp. 265-291, DOI: 10.1016/ j.cma.2014.08.025.

Nguyen-Thanh, Nhon, Kiendl, J., Nguyen-Xuan, H., Wüchner, R., Bletzinger, K. U., Bazilevs, Y., and Rabczuk, T. (2011). "Rotation free isogeometric thin shell analysis using PHT-splines." Computer Methods in Applied Mechanics and Engineering, Vol. 200, No. 47, pp. 3410-3424, DOI: 10.1016/j.cma.2011.08.014.

Pastsakorn, K., Hashizume, Y., and Matsumoto, T. (2002). “Lateral load tests on model pile groups and piled raft foundations in sand.” In Proc. Int. Conf. Physical Modelling in Geomechanics, St. John's, Canada, pp. 709-714.
Poulos, H. G., Small, J. C., and Chow, H. (2011). “Piled raft foundationsfor tall buildings.” Geotechnical Engineering Journal of the SEAGS and AGSSEA, Vol. 42, No. 2, pp. 78-84.
Randolph, M. F. and Clancy, P. (1993). “Efficient design of piled rafts.” In Proceedings 2nd International Seminar Deep Foundation at Ghent, Belgium, pp. 119-130.
Saeedi Azizkandi, A., Baziar, M. H., Modarresi, M., salehzadeh, H., and Rasouli, H. (2014). “Centrifuge modeling of pile-soil-pile interaction considering relative density and toe condition.” Scientia Iranica, Vol. 21, No. 4, pp. 1330-1339.
Saeedi Azizkandi, A., Baziar, M. H., Rasouli, H., Modarresi, M., and Shahnazari, H. (2015). “Centrifuge modeling of non-connected piled raft system.” International Journal of Civil Engineering, Vol. 13, No. 2, pp. 114-123, DOI: 10.22068/IJCE.13.2.114.
Sawada, K. and Takemura, J. (2014). “Centrifuge model tests on piled raft foundation in sand subjected to lateral and moment loads.” Soils and Foundations, Vol. 54, No. 2, pp. 126-140, DOI: 10.1016/ j.sandf.2014.02.005.
Shahnazari, H., Shahin, M. A., and Tutunchian, M. A. (2014). “Evolutionarybased approaches for settlement prediction of shallow foundations on cohesionless soils.” Int. J. Civ. Eng., Vol. 12, No. 1, pp. 55-64.
Shahnazari, H., Salehzadeh, H., Rezvani, R., and Dehnavi, Y. (2014). “The effect of shape and stiffness of originally different marine soil grains on their contractive and dilative behavior.” KSCE J. Civ. Eng., Vol. 18, No. 4, pp. 975-983, DOI: 10.1007/s12205-014-0286-8.
Tradigo, F., Pisanò, F., di Prisco, C., and Mussi, A. (2015). “Non-linear soil–structure interaction in disconnected piled raft foundations.” Computers and Geotechnics, Vol. 63, pp. 121-134, DOI: 10.1016/
j.compgeo.2014.08.014.
Valsangkar, A. J., Dawe, J. L., Mita, K. A. (1991). “Shake table studies of seismic response of single partially supported piles.” In: Sixth Canadian Conference Earthquake Engineering, pp. 327-34.
Wong, I. H., Chang, M. F., and Cao, X. D. (2000). “Raft foundations with disconnected settlement reducing piles.” Design Applications of Raft Foundations, Chap. 17, Thomas Telford, London, pp. 469-486.
Yamada, T., Yamashita, K., Kakurai, M., Tsukatani, H. (2001). “Longterm behavior of tall building on raft foundation constructed by topdown method.” In Proc. 5th Int. conference on deep foundation practice incorporating PILETALK international 2001, Singapore, pp. 411-417.
Yamashita, K., Hamada, J., and Yamada, T. (2011). “Field measurements on piled rafts with grid-form deep mixing walls on soft ground.” Geotechnical Engineering Journal of the SEAGS & AGSSEA, Vol. 42, No. 2, pp. 1-10.
Yamashita, K., Hamada, J., Onimaru, S., and Higashino, M. (2012). “Seismic behavior of piled raft with ground improvement supporting a base-isolated building on soft ground in Tokyo.” Soils and Foundations, Vol. 52, No. 5, pp. 1000-1015, DOI: 10.1016/j.sandf.2012.11.017.
Yamashita, K., Kakurai, M., Yamada, T., and Kuwabara, F. (1993). “Settlement behavior of a five-story building on a piled raft foundation.” Deep Foundations on Bored and Auger piles, pp. 351-256.
Yamashita, K., Yamada, T., and Hamada, J. (2011). “Investigation of settlement and load sharing on piled rafts by monitoring full-scale structures.” Soils and Foundations, Vol. 51, No. 3, pp. 513-532, DOI: 10.3208/sandf.51.513.
Yamashita, Kiyoshi, Junji Hamada, Sadatomo Onimaru, and Masahiko Higashino (2012). “Seismic behavior of piled raft with ground improvement supporting a base-isolated building on soft ground in Tokyo.” Soils and Foundations, Vol. 52, No. 5, pp. 1000-1015, DOI: 10.1016/j.sandf.2012.11.017.

SCOUR EFFECTS ON LATERALLY LOADED PILES IN SAND AND POTENTIAL REMEDIAL MEASUREMENTS

Ammar A. Mohammed, Sultan Qaboos University, Oman, 3malsharif@gmail.com
Yahia E-A. Mohamedzein, Sultan Qaboos University, Oman, yahiaz@squ.edu.om, Phone 0096824142577

ABSTRACT

The effect of scour on laterally loaded piles installed in sand is investigated using laboratory model tests. The model test was performed in a large tank. The influence of different scour depths and the use of riprap as a potential remedial measures, were studied. The scour depth was varied from 1D to 3D (where D is the pile diameter). A substantial reduction in ultimate lateral capacity of the pile due to scour is observed. The percentage decrease of the lateral load capacity (PDC) reaches almost 20% when the scour depth increases from 0 to 3 D. The countermeasure used in this study (i.e. riprap) has a significant influence on the lateral load resistance for the scoured piles. The riprap improves the ultimate lateral resistance of the pile for the 3D scour case from 52 to 116 N.

Keywords: bending moment, deflection, dune sand, laboratory model, laterally loaded piles, scour

INTRODCTION

Piles are generally used to transmit vertical and lateral loads to the surrounding soil media. Piles that are used to support structures such as bridge piers, transmission-line towers, high rise buildings, retaining walls and offshore structures are normally subjected to lateral loads. These piles or pile groups should resist not only vertical movements but also lateral movements. The load capacity of the pile foundation depends mainly on the interaction between the pile and the surrounding soil, so the lateral resistance decreases as the embedded pile length decreases or unsupported length increases.

Scouring in cohesionless soils increases the unsupported length and therefore reducing the lateral resistance of the pile. Scour is basically a process of soil erosion by the action of flowing water. Lagasse et al. (2006) reported that approximately 60% of the bridge failures in the United States results from scouring effects. Thus, understanding the fundamental of scouring phenomena will help in proper design of any structure exposed to such condition. Extensive research had been done to determine the scour depth (Avent and Alawady 2005; Lauchlan and Melville, 2001; Richardson and Richardson, 1993; Richardson and Davis, 2001). However, limited studies have been undertaken to evaluate the lateral response of piles under scour conditions (Kishore et al., 2009; Ni et al. 2011; Lin et al., 2010; Li et al. , 2013; Lin et al., 2015; Qi et al., 2016). In current practice, when pile foundations under scour conditions are analyzed, soils around the pile foundations are totally removed to the scour depth, which will lead to a conservative analysis (Lin et al., 2015). Li et al. (2013) used the three-dimensional (3D) finite-difference method to evaluate the behavior of laterally loaded piles in marine clays at different scour-hole dimensions, such as scour depth, scour-hole width, and slope. They concluded that the reduction in the lateral resistance varies from 14% to 78%, depending on the scour depth level and lateral deflection level. The objective of this paper is to study the variation of the lateral capacity of piles installed in dune sand under different scour conditions. To achieve this objective, a fully instrumented hollow steel pipe pile models were installed into dune sand and subjected to lateral loading under different scour conditions. The scour was varied from 0 to 3 times the pile diameter. Model tests were also performed to study the benefits of using riprap as a countermeasure to prevent the scour.

© 2018 Deep Foundations Institute

SOIL MATERIALS

Two types of soils were used in this study: dune and coarse sands. The dune sand is a poorly graded sand (SP) with 2% fine, a coefficient of uniformity (C_u) of 2.1 and a coefficient of curvature (C_c) of 1.0. The coarse sand is almost passing sieve No 4 (4.75 mm) with 1.95% fines. It has a coefficient of uniformity (C_u) about 6.0 and coefficient of curvature (C_c) of 1.16 and can be classified in the border line between poorly and well graded sand (SP-SW). Figure 1 shows the grain size distribution for both sands. The figure also shows the grain size distribution of the riprap that was used as a countermeasure of erosion.

PILE MATERIALS

Steel pipe piles are commonly used in practice and therefore they were used in this study. The outer diameter of the pile is 33.5mm with 3mm wall thickness and has a length of 670 mm (i.e. 20 times the diameter). Table 1 shows the properties of the steel pile.

TEST SET-UP AND INSTRUMENTATION

The test tank used in this study was a square tank. It was designed using 18 mm plywood and stiffened at its edges with steel angle to protect the tank from bulging when filled with sand. The tank dimensions were selected to ensure that there are no boundary effects on the results. The tank width, length and height are 1.0, 1.0 m 0.8 m, respectively (volume 0.8 m^3). A pulley arm was attached to the tank to facilitate the loading. The pulley arm was made from a 3mm steel angle. Figure 2 shows a schematic diagram of the experimental setup for a single pile and Figure 3 shows a photograph of the tank and the pile.

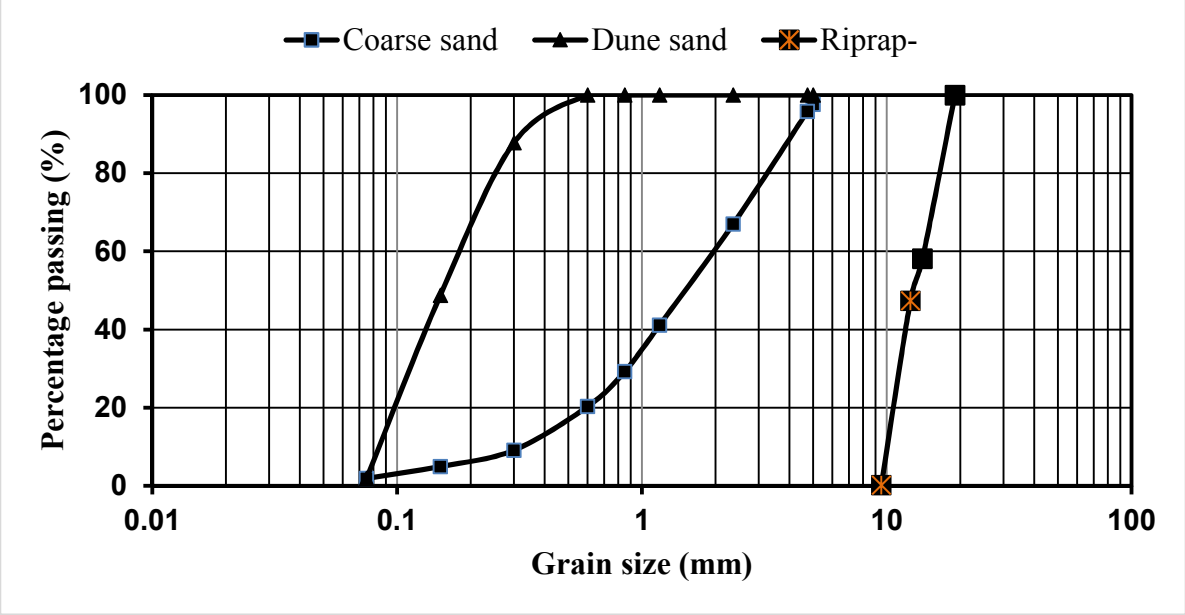


Figure 1. Grain size distribution for coarse, dune sand and riprap

Table 1. Pile properties

Length, L (mm)	Outer diameter, D(mm)	Wall thickness,(mm)	Moment of inertia, I_p,(mm^4)	Poisson's ratio, v	Elastic Modulus, E_p,(MPa)
670	33.5	3	33749	0.3	$210x10^3$

Instrumentation

Figure 2 shows the layout of the instrumentation used which consisted of strain gauges and liner variable differential transducer (LVDT). Five strain gauges of type FLA-10 were attached to the pile surface along its embedded length. The strain gauges were attached to measure the deformation along the length of the pile. The LVDT was used to measure the deflection of the pile. The LVDT core length was 100 mm, and was fixed at 40 mm above the soil surface. The LVDT was adjusted in order to measure the displacement during the loading and unloading stages. The lateral load that applied on the single pile was provided by dead weights, using a steel wire and a pulley, as shown in Figure 2. The loading point was 25 mm above the soil surface. The strain gauges and LVDT readings were collected by a data logger which was connected directly to a computer and automatically recorded the readings in 10 minutes intervals during the test.

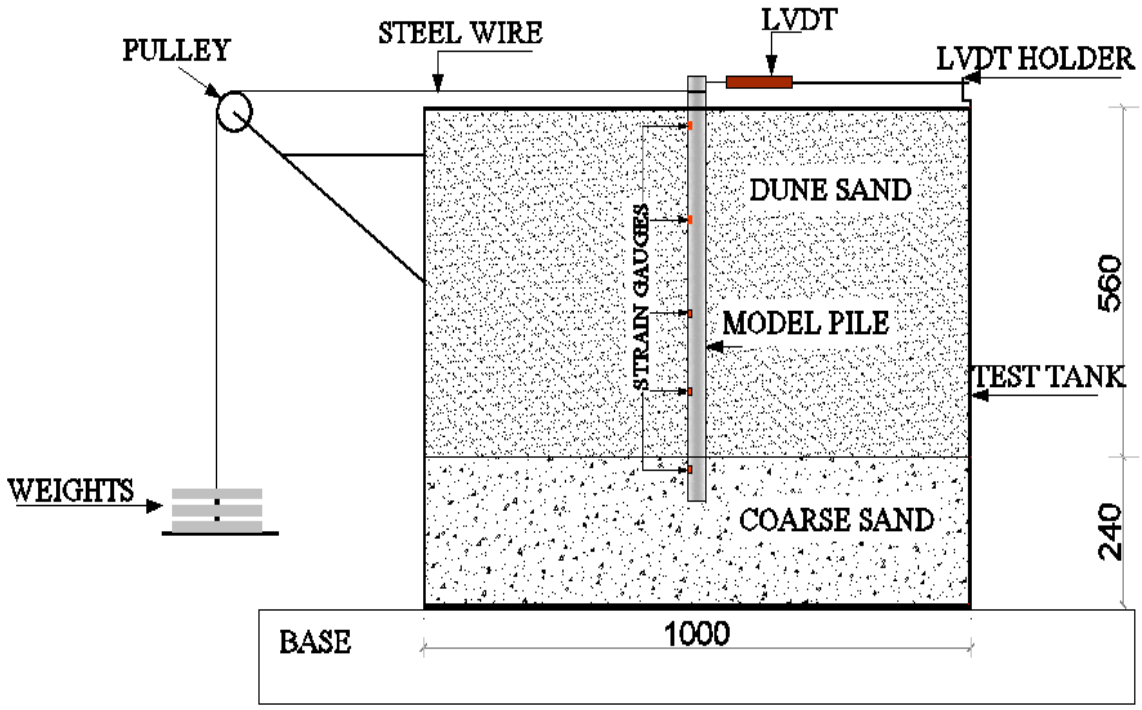


Figure 2. Schematic view of test set-up and instrumentation (Units in mm)

SOIL PLACEMENT

The coarse sand was placed at the bottom of the test tank to a depth of 170 mm. The coarse sand was intended to provide a suitable bearing formation for the pile. The pile was then placed at the required level guided by a frame to ensure the vertical alignment of the pile. After securing the pile in place, more coarse sand was added up to 240 mm (10 % of the pile length was embedded in the coarse sand). By using sand-raining technique dune sand was filled up to 800 mm (top surface of the tank). During the raining of the dune sand the density was measured at different depths by small containers with known volume.

In the case of scouring tests the sand was filled up to the top surface of the tank then the soil was removed to form the scour hole with specific width and scour depth. Angle of repose of dune sand (i.e. about 26.5^{o}) was used as slope angle of the scour hole for all the tests.

TEST PROCEDURE

After the test setup, the LVDT was attached to the top of the pile. The load was applied in 4 to 5 increments, with an incremental load of about 10 N and the load was held constant for a duration of 6 hours for each load step. This time duration was selected based on several tests and it was found no variation in the pile displacement after six hours. The lateral load was applied until the top lateral deflection reaches 5% of the pile diameter (1.675 mm) and the corresponding load was taken as the lateral-load capacity of the pile. This 5% was considered large enough to cause a safety problem in practice (Ni et al., 2011). The unloading stage follows the loading stage with the same loading rate.

TESTING PROGRAM

The testing program was intended to study the effect of different scour levels and also to explore the potential use of the riprap as a countermeasure. The scour depth was varied from 1 to 3D (where D is the diameter of the pile), thus covering practical depth reported in the literature. Also test were performed with riprap as a countermeasure to scour.



Figure 3. Photograph of test tank and pile

ANALYSIS OF THE RESULTS

The measured data during lateral load testing included load–deflection curves at the loading point and the strain gauge readings a long the pile length for each load increment. The loading point was at 25 mm above the soil surface. The measured data, and hence the performance of piles under scour, could be presented in terms of: load–deflection curves at top of pile and the variation of deflection, bending moment, shear force and soil pressure along the length of the pile. The load–deflection curves were obtained directly from the readings of the LVDT and the measured load. The variation of the deflection, bending moment, shear force and soil pressure with depth were obtained from manipulation of the readings of the strain gauges. The collected strain data consisted of values of microstrains for each load increment at discrete points along the model pile length. The bending moment can be obtained directly from the strain gauge readings. First the curvature (Φ) was related to strains assuming linear elastic material as:

$$\Phi = \frac{\varepsilon}{(D/2)} \quad (1)$$

Where: D = Pile Diameter, ε = Strain gauges readings.
Then the bending moment (M) can be obtained from the curvature as:

$$M = EI * (\Phi) \quad (2)$$

Where: E = Modulus of elasticity of the pile (kN/m^2), I= Moment on inertia of the pile cross section (m^4).

Through double integration of the curvature, the deflection (y) along the pile length can be obtained, using two boundary conditions, as:

$$y = \int \int \frac{M}{EI} dz\, dz \quad (3)$$

The soil pressure (p) can be obtained using double differentiation of the moments along pile length as:

$$p = -\frac{d^2M}{dz^2} \quad (4)$$

To evaluate the reduction of the pile capacity due to scour, a quantity termed the percentage decrease of lateral load capacity (PDC) was proposed by Ni et al. (2011) as follows:

$$PDC = \frac{L_{CO} - L_{CS}}{L_{CO}} * 100\% \quad (5)$$

Where L_{CO} and L_{CS} = lateral load capacity of the pile without scour and with a certain scour depth, respectively.

RESULTS AND DISCUSSION

Load–deflection curves

Figure 4 depicts the lateral load versus top deflection of a single pile without scour and under different scour depths. It is clear that for the same load level the deflection increases with the increase in scour depth. This is physically acceptable because the soil resistance is reduced due to sand removal around the

pile up to the scour depth. Similar results were obtained by other researchers (Lin et al., 2015; Li et al., 2011).

Also the scouring of the soil around the pile severely decreases the lateral load capacity of the piles. For example, the lateral load capacity is 76 and 59 N for scour depths 0D, and 3D, respectively, when the allowable lateral deflection (δ) is set as 5% of the pile diameter. When the scour depth is 3D, the pile is losing around 20% of its original lateral load capacity when compared to that without scouring. Figure 4 shows that the slope of the curves decreases as load level increases.

Figure 5 shows the PDC (as defined by Equation 5) for the piles with different scour depths. The quantity PDC varies from 3% to 20% when the scour ranges from 1 to 3 times the pile diameter. This means that approximately 3% to 20% of the load capacity was lost when scouring of the soil occurs around the pile foundation. Therefore, care should be taken when designing the piles to resist the lateral load especially when a pile foundation is expected to face a large lateral force, such as during floods and debris flow events.

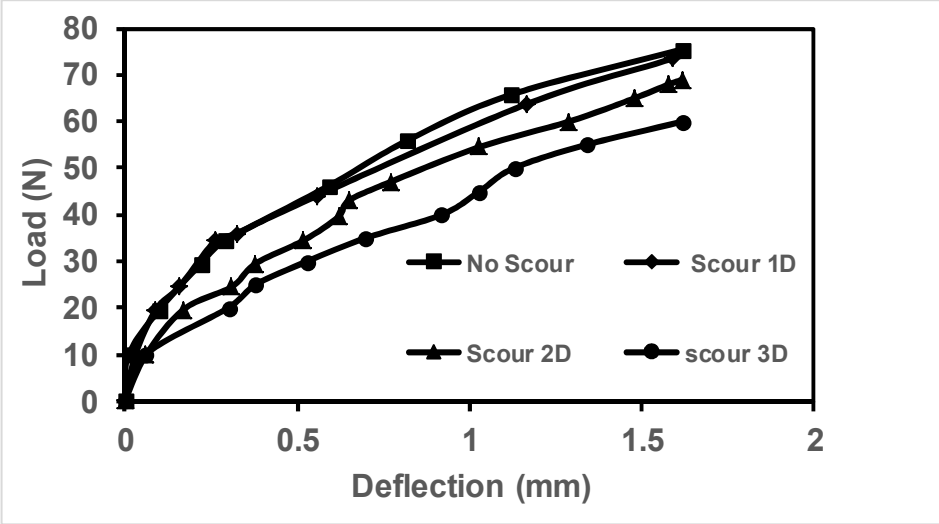


Figure 4. Comparison of top lateral deflection for a single pile

Bending moment diagrams

Bending moments of piles were determined for different scour depths and load levels. A simple Matlab Script was written to calculate the moment, shear force and soil pressure form the strain gauge readings. Figures 6 and 7 present the moment diagrams for different load levels for the case of no scour and 3D scour. These figures clearly show that as the load level increases the moments increases along the embedded length up to a certain level then starts to decrease. It can be observed that the maximum moment location is shifted up (from 0.51L to 0.54L) as the load level increases. The effects of scour depth is clear in Figure 8, at a given load, the moment increases as the scour depth increases. The increase in moments is due to removal of top soil which resist the pile movement.

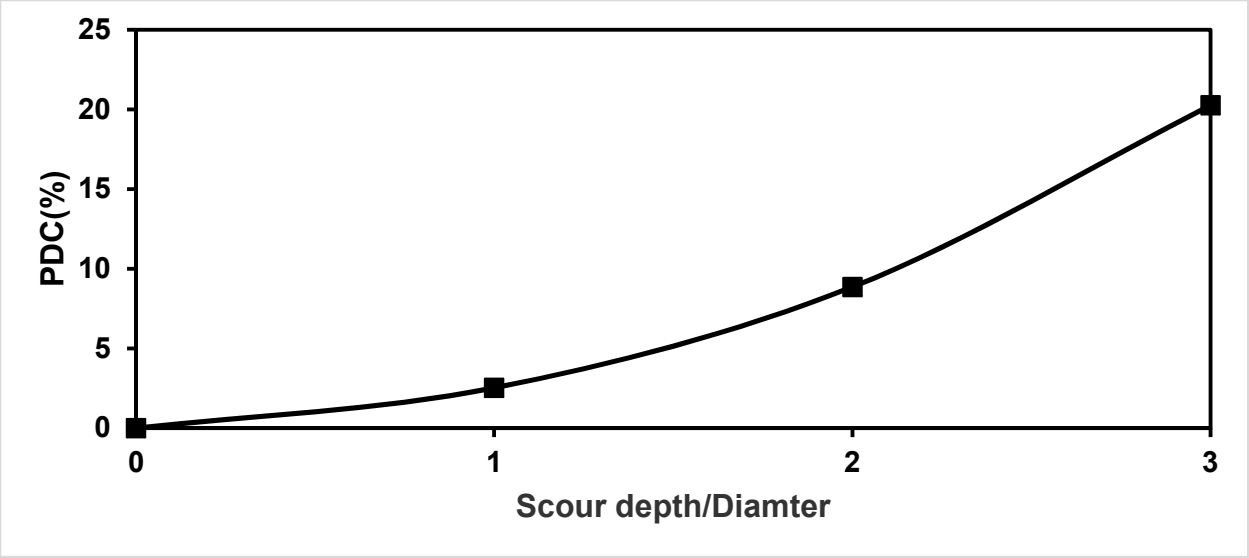


Figure 5. Percentage decrease of lateral load capacity for a single pile at δ/D=5%

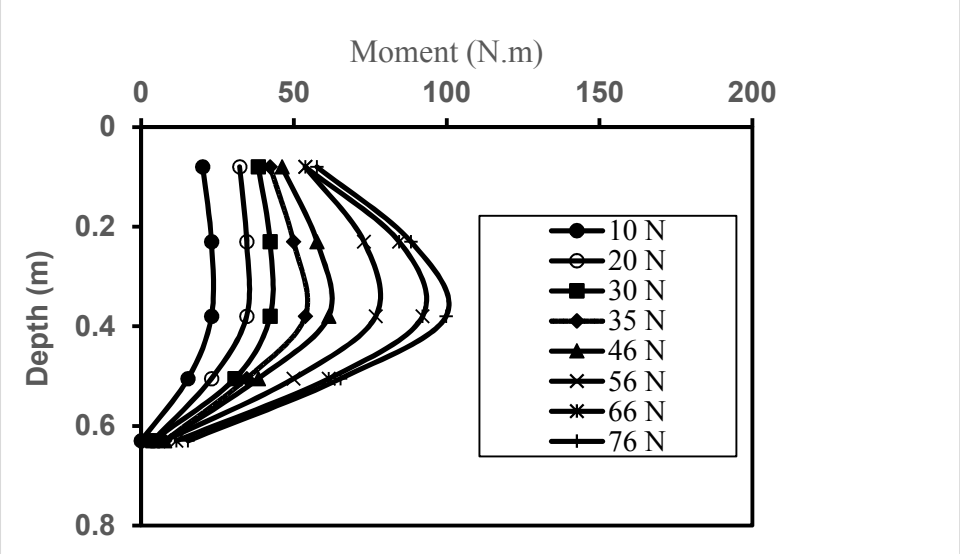


Figure 6. Variation of moment with depth for a single pile without scour

USE OF RIPRAP AS A COUNTERMEASURE

The frequently used armoring countermeasure is the riprap (Lauchlan and Melville, 2001). The grain size distribution of the riprap is shown in Figure 1. The dimensions of the riprap (for 3D scour depth) are: depth of riprap is 3D (about 100 mm) and radius of hole at surface is about 200 mm. The load- deflection curve for a pile with riprap is shown in Figure 9. The figure indicates that the ultimate lateral load is increased significantly compared to the case with scour. In the case of the riprap, the improvement that occur in the resistance was almost 100% when compared with the case with 3D scour.

The distribution of the bending moment with depth for the case of riprap is similar to the cases shown earlier but, the magnitudes are different. Figure 10 compares the moment at 3 different cases (without scour, with 3D scour and with riprap) at the same load level. It can be observed that the moment was higher in the case of 3D scour followed by the case without scour and the case with riprap, respectively. This is because the higher strength of the riprap and because of the increased confining stress of the soil underneath the riprap which accordingly increased the lateral resistance.

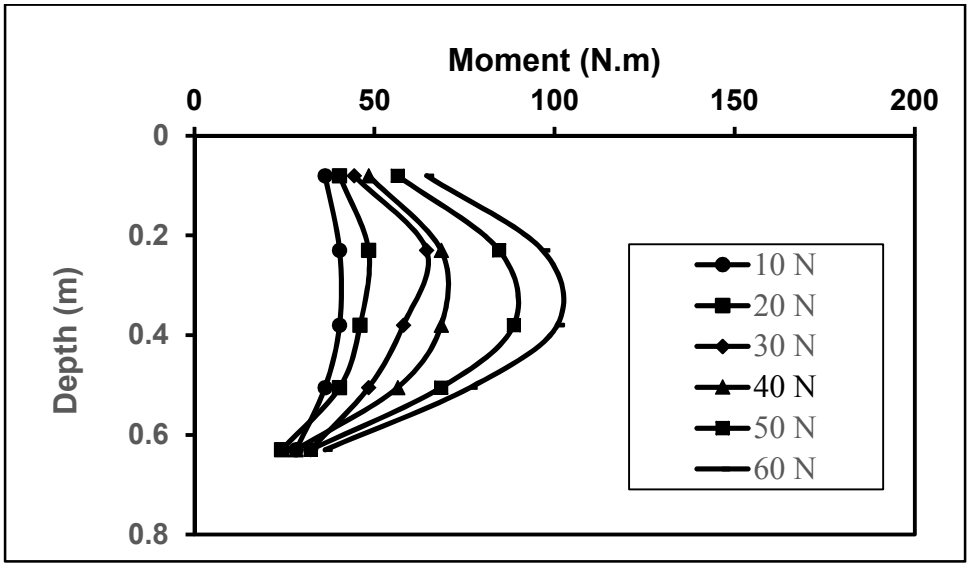


Figure 7. Variation of moment with depth for a single pile with 3D scour

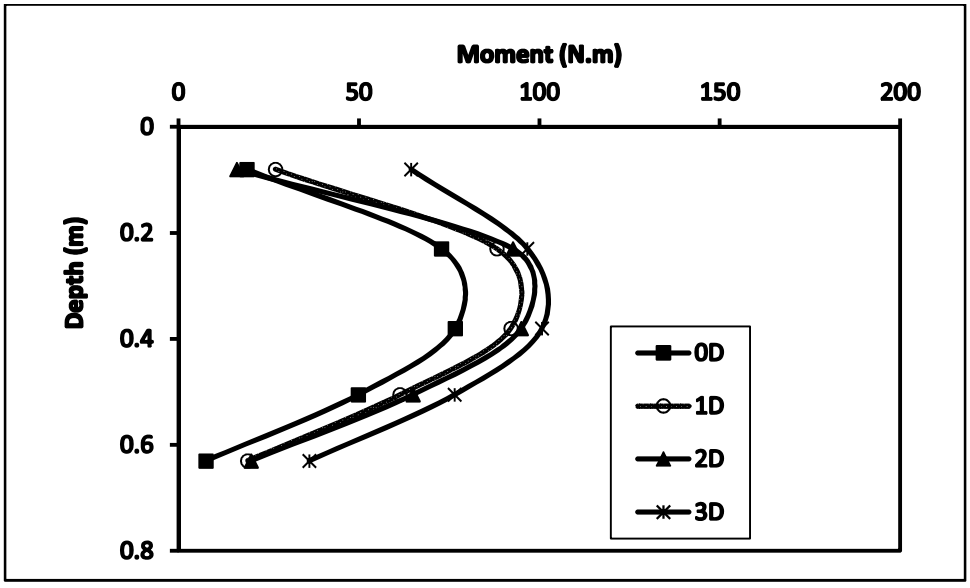


Figure 8. Comparison of moment variation with depth for different scour depths, without scour (Applied load 60 N)

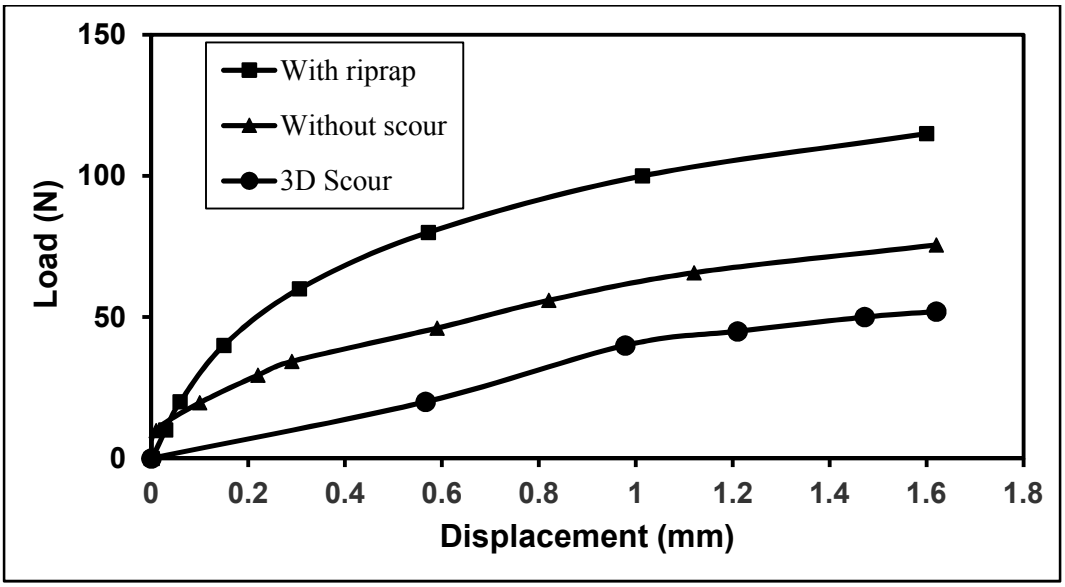


Figure 9. Comparison of load-deflection curves for different cases

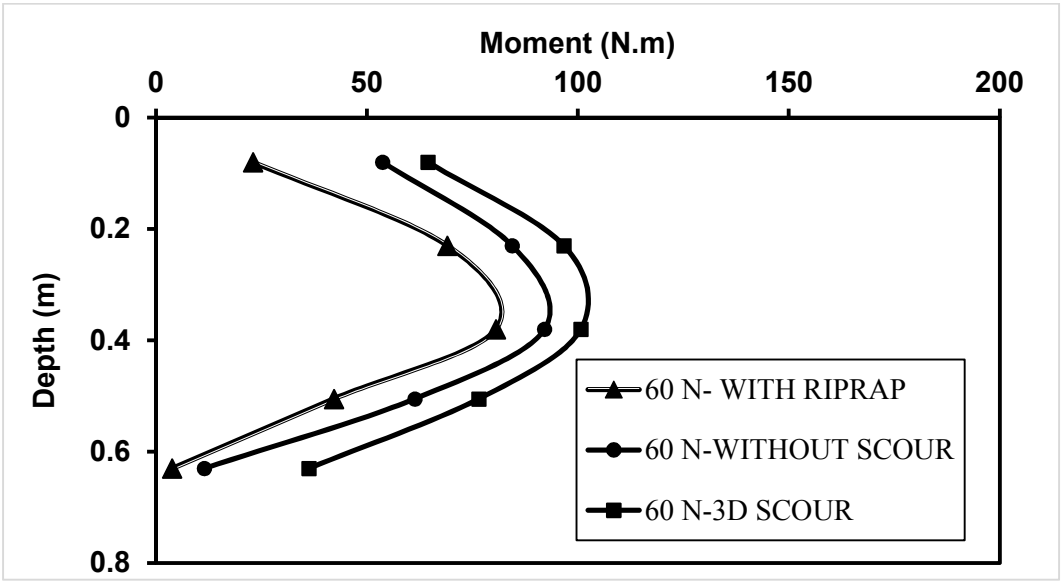


Figure 10. Comparison of moment variation with depth for different cases

CONCLUSIONS

The following conclusions were drawn from the model test results:

1- The scour influenced the responses of laterally loaded piles significantly. The lateral displacement at the top of single pile increases at an increasing rate with the scour depth, specially at a higher loads. The ultimate lateral load capacity of the pile decreases substantially

with the scour depth and the decrease could reach 20% when the scour depth increases from 0 to 3 D.

2- The bending moments increases as scour depth increases.
3- The countermeasure used in this study (i.e. riprap) has a significant influence on the lateral load resistance for the scoured piles. The riprap improves the ultimate lateral load of a single pile for the 3D scour case from 52 N to 116 N.

REFERENCES

Avent, R. R and Alawady, M. 2005. Bridge scour and substructure deterioration: Case study. Journal of Bridge Engineering, *10*(3), 247-254. doi:10.1061/(ASCE)1084-0702(2005)10:3(247).

Kishore, Y. N., Rao, S. N. and Mani, J. S. 2009. The behavior of laterally loaded piles subjected to scour in marine environment. KSCE Journal of Civil Engineering, *13*(6), 403-408.

Lagasse, P. F., Arneson, L. A. and Zevenbergen, L. W. 2006. Research needs for scour at bridge foundations -an update. World Environmental and Water Resources Congress 2006, May 21-25, 2006, Omaha, Nebraska, United States.

Li, F., Han, J. and Lin, C. (2013). Effect of scour on the behavior of laterally loaded single piles in marine clay. Marine Georesources & Geotechnology, *31*(3), 271-289.

Lin, C., Bennett, C. , Han, J. and Parsons, R. 2010. Scour effects on the response of laterally loaded piles considering stress history of sand. Computers and Geotechnics 37 (2010) 1008–1014

Lin, C., Bennett, C. , Han, J. and Parsons, R. 2015. Effect of soil stress history on scour evaluation of pile- supported bridges. Journal of Performance of Constructed Facilities, 29(6), 4014178. doi: 10.1061/(ASCE)CF. 1943-5509.0000681.

Lauchlan, C. S. and Melville, B. W. 2001. Riprap protection at bridge piers. Journal of Hydraulic Engineering, ASCE, 127(5), 412-418.

Ni, S. H., Huang, Y. H. and Lo, K. F. 2011. Numerical Investigation of the Scouring Effect on the Lateral Response of Piles in Sand. Journal of Performance of Constructed Facilities, ASCE, 26(3), 320-325.

Qi, W. G. , Gao, F. P., Randolph, M. F. and Lehane, B. M. 2016. Scour effects on p–y curves for shallowly embedded piles in sand. Géotechnique, 66, No. 8, 648–660.

Richardson, J. and Richardson, E. 1993. Local scour at bridge abutments - discussion. Journal of Hydraulic Engineering, ASCE, 119(9), 1069-1071.

Richardson, E. V. and Davis, S. R. 2001. Evaluating scour at bridges: Federal Highway Administration Hydraulic Engineering Circular No. 18. Publication FHWA NHI, 01-001.

UNCONVENTIONAL GEOTECHNICAL INVESTIGATION FOR CONSTRUCTION OF NEW GENERAL CARGO TERMINAL AT PORT OWENDO, GABON

Aditya S. Khatavkar[1], Prakash S. Bansod[2]

1. **Design Engineer, Afcons Infrastructure Ltd, Andheri, Mumbai.**
2. **Assistant General Manager, Afcons Infrastructure Ltd, Andheri, Mumbai.**

Abstract: A 420 m x 40 m Berth and 13hectare (Ha) Container stacking yard is founded on 1400 mm φ bored cast-in-situ reinforced concrete piles. These piles were installed through the overburden material into the underlying rock in the onshore/offshore areas. As a part of work, two initial Pile Load tests with working load of 980 MT were carried out and tested to a load of 2450 MT. A total of 675 piles are in scope of work out of which 292 numbers are constructed as Marine piles using Jack-up Platform and 383 numbers of Land based piling by filling the backyard area by locally available sand. Out of two Pile Load Test one was Land based Pile Load Test and other was Marine Simulated Pile Load Test. There were apprehensions about quality of very weak to weak siltstone rock samples obtained during the boring of Piles which eventually resulted in increase of pile length for few initial piles. Solution to this problem by conducting unconventional investigation and optimization of pile length is described briefly in this paper.

Keywords: siltstone, marine simulated pile load test, core barrel, UCS tests.

1.0 INTRODUCTION

Afcons Infrastructure Limited had constructed New General Cargo Terminal at Port Owendo in Gabon for M/s Gabon Special Economic Zone, Gabon (GSEZ). Gabon is a French colonized country which is situated on the equator on the west coast of Africa. Port Owendo is situated where Gabon estuary meets the Atlantic Ocean. Pretender detailed Geotechnical investigation was carried by M/s Geofor Fugro using Jack-up platform. During execution of piling works, client's representative had some apprehensions regarding the quality of rock which was extracted from the bored muck. To validate the strength of rock with the geotechnical investigation carried out earlier, an Unconvention Geotechnical Investigation were carried out in working pile bore by using available pile boring equipment with 600 mm φ rock core barrel as an attachment. And rock core samples were extracted for testing its strength. Requirement of this Unconventional Investigation and its process is briefly described in this paper.

2.0 GEOLOGICAL SETUP

After award of work Afcons decided to carry out additional investigation. A total of 22 numbers of borehole were drilled by M/s Geofor Fugro which include 11 boreholes on land and 11 boreholes in sea. The locations of bore holes are indicated in fig.1. The geology of the location consists of top soil which is amorphous peat/organic clay, soft to very soft, with SPT N value varying from 1 to >10. The underlying rock consists of very weak to weak sandstone to siltstone. UCS of rocks is varying from 0.5 MPa to about 12 MPa with an average design value of about 6 MPa weak rock in land and 4 MPa very weak rock in sea portion. Various tests were performed on soil which consists of following:

2.1 FIELD TESTS

- Standard Penetration Test (SPT)
- Vane Shear Test (SPT)
- Menard Pressure Meter Test (PMT)

2.2 LABORATORY TESTS

- Density and Moisture content of soil and rock
- Plastic limit and Plasticity Index of soil
- Particle Density determination-Pycnometer of soil
- Particle Size Distribution- Wet sieving and Hydrometer
- Uniaxial Compressive Strength of rock samples
- Water absorption and porosity of rock samples
- Modulus of Elasticity of rock
- Point Load Strength Index test on rock

© 2018 Deep Foundations Institute

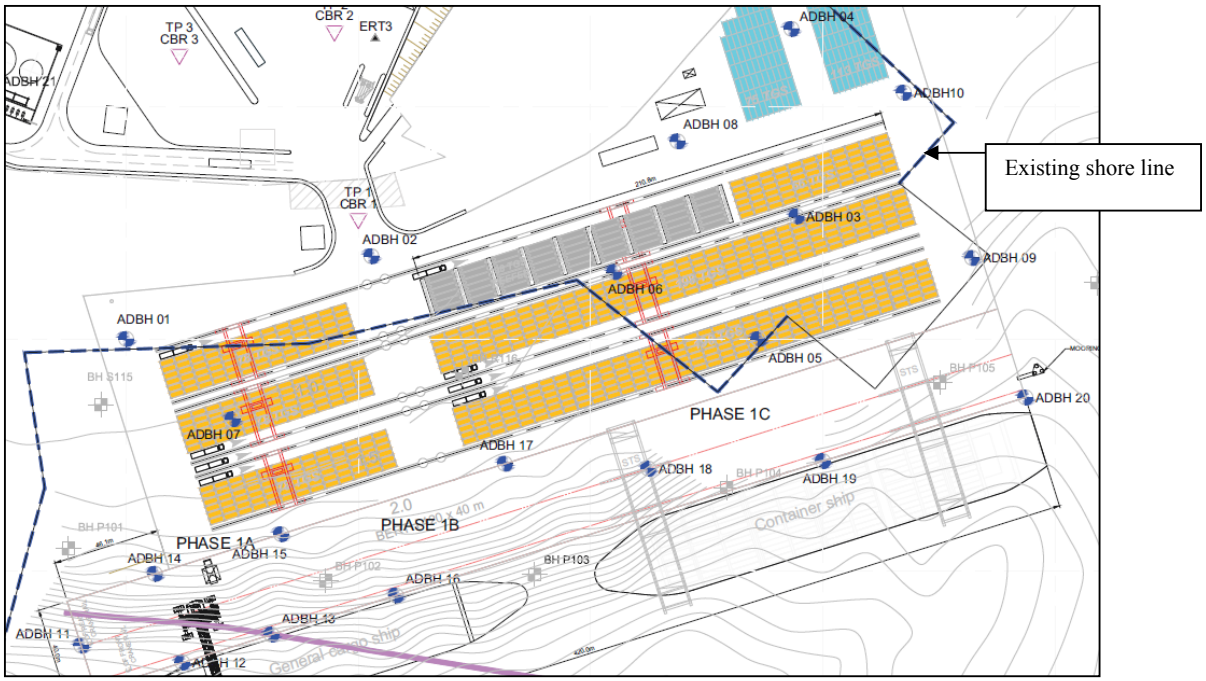


Fig. 1 Borehole locations plan

3.0 DESIGN OF BORED CAST IN SITU PILE

Bored cast-in-situ piles were of 1400 mm φ suggested by Afcons Infrastructure. Design load on pile was calculated as 980 MT with piles socketed in weak to very weak sandstone, siltstone.
Design consultant, Royal Haskoning designed the geotechnical capacity of pile based of available geotechnical investigation report. Since considerable variation of strata was observed in geotechnical investigation report, Royal Haskoning suggested a minimum 6D socket in weak rock having average Unconfined Compressive Strength of rock as 6 MPa and above for piles on land and socket length of 9D-10D for offshore piles in very weak rock where UCS values was of order of 4 MPa and above.

3.1 LAND PILE LOAD TEST

Piling activity started on 9th of March 2016 with boring of first test pile as a part of Initial Pile Load Test. This 1st Pile Load test was for Land based piles. According to design, minimum 6D socket was provided to Test pile 1 and Pile Load Test was commenced from 12th to 15th April 2016. A Report of Pile Load Test was prepared by Afcons and submitted to consultants. Consultants carried back analysis by CEMSET curve fitting procedure and concluded that pile had achieved ultimate capacity of 4000 MT as per CEMSET analysis. Total settlement of pile was 5.6 mm and net settlement was 0.75 mm. CEMSET is a computer program developed by Cementation Piling Foundation Ltd to estimate ultimate pile capacity of a single pile using results of pile load tests conducted in conventional manner. This method has been described by WGK Flemming in 1991 in Geotechnique 42, No.3, (411-425).

3.2 MARINE SIMULATED PILE LOAD TEST

New General Cargo Terminal consists of Container berth which was in sea portion and back yard which was on land. As a part of Initial Pile load test, Marine simulated pile load test was suggested. In this test, Marine condition was simulated on the pile which was casted on land as per IS 2911 (Part 4): 2013. A provision of oversized liner of 1600 mm φ till rock start level i.e.-6.35 m below Chart Datum (CD) was installed. And then pile of 1400 mm φ was socketed in weathered rock with 6D socket length. However effect of overburden can be neglected for piles socketed in rock. Schematic arrangement of Marine simulated pile load test is shown in figure 2.

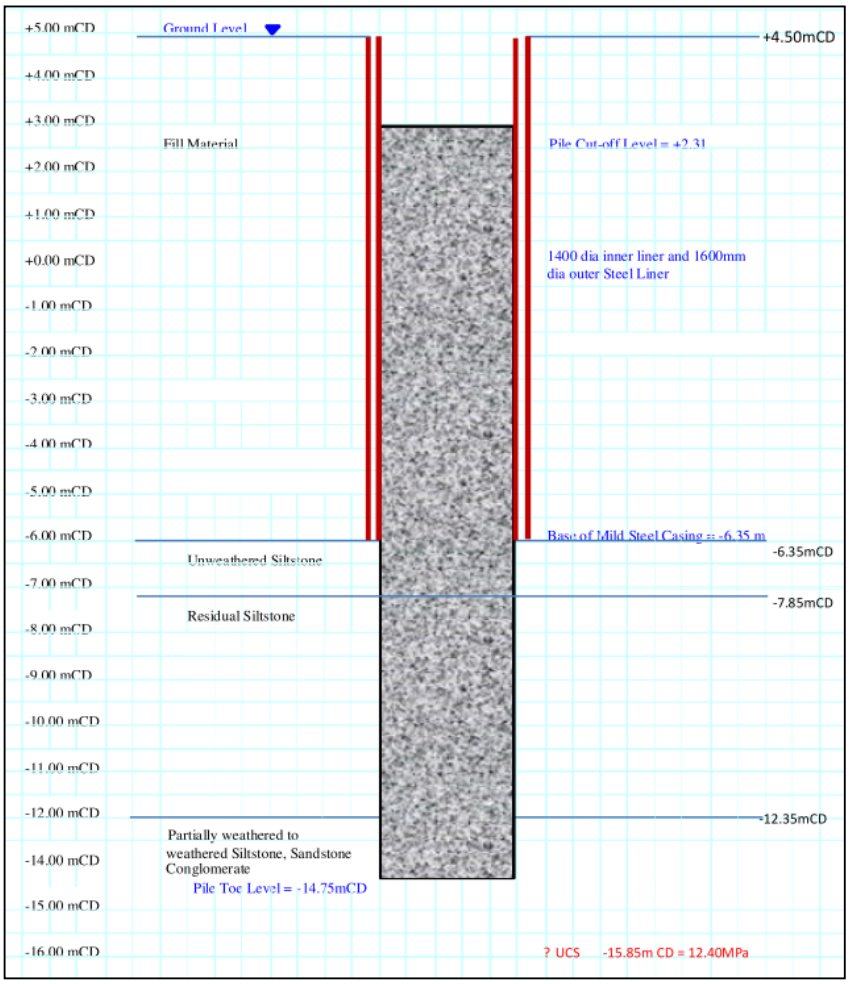


Fig.2 Schematic sketch of Marine simulated pile load test

Borehole adjacent to Marine simulated pile load test was ADBH-03; description of strata is given in Table 1.

Table 1: Description of Borehole ADBH-03.

Layer no	Top level m (CD)	Base Level m (CD)	Description
1	+4.65	-6.35	Recent fill, comprised of clayey silt mixture
2	-6.35	-12.35	Unweathered Siltstone to Residual Siltstone
3	-12.35	-14.75	Partially weathered to moderately weathered Siltstone, Sandstone
4	-14.75	-30.35	Partially weathered to moderately weathered Siltstone, Sandstone, Conglomerate

Table 2: Results of Pressure meter tests for ADBH-03.

Level m (CD)	Limit Pressure (PL) MPa	Menard Modulus (Em) MPa
-8.25	5.05	202.72
-10.75	7.40	351.82
-13.75	7.26	418.70
-16.75	7.22	202.92

Pile was terminated at -14.75 m CD and during confirmatory Geotechnical investigation work available UCS was at -15.85 m CD and -19.45 m CD of 12.4 MPa and 16.76 MPa respectively. **No UCS value was available in the socket length of pile since RQD in the portion was 0%.** Instead, Pressure meter test was performed where it was difficult to extract rock samples. The results of pressure meter test are given in table 2.

4.0 DIFFICULTIES FOR DECIDING TERMINATION LEVEL OF PILE

Type of rock described in geotechnical investigation was residual siltstone to sandstone having very low UCS values of less than 12.5 MPa. BAUR BG20H integrated piling rig was used for boring. For drilling in rock, Rock auger was used. Because of continuous rotation, the weak siltstone/sandstone used to get pulverised into dry powder (as shown in fig 3), and immediately in presence of water the dry powder used to get converted into a paste like substance (as shown in fig 4). Now the encountered material appeared to be sand or silt and gets crushed by bare hand.



Fig.3 Rock getting Pulverized in the form of dry powder because of boring with rock auger



Fig. 4 Formation of paste in presence of water

This appearance of siltstone/sandstone caused mis interpretation of strata and created confusion in the mind of client's representative. The material encountered from pile was stated as sand and there was a doubt to differentiate clearly between rock and sand. Many alternatives were tried to describe and differentiate between sand and rock. Few of them are described below in the paper.

4.1 PILE PENETRATION RATIO (PPR)

IRC 78:2014 give guidelines for termination of piles in weathered rock.

$$PPR = \frac{2\pi n T t}{A P} \qquad \text{...eqn 1}$$

Where, n= RPM of rotary rig, T= Torque in 'T-m' for corresponding 'n', t= Time in minutes, A= Area of pile in 'm^2', P= Penetration in 'cm'.

As a trial, Energy criteria and Pile Penetration Ratio (PPR) was adopted as a quality control tool for deciding termination of pile in rock. But, this failed miserably and even with PPR it was not clear whether the material encountered is rock or not. The energy and rate of penetration obtained from few initial piles are stated in tabular form in table 3.

Table 3: Pile Penetration Ratio as per IRC 78:2014

Relation between Torque generated (T) vs. rotation of Kelly per minute (N) can be extracted from specification of equipment used.

Pile no	Energy spent	Penetration Rate	Actual rock socket length	Theoretical rock socket length (6D)
	T.m/m^2	m/hr	m	m
Test Pile 1	110438.78	4.89	10.68	8.40
Reaction pile 1	168204.08	1.51	10.19	8.40
Reaction pile 2	185408.16	1.77	10.60	8.40
Reaction pile 3	67230.61	3.08	8.52	8.40
Reaction pile 4	108987.76	2.81	9.65	8.40
Test Pile 2	120918.37	1.72	8.50	8.40
Reaction pile 1	159612.24	1.62	10.65	8.40
Reaction pile 2	152357.14	2.00	10.95	8.40
Reaction pile 3	176540.82	1.44	10.80	8.40
Reaction pile 4	113663.27	2.20	10.40	8.40
		Average	10.09	8.40

Here energy is calculated which was spent to bore pile of 1400φ and rate of penetration in rock socketed portion.

4.2 PILE CAPACITY CALCULATIONS BY PRESSURE METER TEST RESULTS (PMT)

Pressure meter is a French invention by Louis Menard, Since Gabon was a French colony, and Pressure Meter tests are very commonly used in stiff soils and in very weak to weak rocks wherever the samples are not extracted for conducting UCS tests. Table 2 shows results of pressure meter tests performed in borehole ADBH-3. An attempt was also made to calculate geotechnical capacity of pile based on PMT using IS 14593: 1998 with guidelines given by Michel Bustamante et.al. The capacity of test pile -2 was calculated as **1176 MT which was greater than designed capacity of 960 MT**.

4.3 DIFFERENTIATING BETWEEN ROCK AND SAND BY STANDARD PENETRATION TESTS (SPT)

SPT is one of the renowned, easy, convenient, conventional and commonly used reliable field tests. Meanwhile, SPT tests were performed in the working pile just after start of rock level. The method adopted for performing test in working pile was reverse SPT. A total 100 numbers of blows are used out of which first 20 numbers of blows are considered as sitting blows and thereafter penetration was calculated for every 20 numbers of blows. Extrapolated SPT N is calculated for 60 numbers of blows and last 20 numbers of blows are rejected. N extrapolated were carried out which was more than 400 which showed that the material encountered from the pile was definitely a weak to very weak rock. Figure 5 shows the SPT sample extracted from a working pile during performing SPT tests.



Fig.5 Sample extracted from Split Spoon sampler after performing SPT test

4.4 UNCONVENTIONAL GEOTECHNICAL INVESTIGATION

Since PPR is based on various factors like sharpness of bullets used for boring, skills of operator and accuracy of observed. It was pretty clear that PPR was not working as a proper guide for deciding pile termination level and socket length was getting increased. Marine simulated Pile load test was just completed and interpretation was under process. Theoretical calculation of pile capacity was submitted for clients review. And from SPT tests, client's representatives were convinced about presence of rock, but still a hint of doubt was there regarding UCS value of rock which was required to be 6 MPa and above.

An unconventional geotechnical investigation was carried out by extracting rock samples from working pile. I initially attempts were made to obtain cores of rocks using piling rig and 1400 mm φ rock core barrel. A it proved very cumbersome and time consuming, rock core samples of 600 mm φ were obtained by using same piling rig and 600 mm φ rock core barrel and running the machine at a slower speed at about 7-8 RPM. Each coring run was maintained up to 1m length and big chunks of rock were obtained from working pile from the entire socket length portion. This was arranged in a chronological order as shown in fig 6. Level of rock samples was marked by paint on it.



Fig.6 Sample rock core extracted from 600mm φ core barrel from working pile

These rock samples were taken to laboratory and the rock was drilled with diamond cutting bit to obtain a sample of about 6 cm dia and L:D ratio of 2. Figure 7 & 8 shows the sample extracted from 600 mm φ rock core barrel and residual stone after extraction of sample. These rock samples were tested in presence of client's representative. The UCS values obtained from this pile are shown in table 4.



Fig.7 100mm φ Rock sample extracted from 600mm dia rock core barrel



Fig.8 Residual rock after extraction of 100mm φ sample for UCS

Table 4: UCS values obtained from working pile.

Sr no	Depth	Diameter	Height	Weight	Failure Load	Area	UCS	density
	M (CD)	cm	cm	gm	kN	cm2	Mpa	gm/cm3
1	-1.00	6.03	11.15	695.50	10.00	28.58	3.50	2.18
2	-1.60	6.04	10.26	628.10	5.00	28.65	1.75	2.14
3	-2.10	6.06	11.37	722.90	16.00	28.86	5.54	2.20
4	-2.49	6.06	12.00	765.60	6.00	28.86	2.08	2.21
5	-2.49	5.97	12.00	853.30	12.00	28.01	4.28	2.54
6	-3.44	6.05	11.71	810.70	42.00	28.77	14.60	2.41
7	-3.99	6.06	9.41	656.30	33.00	28.86	11.43	2.42
8	-4.54	6.04	12.09	816.10	25.00	28.67	8.72	2.35
9	-5.84	6.05	12.01	814.20	26.00	28.77	9.04	2.36
10	-5.84	5.74	10.92	697.50	15.00	25.88	5.80	2.47
11	-6.40	6.00	8.55	525.00	13.00	28.27	4.60	2.17
12	-7.37	6.02	10.66	695.55	17.00	28.48	5.97	2.29
13	-7.84	6.05	12.02	782.30	12.00	28.77	4.17	2.26
14	-8.24	6.04	12.00	797.30	25.00	28.67	8.72	2.32
15	-8.74	6.04	10.30	655.80	12.00	28.67	4.19	2.22
16	-8.74	6.02	12.16	790.10	13.00	28.48	4.56	2.28
17	-9.54	6.05	12.00	776.60	17.00	28.77	5.91	2.25
18	-10.54	6.05	11.06	748.50	27.00	28.77	9.39	2.35
19	-13.54	5.92	9.11	511.90	2.50	27.54	0.91	2.04
20	-14.04	6.02	12.06	776.50	20.00	28.48	7.02	2.26
21	-14.54	5.60	11.68	753.20	25.00	24.63	10.15	2.62
22	-15.24	5.94	11.96	726.60	10.00	27.73	3.61	2.19
						Average	**6.18**	**2.30**

UCS is varying over a wide range with minimum value of 0.91 MPa and maximum 14.60 MPa with average value of more than 6 MPa. This is clearly observed in table 4. Figure 7 shows cores obtained from big chunks of rocks

4.5 STARTING OF ROCK SOCKET LENGTH

The conflict of start of rock was solved by very simple way. Since, top soil consists of amorphous peat/organic clay, soft to very soft, in nature and then weak rock is encountered. Liner was driven by vibro hammer at the pile location. Driving was very smooth in clay and as the strata improves, liner shows refusal and further penetration of liner was not observed. **Start of rock is decided just about 1m below liner bottom level.**

5.0 IMPACT ON COST SAVING

5.1 SAVING IN ROCK SOCKET LENGTH

For initial 11 numbers of piles, rock socket length was 17.313 m. Where all trial and error methods were adopted for deciding termination of pile. After unconventional geotechnical investigation, UCS of rock was confirmed and socket length of pile was drastically reduced from 17.313 m initially to 10.90 m. Although this is more than 6D but this also includes some weak patches encountered in between. With this way rock socket of all 675 piles including land and marine piles were carried out. **Therefore, cost for boring in rock of about 4258 running meters was saved.**

5.2 SAVING IN TIME

Design consultant was taken into confidence and a mutual understanding was build between Afcons engineers and clients representative in presence of design consultant for determination of pile termination level and differentiating between rock and soil. This saved the time of Afcons engineers to wait for client's representative every time during start of rock touch level and inspection of every pile. Also boring in rock was reduced which further saved time as well as excess wear and tear of equipment and wastage of energy in terms of fuel.

6.0 FUTURE ADOPTION OF IDEA

This unconventional investigation proved very effective in saving the time and cost of project. This same concept is under process in **'Construction of Container berth and Fishery jetty at Vizhinjam, Kerala'**. In this project, there are limited data of geotechnical investigation and bore logs were unable to perform because of time constrain. Using this unconventional geotechnical investigation, UCS values of rock can be extracted by drilling in working pile and then testing of these rocks can be done for further reduction in socket length.

7.0 CONCLUSIONS

Reduction of socket length was made possible by performing various field tests, laboratory tests and theoretical calculations. PPR, calculations by pressure meter test, performance of field SPT test, performing Marine simulated pile load test and then unconventional geotechnical investigation. Simultaneously, all the activities were carried out and it was proved that the paste/pulverized type material extracted during boring of pile was a residual sand stone/ siltstone and not just sand.

In order to decide the termination level of bored cast-in-situ piles in very weak to weak rocks, it is important to decide following two factors.

1. Starting point of rock socket.
2. Socket length design in relation to strength characteristics of very weak rock.

From the above mentioned points, starting point of socket length was decided as 1 m to 1.5 m below the termination level of permanent liner installed using vibro hammer. In weak rocks at land portion where average UCS was of order of 6 MPa, socket length of 6D was adopted and in the Marine portion where very weak rock which was slightly weaker with average UCS of 4 MPa, socket length of 9D was adopted. By adopting this methodology, the work of construction of 675 piles was successfully completed in the period between March 2016 and March 2017. And commercial operations from this berth have commenced from March 2017.

Acknowledgement: We thank Dr. Sunil S. Basarkar (General Manager, Afcons Infrastructure ltd) for comments that greatly improved the manuscript and Dr. Dasaka Murty (Associate Professor, Indian Institute of Bombay) for encouraging writing this paper.

REFERENCES

IRC 78:2014. 'Standard specifications and code of practice for road bridges'.

IS14593:1998. 'Design and construction of bored cast-in-situ piles founded on rock'

IS 2911(Part-4):2013. 'Design and constructions of pile foundations'

Michel Bustamante et.al "Pile design and failure using the Menard Pressure meter an Up-date", IFCEE 2009, French contribution- Foundation design with Menard Pressure meter tests.

A MODEL STUDY OF MICROPILE GROUPS SUBJECTED TO LATERAL LOADING UNDER DIFFERENT RELATIVE DENSITY

Zakir Hussain, Research scholar, Civil Engg. Deptt, Assam Engineering College, Guwahati, Assam, India, Ph.: +919864018992, email: zakirhussain.ray@gmail.com
Binu Sharma, Professor, Civil Engg. Deptt, Assam Engineering College, Guwahati, Assam, India, Ph.: +919864155359, email: binusharma78@gmail.com
Takiur Rahman, M.E. Student, Civil Engg. Deptt, Assam Engineering College, Guwahati, Assam, India, Ph.: +917002329793, email: takiur777@gmail.com

ABSTRACT

Many old structures like high rise buildings and bridges are unsafe and need to be strengthened in highly seismic prone zones. Strengthening of existing foundations of structures is difficult as it involves excavation, temporary support system below the foundation level, limited head room, risk of collapse of the structure during excavation. In such cases micropiles are the best solution for strengthening of vulnerable structures. Different investigations report different and contradictory group effects on micropiles subjected to vertical and lateral loading. This work is a model study to investigate the behaviour of micropile groups subjected to lateral load installed in loose sand (relative density 30%) and in dense sand (relative density 80%). The group behaviour is found to be a function of relative density of sand, length to diameter (L/D) ratio and spacing of the micropile groups. In loose sand ultimate lateral load carrying capacity of micropile groups as well as efficiency is highest in 2D spacing followed by 4D and 6D spacing. Positive group effect is seen at 2D spacing for 30% relative density and at 6D spacing for 80% relative density and also by a few piles of higher L/D ratio at 4D spacing at 80% relative density. Rest of the piles show a negative group effect.

Keywords: Micropiles, length to diameter ratio, spacing of piles, relative density of sand.

INTRODUCTION

Micropiles are basically piles of diameter less than 250 mm. It is constructed by pressure grouting technique by pumping concrete or mortar into the reinforcement (diameter 16-32 mm). The grout is either injected or placed under certain pressure (pressure grouting above 0.8 Mpa to 1 Mpa). The soil near the micropiles generally forms a composite block to resist the applied loads. This leads to a group capacity or network capacity that differs from the total overall capacity of individual piles forming the group or network.

Micropiles are mainly used for two basic purposes i.e. seismic retrofitting or as a structural support which are generally technically viable and economically feasible in many situations. It is widely used in construction purposes due to the facts that the equipment is light in weight, exhibits a flexible layout and requires a low headroom area and can easily access congested areas where it is difficult to construct conventional piles. Micropiles were first established in Italy in the year 1950 and were used as a technique to underpin old historic buildings and monuments. Lizzi (1983) denoted micropiles as root piles and in network effect as reticulated root piles. Root piles and reticulated root piles were used widely by Lizzi in the year 1952. This technique was introduced in the year 1970 in U.S. Micropile became popular after 1980's when it gained popularity and acceptance as a method to underpin existing structures.

Micropiles have a high skin friction, due to which the load carrying capacity of micropiles is higher than that anticipated by conventional bearing capacity theory. Micropiles are used for underpinning because of its "quick response" to the slightest movement of the structure. The settlement of micropiles are few mm for load value even upto crushing strength. With respect to the seismic behaviour, micropile system

© 2018 Deep Foundations Institute

exhibits flexible type of behaviour under dynamic loading. Another important feature of micropile is that retrofitting methods that uses micropiles can be used in liquefied ground also. Due to its small diameter it can be constructed at any ground condition and with equipments generally smaller than that required for conventional piles.

BRIEF LITERATURE REVIEW

Several researchers (Schlosser and Juran 1979; Lizzi 1983; Soliman and Munkofh 1988; O'Neill and Pierry 1989; Bruce 1995; Ting and Nithiraj 2001; Kershaw and Luna 2018) have reported on micropile technology, application and soil micropile interaction in literature. Lizzi (1985) reported model test results of group efficiency of micropile on coarse sand. Lo (1967) observed that the group effect was not consistent, but most of the piles presented positive group effect. A series of centrifugal tests conducted on micropile group and network system in loose to medium sand was reported by Benslimane "et al." (1998). Nishitani "et al." (2002) described seismic retrofitting by micropile method. Yamana "et al." (2000) reported about the efficiency of micropiles for seismic retrofit of foundation system. Deshmukh "et al." (1990) worked on design and construction of mini grouted piles (micropiles) in Bombay region. Sharma (2011) did a model experimental study of group micropiles of different length to diameter ratio installed in sand bed of 50% relative density and subjected to lateral loading and oblique pull. Sharma and Buragohain (2013) reported about the behaviour of micropile groups under oblique pull out loads in sand. Mitrani and Madabhushi (2005) investigated inclined grouted micropiles and studied its effect on liquefaction remediation of soils.

In this investigation a model experimental study has been conducted on micropiles. Single micropiles of various length to diameter (L/D) ratio, and micropile groups of different L/D ratios as well as centre to centre spacing were installed in sand beds of relative densities 30% and 80%. The piles and the pile groups were subjected to lateral loading condition. The object was to study the response of the pile group due to the relative density of the sand, spacing of the piles and L/D ratio of the piles.

EXPERMENTAL SET UP

Properties of sand

Micropiles of different L/D ratios were installed in sand bed inside a model tank of size (1.7mx1.5mx0.93m). The physical properties of the sand used in the model tank are shown in Table 1. To achieve uniform relative density throughout the tank, rainfall technique was applied. Sand was allowed to fall freely through a strainer from a fixed height of 30 cm and 90 cm respectively to obtain relative densities of 30% and 80% respectively. The density and angle of internal friction (Φ) of sand with relative density 30% was found out to be 1.37 gm/cc and 34˚ respectively and for relative density of 80%, density and angle of internal friction (Φ) was found out to be 1.83 gm/cc and 43.5˚ respectively.

Installation of Micropiles

Micropiles were casted through an aluminium pipe of external diameter 12 mm and internal diameter 10 mm with a 60˚ conical wooden shoe attached at the bottom end of the pile to obstruct sand from entering into the casing during installation. The reinforcement used is a 1.5 mm mild steel rod. The pipe casing was pushed manually into the sand bed vertically. Then the reinforcement is placed into the casing and grouting is performed with cement slurry of water cement ratio of 0.6 under a constant gravity head of 100 cm. The casing pipe was initially filled up upto 100cm by cement slurry, then gradually lifted up by 2cm and additional cement slurry equivalent to 2cm height was poured from the top. This was done in order to maintain a constant slurry head of 100cm. This process was repeated till the whole pile was grouted and the casing taken out. Wooden frameworks were used to construct pile caps which were reinforced with steel wire mesh.

Table 1. Properties of Sand

Sl. No.	Properties	Value
1	Effective Grain Size (mm)	
	i) D_{10}	0.22
	ii) D_{30}	0.32
	iii)D_{60}	0.46
2	Uniformity Coefficient, C_u	2.08
3	Coefficient of Curvature, C_c	0.98
4	Specific Gravity of Soil, G_s	2.67
5	Maximum Voids Ratio, e_{max}	0.88
6	Minimum Voids Ratio, e_{min}	0.68
7	Voids Ratio, e under Relative Density 30%	0.81
8	Voids Ratio, e under Relative Density 80%	0.65
9	Density under Relative Density 30% (gm/cc)	1.37
10	Density under Relative Density 80% (gm/cc)	1.83
11	Angle of Internal Friction for Relative Density 30%	34^0
12	Angle of Internal Friction for Relative Density 80%	43.5^0

Measurement of Load and Deflection

Load was applied to the pile cap with the help of a mechanical jack, and load was measured with the help of proving ring and displacement was measured with the help of a dial gauge. The mechanical jack was fixed in a horizontal cross beam with nuts and bolts in such a way that it is convenient to slide when necessary. An adjustable collar was used to connect one end of the tip of the lever arm of mechanical jack and the other end is connected with one end of the proving ring. The proving ring, having a constant of 0.99kg (approximately 9.8N)/div, is fixed to the collar with the help of a bolt. The other end of the proving ring was fixed with a ball and socket arrangement for the application of the loads to the top of the pile cap. The lateral loading arrangement is shown in Fig.1 photo.

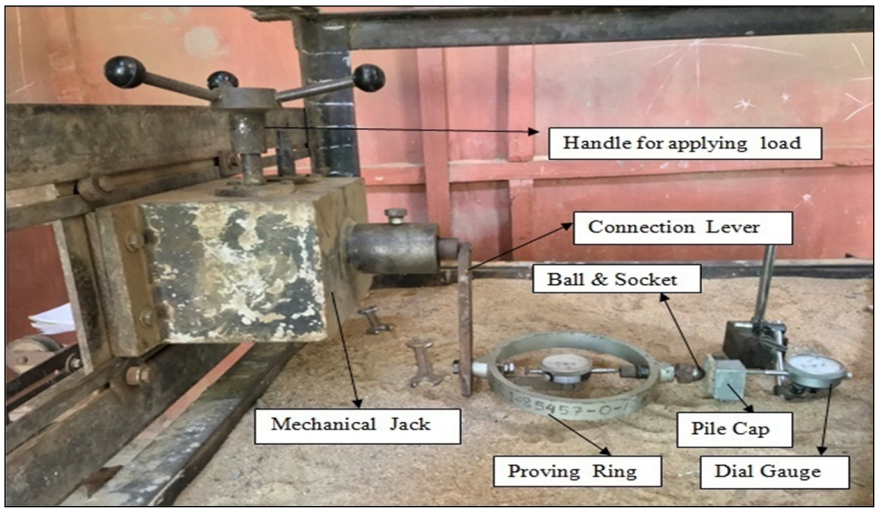


Fig. 1. Lateral Loading Arrangement

TEST RESULTS

A model of 64 micropiles was installed in the model tank. Single micropiles and group micropiles were casted for L/D ratios of 12, 18, 24, 30, 36, 48, 60 and 80. The micropile groups were in a square grid pattern of four piles per group, with a centre to centre spacing of 2D, 4D and 6D respectively. Both single and group micropiles were installed in sand bed having relative density of 30% and 80%. The lateral load versus displacement plots of a single pile and a group pile (spacing 4D) of L/D ratio 24 and relative density 30% are shown in Fig. 2-3. Ultimate resistance of the single piles and pile groups under lateral load has been taken as the point on the lateral load versus lateral displacement curve at which the curve maintains a continuous displacement increase with no further increase in lateral load.

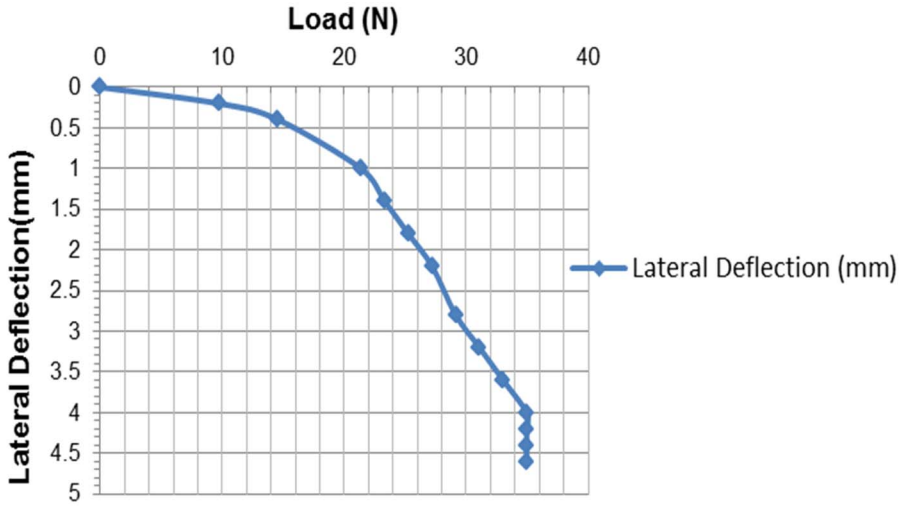


Fig. 2. Plot of Load versus Lateral Deflection for Single Pile of L/D 24 at 30% Relative Density

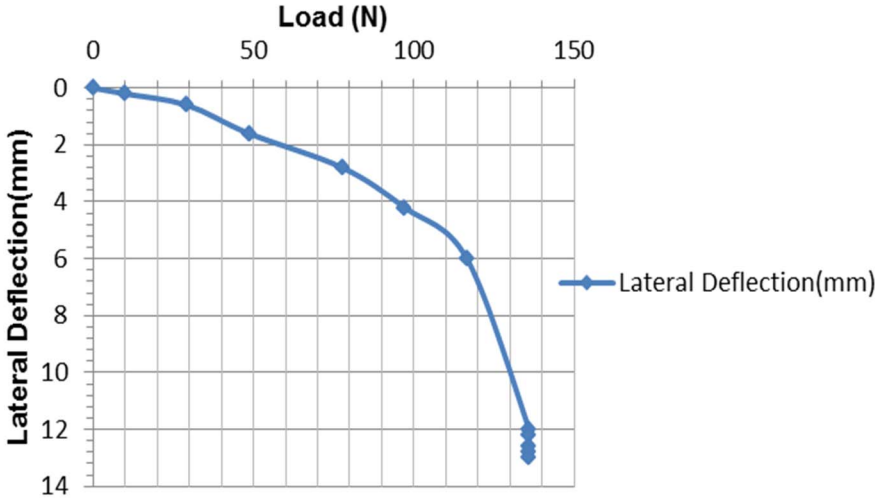


Fig. 3. Plot of Load versus Lateral Deflection for Group Pile of L/D 24, Spacing 4D at 30% Relative Density

A graph of the ultimate lateral load versus L/D ratio of single micropiles is shown in Fig. 4 where it can be seen that the ultimate lateral resistance of all the piles at relative density 80% is higher than at a relative density of 30%. Again it is seen that the ultimate lateral resistance increases at a high rate upto L/D ratio of 48 and after that the ultimate lateral resistance significantly decreases and becomes insignificant. For 80% relative density it is seen that the ultimate lateral resistance increases at a high rate upto L/D ratio of 60 and after that the increase is not significant. Both soil failure and structural failure were observed which are further discussed in the mode of failure of micropile goups.

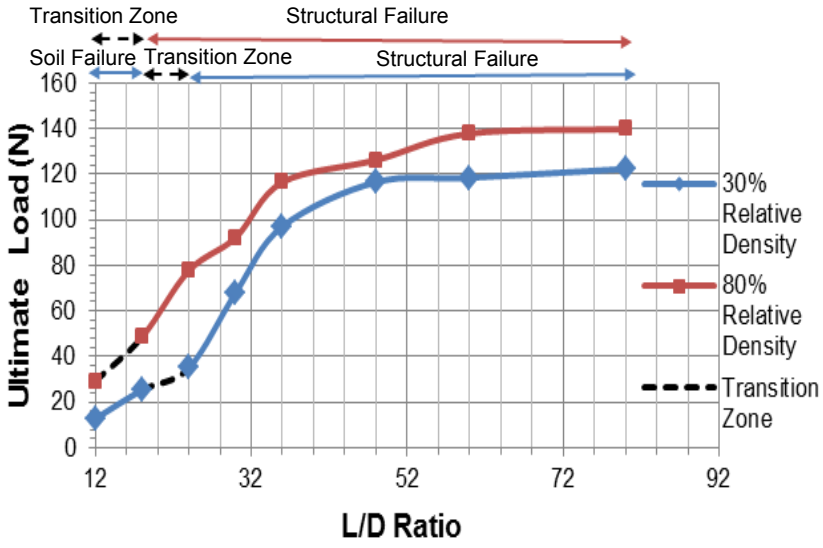


Fig. 4. Plot of Ultimate Lateral Load versus L/D Ratio of Single Micropile

Fig. 5-7 shows the variation of ultimate lateral resistance with length to diameter ratio of the micropile group at three different spacing and at relative densities of 30% and 80%. It is seen that ultimate lateral resistance increases rapidly with a high rate upto L/D of 36 and from L/D ratio of 48 to L/D ratio of 80 the rate of increase is insignificant. Similar are the trend for micropile groups of 4D and 6D spacing. This is in agreement with the findings of laterally loaded piles that increasing the pile length beyond a particular length is not necessary. The L/D ratio of the micropile groups at which the increase of ultimate load becomes constant is not clear from the experimental study. L/D ratio of the micropile groups could not be further increased due to the limited depth of the tank which is 0.93m. For micropile groups in sand bed of 30% relative density it is seen that the group capacity is high at 2D spacing followed by 4D and 6D spacing whereas for 80% relative density it is seen that the group capacity is high at 6D spacing followed by 4D and 2D spacing.

In Figure 5 it is seen that for 2D spacing group capacity is high at 80% relative density for L/D ratio upto 30. For L/D ratio 40 to 80 group capacities is same for both 30% and 80% relative density. Sand at relative density 30% is loose sand or contractive sand. On insertion of the aluminium casing at 2D spacing, the sand within the block, contracts. Since the piles are grouted at a gravity head, due to the penetration of the fluid part of the mix into the surrounding soil, a strong composite pile group block formation occurs at 2D spacing. This results in high group capacity at 2D spacing for all the L/D ratio at 30% relative density. Again sand at relative density of 80% is dense sand or dilative sand and on insertion of the aluminium casing at 2D spacing, the sand within the block dilates. So the same strong composite pile group block formation occurs at 2D spacing upon grouting. This leads to the same ultimate lateral resistance at 2D spacing for L/D ratio 36 to 80 for both 30% and 80% relative density, where it is

observed that these piles actually fail under structural failure. For L/D ratio of 12 to 30, the piles fail by soil failure which occurs due to passive resistance of the soil being exceeded.

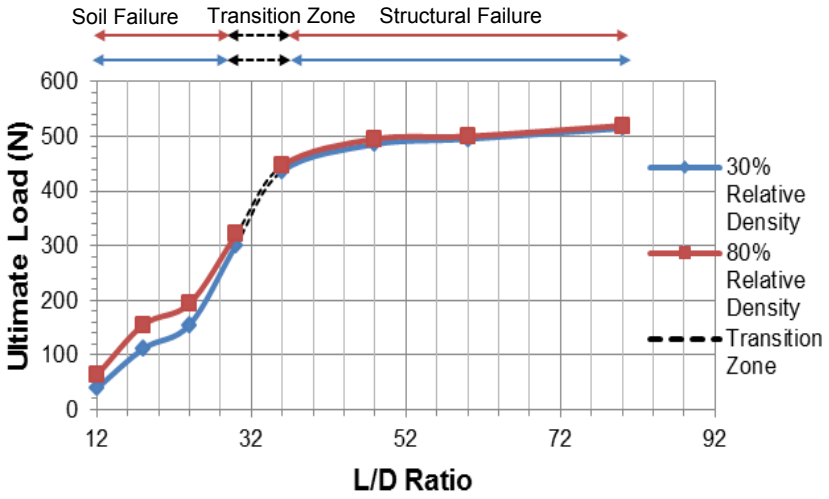


Fig. 5. Plot of Ultimate Lateral Load versus L/D Ratio for 2D Spacing

Effect of relative density is seen in 4D and 6D spacing in Fig. 6-7. At 80% relative density ultimate lateral load comes out to be more than at 30% relative density at this two spacing. Side resistance of a pile is dependent upon the normal stress on the interface between pile and sand and the critical state strength of the sand. The normal stress of the interface is dependent upon the state of the sand when it is subjected to shearing. Dense sand would expand under shearing and loose sand would contract. Volume changes in sand would result in a variation of normal stress along the surface. Dilative sand would result in an increase in normal stress along the surface and contractive sand would result in a decrease in normal stress. Stress overlapping phenomenon is another parameter which influences group capacity. Again the grouting of the piles results in a strong grout to ground bond around the periphery of the piles. At this stage, parameters which have actually contributed more to give a high value of ultimate lateral resistance at 6D spacing at 80% relative density cannot be ascertained. Further investigations are needed in this direction.

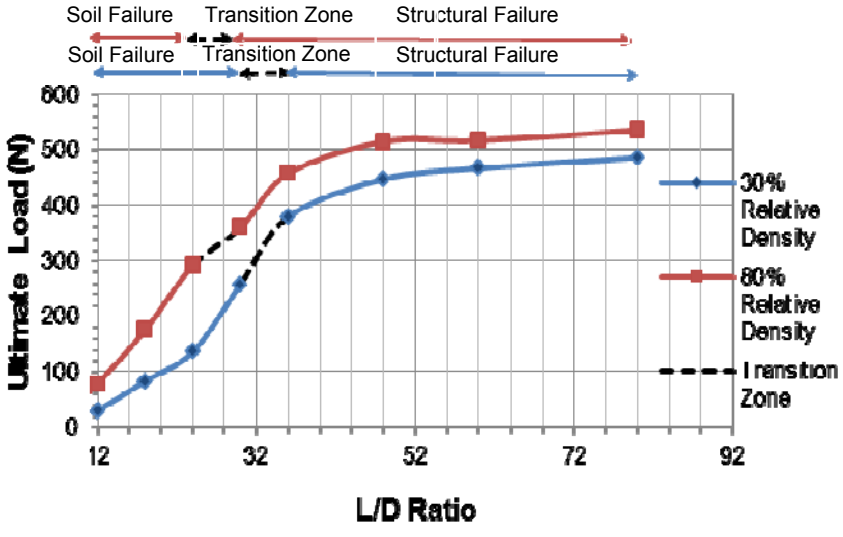


Fig. 6. Plot of Ultimate Lateral Load versus L/D Ratio for 4D Spacing

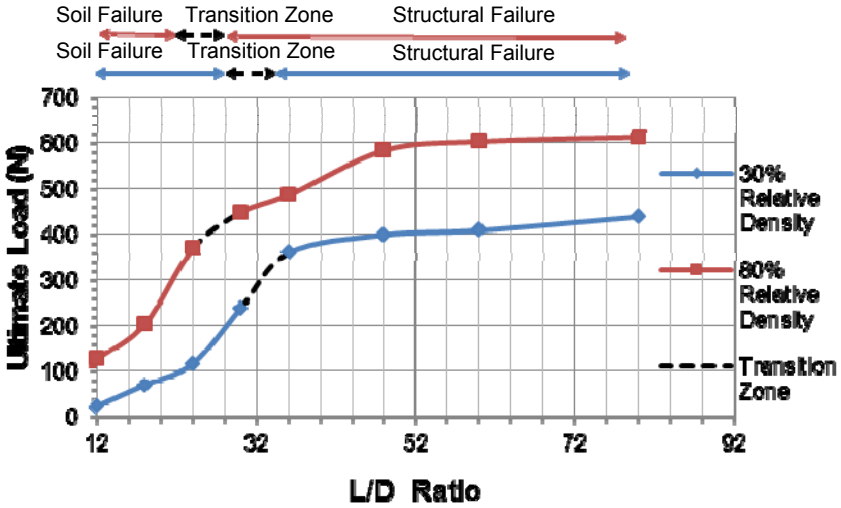


Fig. 7. Plot of Ultimate Lateral Load versus L/D Ratio for 6D Spacing

Mode of Failure of Micropile Groups

In piles installed in cohesionless soil and subjected to lateral load, two types of failure are observed. One type of failure is soil failure and the other is fracture of piles by formation of plastic hinges. Soil failure can be generally seen in short piles. When lateral load is applied on a short pile the pile rotates and a passive resistance is developed at the opposite faces. Failure basically occurs at the toes when the passive resistance at the head and toe is exceeded. The second type of failure is observed by a long pile. In case of a long pile it cannot rotate due to the development of high cumulative passive resistance developed at the lower part of the pile and structural failure occurs at the point of maximum bending moment. In this study, structural failure was generally observed by development of cracks at the pile body at positions of 0.2 to 0.4 times the pile depth. At relative density of 30% pile groups from L/D 12 to L/D 30 failed by soil failure and the pile groups from L/D 36 to L/D 80 failed by structural failure. At relative density of 80% pile groups from L/D 12 to L/D 24 failed by soil failure and the pile groups from L/D 30 to L/D 80 failed by structural failure. The spacing of micropile groups had no effect on the mode of failure of the pile groups. In case of single piles (Sharma 2009), it was found that the piles upto L/D ratio 18 failed by soil failure and the rest of the piles by structural failure. Therefore it is observed that length/diameter (L/D) ratio is a major influencing factor in the mode of failure of free head single micropiles and micropile groups. A typical structural failure is shown in Fig.8. In between soil and structural failure, there is a transition zone where piles having L/D ratio in this zone may fail either by soil or structural failure.



Fig. 8. Structural Failure of Laterally Loaded Pile Group (L/D 80) at Relative Density 80%

GROUP EFFICIENCY

A lot of research work has been carried out regarding the group efficiency of micropiles. However the results have not been consistent so far. Efficiency of micropile groups in this study has been defined in the same way as for conventional piles as given in equation 1.

$$\eta = \frac{Q_g}{n\,Q_s} \qquad [1]$$

where η = efficiency of the pile group, Q_g is = the group capacity , Q_s = capacity of a reference pile that is identical to a group pile but is isolated from the group and n is the number of micropiles in the group.

For the present study, single micropiles of the same L/D ratio as micropile groups were tested. The variation of efficiency with L/D ratio is shown in Fig. 9, where it is seen that in case of micropile groups efficiency increases with increase in L/D ratio initially. However beyond a certain L/D ratio the increase in efficiency comes out to be insignificant. This observation is seen for both 30% and 80% relative density. It is further seen that the efficiency is highest in 2D spacing, followed by 4D and 6D spacing for 30% relative density. Similar observation is also reported by Lizzi (1979) where it has been shown that in case of lateral loading, micropile groups showed positive group effect at 2D spacing and moreover the efficiency came out to be high at this spacing compared to other spacing. However the state of the sand was not mentioned in the work.

The efficiency is highest for 6D spacing, followed by 4D and 2D spacing for 80% relative density. Moreover, a higher efficiency is seen at 80% relative density compared to 30% relative density for the three different spacing. Positive group effect is seen at 2D spacing for 30% relative density and at 6D spacing for 80% relative density and also by a few piles of higher L/D ratio at 4D spacing at 80% relative density. Rest of the piles show a negative group effect.

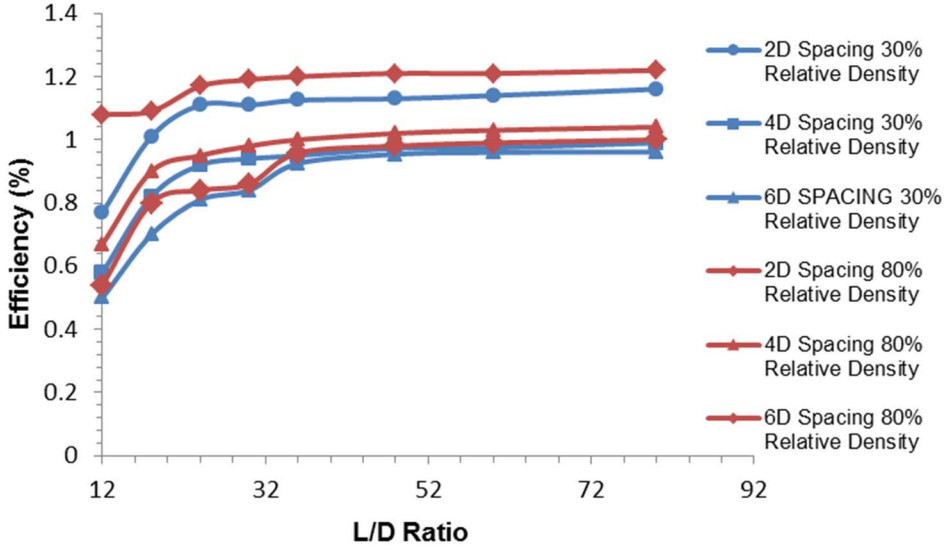


Fig. 9. Variation of Efficiency with L/D Ratio

CONCLUSIONS

A study of micropile group behaviour under lateral loading shows that length to diameter ratio of the piles, spacing of the pile groups and relative density of the sand are important parameters which influences the

pile group behaviour. Ultimate lateral load and efficiency comes out to be more at 2D spacing at 30% relative density and at 6D spacing at 80% relative density. Positive group effect is seen at 2D spacing for 30% relative density and at 6D spacing for 80% relative density and also by a few piles of higher L/D ratio at 4D spacing at 80% relative density. Mode of failure of the micropile groups is affected by the length to diameter ratio of the piles and the relative density of sand. There is no effect of spacing of the piles in the mode of failure of the pile groups.

REFERENCES

Bruce, D.A., 1995. Small-diameter Cast-in-place Elements for Load-Bearing and In Situ Earth Reinforcement, in Ground Control and Improvement by Xanthakos, P.P. Abramson, L.W. and Bruce D.A. John Wiley and Sons, New York, Chapter 6. pp. 406–492.

Benslimane, A., Juran, I., Hanna, S. and Drabkin, S., 1998. Seismic Behaviour of Micropile System, Proceedings of Sessions of Geo-congress 98, October 18-21, 1998, Boston, Massachusetts.

Deshmukh, A.M. and Ganpule, V.T. (1990). "Design and Construction of Mini Grouted Piles in Bombay Region", Pile Talk International, July : Jakarta, Indonesia, pp. 17–22.

Kershaw, K. and Luna, R., 2018. Scale Model Investigation of the Effect of Vertical Load on the Lateral Response of Micropiles in Sand, DFI Journal, received 17 Oct 2016, accepted 02 Apr 2018, published online: 27 Apr 2018

Lizzi. F. and Carnavale. G. 1979. Network of Root Piles for the Consolidation of Soil : Theoretical Aspects and Test Models. International Symposium on Soil and Reinforcement ENPC-LCPC, Paris.

Lizzi, F. 1983. The Reticolo Di PALI RADICE (Reticulated Root pile) for the Improvement of Soil Resistance Physical Aspects and Design Approaches-VIII ECSMFE, Helsinki, pp 521-524

Lizzi, F. 1985. Pali Radice and Reticulated Pali Radice. Ed. By Thornburn, S. and Hutshinson, J. F., Surrey University Press. pp. 84-141.

Lo, 1967. Discussion to paper by Y.O. Beredugo. Canadian Geotechnical Journal, Volume 4 pp. 353-354.

Mitrani, H. and Madabhushi, G.P.S. 2005. "Centrifuge Tests Investigating Inclined Grout Micropiles as a Method of Liquefaction Remediation for Existing Buildings." *Proceedings of ASCE Geo–Frontiers Conference.* pg. NA, (doi 10.1061/40779(158)14).

Nishitani Masahiro, Umebara Takeshi and Fukui Jiro, 2002. Development of Seismic Retrofitting Technologies for Existing Foundation, Http://www.pwri.go.jp./eng/Kokusai/conference/Nishitani 021020-1-pdf-pwri japan.

Nayak, N.V. and Ketkar, 1992. Consultancy and Construction Capabilities in Geotechnical Enginering Investigation, 13th ICSMFE, New Delhi, 1983.

O'Neil, M.W. and Pierry, R.F., 1989. Behaviour of Minigrouted piles used in Foundation Underpinning in Beaumont Clay, Houston, Texas, U.S.A., Proceeding of the International Conference Piling and Deep Foundation, London/15, 1 May pp. 101–109.

Schlosser, F. and Juran, I., 1979. Design Parameters of Artificially Improved soils, ECSMFE, Vol. 5, pp. 197– 225. BRIGHTON.

Soliman, N. and Munkofh, G., 1988. Foundation on Drilled and Grouted Minipiles–A Case History. Proceeding 1st International Geotechnical Seminar on Deep Foundations on Bored and Auger Piles, GHENT/7-9 June, pp. 363–369.

Sharma, B., 2009. A Model Study of Micropiles Subjected to Lateral Loading Condition, IGC 2009, Guntur, India

Sharma, B., 2011. A Model Study of Micropiles Subjected to Lateral Loading and Oblique Pull. Indian Geotechnical Journal. Vol. 41, No.4. : 196-205.

Sharma, B and Buragohain, P., 2013. Behaviour of Micropile Groups under Oblique Pull Out Loads in Sand. Indian Geotechnical Journal. DOI 10.1007/s40098-013-0091-1.

Ting, W.H. and Nithiraj, R., 2000. Underpinning a Medium Rise building with Micropiles - A Case History, Volume–31, Geotechnical Engineering Journal of South East Asia Geotechnical Society Sponsored by Asian Institute of Technology.

Yamane, T., Nakata, Y., and Otani, Y., 2000. Efficiency of Micropiles for Seismic Retrofit of Foundation System, 12th World Conference on Earthquake Engineering, Auckland, New Zealand, pp.1-8.

ADVANCED NUMERICAL MODELLING OF DEEP EXCAVATION SUPPORTING SYSTEM USING CONTIGUOUS PILE WALL

George Tharakan Idiculla[1] and Satyanarayana Murty Dasaka [2]

1 Research Scholar, Department of Civil Engineering, Indian Institute of Technology Bombay, Mumbai; e-mail: 25.george@gmail.com
2 Associate Professor, Department of Civil Engineering, Indian Institute of Technology Bombay, Mumbai; e-mail: dasaka@civil.iitb.ac.in

ABSTRACT

The use of contiguous pile walls for deep excavation supporting system has become common in geotechnical engineering practice around the world. The implementation of contiguous piles (piles with a gap between them) for deep excavation support is most suitable for cohesive soil, where ground water table is located below the base of excavation. The Soil Arching plays an important role in stabilizing the soil in between the adjacent piles. The Mohr-Coulomb model is routinely used in the numerical analysis of deep excavations, due to its simplicity. Use of an advanced soil model may be prudent to capture realistic soil response during the excavation process. The Hardening Soil model is an effective and better model to simulate the real soil behavior in terms of stress dependency, non-linearity and inelasticity. The present study highlights salient advantages of Hardening Soil model over Mohr-Coulomb model in the numerical modelling of deep excavation supporting system using discrete piles with a gap between them.

INTRODUCTION

The demand of deep excavations in the case of basements of high-rise buildings, tunnel stations, underground parking and other underground structures is progressively increasing over the years. Sheet pile walls and concrete diaphragm walls are popular forms for deep excavation supports in soft soil. Furthermore, soldier pile and lagging walls, reinforced concrete (cast-in-situ or prefabricated) retaining walls and jet-grout walls (or deep soil mixing) with anchors or struts are also being used as deep excavation support system. Various factors affecting the selection of deep excavation support system are size of excavation, ground water level, settlement of adjacent ground, soil properties and displacement criterion. Recent advancement in area of deep excavations is the replacement of traditional deep excavation support systems with contiguous piles (Keawsawasvong and Ukritchon 2017; Gaba et. al. 2003). This application of contiguous pile walls for deep excavation support is most suitable for cohesive soil where ground water table is below the excavation level. The wall consists of discrete column piles with a gap between them and these piles are typically installed into the ground before the excavation.

The phenomenon of soil arching contributes to the stability of soil mass between the adjacent piles in contiguous pile wall system. Application of piles for deep excavation support resembles the active trapdoor mechanism, but in the horizontal direction. Many researchers (Evans 1983; Costa et al. 2009; Smith 2012; Iglesia et al. 2013; Wang et al. 2017) had carried out experimental studies on soil arching mechanism to understand the transfer of stress from yielding portion of geo-material to the stationary portion using conventional trapdoors. The deformation characteristics at the soil gap between the laterally loaded piles used in slope stabilization and deep excavation support were studied in the past few decades (Ito and Matsui

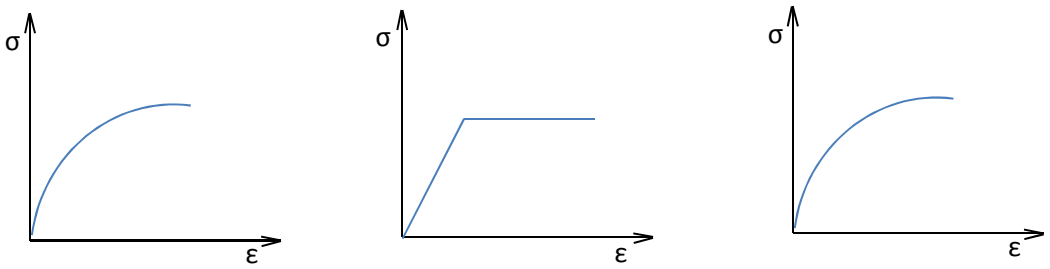
© 2018 Deep Foundations Institute

1975; Vermeer et al. 2001; Haema and Tanseng 2010; Richards et al. 2016; Keawsawasvong and Ukritchon 2017). The aim of the present study is to further understand the behaviour of anchored contiguous pile wall used for deep excavation support, by employing numerical modelling using PLAXIS 3D. Two constitutive models, viz. Mohr-Coulomb and Hardening Soil models have been used in the present study. The study also aims to highlight salient advantages of Hardening Soil model over Mohr-Coulomb model in numerical modelling of the particular problem.

THE MOHR-COULOMB AND THE HARDENING SOIL MODELS - AN OVERVIEW

The Mohr-Coulomb is a linear elastic-perfectly plastic model, which can be used as first approximation of soil behavior. The soil behavior will be elastic and obeys Hook's law for isotropic linear elasticity for the stress states within yield surface. Hence, the real soil behaviour of stress dependency on the elastic stiffness cannot be depicted using Mohr-Coulomb model.

Figure 1 shows the stress-strain behavior of real soil and the patterns, which can be observed using Mohr-Coulomb and Hardening Soil models.



(a) Real Soil **(b) Mohr-Coulomb model** **(c) Hardening Soil model**

Figure 1. Stress-strain behaviour of real soil, MC soil and HS soil

Mohr-Coulomb yield criterion comprises of six yield functions (Equations 1-6), which are derived in the form of principal stresses and the model parameters cohesion, C and friction angle, Φ (Smith and Griffiths 1982).

$$f_{1a} = \frac{1}{2}(\sigma'_2 - \sigma'_3) + \frac{1}{2}(\sigma'_2 + \sigma'_3)\sin\Phi - C\cos\Phi \leq 0 \quad (1)$$

$$f_{1b} = \frac{1}{2}(\sigma'_3 - \sigma'_2) + \frac{1}{2}(\sigma'_3 + \sigma'_2)\sin\Phi - C\cos\Phi \leq 0 \quad (2)$$

$$f_{2a} = \frac{1}{2}(\sigma'_3 - \sigma'_1) + \frac{1}{2}(\sigma'_3 + \sigma'_1)\sin\Phi - C\cos\Phi \leq 0 \quad (3)$$

$$f_{2b} = \frac{1}{2}(\sigma'_1 - \sigma'_3) + \frac{1}{2}(\sigma'_1 + \sigma'_3)\sin\Phi - C\cos\Phi \leq 0 \quad (4)$$

$$f_{3a} = \frac{1}{2}(\sigma'_1 - \sigma'_2) + \frac{1}{2}(\sigma'_1 + \sigma'_2)\sin\Phi - C\cos\Phi \leq 0 \quad (5)$$

$$f_{3b} = \frac{1}{2}(\sigma'_2 - \sigma'_1) + \frac{1}{2}(\sigma'_2 + \sigma'_1)\sin\Phi - C\cos\Phi \leq 0 \quad (6)$$

The criteria, $f_i = 0$ for all yield functions together represents a hexagonal cone on principal stress space as shown in Figure 2a.

Hardening Soil model is an advanced soil model to simulate the behaviour of different types of soil, both stiff soils and soft soils (Schanz 1998, Brinkgreve et al. 2004). Nonlinear, inelastic and stress dependent behaviour of soil can be captured using Hardening soil model. The variation of elastic stiffness with the stress is taken into account in the Hardening Soil model, whereas the elastic stiffness is considered as constant value in Mohr-Coulomb model. The yield surfaces are not fixed on principal stress space, but can expand as the soil undergoes plastic straining. The Hardening Soil model supersedes the Mohr-Coulomb model: firstly by using the theory of plasticity rather than theory of elasticity; secondly by including soil dilatancy; and thirdly by introducing a yield cap. Some basic characteristics of the Hardening Soil model and its input parameters for the numerical modelling are shown in Table 1.

Table 1. Basic characteristics of HS model

Basic characteristics	Input parameters
Stress dependent stiffness according to a power law	m
Plastic straining due to primary deviatoric loading	E_{50}^{ref}
Plastic straining due to primary compression	E_{oed}^{ref}
Elastic unloading / reloading	E_{ur}^{ref}, ν_{ur}
Failure according to Mohr-Coulomb failure criterion	C, Φ, ψ

The hyperbolic relationship (Figure 3) between the vertical strain, ε_1, and the deviatoric stress, q, in primary triaxial loading is the basic idea for the formulation of Hardening Soil model. The yield curves obtained from a standard triaxial test can be described by:

$$-\varepsilon = \frac{1}{E_i}\left(\frac{q}{1-q/q_a}\right) \qquad \text{for } q < q_f \tag{7}$$

q_a is asymptotic value of shear strength and E_i is the initial stiffness which is related to E_{50} by:

$$E_i = \frac{2E_{50}}{2-R_f} \tag{8}$$

$$E_{50} = E_{50}^{ref}\left(\frac{C\cos\Phi - \sigma_3^{'}\sin\Phi}{C\cos\Phi + p_{ref}\sin\Phi}\right)^m \tag{9}$$

E_{50}^{ref} is a reference stiffness modulus corresponding to a reference confining pressure, p_{ref}. The ultimate deviatoric stress, q_f and the quantity q_a in Equation 7 are defined as:

$$q_f = \left(C\cot\Phi - \sigma_3^{'}\right)\frac{2\sin\Phi}{1-\sin\Phi} \tag{10}$$

$$q_a = \frac{q_f}{R_f} \tag{11}$$

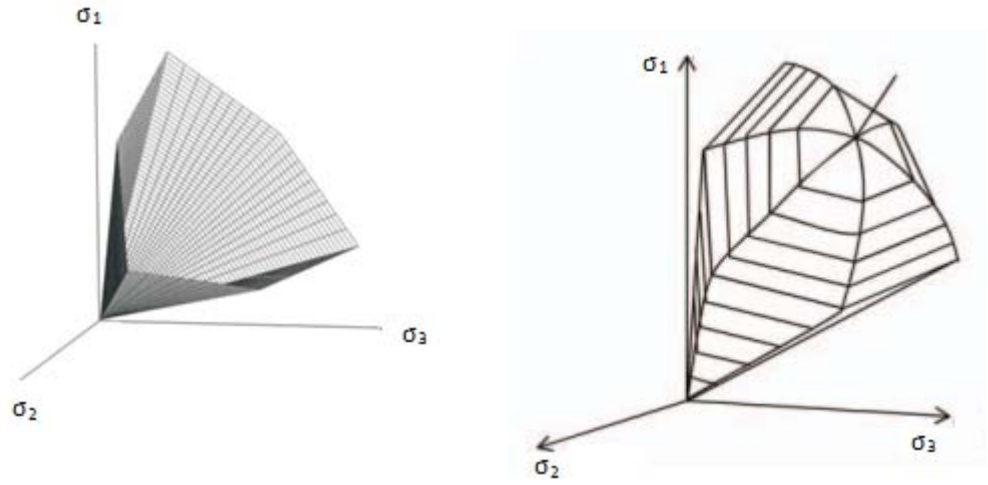
R_f is the failure ratio which is lesser than 1.

For unloading and the reloading stress paths, another stress dependent stiffness modulus is used:

$$E_{ur} = E_{ur}^{ref}\left(\frac{C\cos\Phi - \sigma_3^{'}\sin\Phi}{C\cos\Phi + p_{ref}\sin\Phi}\right)^m \tag{12}$$

E_{ur} is the reference Young's modulus for unloading and reloading, corresponding to reference pressure, p_{ref}. In many practical cases, it is appropriate to set E_{ur}^{ref} equal to $3E_{50}^{ref}$.

The Hardening Soil model has two yielding surfaces as shown in Figure 4. The first one deals with the yielding due to shear stress and the second one handles the expansion of the cap due to changes in mean effective stress, p´. The 3-dimensional yield surface is shown in Figure 2b.



(a) (b)

Figure 2. Yield surface in principal stress space:
(a) Mohr-Coulomb model (After Smith and Griffiths 1982)
(b) Hardening Soil model (After Brinkgreve et al. 2004)

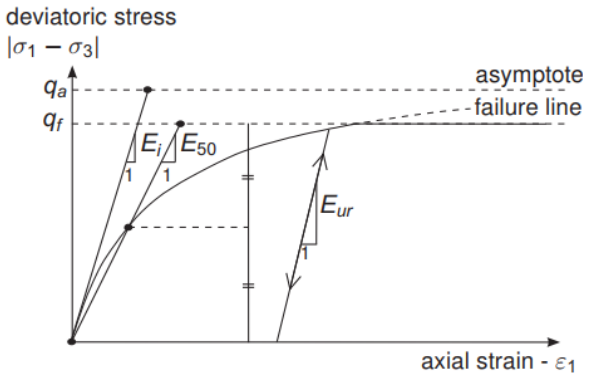


Figure 3. Hyperbolic stress-strain behaviour in primary loading for a standard drained triaxial test (After Duncan and Chung 1970)

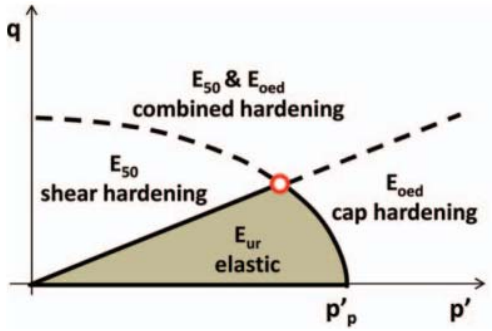
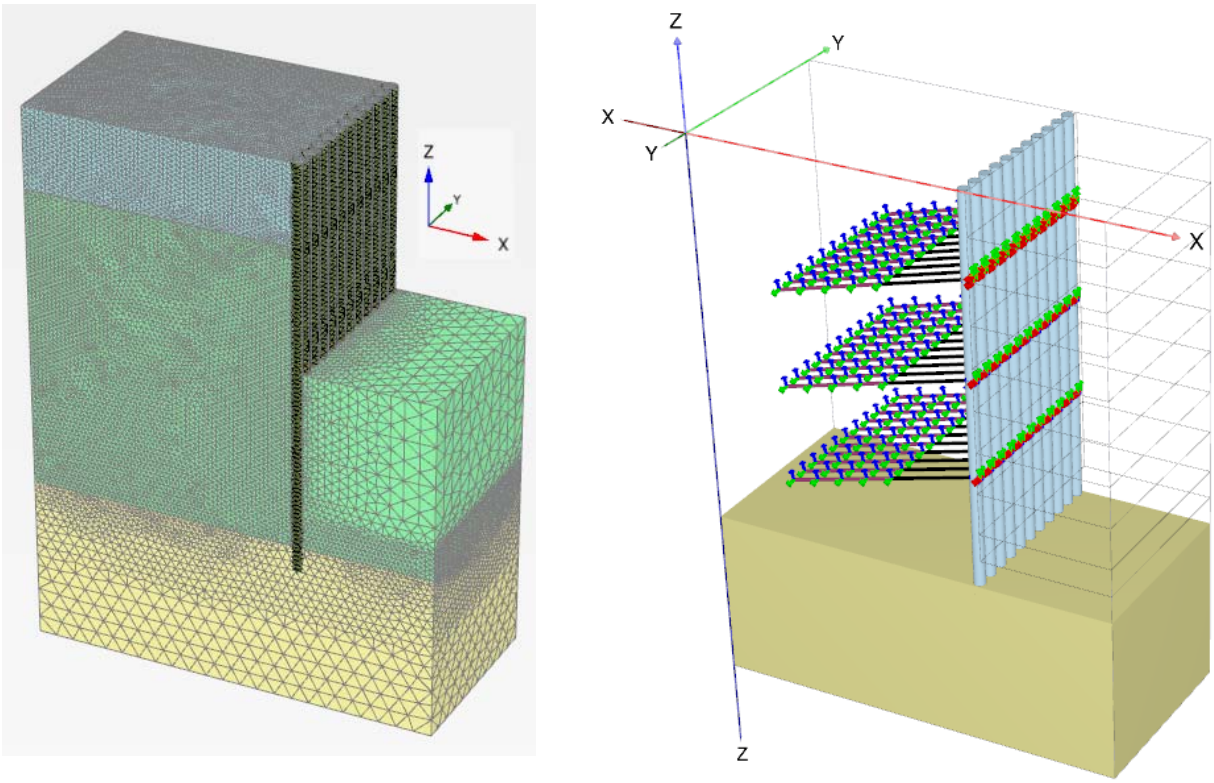


Figure 4. Illustration of double yield surfaces of HS model (After Brinkgreve et al. 2004)

NUMERICAL MODELLING

The number of case studies available on the application of contiguous pile wall for deep excavation support reported is very limited. However, its successful implementation as deep excavation support system is frequently done in Santiago, Chile (Saez and Ledezma 2011; Prado et al. 2012). Deep excavation of 26 meters depth supported by contiguous piles of 0.8 m diameter and 0.5 m clear gap between them is numerically modelled in the present study using Plaxis 3D. The soil profiles are modeled using both Mohr-Coulomb and Hardening Soil model and the results are compared. The contiguous piles are modelled as linearly elastic non-porous material. Piles are supported by three layers of anchors at depths 6 m, 13 m and 20 m. These supporting anchors are modelled using embedded pile element for the grouted part and node-to-node anchor element for un-grouted part. A fines content of 3%, with a plastic index between 5 and 20 and coarse grains of up to 30 cm of nominal size (Rodriguez-Roa 2000) characterize the Santiago gravel. A 1.5–3.0 m thick deposit of low-plasticity clay of medium to high consistency overlies this gravel deposit. From the ground surface down to a depth of 5–7 m, the gravel contains low-plasticity silty fines, with a cohesion of about 20 kPa, and an angle of internal friction of 45º. The upper gravel layer is known as the second deposit of the Mapocho River. Below this stratum, there is a denser gravelly deposit with a very similar particle-size distribution. Many authors (Kort et al. 1979; Ortigosa et al. 1982; Rodríguez-Roa 2000; De la Hoz 2007) studied the mechanical properties of this material. The ground water table observed at the site is at a depth of around 22 m. Soil layers and piles are modelled by 10-node tetrahedral elements and 12-node interface elements to model pile-soil interface. 302921 elements and 425303 nodes were generated to model the site of dimensions 30 m x 14 m x 40 m (length x width x depth) and is shown in Figure 5a.



(a) (b)

Figure 5. Numerical modeling:
(a) Finite element meshing;
(b) 13 phases of 26 m deep excavation (soil layers are hidden to show the contiguous pile wall and supporting anchors).

Excavation process is replicated numerically by a thirteen-phase process:

Phase 0 – Application of initial soil conditions.
Phase 1 – Installation of piles.
Phase 2 – Excavating up to 3 m depth.
Phase 3 – Excavating up to 6 m depth.
Phase 4 – Installation of first layer of anchors at 6 m depth.
Phase 5 – Excavating up to 9 m depth.
Phase 6 – Excavating up to 12 m depth.
Phase 7 – Excavating up to 15 m depth.
Phase 8 – Installation of second layer of anchors at 13 m depth.
Phase 9 – Excavating up to 18 m depth.
Phase 10 – Excavating up to 21 m depth.
Phase 11 – Installation of third layer of anchors at 20 m depth.
Phase 12 – Excavating up to 24 m depth.
Phase 13 – Excavating up to 26 m depth.

RESULTS AND DISCUSSION

Soil elements (Points P_1, P_2 and P_3) at the midway between the piles at different depths (5 m, 10 m and 20 m), which are adjacent to the exposed face of excavation are taken into consideration (Figure 6). The variation of lateral stresses in the direction of flow of soil (σ_{xx}) and the variation of Young's modulus (E) with the phases of excavation are illustrated in Figure 7.

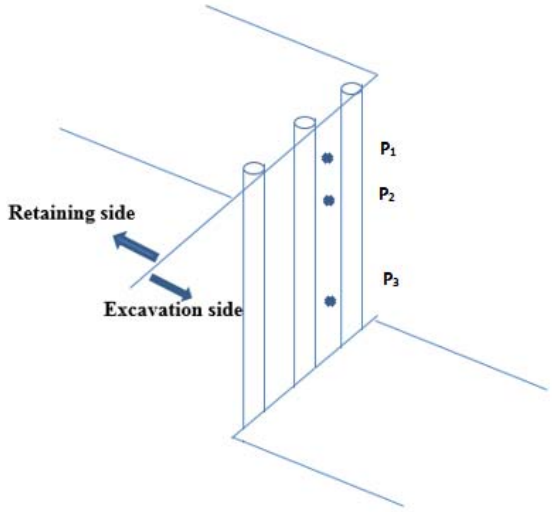
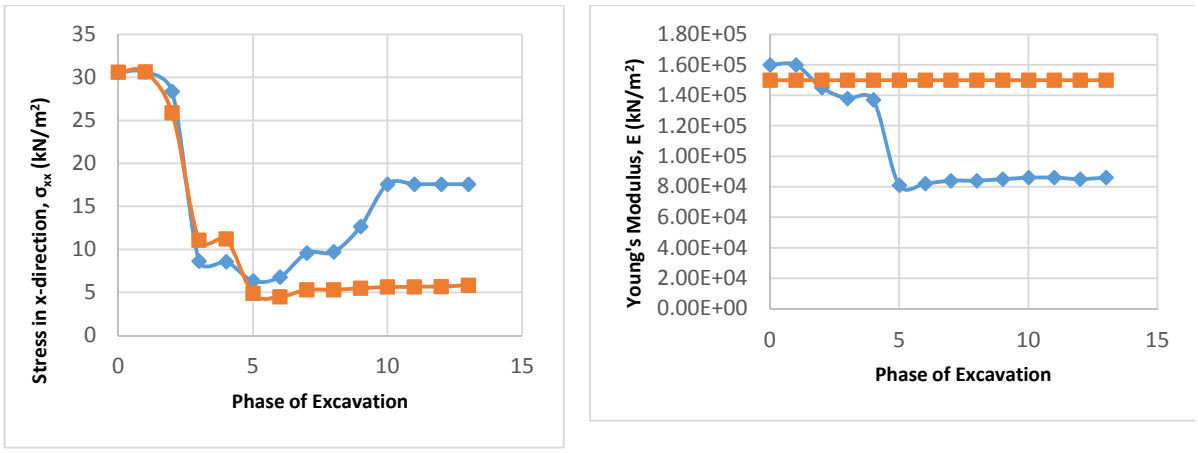


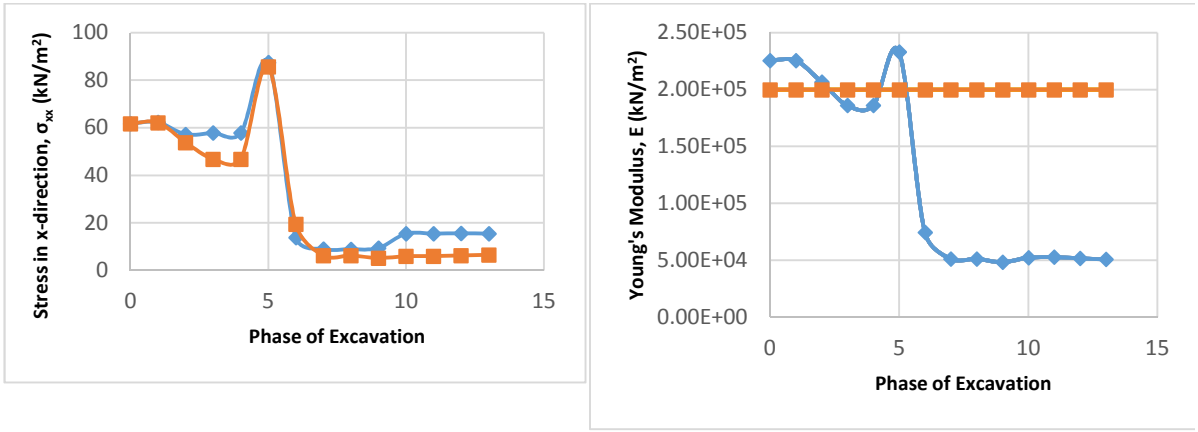
Figure 6. Points considered for the comparative study

Significance of modelling nonlinear behaviour before failure

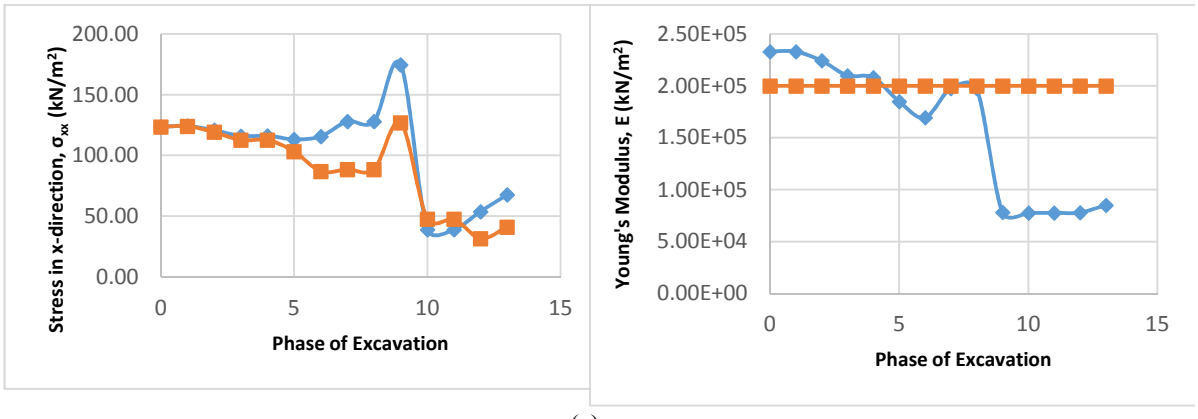
In the Mohr-Coulomb model, soil remains elastic until the stress state of the soil reaches yield surface. Upon reaching the yield surface, it switches to plastic state. However, the real soil behaviour is elastic-plastic (i.e. nonlinear) even before approaching the yield surface. The Hardening Soil model captures this nonlinear behaviour by varying the Young's modulus during primary loading. Figure 7 depicts the variation in stiffness in Hardening Soil model whereas the stiffness is constant in the Mohr-Coulomb model.



(a)



(b)



(c)

Mohr- Coulomb model Hardening Soil model

Figure 7. Variation of lateral stress (σ_{xx}) and Young's modulus (E) at the soil gap between the piles with the phases of excavation: (a) at 5 meter depth; (b) at 10 m depth; and (c) at 20 m depth.

Modelling of Stress-dependent stiffness in HS model

The nonlinearity in stress-strain behaviour in the Hardening Soil model in turn depicts the stress dependency of Young's modulus. As the stage wise excavation is progressed, the lateral stresses on the soil elements at the gaps between the adjacent piles get relieved from top to bottom, up to the depth of excavation. This reduction in the lateral stresses in the direction of soil flow, with the stages of excavation is illustrated in Figure 7. The stress dependency of the soil stiffness in the Hardening Soil model can be evidenced in the graph, whereas the Young's modulus remains constant when Mohr-Coulomb model is adopted.

Modelling of Unloading-reloading behaviour using HS model

An elastic Mohr-Coulomb soil sample may produce improper response for certain stress paths. From Figure 8b, it can be noted that the strain in the direction of deformation of soil at 10 m depth increases from excavation stage 2 to 4 and then drastically decreases to a negative value in excavation stage 5. This behaviour is not observed in numerical model with the Hardening Soil model and in the field as well. Also, more heaving is observed at the excavation side when the Mohr-Coulomb model is used.

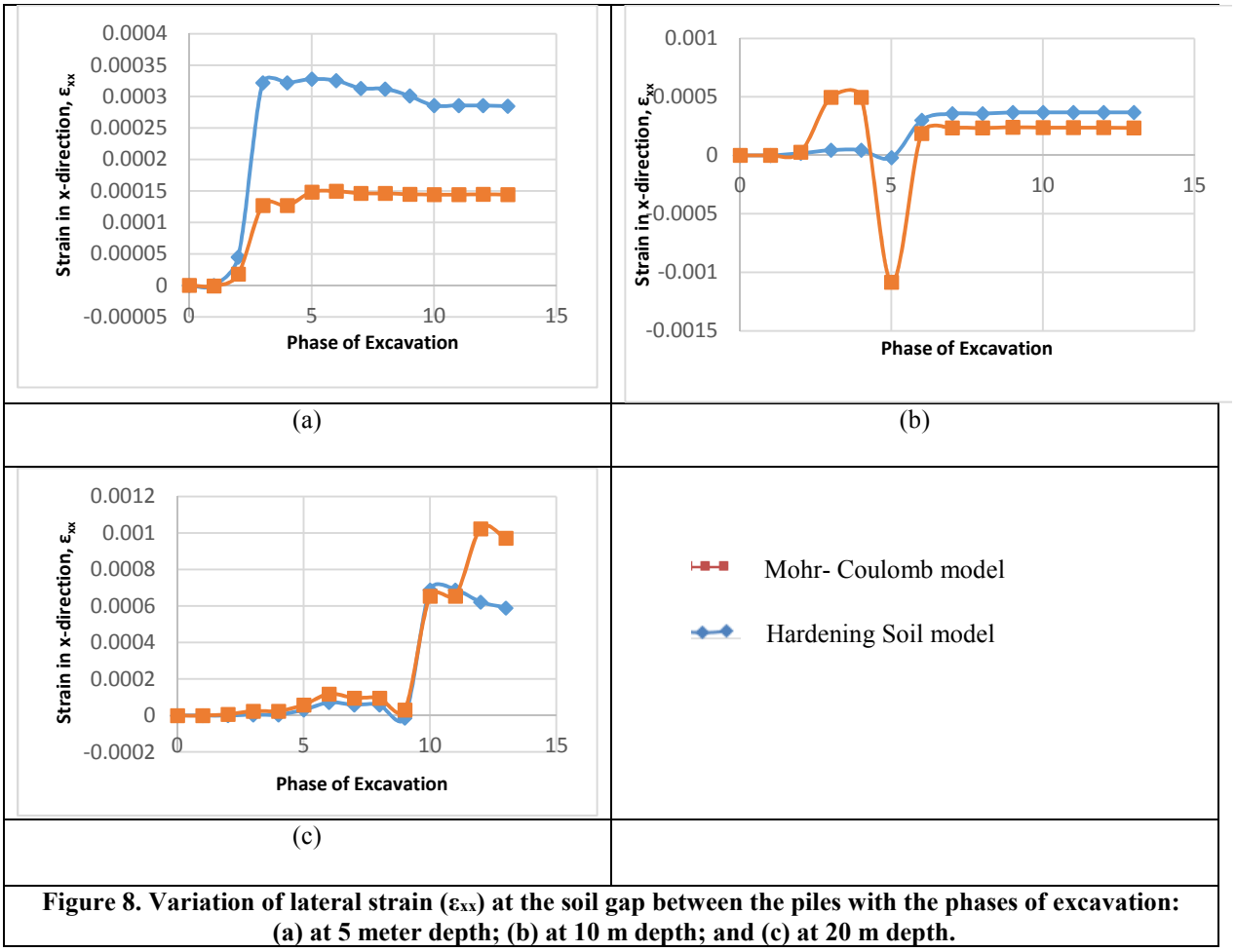


Figure 8. Variation of lateral strain (ε_{xx}) at the soil gap between the piles with the phases of excavation: (a) at 5 meter depth; (b) at 10 m depth; and (c) at 20 m depth.

Mohr-Coulomb model - Effect of Poisson's ratio

The uncertainty in the value of Poisson's ratio may not affect the results to a larger extent in numerical model with Hardening Soil model. As the Hardening Soil model is nonlinear elastic-plastic model, the plastic strain component is not affected by the Poission's ratio. Poisson's ratio affects only the elastic strain component. By varying the Poisson's ratio from 0.2 to 0.4, the lateral deflection of contiguous pile wall is doubled.

Influence of Soil model on the deformations on soil

In numerical modelling, the deformations are obtained from the ratio of stress to soil stiffness. The soil stiffness may increase or decrease with the nature of stress path. This variation in stiffness which happens in reality will not be taken into consideration for computing the deformations of soil when Mohr-Coulomb model is used. The Hardening Soil model accounts for this variation in stiffness and hence give more accurate values of deformations.

CONCLUSIONS

Discontinuous piles are frequently being used for deep excavation support, mainly for cohesive soils with water level deep below the ground surface. Numerical modelling is carried out in the present work replicating contiguous pile wall system used in Santiago, Chile. The Mohr-Coulomb and the Hardening Soil models are used to model the soil layers and a comparative study is presented. The Mohr Coulomb model assumes soil to be elastic perfectly plastic and is commonly used to model soil behaviour. The Hardening Soil model is a second order nonlinear, elastic-plastic model which nearly predicts the real soil behaviour. As stress-dependency of stiffness is taken into account in the Hardening Soil model, it overcomes many of the shortcomings of Mohr-Coulomb model.

REFERENCES

1. Brinkgreve, R. B. J. (2004). "Time-dependent behaviour of soft soils during embankment construction- a numerical study." *Proceedings NUMOG IX.* pp: 631-637.
2. Costa, Y. D., Zornberg, J. G., Bueno, B. S. and Costa, C. L. (2009). "Failure mechanisms in sand over a deep active trapdoor." Journal of Geotechnical and Geoenvironmental Engineering, 1741 (53).
3. De La Hoz, K. (2007). Estimación de los parámetros de resistencia al corte en suelos granulares gruesos. Tesis de Magister en Ciencias de la Ingeniería, *Universidad de Chile (in Spanish).*
4. Duncan, J. M., and Chang, C. Y. (1970). "Non linear analysis of stress and strainin soil." *ASCE Journal of Soil Mechanis and Foundation.* 96, pp: 113-118.
5. Evans, C. H. (1983). "An examination of arching in granular soils." M.Sc. Thesis.
6. Gaba, A. R., Simpson, B., Powrie, W., and Beadman, D. R. (2003). "Embedded retaining walls z guidance for economic design." London: CIRIA.
7. Haema, W. and Tanseng, P. (2010). "Influence of pile spacing on soil resistance of contiguous bored pile wall." The 21th National Convention on Civil Engineering, Ubon Ratchathani, Thailand.
8. Iglesia, G. R., Eienstein, H. H. and Whitman, R. V. (2013). "Investigation of soil arching with centrifuge tests." Journal of Geotechnical and Geoenvironmental Engineering, 140(2).
9. Ito, T., and Matsui, T. (1975). "Methods to estimate lateral force acting on stabilizing piles." Soils

and Foundations, 15 (4), 43-59.
10. Keawsawasvong, S. and Ukritchon, B. (2017). Undrained limiting pressure behind soil gaps in contiguous pile walls. Computers and Geotechnics 83: 152–158.
11. Kort, I., Musante, H., and Fahrenkrog, C. (1979) "In situ mechanical properties measurements of gravelly soil used in an interaction and foundation model for the Santiago Metro." *Proceedings of the 6th Panamerican Conference on Soil Mechanics and Foundation Engineering, Perú, 217-224.*
12. Nethero, M. F. (1982). "Slide control by drilled pier walls. In Application of walls to landslide control problems." Edited by Reeeves, R. B., *American Society of Civil Engineers,* pp: 61-76.
13. Ortigosa, P., Musante, H. and Kort, I. (1982) "Propiedades mecánicas de la grava de Santiago." *1° Congreso Chileno deIngeniería Geotécnica, Santiago: 442-54, 1982 (in spanish).*
14. Pardo, G., Saez, E. and Ledezma, C. (2012) "Seismic response of a pile supported excavation on Santiago gravel" *15 WCEE, Lisboa*
15. Poulous, H. G (1995). "Design of Reinforcing piles to Increase Slope Stability." *Canadian Geotechnical Journal.* 32: 808-818.
16. Richards, D. J., Wiggan, C. A. and Powrie, W. (2016). "Seepage and pore pressures around contiguous pile retaining walls." Geotechnique 66, No. 7 : 523-532.
17. Rodríguez-Roa, F. (2000). "Observed and calculated load-settlement relationship in a sandy gravel." *Canadian Geotechnical Journal, Vol. 37, No. 2, pp. 333-342.*
18. Rollins, K. M., and Rollins, R. L. (1992). "Landslide stabilisation using drilled shaft walls." Edited by Geddes, J. D. *Ground movements and structures.* vol 4,pp: 755-770.
19. Saez, E. and Ledezma, C. (2011) "Dynamic presures on pile-supported excavations in Santiago Gravel" *5th International Conference on Earthquake Geotechnical Engineering, Santiago, Chile.*
20. Sharafi, H. and Sojoudi, Y. (2016). "Experimental and Numerical Study of Pile-Stabilized Slopes Under Surface Load Conditions" *International Journal of Civil Engineering.*
21. Smith, C. C. (2012). "Limit loads for a shallow anchor/trapdoor embedded in a nonassociative Couilomb soil." International Journal of Soil Mechanics, 62(7):563-571.
22. Smith, I. M. and Griffiths, D. V. (1982) "Programming the Finite Element Method." *Wiley and Sons, Chisester,U. K, second edition.*
23. Sommer, H. (1977). "Creeping slope in a stiff clay." *Proceedings Special Session No. 10, 9th International Conference on Soil Mechanics and Foundation Engineering, Tokyo.* pp: 113-118.
24. Vermeer, P. A., Punlor, A. and Ruse, N. (2001). Arching effects behind a soldier pile wall. Computers and Geotechnics 28: 379-396.
25. Wang, L., Leshchinsky, B., Evans, T. M. and Xie, Y. (2017). "Active and passive arching stress in C'-Φ' soils: A sensitivity study using computational limit analysis." Computers and Geotechniques, 84: 47-57.

ALTERNATIVE PILING METHODS - CHANCES FOR TECHNICAL AND ECONOMICAL SOLUTIONS

Franz-Werner Gerressen, BAUER Maschinen GmbH, Schrobenhausen, Germany, Franz-Werner.Gerressen@bauer.de

ABSTRACT

Everybody knows about piling using hydraulic drill rigs and using the so called Kelly drill mode. Kelly drilling has a lot of advantages as it can work with a wide range of tools facing almost all types of soil and rock. It can also deal with diameters up to 3.000 mm and bigger or depth of +100 m.
But there is a big concern about Kelly drilling as the installation process is relatively slow.

Therefore, alternative Piling Methods like Continuous Flight Auger Piles (CFA), Cased Continuous Flight Auger Piles (CCFA) and Full Displacement Piles (FDP) provide a lot of chances in terms of installation performance and therefore cost, and even more important, time saving potentials. The paper will show where these systems may be an interesting alternative to the traditional Kelly Drilling. Of course there are as well limitations in using these methods which should be known and considered.

The paper will describe these methodologies, reference projects will allow showing the results in time and cost saving in using these methods, but it will also show the limitations for these methods.

Keywords: Bored Pile, Kelly Drilling, CFA, FDP, CCFA, Single Pass Drilling

INTRODUCTION

In the changing construction environment, companies are searching for new technologies or improvement of existing once to complete their projects in shorter time frames. Especially with the focus of increasing urbanization, the aim of fast construction becomes more and more important. Looking into the field of pile installation, either for foundations or for pile walls, significant progress has been undertaken in the last years with the development of increasingly powerful drilling rigs, tools for more efficient quality control and safe pile installation. These developments provide piling companies an increased number of options for the execution of specialist foundation projects when using single pass applications like CFA, CCFA and FDP.

ALTERNATIVE PILING METHODS

Alternative piling methods provide chances not only for technical and economical solutions, but moreover for time saving potentials, are the so called single pass methods CFA, CCFA and FDP. Single pass means in general, that the tool is pushed and rotated into the ground to the final depth in one stroke. After reaching the final depth, concreting is started and concrete is pumped continuously while the tool is withdrawn. In the following, the three methodologies will be explained more detailed.

Continuous Flight Auger Piles (CFA)

CFA piles are cast-in-situ piles, where a hollow-stem continuous flight auger is rotated and driven into the ground at a controlled speed to the specified pile depth (Figure 1, Steps 1-3). Concrete is then pumped under continuous positive pressure through the hollow stem of the auger to fill the borehole as the auger is withdrawn (Figure 1, Step 4). Once the auger is completely out of the borehole, a reinforcing cage can be inserted and driven into the fresh concrete to the designed depth (Figure 1, Step 5).

© 2018 Deep Foundations Institute

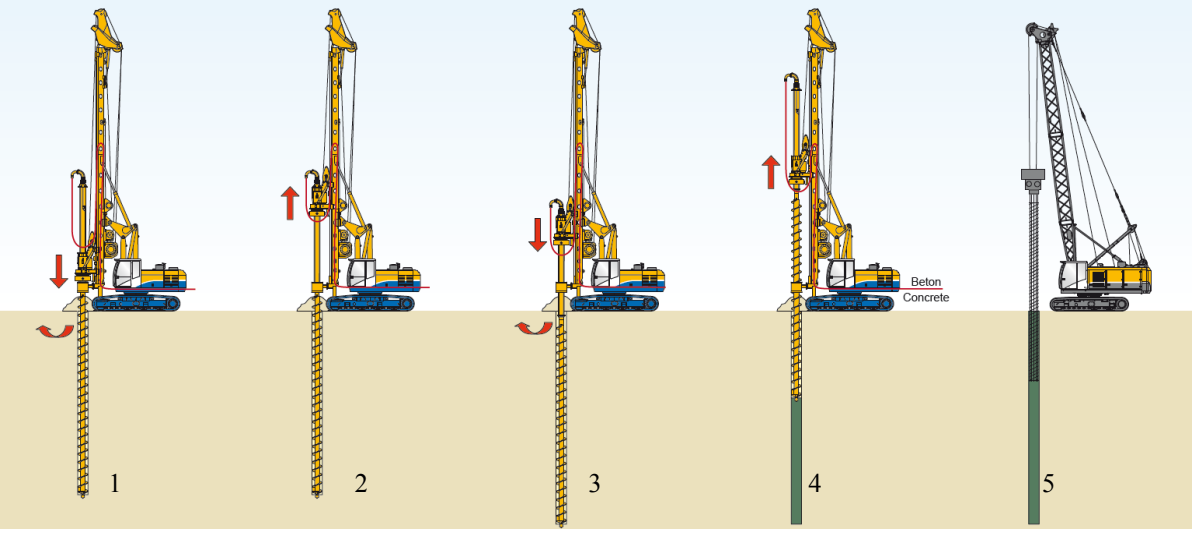


Figure 1: CFA Installation Process

The method is suitable for cohesive soils and granular soils with sufficient cohesive content to allow the soil transport on the auger, were the undrained shear strength "cu" should be above 15 kN/m² and no boulder should be present.

Main application for CFA piles is the use for foundations; the use for pile walls is restricted.

Cased Continuous Flight Auger Piles (CCFA)

The basic principle of a CCFA pile is that a continuous flight auger in combination with an outer casing is drilled simultaneously, but in opposite directions into the ground to the required depth (Figure 2, Step 2). These characteristics led to the common term Cased Continuous Flight Auger Pile (CCFA). The spoil is transported upwards by the auger flights surrounded by the casing and exits through openings at the top of the casing. Once the final depth is reached (Figure 2, Step 3) the concrete pump is activated and concrete is pumped through the hollow stem of the auger. After completion of concreting the drill string has to be cleaned (Figure 2, Step 4). The cleaning is done by rotating the casing and the auger in the opposite direction than during drilling. In some geology it can be beneficial to postpone the cleaning after reinforcement installation (Figure 2, Step 5).

This procedure requires double rotary drive systems to run auger and casing at the same time. Actually, different setups of double rotary drive systems exit. One option is the use of two rotary drives, either working independent or dependent to each other. With a specific geometry this system is also known as Front of Wall (FoW) system. Another option is to use one rotary drive in combination with a torque multiplier. The torque multiplier is a mechanical unit attached to the cardanic joint below the rotary drive. The ratio is fixed at 1:2, so that the torque multiplier doubles the incoming torque, halves the speed and inverts the direction of rotation of the casing.

Similar to CFA, the CCFA method is suitable for cohesive soils and granular soils with sufficient cohesive content to allow the soil transport on the auger, were the undrained shear strength "cu" should be above 15 kN/m² and no boulder should be present. Rock socketing is possible to UCS values of approx. 20 MPa.

Main application for CCFA piles is the use for pile walls, secant and tangent, as support for deep excavations. Of course, CCFA piles can also be used for foundations as well.

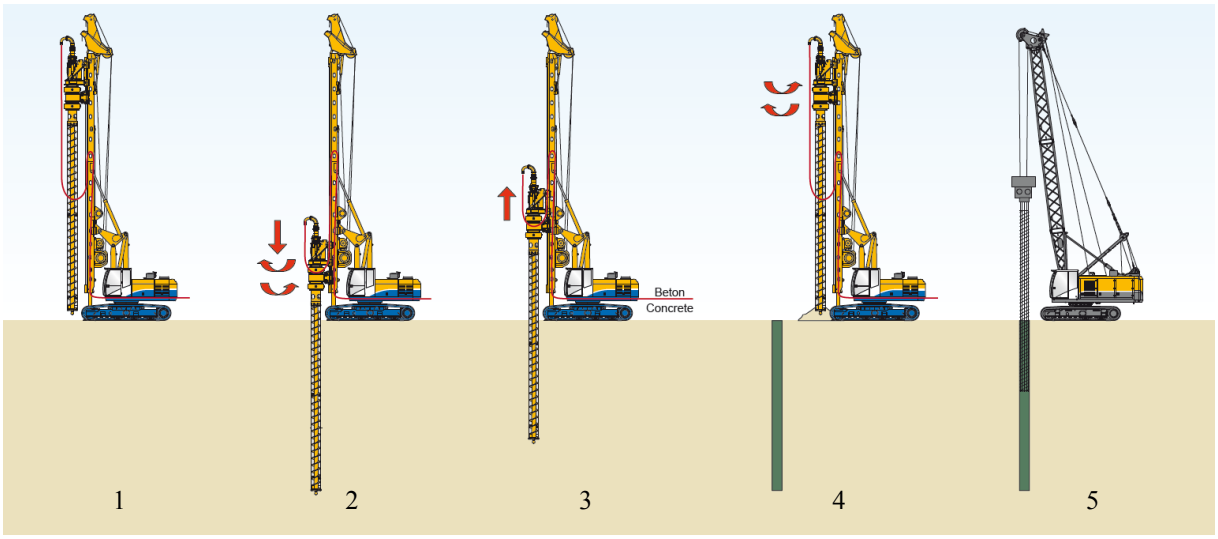


Figure 2: CCFA Installation Process

Full Displacement Piles (FDP)

The hollow stem displacement tool is rotated and drilled into the ground (Figure 3, Step 2-3), by the torque generated by the rotary drive of the drilling rig and the crowd pressure generated by the crowd winch, at a controlled rate of penetration to the specified depth. Penetration depth can be increased using an optional Kelly extension (Figure 3, Step 3). Upon reaching the required depth, concrete is pumped into the hollow stem of the FDP drill string As soon as the hollow stem is completely filled with concrete, the process of withdrawing or extracting the auger at a steady rate begins (Figure 3, Step 4). During the concreting and extraction phase the FDP tool is rotated in the same direction as in the drilling phase.
As soon as the drill string has been completely withdrawn from the bore, a reinforcement cage can be inserted into the fresh concrete and driven to the specified design depth (Figure 3, Step 5).

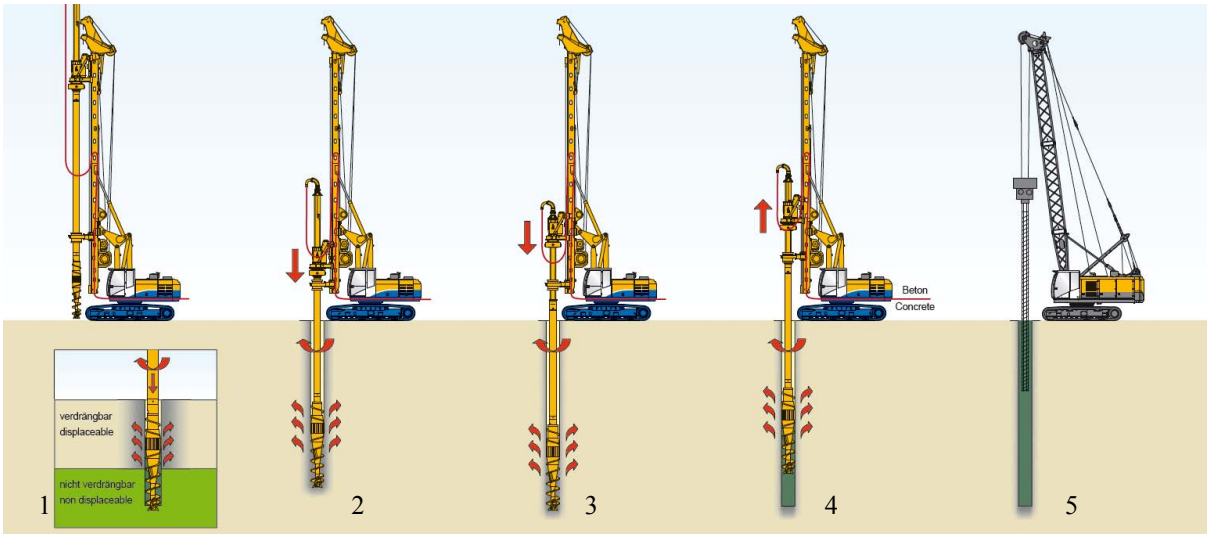


Figure 3: FDP Installation Process

As a variation of the system, using different kind of FDP drill string, steps four and five can be swapped. In this case, the reinforcement cage is inserted through the hollow stem prior to concreting and an ensured

installation of the reinforcement cage in the center of the pile to final depth takes place. By installing the reinforcement cage through the stem, at the bottom of the drill string an artificial bit is push away and will remain in the ground. Therefore, the system is also called FDP Lost Bit.

The FDP method is suitable for displaceable soils in a range of approx.:

- SPT < 30 or CPT < 15 MPa (for granular soils)
- SPT < 15 or CPT < 1-2 MPa (for cohesive soils),

And undrained shear strength cu > 15 kN/m²

Main application for FDP piles is the use for foundations or ridged inclusions; the use for pile walls is not possible.

ADVANTAGES, LIMITS AND CONSIDERATIONS

Single pass methodologies provide a lot of chances in terms of installation performance and therefore cost, and even more important, time saving potentials. Reason for that is that the penetration is taking place in one step, therefore, much faster as possible using the well-known Kelly drilling method.
Also the concreting process is much faster, as the drilling tool acts like a tremie pipe during the extraction process, where concreting and extraction of the tool runs simultaneously.

Besides the fast installation process, which is valid for all three methods described, there are exemplarily some specific advantages which should be named:

- **Verticality** of CCFA when using for secant pile walls:
  The verticality of the pile is controlled and influenced by the outer casing. Attention must be paid to the accurate alignment of the casing. The relative stiffness of the combined drill string is significantly higher than that of a CFA auger. The counter rotation of the casing and auger also has a beneficial stabilizing effect. Therefore, the alignment of the pile wall reaches the same quality as known for the installation with cased Kelly drilling.

- **Increased Load Capacity** of FDP piles:
  Due to the fact that the soil is displaced in the surrounding area of the pile, significant densification of the surrounding soil take place. This leads to an increase in skin friction and therefore an increase in pile capacity. This allows a much more time saving and economical design as the number of piles can be reduced or the diameter can be adjusted.

- **Spoil Reduction** when using FDP piles:
  Due to the fact that the loosened material is fully pushed into the surrounding soil material and compacted by the displacement body during the drilling process, practically no vertical soil transport to the surface takes place which creates an almost spoil free production (Figure 4, left). Due to that, this system in particularly is well suited for operation in contaminated areas.



Figure 4: Comparison of spoil for FDP (left) and CFA (right)

Assistance Systems allow the control of the installation process. Most rigs can be equipped with electronic software for use with the so called "Drilling Assistant", which modulates the optimum rate of penetration and crowd force during the drilling process for an optimal speed of rotation of the drilling tool, especially working in single pass methods like CFA, FDP and Cased CFA. The desired initial parameters can be input by the rig operator with the help of simple onscreen menus.
For instance, the system avoids for a system like CFA-Drilling unwished situations like the well-known over-rotated and excessive soil removal, known as “over-flighting" (Figure 5). That means penetration speed is to low compared with rotation speed. This leads to a situation, where the surrounding soil get loosened and the load capacity of the pile might be reduced. In addition, beside the increased amount of spoil, also significant overconsumption of concrete can be observed. Both leads to increased cost for pile installation. Moreover, as a worst case scenario, this can cause ground around the tool to become unstable and ground settlement induced.

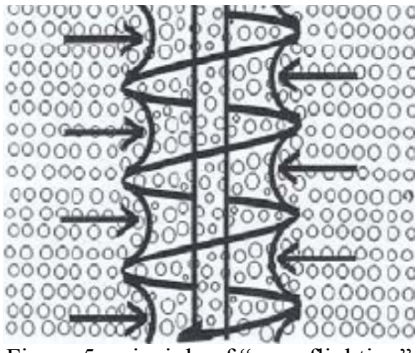


Figure 5: principle of “over-flighting”

By using the "Concreting Assistant", the speed of extraction and volume of concrete can be adjusted. This involves measuring the volume of concrete continuously throughout the concreting process and automatically regulating the speed of extraction based on the concrete flow rate. Of course, also the concrete pressure is monitored and controlled during the concreting process. As control of all relevant parameters takes place, concrete overconsumption can be reduced and blockages can be avoided.

Concrete/Grout and Reinforcement

Concrete/Grout and reinforcement need to be well designed and prepared when using single pass applications. Concrete, or grout, need to have a certain workability, especially to allow the installation of the reinforcement cage immediately after finishing the concreting process. Typically, the max. aggregate size is limited. In terms of the reinforcement, the cage needs to have a specific design and stability allowing the installation into the fresh concrete without damages, even when using a small vibrator in case self-weight is not sufficient.

Range of application

Besides the limitations defined by the soil conditions mentioned before, the single pas methods are also limited in depth and diameter. The limiting factor on the one hand side is the mast height of the used equipment, which can be slightly increased by using extension systems for CFA and FDP, on the other hand to the required retraction force to get the tool out of the ground including the weight of the soil and the lateral friction.

As guidance it can be said, that typical diameters for CFA are up to 880 mm. In some cases diameters of 1,200 mm could be seen as well. Typical depth is up to 30 m, in some cases depth of 50 m and more were carried out.

For the FDP method, the diameter is typically in a range of 400 to 600 mm, very rarely 700 mm. Depth of approx. 35 m could be seen already.
The use of CCFA, mainly for secant pile walls, is in a range of up to 1,200 mm. Depth limit is 25-30 m, very much dependent on the equipment.

These numbers for sure are not fixed, as development of equipment and tools as well as project demand force further development.

JOBSITE EXAMPLES

Reference for CFA

For the modernization of a sugar refinery in Poland, a new storage silo for saccharose need to be build. The foundation works for the new silo were carried out using a BG 24 with three meter mast extension, an eight m long concreting Kelly and auger cleaner (Figure 6).

The original design concept of Kelly bored piles was modified the way, that 120 CFA piles, diameter 1,000 mm, to a depth of max. 21.5 m were installed. These piles were partly reinforced to a depth of 9-12 m, installed into the fresh concrete, using a crane and small vibrator, immediately after finishing concreting.

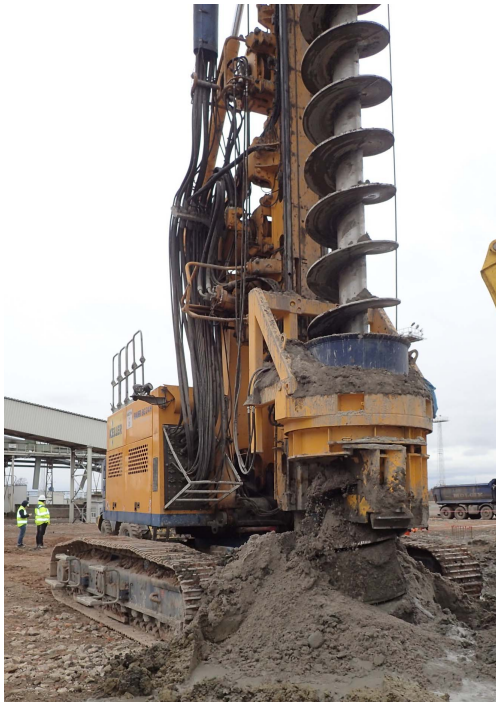


Figure 6: BG24 H with CFA and Auger cleaner

Despite the challenging ground conditions, more than 200 linear meters of CFA piles per day could be achieved and therefore met the expectations for time saving. Average installation time for one pile was approx. 50 min. It could be seen that sufficient torque and puling force is essential to guarantee a successful pile installation.

Reference for FDP

For a project in Padua, Italy, an extension of warehouses and a two story parking lot was planned. The table below shows as well the original design using standard drilled piles in combination with Micropiles as the alternative design of using the FDP piles (Table 1). The alternative design shows all the effects in savings which can be expected by using the FDP method, as there are savings in time, concrete and spoil. The job was executed using a BG 24 (Figure 7) with lattice boom extension using the FDP Lost Bit system to ensure the installation of reinforcement for the full length (24 m).

Design Comparison

	ORIGINAL DESIGN	ALTERNATIVE DESIGN
Piles	Bored piles 800 mm	FDP 610 mm "Lost bit"
Depth	23.44 m	24 m
No of piles	216	372
Micropiles 250 mm		
Depth	23.5 m	--
No of piles	446	0
Spoil volume	3,065 m³	400 m³
Concrete volume	2,527 m³	2,446 m³
Grout volume	398 m³	0
Estimated time	74 days	47 days

Table 1: Comparison of original to alternative design



Figure 7: BG24 H FDP Lost Bit

References for CCFA

In the last decade secant pile wall piling projects swopped from the traditional Kelly Drilling to the CCFA drilling frequently. Many piling projects using CCFA piles for secant pile walls have been completed with great success in the UK, Germany and Italy. The typical diameters for the piles have been 750 mm or 880 mm. The tendency for bigger diameters can be seen. In the following we will see two examples showing the potentials in time saving due to the achievable performance.

First of all, a project reference in Bath, UK. It was expected to install 4 piles, 18 m in length, for every single day. However, a peak performance of 14 piles per day was achieved with an average of 8 piles per day over the whole project. Figure 8 shows a BG 36 with BTM 400 during the operation, using the pile chute system for safe soil transport



Figure 8: BG 36 with BTM 400, with pile chute system

In Naples, Italy, several excavation pits with secant pile walls were built during the new development of a new subway using CCFA. These pits are needed for the mechanical equipment of the air ventilation system of the tunnel. Exemplarily, the following table 2 shows the installation steps and required time for the installation comparing primary and secondary piles to a depth of 15 m.

	unreinforced	reinforced
Positioning	2 min	2 min
Drilling	8 min	16 min
Concreting	9 min	9 min
Installation of reinforcement		35 min
	1 min	
Total:	20 min	62 min

Table 2: Pile construction durations

As it can be seen, the installation of the reinforcement cage took quite long. Reason for that was the fact, that due to the very confined jobsite situation, the cages were delivered in three sections and had to be connected two times during installation.

However, although space on site was very limited (see Figure 9), the works were carried out without any problems. In this confined environment also the benefit of using flushed the air during drilling to dry the spoil meant no special facilities for the collection and control of water on the surface were needed.

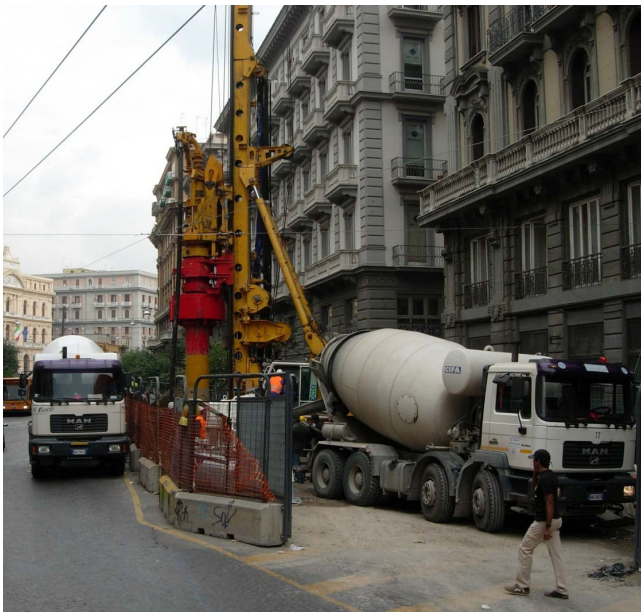


Figure 9: BG 28 with BTM 400, 15 m pile length, diameter750 mm

The spoil fell down through the soil discharge chute. The required length to keep the chute just above the ground surface is adjusted by a small winch. Therefore, it was possible to bypass the traffic directly along the adjacent street and pavements.

CONCLUSION

Single pass piling methods, as shown before, provide a lot of opportunities to the foundation market. Especially in terms of time saving potentials, the described methods are welcome alternatives to the conventional piling methods. It could be seen, that all these methods provide as well high cost saving potentials, due to achievable performance, design adjustments and material cost savings. Therefore, wherever the demands of timesaving is increasing and the soil and other relevant job site requirements would allow to use of one of the single pass methods, it should be considered to take this decision.
Doing that, single pass piling methods will become more and more important. But, especially at the beginning of projects the team needs to gain some experience to adjust the method to the soil conditions. The drilling rig must have sufficient torque, pull down and extraction force to keep the drilling process steady at all times, even in difficult soil conditions. A consistent and reliable concrete supply must be organized as part of the work preparation to ensure a constant operating sequence. Good communication and coordination among the crew on site is important and changes in staff should be avoided.

These improvements and advances contribute to a better quality product. However, these will only be successful if used properly. Therefore the importance of training, understanding and briefing to all personnel involved is vital to its success.

REFERENCES

Fleming, W. G. K. (1995), The understanding of continuous flight auger piling, its monitoring and control. Proceedings of the Institution of Civil Engineers - Geotechnical Engineering: 157 - 165..

F.-W. Gerressen, P. Platzek, 2010, Overview of the state of the art of double rotary drilling methods, Geotechnical Challenges in Urban Regeneration, London, UK

F.-W. Gerressen, H. Kopfmüller, 2016, FDP – Full Displacement Piling - an alternative Method - Principles and Applications, Sefe 8, Sao Paulo, Brazil

F.-W. Gerressen, 2018, Electronic support in installation of special foundation products - Ensuring safe production and increasing quality control, DFI-EFFC International Conference on Deep Foundations and Ground Improvement, Rome, Italy

BASE GROUTING OF BORED CAST-IN-SITU PILES AT THE RAILWAY BRIDGE OVER THE RIVER RUPSHA, BANGLADESH: A CASE STUDY

Vignesh R, Engineering Manager, L&T Construction, Chennai, rvignesh@lntecc.com
Rahul S, Asst. Engineering Manager, L&T Construction, Chennai, RAHUL-S@lntecc.com
Visakan R, Engineering Manager, L&T Construction, Chennai, VISAKAN@lntecc.com

ABSTRACT

The alignment of the new rail line, which connects Khulna port and Mongla city, passes across the river Rupsha, which necessitates for a railway bridge near the existing road bridge. Pile foundation is designed as bored cast in-situ pile of diameter 1.5 m at the approach bridge and 2.5 m diameter at the main bridge portion. The prevailing geotechnical condition at the bridge location consists of strata of soft to medium silt/clay, poses great challenges in designing and execution of pile foundations. Pile load test, which was conducted on 1.5 m diameter pile of 40 m long pile, proved the inadequacy of the pile to achieve the required design capacity of 570 tons and it experienced huge settlement. Hence to meet the required capacity without increasing the length of pile substantially, base-grouting technique was implemented based on subsequent load tests on piles of various lengths with and without base-grout have been conducted. The test results on the base-grouted pile were satisfactory over non-grouted piles. This paper describes the experience gained in pile foundation with base grouting and the comparative study between base-grouted and non-grouted piles.

Keywords: Pile foundation, base grouting

1. INTRODUCTION

Mongla port, which is the second largest seaport of Bangladesh, is gaining importance as the major port at Chittagong has become overloaded to its maximum shipping activities. Besides, due to the geographical advantage of the Mongla port, the port has high potential of becoming a regional port as it can handle cargo transportation across the border to Nepal and Bhutan. Under these circumstances, Bangladesh Government has decided to link Mongla port and Khulna city with railway line to make the port more effective and economical. The alignment of the proposed railway line passes across the river Rupsha which necessitates for a railway bridge near the existing road bridge.

The alignment of the railway line and the bridge crossing is given in the Fig. 1. The general arrangement drawing of the bridge is given in the Fig. 2. The entire bridge consists of viaduct of 4413 m and the main bridge portion of 717 m.

Sensitivity: Unclassified

© 2018 Deep Foundations Institute

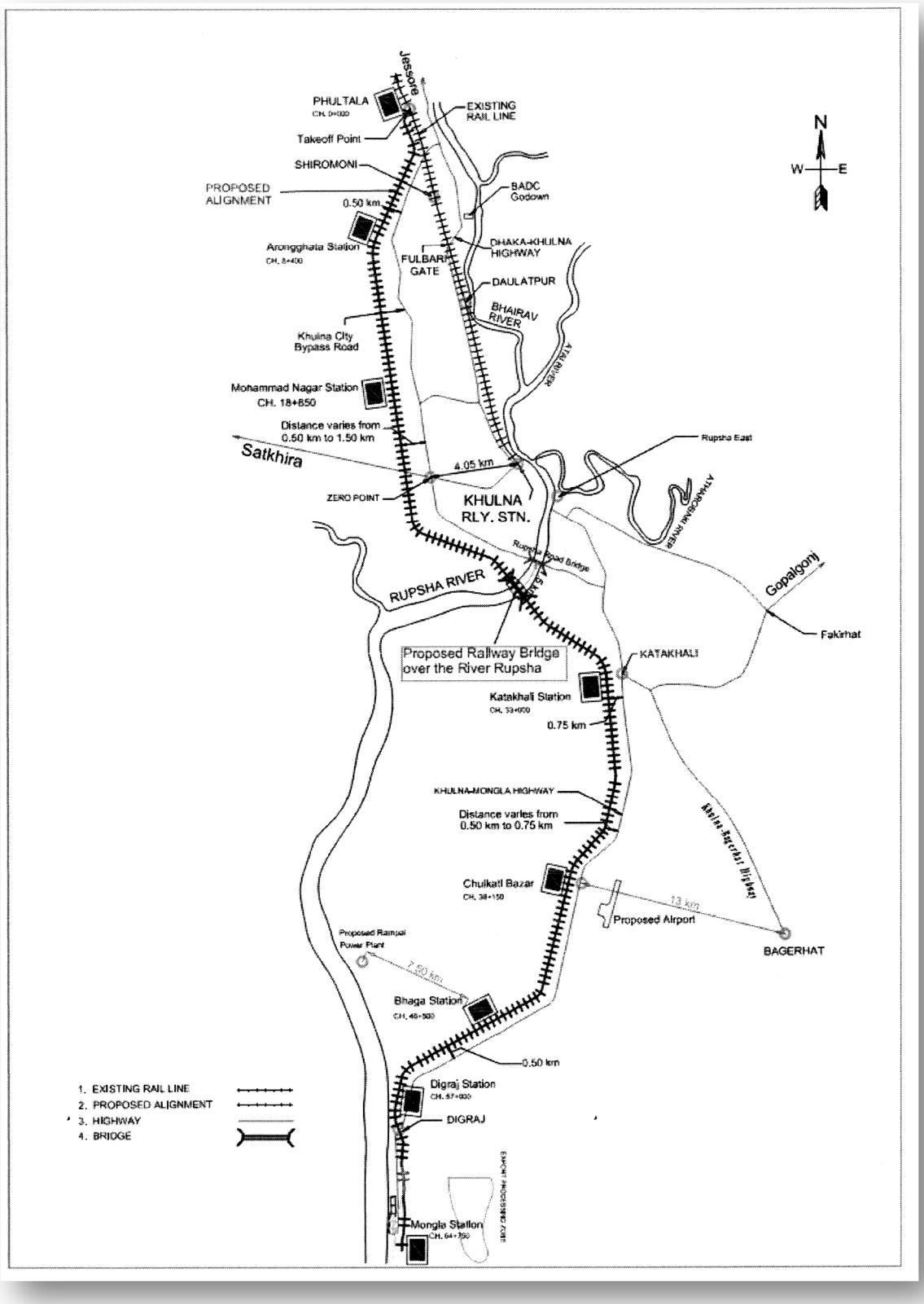


Fig. 1. Alignment of the railway line connecting Mongla Port and Khulna city

Sensitivity: Unclassified

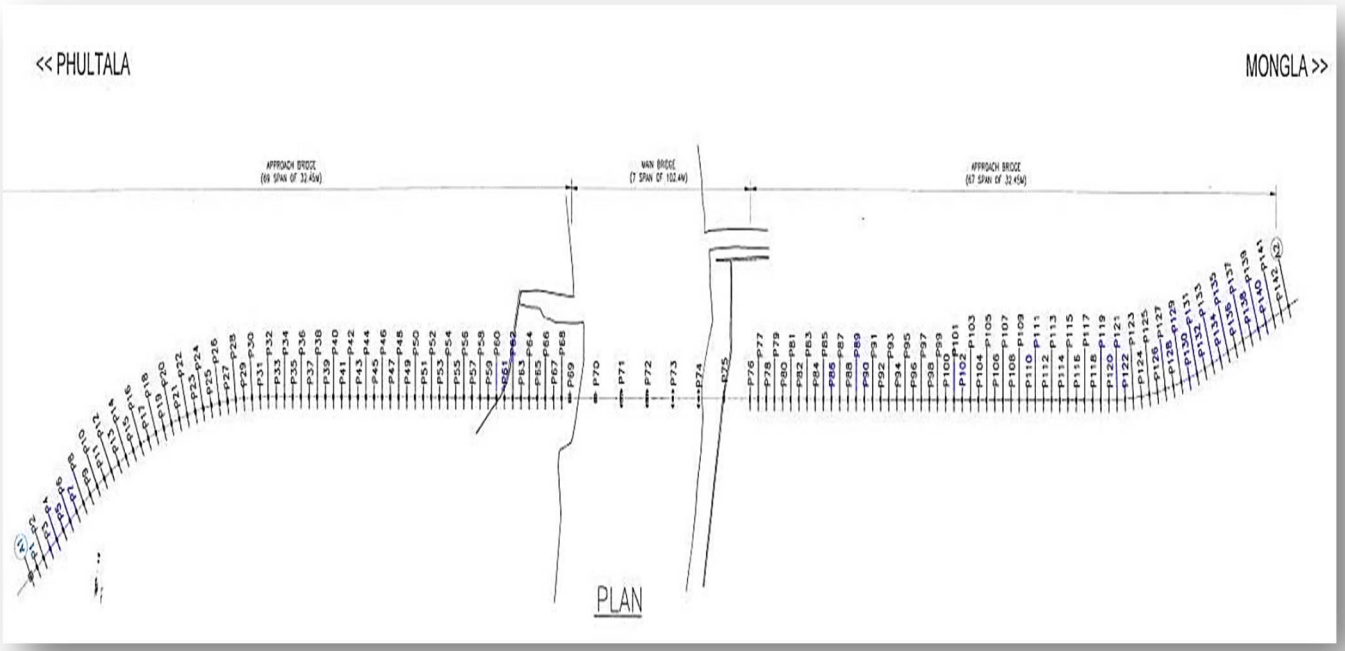


Fig. 2. Plan of the general arrangement of the bridge

2. SUB-SOIL CONDITION

In general, the subsoil profile consists soil with very poor bearing capacity in the top 15 m below the ground level in the viaduct portion. The presence of weak patch of soil most of the stretched pose a great challenge in designing the toe level of the pile. Table.1 give the general sub-soil profile of the entire stretch of the bridge alignment.

Table 1. General Subsoil Profile along the bridge alignement

Portion	Layer	Depth from EGL (m)	Soil Type	SPT 'N' Range
Viaduct	1	0-15	Silt/ Sandy Silt	0-9
	2	15-35	Silty Sand	15-30
	3	35-50	Silt	5-15
	4	50-75	Silty Sand	35-55
Main Bridge	1	0-15	Silty Sand	15-20
	2	15-30	Silt	5-15
	3	30-100	Silty Sand	35-75

Sensitivity: Unclassified

3. FOUNDATION

In the viaduct portion, pile of 1.5 m dia and length of 40 m is proposed as the foundation during the initial stage of the project. The pile is designed for the capacity of 400 T to 570 T depending on the locations. In the main bridge portion, pile dia of 2.5 m and length of 69 m is proposed. The length and the capacity of piles proposed for piers is given in the Table 2.

Table 2. Length and the load carrying capacity of pile at various pier

Pier	Length (m)	Safe Load Carrying capacity (T)	Remarks
P1 – P14	40	460	Viaduct
P15 – P28	40	480	
P29 – P51	40	525	
P52 – P67	40	570	
P68 - P75	69	1000	Main Bridge
P76 – P91	40	570	Viaduct
P92 – P107	40	525	
P108 – P128	40	480	
A1 & A2	40	400	Abutments

4. PILE LOAD TEST

The vertical load carrying capacity of the piles were determined by conducting intial load test on test piles using cyclic method and reaction for the load was obtained by kentledge method for testing. The first initial pile load test (TP-01) was conducted on a 40 m test pile near P-65. The test result shows that the pile load capacity of 312 T was achieved against the required capacity of 570 T.

Following the failure of the test pile to meet its required capacity, pile group configuration was changed to 8 nos of 52 m long pile instead of the original configuration of 6 nos of 40 m long pile and the pile load capacity is revised to 440 T. To verify load carrying capacity of 52 m pile, second load test (TP-02) conducted near to the location of TP-01. The test result ended up in test pile achieving a load carrying capacity of 480 T. In order to avoid the number of piles, alternative methods were looked for and base grouted piles were proposed after studying its effectiveness in the surrounding region. Two more pile load tests were carried out near to the first two tests – TP-03 (45 m long) and TP-04 (52 m long).

Sensitivity: Unclassified

5. BASE GROUTED PILES

Sleeve-Port (Tube-Á-Manchette) grout distribution system is used in the base grouting of the piles. Four "conduits" of 38 mm steel pipes were installed along with the reinforcements. General arrangement drawing of the base grouted pile is shown in the Fig. 3.

Each conduit has openings in the bottom horizontal portions and is covered by rubber sleeves to prevent the closing of the orifices during installation.

Grouting was done in stages; first stage was of permeation grouting which is a process of injecting cement-based grouts into a soil to improve the strength and reduce the permeability of the soil underneath the pile tip by introducing grout. This is followed by grouitng in three to four stages through each conduit separately.



Fig.3. General Arrangement drawing of base grouted pile

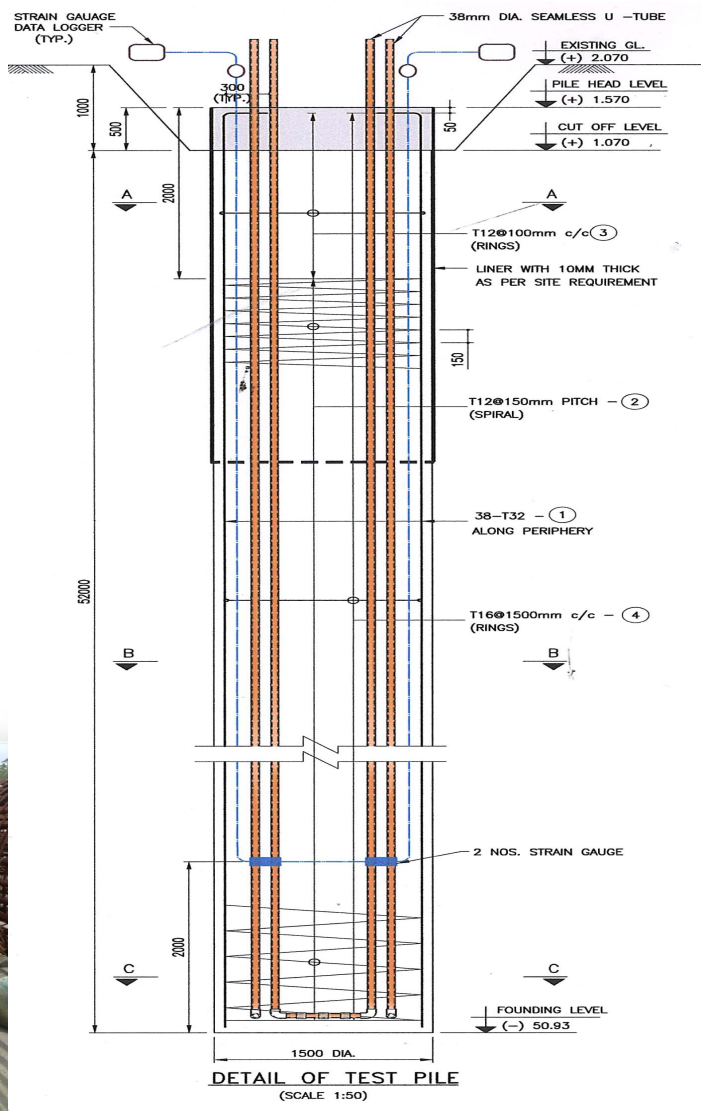


Fig.4. Arrangement of Grout pipes with reinforcement cage

6. COMPARATIVE STUDY OF BASE GROUTED AND UNGROUTED PILES

Four initial test piles results are analysed to understand the behavior of base grouted piles. Table 3 gives the details of the test piles of TP-1 to TP-04.

Sensitivity: Unclassified

Table 3. Details of the test piles

S. No	Test Pile Id	Location	Length (m)	Dia. (m)	Remarks
1	TP-01	Near to P-65	40	1.5	Un-grouted
2	TP-02	Near to P-65 & P -66	52		Un-grouted
3	TP-03	Near to P-63	45		Grouted
4	TP-04	Near to P-67	52		Grouted

The load vs settlement curves of the four tests are given in the Fig. 5.

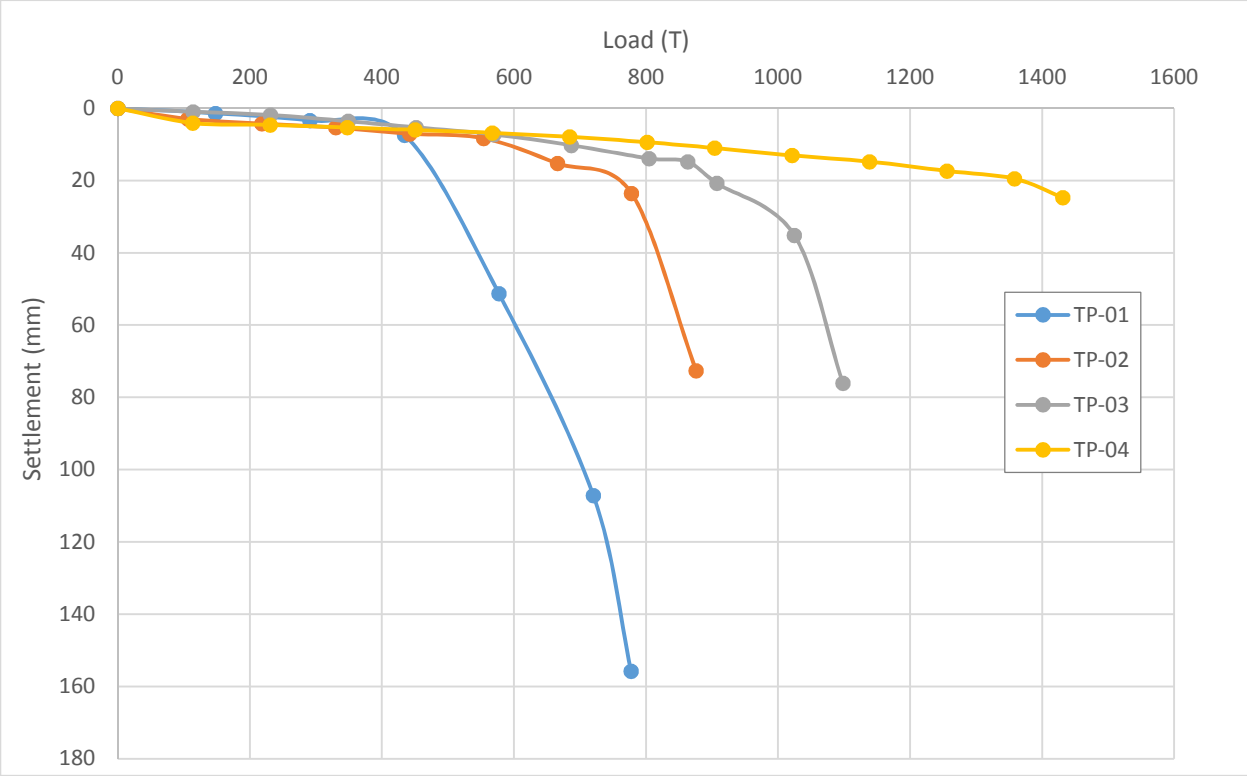


Fig. 5. Load vs settlement of TP-01 and TP-03

To study the improvement in the load carrying capacity of base grouted piles, the behavior of test piles TP-01 and TP-03 are compared as the length of piles are almost of same length. A better comparative study is made by analyzing the load vs settlement behavior of TP-02 and TP-04.

6.1 TP-01 and TP-03

The safe vertical load carrying capacity of the pile is calculate as per the IS: 2911 (Part IV) 2013. As per the code, safe vertical load carrying capacity of the pile is minimum of 2/3 of load at which total displacement is 18 mm or 2% pile diameter whichever is less, and 50% of final load at which the total displacement is equal to 10% pile diameter. The Fig. 6 gives the load vs settlement curves of TP-01 and

Sensitivity: Unclassified

TP-03. Table 4 gives the load at 18 mm total settlement and the load at total settlement of 10 % pile diameter.

The safe vertical load carrying capacity of TP-01 and TP-03 are calculated as 312 T and 593 T respectively. Therefore, the improvement ratio of safe vertical load carrying capacity of base-grouted pile TP-03 to that of un-grouted pile TP-01 is found to be 1.90. The calculated improvement ratio may be overestimated as the length of base grouted is more than the un-grouted pile.

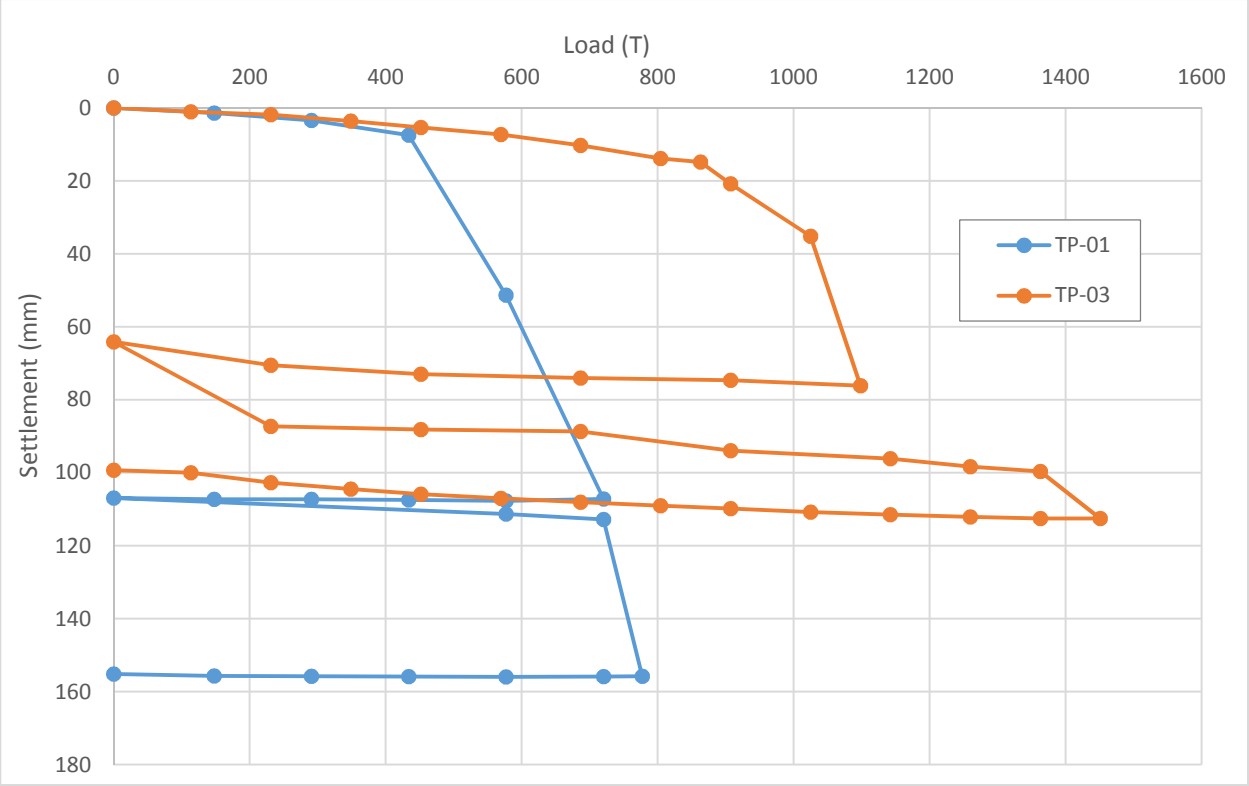


Fig.6. Load vs settlement of TP-01 and TP-03

Table.4. Loads at settlement of 18 mm and 10% pile diameter for TP-01 and TP-03

Test Pile ID	Load at 18 mm total settlement (T)	Load at total settlement 10% of pile diameter (T)
TP-01	468	770
TP-03	890	-

6.2 TP-02 and TP-04

The Fig.7 gives the load vs settlement curves of TP-02 and TP-04.Table 5 gives the load at 18 mm total settlement and the load at total settlement of 10 % pile diameter. The safe vertical load carrying capacity of TP-02 and TP-04 are calculated as 480 T and 890 T respectively. Therefore, the improvement ratio of

Sensitivity: Unclassified

safe vertical load carrying capacity of base-grouted pile TP-04 to that of un-grouted pile TP-02 is found to be 1.438. Unlike the comparative study of TP-01 and TP-03, TP-02 and TP-04 are of same lengths. Hence, improvement ratio of 1.438 gives a more accurate and reliable value.

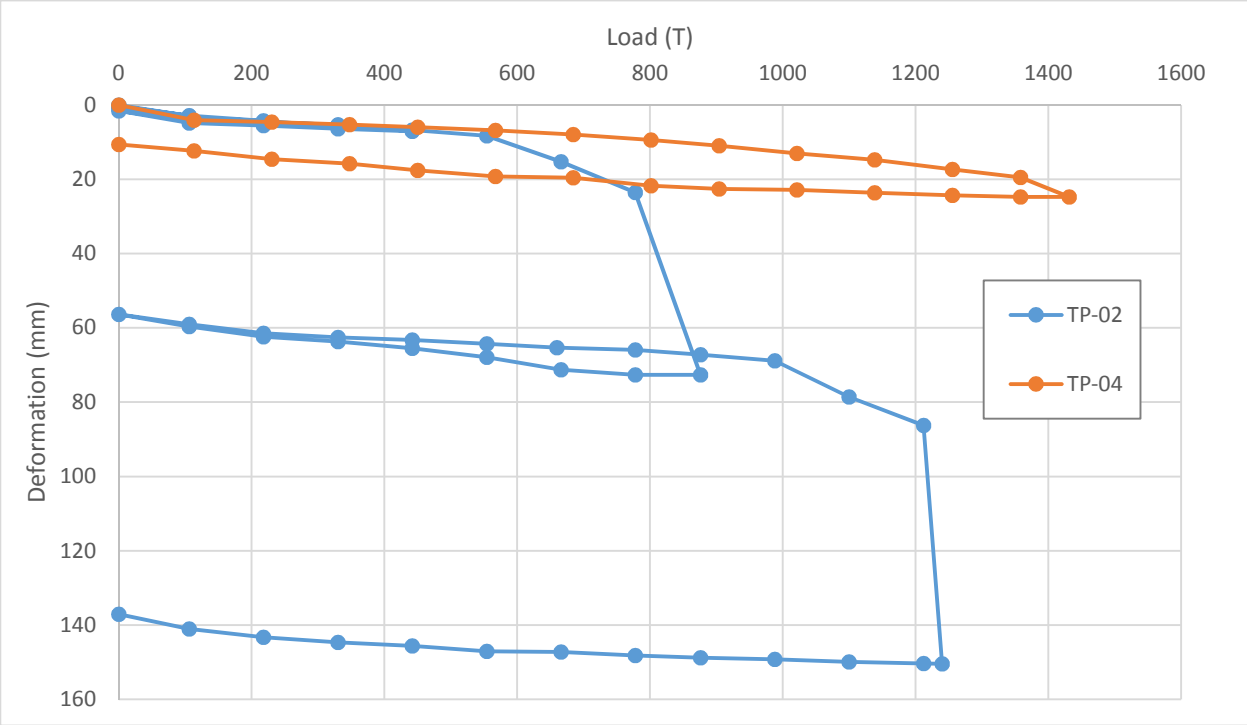


Fig.7. Load vs settlement of TP-02 and TP-04

Table.5. Loads at settlement of 18 mm and 10% pile diameter for TP-02 and TP-04

Test Pile ID	Load at 18 mm total settlement (T)	Load at total settlement 10% of pile diameter (T)
TP-02	720	1230
TP-04	1335	-

6.2.1 Shaft friction and end bearing

The shaft friction and the end bearing components of the ungrounded pile TP-02 was determined from the load v/s settlement curves obtained from the various cycles of loading. The graphical method described in the IS: 2911(Part 4): 2013 was adopted to calculate shaft friction and end bearing components. Fig. 8a gives the skin friction and end bearing components of ungrouted test pile TP-02.

The strain gauges were installed at the bottom of the base grouted test pile TP-04. The load measured by strain gauges give the end bearing components and skin friction component is calculated by deducting the

Sensitivity: Unclassified

measured end bearing from the total load which is applied at the pile top. Fig 8b gives the skin friction and end bearing components of base grouted test pile TP-04.

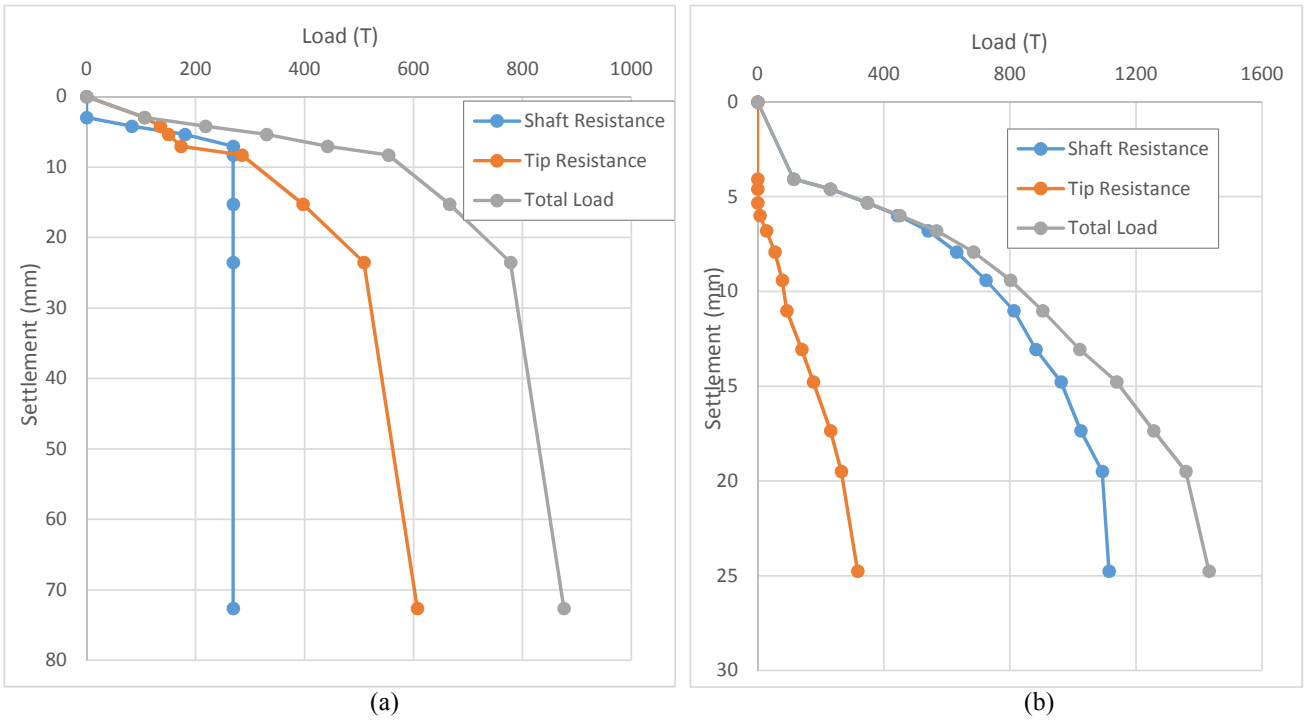


Fig.8. Shaft friction, tip resistance and total load at the pile top of (a) ungrouted and (b) base-grouted pile

7. CONCLUSION

The results obtained from pile load tests on ungrouted and base-grouted piles are studied and load v/s settlement behavior of base-grouted piles are compared with that of ungrouted piles and the comparison has proved that base-grouting technique is most effective way and which represented as an alternate for long pile / additional pile requirement in the project.

Consequently based on the initial load tests conducted in the vicinity of P-65 location, it was concluded to apply base-grouting technique to all working piles throughout the project, i.e., approach viaduct and main bridge pile foundation.

However base-grouting technique in the test pile for the initial pile load test was applied by experimental process, but considering the uncertainty of the long term Behaviour of the grout, strict quality control monitoring was employed in the project to ensure that the grout applied for the working piles has durability through the service life of the bridge structure.

Sensitivity: Unclassified

To verify the performance of the working piles, routine load test was conducted by static and dynamic method and the test results were observed that the vertical load carrying capacity of the piles has been increased to 1.4 times by base grouting.

8. REFERNCES

AASHTO (2012), *AASHTO LRFD Bridge Design Specifications, Customary U.S. Units*, 6th Edition, with 2013 Interim Revisions, Publication LRFDUS-6, American Association of State Highway and Transportation Officials, Washington, DC, 1938 pp.

API Recommended Practice 13B-1 (2009), "Recommended Practice for Field Testing Water-based Drilling Fluids," American Petroleum Institute, Section 1, Fourth Edition, 91 pp.

ASTM Standard C150 (2012), "Standard Specification for Portland Cement," ASTM International, West Conshohocken, PA, DOI: 10.1520/C0150_C0150M-12. <www.astm.org>

ASTM Standard C204 (2011), "Standard Test Methods for Fineness of Hydraulic Cement by Air-Permeability Apparatus," ASTM International, West Conshohocken, PA, DOI: 10.1520/C0204-11. <www.astm.org>

ASTM Standard D1143 (2013), "Standard Test Methods for Deep Foundations Under Static Axial Compressive Load," ASTM International, West Conshohocken, PA, DOI: 10.1520/D1143_D1143M. <www.astm.org>

ASTM Standard D4380 (2012), "Standard Test Method for Density of Bentonitic Slurries," ASTM International, West Conshohocken, PA, DOI: 10.1520/D4380-12. <www.astm.org>

ASTM Standard D6910 (2009), "Standard Test Method for Marsh Funnel Viscosity of Clay Construction Slurries," ASTM International, West Conshohocken, PA, DOI: 10.1520/D6910_D6910M-09. <www.astm.org>

ASTM Standard C109 (2013), "Standard Test Method for Compressive Strength of Hydraulic Cement Mortars (Using 2-in. or [50-mm] Cube Specimens)," ASTM International, West Conshohocken, PA, DOI: 10.1520/C0109_C0109M. <www.astm.org>

ASTM Standard C476 (2010), "Standard Specification for Grout for Masonry," ASTM International, West Conshohocken, PA, DOI: 10.1520/C0476-10. <www.astm.org>

Sensitivity: Unclassified

BEHAVIOR OF SINGLE PILE AND PILE GROUPS SUBJECTED TO ABRUPT COLLAPSE OF A RETAINING WALL

Kranthikumar A., Research Scholar, IIT Roorkee, Roorkee, Uttarakhand, India, +91-9440664767, kranthikumar0143@gmail.com
Ravi S. Jakka, Associate Professor, IIT Roorkee, Roorkee, Uttarakhand, India, +91-9458947076, rsjakka@gmail.com
Rajesh P. Shukla, Research Scholar, IIT Roorkee, Roorkee, Uttarakhand, India, +91-9410987732, rpshukla.2013@iitkalumi.org

ABSTRACT:

Retaining walls are often used to support the unstable backfill soil. In certain circumstances, structures like high rise buildings, bridge and bridge abutments, transmission towers and offshore platforms are constructed adjacent to retaining walls. Pile foundations are generally used to support these type of structures. Retaining walls near these foundations may suddenly fails sometimes, and they can affect the stability and safety of nearby structures and foundations. In this study, experiments are done on small scale model piles to determine the settlement of pile foundations exposed to the movement of soil induced from the abrupt collapse of a retaining wall. Various factors affecting the behavior of single piles and pile groups are considered. Embedment ratio and critical height of collapsed retaining structure are the two most important factors affecting the settlement of piles. The settlement of piles increases with the increase in height of retaining wall collapsed. In piles of embedment ratio 10, the settlement increases with increase in the spacing, and increase in number of piles, while piles of embedment ratio 20 show behavior opposite to the piles of embedment ratio 10. In general, settlement of piles decreases about 20 to 50 % with the increase in embedment ratio of piles group. Piles group with small embedment ratio affected more severely due to abrupt collapse of retaining wall than the piles of large embedment ratio. The increase in the settlement with the increase in the height of collapsed retaining wall is relatively more noticeable as compared to increase in lateral displacement.

Keywords: Retaining Wall, Soil Displacement, Pile Groups, Experimental Testing

INTRODUCTION

Pile foundation is a deep foundation, and commonly used in cases of large structural loading, unavailability of good soil at shallow depth and under various other adverse conditions. Piles are subjected to variety of loadings, such as vertical, lateral and combined loading. On the basis of mechanism of load transferring, laterally loaded piles are considered into two categories; passive and active piles (De Beer and Wallays, 1972). Piles transferring the loads to the soil are active piles, and piles sustaining the loads coming from the soil are passive piles. The loading on passive piles is induced from soil movement induced due to underground construction, mining, landslides, tunnelling, liquefaction, embankment loading and various other construction activities (Ong, 2004). In metropolitan cities, new structure frequently constructed near to existing one, and a large excavation is required for carrying out new construction. Lateral loads generated by the soil movement can induce additional deflections, settlement and bending moment in piles, which may further reduce the structural integrity of the piles (Hannink and Van Tol, 1988). For the construction of new buildings and other structures, excavations near existing structures is increased significantly in more urbanized areas. These exccavations made significant effect on the foundaations of these existing buildings (Lin et al., 2016; Liyanapathirana and Nishanthan, 2016; Zheng et al., 2012). To minimize the

© 2018 Deep Foundations Institute

excavationinduced impact on the environment, protective measures must be taken to control wall deformations and related soil movements. A number of field studies are reported in the literature, where stability of pile foundations was degraded due to excavation of soil (Finno et al., 1991; Poulos, 1997; Kok et al., 2009). Apart from these field studies, a good number of theoretical and experimental studies were also carried out to determine the piles behaviour subjected to the soil movement introduced by excavation and construction activities (Leung et al., 2000; Goh et al., 2003; Leung et al., 2003; Leung et al., 2006a; 2006b; Ong et al., 2006; 2009). A detailed review of work on passive piles is provided by Kok et al. (2009). These studies determined the pile response in term of lateral displacement and induced bending moment. Though, an excavation can induce both the lateral displacement and settlement in the pile foundation, only a few studies considered the settlement of piles (Shukla and Patra, 2015; Korff et al., 2016). Shukla and Patra (2015) measured the settlement of axially loaded pile groups, and found that the behaviour of piles is depending significantly on the embedment ratio of pile groups. The results were presented in the respective units, consequently the results cannot be used directly. Numerous protective measures have already been extensively investigated; however, despite the frequent use of pile rows in practice, little is known about the use of a pile row as a measure to protect the environment and the structures in close proximity to an excavation. Literature review stipulates that the only a few studies determined the settlement of piles group due to soil movement, and most of studies had considered only limited parameters. Furthermore, previous studies considered the soil movement supported with stable retaining wall. However, it is also possible that the retaining can fail itself which was constructed to support the piles foundation against various activities inducing the soil movement. This condition can be easily arise in hilly region, mining regions and metropolitan cities where, the retaining wall may fail itself due to failure of slopes, large volume excavation, and due to other construction activities. Settlement of piles and pile groups induced due to abrupt collapse of retaining wall is studied. A detailed testing is performed by varying critical parameters affecting the settlement behavior of pile and pile groups near the vicinity of retaining wall.

EXPERIMENTAL SETUP

All model tests were conducted in a 1-g environment. Initially, the load carrying capacity of piles and pile groups were evaluated by compression testing. Based on the compression test results, safe load was determined for single piles and pile groups. Rain fall method was used to pour the sand into the tank at a desirable density. The model piles were made of hollow circular aluminum tubes of 1 mm thickness and 30 mm internal diameter is used for testing. The diameter of piles was maintained constant throughout the testing. Piles of length of 320 mm and 640 mm were used in the testing to consider the effect of embedment depth of piles on the settlement of piles group. Piles were marked to the two third of embedment ratio, and piles group was assembled to the pile cap at the outside of tank. Marks were made on the tank walls also to identify the tip level of piles during the sand filling. Sand was filled just below the marked level on tank walls, and piles were suspended at the prerequisite level into the tank using the two flat steel plates and number of C-clamps. This step requires utmost care so as to retain the pile cap perfectly horizontal. The level of pile cap was tested using a sprit leveler to avoid the tilting. Perfectly horizontal pile cap helps to apply the loads vertically on pile before collapse of retaining wall. Sand filling was again started and continued till it filled the tank up to the marks on the piles. As piles are adequately embedded in the sand, both flat plate were detached cautiously from the pile cap by releasing the C clamps. To make sure that pile cap remains perfectly horizontal during the filling process, level of pile cap was checked intermittently and sand filling was again continued up to just below the pile cap. Four dial gauges were attached at the pre-determined location using steel columns and two steel plates. A plate was attached to the pile cap of row piles in order to support the loading. Level of pile cap was checked once again before the application of loading. Safe load determined from the compression test was applied directly on piles cap. To verify that the loading stage has not changed the density of sand, density of sand was checked before and after loading stage. The density of sand was checked using a dynamic penetrometer. Before heading to simulate the collapse of retaining wall, the whole setup was maintained idle for a sufficient time to allow the settlement

of piles induced due to application of loading on pile. The parts of wooden shutter were released to simulate the abrupt collapse of retaining structure. Dial gauge readings were recorded after the collapse of retaining structure. Displaced soil profile was also recorded by means of vertical lines drawn on the tank wall. These vertical lines were marked to measure the distance from the wooden shutter. Fig. 1 shows the basic outlet of model testing setup and pile group configurations used in the testing. A few tests are repeated to check the validity of the results and then detailed testing is carried out by varying different parameters. Table 1 shows the properties of the surrounding soil used in the testing.

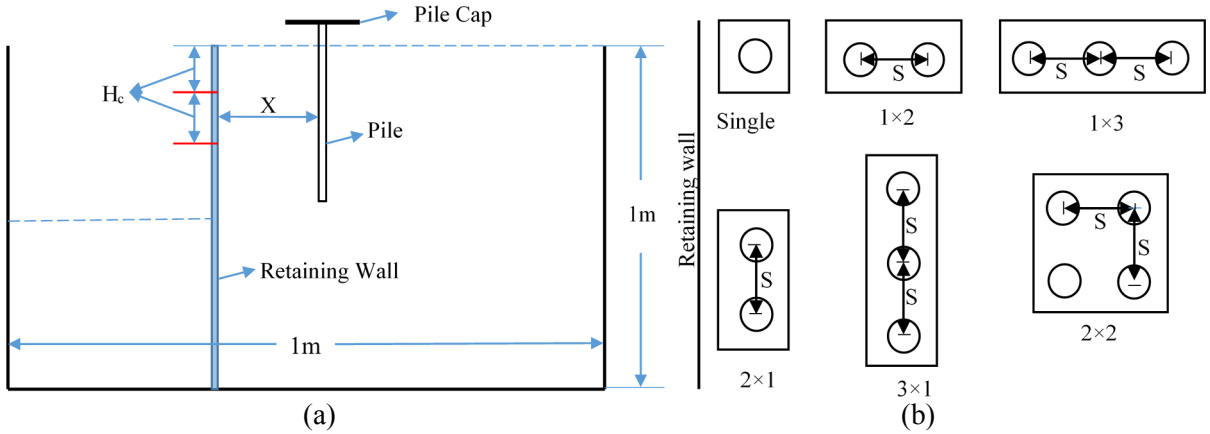


Fig. 1. (a) Basic model used in the testing; (b) Pile configurations used in testing

Table 1. Material properties of the pile and surrounding soil

Properties of Sand	Value	Units
Maximum density	16.80	kN/m^3
Minimum density	14.40	kN/m^3
Unit weight	15.61	kN/m^3
Relative density of sand	54.30	%
Angle of internal friction	34.00	^{0}
Uniformity coefficient	1.70	-
Coefficient of curvature	0.97	-

RESULTS AND DISCUSSIONS

Lateral displacement of piles is represented in dimensionless form as a ratio of pile displacement to the height of retaining structure failed. Similarly, the distance between piles and retaining structure was also expressed in terms of height of the retaining structure. Figure 2 shows the instrumental setup for an unloaded single pile before and after collapse of retaining structure. Testing is carried out by varying different parameters which effect the settlement behavior of piles. Parameters considered in the testing are mentioned in Table 2. The vertical and lateral displacement response of pile foundation subjected to collapse of retaining wall was determined and presented in dimensionless form. The effect of various parameters on settlement response of pile is discussed below:

Effect of distance between retaining wall and pile group:
Figure 3 shows that the settlement of pile group decreases nonlinearly with increase in distance of piles from the retaining wall. Earlier studies also found that the settlement and lateral displacement decreases with increase in the distance of piles from excavation surface and retaining wall. The confining pressure and skin friction increases with increase in the distance of piles from retaining wall, consequently it decreases the settlement of piles. Velocity of soil movement near to the collapsed retaining wall is high and

it impart higher force and moment on the piles, and consequently it causes higher settlement in case of piles group resting near to the retaining wall. From Figures 3 (a) and (b), it is perceived that in piles of small embedment ratio, the increase in settlement is relatively higher when distance between piles and retaining wall is decreasing.

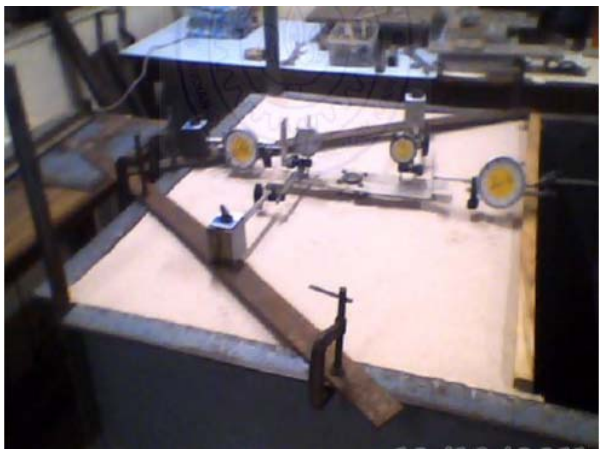
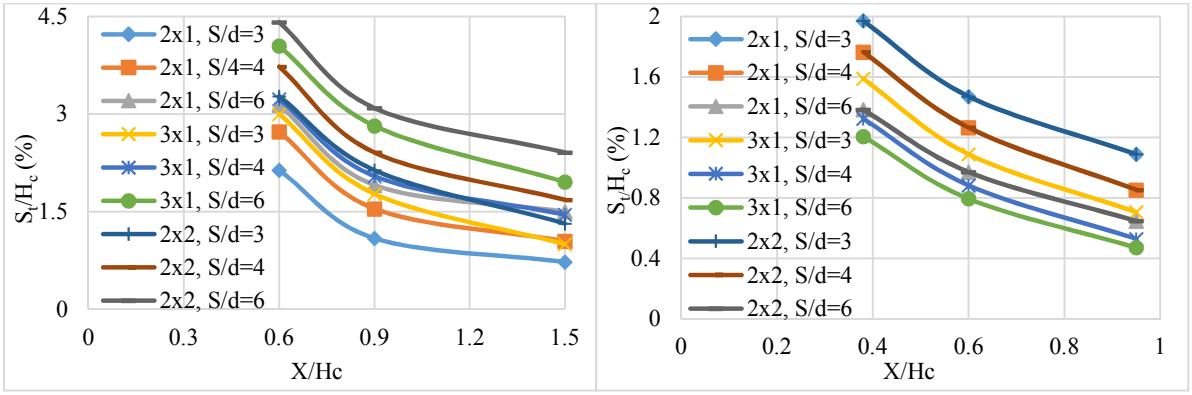


Fig. 2. Instrumented setup for a pile before collapse of retaining wall

Table 2. Nominal height of retaining wall used in the analysis

Length of pile, L (cm)	Number of wooden planks to be loosen	Height of retaining wall, H_c (cm)	Nominal height of retaining wall (H_c/L)
32	0	0	0
	1	10	0.312
	2	22	0.687
64	0	0	0
	1	10	0.156
	2	22	0.344
	3	34	0.532



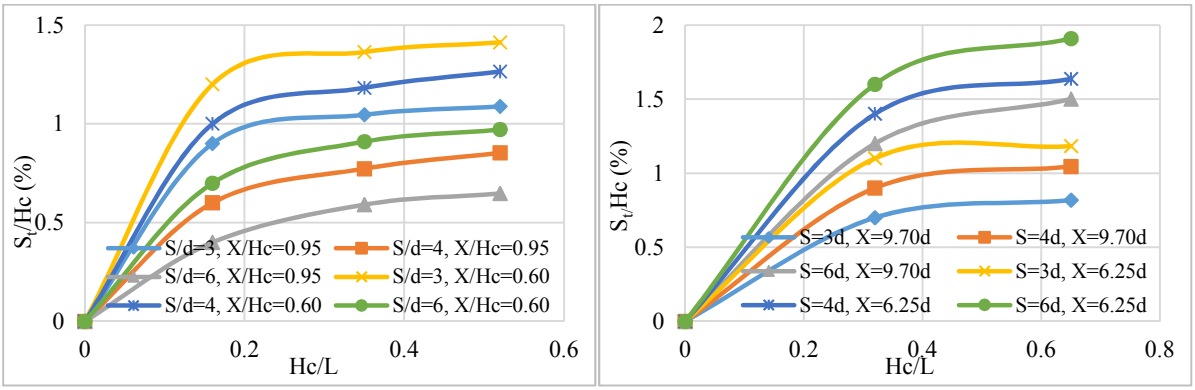
(a) (b)

Fig. 3. Effect of distance between retaining wall and pile groups; (a) L/d=10; (b) L/d=20

Effect of critical height of retaining wall:

Effect of critical height of retaining wall is shown in Figure 4. Induced force due to abrupt collapse of retaining wall increases with increase in the height of retaining structure collapsed, and it leads to increase in the settlement of piles. The increase in the depth of soil movement increases the plastic flow of soil over

the piles. The plastic flow over the soil also increases with increase in the height of retaining wall and it further increases the magnitude of piles settlement. It can be also observed that the piles group with small embedment ratio (L/d=10) more severely affected from soil movement than longer piles (L/d=20).
For a small height of collapsed retaining wall, the developed initial strains are within elastic limit. Increasing the height of retaining wall collapsed causes to deformation of soil mass plastically with a large rate of stains. At this stage, the pressure reduces to smaller value, and thereby the rate of increase in the settlement is also reduced. It can be easily seen from the Fig. 4 this stage is reached at the nominal height (H_c/L) of 0.16 and 0.32, respectively for piles of embedment ratio 20 and 10 respectively.



(a) (b)

Fig. 4. Effect of critical height of retaining wall; (a) 2×1 pile group, L/d=20; (b) 2×1, L/d=10

The effect of increase in the height of collapsed retaining wall on piles settlement becomes nominal after a particular height in case of piles group of large embedment ratio. However, in piles group of small embedment depth, the piles generally show the continuous increase in the settlement. The magnitude of settlement is also relatively large in piles of embedment ratio of 10 as compared to piles of embedment ratio 20. The end bearing of piles group of longer length affected relatively less as compared to piles of small embedment depth. Even the magnitude of shaft friction leftover after collapse of wall is more in case of longer piles than the shorter piles. Because of these facts the piles of small embedment affected more severely due to soil movement induced from collapse of retaining wall than longer piles group.

CONCLUSIONS

A small scale laboratory testing is performed to determine the critical parameters affecting the behavior of piles under sudden collapse of retaining wall near pile foundations. It is found that height of collapse of retaining wall and embedment depth of pile are two critical parameters those mainly affect the settlement of piles and pile group. Vertical and lateral displacements of piles increased with increasing the height of collapsed retaining wall. The settlement behavior of piles of embedment ratio 10 is dissimilar to the piles group of embedment ratio of 20. In case of longer piles, the settlement is decreased with increase in the spacing and piles number. On the other hand, the settlement of pile groups of smaller length increases with increase in these parameters.
Settlement of piles decreases with increase in the distance of piles from excavation surface and retaining wall for a constant embedded depth ratio. For a L/D = 10, settlement decreased from 50 to 33 % with increase in effect of distance between pile and retaining wall (X/H_c) from 0.6 to 1.5, respectively. Settlement decreases 50 % with increase in embedded depth of pile in pile group.
The effect of pile spacing on the piles group settlement decreases with increasing in the piles number in a piles group. The settlement is relatively large for the small distance between retaining wall and piles and it reducing with increase in this distance. In a piles group, the influence of distance between retaining wall and piles is reduced with increasing piles number.

REFERENCES

1. De Beer, E.E., and Wallays, M., 1972. Forces induced in piles by unsymmetrical surcharges on the soil around the pile. In Proceedings of 5th European Conference on Soil Mechanics and Foundation Engineering, 1, Madrid.
2. Finno, R.J., Lawrence, S.A., Allawh, N.F., and Harahap, I.S., 1991. Analysis of performance of pile groups adjacent to deep excavation. Journal of Geotechnical Engineering, 117(6): 934–955.
3. Goh, A.T.C., Wong, K.S., Teh, C.I., and Wen, D., 2003. Pile response adjacent to braced excavation. Journal of Geotechnical and Geoenvironmental Engineering, 129(4): 383–386.
4. Hannink, G., and Van Tol, A.F., 1988. Large horizontal displacements of houses in Rotterdam. In Proceedings 2nd International Conference on Case Histories in Geotechnical Engineering, St. Louis, Missouri, 1409–1415.
5. Kok, S.T., Bujang, B.K.H., Jamoloddin, N., Saleh, M.J., and Gue, S.S., 2009. A case study of passive piles failure in open excavation, DFI Journal, 3(2): 50–57.
6. Korff, M., Mair, R.J., and Van Tol, F.A.F., 2016. Pile-soil interaction and settlement effects induced by deep excavations. Journal of Geotechnical and Geoenvironmental Engineering, 142(8): 04016034.
7. Leung, C.F., Chow, Y.K., and Shen, R.F., 2000. Behavior of pile subject to excavation induced soil movement. Journal of Geotechnical and Geoenvironmental Engineering, 126(11): 947–954.
8. Leung, C.F., Lim, J.K., Shen, R.F., and Chow, Y.K., 2003. Behaviour of pile groups subject to excavation induced soil movement. Journal of Geotechnical and Geoenvironmental Engineering, 129(1), 58–65.
9. Leung, C.F., Ong, D.E., and Chow, Y.K., 2006a. Pile behaviour due to excavation induced soil movement in clay. I: Stable Wall. Journal of Geotechnical and Geoenvironmental Engineering, 132(1): 36–44.
10. Leung, C.F., Ong, D.E., and Chow, Y.K., 2006b. Pile behaviour due to excavation induced soil movement in clay. II: Collapsed Wall. Journal of Geotechnical and Geoenvironmental Engineering, 132(1): 45–53.
11. Lin, D.G., Liu, W.T., and Chou, J.C., 2016. Mechanical behaviors of piled-raft foundation and diaphragm wall in deep excavation of Tapei Metropolitan. Journal of Marine Science and Technology, 24(5): 980–991.
12. Liyanapathirana, D.S., and Nishanthan, R., 2016. Influence of deep excavation induced ground movements on adjacent piles. Tunnelling Underground Space Technology, 52: 168–181.
13. Ong D.E.L., 2004. Pile behaviour subject to excavation-induced soil movement in clay. Ph.D thesis, Department of Civil Engineering, NTU, Singapore.
14. Ong, D.E.L., Leung, C.F., and Chow, Y.K., 2006. Pile behavior due to excavation induced soil movement in clay. I: Stable wall. Journal of Geotechnical and Geoenvironmental Engineering, 132(1): 36–44.
15. Ong, D.E.L., Leung, C.F., and Chow, Y.K., 2009. Behavior of pile groups subject to excavation-induced soil movement in very soft clay. Journal of Geotechnical and Geoenvironmental Engineering, 135(10): 1462–1474.
16. Poulos, H.G., and Chen, L.T., 1997. Pile response due to excavation induced lateral soil movement. Journal of Geotechnical and Geoenvironmental Engineering, 123(2): 94–99.
17. Shukla, R.P., and Patra, N.R., 2015. Settlement of pile groups exposed to excavation induced soil movement. Electronic Journal of Geotechnical Engineering, 20(10); 4293–4304.
18. Zheng, G., Peng, S.Y., Ng, C.W.W., and Diao, Y., 2012. Excavation effects on pile behaviour and capacity. Canadian Geotechnical Journal, 49(12): 1347–1356.

BIDIRECTIONAL STATIC AXIAL PILE LOAD TEST: GARCA RIVER BRIDGE – BRAZIL

Paul George Alexander C., GEO - Ground Engineering Operations India Pvt Limited, paul.alexander@geosoil.com

ABSTRACT:

The Bi- Directional Load Test provides us with the Unique ability to determine both the skin friction and the end bearing capacity of a bored pile at a single test simultaneously. To understand this methodology and the advantages of this pile load test a case study was conducted on an of shore pile across the River Garcia in Brazil. Where the pile was 1.4 m in Día, 20m in depth and had a working load of 8000kN. The methodology included the installation of load cells in the reinforcement at the fabrication stage which was completed in one single day and the test which was conducted at the end of 28 days. The testing was done to the twice of the piles working loaded which was exactly 16632kN. The results gathered at both the skin friction and end bearing was recorded and found satisfactory. The installation of the load cells and the entire testing process was conducted in less than 48 hrs. This test's methodology is different to the conventional load test as there is no limit to the load that can be applied to the pile. This paper submitted with the intention that the paper will help us develop a better understanding of the methodology of the Bi- Directional load test, advantages and limitations, feasibility, interpretation of the results in hope that this will be a valuable addition to our esteemed field of deep foundations.

Keywords:

Bi-direction. Load test, load cells, bored pile
:

INTRODUCTION:

This paper includes the case study done on the Bi-directional load test done on a working pile in off-shore conditions to observe the advantages and limitations of the load test type that has been accepted in various parts of the world and to study the impact and changes that this type of load test could provide to the dynamic and divergent Indian market.

The Bidirectional static axial plate load test consists of inserting the dynamic expansive cells in the reinforcement of the pile and concreting the pile and after 28days of concreting. During the testing the load cells are expanded within the pile and measuring the displacement achieved by the pile. Unlike other load tests in this test both the skin friction and the end bearing capacity can be recorded simultaneously hence the name Bi-directional.

One test was chosen to study the Bi-directional load test. The piling work on the river bridge of Garca in Brazil consisted the challenging situation in which executing a conventional load test will be more difficult and the team decided to conduct the Bi-directional load test due to difficult conditions.

Pile Details:

The pile was done in offshore conditions in running river water the pile was of depth 20 m and with a dia of 1.4 m. The required working load of the pile was set at 8000 kN so the load test was determined to be done at 16000 kN which is double that of the design working load. The soil strata was mainly consisted of fractured rock and weathered rock.

© 2018 Deep Foundations Institute

The Pile was done with hydraulic rig and the pile was in middle of the river, the excavation of the pile started and completed without any incidences as the Polymer fluid and the Polymer engineer was available at the site to monitor the stability. During the process of the excavation the pile reinforcement cage was introduced with dynamic expansive cell at the depth of 7m from the bottom by sectioning the reinforcement. Once the excavation is completed the pile toe was thoroughly cleaned with the cleaning agent provided by the polymer supplier was used and the proper cleaning of the toe was ensured by calculating the density gradient of the fluid. A clean pile toe is mandatory to measure the end bearing load of the pile in order to ensure the proper reaction for the load cells when it is expanded.

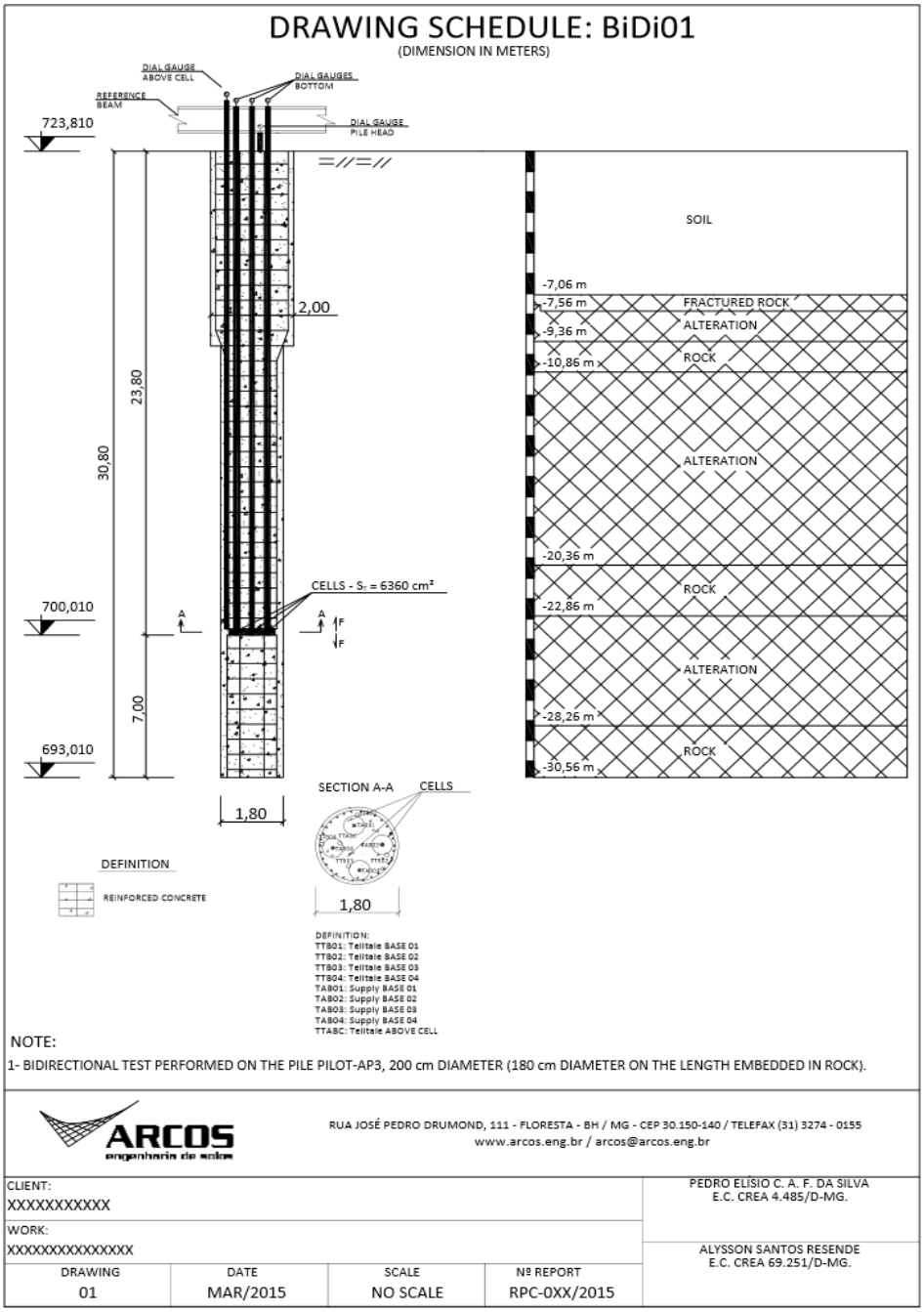


Fig 1: Soil strata of the Pile

FIRST PHASE:

Defining cell assembly and equilibrium position:

The reinforcement drawing and the applicable soil strata details were delivered by the clients team in advance in order to determine the equilibrium position of the pile so that the load cells position can be fixed. The working load of the pile and the test load of the pile was provided in advance by the client and the ARCOS designer determined the equilibrium position at 7m from the bottom of the pile.

Once the equilibrium position of the pile was determined and the test load was computed the number of load cells was determined to be three.

The load cells were fabricated at Belo Horizonte in accordance with the project and then was shipped to site with all the other auxiliary materials that are required to conduct the test.

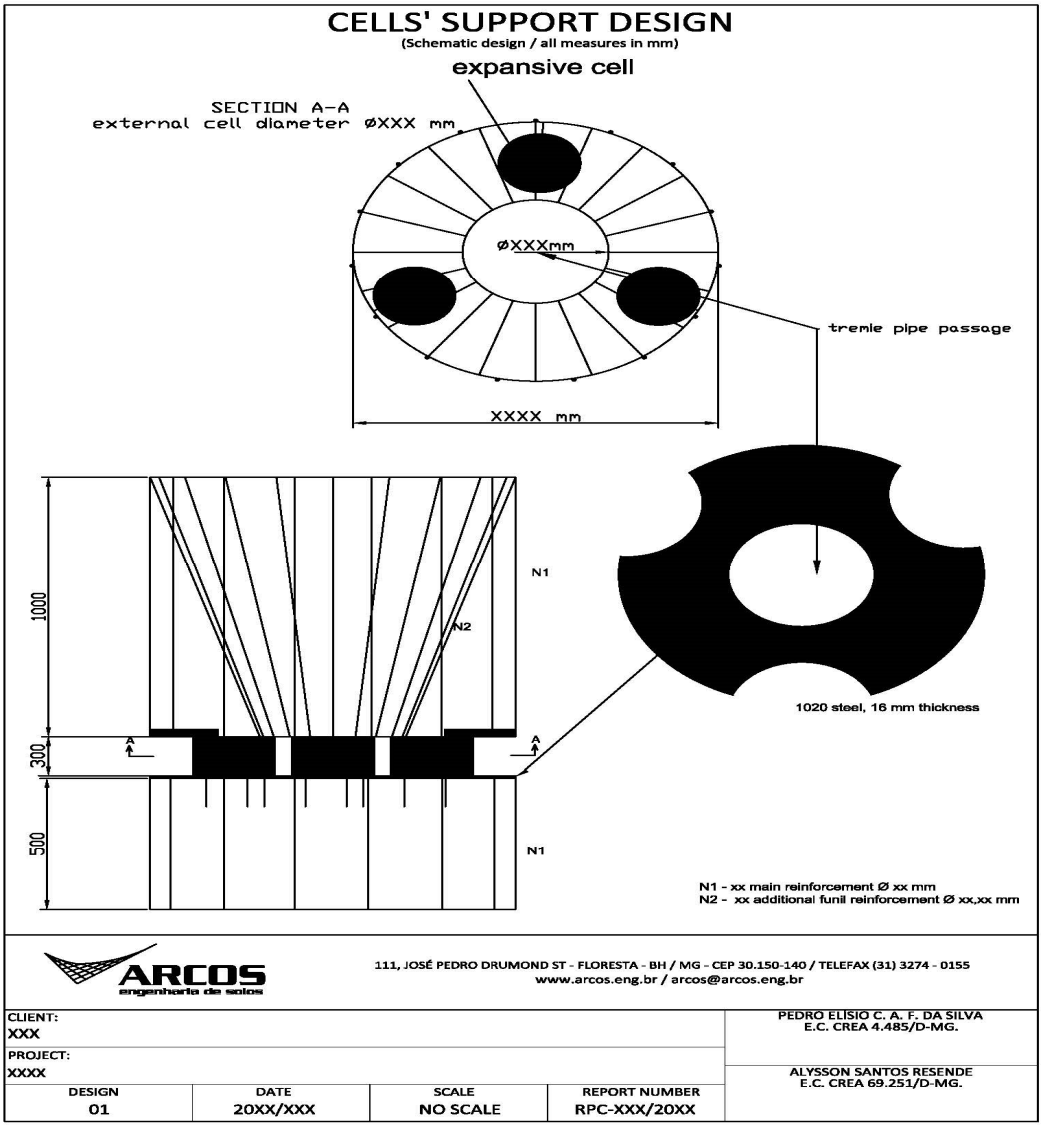


Fig 2: Cell Assembly with the support plate

SECOND PHASE:

Fixing of the cell assembly:

The steel reinforcement cage shall be sectioned at 7m from the bottom of the pile at the location of the cell, so the cell assembly could be welded or clipped at this point of the cage. (Alternatively, reinforcement cage shall be prepared in two parts in such a way to enable fixing of cell assembly). The bearing plates are designed specifically and individually for each project.. The cells are accurately positioned on the bearing plate and welded into place. Temporarily lifting arrangements are often used to facilitate handling of the plates and cells.



Fig 3: Load Cell Assembly with tremie Cone

Fixing of Ancillary Materials:

1- An individual pressure supply pipe for each cell is fixed. The cells are connected in parallel with an external manifold that guarantees that the same flow and pressure are applied in the cells.

2- Adequate guide pipe(s) like PVC are connected to cell upper level and extended to the pile top to measure cell upper displacement through telltale rods inserted at time of testing in PVC pipes. PVC pipes are clamped to cage reinforcement.

3- Adequate guide pipes like PVC are connected to each cell lower level and extended to the pile top to measure cell bottom displacement through telltale rods inserted at time of testing in PVC pipes.



Fig 4: Load cells inside the excavation



Fig5 : Fixing of PVC pipe along with load cells.

Lifting of Cage:

1. The lifting of each cage to vertical should be carried out using a lifting beam or several pick points to ensure the cage remains reasonably straight during lifting.

2. A suitable number of spacers should be used to ensure that the reinforcing cage remains central to the bore as the cage is lowered.

3. The reinforcing cage or a support assembly will have extended beyond the concrete cut off level to above ground level, where appropriate, to support telltales, instrumentation wiring, and hydraulic supply lines above the concrete level for testing purpose.



Fig 6: Lifting of Reinforcement Cage along with the load cells

Precautions:

- Ensure clean bore hole including Pile Toe before concreting. This is Mandatory.
- Maintain concrete's properties with desired slump while tremie concreting;
- Signalize the work area and mark it if necessary for pile to be executed for running the test;
- Keep the work area clean and unobstructed.
- Pile should be executed according to construction methodology approved by Engineer;
- Necessary Pile platform in case of marine piles and work area to be provided to fix the reference beams and placing instrumentation for fixing, running the test.
- Equipment shall be protected against the weather so there is no variation of the test results**.**
-

THIRD PHASE:

Conducting the Load Test:

The load test may be conducted as per the requirement of the site. But the recommended days of waiting is 28 days for the full load test. In this pile the test was done after the 28 days from the day of casting of the pile.

1- Reference beams / frame are set up properly for instrumentation set up.
2- Initially, tell-tales shall be installed in the guide PVC pipes and telltale are connected to dial gauges and mounted on the reference beam to measure displacements at designated points.
3- The tell-tales are extending from the cell top to the ground surface to measure the displacement of the pile above the cell, also tell-tales attached to the bottom cell plate to measure the pile toe movement. The pile head movement shall be measured with a separate gauge to record pile head displacement.
4- Pressure pipes extended to pile top are connected to main pressure line of supply pump.
5- A calibrated, high-pressure gauge will be used to read the pressure on the pump.

6- The cell will be pressurized with hydraulic fluid, typically water and pump by oil. An electric pump is used to pressurize the galvanized pipes connected to cells.
7- The load test commences by applying hydraulic pressure to cell connected pressure pipes using an electrical pump with pressurizing the cells to break the concrete to create fracture zone which separate the two elements of the pile at cell level.
8- It is to be noted that the loads applied by bi directional hydrodynamic expansive cells act in two opposite directions, resisted by upper skin friction above the cell and by the combined end bearing and lower skin friction below the cell assembly.
9- Load Increments**:** The loading was done in equal increments at equal intervals at the rate of 20 kgf. In this test quick loading method was applied and the entire load of 16632 kN was applied in 5 hrs and 20 mins
10- Maintaining Full Load**:** The full test load 16632 kN was maintained and held for 1 hour.as per consultant/Engineer In charge directives.
11- Load Decrements**:** The unloading of the test was done in equal parts of 2000kN at equal intervals of 15mins
12- Maintaining Zero Load: The zero load was maintained for 30 mins
13- The testing is deemed completed once either one of the following situations occur:

a. A predetermined maximum test load has been applied.
b. The Cells approaches its maximum nominal stroke of 150 mm.
c. Ultimate capacity of the pile above or below the cell's location has been reached.

Precautions:

Air Purge: Air purge is carried out to ensure there is no air trapped through the pressure pipe. To ensure this, the supply of water in the pipe shall be injected slowly and repeatedly. The amount of water must be at least equal to the volume of cell and pressure pipe.
Injection of water: At the start of the test, the cell system is saturated by injecting water to the cell-pressure pipe.
Grouting:
When doing the test, it is mandatory to grout of the pile in case of working pile as it is a destructive test. In this test the cement grout was used a total of 115l of cement grout was used to fill all the voids and pipes of the tests.
The grout is a cement slurry with a water/cement radio of 0.50 that is prepared in a mixer after the test.
With the support of an injection pump, one extremity of a 1/2-inch hose is connected to the pump and the other inserted into the iron pipe (1-inch) to grout the space inside the cell and the pipes as well. The hose works as a tremie tube, so the grout is injected under low pressure (0,5 to 2 kgf/cm²) from the bottom to the top expelling all oil and water from the cells and pipes and leaving the grout inside.
The PVC pipes are also connected to the injection pump which injects grout under pressure (0,5 to 2 kgf/cm²) to fill the voids. Being the PVC pipes connected to each other by the fracture zone, the system works as a return line, so the grout is injected in a pipe and goes out in another. If the return line is obstructed, all PVC pipes shall be individually injected until reaches the pressure of 10 kgf/cm^2. That guarantees that all voids are fulfilled.

FOURTH PHASE:

Reporting of the Test Results:

- The test detailed report indicates all information required by the engineer such as project identification and location, test site location, date and type of test, methodology used, pile data, description of measurement instrumentation, test data, tables, various graphs and results.
-

- The following test results along with curves shall be delivered along with detailed report:

1. Cell Top displacement VS Load
2. Cell Bottom displacement VS Load
3. Pile Head displacement VS Load
4. Lateral side shear (skin friction) above cell VS displacement of above cell
5. The equivalent top loaded load VS Settlement curve (similar to static load test)



Fig 7: Graph of Load Applied and Displacement (Loading)

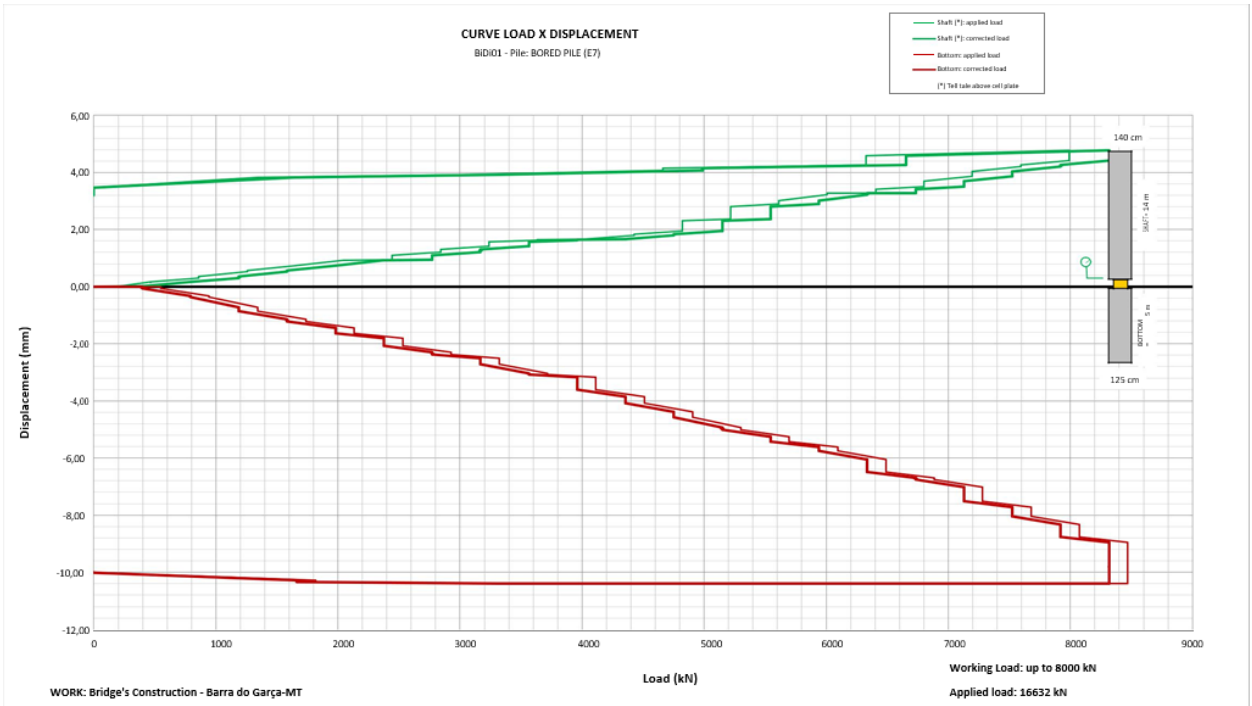


Fig 8: Graph of Curve load with displacement (Unloading)

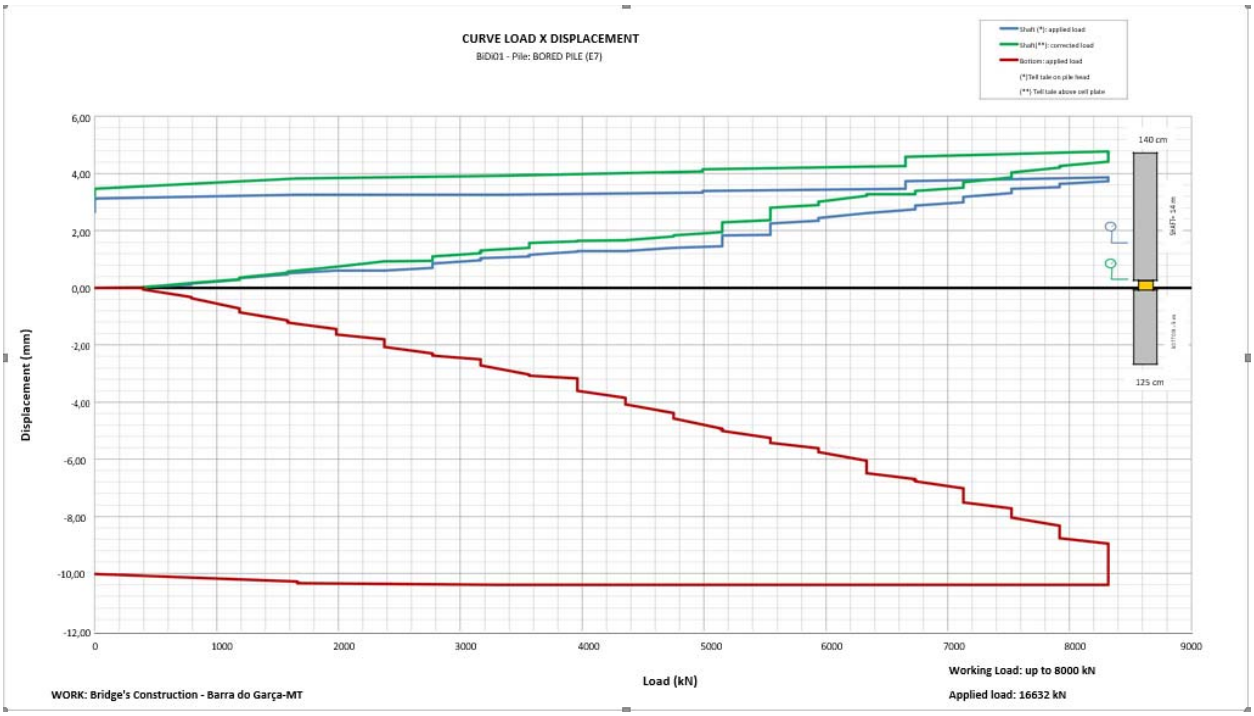


Fig 9: Graph of Load and Displacement (Combined)

. **Conclusions:**

1. The pile qualified the test as it sustained twice the working load and the displacement was within the specifications.
2. The pile required less time for installation of the load test equipments and the ancillary set up.
3. Most of the setup required were done simultaneously along with the pile excavation.
4. Off- shore conditions did not require any major setup.

Advantages:

- The bi directional load test required less equipment and man power to execute the test.
- The load applied did not have any limitations.
- The test was concluded much more quickly.
- The preparations that were required for a load test at an off shore location was minimum and very easy.
- The risk involved in performing the test was minimum.
- The reports were available immediately after completion of the test
-

Limitations:

Eventhough there are no direct disadvantages in this process there are some limitations when engaging the bi-directional load test at a divergent market like India.

1. The Project owner or the Consultant would like to choose a pile for load test at random. In the case of Bi-directional load test that is not possible. About 100 % of the preparations involved are to be done prior to the concreting was done.
2. This test involves sectioning of main bars in the reinforcement cage. That might be a problem with some of the consumers if it was not explained properly.
3. This test needs to be done by the qualified Engineers and designers in the ARCOS only as there are many patents involved and the load test are manufactured by themselves. Unlike the conventional static load test where the contractor can conduct the tests themselves by training their staff in the load test.

ENGINEERING ASPECTS OF JET GROUTING AND ITS APPLICATIONS FOR SEEPAGE CONTROL

Akhila Manne, Sr. Geotechnical Engineer, Keller India, akhila@kellerindia.com
PVSR Prasad, Geotechnical Manager, Keller India, prasad@kellerindia.com
Madan Kumar Annam, Head of Engineering, Keller India, madankumar@kellerindia.com

ABSTRACT

Jet grouting technique is applied for modifying the existing ground or to construct load bearing member or a barrier without prior excavation. The jet grouting process employs hydraulic-induced mixing of cement slurry with the native soil and is commonly used for providing seepage control, limiting subsidence over tunnel excavation sites, and underpinning existing structures threatened by subsidence etc. In specific to seepage control, the structural barriers resulting due to jet grouting in the in-situ soil help increase the imperviousness of the in-situ soil and acts as a barrier to water flow. Achieving the required diameter, strength, permeability etc. of the jet grout barrier depends on jet grouting parameters such as grout pressure, lifting speed, number and diameter of nozzles and grout mix. In addition to the operating parameters, column geometry, depth of treatment, effective quality control plan plays important role in achieving a reliable seepage control barrier. This paper discusses the engineering aspects of jet grouting in specific to address seepage control application of in-situ soil. The technological process, construction parameters and construction method for formation of impervious wall for seepage control are discussed in detail along with case history of one of the multipurpose irrigation project in India.

Keywords: Ground improvement, jet grouting, cement stabilization, seepage control

INTRODUCTION

Grouting techniques have a long history of usage in dam construction and can be applicable to address challenges in seepage remediation. Jet grouting is widely recognized as the most suitable ground improvement technique for its applicability to majority of soil types. The technique enables the arrangement of grout columns in various geometrical configurations, employability for new facilities as well as for existing ones and for wide ranges of soils. Jet grouting application is proven technique for seepage control in dam foundations, foundation retrofitting, subsidence control, contaminant barriers, tunneling and mining operations, offshore construction, etc.

Process of jet grouting (JG) consist of disaggregation of soil and mixing it with a cementing agent or binder. This is achieved by high pressure jets of grout comprising of a water/binder suspension injected through a nozzle, by which the soil around the borehole is eroded. The eroded soil is brought into suspension and these particles are rearranged and mixed with the cement suspension, which subsequently sets and hardens to form a stabilized jet grout column. This paper focuses on the engineering aspects of jet grouting for the creation of cut-off wall for seepage control. Fig. 1 shows application of jet grouting works especially in dam foundations for seepage control.

JET GROUTING TYPES

The design of grout column is based on the soil conditions (Fig. 2) and its application for a specific project. Accordingly, different jetting techniques namely single, double and triple fluid type systems. These are classified based on the number of fluids injected into the subsoil i.e. water & grout or air & grout, water, air & grout. The grouting process is influenced by the soil conditions i.e., grain size distribution, organic content of soil, ground water, geometrical form and quality of the jet grout columns required.

The most recognized systems of jet grouting are the S, D and T jet systems that correspond to single, double, and triple jetting methods respectively (see Fig. 3). The S process is used for small to medium

© 2018 Deep Foundations Institute

sized columns. D jet system employs simultaneous cutting and mixing of the soil using grout suspension combined with air jet. The T jet system performs simultaneous cutting and mixing of soil along with water and air jets.

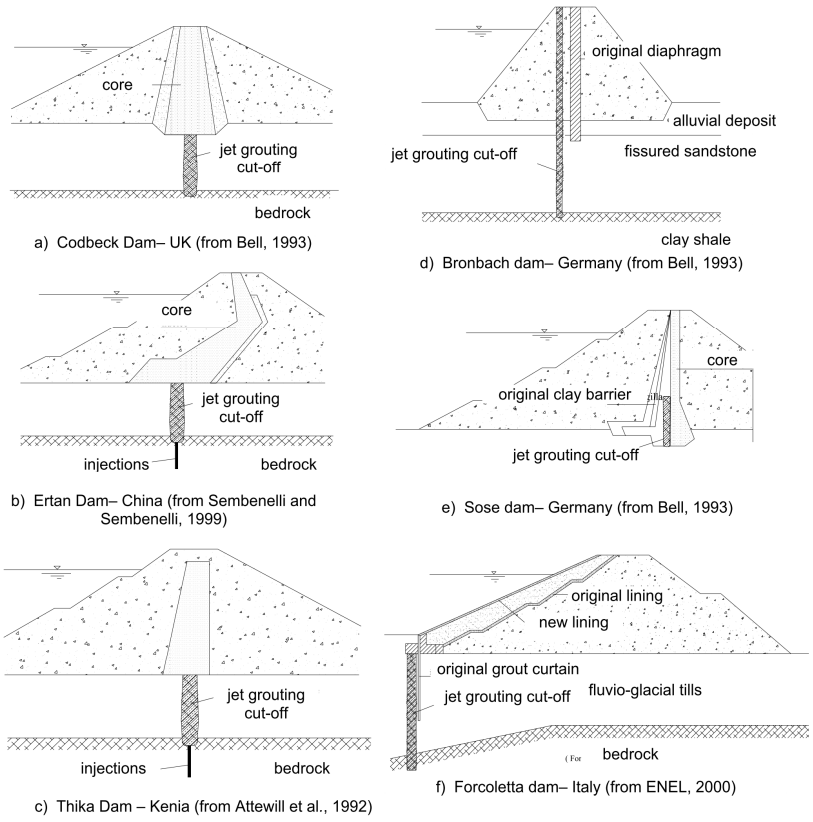


Fig. 1. Cross-sections of jet grouting cut-offs in dams (Croce and Modoni, 2007)

Typical range of diameters of the jet grout columns using various jetting systems are presented in Table 1.

Table 1 Typical diameters for different systems

Soil Type	Diameter (m)	
	Single Jet	Double/Triple Jet
Gravel	0.6-1.2	1.0-1.6
Sandy Gravel	0.5-1.0	0.9-1.8
Silty Clay	0.5-1.0	0.8-1.5
Clayey Silt	0.4-0.6	0.7-1.0
Clay	0.4-0.8	0.6-1.2

PROCESS OF JET GROUTING

Drilling is the first step in the jet grouting process which consist of eroding the soil and jetting of binder suspension (usually cement and or bentonite plus water) into the soil. The jetting process helps to achieve the required mechanical properties of the jet grouting columns. Schematic of the jet grouting process is presented in Fig. 4.

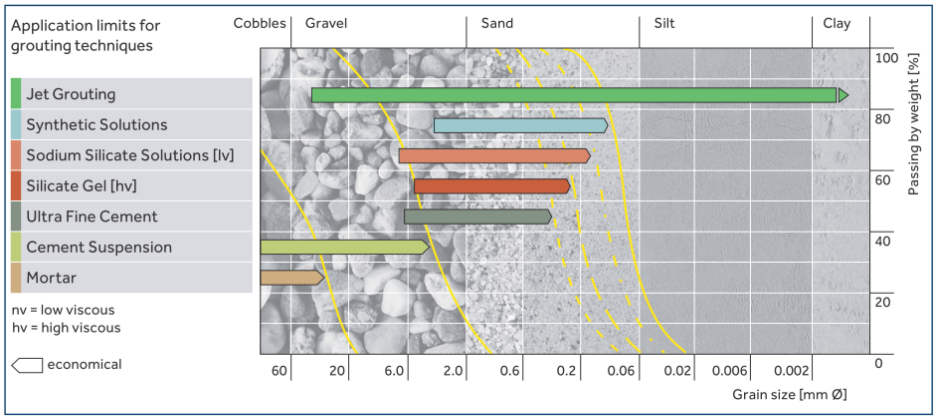


Fig. 2. Jet grouting applications in various soil types

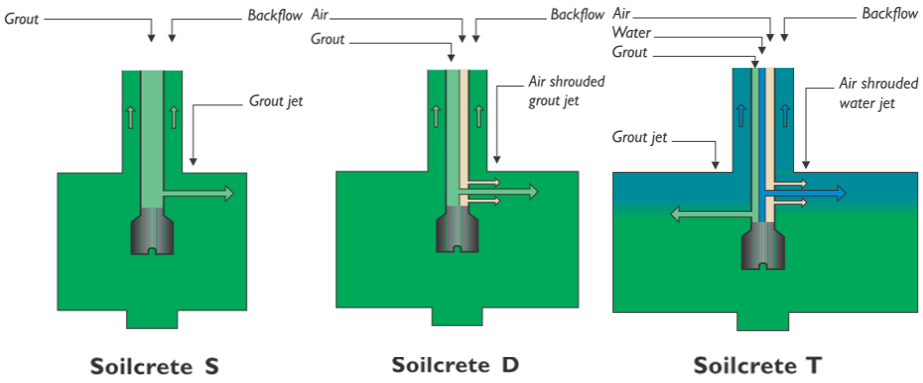


Fig. 3. Jet grouting systems

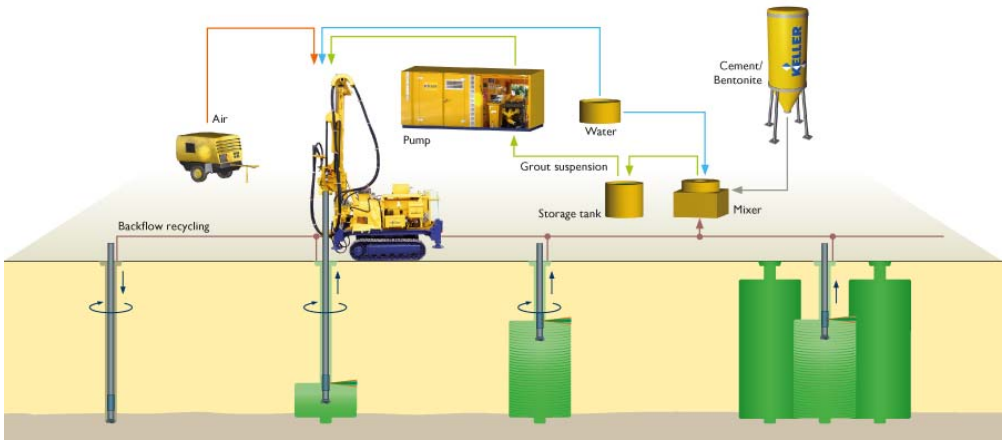


Fig. 4. Jet grouting process

OPERATION PARAMETERS AND SUITABILITY

The jetting is carried out as a 'bottom-up' operation in which the drill string (Fig. 4), with the jetting monitor attached at the base, is slowly raised and rotated while injecting the grout to form a column of soil/cement. During jetting, the spoil returns (excess material from the soil/grout mix) rises to the top of the drill hole. The jet grout column characteristics (diameter, composition, permeability, strength,

effective thickness of the cut-off wall etc.) are majorly dependent on the jetting parameters employed and type of soil encountered. These include rotation and extraction speeds, jetting pressure and grout flow rate, the grout mix, as well as soil type, grain size distribution and consistency of the in-situ soils. Typical operational parameters are indicated in Table 2.

Table 2 Typical operational parameters for various JG systems (Lunardi, 1997)

System	Fluid	Pressure, bar	No. of Nozzles	Withdrawal Rate (cm/min)	RPM	Discharge (l/min)
Mono	Grout	400-550	1-2	15 - 100	5 - 15	70 - 600
Bi	Grout	400-550	1-2	10 - 30	4 - 8	70 - 600
	Air	10-12	1-2	10 - 30	-	-
Triple	Grout	50-100	1-2	6 - 15	4 - 8	80 - 200
	Air	10-12	1-2	6 - 15	-	-
	Water	400-500	1-2	6 - 15	-	40 - 100

SEEPAGE CONTROL BY JET GROUTING

Seepage control practices in geotechnical and geo-environmental engineering can be generally classified into four categories (Chen et al.,2010), as per the following:

1. Creating impervious barrier with low permeability and high critical hydraulic gradient
2. Provide filters and lower the hydraulic gradient
3. Control the effective water level fluctuation
4. Creating hydraulic containment to arrest flow of water

Jet grouting discussed here belongs to the first type of seepage control method where the seepage is controlled through low permeable barrier. Jet grout cut-off walls act as a sealing structure. The sealing effect of grout against water ingress is generally achieved by selecting a suitable grout suspension and if necessary by the addition of bentonite. The type and quantity of the injected grout material as well as the kind and volume of the remaining soil particles in the grouted mass guide the sealing properties.

Pattern and length of jetted columns for seepage control

Cut-off walls represent extension of a dam's water proofing system into the subsoil which is made by connecting several vertical overlapped elements. Waterproofing of coarse alluvial deposits below cofferdams is performed by building diaphragm consisting of rows of overlapping jet grout columns extending down to impervious layer or to required design depth. Different patterns of jet grout columns are presented in Fig. 5. The depth of cut-off walls is usually established based on the reservoir storage and target hydraulic gradient.

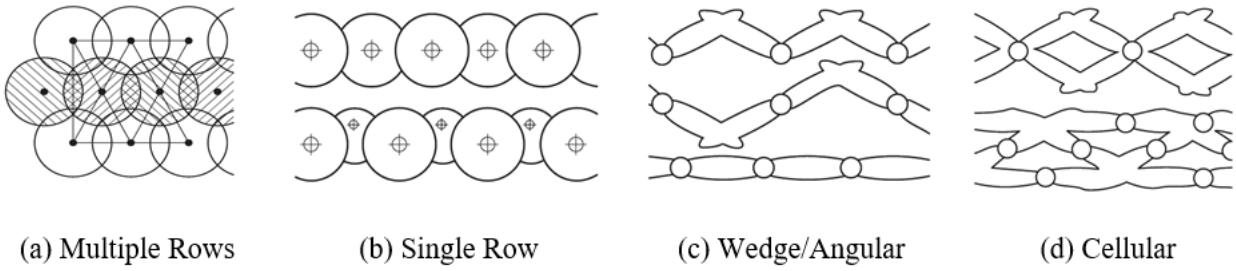


Fig. 5. Different patterns of jet grout columns

Engineering aspects

Strength is a general index used for identifying the quality of engineering material. Strength is often used as quality control check for cement-bentonite materials typically the unconfined compressive strength. However, strength requirement for cut-off walls vary substantially from 10kPa-500kPa. A realistic minimum strength for many applications using bentonite-cement mixes is 50kPa. Jefferies (2012) based on his study suggests a minimum strength for slurry trench cut-off walls at 28 days as 100kPa. However, the strength of samples collected from jetted columns show wide variation and this scatter is much more in cement-bentonite mixes (Jefferis, 2012; BRE,1999). The variation is attributed to the presence of soil from the ground dispersed into the slurry.

Permeability is the most important parameter in seepage control applications. In cut-off walls, the material of the elements (panels, piles, jet-columns etc) have very low permeability ($<10^{-7}$m/s) and are to be practically impervious. The trend of variation of permeability with time is quite interesting based on the binder used for jetting. The permeability of cement-bentonite materials tends to decline under continued permeation with water.

CASE STUDY: SEEPAGE CONTROL FOR IRRIGATION PROJECT IN INDIA

The following case study discusses application of jet grouting for seepage control for temporary cofferdams in one of the multipurpose irrigation projects in India. JG was used to construct a 600mm thick barrier, with 2m diameter jet grouting columns at 1.5m c/c distance. Grout columns were designed for a permeability less than 10^{-6} m/s.

Total JG treatment area covers approximately 66000 sq. m and designed to act as a cut-off wall for cofferdams in upstream and downstream area. The site is situated across the widest bank of a perennial river and comprises predominantly of well graded sands up to 20m and underlaid by silty clays/ clayey silts towards the banks. The grout columns were constructed by double fluid method to achieve a diameter of 2m and using fresh on fresh sequence (Fig. 6) in single row pattern. An extensive testing programme consisting of field and laboratory testing were performed for the quality control of jet grout column construction. Prior to installation of columns at site, site specific detailed laboratory study was conducted on the design of mix and permeability values for the designed mix. After successfully achieving the performance criteria in the laboratory, field trials were conducted to establish the operational parameters apart from the performance criteria. The details are covered in the following section.

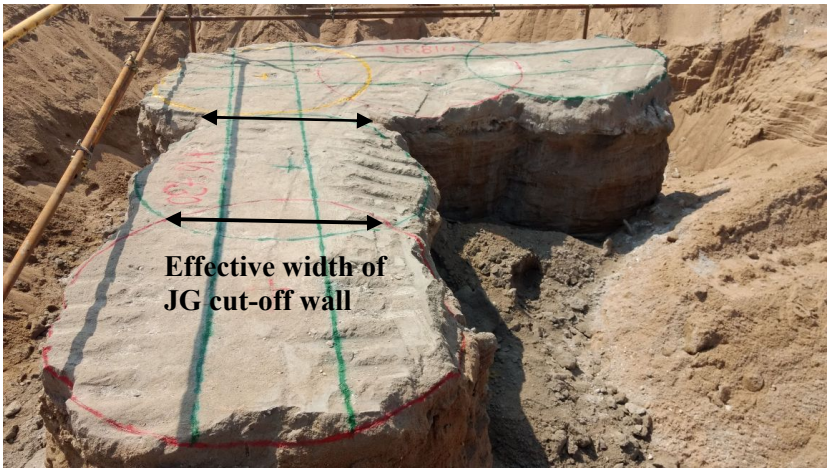


Fig. 6. Exposed jet grout columns at irrigation project site

Quality control aspects

The ideal operational parameters for a project site are to be established based on initial trials and experience. The grout properties such as viscosity, density and bleed are initially tested in laboratory study (Fig. 7) before adopting the grout mix at site. These properties were tested at site frequently to ensure consistency of the mix in the whole project. Jetting pressure and withdrawal rates can be monitored at the site with real time data acquisition systems (**Error! Reference source not found.**). Apart from these parameters, to ensure the formation of diameter of jetted column including verticality, ACI (Acoustic column inspector) testing (Fig. 7), Inclinometer test, tell-tale tests (Fig. 9) and visual column inspection (Fig. 7) were conducted. Various trial columns were installed to check if the required diameter are formed in the in-situ soil. The ACI test/tell-tale test confirm the diameter formation whereas inclinometer test/ records are used to ensure the verticality of the column which confirms the assumed column overlap throughout the depth of treatment.

Production column works were initiated at the site after selecting suitable parameters using the bi/double jet system and confirming the grout mix design. The parameters used in this project fall in the range mentioned in Table 2. The grout mix consists of cement and bentonite as binders. The hydration of bentonite is maintained well to achieve a uniform and pumpable mix with consistent properties throughout the production duration. During the installation of columns, verticality check is performed for every 1 in 20 columns and deviation is maintained within 1:100. Also, the grout mixed with the in-situ soil termed as 'spoil grout' is collected at various depths of the column and sampled for permeability testing. The collected samples were cured and tested at various ages such as 28, 56, 90 days etc. The test is conducted as per ASTM D 5084 -10 using the variable head concept. Fig. 10 summarizes the permeability test results on the spoil grout samples after 56 days of curing. At 56 days the target permeability of the jet grout columns is achieved and is less than 10^{-8} m/s



Fig. 7. Jet Grouting QA-QC testing adopted in irrigation project

Page: 2 / 2

Site Name:	**polavaram**		
Site Number:	**896**	**Machine Inv. Nr.:**	**41000493**
Point Number:	**test34**	**Machine Type:**	**KB6 Nr.: 005**
Shift:	**1**	**Prozess ID/Version**	**6100 V2.67.2.00**
Date/Time local:	**25.11.2017 14:29:35**		

KELLER

Keller India

JETTING

Events No	Description	Time [hh:mm:ss]	Depth [m]	Grout Drilling [l]	Grout Column [l]	Grout Point [l]
1	Point Start	14:29:35	0,73	0	0	0
2	Zero Depth	14:29:41	0,73	0	0	0
3	Column Start	14:59:08	11,05	709	0	709
4	Column End	15:49:16	0,55	709	20715	21425
5	Point End	15:49:17	0,55	709	20715	21425

Duration Point [hh:mm:ss]:	01:19:40	**Grout Point [l]:**	21425	**Max. Depth [m]:**	11,06
Duration Drilling [hh:mm:ss]:	00:29:31	**Grout Drilling [l]:**	709	**Column Length [m]:**	10,50
Duration Column [hh:mm:ss]:	00:50:07	**Grout Column [l]:**	20715		

Remarks:

Fig. 8. Monitoring grout consumption and column length in the irrigation project

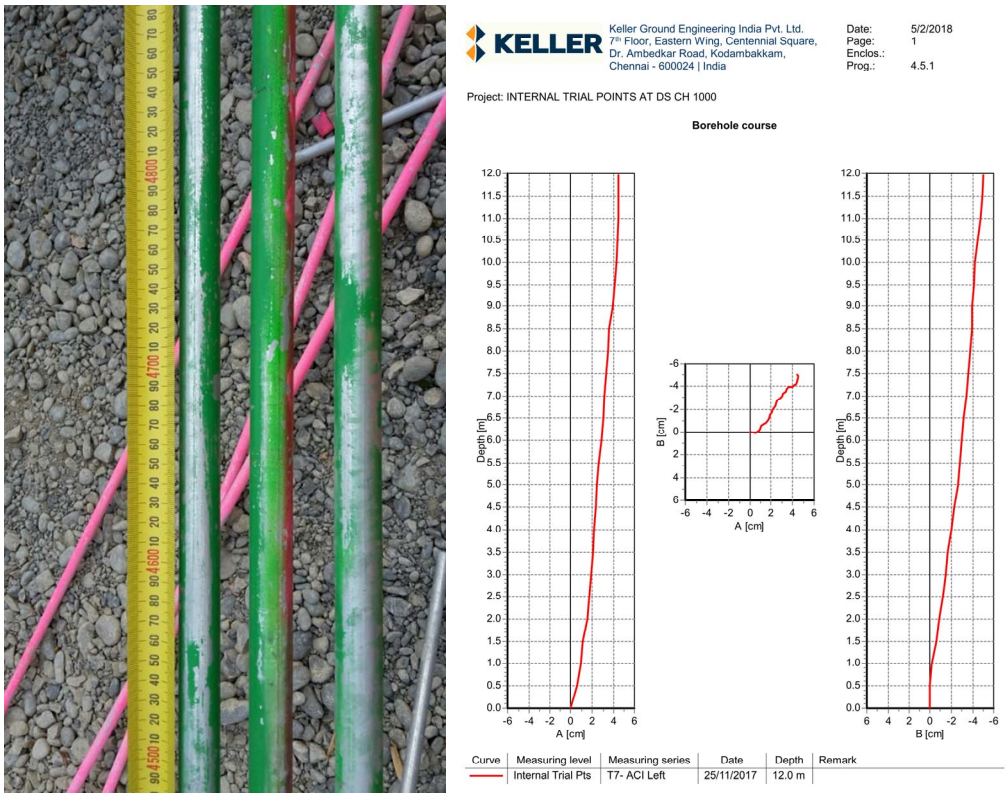


Fig. 9. Feeler Rods for tell-tale test/ACI testing and typical record for inclination test

Challenges in execution of JG columns

One of the major challenges faced during the project were maintenance of verticality. The limit for minimum deviation is to be stringently maintained to produce a low permeable barrier of designed width. Also, while installing the columns, proper interlocking between the columns is necessary to prevent

seepage. For this, there cannot be formation of cold joints between the JG columns. The collection of huge number of spoil grout samples at various depths of the columns and testing of the same after achieving the required age is not simple. Jetting of grout mix at high pressure (~400bar) to achieve required column diameter and for proper mixing of in-situ soil with grout is quite risky in terms of safety. Therefore, stringent safety precautions were required in this project. Apart from maintenance of the high quality standards, the major challenges faced in the project are working in the wide river bank with stringent deadlines before the site is flooded. In jet grouting projects, it is also a challenge to maintain relevant operational parameters in highly stratified soils and maintenance of design diameters in stratum with varying stiffness.

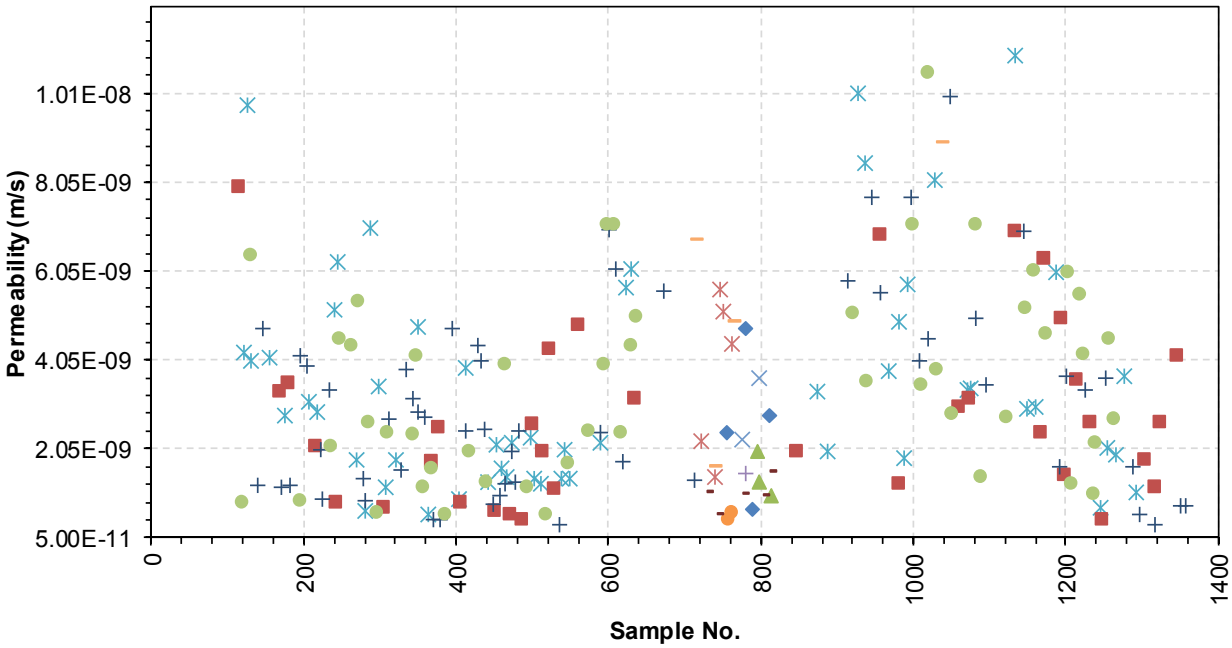


Fig. 10. Permeability test results on field samples at 56 days

CONCLUSIONS

Jet grouting technique is a proven application to address challenges in seepage remediation. This technique is one of the widely recognized ground improvement method, for its applicability to most soil types and solution to various challenges in the field of geotechnical engineering. The technique is flexible and capable of conforming to different types of waterproofing systems. It is widely used for seepage control as, the treatment can be executed without disturbing the nearby existing structures and even without lowering the reservoir water level. In this paper, the crucial parameters (operational and mechanical) in design point of view are discussed and different systems for executing jet grouting are also elaborated. Apart from the engineering parameters effective quality control measures to be followed at project site and seepage control applications also discussed along with a case study of a multipurpose irrigation project in India.

REFERENCES

ASTM, D. 5084-03. 2003. Standard test methods for measurement of hydraulic conductivity of saturated porous materials using a flexible wall permeameter. Annual Book of ASTM Standards, 4, 08.

Building Research Establishment (BRE), Construction Industry Research, & Information Association. 1999. Specification for the construction of slurry trench cut-off walls as barriers to pollution migration. Thomas Telford.

Chen, Y., Hu, R., Zhou, C., Li, D., Rong, G., & Jiang, Q. 2010. A new classification of seepage control mechanisms in geotechnical engineering. *Journal of Rock Mechanics and Geotechnical Engineering*, *2*(3), 209-222.

Croce, P., & Modoni, G. 2007. Design of jet-grouting cut-offs. *Ground improvement*, *11*(1), 11-20.

Jefferis, S. 2012. Cement-bentonite slurry systems. In Grouting and Deep Mixing 2012, pp. 1-24.

Lunardi, P. 1997. Ground improvement by means of jet-grouting. Ground improvement, 1(2), 65-85.

EVALUATION OF SLOPE STABILITY FAILURE ON RECLAMATION BUND - A CASE STUDY

Vinay Kumar M, Geotechnical Engineer, E-mail:mvk08486@gmail.com

Jeevan Reddy, Senior Engineer-Geotechnical, AECOM India Pvt Limited, E-mail: M.Reddy@aecom.com

Aminul Islam, Assistant General Manager, ITD Cementation India Limited, Mumbai, E-mail: aminul.islam@itdcem.co.in

ABSTRACT

A large container terminal is constructed at the port terminal in western coast of India by reclaiming the sea. The slope stability analyses have been performed for perimeter bund which is having a length of about 11km. The terminal is developed over marine clay and the maximum thickness of very soft to soft clay is around 24 m. The soft marine clay is susceptible to large settlements and slope failure during temporary & permanent condition. The ground improvement by prefabricated vertical drains (PVD) and preload is adopted to mitigate the aforesaid issues. In addition to the above, high tensile woven geotextile is also used at the perimeter bund to ensure adequate factor of safety against slip failure. This paper examines two failures of embankment slopes. The geotechnical investigation has been carried out at the collapsed region and itis observed that soil strength is inadequate to support the self-weight of the embankment along with preloaded surcharge.

Keywords: Ground improvement, Shear strength, Slope stability, Reclamation, Slope failure

INTRODUCTION

The onshore terminal area is developed by reclaiming about 100 Ha of land over very soft to soft marine clay to accommodate container stack yards and associated structures such as rail container, port buildings, workshops, roads and other utility buildings.

The project consist around 11km permanent perimeter bund and slope stability analyses has been carried out to design the embankment geometry and ground improvement under the embankment. Total perimeter bund is divided into number of zones based on the use of individual sets of selected design parameters, thickness of marine clay, individual service live loadings and functional requirement in future.

Consolidation happens when the water in soil is squeezed out from the soil matrix by impressing preload on soft clay. In this process the soil decreases its volume and large settlement take places during construction. It reduces the post construction settlement and enhances the bearing of the soil.

The construction of embankment height of 12m during preload condition is colossal challenge and ensuring the stability of the embankment is most critical task. The construction of embankment height is divided into three stages and adequate pause period is allowed at the intermediate stage. The gain in shear strength is calculated as per Skempton & Henkel method [1] and pause period is estimated as per IS 15248-Part 2 [2] to achieve the desired degree of consolidation. The stability of the embankment for each stage of construction is analyzed considering the improved shear strength after allowing the designed pause period at the intermediate stages.

GEOTECHNICAL INSTRUMENTS

Geotechnical instruments are installed after reclamation of stage-1/working level to monitor the ground improvement works and lateral movement of slope during construction. The type of instruments and other details are presented in Table 1. Typical geological profile along with the indicative location of geotechnical instruments are shown in Figure.1.

© 2018 Deep Foundations Institute

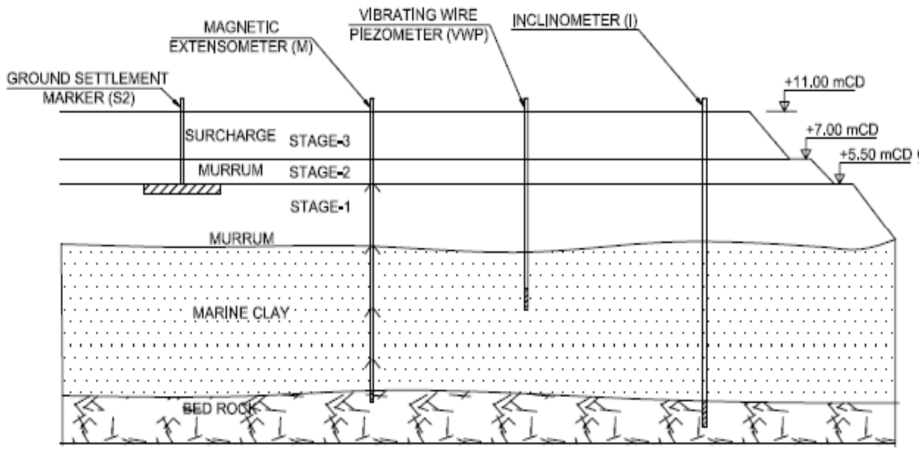


Figure.1. Geological Profile along with Location of Instruments

Table 1 Type of Geotechnical Instruments

Sr. no.	Type of Instrumentation	Purpose	Remarks
1	Ground Settlement marker (S2)	To measure settlement	-
2	Magnetic Extensometer (M)		
3	Vibrating Wire Piezometer (V)	To measure the pore water pressure	-
4	Open Stand pipe (O)		
5	Inclinometer (I)	To measure the lateral deformation of slope/embankment	Installed at perimeter bund

SLOPE STABILITY

The slope stability analyses are carried out using the industry recognized software of Slope/W developed by Geoslope [3] for perimeter bund. The software program implements several methods for analyses of random circular, non-circular slip and sliding failure surfaces, the Morgenstern-Price Method [4] is used to calculate factor of safety. In the Morgenstern-Price Method, compatibility of both moment and force equilibrium is enforced; this provides a higher level of reliability than methods that compute moment or force equilibrium alone.

The minimum required factor of safety (FOS)and service loading depicts in Table 2.

Table 2. Loading and FOS for Slope Stability Analyses

Service Life	Loading type	Service Load or Impose Load	Min FOS
Temporary Condition	Static	Self-weight of the embankment and 10kPa as construction load	1.3
Permanent Condition	Static	Self-weight of the embankment and 30kPa as load due to traffic movement	1.5
	Seismic	Self-weight of the embankment and 15kPa as load due to traffic movement	1.1

CASE STUDY 1

Background

Generally most critical stage for stability analysis of an embankment is when the entire surcharge is installed. In this stage imposed load reaches the maximum and underneath soft clay unimproved or partially improved.

The failure of the slope is noticed immediate after placement of surcharge up to final level. The additional geotechnical investigation is carried out to verify the shear strength of underneath the soft

clay. As per IS 4434, field vane shear tests are conducted in each borehole at 1.0 to 1.5m interval along the full depth of the soft marine clay. The Borehole location and photograph of the collapsed slope are shown in Figure2and Figure3.

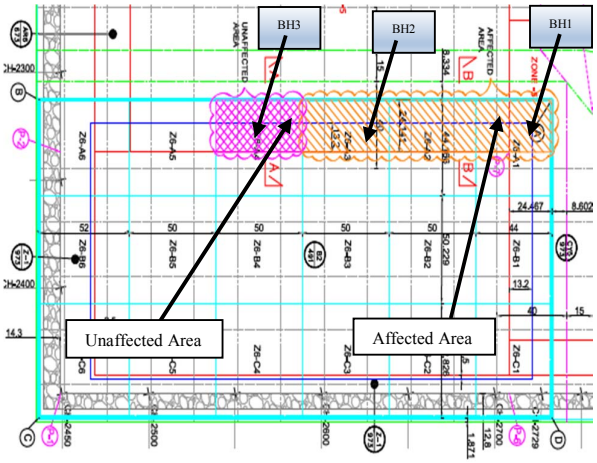


Figure. 2. Layout of Collapsed Slope



Figure. 3. Photo of Collapsed Slope

Analysis of Failure

After analysis of the post failure geotechnical investigation data and review of adopted construction methodology, the following probable causes of failure was identified

1. The collapsed edge was a temporary perimeter bund. It was created due to sequence of reclamation and hand over time schedule for adjacent areas. The temporary perimeter bund is not envisaged and hence not considered in design.
2. Unplanned excavation nears to the toe of embankment which has been undermined the toe of the edge slope and hence affected its stability.
3. The berms widths were insufficient for ensuring edge stability.
4. The intermediate pause period at stage 1 and stage 2 of filling were insufficient to allow the marine clay to gain strength.

Conclusion and Adopted Way Forward

The perimeter bund is constructed in stages to ensure the edge stability and the succeeding stage is constructed after underneath soil attains the required strength to support the additional surcharge height. The factor of safety at each stage is computed to demonstrate that the achieved FOS is greater than minimum requirement i.e. 1.3.A stipulated pause period is allowed in each intermediate stage to dissipate the excess pore water pressure which is generated due to the surcharge load. As the excess pore water pressure dissipates degree of consolidation & shear strength increases. The gain in shear strength depends on the allowed pause period. The additional borehole is carried out at each stage of construction to ascertain actual gain in shear strength. The gain in shear strength of soil is estimated based on Skempton & Henkel method [1]. In the event when the achieved gained shear strength is great than theoretically estimated gained shear strength then proceeds for next stage of construction. Nevertheless if achieved gained shear strength less than theoretically estimated gained shear strength then pause period is extended and retests are carried out prior to proceed for next stage of construction.

The rapid rate of surcharge filling generates excess pore water pressure and also reduces factor of safety. The rate of surcharge filling is restricted up to maximum of 0.5 m height of fill per day. This moderate rate of surcharge placement allows dissipating the excess pore water pressure gradually.

Sequence of reclamation as well as subsequent hand over time schedule for future work is reviewed and temporary perimeter bund identified. According to the geotechnical parameter at that section temporary perimeter bund is designed and adequate berm width and appropriate pause period at the

intermediate stage is provided. The output of slope stability analysis for temporary perimeter bund using Slope/W software is presented in Figure 4.

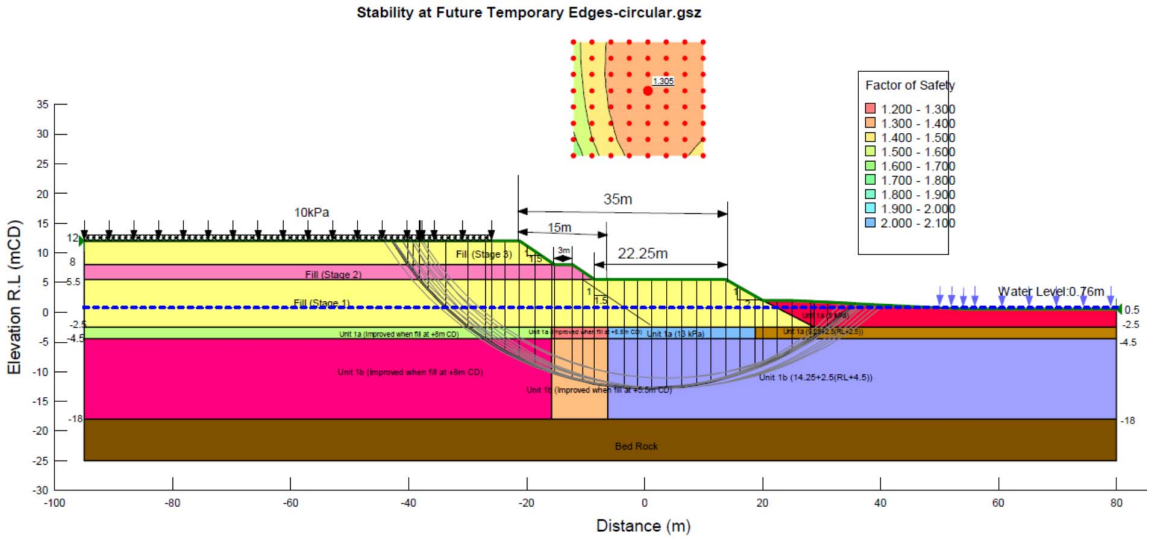


Figure. 4. Slope stability analysis and cross section

CASE STUDY 2

Background

The geotechnical investigation was carried out prior to the reclamation to establish the design parameters. Field vane shear test [5] and static cone penetration tests [6] were conducted. Based on geotechnical parameters, the embankment is designed and three stage of construction is considered. A pre-decided pause period is adopted for each stage and gain in shear strength is estimated as per Skempton & Henkel method [1]. It has been noticed during slope stability that final stage of construction is most critical.

Nevertheless, the embankment slope is collapsed during placement of surcharge at final stage. A detailed survey was carried to understand the behavior of the failure pattern. The location of failure zone is presented in Figure 5 and the failure surface is depicted in Figure 6.

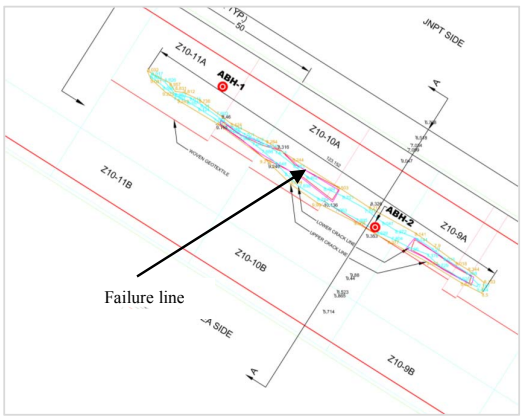


Figure. 5. Location failure zone

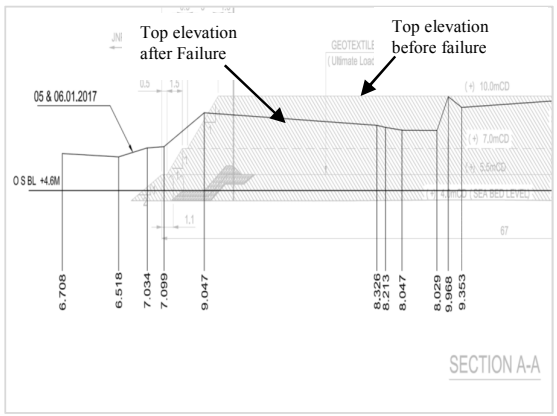


Figure. 6. Cross section of failure zone

Analysis of Failure

The additional boreholes namely ABH 1 and ABH 2 are carried out at the failure zone and the location of boreholes and photograph of collapsed are shown in above Figure 5.

The achieved shear strength value from borehole ABH1 and ABH2 is plotted in Figure 7 and compared with the theoretically estimated gained shear strength profile prior to placement of

surcharge at final stage. It is observed that the achieved shear strength less than the estimated gained shear strength and it causes the collapse of embankment. Based on the achieved shear strength value from ABH1 and ABH2, the design parameters are revised and modify design line is established. It is presented by green dotted line in Figure 7.

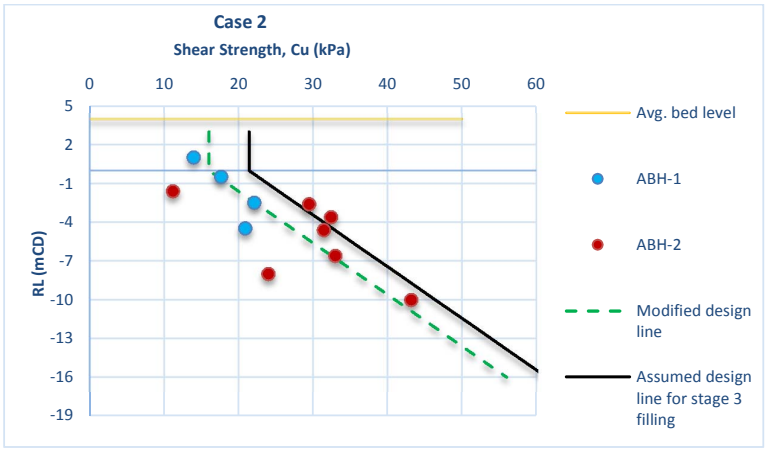


Figure. 7. Shear strength profile along depth of soft clay



Figure. 8. Photo of Collapsed Slope

Conclusion and Adopted Way Forward

The achieved rate of gain in shear strength is significantly lesser than what theoretically assumed and this results higher pause period at the intermediate stages. The additional borehole to ascertain the gain in shear strength has not been carried out.

The modified design line is considered and the stability of the embankment is reanalyzed. The output of the Slope/W software is presented in the Figure 9. The pause period at the intermediate stage is augmented to the increase the gain in strength and enhance factor of safety against slip failure.

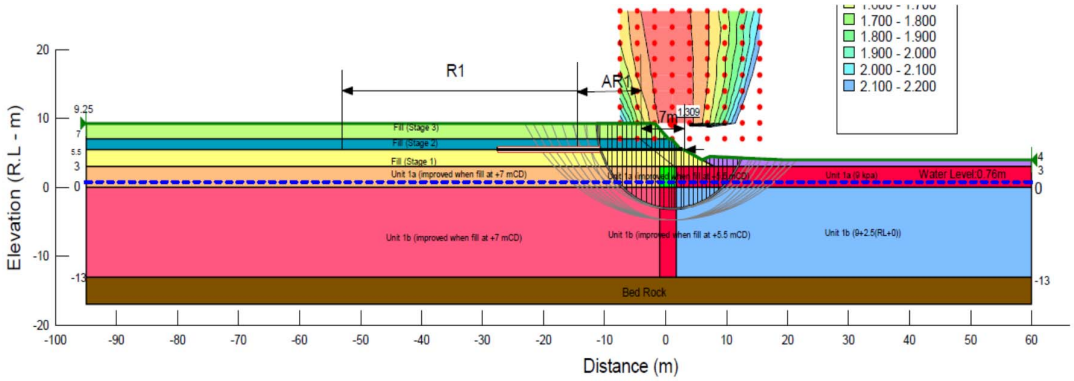


Figure. 9. Output of stability analysis for collapsed zone

The top elevation of surcharge at the final stage is reduced by 750mm to minimize the imposed load on the soft clay. However, the top elevation of surcharge is monitored regularly and it is ensured that depth of soil above finish ground level is not less the depth of soil equivalent to the service load. In case depth of the surcharge over finished ground level is reduced then additional thickness of surcharge layer is placed.

REFERENCES

[1] Skempton, A.W and Henkel, D.J. The post Glacial clay of the Thames Estuary at Tilbury and Shell haven, Proc. 3rd ICSMFF, Zurich, Vol 1.1953.302-308

[2] IS 15248 Part 2- 2004; Design and construction of ground improvement- guidelines: pre-consolidation using vertical drains.

[3] Stability modelling with Slope/W Manual. Geo-Slope International Ltd., December 2012.

[4] Morgenstern, N.R., and Price, V.E. 1965. The analysis of the stability of general slip surfaces. Géotechnique, 15(1): 79-93.

[5] IS 4434 -1978: Code of practice for in-situ vane shear test for soils

[6] ASTM D5778 – 12Standard Test Method for Electronic Friction Cone and Piezocone Penetration Testing of Soils

FOUNDATION ANCHORING FOR STABILITY IN BROWNFIELD SITE

Manos De, Tata Consulting Engineers Limited, Jamshedpur, Jharkhand, India, Phone - (0657)6696303, email - mde@tce.co.in
Soumik Chakraborty, Tata Consulting Engineers Limited, Jamshedpur, Jharkhand, India, Phone - (0657)6696632, email - soumikc@tce.co.in
Anup Kumar Mandal, Tata Consulting Engineers Limited, Jamshedpur, Jharkhand, India, Phone – (0657)6696648, email – akmandal@tce.co.in
Shuvranshu Rout, Tata Consulting Engineers Limited, Jamshedpur, Jharkhand, India, Phone - (0657)6696673, email - skrout@tce.co.in
Pradip Kumar Nandi, Tata Consulting Engineers Limited, Jamshedpur, Jharkhand, India, Phone – 9204394152, 7481826505, email – pknandi@tce.co.in

ABSTRACT

Executing projects in brown field site conditions throws up many challenges requiring innovative approach for feasible solutions. In the present case foundation for a heavily loaded storage silo support structure was required to be designed at a site with numerous closely located existing services. The required foundation plan area was under adjacent existing road which was planned to be temporarily diverted. However at time of execution temporary shutdown of part of the road was not allowed by plant operation. Also during excavation presence of an underground water pipe was revealed and this pipe could not be diverted or temporarily rerouted since it was vital for operation of existing plant. The foundation layout had to be modified to avoid disruption to these facilities but because of the critical loading conditions from superstructure, reduction in foundation area was resulting in loss of required stability of the foundation. Since the governing condition for inadequate stability was found to be overturning effect from moment under seismic conditions, alternative design for the foundation within available footprint space was carried out by providing rock anchors. The anchors were provided along the periphery of the foundation to maximize the stabilizing effect. This paper presents the case study on the evaluation of the layout and construction restrictions on the designed foundation, planning and design of the alternative solution to suit site conditions and provide the required factor of safety for stability of the foundation, design of the anchors and installation procedure, load testing of anchors and finally constructing the foundation within the limitations. The implemented solution achieved the desired safety of the foundation while maintaining all facilities in the operating plant unhindered.

Keywords: coke dry quenching, dust storage silo, rock anchor, anchor pull out test

INTRODUCTION AND BACKGROUND

Development in Steel Industry is a very important aspect in the growth of industrial infrastructure. However, the various aspects of land acquisition, logistics of the movement of huge quantities of materials required and also environmental concerns have placed restrictions on availability of new land for setting up new plants. This has prompted the plant owners to plan for capacity expansion within existing plant boundaries. Additionally, to meet the stringent emission and effluent norms, the new plants

© 2018 Deep Foundations Institute

are adopting state of art technologies to not only meet the current standards but even plan for further stringent norms that would come into effect in future to enable the plant to operate successfully throughout its design life.

The property owner had earlier installed a Coke Wet Quenching (CWQ) for their Coke Plant. Subsequently for utilization of waste heat from coke cooling process and improve environmental performance the owner decided to install Coke Dry Quenching (CDQ) system. The facilities for the new plant are to be constructed while the existing CWQ will remain in operation. This imposed various constraints on the layout of the units for the new plant from aspects of foundation construction feasibility close to existing and operating plant, logistics for movement of both construction and maintenance equipment and maintain complete safety of the new construction and existing plant. It is against this background that this challenging design concept for one critical unit of the new plant was prepared.

LAYOUT OF THE PLANT

The units of the new plant are located within the operating zone of existing coke oven plant and adjacent to many of the existing facilities in operation. The new plant consists of various units like lifting crane structure for hot coke bucket, coke dry quenching chamber, conveyor tunnels, air blower fan, dust catcher chambers, steam generating boiler, dust extract system equipment, dust storage structures and various utility structures for conveying pipes and cables. The plant layout is shown in Fig.-1 below:

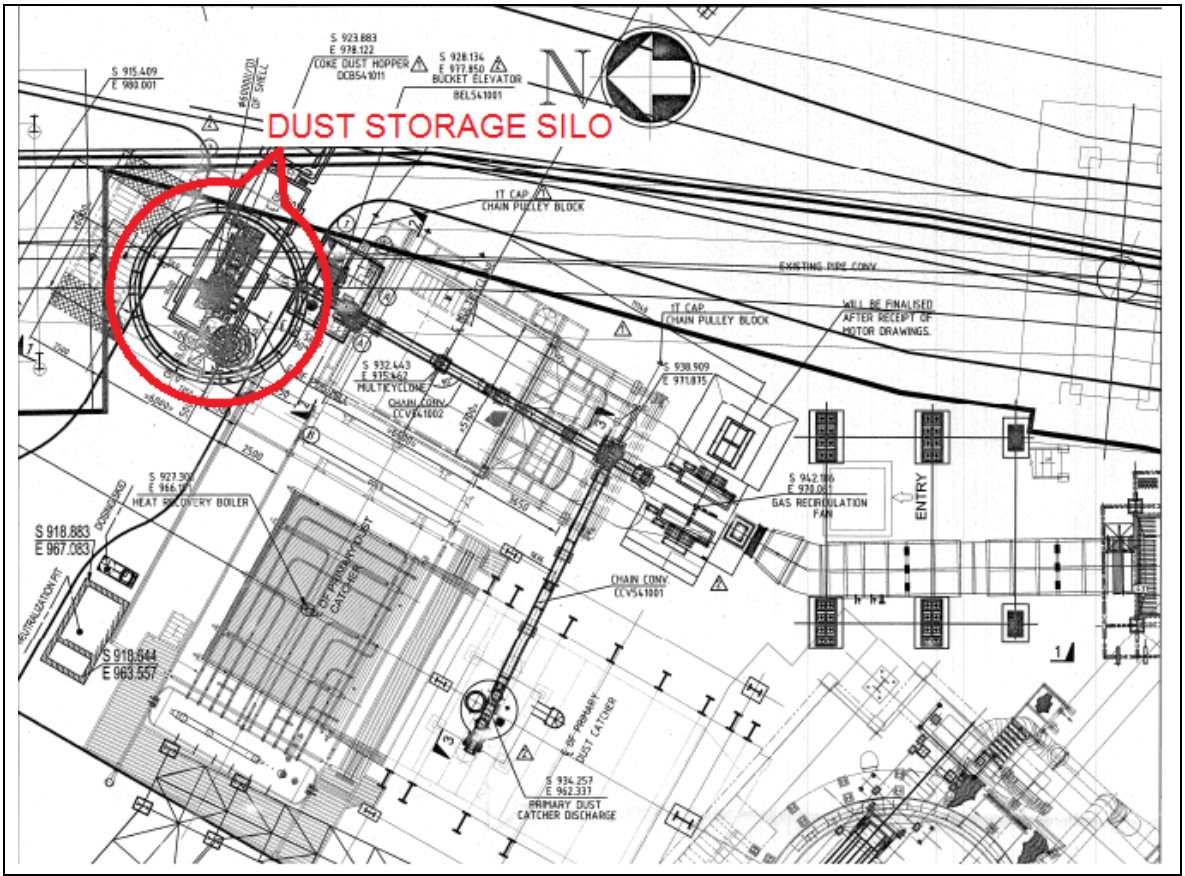


Fig. 1. Layout of Plant for Coke Dry Quenching System

The plant component that is the object of this present study is the coke breeze silo, this item is marked 10-16 in the layout. The purpose of this equipment is to collect the dust generated during movement and transfer of coke during its cooling process in the chamber, from the silo the collected dust is to be removed by trucks. From the layout, it can be seen that the dust silo is located below an existing conveyor gallery close to one of the existing trestle foundations and adjacent to foundations for the boiler and secondary dust catcher of the new plant. Due to space constraints, the units had to be placed as close to each other as allowed by process safety requirements causing severe strain on foundation design, detailing and construction. The situation is further aggravated by the presence of some additional underground utilities that are not mapped and these were detected only during the actual construction stage. The foundation for this dust storage silo had to be designed within these constraints.

LAYOUT OF THE SILO FOUNDATION

The silo supporting structure comprises of four columns and there is an adjoining staircase with two independent columns and the other part of the staircase structure is supported on two of the silo supporting columns. Overall the silo and stair support structure comprising six columns are founded on a common raft foundation. The general arrangement of the structure is shown in figures 2 and 3 respectively.

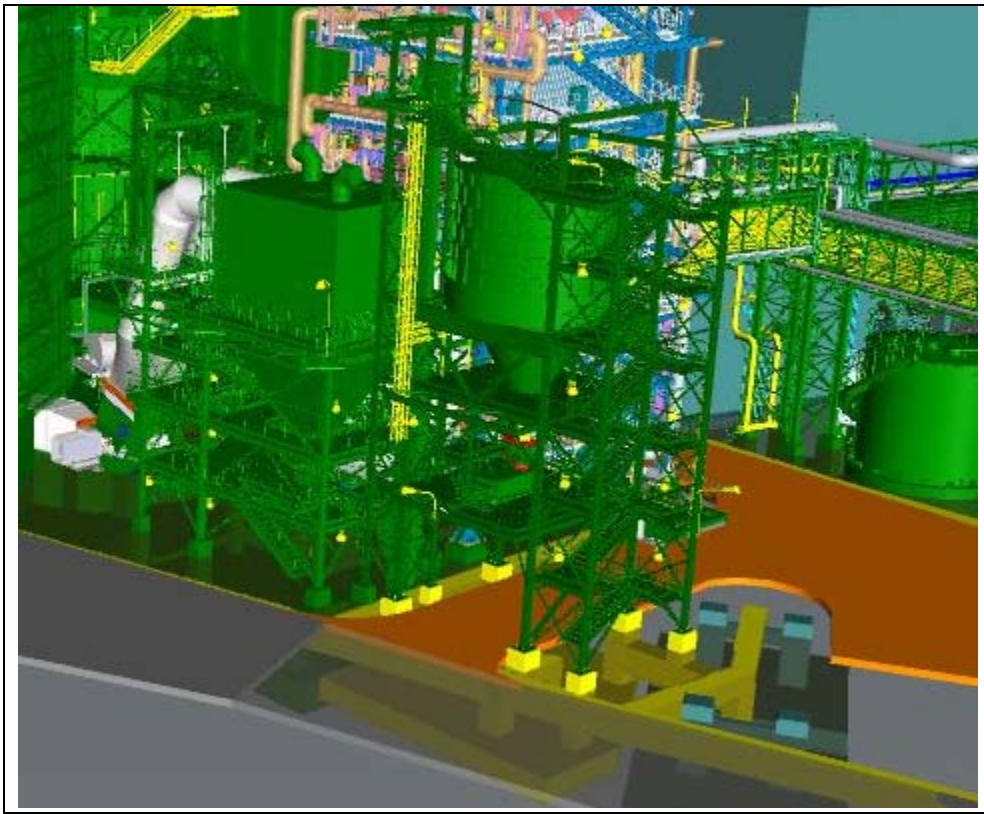


Fig. 2. Snapshot of 3D Model showing Coke Breeze Silo Structure and Foundation

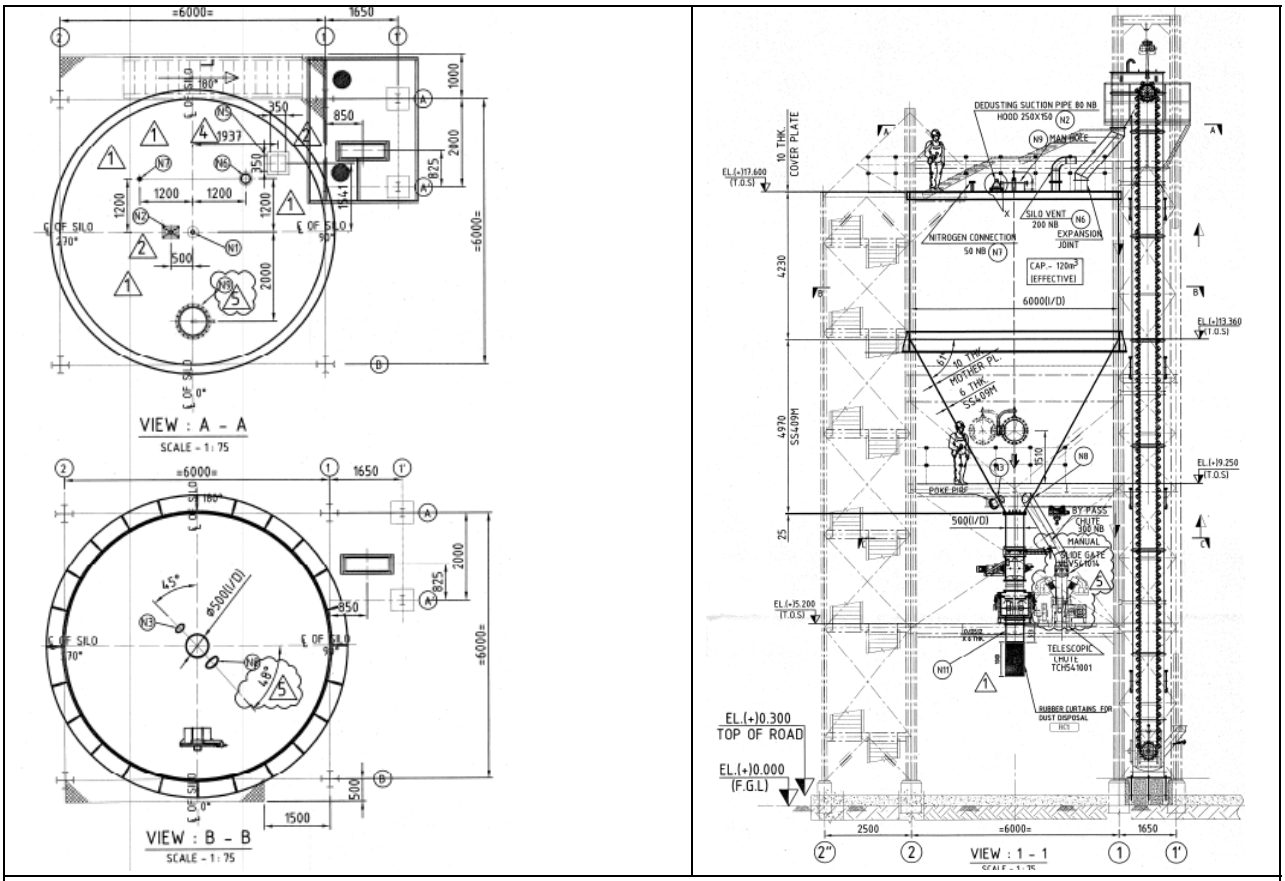


Fig. 3. General Arrangement of Coke Breeze Silo structure

GEOTECHNICAL CHARACTERIZATION AND DESIGN OF THE SILO FOUNDATION

Geotechnical investigation at the site was carried out to determine adequate founding depth and ascertain soil parameters to be used for the foundation design. Borehole no. 12 is the closest point of investigation to this foundation. The typical geological formation at the design level of base of foundation was of basically metamorphic mica schist rock. Highly fractured mica-schist was found to occur from depth of 2.5m to 6.5m below ground with SPT value > 100, core recovery of 60% and RQD value of 35. This is followed by partly weathered slightly fractured mica schist from 6.5m to 14.0m below ground level with occasional quartz lamination. The rock parameters in this zone are SPT > 100, core recovery of 66% and RQD value of 48. Bulk density of the rock at foundation level is 25kN/cum and minimum compressive strength is 10.1 MPa. The design value of bearing capacity of foundation in this layer was considered as 250kN/sqm.



FIELD BOREHOLE DATA-SHEET

Project : Geotechnical Investigation work for proposed Coke Dry Quenching Plant for Coke Oven Battery No. 10 & 11, TSL, Jamshedpur

Location/Site : COB#10

Borehole No : 12

Commenced on : 07.11.2014

Completed on : 20.11.2014

Co-ordinate : S 929.370, E 970.805

R.L. of Existing Ground : 163.500m

Borehole Diameter : 150mm/Nx

Soil Boring termination depth : 2.50m below EGL

Drilling termination depth : 25.00m below EGL

Ground Water : Struck at / Sealed at

Standing Water Level : 1.70m Below EGL

Method of boring : Shell & Auger/Rotary Drilling

Depth in metre	Description of soil	Thickness of layer in mtr.	Details of soil sampling			Penetration (in cm)			'N' value	Remarks
			Ref. No.	Type	Depth (m)	15	30	45		
Below EGL	Dark Grey, heterogeneous fill materials consisting of hard slag, coal pieces, cinders, small concrete pieces etc.	0.75	3086	P	0.50	47/5cm	-	-	>100	150mm diameter borehole
0.75			3088	P	1.50	10	27	33	60	
0.75	Highly weathered, brownish grey Micaschist	1.75	3100	W	1.70	-	-	-	-	
2.50			3090	P	2.50	52/3cm	-	-	>100	

Depth in metre	Description of soil/rock	Thickness of layer in meter	Type & size of Bit	Run (m)	Depth (m)	Recovery (%)	RQD (%)	'N' value	Remarks
2.50	Weathered, greenish grey, highly fractured Micaschist	4.00	DIA/NX	1.00	2.50 - 3.50	50	Nil	-	
			SPT Conducted at 3.50 - 3.54m depth.					>100	53/4cm
			DIA/NX	1.50	3.50 - 5.00	67	29	-	
			DIA/NX	1.50	5.00 - 6.50	49	27	-	
6.50			DIA/NX	1.50	6.50 - 8.00	73	48	-	
6.50	Partly weathered, light bluish grey, slightly fractured Micaschist, quartz lamination was found between 7.50m and 7.75m depth	7.50	DIA/NX	1.50	8.00 - 9.50	100	67	-	
			DIA/NX	1.50	9.50 - 11.00	70	63	-	
			DIA/NX	1.50	11.00 - 12.50	40	28	-	
14.00			DIA/NX	1.50	12.50 - 14.00	53	32	-	
14.00	Hard, bluish grey Gneiss with traces of laminated quartz	3.00	DIA/NX	1.50	14.00 - 15.50	60	40	-	
17.00			DIA/NX	1.50	15.50 - 17.00	67	53	-	
17.00	Hard, light bluish grey Micaschist with traces of laminated quartz	8.00	DIA/NX	1.50	17.00 - 18.50	80	60	-	
			DIA/NX	1.50	18.50 - 20.00	90	63	-	
			DIA/NX	1.50	20.00 - 21.50	87	65	-	
			DIA/NX	1.50	21.50 - 23.00	83	67	-	
			DIA/NX	1.50	23.00 - 24.50	87	73	-	
25.00			DIA/NX	0.50	24.50 - 25.00	100	100	-	

Fig. 4. Geotechnical characterization at location of Silo Foundation

The initial foundation design was carried out as a shallow raft foundation. The contact area of the raft was provided as required to distribute the loads from the superstructure safely to the foundation. The designed solution for the foundation had already considered the site constraints known at the time of design – proximity to adjacent existing conveyor gallery supporting tower foundation, existing road and other obstructions. The shaded portion in figure 5 shows the foundation area under road. The foundation design had been carried out with due consideration for these constraints by providing bridging beams and irregular shaped foundation. It was agreed with construction contractor and owner that partial shutdown of the road would be allowed for the construction.

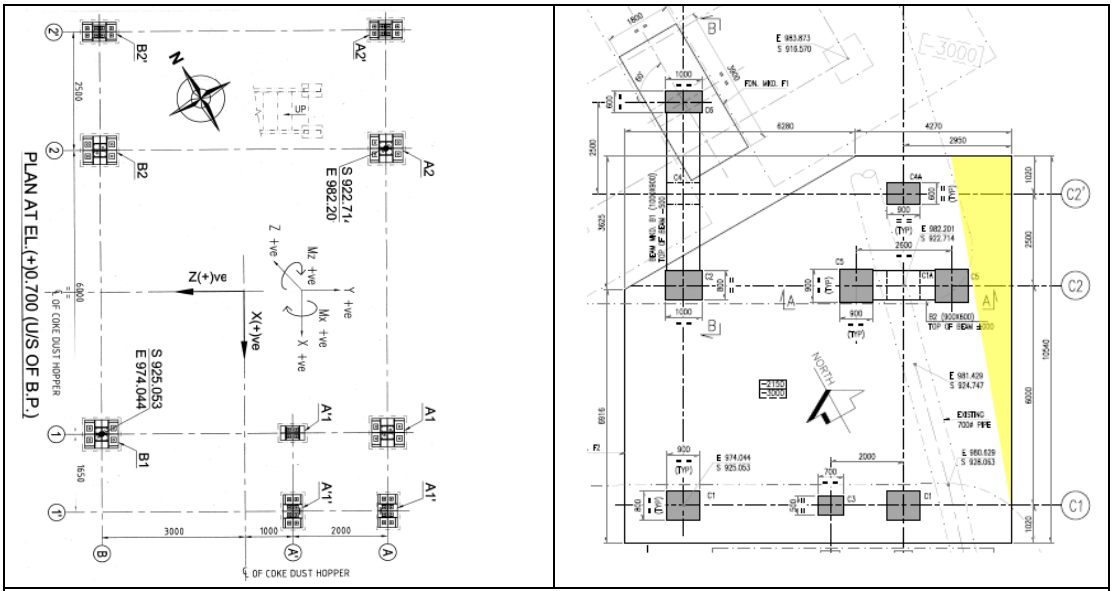


Fig. 5. Base Plate Layout and Silo Foundation Plan

CHALLENGES TO CONSTRUCTION

Additional hurdles to planned design and construction program were encountered when field work was started. The first unknown obstruction encountered was occurrence of a 700mm diameter live water carrying pipe which could not be rerouted. Foundation design was modified to bridge over the water pipe line with a bridging beam to receive the pedestal for supporting the column leg of the silo structure. The second difficulty encountered was of more critical nature when it was understood that the plant operation would not be able to provide required partial shutdown of the road under which the foundation raft had to be constructed. This constraint resulted in loss of contact area of the foundation raft. This was further aggravated by inability of the contractor to excavate safely under the water pipe so that the foundation outline was further reduced to clear the edge of the pipe. This loss of contact area proved to be very critical since the fully loaded silo was subject to high seismic forces on the column bases and the reduced area caused tension and uplift in the foundation. The design had become unsafe and called for special measures to ensure stability. The shape of the foundation that was found feasible to suit the construction constraints is depicted in figure 6.

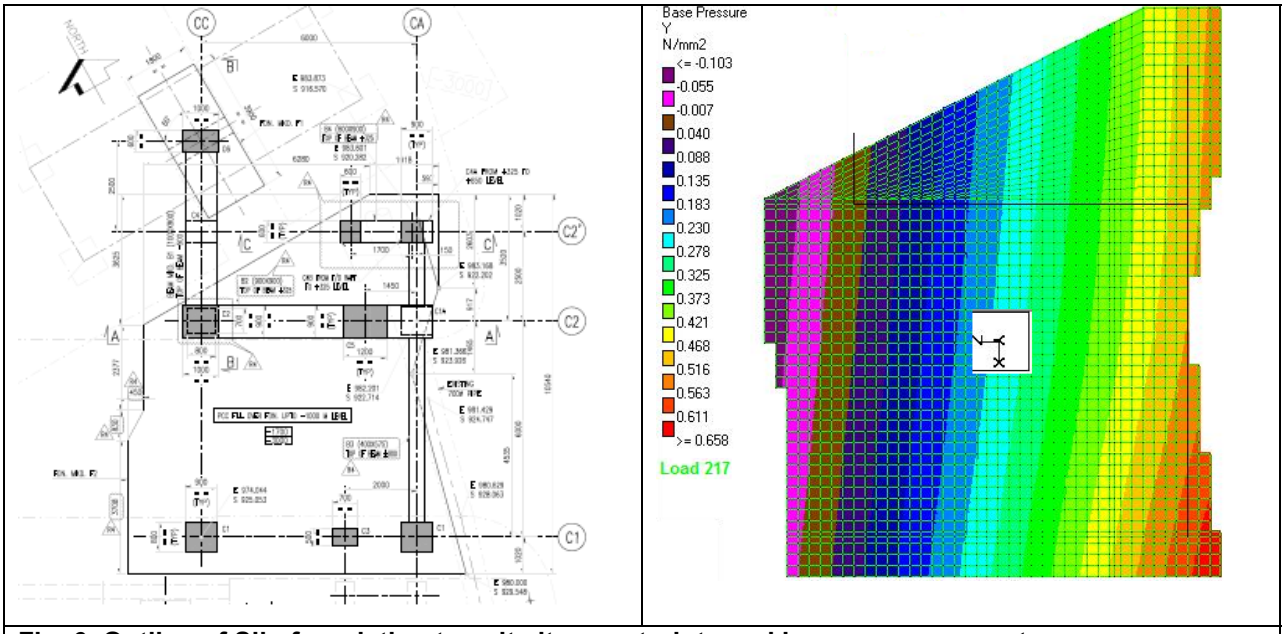


Fig. 6. Outline of Silo foundation to suit site constraints and base pressure contour

REVISED DESIGN OF THE FOUNDATION WITH ROCK ANCHORS

The revised design had to take into account the available foundation outline that suited the site constraints for construction. The vertical loads (Y-direction) from the superstructure on the foundation for the critical cases are presented in Table 1:

Table 1. Load Data for Columns of Silo Supporting structure

Column grid	Empty Silo (kN)	Silo Full (kN)	Siesmic load (+X, kN)	Siesmic load (+Z, kN)
CA-C1	-317	-519	355	562
CA-C2	-373	-618	-319	507
CA-C2’	-221	-567	665	179
CC-C1	-344	-638	-209	-729
CC-C2	-263	-403	-308	-554
CC-C2’	-185	-273	607	-115

Upward loads are with +ve sign, Downward loads are with (-)ve sign

The high values of seismic loads were causing uplift and overturning effects on the foundation and tension in the soil support below the raft. This can be seen in the analysis output showing base pressure diagram in figure 6 where considerable zone is found to be in tension zone (base pressure has negative value). To overcome this stability problem, use of rock anchors was resorted to. The anchors selected had the following design parameters
Anchor make: HILTI
Anchor family: Chemical type
Anchor type: RE 500
Anchor rod type: 16mm rebar
Embedment depth: 300mm
Base material (for anchorage design): Rock
Proof load: 36 kN
Pull out test was conducted on samples of the anchor bars under supervision of the manufacturer to establish the allowable load. Three samples were tested at site using 58.8 ton rebar tester equipment number 797-06 till the value of proof load. No failure of the anchors was observed. Hence the design proof load was adopted as allowable pull out load on each anchor.

Revised analysis of the raft was carried out by providing anchors under the base raft at pre-determined locations. Tension was found along the peripheral elements of the foundation raft only and hence anchor layout was planned along the periphery of the raft. The anchors are modelled as tension only springs with spring constant calculated as follows

Spring constant $K_y = F_y/ \Delta_y = A*E/L = 201*10^{-6}*2*10^8/0.3 = 134000$kN/m

The anchors are embedded 300mm into the rock layer as confirmed by the pull out load test and are projected 600mm into the raft concrete. The projection length into concrete was worked out on the basis of required development length of the rebar to fully transfer the design load of 36kN.

Discussion on Design Basis

The selection and design of the rock anchors was developed based on the guidelines of US Army Corps of Engineers document. Out of the two types of anchor systems – tensioned anchor system and un-tensioned anchor system; the latter system of rock dowels was selected for this application. The dowels and rock

mass interact through development of cohesive and frictional forces along the column of grout which provides the bond forces between the dowel rod and the rock mass. The anchorage action of dowel is activated by tendency of anchor to displace or potential partial shear failure.

Calculation for rock anchor length

Calculation for anchorage length of rebar in rock:
Maximum load in anchor bar F = 10.6 kN = 10600 N
Diameter of drill hole d = 20 mm
Compressive strength of rock = 10.1 MPa
Compressive strength of grout = 40 MPa
Ultimate bond stress τ_{ult} = 1/10 (Min of compressive strength of rock and grout) = 1.01 MPa
Working bond strength $\tau = 0.5*\tau_{ult}$ = 0.5 MPa
Required anchor length $L = F /(\pi *d *\tau) = (10600)/(\pi *20*0.5)$ = 337.4mm. Actual minimum anchor length provided is 75mm in plain concrete below foundation + 300mm into rock mass.

Calculation for development length of anchoring rebar into concrete (as per clause 26.2.1, IS 456: 2000)
Design load in anchor bar = 36 kN = 36000 N
Sectional area of rebar (16mm diameter) = 201 sq mm
Stress in rebar σ_s = 36000/201 = 179.1 N/sq mm
Foundation concrete grade M25, Anchor bar grade Fe 500 (deformed bar)
Design bond stress (clause 26.2.1.1) τ_{bd} = 1.6*1.4 = 2.24 N/sq mm
Required development length $L_d = \phi * \sigma_s/ (4*\tau_{bd}) = (16*179.1)/(4*2.24)$ = 319.83mm against which 600mm inserted length into raft concrete is provided.

The revised analysis with ground anchors showed that the maximum load in an anchor is 10.6kN. This provided a factor of safety of 36/10.6 = 3.4 which is found adequate for required margin of safety.

SUMMARY AND CONCLUSION

The component of design presented in this study reflects a typical problem encountered in brownfield site conditions where there are many challenges to construction due to interferences from existing facilities with numerous above and below ground obstructions and restrictions imposed by plant operations. The solution presented for the problem is a case study in application of sound engineering principles to overcome such constraints. This solution enabled the foundation design to be performed with required safety of supported structure and equipment and also to meet the challenges faced by in construction and enable successful implementation of the solution. The modified layout enabled construction to be completed without disturbance to existing utilities, with no shutdown of the road thus maintaining regular operation activities in the plant and without compromise of safety of the construction work. The final layout and details of the rock anchoring scheme are shown in figure 7.

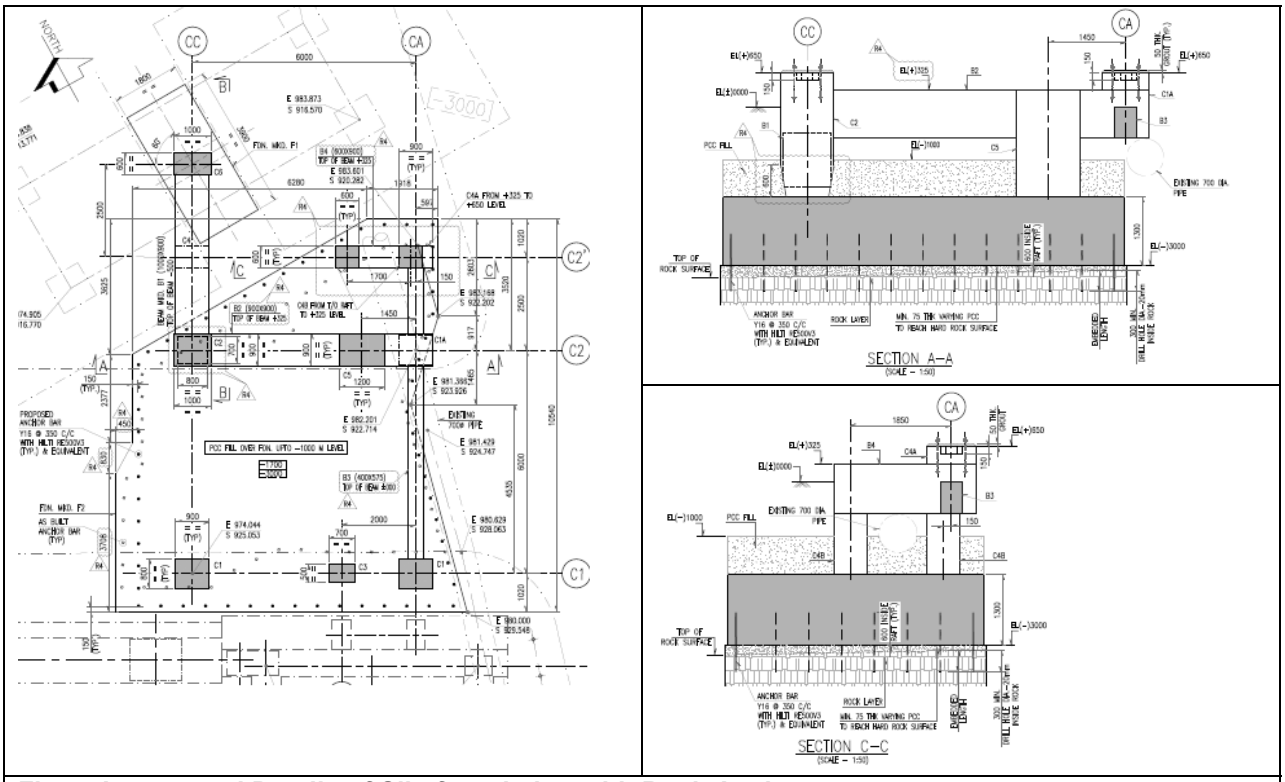


Fig. 7. Layout and Details of Silo foundation with Rock Anchor

ACKNOWLEDGEMENTS

We would like to thank Tata Steel Limited, Jamshedpur, India for facilitating necessary approvals to Tata Consulting Engineers to work as "Consultant" in such a complex project and continuous support on site specific inputs throughout project execution. We would like to thank the Engineering support team of HILTI India Pvt Ltd, Gurgaon, India for design and supply of the anchors and carrying out the field tests at site to verify the pull out load of the anchors.

REFERENCES

US Army Corps of Engineers, Washington, November 1994, Course No. G09-001, Rock Foundations Engineering and Design

Nabil Ismail, January 1982, Design of Shallow Rock-anchored Foundations, Canadian Geotechnical Journal 19(4):463-471

Shi Yan, Bi-Cheng Song, Wei Sun, Han Yan and Qi-Le Yu, 2013, Stress State Analysis on a Rock Anchor RC Foundation of Wind driven Generator, proceedings, World Congress on Advances in Structural Engineering and Mechanics

HYDRAULIC LATERALLY EXTRUDED PILE: A METHOD TO ENHANCE THE BEARING CAPACITY OF PILE

[1] Dinesh Bishnoi, [2]Venkateswarlu.P, [3]Swapnali S. Pawar, [4]Upendra M, [5]Jignesh B. Patel

[1,2,3,4] Post Graduate student, [5]Assistant Professor, Applied mechanics department, SVNIT, Surat, Gujarat, India, Phone Number: [1]+91 8780093039, [2]+91 9904849487, [3]+91 7666469660, [4]+91 8178518767, [5]+91 9725757937.
E-mail:[1]dineshbishnoi664@gmail.com, [2]pvenkateswarlu95@gmail.com, [3]swapnali9660@rediffmail.com, [4]upendarjntuk@gmail.com, [5]jig8107@gmail.com .

ABSTRACT

Constructions of foundation for heavy structure within confined spaces or on the areas which consist of problematic soil is a challenge. Pile foundation is one of the solutions for the mentioned problem but for heavy structures plain pile may be uneconomical. In the present study a new pile (Hydraulically Extrude Pile (HEP)) is proposed, which acts as a plain pile while driving operation and after reaching the desired depth, extrusions along its shaft are embedded in to the soil. These extrusions provide additional bearing resistance to the pile. Plain pile and HEP were tested at three different relative densities (30%, 45% and 60%). The ultimate loads corresponding to 6mm (5 % failure criterion) settlement were determined for both the piles at the above relative densities. The test results show that the HEP provided an increase in capacity of about 37% when compared with plain pile. As the relative density increases, the bearing capacity ratio of HEP and plain pile also increases.

Keywords: Hydraulically Extruded Pile, Bearing capacity, Extrusions

INTRODUCTION

India is one of the fastest developing countries; the construction of heavy infrastructures and high rise buildings is increasing continuously. Construction of foundation to support these heavy structures within confined spaces or on the problematic soil is a challenge. Pile foundation is one of the solutions for the above mentioned problem but for heavy structures, plain pile becomes uneconomical due to wider and longer piles. Thus there is need to enhance the capacity of pile by making some modifications in plain pile.

Considerable research has been conducted on the behavior of helical piles and anchors in various soil conditions using numerical modelling, laboratory and in situ tests (Abdelghany and EI Naggar, 2011; Ghaly et al., 1991; Iskander and Hassan, 1998; Juran and Komornik, 2006; Kurian and Shah, 2009; Livneh and EI Naggar, 2008; Tsuha et al., 2007, 2012; Wang et al., 2013).

Koutsoftas (2002) studied several case histories on high capacity piles in very dense sand. One of the case had tubex piles of 406mm OD, 7.9mm thickness driven to depth of 14m. The results of load test data showed that tubex piles can develop very high capacities and can achieve significant penetrations into dense soils. The greater penetrations allow much higher capacities and compensate for the higher unit costs.Gorasia et. al. (2012) conducted series of tests on ribbed piles having variable rib spacing in kaolin clay. He reported that an increased ultimate bearing capacity can be achieved by modifying the profile of the shaft. There was an increase in capacity of about 3% to 57% for different rib spacing compared with the plain pile. The ribbed piles capacity was shown to be reduced with a large rib spacing (40mm) but consistently increase as the rib spacing was reduced. Furthermore, the difference between the improvement in the 10mm and 20mm spaced ribs was only 1%. This suggests an optimum spacing has been found since the additional work required to install closer spaced ribs only increased the piles

© 2018 Deep Foundations Institute

improvement by a small amount. A wider range of geometries will need to be tested to verify this. Qian et. al. (2017) studied the behavior of ribbed piles under pull-out tests. Both physical and numerical modelling were done to study the effect of S/D ratio in ribbed piles and to know the failure mechanism of ribs. Shear wedges were formed ahead of the ribs and these wedges connect to each other to form larger shear zones around the pile to increase the pile resistance.

Under reamed piles are also efficient in increasing the capacity of the pile. Cai et. al. (2006) performed a series of static load tests to analyze the bearing capacity of bored piles with straight shaft and another with reamed enlargements. He found that compared to a reamed enlargement installed in clay soil, the reamed enlargement installed in sandy soil greatly loosened the soil around pile and resulted in lower value for bearing capacity.

The main objective of the study is to investigate the effect of extrusions on bearing capacity of pile and understand the settlement behavior of hydraulically extruded pile. To compare the results of both the piles (plain and HEP pile) in terms of bearing capacity and check the effectiveness of proposed pile.

About hydraulically extruded pile (HEP)

Considering the findings of the mentioned authors a new pile named as Hydraulically Extruded pile (HEP) is proposed. HEP utilizes the advantage of tubex pile with additional provision of extrusions inside the annular space of pile. HEP acts as a plain pile while driving operation and after reaching the desired depth, extrusions along the shaft are embedded into the soil. These extrusions will provide multiple number of end bearing resistance to the pile and will also densify sand along the shaft due to displacement of sand by them. These extrusions also enable a large part of soil to bear the load and enhance the capacity of the pile. HEP can lead to economical and efficient solution by reduction in length and section of plain pile. In this paper the behavior and ultimate load capacity of HEP is compared with the plain pile. Effectiveness of HEP at different relative densities is also studied.

MATERIALS

Sand

Relatively uniform sand was used in the study.The specific gravity of the soil is 2.611. The particle size distribution is shown in Fig.1 and physical properties of the sand is shown in Table.1.The sand is classified is poorly graded sand (SP) according to USCS classification system. All the tests were performed as per Bureau of Indian Standards (BIS).

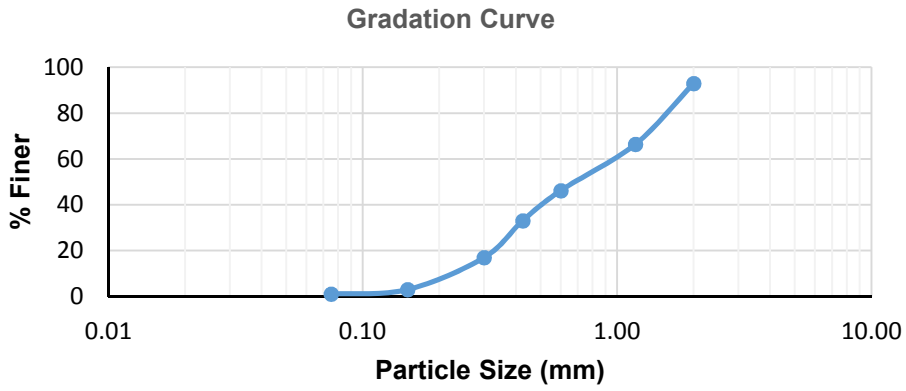


Fig. 1. Particle size distribution curve of the sand

Table 1. Physical properties of soil

Property of sand	Value
Specific Gravity (G)	2.611
Effective size of particle (D10), mm	0.21
Mean size of particle (D50), mm	0.7
Coefficient of uniformity (Cu)	4.76
Coefficient of curvature (Cc)	0.76
USCS classification	SP
Minimum unit weight (γ_{min}), kN/m^3	14.87
Maximum unit weight (γ_{max}), kN/m^3	17.87
Angle of internal friction at 30% Relative density (φ)	28.44
Angle of internal friction at 60% Relative Density (φ)	38.29

Model pile

The model pile used in the study was made up of Poly Vinyl Chloride (PVC) of hollow section. The outer diameter and height of the pipe are 120 mm and 320 mm, respectively. The thickness of pipe is 3mm for both the piles. Two types of pile were used in the present study shown in Fig 2(a). The details of Piles are shown in Table 2.



(a) **(b)**

Fig. 2. (a)Plain pile and hydraulically extruded pile (HEP) with expanded extrusions. (b) Details of HEP.

Pile 1 (Plain Pile) is simple cylindrical in shape with closed end at the end became the simple bearing pile.
Pile 2 (Hydraulically Extruded Pile) consist of an arrangement in the annular space for the provisions of the extrusions. Plastic syringes were used as extrusion material. Total 4 nos. of extrusions were provided in two layers at vertical spacing of 50 mm and 100 mm from the bottom of the pile as shown in Fig. 2(b). The length of extrusions embedded into the sand was 55mm from the face of the pile.

Table 2. Details of piles

	Total Length (mm)	Effective Length (mm)	Outer Diameter (mm)	Thickness (mm)	Provision of extrusions
Pile 1	320	270	120	3	No
Pile 2	320	270	120	3	Yes

Model box

A cubical box of size 600mm×600mm×600mm (shown in Fig. 3) was prepared to conduct model compressive test on piles. The dimensions of the box were selected by considering the boundary effects from the pile. Three sides were made up of steel plates (1.02mm thickness) and fourth side was made up of acrylic glass sheet (6mm thickness) to check the relative density distribution throughout the depth.



Fig.3 Model box used for the present study

METHODOLOGY

The sand was placed in the box by rainfall technique to achieve constant relative density throughout the depth. Several trials were performed on mould of capacity 3000×10^3 mm^3 from heights of 50mm, 250mm, 450mm, and 650mm through a sand pouring jar having 20mm diameter hole. The respective relative densities obtained were 30%, 53%, 65%, and 73%. Back computations were done to determine the height of fall for relative density of 30%, 45% and 60%. The height of fall, relative density, unit weight and angle of internal friction is presented in Table 3.

Table 3. Height of fall for different relative densities

Relative density (%)	Height of free fall (cm)	Unit weight of soil (kN/m^3)	Angle of friction (φ)
30	5	15.69	34.67
45	17.5	15.98	36.25
60	36.31	16.54	37.17

Preparation of sand bed

Constant heights were maintained while filling the tank to achieve respective relative densities uniformly throughout the depth. Proper care has been taken for the preparation of sand bed. The top of the sand bed was leveled and checked with level tube. The surface of the sand bed is horizontal. Inclined sand bed may cause the pile installation in tilting with horizontal line. The sand was filled in the box up to height of 500 mm by rainfall technique besides the loading frame.

Installation of pile

After the completion of sand bed, the pile is driven into the sand up to depth of 270 mm from top of sand with the help of hammer driving. The weight of the hammer is 3.5 kg and the height of free fall is 300 mm. The blows were given to the pile by placing cover steel plated at the top of the pile. Blows were given at the center of the pile at constant rate. Total number of blows required to penetrate the pile into the sand were vary from relative densities. For 30 %, 45 % and 60 % relative densities the average numbers of blows are 70, 90, and 110 respectively. For the plain pile and hydraulic pile after the installation of pile the entire model box pushed on center to the loading frame. For hydraulic pile, before applying load the extrusions were pushed out into the sand by hydraulic pressure at outside one by one starting from bottom extrusion.

TESTING PROGRAM



Fig. 4. Details of the test set-up assembly used for performing compressive tests on piles

Total six numbers of tests were performed on both the plain and hydraulic pile. After installing the pile into the prepared sand bed, the model box along with pile was centered to the loading frame to apply compressive load to the pile. First loading shank is connected to the load cell and load cell connected to the metal rod of 50 mm diameter to transfer the load to the pile as shown in the figure 3. The pile was instrumented with a multi-speed loading frame having load cell of 1-ton capacity with precision of 1kg, was used to perform compressive tests on the piles. A linear variable displacement transducer (LVDT) having precision up to ±0.01mm were used to measure the settlement of the pile. Loads were recorded at an interval of 0.02 mm settlement. The load was applied to the pile at a strain rate of 2.2 mm/min. The whole set-up is shown in Fig. 4.

RESULTS AND DISCUSSIONS

A total of six numbers of compressive tests were performed using the above mentioned box and loading frame. Three tests were performed with the plain pile and three tests were performed on the hydraulically extruded pile at relative densities of 30%, 45% and 60%.

Loading and displacement relationship

The Load-Settlement behaviors of both the piles at three different relative densities were shown in Figs. 5, 6, and 7. From the plots, observed that the load taken by the Hydraulically Extruded Pile (HEP) is significantly higher than the plain pile for all the three relative densities. The increase in capacity of pile is due to the contributions from the embedded extrusions into the soil. These extrusions provide additional multiple numbers of end bearing resistance to the pile thus enhancing its capacity.

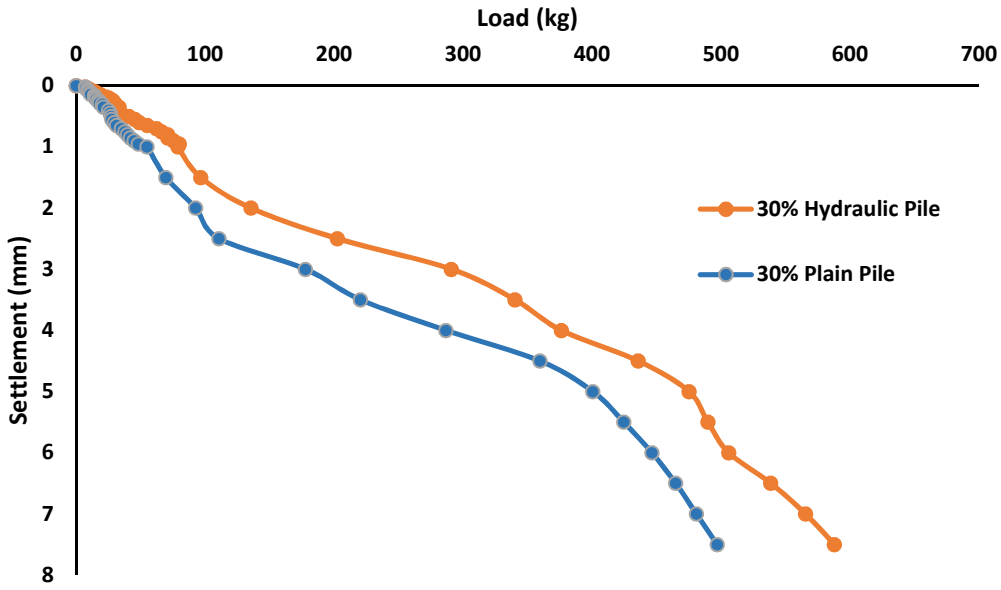


Fig. 5 Load-settlement behavior of plain pile and HEP at 30% relative density

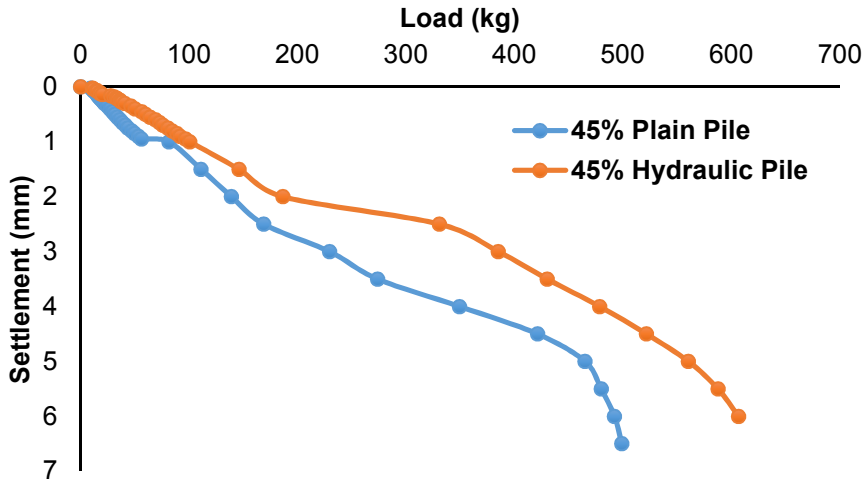


Fig. 6. Load-settlement behavior of plain pile and HEP at 45% relative density

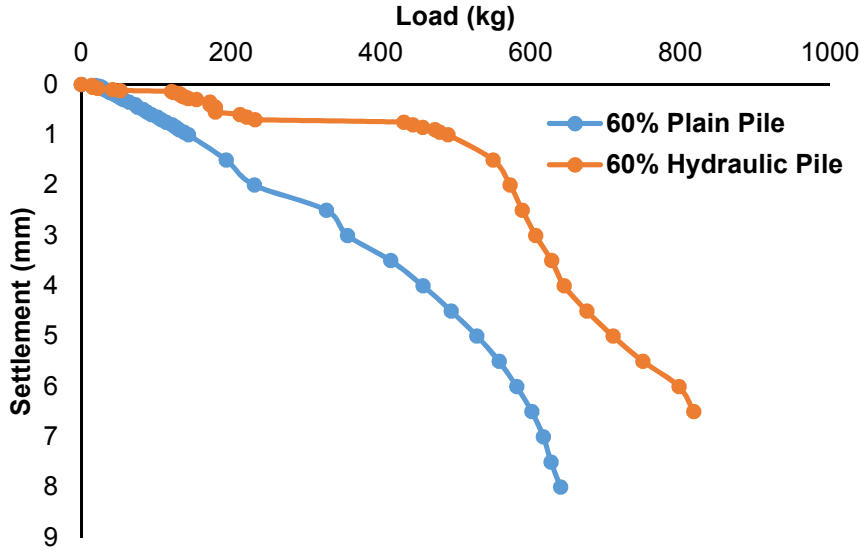


Fig. 7. Load-settlement behavior of plain pile and HEP at 60% relative density

Fig. 8 shows the load taken by HEP and plain pile for all three different relative densities corresponding to a settlement of 6mm. The 6mm settlement criterion was selected (5% failure criterion, Mohajerani 2016) which is 5 % of the pile diameter. It was observed that with the increase in relative density the capacity of both the pile increases but the increase in HEP is significantly higher than the plain pile. Table 4 summarizes the load corresponding to 6mm settlement for both the piles. The percentage increase in capacity of HEP over plain pile increases from 13.3% to 37.25 % at 30% and 60 % relative density, respectively.

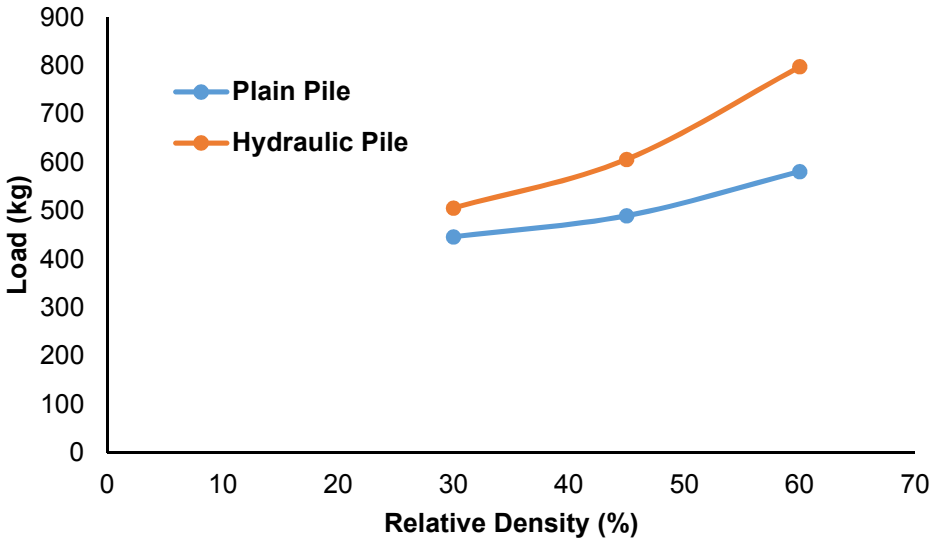


Fig. 8. Load taken by plain pile and HEP corresponding to 6mm settlement at 30%, 45% and 60% relative density

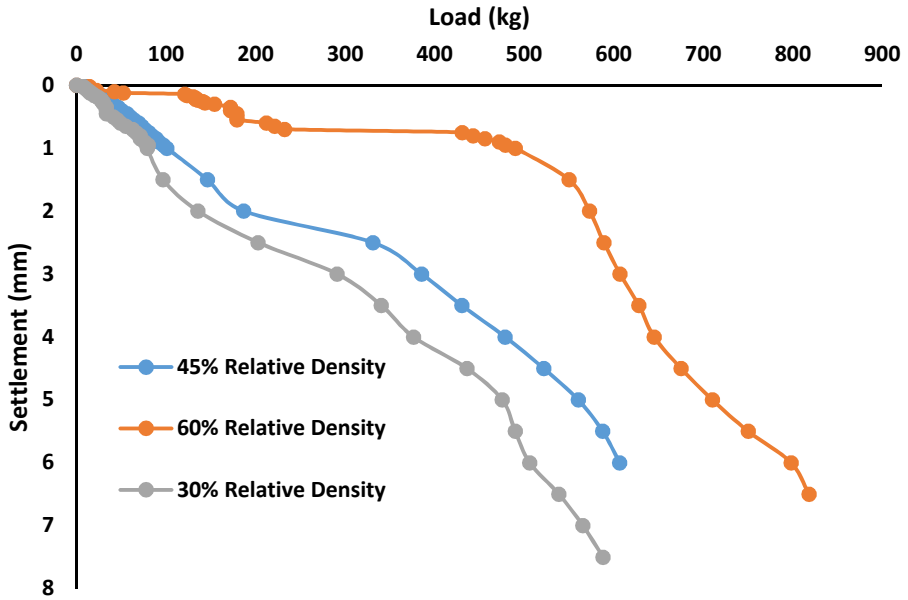


Fig. 9. Load-settlement behavior of HEP at three different relative densities

From Fig. 9 shows that there is a critical settlement after which the extrusions contribute to the load capacity of the pile. For 45% and 60%, the critical settlement is 2mm and 0.8mm respectively. For 30% relative density, no critical settlement is observed. After critical settlement, the pile takes significantly high loads and also prevents the settlement of pile up to some extent. Further settlement of the pile causes HEP to behave similar to plain pile.

Table 4. Test results of Hydraulically Extruded Pile and Plain pile

Relative Density	Load (kg)		% Increase
	Plain pile	Hydraulic Pile	
30	446.5	506	13.33
45	490	606.5	23.78
60	581.4	798	37.25

CONCLUSIONS AND DISCUSSION

Comparative study of hydraulically extruded pile and plain pile was done in the present paper. Effectiveness of HEP over plain pile was studied by performing small scale physical model tests. The modelling results provided the following findings:

i. By providing extrusions, the bearing capacity of pile can be increased significantly compared to plain pile. These extrusions provide additional multiple number of end bearing resistance to the pile.
ii. The load carrying capacity of HEP increases with the increase in relative density of sand. At 60% relative density there was increase of 37.25% in bearing capacity of HEP over plain pile.
iii. The tests showed that there was a critical settlement of pile after which the extrusions becomes active and started taking load. After the critical settlement, there is considerable reduction in further settlement of pile.

Thus with the modification in the geometry of pile its bearing capacity can be increased significantly. It is noted that the above findings and conclusions were made based on the PVC pile and plastic extrusions. Further tests need to be carried out with different pile material and stiffer extrusion material. The effect of shape and spacing of extrusions can be studied so that the extrusions can be utilized fully.

ACKNOWLEDGMENTS

The technical support from the Sardar Vallabhbhai National Institute of Technology (SVNIT) laboratory is gratefully acknowledged.

REFERENCES

Abdelghany Y and El Naggar H (2011). Steel fibers reinforced grouted and fiber reinforced polymer helical screw piles – a new dimension for deep foundations seismic performance. In Geo-Frontiers 2011: Advances in Geotechnical Engineering (Han J and Alzamora DE (eds)). ASCE, Reston, VA, USA, Geotechnical Special Publication no. 211, pp. 103–112.

Demetrious, C.K., 2002. High capacity piles in very dense sands. ASCE International deep foundation congress, February 14-16, 2002, Orlando, Florida, United States.

Gorasia, R.J., McNamara, A.M., 2012. High shear capacity ribbed piles. Proceedings of the Institute of Civil Engineers: Geotechnical Engineering, 169(3), p.p. 264-275.

Ghaly A, Hanna A and Hanna M (1991). Uplift behavior of screw anchors in sand. I: dry sand. Journal of Geotechnical Engineering 117(5): 773–793.

Indian Standard (1980). IS 2720: 3: Sec 2Methods of test for soils - Part 3: Determination of Specific Gravity-Section 2:Fine, Medium and Coarse Grained Soils. Bureau of Indian Standards, New Delhi, India.

Indian Standard (1983). IS 2720:14Methods of test for soils - Part 14: determination of density index (relative density) of cohesionless soils. Bureau of Indian Standards, New Delhi, India.

Indian Standard (1985). IS 2720:4 Methods of test for soils - Part 4: grain size analysis. Bureau of Indian Standards, New Delhi, India.

Indian Standard (1986). IS 2720:13Methods of test for soils - Part 13: direct shear test. Bureau of Indian Standards, New Delhi, India.

Iskander M and Hassan M (1998). State of the practice review: FRP composite piling. Journal of Composites for Construction, ASCE 2(3): 116–120.

Juran I and Komornik U (2006). Behavior of Fiber-Reinforced Polymer Composite Piles under Vertical Loads. U.S. Department of Transportation, Federal Highway Administration, Washington, DC, USA, Publication No. FHWA-HRT-04-107.

Kurian NP and Shah SJ (2009). Studies on the behaviour of screw piles by the finite element method. Canadian Geotechnical Journal 46(6): 627–638.

L. Cai, Y. Li, H. Zhou, 2006. Discussion on the bearing capacity of bored pile with reamed enlargements. ASCE, Geoshanghai International Conference 2006, June 6-8, 2006. Shanghai, China.
Mohajerani , A., Bosnjak, D. and Bromwich D., 2016. Analysis and design methods of screw piles: A review. Soils and Foudations © The Japanese Geotechnical Society, 56(1):115-128

Livneh B and El Naggar MH (2008). Axial testing and numerical modeling of square shaft helical piles under compressive and tensile loading. Canadian Geotechnical Journal 45(8): 1142–1155.

Mohajerani , A., Bosnjak, D. and Bromwich D., (2016). Analysis and design methods of screw piles: A review. Soils and Foudations © The Japanese Geotechnical Society, 56(1):115-128.

Qian, Gao, Wang, Xue, Huang, 2017. Physical and numerical pull-out modelling of ribbed piles. Proceeding of the Institute of Civil Engineers: Geotechnical Engineering, 170, February 2017 Issue GE/ pages 51-61.

Tsuha CHC, Aoki N, Rault G, Thorel L and Garnier J (2012) Evaluation of the efficiencies of helical anchor plates in sand by centrifuge model tests. Canadian Geotechnical Journal 49(9): 1102–1114.

Wang D, Merifield RS and Gaudin C (2013). Uplift behavior of helical anchors in clay. Canadian Geotechnical Journal 50(6): 575–584.

JET GROUTED COLUMNS-GROUND IMPROVEMENT FOR LIQUEFACTION RESISTANCE – A CASE STUDY

Jibi C Yohannan, Va Tech Wabag, India, Email: c_jibiyohannan@wabag.in
Viswanathan N, Va Tech Wabag, India, Email: n_viswanathan@wabag.in
Miguel Dimadura, SEGCON, Philippines, Email: dimaduramiguel@gmail.com

ABSTRACT

This paper presents a case study of soil treatment carried out to mitigate liquefaction potential of the site for a Sewage Treatment Plant at Tunasan, Muntinlupa City, Philippines. The assessment was carried out using LiquefyPro software to determine the liquefaction potential and estimated settlement of soil deposit due to seismic loads of PGA 0.71g. Design approach using Baez (Advances in the Design of Vibro Systems for the Improvement of Liquefaction Resistance) was followed using the stress concentration criteria to eventually co-relate to a new factor of safety for the improved site with jet grouted columns. After installation, using high pressure jet injection system, cores were taken to evaluate the diameter formed and the compressive strength of the soil cement columns to validate the design.

Keywords: Liquefaction, Ground improvement, Jet Grout columns,

INTRODUCTION

The site for proposed sewage treatment plant is situated south of Magdaong River and adjacent to Muntinlupa Science High School, Tunasan, Philippines. (Fig-1) The city, in general, is underlain by alluvium (Holocene), marine and terrestrial sediments (Pilocene-Pleistocene), and volcanic piedmont deposits (Pliocene- Quartenary) Alluvium deposits on the east side of the area are basically from deposition of sediments as the river streams following into Laguna Lake. Nearest seismic source is the West Valley Fault (WVF), a type A source, located well with in 5km distance, and to the east of the project (Fig-2).



Fig-1. Site Location



Fig-2. West Valley Fault

A Seismic hazard assessment study was conducted to establish design acceleration parameters corresponding to the Maximum Considered Earthquake (MCE) as defined in ACI 350.3.06 by GEOSEED. Results of the site spectra were then compared with code (NSCP-2010) spectra and concluded a high PGA 0.71g.

© 2018 Deep Foundations Institute

The results of the geotechnical investigation shows that the site is underlain by loose sands and silts, interspersed with medium stiff to stiff clay. Considering the location of the area near the lake shore, and the proximity of a seismic source capable of generating high-magnitude earthquakes, it is evident that the loose to medium dense sands (SPT N-value = 4 to 27) within the site subsurface are susceptible to liquefaction. Liquefaction analysis considering SPT data was undertaken using LiquefyPro software. This is based on the most recent methods recommended by the National Center for Earthquake Engineering Research (NCEER) Workshop on Liquefaction and Special Publication 117 (Guidelines in Analyzing and Mitigating Liquefaction in California).

PRE-TREATMENT AND POST-TREATMENT LIQUEFACTION ANALYSES

The objective is to determine the extent of material prone to strength loss with seismic loading, and to estimate the induced settlement in the event of an earthquake. The analysis is directed to implement the findings from soil investigations conducted and the subsequent Probabilistic Seismic Hazard Analysis. To expedite the calculations, LiquefyPro v.5 (Civil Tech) was used. The program determines the liquefaction potential and estimated settlement of soil deposit due to seismic loads. The evaluation requires the input mainly of CPT, BPT or SPT data, design earthquake parameters, groundwater location, and soil classification. The PGA value for liquefaction potential is calculated using 100% code-based response spectra (NSCP 2010). The calculated PGA value of 0.5676g, which is based on the zero (0) time period, is then multiplied by an importance factor of 1.25 resulting to a PGA value of 0.71g. The Factor of Safety (FS) for liquefaction potential is calculated as the ratio of the Cyclic Resistance Ratio (CRR) to the Cyclic Stress Ratio (CSR). Liquefaction-induced settlements are based on the Ishihara and Yoshimine (1990). (FS = CRR M / CSR fs).

SOIL PROFILE

The soil profile for borehole BH-3 as presented hereunder (Fig-3b). The first 9m is composed of sand. Except for the 1.5m intervening sand layer, the material from Elev. -9.0m to -22.5m is composed of silt. Its consistency varies from stiff to very stiff whereby the PI is larger than 18 up to around 18m. The lower layering is a sequence of alternating layers of sand and silt. Groundwater table is measured at around 0.3m below the natural grade line.

LIQUEFACTION ANALYSES

Liquefaction analyses are typically done on the upper 15m strata as per earlier methods by Seed and Idriss (1971), with the procedure even extendable to 20m depth. In practice, liquefaction investigation beyond 24m are generally waived due to limitations of both empirical and detailed modelling methods, known decreased impact with depth and difficulties of mitigating deep liquefaction. For this study, the depth of analysis was limited to 20m.

For the required program input (LiquefyPro v.5), the following information, including the document sourced, are as follow:

1. SPT N values, Groundwater Location and Soil Classification from Geotechnical Investigation Report Proposed Tunasan STP Project
2. Peak Ground Acceleration - 0.71g
3. Moment Magnitude – 7.2 by the West Valley Fault
4. Overburden pressure – given by H of fill, with the net foundation load converted to an equivalent soil height.
5. Soil Unit Weight – total unit weight of soil. To facilitate data entry, an average value of 19 kN/m3 was used globally.

6. Fines % - percentage of soil passing No. 200 sieve (Grain Size Analysis, Final Report). This value is used to correct the cyclic resistance of the soil known to increases due to the presence of fine grained material.

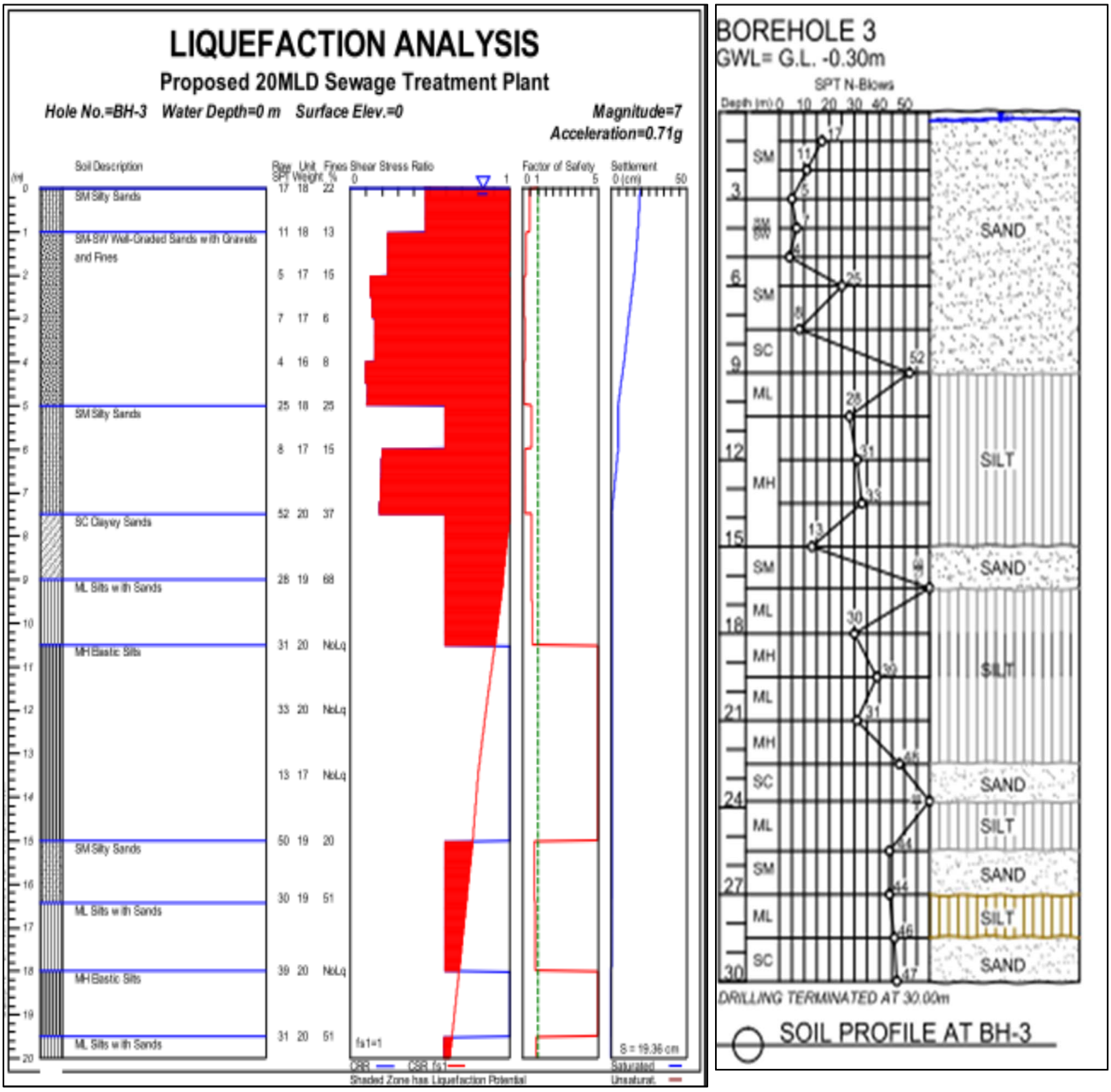


Fig. 3 (a) **Pre Treatment Liquefaction Analysis Graph,** (b) **Bore log of BH-3**

LIQUFACTION ANALYSIS FINDINGS

Based on the parameters and soil information used, the location of liquefiable material and the estimated induced settlement are as plotted in Fig. 3a for BH number 3. Areas with Factor of Safety less than 1.0 are deemed liquefiable in the event of an M7.2 earthquake by the West Valley Fault. For BH3, liquefiable material is generally confined between -3.0m to -20.0m.

However, since the induced settlement of the stretch from -9.0m and below is only 2.5cm and its effect at the upper layer could be curbed by arching effect and distance, this lower liquefiable layer shall be left untreated. Further, if PI>18 is invoked as non-liquefiable (Bray), the layers from -9.0m to -15.0m would not yield to any settlement. As such, the liquefiable layer that needs soil treatment is from -3.m to -9.0m. The summary of liquefaction analysis and computed settlement (averaged values 7.52 to 19.36cm) of various boreholes are tabulated below. (Table-1).

Table 1. Average computed settlement for various boreholes

Borehole	*Average Liquefiable Depth Region*, m*	*Average Computed Settlements, cm*
BH-1	0.0 – 4.0 / 5.0 – 6.0 / 7.5 – 9.0 / 13.5 – 20.0	12.91
BH-2	0.0 – 4.0 / 5.0 – 10.5 / 12 – 19.5	15.07
BH-3	0.0 – 10.5 / 15.0 – 18.0 / 19.5 – 20.0	19.36
BH-4	0.0 – 5.0 / 7.5 – 9.0 / 15.0 – 18 / 19.5 – 20.0	7.52
BH-5	0.0 – 5.0 / 7.5 – 13.5 / 15.0 – 18.0 / 19.5 – 20.0	13.98

OPTIONS STUDIED TO MITIGATE LIQUEFACTION

Following three options were considered for mitigation-

- Stone columns
- Pile
- Jet grouted column or Deep cement mixing

Based on economy of the method, Stone columns were found the most economical and Piles of high cost. The final option was guided by:

- Soil profile
- Local equipment availability,
- Pre and post installation and test regime procedures for similar ground improvement techniques,
- Economic considerations.

Depending on the specific site condition and method of installation few options were more influential than others. In the case of low permeability silty soils not densifiable by the action of vibrations from the stone, the stress concentration criterion would be more relevant for a viable solution. Considering the above Jet grout columns were finally chosen.

DESIGN APPROACH ON JET-GROUTED COLUMNS TO MITIGATE LIQUEFACTION

Based on the paper of Baez (*Advances in the Design of Vibro Systems for the Improvement of Liquefaction Resistance*), the rigidity property of the vibro-concrete columns and its stress concentration criterion can be applied to the jet-grouted columns. As such, the design for stress concentration criterion (no densification and drainage) has been followed for the design of jet-grouted column system. Shear modulus ratio (G_r) is calculated as the proportion between the shear modulus of jet grout column (G_{jg}) and the shear modulus of the surrounding soil (G_s). ($G_r = G_{jg} / G_{s)}$. Area replacement ratio, (A_r) is taken as the ratio of Area of jet grout columns (A_{gc}) to that of total area (A). ($A_r = A_{gc} / A$). The recommended reduction factor (function of area replacement ratio and shear modulus ratio) is applied to the CSR (cyclic stress ratio) in the pre-treatment liquefaction analysis and subsequently a new factor of safety is obtained. Average soil modulus of elasticity, E_s of surrounded soil is taken as15 kPa. Average modulus of elasticity of column is taken as 1500 kPa.

The shear stresses of the columns are calculated whereby the maximum shear stress of the former liquefiable layers serves as a control for the establishment of the required shear strength of the column.

The column shear stresses are the soil shear stresses (calculated in the LiquefyPro program) multiplied by the modular ratio and reduction factor.

The spacing and diameter of columns selected such a way that the liquefiable layers are no longer liquefiable after the installation of the columns. In order to fulfil the liquefaction mitigation and allowable column stress, the square spacing of 1.7m has been selected with column diameter of 0.8m.

A sample of the calculation for the Pre and Post Factor of safety for few layers is attached in Table-2 below.

Table-2. Factor of Safety Pre-Treatment (FS) and Factor Safety Post-Treatment (FS1)

Depth	CRR	CSR	FS	Judgment	CSR1	FS1	Judgment1	σ, kPa	τ, kPa	τsc, kPa
8.18	0.33	0.72	0.46	Liq	0.1672609	1.9729651	Non-Liq	121.1847	87.252984	405.38934
8.2	0.33	0.72	0.46	Liq	0.1672609	1.9729651	Non-Liq	121.38735	87.398892	406.06725
8.23	0.33	0.72	0.46	Liq	0.1672609	1.9729651	Non-Liq	121.59	87.5448	406.74516
8.25	0.33	0.72	0.46	Liq	0.1672609	1.9729651	Non-Liq	121.79265	87.690708	407.42307
8.28	0.33	0.72	0.45	Liq	0.1672609	1.9729651	Non-Liq	121.9953	87.836616	408.10098
8.3	0.33	0.72	0.45	Liq	0.1672609	1.9729651	Non-Liq	122.19795	87.982524	408.77889
8.33	0.32	0.72	0.45	Liq	0.1672609	1.9131783	Non-Liq	122.4006	88.128432	409.45679
8.35	0.32	0.72	0.45	Liq	0.1672609	1.9131783	Non-Liq	122.704575	88.347294	410.47366
8.38	0.32	0.72	0.45	Liq	0.1672609	1.9131783	Non-Liq	122.907225	88.493202	411.15157
8.4	0.32	0.72	0.45	Liq	0.1672609	1.9131783	Non-Liq	123.109875	88.63911	411.82947
8.43	0.32	0.72	0.45	Liq	0.1672609	1.9131783	Non-Liq	123.312525	88.785018	412.50738
8.45	0.32	0.72	0.45	Liq	0.1672609	1.9131783	Non-Liq	123.515175	88.930926	413.18529
8.48	0.32	0.72	0.45	Liq	0.1672609	1.9131783	Non-Liq	123.717825	89.076834	413.8632
8.5	0.34	0.72	0.47	Liq	0.1672609	2.0327519	Non-Liq	123.920475	89.222742	414.54111

Maximum shear stress in the Jet columns was found to be around 510 kpa. Hence the Shear strength of the installed Jet columns needs to be more than this value. The shear strength is taken as 20% of the UCS. Expected UCS of jet grout columns ranges from around 1.75 MPa to 3.0m MPa, reflecting the increasing strength properties of the soil with depth and which is verified at site by testing drilled core of finished columns. Hence the shear strength varied from 0.2x UCS, i.e., 350 kPa to 600 kPa. For the installed jet columns UCS were carried out on extracted core samples.

INSTALLATION

Figures 4 to 8 shows various sequence of work related to installation and testing.

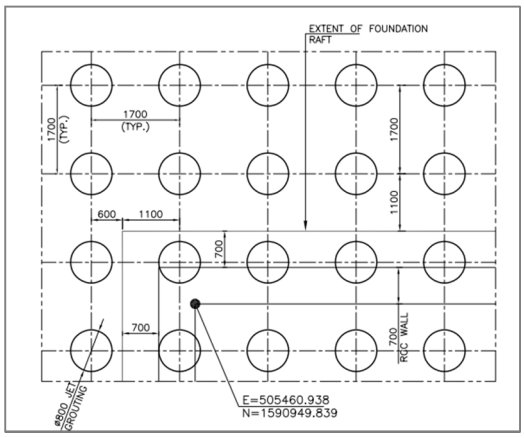


Fig-4- Layout (Part)- Jet grout columns



Fig-5 Jet grout columns under installation



Fig-6- Installed Jet column diameter measurement



Fig-7 Cores Extracted from Jet grout columns

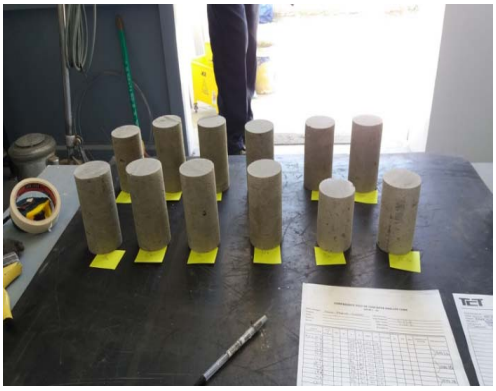


Fig-8- Cores prepared for UCS testing



Fig-9-Tested cores

FIELD TEST AND PERFORMANCE ACCEPTANCE CRITERIA

In order to verify the design assumptions, trial tests are conducted after installation of jet-grouted columns and performance of specific checks. The important factors verified are the Unconfined Compression Strength (UCS) value and achieved diameter of the columns. For the determination of the material strength of the jet-grouted columns achieved in the prevailing site conditions as well as the achieved diameter, coring of the columns after the curing period and sampling of cored samples were undertaken. The cored samples taken at specified depths brought to the laboratory for unconfined compression tests.

For UCS Strength check
After a curing period of at least 10 days, coring through the entire length carried out. Four (4) cored samples taken from the depths at the centre (or near centre if the central tube is placed for injection process) of the column –which would represent each quarter of the whole length. The samples would be drawn from the centre of each quarter. These shall be brought to the material laboratory for Unconfined Compression Test. Diameter of cores to be 50mm.

Acceptance Strength Criteria, UCS
As the shear strength is taken is 0.2 of the UCS, the test results should ideally have this magnitude for the particular depth as reflected in the liquefaction analysis. Core samples prepared and tested as per ASTM C42 and core strength results shall be stated with due corrections done for height/diameter ratio as per ASTM C42. Equivalent cylinder strength for UCS = UCS(Test) = Core Test strength/0.85. The above, UCS (Test), found more than the UCS (Design), i.e, design strength for the representative quarter.

Diameter Size Inspection
The diameter size sufficiency can be verified by coring through the column at an internal position tangent with the circumference of a 0.8m-column at 2 positions diametrically opposite. This coring is only to validate the formation of diameter of the columns. Diameter of cores to be 50mm.

Acceptance Minimum Diameter Size
Achieved diameter size shall be assessed based on the continuity and quality of the cored materials. Should there be a decrease in size, the top layers can be excavated to visually inspect the extent of the jet-grouting and further evaluation shall be made.

Visual Inspection of column
Likewise, for these trial positions, excavation shall be carried out around the 2 positions until a safe depth of around 2 to 3 meters. Hence, inspection at the upper portion should be sufficient.

Table-3- Required design UCS values for each quarter along length of Jet column

Test Quarter	Tc=Shear strength as per Design- kPa	UCS as per design = Tc/0.2 kPa
1	300	1500
2	390	1950
3	460	2300
4	510	2550

Tested cores met the design requirement of UCS values and thus the shear strengths.

CONCLUSION

Jet grout columns of 0.8m diameter with length varying from 8.0 m to 15.0m with square grid spacing of 1.7m X 1.7m was proposed for various units based on the structure loading and soil profile. The resulting design area replacement ratio satisfied both liquefaction mitigation and shear strength requirements as well as settlement criterion under normal conditions. The design parameters were verified at site after completion of jet grouting column installation for the column diameter, UCS. The results showed that the tested cores of the Jet grouted columns met the design requirement for the UCS and thus the shear strength of Jet grouted columns. The ground improvement thus followed using the concept of "Stress concentration" (no densification and no drainage) as evolved by Baez were found to provide the solution toward liquefaction mitigation due to the increased shear strength of the composite sub soil.

ACKNOWEDGEMENTS

The authors would like to acknowledge the appreciation to M/s Bauer Foundations Philippines, M/s Wabag Philippines site team and support staff who successfully delivered this project and M/s SEGCON Philippines, M/s ARUP Philippines for their technical assistance.

REFERENCES

Baez, J.I. and Martin, G.R. (1993) Advances in the design of Vibro-systems for improvement of liquefaction resistance. Proceedings of the Symposium on Ground Improvement, Canadian Geotechnical Society, Vancouver

Youd, T.L et al, (1997), NCEER workshop on evaluation of liquefaction resistance of soils, National Center for Earthquake Engineering Research Technical Report NCEER-97-0022, p. 276

ACI 350.3-06 Seismic Design of Liquid-Containing Concrete Structures and Commentary

NSCP-2010 National Structural Code of the Philippines

GEOSEED Report- Site Specific MCE Seismic Design Parameters for the 20 MLD Muntinlupa STP, Tunasan, Metro Manila

Geo-Institute of ASCE, Grouting Committee, Jet Grouting Task Force- Jet Grouting Guideline

MITIGATION OF LIQUEFACTION POTENTIAL USING VIBRO COMPACTION

Tanmay Gupta, Keller Ground Engineering India Pvt. Ltd., Mumbai, Maharashtra, India, +91-8828231006, tanmay@kellerindia.com
Madan K. Annam, Keller Ground Engineering India Pvt. Ltd., Mumbai, Maharashtra, India, +91-8754509036, madankumar@kellerindia.com
Valluri Sridhar, Keller Ground Engineering India Pvt. Ltd., Mumbai, Maharashtra, India, +91-9967063113, sridhar@kellerindia.com

ABSTRACT

Earthquakes are one of the most disastrous natural event. It remains an area of research to predict the earthquakes, but always there is room for learnings from the earthquakes. One such risk is the liquefaction potential of soils in loose sand deposits with shallow ground water table. Addressing liquefaction mitigation in foundation design is one of the greatest challenges for practicing foundation engineer. The mitigation of liquefaction potential could be achieved by several methods predominantly with vibro compaction or dynamic compaction and vibro stone columns etc. The work in this study highlights the liquefaction evaluation procedure and its mitigation using vibro compaction. Soil investigation works using eCPTs were conducted before the start of the works to evaluate the seismic vulnerability of soil in terms of liquefaction potential. Field trials were conducted at site to arrive at optimum design of vibro compaction. High quality control using computerized output was monitored to achieve the required compaction of the soil. The amount of backfill required resulting from subsidence of surface was recorded to ensure the effectiveness of vibro compaction work. After ground improvement, soil investigation works were conducted to assess efficacy of vibro compaction. Subsequently, full size plate load tests were conducted to check the improved load settlement characteristics of improved ground. Based on the findings of this study, vibro compaction proved as an effective ground improvement technique to mitigate the liquefaction potential of soil, especially in loose sandy deposits.

Keywords: Earthquake, Liquefaction, Vibro Compaction, Ground Improvement

INTRODUCTION

Liquefaction is the phenomenon where soil loses its stiffness and starts to behave like a liquid. Cohesionless soil deposits present in seismically active zone with shallow ground water table possess a risk of liquefaction. Disastrous earthquakes like Niigata (1964), Christchurch (2011), Bhuj (2001), etc. have prompted practicing engineers to address the stability of structure during and after the earthquakes.

The design of foundations in such areas shall address the mitigation of liquefaction potential. This paper, in its first part addresses the methodology of evaluation of liquefaction potential of soil according to IS 1893: 2016, is covered. After evaluation of liquefaction potential, ground improvement using vibro compaction is discussed to mitigate the liquefaction potential (Belani et al. 2003). Finally, a case study is presented where liquefaction potential was evaluated and subsequently mitigated using vibro compaction. The case study is selected from an industrial plant located in North Eastern India.

LIQUEFACTION EVALUATION AND MITIGATION

Liquefaction evaluation is a field of ongoing developments (Idriss et al. 2014, Seed et al. 2003). It is likely to be triggered when loose saturated cohesionless soil experiences cyclic stresses. Liquefaction triggering depends on intensity and duration of cyclic loading, soil *in-situ* density and the presence of ground water table.

© 2018 Deep Foundations Institute

The current study deals with the simplified procedure mentioned in IS 1893: 2016 for evaluation of liquefaction potential. The liquefaction evaluation is based on the calculation of factor of safety. The factor of safety against liquefaction is the ratio of resisting force to driving force. The resisting force is a function of the soil stiffness and driving force is a function of earthquake characteristics.

The resisting force of soil is evaluated in terms of CRR (Cyclic Resistance Ratio). CRR is the ratio of soil's capacity against liquefaction to the initial effective stress. CRR is calculated from *in-situ* soil investigation tests like cone penetration test (CPT), standard penetration test (SPT) with grain size distribution and shear wave velocity test. This paper is focused on evaluation of liquefaction potential using cone penetration data.

The driving force is evaluated in terms of CSR (Cyclic Stress Ratio). CSR is the ratio of earthquake driven shear stress to the initial effective stress. CSR is calculated for an expected ground acceleration (a_{max}) and earthquake magnitude. Following section presents stepwise procedure to evaluate the liquefiable depth based on guidelines recommended by IS 1893 (2016).

Factor of safety (FOS) is calculated as CRR/CSR. The final output from liquefaction evaluation is the liquefiable depth of soil deposit. Liquefiable depth is defined as the depth beyond which FOS is greater than or equal to 1. The detailed flowchart for evaluation of liquefaction potential is presented in Fig. 1. After evaluation of liquefiable depth based on these guidelines, next challenge is to mitigate the liquefaction potential of soil.

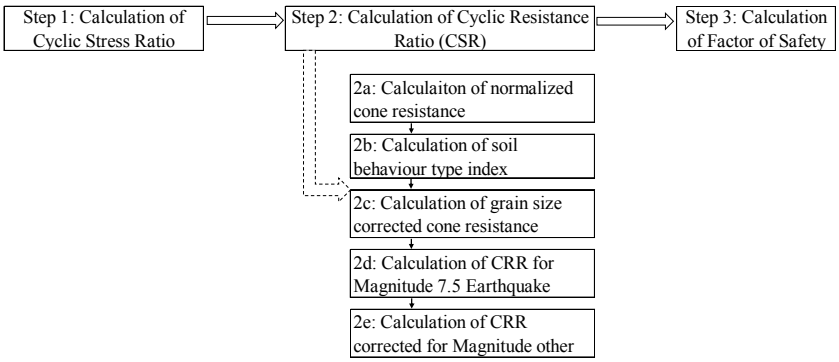


Fig. 1. Flow chart for evaluation of liquefaction potential

Mitigation of Liquefaction

There are three key terms in definition of liquefaction as described earlier. These are loose, saturated and earthquake loading (cyclic stress on soil). The mitigation of liquefaction could be achieved by addressing any one of these three parameters (Ground Improvement Committee 2013; Belani et al. 2013; Seed et al. 2003).

- Densification of loose deposit to required level shall mitigate the liquefaction potential (Baez et al. 1993; Annam et al. 2012)

- Providing drainage path in form of earthquake drains shall inhibit the build-up of pore pressure. Pore water pressures in saturated cohesionless soils when become equal or close to applied stress, causes zero or very low effective stress which is termed as liquefaction. These drainage paths will not allow pore water pressure to rise up beyond certain level which shall mitigate the liquefaction potential of soil (Baez et al. 1992; Murali Krishna et al. 2018; Seed et al. 1976).

- Reinforcing the soil with higher stiffness elements. These higher stiffness elements will share certain part of earthquake stress resulting in reduced earthquake stress on soil (Priebe 1995; Kirsch et al. 2017).

This paper deals with the densification of the loose sand deposits to mitigate the liquefaction potential. One of the means to achieve densification is vibro compaction which is discussed in detail in next section.

GROUND IMPROVEMENT USING VIBRO COMPACTION

As discussed in previous section, one of the measures to mitigate the liquefaction potential of soil is to densify the loose sand deposits. The target densification requirement shall be based on factor of safety evaluated from the liquefaction evaluation procedure. The soil is said to be non-liquefiable if factor of safety post improvement is greater than or equal to 1.

Ground improvement using vibro compaction increases the resistance of the soil towards liquefaction. This process causes the rearrangement of soil particles in denser configuration. Unlike surface compaction, vibro compaction generates horizontal forces at required depth. This is particularly advantageous when design depth is more than the influence zone of surface compaction. In this process, a vibrating probe is penetrated in the ground which generates strong lateral forces. The rearrangement of soil particles in denser configuration is possible only when these lateral forces imparted by vibrator exceeds the interparticle friction of soil. Water jets are used in this process to assist the penetration of vibrator to required depth. Use of water also causes generation of excess pore water pressures which reduces interparticle friction. This technique, also called as vibro floatation, was first developed in 1930s in Germany.

Suitability

Vibro compaction is ideally suited for soils having fines less than 20 % (preferably less than 10%). The clay content shall be less than 2-3 % (Saito 1977). Figure 2 shows applicability of vibro compaction for different soil types based on gradation.

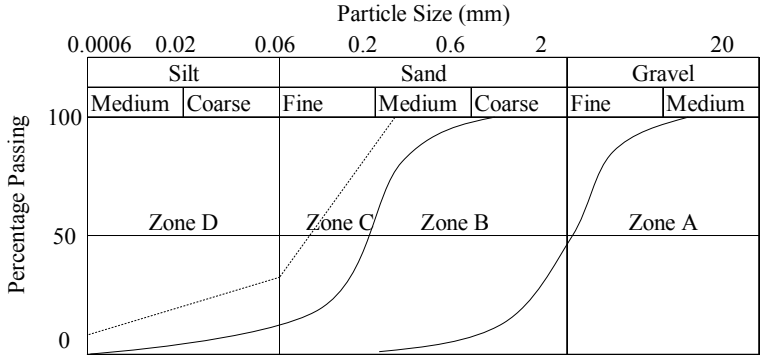


Fig. 2. Suitability of vibro compaction (redrawn from Woodward, 2005)

Zone A: Vibro compaction appropriate, but penetration difficult
Zone B: Most suitable for vibro compaction
Zone C: Vibro compaction feasible, but longer time required
Zone D: Vibro compaction not feasible – use stone columns (Kirsch et al. 2017)

Mechanism

Vibro compaction depends not only on the soil characteristics but also on the vibrator power, time of compaction and confinement around the compaction zone. The soil properties which influence the efficiency of vibro compaction are initial density, grain size, depth of compaction and permeability. The vibrator characteristics affecting vibro compaction are frequency, amplitude and acceleration of vibrations. The duration of vibrations also affects the degree of compaction achieved (Han 2015).

The vibratory forces are attenuated as the radial distance from the vibrator increases. At acceleration of about 0.5g, the dynamic stresses induced by vibrator overcomes the interparticle friction and the structure of granular soils is destroyed. Soil becomes fluidized at acceleration more than 1.5g and acceleration of more than 3.0g causes soil dilation. Rodger (1979) idealized the response of granular soils to vibration as shown in Fig. 3.

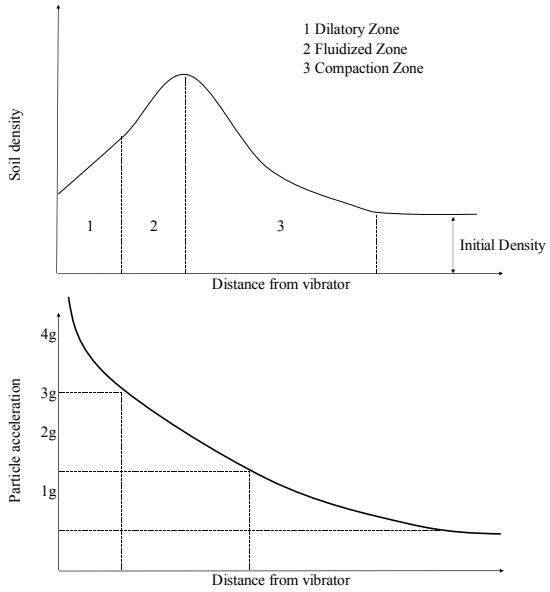


Fig. 3. Idealized response of cohesionless soil around vibrating probe (redrawn from Rodger 1979)

In fluidization zone of soil around the probe, the shear strength of soil is reduced but doesn't reach zero value. Thus, the vibrations are transmitted from soil particles' contact which are continuously made and broken. With use of water or below water table, pore water pressures are generated which when exceeds the rate of dissipation, results in fluidization of soil.

The plastic (dilatory and fluidized) zone is followed by compaction zone. The boundary between plastic and compaction zone is where maximum densification happens. The compaction zone extends to the point where no further densification happens.

Surface Manifestation

During vibro compaction process, there is substantial reduction in void ratio of soil owing to rearrangement of soil particles in denser configuration. This reduction in void ratio and subsequently volume of soil is evident at ground surface in form of conical crater. The depth of this crater is maximum close to the probe point and reduces radially from probe point. The subsidence of this ground level is accounted for by continuously feeding coarse graded sand at ground level. The addition of sand helps in maintaining the ground level uniform and assists in compaction efficiency at shallow depths.

CASE STUDY: INDUSTRIAL PLANT IN NORTH EASTRN STATES

This section deals with application of vibro compaction technique for one of the project site situated in North East India. An industrial plant was proposed to be constructed at the project location. Based on the geographic location, the site falls under Zone V as per IS 1893 (2016). Soil at proposed project location was essentially sand having percentage fines less than 10 percent. Ground water table was observed at an average depth of 1m below the ground level. This section describes the details of the project structures, soil characterization, performance criteria and successful implementation of vibro compaction.

Site Details

The industrial plant is in a public-sector refinery. The site falls under earthquake Zone V as per IS 1893 (2016). Structures proposed at this industrial plant includes compressor room, substation building, admin building etc. The performance criteria for this plant is summarized in Table 1:

Table 1. Performance criteria for proposed industrial plant

A. Loading Intensity	
• Isolated foundations	: 25 T/m^2
• Raft foundations	: 20 T/m^2
B. Post Construction Long term total permissible Settlements	
• Isolated foundations	: 25mm
• Raft foundations	: 40mm
C. Liquefaction mitigation	
• Seismic zone	: Zone V
• FOS to mitigate Liquefaction	: 1.0
• Peak ground acceleration for Liquefaction Analysis	: 0.36g
• Earthquake Magnitude	: 7.5

The peak ground acceleration was taken as per IS 1893 guidelines. The earthquake magnitude was considered as 7.5 based on the severity of the location.

Soil Details

The soil investigation works were conducted using eCPTs. The eCPTs were penetrated till dense sand strata. Based on eCPT data and interpretation (Robertson 2016), the soil is observed to fall in sandy silt to silty sand zone. The layout of eCPTs is presented in Fig. 4 and typical eCPT plot is presented in Fig. 5.

The liquefiable depth as calculated from previous sections was observed to be varying from 11m to 12m below the existing ground level. Following the evaluation of liquefaction potential, ground improvement using vibro compaction was proposed to mitigate the liquefaction potential of soil.

Mitigation of Liquefaction

Vibro compaction densifies the soil and mitigates the liquefaction potential of soil. A trial grid with design spacing of 2.75m c/c triangular was first executed and site. The results from before and after vibro compaction were compared and FOS was evaluated. FOS evaluated from trial locations was found to be greater than 1 post vibro compaction works.

For purpose of liquefaction mitigation, it was recommended to treat the area surrounding the footing for confinement purpose. The lateral confinement extent was taken as two thirds the depth of liquefaction beyond the footing edge (Kirsch et al. 2017).

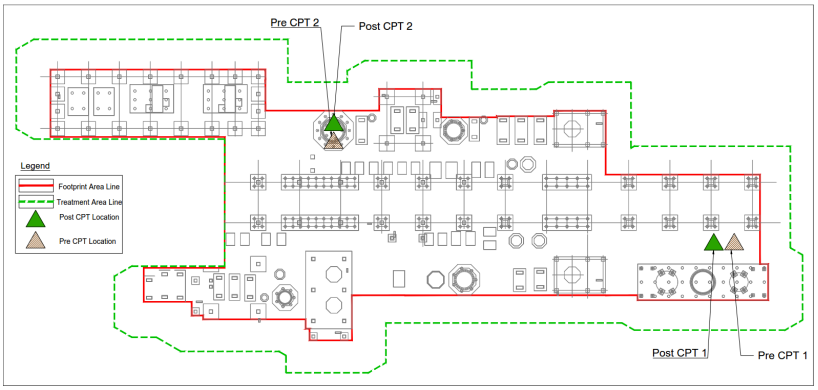


Fig. 4. Location plan of eCPT

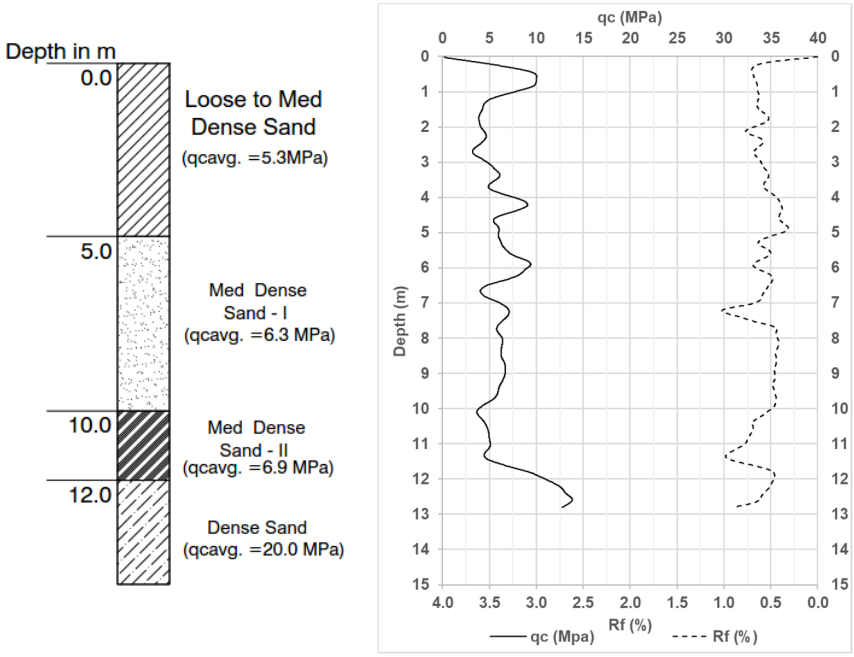


Fig. 5. Soil summary for the industrial plant

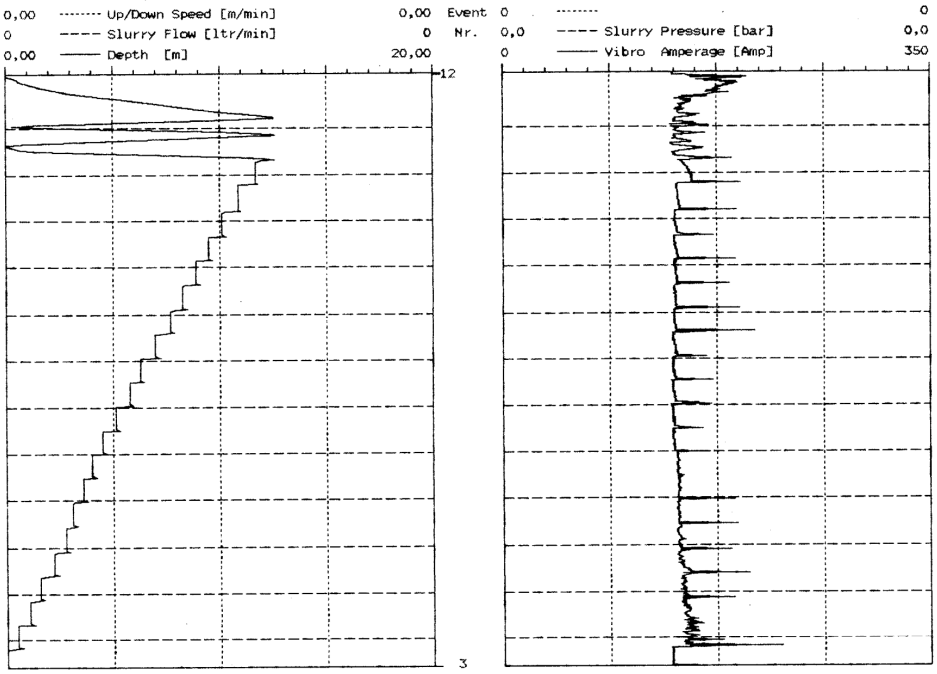
Quality Assurance and Control

M4 Graph

Quality control using M4 graphs provides real time monitoring for vibro compaction process. This graph gives output in form of depth vs time, depth vs compaction effort, time taken at each depth and total time taken for each probe point. These graphs are continuously reviewed during field trials and parameters are frozen to be followed for main works. Each soil type responds to vibration effect in different time. The time for which vibrator shall be hold at constant depth is fixed during these field trials. A typical M4 graph is presented in Fig. 6.

Backfill Monitoring

The subsidence of ground surface is observed in form of conical crater. Coarse graded sand is continuously fed from the ground level at probe point to compensate for the volume reduction. At this site, around 10 to 11 percent of sand volume in terms of complete volume of treatment was compensated on account of decrease in soil volume. The backfill monitoring also serves in visualization of efficiency of vibro compaction.



Event Nr	Art	Event Designation		Time Hour:Min:Sec	Depth [m]	Elec. Energy [kVAh]	Slurry Probe [cbm]	Slurry Column [cbm]
01	09	PROBE	START	15:00:38	0,0	0,00	0,00	0,00
02	13	DEPTH	ZERO	15:00:39	0,0	0,02	0,00	0,00
03	10	PROBE	END	15:25:55	0,0	40,29	0,00	0,00

End Probe Number: 445 Max.Depth: 12,7 m Duration: 25,26 min
Column Length: 12,7 m

Fig. 6. Typical M4 graph used for quality control

Pre and Post Soil Investigation

Post soil investigation using eCPTs were conducted to observe the efficacy of vibro compaction process. The post eCPTs were conducted in shadow zone or least influential zone which is the centroid of the triangle formed by the triangular grid pattern.

As evident from the eCPTs in Figs. 7-8, improvement in range of 1.5 to 2 times was observed after vibro compaction. It shall be noted that at some depths, friction ratio close to 1 percent was observed which signifies presence of silt/clay in sand deposit. This presence of silt/clay traces is evident around 6m depth where low improvement factor is observed. The post eCPT data was then used to evaluate the liquefaction potential of the improved ground.

The factor of safety as calculated for post eCPTs was greater than 1 for most of the depths. This increase in cone resistance positively shows that vibro compaction is effective in mitigation of the liquefaction potential of soil.

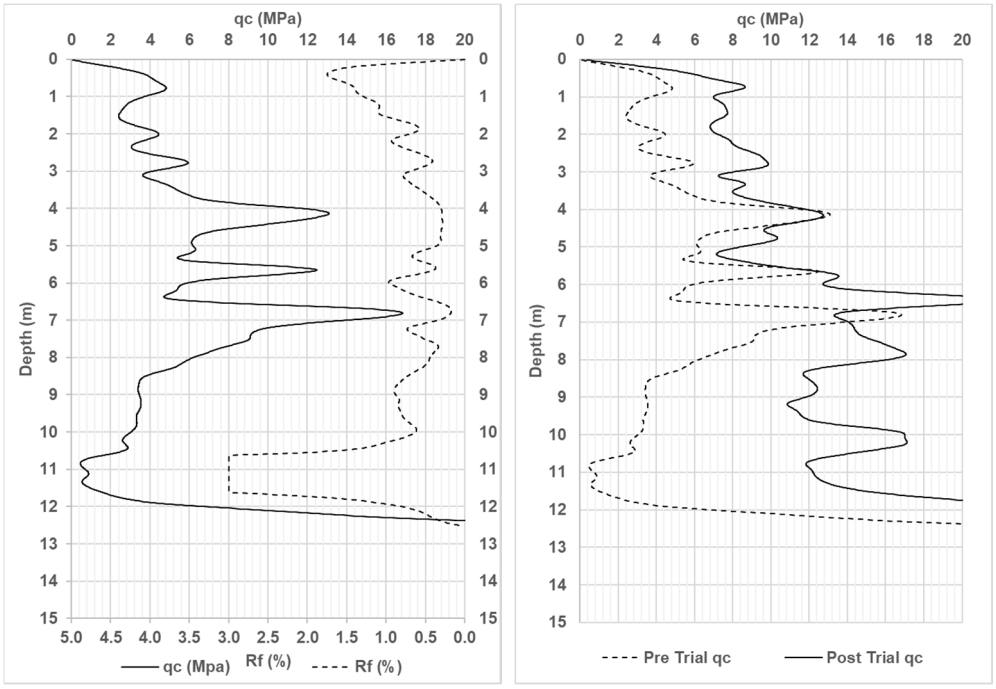


Fig. 7. Before improvement eCPT plot and comparison of pre and post cone resistance (q_c) for trial works

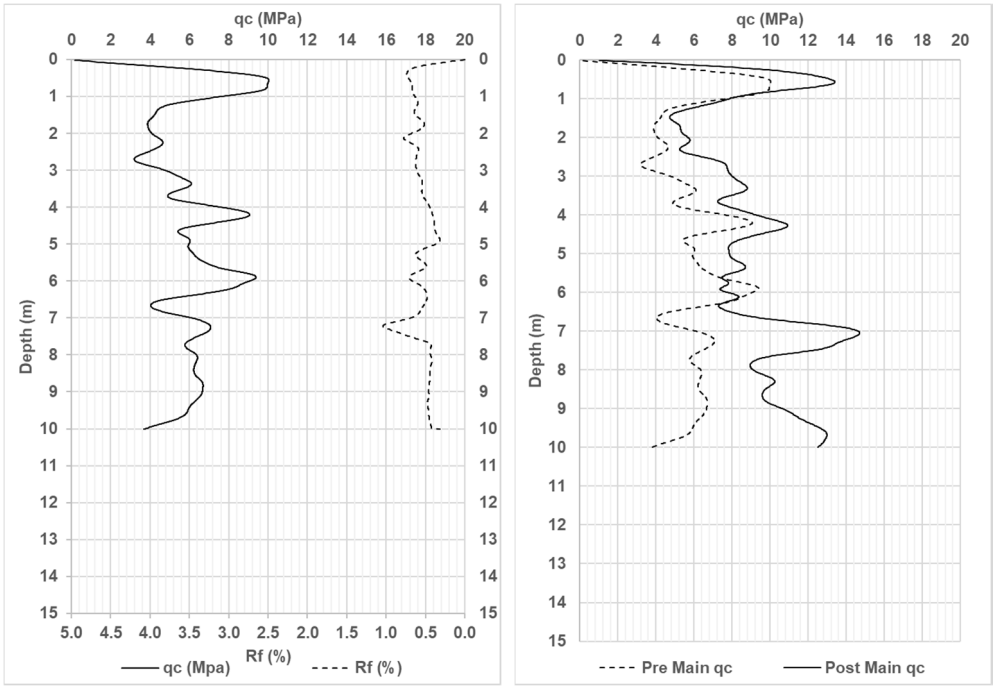


Fig. 8. Before improvement eCPT plot and comparison of pre and post cone resistance (q_c) for main works

Plate Load Test

One of the geotechnical concerns to be addressed in design of vibro compaction was to improve the soil bearing capacity and reduce the settlements. Plate load tests were conducted at site after vibro compaction works to demonstrate the improved load settlement behavior of soil. As observed from plate load test results, the settlements from the test plate were well within permissible limits as tabulated in Table 2.

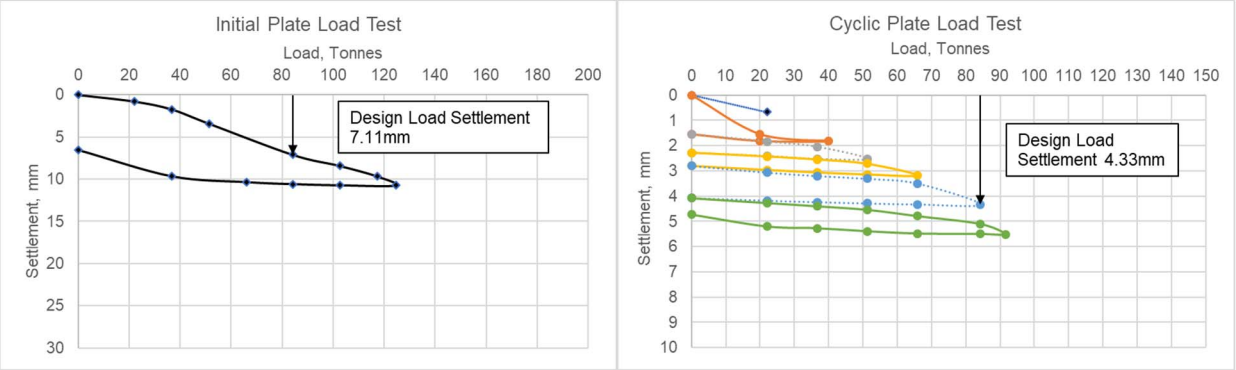


Fig. 9. Plot of load settlement curve from plate load tests

Table 2. Summary of plate load test results

Plate Load Test	Design Load Intensity, kPa	Settlement @ Design Load, mm	Test Load Intensity, kPa	Settlement at Test Load, mm	Rebound, mm	Net Settlement, mm
Initial	250 kPa	7.11	375 kPa	10.75	4.23	6.52
Cyclic	250 kPa	4.33	275 kPa	5.51	0.78	4.73

SUMMARY AND CONCLUSION

This paper presents an approach for practicing geotechnical engineers on mitigation of liquefaction potential of soil. Liquefaction evaluation procedure was discussed in detail according to latest Indian Standard guidelines. Based on the liquefaction analysis and soil conditions, ground improvement using vibro compaction was proposed to mitigate the liquefaction potential of soil.

High standard quality procedures were adopted before and after ground improvement works. Soil investigation works were conducted after ground improvement to demonstrate the efficacy of the treatment technique. Post eCPTs were analyzed and factor of safety greater than 1 was obtained. Plate load tests were then conducted at site to observe the load settlement behavior of improved ground. Results from plate load test successfully verified the intended performance criteria for the structures.

Based on the post improvement liquefaction evaluation and observed load settlement graph, it is concluded that vibro compaction was effectively employed to achieve required densification. The results from this study establishes that similar soil could be treated using vibro compaction.

REFERENCES

ASTM D 5778, 1995. Standard Test Method for Performing Electric Friction and Piezocone Penetration Testing of Soils. ASTM International, West Conshohocken, PA

Baez J.I., and Martin G., 1993. Advances in the Design of Vibro Systems for the Improvement of Liquefaction Resistance. Proceedings from Symposium on Ground Improvement, Vancouver Geotechnica1 Society, Canada.

Baez, J.I., and Martin, G., 1993. Quantitative Evaluation of Stone Column Techniques for Earthquake Liquefaction Mitigation. Earthquake Engineering. Tenth World Conference, Balkema, Rotterdam.

Belani, T., Nagrikar, S., and Raj, D., 2013. Study of Extent of Soil Improvement by Employing Vibro Compaction Technique. Seventh International Conference on Case Histories in Geotechnical Engineering, 36.

Boulanger, R.W. and Idriss, I.M., 2014. CPT and SPT Based Liquefaction Triggering Procedures. Report no. UCD/CGM-14/01. Center for Geotechnical Modelling. University of California at Davis, California.
Ground Improvement Committee, 2014. Commentary on the Selection, Design and Specification of Ground Improvement for Mitigation of Earthquake-Induced Liquefaction. The Journal of Deep Foundation Institute, 7(1), 3-12.

Han, J., 2015. Principles and Practice of ground Improvement. A text book.

Idriss, I. M, and Boulanger, R.W., 2010. SPT Based Liquefaction Triggering Procedures. Report no. UCD/CGM-10/02. Center for Geotechnical Modelling. University of California at Davis, California.

Indian Standard 1893, 2016. Sixth Revision, Criteria for Earthquake Resistant Design of Structures, Part 1: General Provisions and Buildings. Bureau of Indian Standards, New Delhi.

Indian Standard 383, 2016. Third Revision, Coarse and Fine Aggregate for Concrete – Specification. Bureau of Indian Standards, New Delhi.

Kirsch, K., and Kirsch, F., 2017. Second Edition. Ground Improvement by Deep Vibratory Methods. A text book.

Murali Krishna, A., Annam, M.K., and Baruah, U.K., 2018. Stone Columns/Granular Piles for Improving Liquefiable Sites: Case studies. Geotechnical Engineering Journal of the SEAGS & AGSSEA, 49(1), 136-142.

Priebe, H.J., 1998. Vibro Replacement to Prevent Earthquake Induced Liquefaction. Proceedings of the 5th Geotechnique-Colloquium, Darmstadt, Germany.

Robertson, P.K., 2016. Cone Penetration Test (CPT)-based Soil Behavior Type (SBT) Classification System — an Update. Canadian Geotechnical Journal, 53, 1910-1927.

Rodger, A.A., 1979. Vibro Compaction of Cohesionless soils. Internal Report, R.7/79. Cementation Research Limited, Croydon, UK.

Saito, A., 1977. Characteristics of Penetration Resistance of Reclaimed Sandy Deposit and Their Change Through Vibratory Compaction. Soils and Foundations, Japanese Society of Soil Mechanics and Foundation Engineering, 17(4), 31-43.

Seed, H.B., and Booker J.R., 1976. Stabilization of Potentially Liquefiable Sand Deposits using Gravel Drain Systems. Earthquake Engineering Research Center. Report no. EERC/76-10. University of California, Berkeley, California.

Woodward, J., 20015. Introduction to Geotechnical Processes. A text book.

Youd T.L. et al., 2001. Liquefaction Resistance of Soils: Summary Report from the 1996 NCEER and 1998 NCEER/NSF Workshops on Evaluation of Liquefaction Resistance of Soils. ASCE Journal of Geotechnical and Geoenvironmental Engineering, 127(10), 817-833.

NEGATIVE SKIN FRICTION ON A PILE - EFFECT OF DRAINAGE CONDITION

Prince **K**umar[1] and **S**atyanarayana **M**. **D**asaka[2]

[1]Postgraduate Student, Department of Civil Engineering, Indian Institute of Technology Bombay, Mumbai; e-mail: princeiitb16@gmail.com
[2]Associate Professor, Department of Civil Engineering, Indian Institute of Technology Bombay, Mumbai; e-mail: dasaka@civil.iitb.ac.in

ABSTRACT

Negative skin friction (NSF) is a common problem in the design of pile, where soft soil presents. The soft soil applies drag on the pile when soil settlement is more than the pile. The NSF is a very complex problem because it depends on several factors. In this paper, finite element method (FEM) is used to simulate and analyse the pile-soil interaction problem of negative skin friction. For the analyses, modified cam-clay (MCC) model, Mohr-Coulomb (MC) model, Hoek-Brown model, and linear elastic model are used for soft clays, sand, rock, and pile, respectively. The model is validated with a known case history. The development of dragload, downdrag, and the location of the neutral plane (NP) are investigated and they match well with field data. Detailed parametric studies on the effect of drainage condition on the location of NP and development of dragload are conducted in this study. From this parametric study, it is observed that the depth of NP is different for one-way and two-way drainage conditions during the consolidation process, but it is same at the end of the consolidation for both drainage conditions. The surcharge load does not have any influence on depth of NP, but dragload increases with surcharge load.

Keywords: Negative skin friction, Drainage condition, Neutral plane, Dragload, Numerical modelling

INTRODUCTION

Pile foundations are very common for heavy structures because they are able to transfer heavy loads to the deep ground. The presence of soft soil is predominant in many countries, generally in coastal areas. Generally, the soil stratum is in layers, and when piles are passing through different layers of soil, the soft soil applies a drag force on pile instead of resisting the load. Because of relative settlement between pile and soil, shear stresses induce on the pile surface. When soil settlement is more than pile settlement, the friction induced on the pile is called negative skin friction, and if the settlement of pile is more than soil settlement, positive skin friction is induced on the pile. The phenomenon of negative skin friction usually occurs when the pile is installed in soft soil that is still undergoing consolidation.

Since 1960s, research on NSF gained momentum and many full-scale tests were conducted in the field between 1960 to 1975. Many research results on NSF were presented at the 7th International Conference on Soil Mechanics and Foundation Engineering held in Mexico in 1969, which in the opinion of Fellenius (1998) “broke new ground”. After that, there were many full-scale tests and laboratory tests were conducted to understand the complexity of NSF on the pile. After 1990s, the centrifuge tests came in trend and some centrifuge tests were conducted on the pile to see NSF effects. It is not surprising that great discrepancy of 57% to 315% between the calculated and measured dragloads have been reported at the MIT symposium (Garlanger and Lambe, 1973). To see the discrepancy between engineers, another symposium the “Wroth Memorial Symposium” was conducted and the calculated dragloads were observed from 98% to 515% of the measured values (Little and Ibrahim, 1993). Poulos (1997) and Fellenius (1998) reported that the dragload is not a problem of ultimate geotechnical capacity but is a serviceability problem. Also, it is a problem for the structural design of pile. So, in the design of pile, the dragload should be considered for structural design and the settlement (downdrag) should be well within acceptable limits.

Many researchers studied NSF on the pile by using numerical analysis. Indraratna et al. (1992) utilized the concept of finite element method to understand the NSF and they observed that the shear stress distribution along the pile shaft was directly controlled by the behaviour of pile-soil interface elements. Lee

© 2018 Deep Foundations Institute

et al. (2002) considered the most important factor, soil slip effect, at the pile-soil interface and this factor governed the development of skin friction in pile shaft. Jeong et al. (2004) considered the mechanism of soil-pile slip and nonlinear analysis was observed more realistic than linear analysis, and Mohr-Coulomb model was used to model the behaviour of sand and clay, and isotropic elastic model for the pile. For full mobilization of skin friction, a limiting relative displacement of 5 mm was assumed. Hanna and Sharif (2006) carried out a parametric study by using a computer program CRISP (developed by Cambridge University). They observed that the effect of time (long or short term) on NP depth was very less and same observation was reported by Indraratna et al. (1992) and Leung et al. (1991). Very recently, Tan and Fellenius (2016) studied soil-structure interaction by using PLAXIS 2D software. They used the axisymmetric model to study NSF on the single pile and hardening soil model was used for all types of soil. They observed out that the transition zone exists above NP, and the NP depth shifts upwards with an increase in axial load on the pile. Moreover, they observed that the ultimate geotechnical capacity of the bitumen-coated pile was reduced.

Commercial finite element code PLAXIS 3D 2016 is used in the present study to carry out numerical modelling of NSF on a single pile. This commercial code is equipped with various constitutive models including some advanced constitutive models which are capable of simulating the non-linear and time-dependent behaviour of soil. In addition to this, PLAXIS is capable of considering pore pressure either in a hydrostatic or non-hydrostatic condition. It can also deal with the complex interaction between the structure and the soil. As PLAXIS distinguishes between drained and undrained soils to model behaviour of permeable sands and highly impermeable clays, excess pore pressures are generated during plastic calculations when undrained soil layers are subjected to change in loadings. Dissipation of excess pore pressures with time can be computed using consolidation analysis available in PLAXIS. All these features make PLAXIS 3D an appropriate program for analysing the NSF problem resulted from the interaction between the pile and the consolidating soil in the current study. In this paper, a wished-in-place single pile is modelled in a consolidating ground by an axisymmetric FEM model. The detailed parametric studies of the effects of drainage condition on the location of NP and on dragload are conducted.

MODELLING OF INTERFACE

In modelling pile-soil interaction, the inclusion of an appropriate interface is crucial, as confirmed by Lee et al. (2002) and Jeong et al. (2004). The properties of interface elements are related to the surrounding soil properties. In PLAXIS, Interface elements are simulated by means of the bilinear MC model. The Coulomb criterion is used to distinguish between elastic and plastic interface behaviour. In case of the linear elastic model, Mohr-Coulomb model, hardening soil model, soft soil model, and Hoek-Brown model, the interface strength is defined by the parameter R_{inter}. The interface can be rigid or flexible. In case of rigid interface, the strength of interface is equal to the surrounding soil strength, which means that the $R_{inter} = 1.0$. In case of flexible interface, the interface strength is less than surrounding soil strength, which means that the $R_{inter} < 1.0$. For Modified Cam-Clay model, the interface strength is defined by effective cohesion c'_{ref}, effective friction angle ϕ', and dilatancy angle Ψ'.

For the interface to remain elastic, where small displacements can occur within the interface, the shear stress τ is given by:

$$|\tau| < c'_i + \sigma_n \tan\phi_i \qquad [1]$$

Where σ_n is the effective normal stress.

For plastic interface behaviour, when permanent slip occurs, τ is given by:

$$|\tau| = c'_i + \sigma_n \tan\phi_i \qquad [2]$$

Where c'_i and ϕ_i are the cohesion and friction angle of the interface. The strength properties of interfaces are related to the strength properties of soil layer. The interface properties are calculated from the soil properties by applying the following rules:

$$c_i^{'} = R_{inter}\, c_{soil} \quad [3]$$

$$\tan\phi_i = R_{inter} \tan\phi_{soil} \leq \tan\phi_{soil} \quad [4]$$

MODEL VALIDATION

In order to check the feasibility of 3D FEM model for negative skin friction problems, a known case history is selected for the verification of a 3D FEM model results. This known pile load test was conducted in Bangkok, Thailand, and reported by Indraratna et al. (1992). The site was located at 10 km east of Bangkok and Indraratna et al. (1992) conducted two full scale instrumented pile load tests. The soil consisted of 2-4 m thick weathered clay, overlying 16 m thick of soft clay followed by medium stiff and stiff clay ranging from 6-8 m thick and then sand. The ground water table was located at 2 m below the ground surface. Two 27 m long instrumented concrete piles were driven by standard drop hammer. The inner and outer diameter of pile is 0.25 m and 0.40 m, respectively. The upper 20 m length of one of the two piles was coated with bitumen. 2 m thick fill was placed around the piles over an area of 24 m × 14 m. The test was monitored for 265 days after placing the embankment and the equivalent average degree of consolidation is 60%. In first 2 months, the settlement of ground surface occurred rapidly and after 6 months it became nearly constant. For the simplicity of the problem, the pile is considered as wished-in-place and the equivalent solid pile of diameter 0.40 m is considered for the study. In this study, the consolidation of soil due to surcharge load is considered.

Numerical Modelling Procedure

The axisymmetric model is considered for the problem. The pile is modelled as a volume element and 10-node tetrahedral elements are used for soil and pile both. The soil is modelled around and below the pile in such way that the outputs are not influenced. These numerical analysis procedures are considered for both validation and parametric studies. The following procedure is followed for the numerical analysis of pile.

1) Generate axisymmetric mesh of the problem. The soil is modelled around and below the pile in such way that the outputs are not influenced. So, the boundary distance from the center of the pile should be sufficient. The local refinement of the mesh is considered and it will be discussed in the next section.
2) Generate initial stresses and water pressures in the model. The lateral initial stresses are considered by K_0 procedure: $\sigma_{ho} = K_0 \times \sigma_{vo}$.
3) The pile material is replaced with concrete material and the interface is considered between soil and pile. The weight of the concrete material is more than the weight of soil so that the stress condition is changed slightly. The pile is considered as wished-in-place and the installation effects are not considered.
4) The fill is placed on the top of the soil to induce the surcharge effect. After placing the fill, the development of excess pore pressures started and when they attained maximum value, drainage is allowed for consolidation of soil.

Mesh and Model Parameters

This study uses the benefit of the symmetric plane and so considered only half of the problem. The axisymmetric model of the single pile is developed by PLAXIS 3D. The soil is modelled using 10-node tetrahedral elements and the interface between pile and soil is modelled by 12-node interface elements. For present analysis the soil properties are same as reported by Indraratna et al. (1992), but the permeability values have magnified in present analysis by 15 times of values adopted by Indraratna et al. (1992). However, these magnified values are in the typical range of Bangkok clay as reported by Horpibulsuk et al. (2007). Table 1 summarises the input soil and pile properties for this analysis. The fill of 2 m is placed on the top of existing ground surface to induce surcharge load. The pile is modelled as a cluster of volume

elements having the dimensions and location of the pile installed at depth. The distance of model boundary from the center of pile is very important for modelling. Trochanis et al. (1988) recommended that the minimum lateral boundary distance from the center of the pile should be 25 times the pile diameter or 0.60 times the pile length, whichever is higher. Similarly, the base of the mesh should be placed below the pile tip by minimum of 0.70 times the pile length. These recommendations are considered for all parametric studies. The roller boundary is considered on sides of the mesh to permit the vertical settlement and the fixed boundary is considered at the bottom of the mesh. The top surface of mesh is considered as a free boundary to allow settlement of soil. The ground water table is at 2 m below the existing ground surface. The hydrostatic pressure is applied below the ground water table and the suction effect is neglected above the water table. The two-way drainage condition is considered for this case history. For clay, modified Cam-Clay model is considered, whereas Mohr-Coulomb model is used for fill and sand. The pile is modelled as linear elastic model. The axisymmetric model of the problem is shown in Figure 1.

The element sizes are very important in FEM analysis. In PLAXIS 3D, there are five global mesh types are available: very coarse, coarse, medium, fine, and very fine. For mesh convergence study, all available mesh sizes with the interface between soil and pile are considered. From obtained results, it is observed that the convergence does not occur. Hence, the global mesh does not work effectively on mesh convergence. Now, the local refinement mesh is used instead of global refinement mesh. The base mesh is "global coarse" and the mesh is locally refined around the pile shaft and near the pile tip. The refinement is done in the zone close to the pile (2.5D from the center of pile and 2.5D below the pile tip). Four different coarseness factors are used for local refinement: 1.0, 0.75, 0.50, and 0.25. The coarseness factor reduces the mesh size locally and the new mesh size is coarseness factor times global mesh size. It is observed that the difference between results of coarseness factor 0.50 and 0.25 is zero. Hence the locally refined mesh works effectively for mesh convergence. For all analyses, the global coarse mesh with 0.50 coarseness factor is considered. After meshing, the total generated number of elements and nodes are 10994 and 18385, respectively.

Table 1 Soil and pile properties for studied case history (After Indraratna et al., 1992)

	Fill	Weathered clay	Soft clay 1	Soft clay 2	Medium to stiff clay	Sand	Pile
Parameters							
Depth (m)	0-2	2-6	6-12	12-22	22-32	32-50	0-27
γ (kN/m^3)	17	17	15	17	19	19	24
K_0	0.4	0.70	0.60	0.60	0.67	0.45	—
OCR	2.7	2.7	1.2	1.3	1.8	—	—
e_o	1.93	2.4	3.8	3.4	1.6	1.2	—
κ	—	0.053	0.084	0.063	0.027	—	—
λ	—	0.182	0.514	0.323	0.116	—	—
M	—	1.05	0.97	0.98	0.90	—	—
ϕ' (^{o})	33	—	—	—	—	33	—
ν	0.2	0.33	0.33	0.33	0.33	0.33	0.33
E (kPa)	4900	—	—	—	—	27440	18×10^6
k (m/day)	0.01	0.01	0.82×10^{-3}	0.39×10^{-3}	0.55×10^{-3}	0.01	—

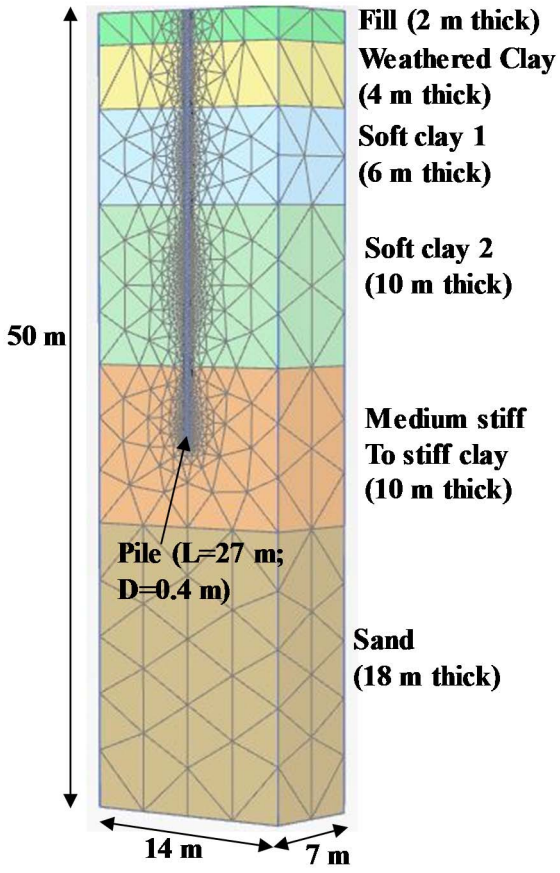


Figure 1 FEM axisymmetric mesh used for validation studies

Soil and Pile Settlements

Figure 2 shows the comparison between predicted settlement of soil and measured soil settlement in field. The soil settlement in the field was measured at 0.25 m from the pile center. The soil settlements after 3, 53, and 265 days are considered in this analysis and compared with field data. This analysis slightly overestimates the settlements in soft clay layer. However, results show comparable trend of the settlement. The predicted soil and pile settlements are shown in Figure 3. From Figure 3, we can observe that the soil settlement varies noticeably with depth, and most of the settlements are because of the consolidation of soft clay layers. The pile settlement is almost constant with depth, it means the elastic settlement is very less. Here, the relative settlement is obtained from the difference between settlement of soil and pile. Moreover, it observed that the relative settlement is zero at depth of 20 m from the top of the pile, and this is called neutral plane depth. The measured NP depth is 21 m, and this analysis underestimates the depth of NP by 4.70 %. The relative settlement below the NP depth is small except long-term case of 265 days.

Axial Load

In Figure 4, the variation of axial load along the pile length from the present study is compared with that of published field study. The axial load is measured after 265 days of consolidation. This study slightly underestimates the axial load in shallow depth but overestimates between 7 m to 20 m depth. However, the trend of predicted values is same as field results. The difference in maximum axial load between field results and that of predicted is only 3.33 %. The maximum axial load transferred on the pile is called dragload and the depth at which the dragload is maximum is called neutral plane depth. We can

also observe that the neutral plane depth is 20 m, which is less than the field value. The neutral plane depth observed from settlement criterion is equal to the value observed from drag load criterion. However, the PLAXIS 3D model is able to simulate the field condition. Hence, PLAXIS 3D is used in the parametric studies on NSF.

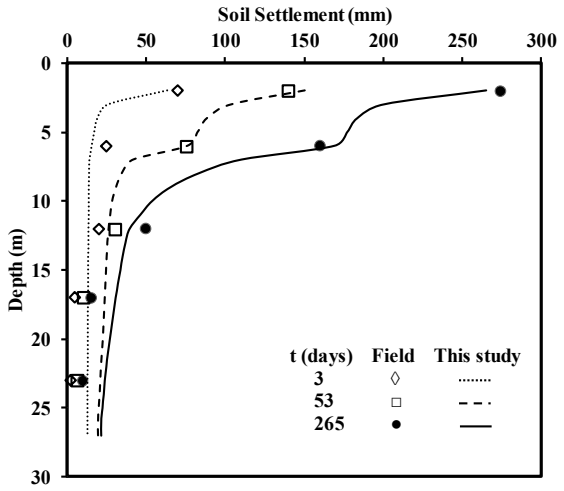


Figure 2 Comparison of predicted ground settlement distribution with field measurements

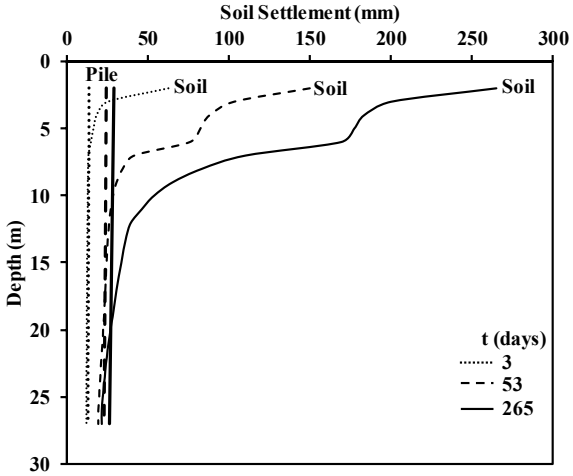


Figure 3 Variation of soil and pile settlements with depth

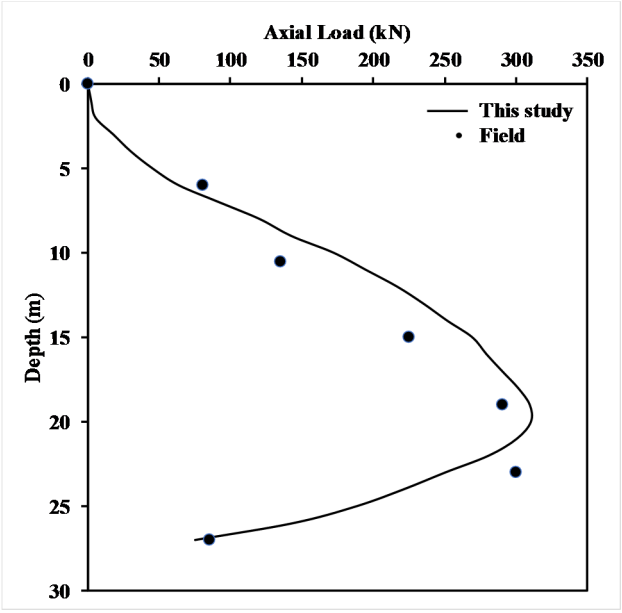


Figure 4 Comparison of predicted and measured load distribution along the pile length

PARAMETRIC STUDIES

The numerical modelling procedures adopted in the parametric studies are same as discussed in the earlier section. The assumed diameter of pile is 1.0 m for all studies. The average degree of consolidation is considered in this study and calculated from settlement criterion. Table 2 presents soil, rock, and pile properties considered for parametric studies. The Hoek-Brown model is used for rock material and required model input parameters are: Young's modulus (E), Poisson's ratio (ν), Uni-axial compressive strength of the intact rock (σ_{ci}), Intact rock parameter (m_i), Geological Strength Index (GSI), Disturbance factor (D).

Table 2 Soil, rock, and pile properties for parametric studies

	Fill	Weathered clay	Soft clay	Sand	Rock	Pile
Parameters						
γ (kN/m^3)	17	17	17	19	25	24
K_0	0.4	0.70	0.60	0.45	—	—
OCR	2.7	2.7	1.3	—	—	—
e_o	1.93	2.4	3.4	1.2	—	—
κ	—	0.053	0.063	—	—	—
λ	—	0.182	0.323	—	—	—
M	—	1.05	0.98	—	—	—
ϕ' (°)	33	—	—	33	—	—
ν	0.2	0.33	0.33	0.33	0.25	0.33
E (kPa)	4900	—	—	27440	9.0×10^6	30×10^6
k (m/day)	0.01	0.0101	0.39×10^{-3}	0.01	—	—
σ_{ci} (kPa)	—	—	—	—	80×10^3	—
m_i	—	—	—	—	20	—
GSI	—	—	—	—	50	—
D	—	—	—	—	0.0	—

Drainage Condition

The detailed parametric studies are conducted on the effect of drainage conditions on the dragload and depth of neutral plane. In the field, the consolidation can happen due to either one-way or two-way drainage. Hence, in this study both drainage conditions are modelled. Sand is considered below the pile in case of two-way and rock is considered in case of one-way drainage to simulate field conditions. The effect of thickness of fill, to represent the surcharge loading, is also considered in this study. Three different pile lengths are considered in the present study, i.e., 15 m, 30 m, and 45 m, which correspond to L/D ratios of 15, 30, and 45, respectively. In addition to this, five different thicknesses of fill layer is considered: 2 m, 3 m, 4 m, 5 m, and 6 m.

Results and Discussion

Effects on NP Depth (L_n)

From Figure 5 (a), we can observe that the NP depth is influenced by drainage conditions and length of the pile. The variation of NP depth with degree of consolidation is different for different L/D ratios. In case of one-way (OW) drainage, the trend of the curve is same for all L/D ratios, but is different in case of two-way (TW) drainage. The effect of different surcharge thicknesses on NP depth is shown in Figure 5 (b). The NP depth varies between 7.7 and 8.2 m after 90% of consolidation. Hence, the fill thickness has a negligible effect on the NP depth.

Figure 6 (a) presents the variation of L_n/L with degree of consolidation for both one-way and two-way drainage. The values of L_n/L in case of two-way drainage are varied between 0.33 to 0.58 and 0.42 to 0.58, in case of one-way drainage. Initially, the NP depths are different in both cases but are same at the end of the consolidation. In case of two-way drainage, the neutral plane depth is lesser as compared to one-way drainage at a lower value of the degree of consolidation. The decrease in the NP depth with degree of consolidation was observed in the field by Indraratna et al. (1992) in case of two-way drainage. The settlement of lower soil layers in case of two-way drainage is more than the one-way drainage, as drainage is allowed from the top only in case of one-way drainage. The final normalised NP depth is different in case of different L/D ratios, but same for L/D ratio of 30 and 45. For L/D ratio of 15, the curve corresponding to two-way drainage is above than that of one-way, but with an increase in L/D ratio, the curves almost meet each other.

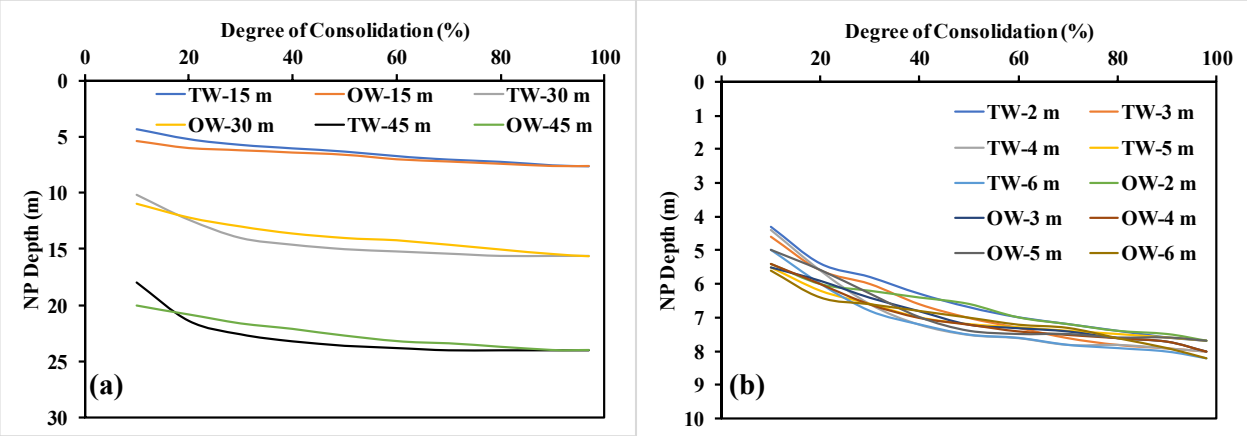


Figure 5 (a) Variation of neutral plane depth with degree of consolidation for 15 m, 30 m, and 45 m pile lengths; (b) Variation of neutral plane depth with degree of consolidation for 15 m pile length under different surcharge thickness; OW- One-way; TW- Two-way.

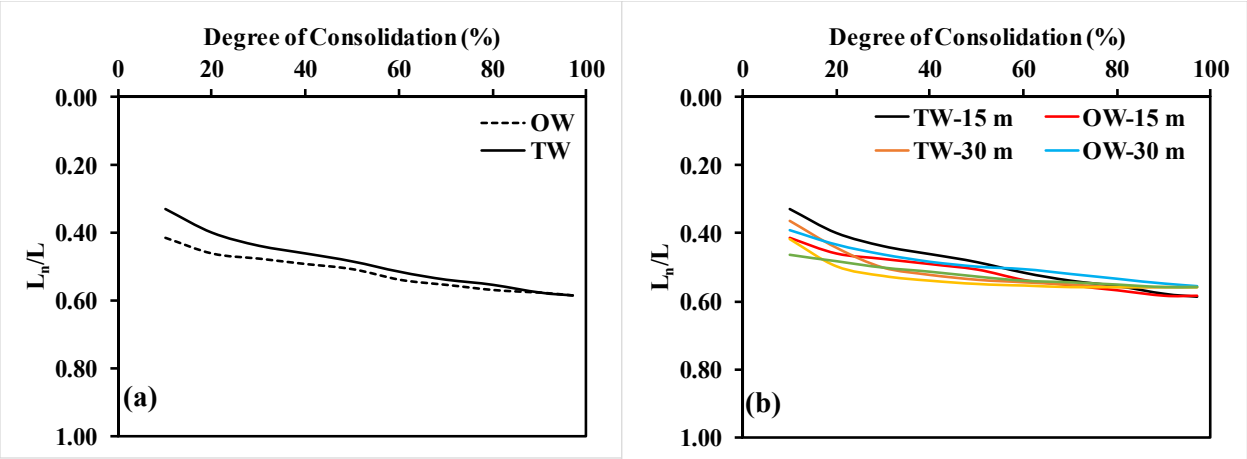


Figure 6 (a) Variation of normalised neutral plane depth with degree of consolidation for 15 m pile length; (b) Variation of normalised neutral plane depth with degree of consolidation for 15 m, 30 m, and 45 m pile length.

Effects on Dragload (F_D)

The variation of dragload with a degree of consolidation for different pile lengths is shown in Figure 7 (a). The trend of the curves is same for all pile lengths, but different under different drainage conditions. The dragload is more in case of one-way than two-way drainage for all pile lengths, but at the end of consolidation, it is same for both drainage conditions. The effect of fill thickness on dragload is also studied. The dragload is observed to increase with fill thickness, as shown in Figure 7 (b). The induced dragload in fill layer is negligible in case of 2 m fill thickness, but significant in case of 6 m fill thickness. Moreover, in case of 2 m fill, the maximum dragload is same in both cases, but from 3 m fill onwards the dragload in case of two-way drainage is more than that of one-way case, and the difference gradually increased. Because of the higher settlement of upper soil in case of one-way drainage, the dragload is more than that of two-way drainage. The settlement of pile is more in case of two-way drainage than one-way drainage during the consolidation process, and they are same at the end of the consolidation, resulting in more dragload in case of one-way drainage initially.

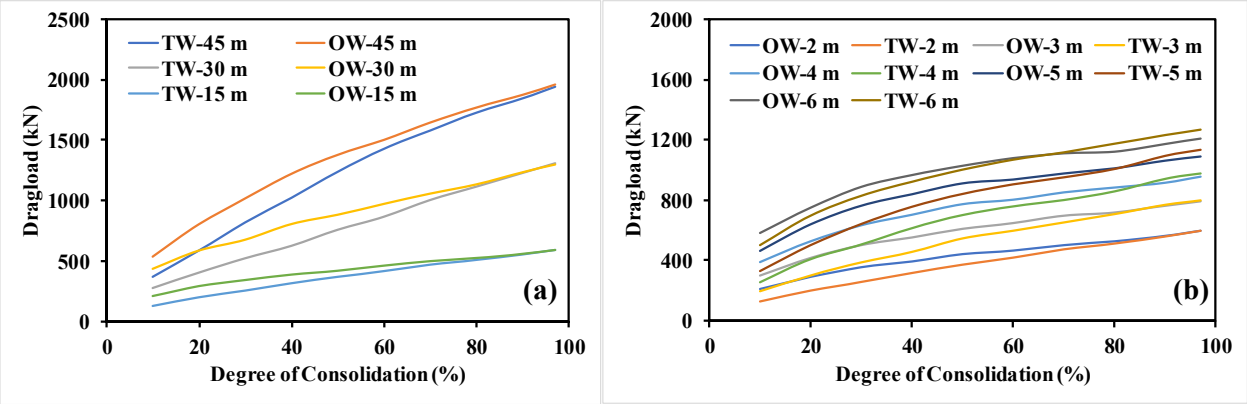


Figure 7 (a) Variation of dragload with degree of consolidation for 15 m, 30 m, and 45 m pile length; (b) Variation of dragload with degree of consolidation for different fill thicknesses.

SUMMARY AND CONCLUSIONS

The NSF on the pile is a very common problem when soft soil exists. The NSF is a very complex problem because it depends on many factors. In this study, the NSF on a single pile is analysed. This study ignores the pile installation effect and considered wished-in-place pile. Numerical studies of NSF on piles are carried out by commercial finite element code PLAXIS 3D. This study shows that the FEM is a perfect tool to analyse NSF problem. The influence of drainage conditions on the development of dragload and depth of NP are studied. The parametric studies of drainage condition include different L/D ratio, different degree of consolidation, and different fill thickness. From the results of the analysis the following conclusions are made:

- The effect of drainage condition on the dragload and NP depth is negligible at the end of consolidation, but at lower degree of consolidation, effect of drainage condition is significant.
- The effect of thickness of fill layer on NP depth is negligible, but it significantly influences the dragload on the pile.

- The variation of NP depths with degree of consolidation is different for different L/D ratios. In case of one-way drainage, the trend of the curve is same for all L/D ratios but different in case of two-way drainage.
- In the design of piles subjected to dragload, the drainage conditions need not be considered, as dragload at the end of the consolidation is same in both one-way and two-way drainage conditions.

REFERENCES

Fellenius, B.H., 1998. Recent Advances in the Design of Piles for Axial Loads, Dragloads, Downdrag, and Settlement. Proceedings of a Seminar by American Society of Civil Engineer, ASCE, pp. 19-37.

Garlanger, J.E. and Lambe, T.W., 1973. Proceedings of a symposium on downdrag on piles, research Report R-73-56, Soil-331, Department of civil Engineering, MIT, Cambridge, Massachusetts.

Hanna, A.M., & Sharif, A., 2006. Drag Force on Single Piles in Clay Subjected to Surcharge Loading. International Journal of Geomechanics, 6(2): 89–96.

Horpibulsuk, S., Shibya, S., Fuenkajorn, K., and Katkan, W., 2007. Assessment of engineering properties of Bangkok clay. Canadian Geotechnical Journal, 44(2): 173–187.

Indraratna, B., Balasubramaniam, A.S., Phamvan, P., & Wong, Y.K., 1992. Development of negative skin friction on driven piles in soft Bangkok clay. Canadian Geotechnical Journal, 29(3): 393–404.

Jeong, S., Lee, J., & Lee, C.J., 2004. Slip effect at the pile-soil interface on dragload. Computers and Geotechnics, 31(2): 115-126.

Lee, C.J., Bolton, M.D. and Al-tabbaa, A., 2002.Numerical modeling of group effects on the distribution of dragloads in pile foundations. Geotechnique, 52(5): 325-335.

Leung, C.F., Radhakrishnan, R., and Tan, S.A., 1991. Performance of precast driven piles un marine clay. Journal of Geotechnical Engineering, 117(4): 637–657.

Little, J.A. and Ibrahim K., 1993. Predictions associated with the pile downdrag study at the SERC soft clay site at Bothkennar, Scotland. Proceedings of the Wroth Memorial Symposium on Predictive Soil Mechanics, pp. 796-818.

PLAXIS 3D Standard User's Manuals, 2016.

Poulos, H.G., 1997. Piles subjected to negative friction: A procedure for design. Geotechnical Engineering, 28(1): 23-44.

Tan, S.A., & Fellenius, B.H., 2016. Negative skin friction pile concepts with soil-structure interaction. Geotechnical Research, 4(3): 137–147.

Trochanis, A.M., Bielak, L., and Christiano, P., 1988. A three dimen- sional non-linear study of piles leading to the development of a sim- plified model. Technical Rep. of Research Prepared for National Science Foundation, Carnegie Mellon University, Pittsburgh.

OPTIMIZATION OF PILE FOUNDATION

A. K. Singh, Associate Professor, Deptt. of Civil Engineering, National Institute of Technology Jamshedpur, Jharkhand (India), Mob. No. : 9430746532, Email: aksingh.civil@nitjsr.ac.in
A. Kumawat, M. Tech. Student, Geotechnical Engg., Deptt. of Civil Engineering, National Institute of Technology Jamshedpur, Jharkhand (India).
A. Kesharwani, M. Tech. Student, Geotechnical Engg., Deptt. of Civil Engineering, National Institute of Technology Jamshedpur, Jharkhand (India), Mob. No. : 7007156080,E-mail: akanksha102@gmail.com

ABSTRACT

Pile is expensive but often necessary for building of large structures, bridges and high rise buildings, etc. therefore it becomes necessary to find the best pile foundation design in terms of performance and economy. In the field, during construction of pile foundation, at some particular location, length of pile is limited to certain depth then by varying parameters like increasing shaft diameter, two piles of smaller diameter, increasing bulb diameter, increasing number of bulbs will give an economical solution for same load. The optimized pile-group design corresponds to the most cost-efficient foundation solution attempting a compromise between the number of piles, their diameter and length as well as the distance between them. That's helps in achieving the most economical design of the pile. Over the past decades, many optimization algorithms have been developed for various engineering problems, but very few attempts, however, have been made in developing an effective optimization methodology for foundation design. In this study, two different design code procedures have been considered in order to assess the performance of the designs obtained during the optimization process, namely IS: 2911 (Part I) and IS: 2911 (Part III). In this work, length of pile is reduced keeping constant load on pile coming from super structure by varying the parameters of pile, volume of earthwork and concrete has been calculated. It has been observed that even after reducing the length of pile (12 m to 9 m), for slightly higher shaft diameter (400 mm to 426 mm), pile foundation is economical.

Keywords: Computer programming; Concrete pile; Under-reamed pile; Pile group; Optimization

INTRODUCTION

In situations where the soil at shallow depth is poor and in order to transmit the load safely, the depth of foundation has to be increased till a suitable soil stratum is met. In view of increased depth, such foundations are called deep foundation such as pile, pier, pile-raft and well. A pile is a relatively small diameter shaft, which driven or cast-in-situ in to the ground. It is expensive but necessary for large structures, high rise buildings, bridges, etc. Therefore, it becomes necessary to find the best pile foundation design in terms of performance and economy (Langroudi et al, 2015; Nikos and Papadrakakis, 2008). Lueng et al (2010) made optimization analyses of piled rafts and freestanding pile groups, where pile lengths are varied across the group to optimize the overall foundation performance. Liu (2012) studied the optimum conceptual design of pile foundations at the initial design stage. A modular method is proposed, which divides the foundation into modules and each module is identified by its characteristics of pile length, diameter, number and layout. Hurd and Truman (2006) developed a three dimensional optimization computer program that designs a foundation system with an optimal number of piles, geometric layout, pile orientation, batter, and size for a given structure subjected to multiple load cases. The optimization procedure controls displacements while reducing the overall weight of the pile foundation design. The foundation cost, of real-world structural systems, can vary from 5 % to 10 % of the construction cost of the superstructure while the number of piles required might exceed several

© 2018 Deep Foundations Institute

hundreds or even thousands (Letsios et al, 2014). At any site, if engineer is facing problems in providing designed length of pile then he will get alternative solution such as larger diameter pile of smaller length, more number of piles of lesser diameter which make the pile foundation economical without compromising the load carrying capacity. Computer program for design of pile foundation allows the user to input data that includes: parameters of pile and properties of soil. Different analytical equations for both cohesive and non-cohesive soil as given in IS: 2911 (Part I) and IS: 2911 (Part III) have been used. Similarly, for reduced length of pile, no. of piles, stem diameter, no. of bulbs, bulb diameter, etc. has been increased and studied at constant pile load and then volume of earthwork and concrete have been computed. In this way cost effective alternative can be selected.

This study presents the optimization of pile foundation using computer program in "C++" that can minimize the cost of pile foundation and time (Ranjan and Rao, 2010; US Army 1991). In present work, program has been developed for checking load carrying capacity by varying the parameters of pile and soil, and then optimized its cost on reduced volume obtained for same load (Hill, 1981; Poulos, and Davis, 1980).

THEORETICAL ANALYSIS

Different derivations have been studied for analysis and design of piles. Piles are design in such a way so that the load coming through the super structure can be transmitted to the soil without causing failure of soil and without causing excessive settlement or failure of pile material under loading.

Ultimate Load Bearing Capacity

The ultimate load bearing capacity (Q_u) of piles in granular soil which can support through the combined resistance of skin friction and point bearing as expressed as follows:

$$Q_u = Q_{pu} + Q_f \tag{1}$$

Where, Q_{pu} - Ultimate point bearing resistance, Q_f - Ultimate skin friction resistance

In cohesive soils the contribution of point bearing is small compared to that of shaft skin frictional resistance. The ultimate load bearing capacity (Q_u) of piles can be calculated by

$$Q_u = (A_P * N_C * C_P + \alpha * c_u * A_s) \tag{2}$$

Where, A_p – Cross sectional area of pile base, N_c – Bearing capacity factor, C_p - Average cohesion at pile tip, α - Adhesion factor, c_u - Average cohesion in embedded length of pile, A_s – Surface area of pile

Ultimate Load Bearing Capacity of Under-reamed Pile

The ultimate load bearing capacity of an under-reamed pile for cohesive soil may be obtained by equation

$$Q_u = A_P * N_C * C_P + A_a * N_C * C'_a + C'_a * A'_S + \alpha * C_a * A_S \tag{3}$$

Where $A_a = \frac{\pi}{4}\left(D_u^2 - D^2\right)$, D_u and D are bulb and stem diameter, C'_a - Average cohesion of soil around the bulbs, A'_S - Surface area of the cylinder circumscribing the bulbs, C_a - Average cohesion of the soil along the pile stem

Estimation of Earthwork and Volume of Concrete for Cast-in-Situ Pile and Under-Reamed Pile

In drilling the holes, cost of earthwork for cast-in-situ pile and under-reamed pile is estimated in terms of depth of bore. Cost per meter cube of concrete and earthwork for cast-in-situ concrete pile and under-reamed pile is estimated in terms of depth of bore hole including the bulbs.

Cast-in-situ concrete pile

Volume of concrete for the shaft portion is given by

$$V_{shaft} = \frac{\pi D^2}{4} * L \quad (4)$$

Volume of pile cap (np = 1) is given as

$$V_{cap} = ((D + 0.2) * (D + 0.2) * t) \quad (5)$$

Where L – Length of pile, t – Thickness of pile cap

For (np = 2)

$$V_{cap} = \left(t * \left((D + 0.2) * \left((D + 0.2) + 2 * D\right)\right)\right) \quad (6)$$

Total volume of concrete for cast-in-situ pile is

$$V_{concrete} = V_{shaft} + V_{cap} \quad (7)$$

Under-reamed pile

Volume of shaft is calculated as given in equation (4) and for remaining portion of bulb, the bulb is considered as a solid of revolution of a trapezoidal section as 1.5 D at the base where it is attached to the shaft and 5 cm at the tip. For uniform under-reaming of bulb by the under reamer, depth of trapezoid is given by:

$$h = (\frac{Du}{2} - \frac{D}{2}) \quad (8)$$

Area of trapezoid is considered equal at any section,

$$\text{Area of trapezoid} = \frac{1}{2} * \left(\frac{Du}{2} - \frac{D}{2}\right) * (1.5D + \frac{D}{4}) \quad (9)$$

$$\text{The average circumference of the solid of revolution formed by the trapezoid} = \frac{\pi(D+Du)}{2} \quad (10)$$

Remaining volume of concrete for n number of bulb is thus given as

$$V_{bulb} = n * \frac{\pi(D+Du)}{2} * \frac{1}{2} * \left(\frac{Du}{2} - \frac{D}{2}\right) * (1.5 * D + \frac{D}{4}) \quad (11)$$

Total volume of concrete for under-reamed pile is given as

$$V_{concrete} = V_{shaft} + V_{bulb} + V_{cap} \quad (12)$$

If the length is restricted, then other parameters may vary for a constant load coming through the super-structure. Corresponding to each safe design, different volumes of concrete have been obtained which directly affects the cost of pile foundation. The safe design corresponding to the least cost will give the most optimum choice for the given load.

RESULT

In the present work, a number of computer programs have been developed for analysis of pile foundation based on IS codes. Computer program allows the user to put data that includes parameters of pile and properties of soil. The value obtained is then compared with the solution given in literature and cost is optimized in respect of volume of concrete. Comparative study has been carried out in which, length of pile is reduced keeping constant load on pile by varying the parameters. Output of computer program for pile in non-cohesive soil ($\emptyset = 40^0$) is given in "Table 1" and ($\emptyset = 35^0$) is given in "Table 2". Variation of volume of concrete with reducing length of pile for ($\emptyset = 40^0$) is shown in Fig. 1 and for ($\emptyset = 35^0$) is shown in Fig. 2.

Result of Cast-in-Situ Concrete Pile (Non-Cohesive Soil)

Table 1. Output of computer program for pile in non-cohesive soil ($\emptyset = 40^0$)

Initial Length of Pile = 12 m $(N_q) = 137$

Sl. No.	Length of Pile (m)	Diameter of Pile (m)	No. of Piles	Q_{safe} (kN)	Volume of Concrete (m^3)
Initial Diameter of Pile = 0.4 m (400 mm)					
	12	0.4	1	1307.5	1.652
1.	9	0.426	1	1310.9	1.440
	8	0.331	2	1316.2	1.630

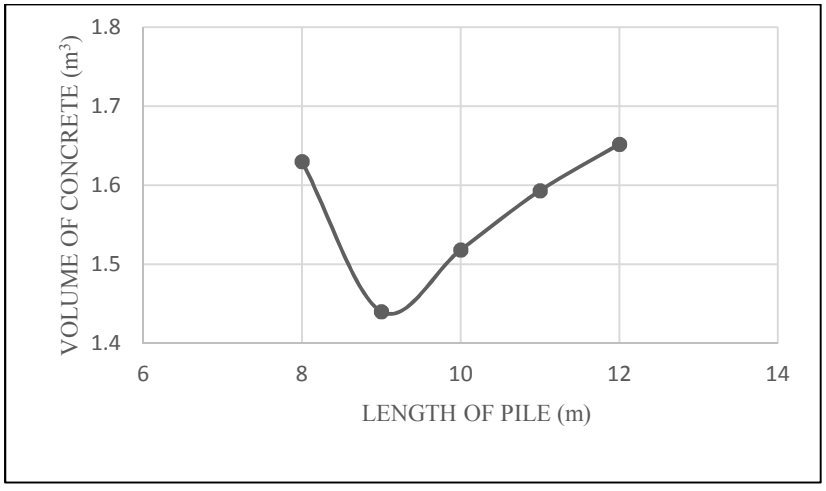


Fig. 1. Variation in volume of concrete with length of pile (D = 400 mm, $\emptyset = 40^0$)

Table 2. Output of computer program for pile in non-cohesive soil ($\emptyset = 35^0$)

Initial Length of Pile = 12 m $(N_q) = 57.5$

Sl. No.	Length of Pile (m)	Diameter of Pile (m)	No. of Piles	Q_{safe} (kN)	Volume of Concrete (m^3)
Initial Diameter of Pile = 0.7 m (700 mm)					
	12	0.7	1	2766.9	4.942
2.	9	0.76	1	2771.5	4.451
	8	0.585	2	2770.8	4.914

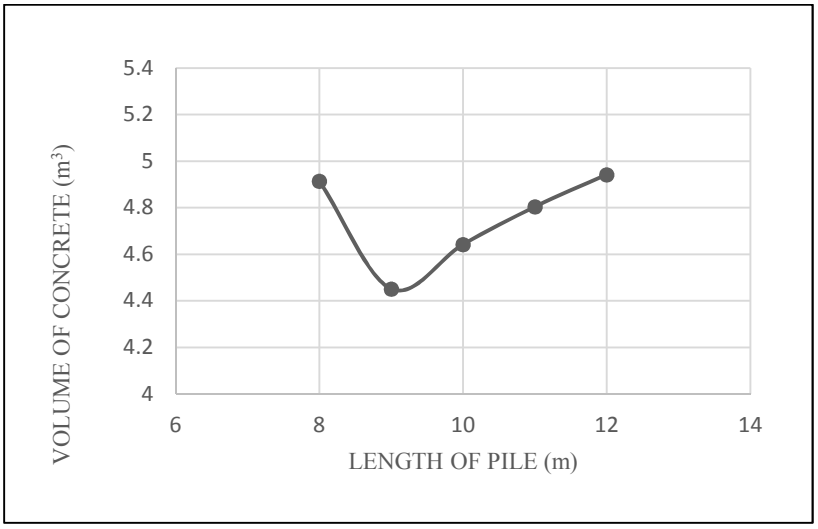


Fig. 2 Variation in volume of concrete with length of pile (D = 700 mm, $\emptyset = 35^0$)

Result of Cast-in-Situ Concrete Pile (Cohesive Soil)

Output of computer program for pile in cohesive soil (c = 30 kN/m^2) is given in "Table 3" and variation of volume of concrete with reducing length of pile for is shown in Fig. 3.

Table 3. Output of computer program for pile in cohesive soil (c = 30 kN/m^2)

Initial Length of Pile = 8 m

Sl. No.	Length of Pile (m)	Diameter of Pile (m)	No. of Piles	Q_{safe} (kN)	Volume of Concrete (m^3)
Initial Diameter of Pile = 0.3 m (300 mm)					
	8	0.3	1	89.06	0.665
1.	7	0.335	1	89.08	0.731
	6	0.202	2	89.17	0.514

Initial Diameter of Pile = 0.4 m (400 mm)					
	8	0.4	1	122.14	1.149
2.	7	0.444	1	122.17	1.249
	6	0.27	2	122.29	0.876

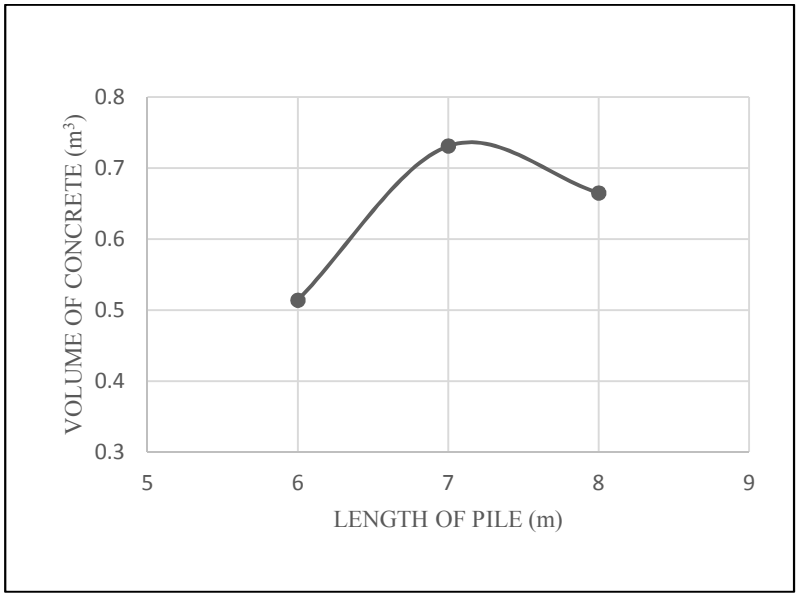


Fig. 3. Variation in volume of concrete with length of pile (D = 300 mm, c = 30 kN/m^2)

Result of Under-Reamed Pile

Output of computer program for under-ream pile in cohesive soil (c = 35 kN/m^2) is given in "Table 4" and variation of volume of concrete with reducing length of pile for is shown in Fig. 4.

Table 4. Output of computer program for pile in cohesive soil (c = 35 kN/m^2)

Initial Length of Pile = 7 m np = 1 n = 2 Q_{safe} = 151.739 kN Volume of Concrete = 1.287 m^3

Sl. No.	Stem Diameter (m)	Bulb Diameter (m)	Q_{safe} (kN)	Volume of Concrete (m^3)
Reduced length of Pile = 6 m				
	0.415	0.830	151.997	1.257
	0.375	0.844	151.924	1.089
1.	0.342	0.855	151.913	0.957
	0.315	0.866	152.516	0.855
	0.291	0.873	152.197	0.766

Reduced length of Pile = 5 m				
	0.429	0.858	151.865	1.206
	0.387	0.871	151.808	1.049
2.	0.352	0.880	151.952	0.923
	0.323	0.888	151.275	0.823
	0.298	0.894	151.195	0.739
Reduced length of Pile = 4 m				
	0.446	0.892	151.945	1.158
	0.399	0.898	152.067	0.998
3.	0.362	0.905	151.741	0.880
	0.331	0.910	151.829	0.784
	0.305	0.915	152.020	0.706

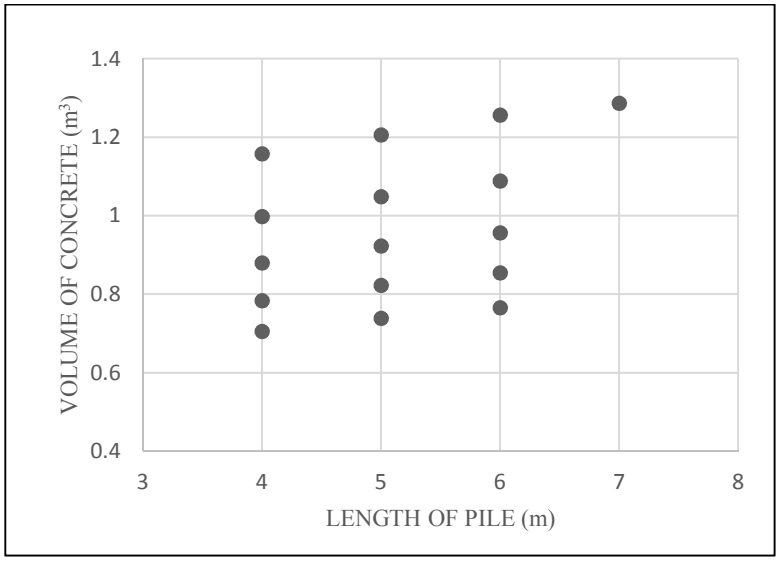


Fig. 4. Variation in volume of concrete with length of pile (c = 35 kN/m^2, np = 1, n =2)

DISCUSSION

In non-cohesive soil, higher load carrying capacity or at least equal load carrying capacity of pile has been found for length of pile decreases from 12 m to 9 m for stem diameter varying from 300 mm - 1000 mm and for variation of Ø of soil from 40^0 to 30^0. Volume of earthwork and concrete is obtained less than the initial volume as shown in "Table 1" and "Table 2"; and Fig. 1 and Fig. 2. Hence, pile of smaller length can also make economical. In case of Ø = 25^0, this above trend has not been found.

If two number of piles of smaller diameter (330 mm) of length 8 m and $\emptyset = 40^0$, same trend has been observed as obtained in case of single pile for stem diameter varying from 400 mm to 1000 mm.

If $\emptyset = 35^0$, this pattern is followed for stem diameter 700 mm to 1000 mm. This trend has not followed for $\emptyset = 30^0$ and $\emptyset = 25^0$. It is happening due to reduction of frictional resistance acting between soil and pile shaft as $\emptyset$ is reducing.

In case of cohesive soil, higher load carrying capacity or at least equal load carrying capacity of pile has been found for length of pile decreases from 8 m to 7 m for stem diameter varying from 300 mm - 1000 mm and for variation of cohesion from 30 kN/m^2 to 50 kN/m^2 but volume of earthwork and concrete is greater than the initial volume as presented in "Table 3" and Fig. 3. Hence, in this option, single pile up to 7 m length is not economical.

If length of pile decreases from 8 m to 6 m for stem diameter 300 mm - 1000 mm and for variation of cohesion from 30 kN/m^2 to 50 kN/m^2, using two numbers of piles, then the volume of concrete and earthwork is less than the initial volume for equal or higher load on pile. Therefore, this option of two piles of smaller length and diameter is economical.

In case of under-reamed pile, higher load carrying capacity or at least equal load carrying capacity of pile has been found for length of pile decreases from 7 m to 4 m for stem diameter 200 mm to 500 mm, bulb diameter 2 to 3 times of stem diameter, number of piles 1 to 2, number of bulbs 2 to 3 and for variation of cohesion 20 kN/m^2 to 35 kN/m^2 and economical since volume of earthwork and concrete is less than the initial volume as shown in "Table 4" and Fig. 4. Same trend has been observed for variation of cohesion from 20 kN/m^2 to 35 kN/m^2 and best economical solution has been observed if number of piles is 2 and number of bulbs is 2 for 4 m length of pile.

CONCLUSIONS

On the basis of study, limited results obtained and rigorous discussion, important conclusions may be drawn as follows:

Non-Cohesive Soil

- In a situation where designed pile length cannot be provided and engineer are compelled to reduce the length of pile even then pile foundation can make economical by slightly increasing the diameter of stem without compromising the load carrying capacity for soil having angle of internal friction greater than 30^0.
- Pile foundation can also make it economical by providing more number of piles of smaller diameter of smaller length for pile diameter 600 mm or higher value without compromising the load carrying capacity for soil having angle of internal friction greater than 30^0.

Cohesive Soil

- Pile foundation cannot be made economical for larger diameter of pile of smaller length as obtained in case of cohesion-less soil.
- It can be made economical satisfying load carrying capacity by adopting more number of piles of smaller diameter and smaller length.

Under-Reamed Pile

- In case of under-reamed pile, high or equal pile load carrying capacity can be achieved by decreasing the length of pile, by reducing the stem diameter and increasing the bulb diameter and make the under-reamed pile foundation economical.

- Pile can also be made economical for more number of piles of smaller diameter and more number of bulbs even after reduced length of pile.

REFERENCES

Hill, J. L., 1981. User's Guide: Computer Program for Optimal Design and Analysis of Pile Foundations (PILEOPT). Instruction Report K-81-5, US Army Engineer Waterways Experiment Station, Vicksburg, MS.

Hurd, A. J. and Truman, K. Z. 2006. Optimization Method of Pile Foundations, Advances in Engineering Structures, Mechanics & Construction, Springer, pp 653–661.

IS: 2911 (Part I/ Sec I), 2010. Driven Cast In-situ Concrete Piles, Bureau of Indian Standards, New Delhi.
IS: 2911 (Part III), 1980. Under –Reamed Piles, Bureau of Indian Standards, New Delhi.

Langroudi G., Marseh P., Heidarpour, Ekramirad and Houssainnezhad, 2015. Dimensional Optimization of Pile Raft Foundation. Research Journal of Recent Sciences.

Letsios, Ch., Lagaros N. D. and Papadrakakis M., 2014. Optimum Design Methodologies for Pile Foundation in London. [J] Elsevier.

Leung, Y. F., Klar, A. and Soga, K. 2010. Theoretical Study on Pile Length Optimization of Pile Groups and Piled Rafts, Journal of Geotechnical and Geoenvironmental Engineering, ASCE, Volume 136 Issue 2.

Liu, X. , Cheng, G., Wang, Bo. and Lin, S., 2012. Optimum Design of Pile Foundation by Automatic Grouping Genetic Algorithms, International Scholarly Research Network, ISRN Civil Engineering Volume 2012, Article ID 678329.

Nikos L. and Papadrakakis M., 2008. Optimum Design of Pile Foundation. Journal Civil-Comp Press.

Poulos, H. G. and Davis, E. H., 1980. Pile foundation analysis and design. John Wiley & Sons Inc.

Ranjan G. and Rao A. S. R., 2016. Basic and Applied Soil Mechanics. New Age, pp. 545-603.

US Army Corps of Engineers, 1991. Design of Pile Foundation. Engineer Manual 1110-2-2906, Washington, DC.

PERFORMANCE OF CONTIGUOUS BORED PILE WALL RETENTION SYSTEM: A CASE STUDY

Vimala Chinnasamy, Sr. Geotechnical Engineer, Keller India, vimala@kellerindia.com
Madan Kumar Annam, Head of Engineering, Keller India, madankumar@kellerindia.com

ABSTRACT

Design of retention system for construction of basements needs technical expertise and well-planned monitoring system to check probable deflections of the retaining structure including subsidence around the excavation pit. The construction of basements with proximity to adjacent structures and busy roads is the most challenging aspect for the practicing engineer. This demand understanding of the complexity of the problem, risk involved and assumptions on soil structure interaction. A simple 2-dimensional analysis using numerical modelling can normally be chosen to assess the exact behavior of the retention structure. Performance of a retention system for deep excavation of 11.5m for three basements having a perimeter of about 215m long, surrounded by high raised buildings is selected for study in this paper. Contiguous bored pile wall with single level inclined ground anchors was adopted as an optimistic temporary retention system in this project after allowing removal of 3.0m of surface soil. A well planned monitoring program was carried out during excavation stages to study the performance of retention system. This paper covers discussions on analysis of retention system using WALLAP and PLAXIS 2D and comparing measured deflections of the wall.

Keywords: Retention system, CBP wall, anchors, WALLAP, PLAXIS 2D, Deflection Monitoring.

INTRODUCTION

In the recent years, deep excavations are widely adopted in India to utilize the underground space for basement construction which can be used for parking, public amenities and metro stations etc. These deep excavations are commonly carried out in congested areas which requires stable retention system to avoid failures of the surrounding structures. The soil within the retention side will experience lot of changes due to excavation inside the site. For an example during excavation stage, the retention soil will experience unloading condition and during installation and pre-stressing of anchors the same soil mass will experience reloading condition. Hence, adequate knowledge on soil-structure interaction is required for analysing the excavation problems. The conventional method of design and analysis of deep excavation problems involves assumptions.

Retention system using Contiguous Bored Pile (CBP) wall with one level of inclined soil anchors were chosen as the cost effective and optimistic solution. Preliminary analysis was carried out using WALLAP and confirmed with PLAXIS 2D during detailed analysis.

This paper presents design and construction of temporary retention system using CBP wall with inclined soil anchors and also covers discussion on performance of the retention system at site.

SOIL STRATAGRAPHY

The subsoil conditions of the project site consist of silty clay / clayey sand, medium dense to dense silty sand and underlain by weathered rock. The ground water table was noticed at 5m below the existing ground level. The site is excavated up to a depth of 3.0m in order to clear the debris of existing old building and also to ensure proper working environment. Also, such removal of the surface will facilitate optimizing the quantities of retention system. The typical subsoil profile is indicated in **Fig. 1**.

ANALYSIS USING WALLAP

WALLAP is a simple, fast and easy software which can be used for the analysis of cantilever as well as anchored retaining walls. Both temporary system (i.e., sheet piles & solider piles) and permanent systems (D wall, CBP wall etc.,) can be designed using WALLAP. The overall stability of wall is

© 2018 Deep Foundations Institute

estimated by limit equilibrium analysis method and the wall movements and bending moments can be estimated either using subgrade reaction analysis or 2D finite element analysis.

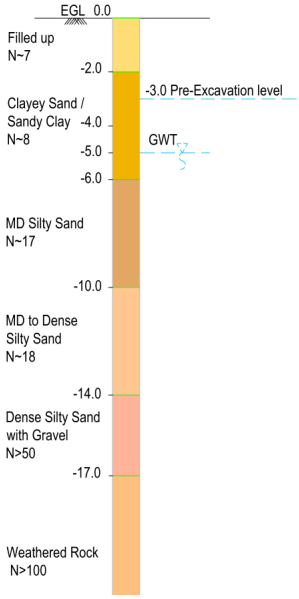


Fig. 1. Subsoil profile

After having results of several options, 750mm diameter of CBP at 820mm centre-to-centre spacing was chosen as an economical solution. The design of CBP was carried out as per procedure stipulated in IS 2911 Part 1 / Section 2 (2010) and IS 456 (2000).

Since this retention system is a temporary wall which was used for the excavation works, capping at the top is ignored and also pre-excavation of 3m was proposed to optimize cost. Based on the similar experience in the past, the anchors were installed 5m below EGL to reduce the bending moment as well as control the wall deflections.

LATERAL SUPPORT

The active earth pressure exerted due to the retention soil and water is more than the resistance provided by the passive pressure due to embedment of CB piles. To counteract the additional load, the lateral support system by means of internal or external supports is required. Hence, the inclined ground anchors of approximately 50T capacity at alternative CBPs were considered as a lateral support. The design of inclined ground anchors was done according to BS 8081 and IS 14268.

The combination of retention piles with inclined ground anchors ensured factor of safety more than 2 against overall stability in WALLAP analysis. A steel waler beam was used to connect all anchors and for prestressing. Grout columns of 150mm diameter were installed behind the CBP wall to control soil erosion due to water seepage. The typical WALLAP model is presented in **Fig 2**.

RETENTION SYSTEM ANALYSIS USING PLAXIS 2D

Since the deep excavation problem involves complex behavior of soil and also to get more confidence of the arrived retention system, it was decided to carryout sensitivity analysis using another software to confirm the outcome of the results. Hence, chosen retention system of 750mm diameter CB piles at 820mm c/c was proof checked by the external consultant using PLAXIS 2D software. The typical model used for PLAXIS is shown in **Fig. 4**.

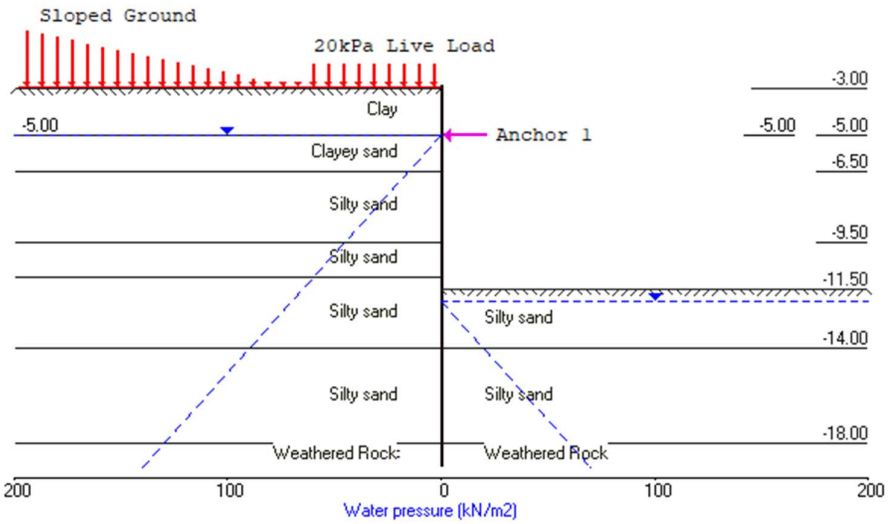


Fig 2. Typical WALLAP model

MODELLING METHODOLOGY IN PLAXIS 2D

The following modelling methodology was used in the PLAXIS 2D analysis.

- The plane strain model with 15 node triangular elements were used as a basic model which is having better distribution of nodes and gives accurate results.
- The most commonly used Mohr coulomb model was used to model the subsoil behaviour.
- Since this site is surround by roads and adjacent structures are 20m away from the retaining wall, surcharge load of 20kPa for the construction activities had been considered.
- In PLAXIS 2D, different sizes of mesh are available such as very coarse, coarse, medium, fine and vey fine. In this analysis fine mesh size was used which will give appropriate results. The connectivity plot of mesh is illustrated in **Fig 3**.

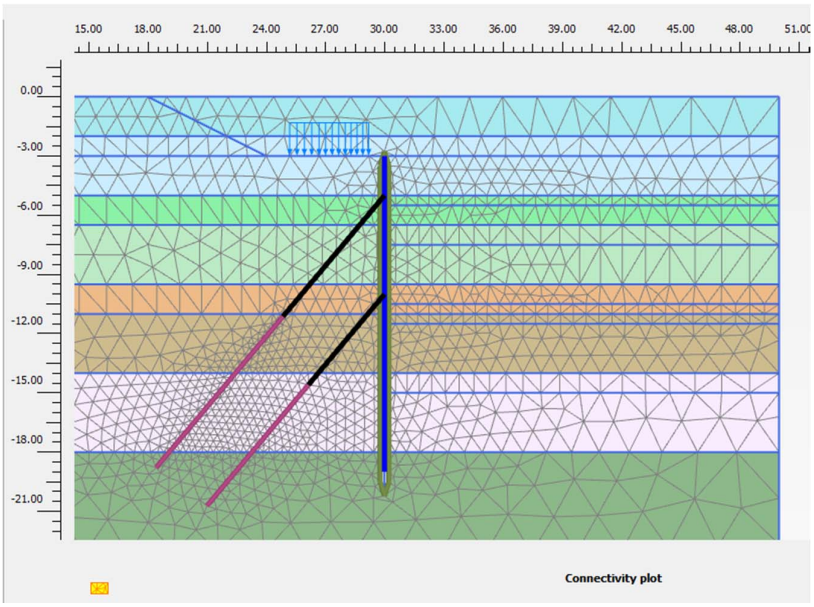


Fig 3. Mesh connectivity plot

The analysis results i.e., bending moment, shear force and deflections obtained from PLAXIS 2D analysis were compared with WALLAP analysis. The results are almost similar, and results obtained from PLAXIS 2D are optimistic when compared to WALLAP analysis.

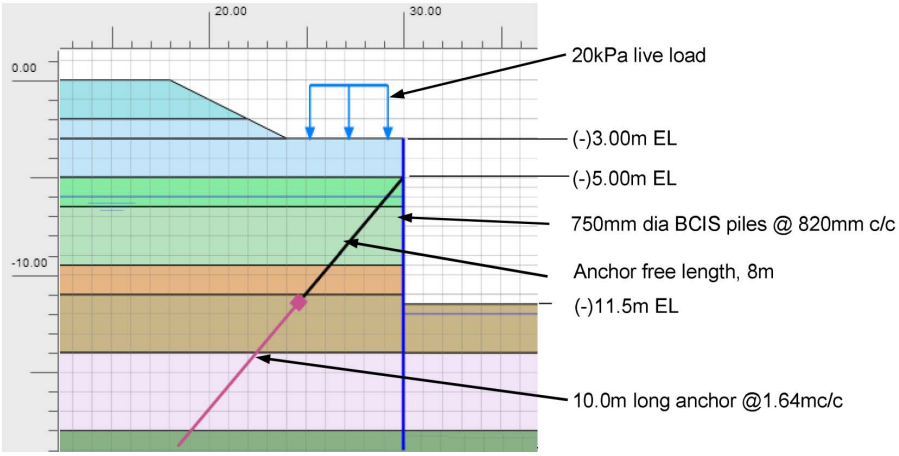


Fig. 4 Typical PLAXIS 2D model

The comparison of results arrived from WALLAP and PLAXIS is presented in **Fig 5**. Hence, the design of retention system was made based on conservative results. The maximum deflection predicted by WALLAP is 32mm whereas the maximum deflection predicted by PLAXIS is 25mm. Typical cross section of adopted retention system is indicated in **Fig 6**.

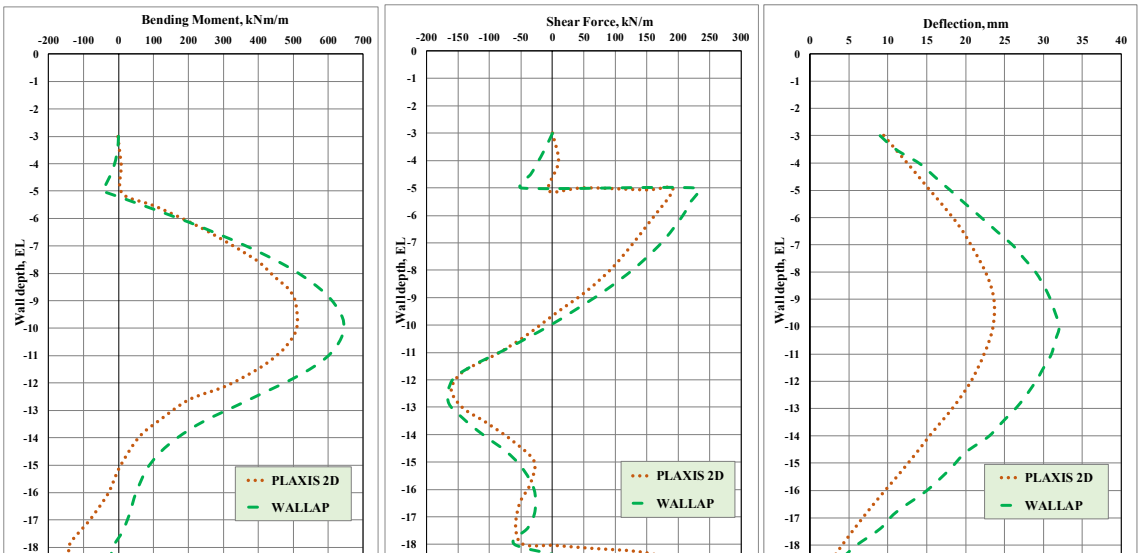


Fig 5. Comparison of analysis results (Bending moment, Shear force and Deflections)

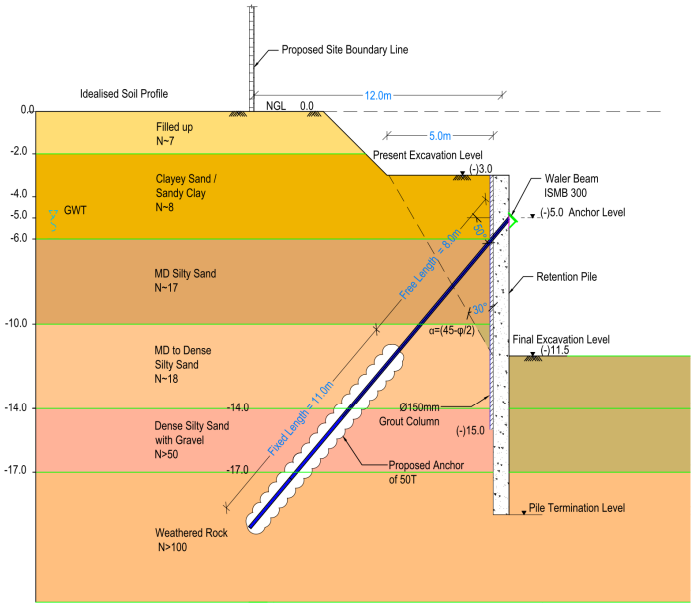


Fig 6. Typical cross section of adopted retention system

MONITORING SYSTEM

The design of retaining wall for deep excavation involves lot of assumptions on the soil and structural behavior which leads to lot of uncertainties in actual conditions. Hence for the excavation problems, it is the design Engineer's responsibility to validate the performance of executed retaining wall by adopting systematic monitoring program at site. This real time monitoring results will build confidence to the design Engineers.

In this project site, totally 26 nos. of monitoring points were established throughout the site at three different levels. The plan and cross section showing monitoring points are shown in **Fig 7**. The monitoring was carried out using a total station instrument. The wall deflections were monitored for a period of 8 months from starting of excavation to till the construction of all basement slabs. The monitoring was carried out on daily basis, during the initial process of excavation. After the stabilization of results, the monitoring works was subsequently reduced to weekly basis.

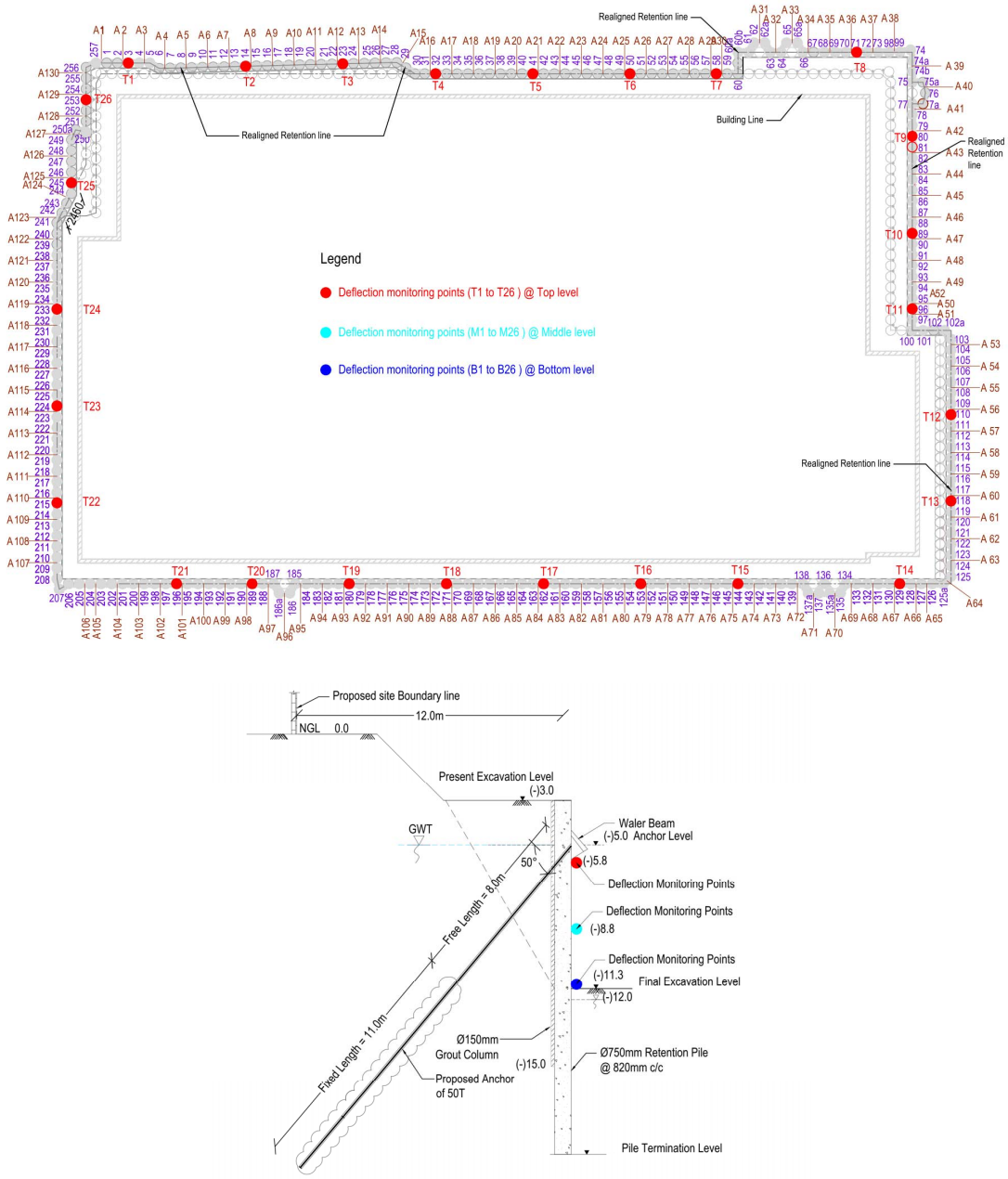


Fig 7. Typical plan and cross section showing deflection monitoring points

The recorded wall deflections and its trend at site is almost comparable with the predicted movement. The maximum wall deflection recorded at site was about 21mm which is almost close to the predicted deflection in PLAXIS 2D (25mm). The comparison of deflections is shown in **Fig 8**. View of the final excavation is presented in **Fig 9**.

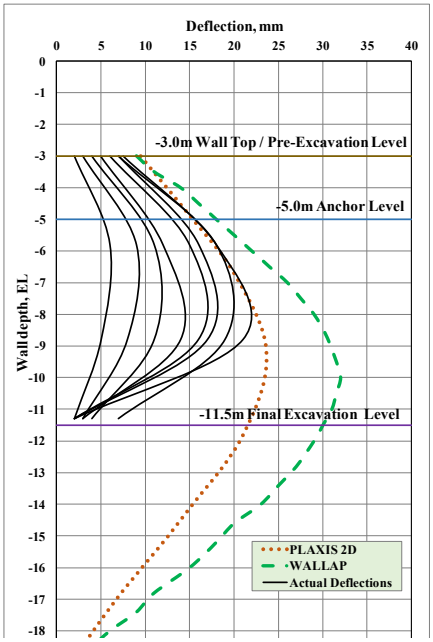


Fig 8. Comparison of predicted and actual deflections

CONCLUSIONS

This paper discussed analysis and design of contiguous bored pile wall with single level ground anchors for a 11.5m deep excavation. Analysis was carried out using two different software (WALLAP and PLAXIS 2D) to have confidence on the behavior of soil structure interaction. The analysis results of both software such as bending moment, shear force and deflections are compared. The importance of wall movement during excavation and monitored results are presented. The actual wall movements observed at site are compared with the deflections predicted by WALLAP and PLAXIS 2D software. The predicted and recorded deflections are comparable and design assumptions are proved accurate. This indicates that the design soil parameters and assumptions considered for the design are accorded with the actual site condition which builds confidence to the practicing engineers.

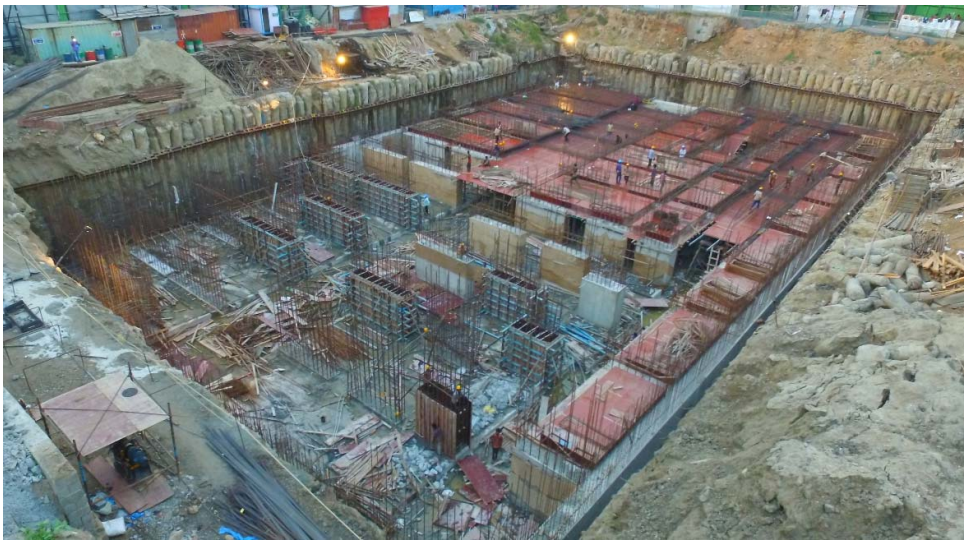


Fig 9. View of the final excavation of the site

ACKNOWLEDGEMENTS

The authors acknowledge with gratitude to Keller management, for their continuous support and encouragement in finalization of theme of this paper including valuable comments and suggestions that helped the authors to refine and improve the quality of the paper. Thanks are also due to Keller India site team for providing photographs and other execution data.

REFERENCES

1. Project soil investigation report, conducted in 2013.
2. Stability analysis report for retention system using Plaxis 2D
3. Design and Construction of pile foundation – code of practice, IS 2911 Part 1, Section 2: 2000
4. BS code for practice for ground anchorages, BS 8081: 1989
5. Guidelines for design of RCC structures, IS 456 2000, SP 16 1980

PRE-STRESSED GROUND ANCHORS FOR UNDERGROUND STATIONS AND EARTH RETAINING STRUCTURES

Nagaraj Kumar BV
Design & Technical Coordinator
Pavai Infra Geotech - TeampT JV
Coimbatore, Tamil Nadu, India
Contact No.: +91-8135855815
E-mail: nagaraj.k@pavaigeotech.com

***Abstract* – Towards the end of 2017, Pavai - TeampT JV began working on Mumbai Metro Line - 03. This phase of the metro project involves the construction of 27 under-ground stations at a depth of 20 to 28 m from ground level, to a cumulative length of 33,500 m. Pavai Infra Geotech, a specialist ground anchor installation agency in association with TeampT, a specialist design consulting firm, acquired earth-retaining structural works in 6 underground stations, namely: BKC, Vidyanagari, SEEPZ Ramp, SEEPZ station, Marol Naka and Vidhan Bhavan. Design of pre-stressed retrievable rock anchors for several stations and TBM launching shaft locations has been completed. The challenge lies in meeting the stringent international standards used in India (BS) and the condition of sensitive working environments, keeping conscious of commercial parameters and practical aspects of execution to specification. This paper discusses the purpose, basic design, detailed design approaches and actual work implementation of pre-stressed ground anchors that are being provided at the Mumbai Metro Line - 03 Project by Pavai Infra Geotech - TeampT JV.**

Keywords – Earth Retaining Structures, Retrievable Rock Anchors, Pre-stressed.

I. INTRODUCTION

The Mumbai Metro Line – 03 project involves the construction of 27 under-ground stations at a depth of 20 m to 28 m from the ground level. Fig. 1 shows the route map of the project. Each station has different soil strata and load bearing requirements for the pre-stressed anchors. Based on the DDC's (Detailed Design Consultant) requirement of type, capacity and maximum working load for each layer, further design is done by Pavai -TeampT JV to the level of each rock anchor's size, number of strands for the pre-stressed rock anchors and other specifications. Once the trial or investigative anchor is done, based on the actual bond stress, further working anchors are designed and executed. In all these stations, the anchors designed and installed are temporary and retrievable.



Fig 1. Mumbai Metro Line-03

II. RETRIEVABLE ANCHOR SYSTEM

Pre-stressed ground anchors are often used as earth retaining devices. However, due to space constraints in this project they are a retrievable type with various acceptance criteria at different stages according to BS standards, since information and guidance is limited in IS 10270 standards.

In this system, the PC strands are encased in plain HDPE pipes and then saddles in U Turn anchor for the purpose of retrieval of anchors. Fig. 2 illustrates the general arrangement of retrievable anchor system.

© 2018 Deep Foundations Institute

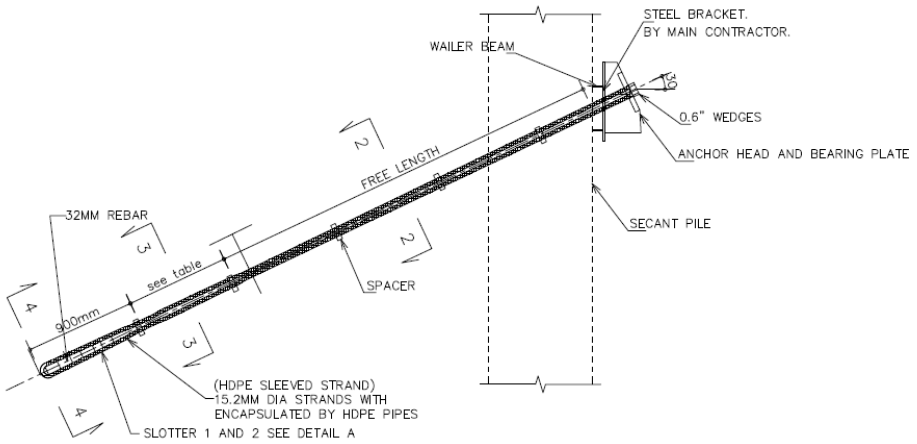


Fig 2. General Arrangement of retrievable U-Turn System

III. COMPONENTS OF ANCHORAGE SYSTEM

All the components of anchorage system are designed and developed in house to meet the ultimate load capacity of each anchor. The performance of the pre-stressed anchors are based on the BS EN 13391-2004 specifications. Fig.3 to Fig. 6 shows the various components of retrievable anchors.



Fig 3. PC Strands as per IS 14268 Class II

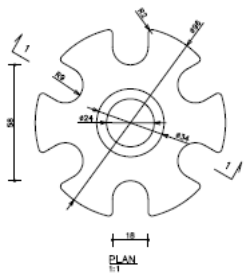


Fig 4. Spacer and centralizer

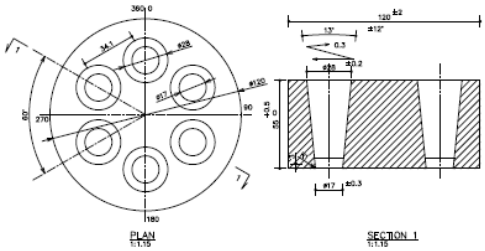


Fig 5. Anchor head

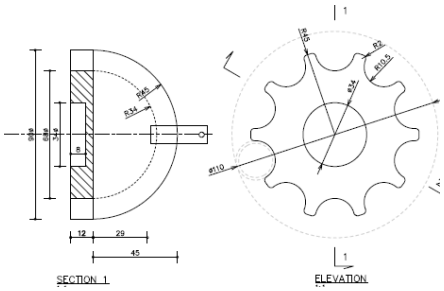


Fig 6. U-Turn Saddle

IV. DESIGN AND WORK FLOW OF PRE-STRESSED ANCHORS

The Work Flow of pre-stressed anchors consist of:

- Fixing the capacity of the anchor based on the actual earth pressure resistance under various conditions.
- Preliminary Design of free length, fixed length and No. of strands for the anchor.
- Installation of Trial Anchors to ascertain the grout-ground interface bond assumed in the preliminary design.
- Design of working anchors.
- Installation of anchors for Suitability and Creep test to ascertain the actual behavior of the working anchor.
- Working Anchor Installation, grouting and stressing work.
- Retrieving of anchors once the service period is completed.

Fig 7. Shows the flow diagram of the pre-stressed rock anchors work.

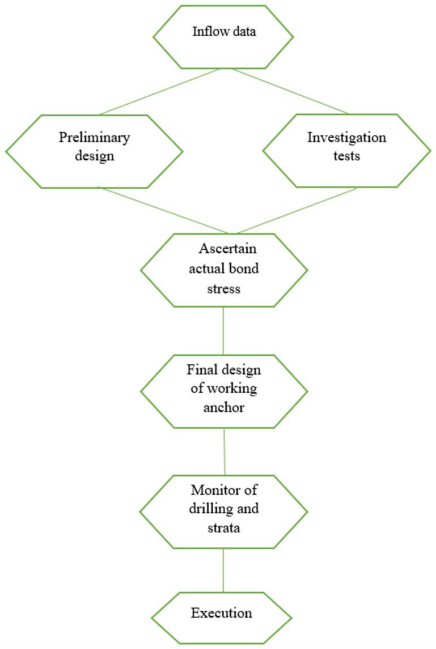


Fig 7 Work Flow of Pre-stressed anchor completion

V. PRELIMINARY DESIGN OF TEST ANCHORS

A. Inflow Data

Before to start the design of test anchors, clients will provide the geotechnical factual investigation reports which will contain the necessary soil strata bore logs with subsurface conditions, regional geological and hydrogeological conditional assessments.

B. Design of Test Anchor

The investigation test anchor locations are proposed by the DDC. At each station, 3 Nos. of test anchors are proposed. The following example (BKC Station) shows the design calculation of test anchor.

Example: (BKC)

Design Load on anchor: 1250 kN
Diameter of bore hole: 150 mm

As per the Geo technical investigation report, the foundation strata at the anchor location is a rock. Hence a rock anchor has been designed as per BS 8081:2015.

The design of Pre-stressed ground anchor involves two parts.

1) *Part-I: Number of Strands*

Diameter of the strand = 15.2 mm
UTS of the strand = 26.54 MT
80% of UTS = 21.23 MT
Design load on anchor = 1250 kN = 127 MT
No of strands required = 127/21.23 = 5.98
Estimate (rounded up) = 6 strands.

2) *Part-II: Fixed Anchor Length*

The fixed anchor length is calculated based on the ultimate skin friction at rock-grout interface. For strong rock, the ultimate skin friction may be taken as 10% of the unconfined compressive strength of the rock up to a maximum value of 4 MPa. In the geotechnical investigation report, it was observed that the average Uniaxial Compressive Strength of the in-situ rock (Volcanic Breccia/Basalt) is 13.53 MPa.

$$q_u = 13.53\ MPa$$
$$\tau_{ult} = 0.1 \times 13.53$$
$$= 1.353\ MPa$$
$$say\ \tau_{ult} = 1.35\ MPa$$

The pull-out capacity of a fixed anchor in rock is given by the following equation,

$$T_f = \pi D L \tau_{ult}$$
$$D = 150\ mm$$
$$\tau_{ult} = 1.1\ MPa$$

According to BS 8081-2015, the minimum required factor of safety on the ground/ grout interface is 3.00 for temporary anchorages.

Hence, the ultimate load on the anchor is

$$T_f = 1250 \times 3.0 = 3750\ kN.$$
$$L = \frac{T_f}{\pi D \tau_{ult}} = \frac{3750}{\pi \times 150 \times 1.35} = 5.89\ m$$

Say 6 m

In retrievable anchor system, one slotter/saddle is required for two strands. The minimum spacing between the saddles of two pairs of strand is proposed as 1 m. Also, as per BS 8081-2015, the fixed anchor length should not be less than 3 m. Hence, for 6 Nos. of strands, a minimum fixed length required is 5 m.

Summary:

No. of strands: 6 Nos.
Fixed Length of anchor: 6 m
Free length of anchor: 18 m
Total length of anchor: 24 m

C. *Summary of Proposed Test Anchors*

The Table 1 shows the summary of the design specifications of Investigation Test Anchor.

Table 1. Summary of Test Anchors

Anchor No.	Tw (kN)	D (mm)	Fixed Length (m)	Free Length (m)	Total Length (m)	No. of Strands
F495	1250	150	6.00	18.00	24.00	6
F497	1250	150	6.00	18.00	24.00	6
F499	1250	150	6.00	18.00	24.00	6

VI. INVESTIGATIVE TEST ANCHOR

A. *Test Method*

The proving tests (investigation tests) on pre-stressed rock anchors are much rigorous tests conducted prior to installation of the working anchors. Investigative tests are conducted to demonstrate the safety and performance of the anchorage for use under the conditions of which it is proposed and also to assess the bond strength characteristics of the in-situ rock.

This method defines the investigative test procedure and assessment of the behaviour of the test anchors. Design of test anchors must have all the conclusions and recommendations proposed for underground station or for the proposed structures.

The method of test anchor execution includes the following:

- Boreholes are drilled with an inclination of degree to an angle that is defined with the horizontal to reach the required rock strata or grade and the geological strata observed in the factual reports.
- The test anchors with specifications as shown in a table (Example) are fabricated and installed in the bore holes according to the preliminary method statement submitted.
- Test anchor stressing operation would be started after the anchor grout has attained the minimum compressive strength of 30 MPa or the age of 14 days (Clause14.6.3.1.2, BS 8081-2015).
- Stressing operation of the test is carried out in 8 cycles up to 80% of the ultimate strength of strands. The load increments and the minimum period of observations are shown in Table 2. Ref (BS 8081).
- Application of force at each increment and the resultant displacements observed were shown in the Fig 12 & Fig 13.

Table 2. Load Increments & Period of Observations for Trial Anchor

Load Increments (%f_{pu})							
1st Cycle	2nd Cycle	3rd Cycle	4th Cycle	5th Cycle	6th Cycle	7th & 8th Cycle	Min. Obs. Period
Initial	10	10	10	10	10	10	1 min
10	20	30	40	50	60	70	1 min
15	25	35	45	55	65	75	1 min
20	30	40	50	60	70	80	15 min
15	20	20	25	30	35	40	1 min
10	10	10	10	10	10	10	1

B. *Installation of Test Anchor*

Test anchors are fabricated as per the approved shop drawing and are installed at borehole locations with specified inclinations to reach the required Grade of Rock/Soil. Stressing jacks are installed on the steel waler beam structure installed on contiguous piling. The photographs taken during the stressing operation were shown in Fig 8 to Fig 10. The resultant elongations are measured using a steel ruler on the stressing jack rams.



Fig 8. Stressing of Test Anchor

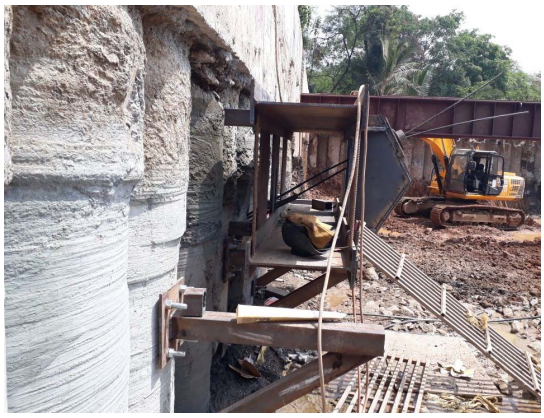


Fig 9. Waler Beam & Stress Block



Fig 10. Stressing Operation



Fig 11. Stressing Jack

C. Observations on Test Anchor Results

The following were the observed from the Investigative Anchor results:

- It is observed during the test anchor work whether the measured elastic elongations at the maximum test load are more than 80% of the theoretical elongations (lower limit) of the free length of anchor and they have not exceeded '110% free length'.
- Confirm if the anchors were successfully stressed up to 80% f_{pu} in 8 cycles and any strand/bond failure was observed.
- During the test if the bond failure does not occur, the loading further increased up to 95 % specified maximum force of any pre-stressed anchorage and terminated.
- Whether displacement creep was observed within the 15 minutes holding time at peak load of each cycle.

PROJECT:	Design and Construction of Underground station at BKC (UGC-05)									
Anchor Reference :	P-493									
Anchor Coil Reference:										
Date of Installation					Jack Piston Area (mm^2)			36698		
Date of Stressing	05.05.2018									
Time of Stressing		Start : 3:20 P.M								
		End : 6:20 P.M								

Working Load	Bond test
Strands Ultimate Load	1564.20
Total Stressing Load (test Load 85% Strand UL)	1329.57
No. of Slotter	3.00
Stressing Load in each Slotter	443.19
Anchor Bond Length (m)	3.00
Slotter Spacing c/c (m)	1.00
Anchor Length (m) L1	23.00
Anchor Length (m) L2	22.00
Anchor Length (m) L3	21.00
Area of Strand A (mm ^2) Actual (Refer MTC)	145.75
Modulus of Elasticity (KN/mm^2) Actual (Refer MTC)	202.44

INITIAL LOAD SEQUENCE	Initial Load (kN)	Gauge P. (Kg/cm^2)	Elongation (mm)		
Load Each Loop Individually & Lock			Th. (Cal.)	Reading	Actual
Step 1			0	12	
Stress Loop L 1	19.3	5.4	15.0	28.0	
Step 2					
Stress Loop L 2	10.1	2.8	7.5	28.0	

Step - 3 (Stress loop L1, L2 & L3)

Cycle	Time	Load			Displacement		Diff. Displacement	Elongation		
Nos.	(min)	%	Force (kn)	Gauge (Kg/cm^2)	Start Time	End Time		Cumulative Displacement	Th. (Cal.)	Remarks
		Initial	29	8.2	28.0	28.0	0	0		
1st Cycle	1	10	156	43.5	35.0	35.0	7	7		
	1	15	235	65.2	44.0	44.0	9	16		
	5,15	20	313	87.0	52.0	52.0	8	24		
	1	15	235	65.2	47.0	47.0	-5	19		
	1	10	156	43.5	36.0	36.0	-11	8		
2nd Cycle	1	10	156	43.5	36.0	36.0	0	8		
	1	20	313	87.0	54.0	54.0	18	26		
	1	25	391	108.7	63.0	63.0	9	35		
	5,15	30	469	130.5	76.0	76.0	13	48		
	1	20	313	87.0	59.0	59.0	-17	31		
	1	10	156	43.5	38.0	38.0	-21	10		
3rd Cycle	1	10	156	43.5	38.0	38.0	0	10		
	1	30	469	130.5	77.0	77.0	39	49		
	1	35	547	152.2	83.0	83.0	6	55		
	5,15	40	626	174.0	98.0	98.0	15	70		
	1	20	313	87.0	68.0	68.0	-30	40		
	1	10	156	43.5	42.0	42.0	-26	14		
4th Cycle	1	10	156	43.5	42.0	42.0	0	14		
	1	40	626	174.0	98.0	98.0	56	70		
	1	45	704	195.7	106.0	106.0	8	78		
	5,15	50	782	217.5	122.0	122.0	16	94		
	1	25	391	108.7	81.0	81.0	-41	53		
	1	10	156	43.5	47.0	47.0	-34	19		
5th Cycle	1	10	156	43.5	47.0	47.0	0	19		
	1	50	782	217.5	124.0	124.0	77	96		
	1	55	860	239.2	133.0	133.0	9	105		
	5,15	60	939	261.0	148.0	148.0	15	120		
	1	30	469	130.5	91.0	91.0	-57	63		
	1	10	156	43.5	53.0	53.0	-38	25		
6th Cycle	1	10	156	43.5	53.0	53.0	0	25		
	1	60	939	261.0	151.0	151.0	98	123		
	1	65	1017	282.7	161.0	161.0	10	133		
	5,15	70	1095	304.5	172.0	172.0	11	144		
	1	35	547	152.2	112.0	112.0	-60	84		
	1	10	156	43.5	59.0	59.0	-53	31		
7th Cycle	1	10	156	43.5	59.0	59.0	0	31		
	1	70	1095	304.5	175.0	175.0	116	147		
	1	75	1173	326.2	186.0	186.0	11	158		
	5,15	80	1251	347.9	197.0	197.0	11	169		
	1	40	626	174.0	125.0	125.0	-72	97		
	1	10	156	43.5	65.0	65.0	-60	37		
8th Cycle	1	10	156	43.5	65.0	65.0	0	37		
	1	70	1095	304.5	177.0	177.0	112	149		
	1	75	1173	326.2	190.0	190.0	13	162		
	5,15	85	1330	369.7	202.0	202.0	12	174		
	1	40	626	174.0						
	1	10	156	43.5						
	1	90	1408	391.4						
	1	95	1486	413.2						

Fig 12. Stressing Report

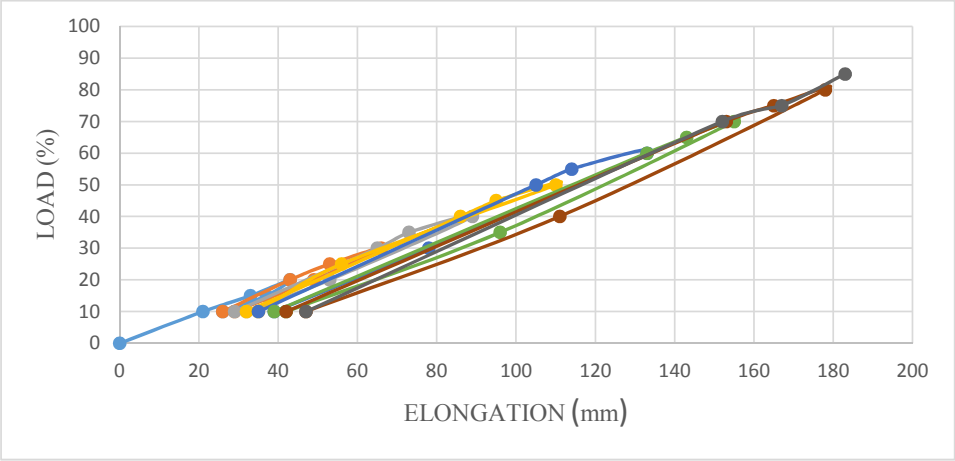


Fig 13. Load vs Observed Elongation graph

D. Conclusions on Test Anchor Results

The following were the conclusions to be drawn from the test anchor results:

- From the test anchor observations it will be understood if the anchors show a satisfactory result in terms of apparent free length calculation and the evaluated ultimate bond resistance values so that the same calculations will be used in the calculation of fixed lengths of working anchors.
- The recommended ultimate bond stress at the rock grout interface would be derived from the actual bond stress calculations.
- Factor of safety: 3.0 (considering the anchors life > 24 months ref BS 8081-2015).
- Allowable bond stress: Actual bond stress /3 = Allowable bond stress MPa.

E. Calculation of Actual Ultimate Bonds Stress

The following example shows the calculation of actual ultimate bond stress from the test anchor results.

Example:

Fixed Length of the anchor: 3.00 m
Free Length of the anchor: 20.00 m
Ultimate Load Applied: 1250 kN
Diameter of bore hole: 150 mm

The pull out capacity of a fixed anchor in rock is given by the following equation,

$$T_f = \pi D L \tau_{ult}$$

$$D = 150\ mm$$

$$L = 3.0\ m$$

$$T_f = 1250\ kN$$

$$\tau_{ult} = \frac{T_f}{\pi D L}$$

$$= \frac{1250 \times 1000}{\pi \times 150 \times 3000}$$

$$= 0.883\ MPa$$

Say 0.88 MPa

Hence, the actual ultimate bond stress at the rock-grout interface is 0.88 MPa.

VII. DESIGN OF WORKING ANCHOR

The following example illustrates the design of working anchor based on the results of investigative test anchor.

Example: (BKC East Wall)

Anchor Level: +1.50 m
Working Load on anchor: 460 kN
Diameter of bore hole: 150 mm

The design of Pre-stressed ground anchor involves three parts.

1) *Part-I: Number of Strands*

Diameter of the strand = 15.2 mm
UTS of the strand (f_{pu}) = 26.54 MT
Allowable stressing load (0.50 f_{pu})
= 50% of UTS = 13.27 MT

Working load on anchor = 460 kN = 46.9 MT
No of strands required =

$$N = \frac{Tw}{0.50 f_{pu}} = \frac{46.9}{13.27} = 3.53$$

Say 4 strands (2 loops)

2) *Part-II: Fixed Anchor Length*

The ultimate bond stress = 0.88 MPa
The pullout capacity of a fixed anchor in rock is given by the following equation,

$$T_f = \frac{\pi D L \tau_{ult}}{FOS}$$

(Clause B.3.5.5, BS 8081-2015)

Factor of Safety = 3.00

$$D = 150\ mm$$

$$\tau_{ult} = 0.88\ MPa$$

$$T_f = 460\ kN$$

$$L = \frac{T_f \times FOS}{\pi D \tau_{ult}}$$

$$= \frac{460 \times 3.0}{\pi \times 150 \times 0.88} = 3.34\ m$$

Say 3.5 m

Load per loop = 460/2 = 230 kN

Fixed length required for each loop = 1.67 m

As per BS 8081, the minimum fixed length shall be 3.0 m

Proposed spacing between the loops = 2.0 m

Proposed fixed length for loop -1 = 5.0 m

Proposed fixed length for loop -2 = 3.0 m

Hence, total bond length (Fixed) = 5.0 m.

3) *Part-III: Free Length*

Proposed free length = 14.00 m

Approximate elevation of competent rock -5.50 m.

Elevation of top of anchor (1st Level) = +1.5 m

Inclination of anchor with horizontal = 30°

Elevation of start of fixed length = 1.5-(14xSin 30°)

= -5.50 m

Hence OK.

Summary:

No. of strands: 4 Nos.

Fixed Length of anchor: 5 m

Free length of anchor: 14 m

Total length of anchor: 19 m

VIII. METHOD OF WORKING ANCHOR, SUITABILITY & CREEP TEST

The on-site suitability test is conducted on PT Rock anchors constructed in exactly the same way as the working anchorages and should be used as reference anchorages against which the performance of the working anchorage can be judged.

A. Suitability Test Method

- *Drilling of bore holes*: The boreholes were drilled with the designed inclination as per the design with the horizontal to reach the required grade of rock and the geological strata observed.
- *Installation of working anchors*: Working anchors with specifications as shown in approved table of anchors are fabricated and installed in the bore holes.
- *Start of stressing and cube strength of the grout*: The stressing operation is started after the anchor grout has attained the minimum compressive strength of 30 MPa or at the age of 14 days (Clause14.6.3.1.2, BS 8081-2015).
- *Maximum load applied during suitability test*: The stressing operations carried out in 3 cycles each up to 1.25 WL (Few cases consultants insist to apply 1.50 Times of WL). After the completion of the 3rd cycle, the strands are stressed up to 1.10 x working load and locked.
- *Lock off load*: In the project most of construction drawings mention the pre-stress force of the anchors. Pre-stress Force is the force at which you need to pull / pre-stress the anchors. Anchor Force F_{SLS} is the maximum force that is expected to be taken by each anchor as per the design analysis. So this force is not relevant to the pre-stressing operations.
- *Table of loading*: The load increments and the minimum period of observations are shown in Table 3.
- *Report*: The forces applied and the displacements observed are shown in the stressing reports

Table 3. Load Increments & Period of Observations for Suitability Test

Load Increment (%Tw)			
1st Cycle	**2nd Cycle**	**3rd Cycle**	**Minimum Period of Observation**
Initial			
50	50	50	1 min
100	100	100	1 min
125	125	125	15 min
100	100	100	1 min
50	50	50	1

B. Conclusions on Suitability Test Anchor Results

The following were the conclusions to be drawn from the test anchor results:

- *Force and bond*: Whether the anchors were successfully stressed up to 1.25 x Tw in 3 cycles (Or 1.50 times). Where any strand or bond failure was observed.
- *Displacement observations*: Whether any displacement was observed within the 15 minutes holding time at peak load of each cycle.
- *Creep* : Any creep/slip was observed after 24 hours of stressing.
- *Load and displacement data***:** The load – displacement data is being plotted on a graph.
- *Apparent free length verification*: The apparent free length from results of the suitability anchors were calculated as shown below.

The apparent free tendon length is given by the following equation (Clause G.2.11.3, BS 8081-2015s)

$$L_a = \frac{AE\Delta_e n}{T}$$

The following example shows the calculation of apparent free tendon length:

Example: (BKC)

Free Length: 5.0 m
Fixed Length: 5.0 m
Grip Length: 1.5 m
Modulus of Elasticity of Strand: 202.44 kN/mm^2
Cross Sectional Area of Strand: 145.75 mm^2
No. of Strands: 2
Peak Cycle Load: 281.3 kN
Datum Load: 22.5 kN
Displacement at peak cycle load: 54 mm
Displacement at Datum Load: 10 mm
Total anchor length: 5 m + 5 m+ 1.5 m = 11.5 m

The apparent free tendon length is given by the following equation,

$$L_a = \frac{AE\Delta_e n}{T}$$

(Clause G.2.11.3, BS 8081-2015)

$$A = 145.75\ mm^2$$

$$n = No.\ of\ Srands = 2$$

$$E = 202.44\ {}^{kN}/_{mm^2}$$

$$\Delta_e = Displ.@\ Peak\ Load - Displ.@\ Datum\ Load$$

$$= 54 - 10 = 44\ mm$$

$$T = Peak\ Cycle\ Load - Datum\ Load$$

$$= 281.3 - 22.5 = 258.8\ kN$$

$$L_a = \frac{145.75 \times 202.44 \times 44 \times 2}{258.8}$$

$$= 10.032\ m$$

From Clause G.2.13, BS 8081-2015, the apparent free tendon length shall not be less than 80% of free length intended in the design nor more than 110% of the intended free tendon length.

80% of tendon length = 0.8 (11.5) = 9.2 m
110% of tendon length = 1.1 (11.5) = 12.65 m

9.2 m < 10.032 m < 12.65 m

Hence, the test anchor **satisfies** the apparent free tendon length criteria.

C. Creep Test

Creep test in continuation to the suitability test is conducted in order to find out the movement of the any part of the fixed anchor with the time duration at a constant load. Once the suitability test is completed the anchor is then locked at 1.1 x Tw and kept observation for time displacement data for residual behaviour up to 24 hours and maximum 10 days.

IX. DESIGN AND PRACTICAL ISSUES & NEW INNOVATIVE METHODS ADAPTED

The various design and practical issues encountered and proposed measures to combat these issues has been discussed below:

A. Factual bore data Vs Actual bore data

Every station building has a factual bore log data which describes the actual strata of a vertical bored hole. These investigative bore holes are done at random and selective locations which might not represent the actual strata thus the bond length and free length calculations are assumptive.

A proposal to *check the actual strata* samples at every casing length and thus taking a decision on bond length to be kept for a particular anchor is made.

B. Actual bond stress:

The actual and allowable bond stress which is derived from test anchors sometimes might be narrowly sufficient and such variations are closely monitored by 3 cycle loading of each anchor during the suitability test conducted at 1 to 5% of the total working anchors quantity.

C. Corrosion Protection:

A proposal to have *special protection* for the temporary anchors with double corrosion protection until these have been de-stressed and removed has been made. Thin layer of grease applied on the surface of the anchor head and strands are then there are sealed with adhesive tapes and cut pieces of PE pipes as shown in Fig 14.



Fig 14. Special Protection

D. Removable Anchor System:

Based on experience, we have developed a loop making machine that gives a radius of 45 mm to 65 mm depend size of anchor and bore hole. This special device assembles the U turn anchor and slotter assembly in complete as shown in Fig 15 & Fig 16.



Fig 15. Special Device for making Loops

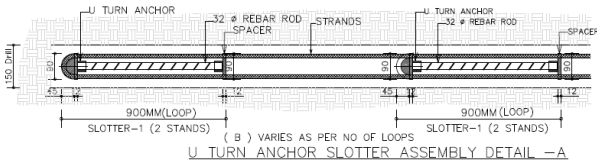


Fig 16. Multi Stage Removable Anchor Mechanism

The differential slotter distance have been developed to each site anchor bond length variations and made successful implementation.

E. Multi Stage Stressing of Anchor:

In order to nullify the slackNess in each loop for the multistage anchors the following method applied successfully.

The removable PT ground anchors consists of strands arranged in loops so that they can be removed after the completion of the construction work. The length of loops are different from each other. Hence, the elongations vary between loops. To ensure that all loops/strands are stressed to the same level, an initial stress of varying magnitude need to be induced in the loops successively. Later, simultaneously all the loops are stressed to the required level. Fig 17. Shows the illustration of multi stage stressing.

The following example illustrates the calculation for the initial force to be applied for loops

(Example)
Working Load: 125 MT
No. of strands: 10 (Example)
Bond length: 9 m
Free length: 10 m
Grip length: 1.5 m
Spacing between loops: 1.5 m (Example Only)
Total length for loop – 1: 20.5 m
Total length for loop – 2: 19.0 m
Total length for loop – 3: 17.5 m
Total length for loop – 4: 16.0 m
Total length for loop – 5: 14.5 m
Force in Each Loop: 260.7 kN (i.e., 50% of UTS)

Elongation:

$$\Delta L = \frac{PL}{AE}$$

P = 260.7 kN

A = 145.75 x 2 = 291.5 mm^2

E = 202.44 kN/mm^2

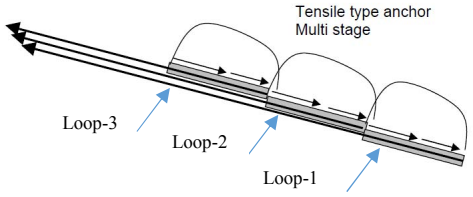


Fig 17. Multi Stage Stressing

The elongations in each loop is shown in the table given below:

Table 4. Elongations in each loop

ΔL_1	90.56 mm
ΔL_2	83.94 mm
ΔL_3	77.31 mm
ΔL_4	70.68 mm
ΔL_5	64.06 mm

Initial load to be given for each loop:

$$\Delta P_1 = \frac{(\Delta L_1 - \Delta L_5)AE}{L_1}$$

$$\Delta P_2 = \frac{(\Delta L_2 - \Delta L_5)AE}{L_2}$$

$$\Delta P_3 = \frac{(\Delta L_3 - \Delta L_5)AE}{L_3}$$

$$\Delta P_4 = \frac{(\Delta L_4 - \Delta L_5)AE}{L_4}$$

$$\Delta P_5 = \frac{(\Delta L_5 - \Delta L_5)AE}{L_5}$$

Table 5. Initial Load for each loop

ΔP_1	76.30 kN
ΔP_2	61.75 kN
ΔP_3	44.69 kN
ΔP_4	24.44 kN
ΔP_5	0 kN

Total initial force: 207.18 kN

- Apply an initial force of 76.3 kN to loop – 1.
- Apply an initial force of 61.75 kN to loop – 2.
- Apply an initial force of 44.69 kN to loop – 3.
- Apply an initial force of 24.44 kN to loop – 4.
- Do not apply any force to loop – 5.
- Now, stress all loops simultaneously.

Thus the slackNess in all loops properly adjusted and uniform load applied for all the loops is achieved.

F. Difficulties Encountered During Drilling:

Drilling for the inclined anchor system is carried with special P6 machines (Fig 18.) fabricated and assembled by Pavai Infra Geotech. These machines are equipped with an innovative mechanism that especially drill the overburden with an extractable casing-cum-drill bit type.

Once rock is encountered, the casing pipe gets fixed and a new drill bit is introduced for further drilling into the hard rock.

While drilling in BKC station (Fig 19.), difficulties such as inability to reach the rock levels and strata samples that did not match the actual expected strata were encountered. In many locations at the Vidhan Bhavan station, water table connected directly to the anchor bore line and took a lot of time for tapping to remove excess water, which delayed drilling and anchoring works.

The issue was combatted by proceeding with drilling works and collecting actual samples for technical personnel inspection as per the DDC. Drilling work was continued until the actual bond length of the anchor was achieved.



Fig 18. Drilling of anchor hole using P6 Machine at Vidhan Bhavan Station

In spite of various issues encountered due to topology, the type of anchor and stringent standards, the co-ordinated efforts by the design and execution team of Pavai-TeampT JV over the last year has helped in proposing workable solutions to such issues. Supplemented by an ergonomically designed anchorage system, and drilling machine used to execute, work has been going on smoothly in all the 6 mentioned stations at the time of submission of this paper.



Fig 19. Installation of anchor at BKC Station

ACKNOWLEDGEMENTS

The author humbly ackNowledges the inputs, help and immense support from L&T Mumbai Metro UGC-01, L&T STEC JV Mumbai Metro UGC-07, J Kumar Mumbai Metro UGC-05 teams and the GCE.

REFERENCES

[1] BS 8081-2015, Code of Practice for Grouted Anchors.

[2] IS 10270-1982, Guidelines for design and construction of prestressed rock anchors.

[3] BS EN 13391-2014, Mechanical Tests for Post Tensioning Systems.

[4] IS 14268-1995, Uncoated Stress Relieved Low Relaxation Seven-Ply Strand for Prestressed Concrete – Specification.

SECANT PILING SHORING SYSTEM-WITH CIRCULAR CONFIGURATION – A CASE STUDY

Rajan Babu C, Va Tech Wabag, Chennai, India, Email: c_rajanbabu@wabag.in
Jibi C Yohannan, Va Tech Wabag, Chennai, India, Email: c_jibiyohannan@wabag.in
Viswanathan N, Va Tech Wabag, Chennai, India, Email: n_viswanathan@wabag.in

ABSTRACT

This paper presents a case study of a Concrete Secant Piling shoring system carried out for a Terminal Lift Pumping Station (TLPS), part of critical works at Al Madina Al Shamaliya Sewage Treatment Plant Bahrain. TLPS rectangular in footprint with diagonal measuring 33m required excavations to depths of (-) 20m. Concrete Secant Piling shoring system with circular configuration of 34.5m diameter was chosen as a suitable method of earth retaining. Concrete hard and soft piles of 900mm diameter spaced at 675mm centres were designed and installed to depths of 3m below the excavation levels of (-)20m. Advantages of the behaviour of a circular shape of the shoring system were used, where the main load paths are hoop compression. This eliminated the requirement of cross bracing and the tie-backs for load transfer.

Performance of the shoring system was continuously monitored during execution for the following-

1. Integrity of concrete for full depth
2. Verticality of pile
3. Position of pile
4. Overlapping of pile between hard and soft pile
5. Cube strength of in-situ concrete

Keywords: Shoring System, Secant piling, Hard and Soft Pile.

INTRODUCTION

As part of the Construction of the Development of a Sewage Treatment Plant at Al Madina Al Shamaliya Island, Northern Budaiya – Kingdom of Bahrain, Terminal Lift Pumping station was to be constructed to receive incoming sewer pipelines. The construction of the pumping station required an unhindered foot print for deep excavation retaining system. This paper present the Secant pile wall as a shoring system which was carried out and performed reliably.

GROUND CONDITIONS

Based on the geotechnical investigation for the location, soil condition generally are non-cohesive, sand upto approximately 10.5m depth and below that weathered calcisiltite / carbonate mudstone. This is modelled as loose, medium and dense sand with Ø and K_0 as mentioned in Table1.

Table 1.

Description	Ø (deg)	K_0=1-(SinØ)	N Value
Loose Sand	30	0.50	<10
Medium Sand	35	0.43	10-30
Dense Sand	40	0.35	>30

© 2018 Deep Foundations Institute

STRUCTURAL ARRANGEMENT

The secant pile wall is 34.5m diameter constructed with 900mm diameter piles Hard/Soft alternate at 675mm c/c as shown in Fig.2 in plan view. The behavior of the wall would be as shown in Fig.1 for the pressures from outside.

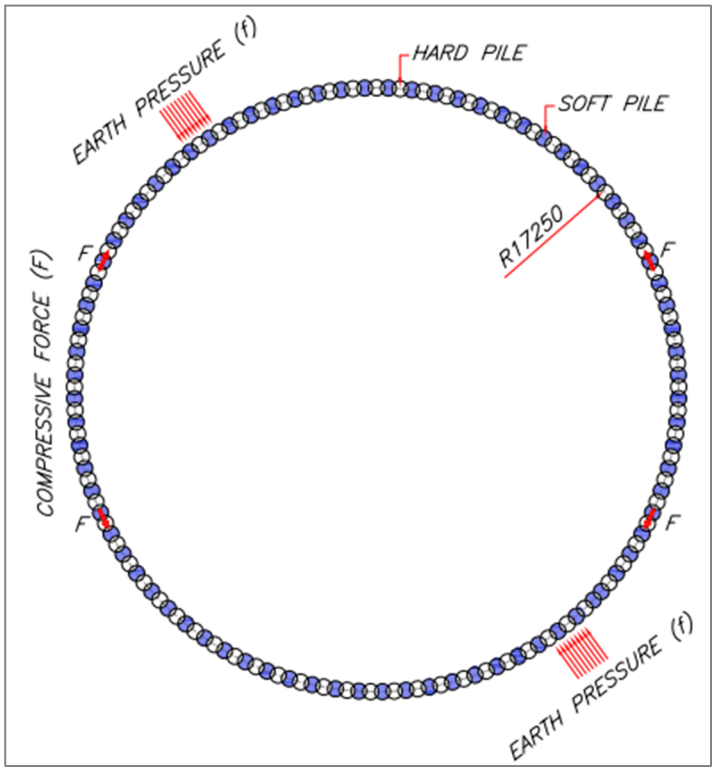


Fig.1 Behaviour of wall for the pressure from outside

Force's 'f' are the lateral loads (earth pressure) acting on the secant pile in radial direction and generates a compressive force in circumferential direction such as F= R x f.

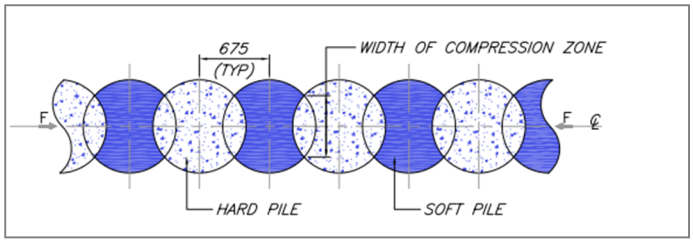


Fig.2 Plan View

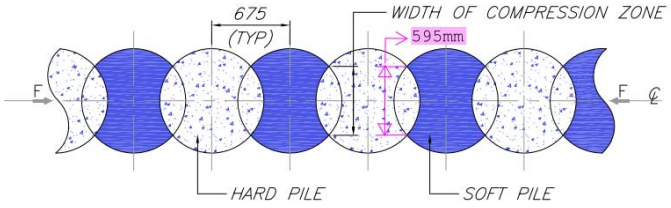
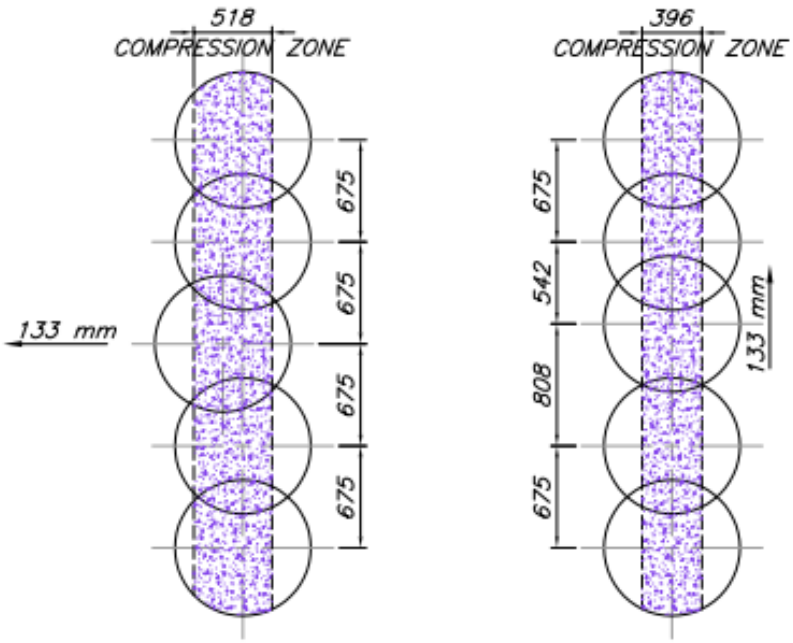
The maximum force which can be transferred through the compressive zone is: Fmax = W x 0.4x Fck (where Fmax is maximum force transferred through the compressive zone, W is the width of compression zone, Fck is Soft pile concrete grade). Soft pile concrete used was fck=20 N/mm2. Where F > Fmax, then an additional Stiffener Ring Beam is provided to take the additional forces.

PILING TOLERANCE

For secant pile walls to be effective it is essential that the overlap between the piles is achieved to prevent soil and ground water ingress. In the case of a circular shaft the overlap needs to be sufficient to provide the necessary resistance to the hoop compression stresses that enable the structure to be self-supporting without any cross bracing system.

In normal Piling practice, a piling contractor can be expected to consistently achieve verticality to a tolerance 1:75. Thus a 20.0m pile can be expected to be 266mm out of placed at the base. This is not considered adequate to achieve a water tight seal, hence a more stringent tolerance of 1:150 was adopted. With 1:150 verticality, the pile can be out of placed at base by 133mm (20,000/150=133mm). To assist the contractor in achieving this tolerance, a guide wall at ground level is provided. The effect of tolerance on the width of the compression zone is highlighted on the sketches shown in Table 2. Based on that, a compression width of 396mm was considered for the design of the secant wall.

Table 2. Effect of tolerance on the width of the compression zone

Case A- No out of place pile, Compression width = 595mm	
Case B1- 133mm Out of place pile in X direction, Compression width = 518mm Case B2- 133mm Out of place pile in Y direction, Compression width = 396mm	

LOADINGS AND PRESSURE DIAGRAM

External earth pressure and liquid pressure variation with height considered for design is indicated in Fig 3.

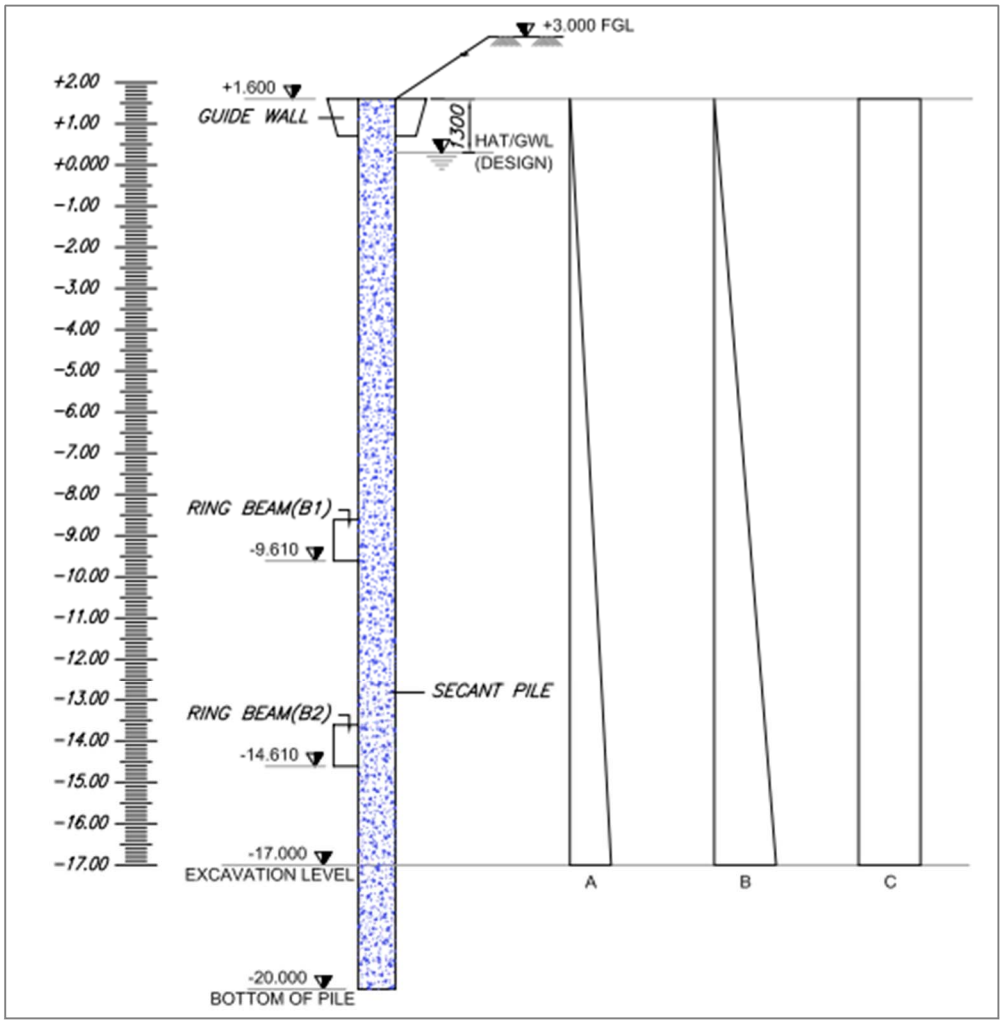


Fig. 3 Lateral forces on secant pile

A=Active Earth Pressure = K0 x h x γsub
B=Hydrostatic Pressure = γ_w x h
C=Pressure due to surcharge = K_0 x q
Using Load factors 1.4 for earth pressure, 1.2 for liquid and 1.6 for surcharge, average $\mathbf{f_{ult}}$ pressure at -14.6m was evaluated as 284.8 kN/m2.
Hoop force due to pressure = F_{ult} = R x f_{ul} = 17.25 x 284.8 = 4913 kN/m
Maximum capacity of Compression zone of 396mm was evaluated as
Secant wall capacity = 396 x 1000 x 0.4 x 20 N/mm2 = 3168 N.
Hence for any excess force more than the capacity, additional Concrete ring beams were added. These concrete ring beams were of concrete grade fck =45 N/mm2.
Two concrete ring beams were provided spaced at 4.6m and the hard pile between these beams were designed for flexure for the balance as shown below-
Pressure on pile = 284.8 kN/m2
Hoop stresses take (3168x100/4913) = 64 %

Balance 36 % is taken in bending of piles to ring beam = 0.36 x 284.8 = 103 kN/m2
The hard piles are designed for the bending moment developed due to this pressure spanning 4.6m.
The ring beams are designed for the shear transferred due to this beam action of the pile.

INSTALLATION

Figure 4 to figure 9 shows the various sequence of work starting from guide wall installation till final ring beam casting including completed shoring system. Since the soil was loose for top 10m depth, we used temporary casing for that depth.



Figure:4 Guide wall arrangement



Figure:5 Guide wall arrangement



Figure: 6 Auguring works



Figure: 7 First stage excavation with capping beam



Figure: 8 second stage excavation with intermediate beam



Figure: 9 shoring system after completion of secant piles

CONCLUSION

This shoring system avoided the cross bracings due to circular configuration, which reduced the construction time and also helped in witnessing hydrotest for full depth of TLPS. The systematic approach in design and site execution with stringent piling tolerance made us to achieve a leak proof secant pile shoring system amidst of high seepage from surrounding sea. Thus the shoring system served the purpose in most effective manner.

ACKNOWLEDGEMENTS

The authors would like to acknowledge the appreciation to Bahrain Foundation Construction Company LLL, Bahrain, and Wabag Belhasa JV Bahrain site teams and support staff that successfully delivered the project and Ismail Khonji Associates and MWH Khonji, Bahrain for their technical assistance on the secant pile wall shafts.

REFERENCES:

Institution of Civil Engineers (ICE) 2007. *Specification for piling and Embedded Retaining walls*

Geotechnical report by *Qatar Engineering Laboratory for AMAS STP site*

SINGLE BORE MULTIPLE ANCHOR SYSTEMS (SBMAS) IN CHALLENGING AND VARIABLE GROUND CONDITIONS

Antonio Marinucci, PhD MBA PE M.ASCE, V2C Strategists LLC and SBMA Ltd., Brooklyn, NY USA, Tel: +1 (401) 261-9102, E: antmarinucci@gmail.com

Devon Mothersille, BEng (Hons) PhD CEng FICE LETAPAEWE, Single Bore Multiple Anchor Ltd and Geoserve Global Ltd., London, UK, Tel: +44 (0) 7961 134943, E: devon.mothersille@sbmasystems.com

ABSTRACT Single bore multiple anchors (SMBAs) are ground anchors that incorporate multiple individual unit tendons of varying lengths, which are installed within a single borehole. Decades of research and practical applications have demonstrated that this configuration facilitates greater efficiency of load transfer to the surrounding ground. Unlike conventional ground anchors, especially in heterogeneous and variable ground conditions, the design of SBMAs can be optimized because the bond length of an individual unit anchor can be designed individually, thereby utilizing and maximizing the inherent strength of the ground. Historically, SBMAs have been used for both permanent and temporary earth support systems, and, where project circumstances dictated, SBMAs have been installed with removable tendons, which permitted the complete removal of the prestressing steel strand (at the end of the anchor's design service life). The installation of SBMAs is congruent with that of traditional ground anchors, and the testing protocol is similar regardless of anchor type. However, unlike conventional ground anchors, the stressing of SBMAs can require a different set up, whereby separate hydraulic jacks are hydraulically synchronized to stress each individual tendon simultaneously so that each unit anchor receives the same load. This paper will provide a general overview of the design, installation, and testing of permanent, temporary, and removable SBMAs along with the applicability for their use and the benefits afforded from using this type of anchoring system. The paper will also present and discuss applications in different ground conditions and test results via mini case histories where SBMAs have been implemented worldwide. The use of specially developed tablet-based software that allows real-time analysis and data management of the anchor testing process will also be presented with reference to SBMAs. Finally, it will be shown that, depending on the ground conditions and project requirements, it is possible that SBMAs can double the capacity of conventional anchors, thereby generating substantial savings in program time and cost.

Keywords: anchors, single bore, multiple anchor, theory, design, case history

INTRODUCTION

For more than three decades, the SBMA system has been used successfully worldwide for anchoring applications in soils and in weak rocks. The system is a ground anchor solution that is applicable to permanent in addition to temporary anchor installations. By effectively distributing the load along the fixed length portion of the anchor, SBMAs efficiently mobilize and maximize ground strength and, in appropriate ground conditions, can double the capacity provided by conventional anchors.

Barley (1997) commented that a conventional grouted anchor with a 10 m (33 ft) long fixed length (i.e., bond length) in soil or rock will, at the test load, need to extend some 30 mm (1.2 in) at the proximal end of the fixed length before any load will be transferred to the distal end of the tendon. Since the elastic behavior of the tendon is dissimilar to that of the grouted soil around it, the resulting differential strains induced during loading cause debonding at the weakest interface, which, in soil and weak rocks, tends to be along the ground-to-grout interface. As the anchor approaches the geotechnical strength limit state (i.e., ultimate ground-to-grout resistance), a highly non-linear profile of bond stress results (Figure 1). For clarity, *resistance* commonly refers to the properties of the ground/grout interface, whereas *capacity* generally refers to the strength properties of the tendon.

© 2018 Deep Foundations Institute

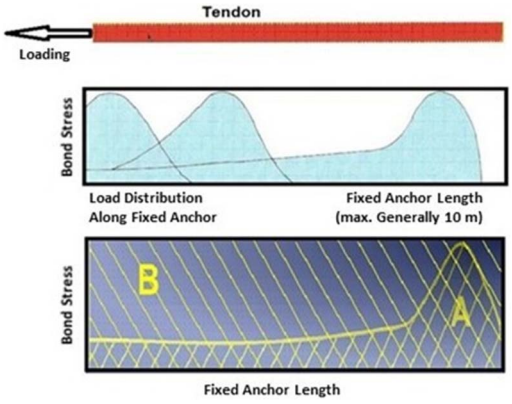


Figure 1. Progressive debonding along a conventional fixed anchor length

Progressive debonding, as the phenomenon is commonly referred, generally results in an inefficient use of the in-situ ground-to-grout bond strength. Under these circumstances as the tendon undergoes elongational deformation, more of the resistance towards the distal end of the fixed length of the anchor is being utilized since the peak bond strength toward the proximal end has been exceeded (Figure 2a). That is, during elongational deformation, the available resistance increases to a peak state; however, once the peak bond strength has been exceeded, the available resistance reduces to a softened strength state and then to a residual strength state with continued deformation. Conversely, SBMAs provide a more optimized anchor system that can transfer the applied loading simultaneously to multiple separate short unit lengths within the fixed length of the anchor with significantly reduced progressive debonding. By doing so, the in-situ ground-to-grout bond strength is mobilized efficiently, resulting in a considerable increase in the capacity of the anchor (Figure 2b).

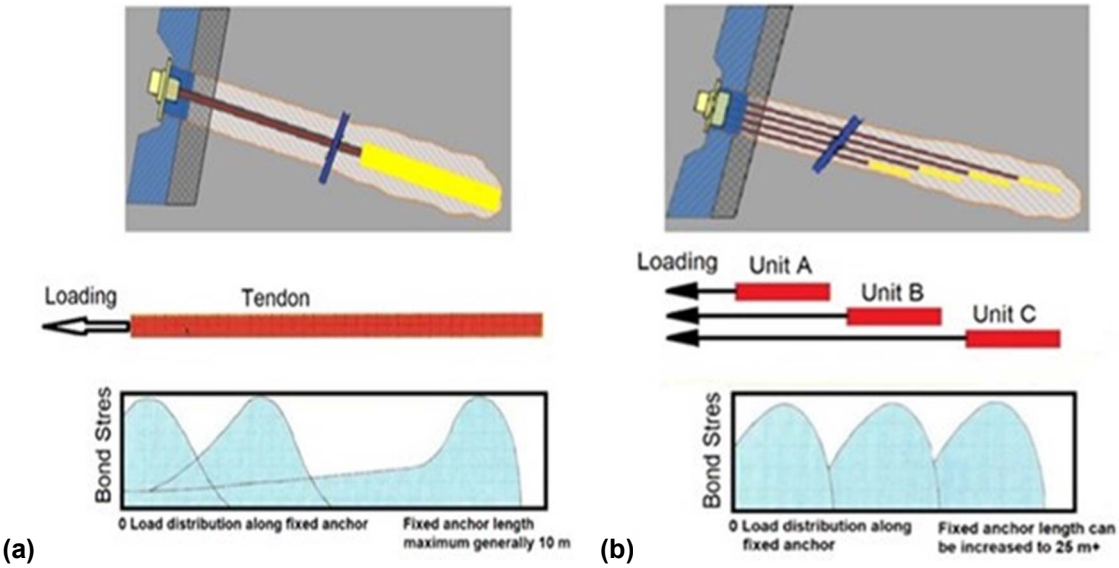


Figure 2. Load distribution in (a) conventional anchors and (b) SBMAs

SBMA systems fall into three basic categories: temporary, permanent, and removable systems. The temporary SBMA system is applicable to projects where the design service life is typically no more than about 2 years. Under normal circumstances (e.g., no aggressive ground conditions), short term protection of the anchor tendon is provided only by the cement grout encapsulating the tendon. The permanent SBMA system comprises a full double corrosion protection in compliance with international codes of

practices and will satisfy the design life of the structure typically up to about 120 years. It is noteworthy that should aggressive ground conditions be encountered, and/or the consequences of failure be categorized as high, similar corrosion protection as for permanent anchors should be implemented for temporary anchor systems. Aggressive ground conditions (i.e., potentially corrosive) are denoted or classified according to the electrochemical properties (i.e., pH [acidic or alkaline], salt content, and resistivity) of the soil, presence or potential of stray electrical currents, type of soil (e.g., organic and calcareous), and presence of debris or industrial waste (e.g., fly ash, cinder, and slag). The SBMA removable anchor is a technology that permits the prestressing strand tendon to be fully removed from the borehole at the end of its design service life. Examples of each system will be presented in the Case History section below.

DESIGN OF SBMAs

The design principles associated with the SBMA system are well documented in the literature, and its load transfer mechanism is recognized by major international codes of practice including in the British Code of Practice for Ground Anchors, BS 8081:1989/2015 (BSI, 1989 and BSI, 2015); European Standard for the Execution of Special Geotechnical Works – Ground Anchors, EN 1537:2013 (BSI, 2013); PTI Recommendations for Prestressed Rock and Soil Anchors, PTI DC35.1-14 (PTI, 2014); and RTA QA Specification R56, Ground Anchors (RTA, 2009).

Ostermeyer and Barley (2003) provide a detailed discussion of the process for the design of SBMAs, and the basic principles are similar to the design of conventional anchors (Eq. 1) with the exception that an efficiency factor (f_{eff}) is introduced in the equation to compute the ultimate anchor load (Eq. 2). The efficiency factor accounts for the non-linear bond stress profile already described (Figure 2).

$$T_{f_conv} = \pi \cdot d \cdot L \cdot \tau_{ult} \tag{1}$$

$$T_{f_SBMA} = \pi \cdot d \cdot L \cdot \tau_{ult} \cdot f_{eff} \tag{2}$$

where, T_{f_conv} is the ultimate capacity of a conventional anchor; T_{f_SBMA} is the ultimate capacity of a unit anchor; d is the diameter of the borehole; L is the fixed length of a unit anchor; and τ_{ult} is the ultimate ground-to-grout bond stress.

Based on the back-analysis of multiple anchors, each with a different fixed length, that were installed in mixed soils and tested to failure, f_{eff} was calculated from the ratio of the actual bond stress to the idealized bond stress area (Area A divided by Area B in Figure 1). Each computed ratio was plotted versus its respective fixed length (where L is in meters), as shown by the data points in Figure 3. A relationship for the efficiency factor with respect to fixed length was established using curve fitting (Eq. 3). The fixed length of conventional ground anchors ranges considerably (L = 6 to 15 m [20 to 50 ft] or longer) depending on the ground conditions and design loading; however, the fixed lengths of the unit anchors are consistently less than those for conventional anchors and typically ranges from 2.5 to 4.5 m (8 to 15 ft). As an example, the efficiency factor ranges from 0.34 to 0.58 for conventional anchors (with L = 6 to 15 m) and ranges from 0.95 to 0.68 for SBMAs (with L = 2.5 to 4.5 m). Moreover, by exploiting the fact that SBMAs can accommodate greater loads than conventional anchors, designers can reduce the overall quantity of anchors required to support the structure.

$$f_{eff} = 1.6 \cdot L^{-0.57} \tag{3}$$

The SBMA system can accommodate variable ground conditions directly and simply by adjusting the fixed lengths of the unit anchors based on the bond strength available. The individual fixed lengths can be designed

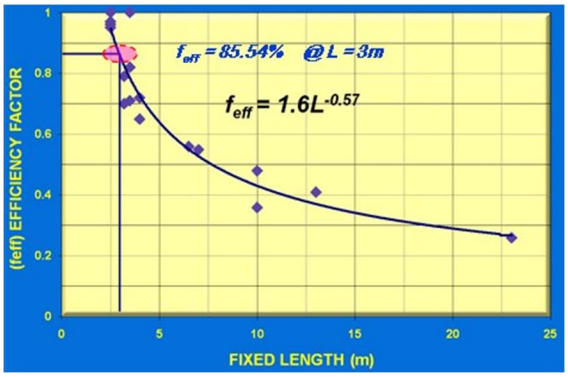


Figure 3. Efficiency factor versus anchor's fixed length (after Barley, 1997)

for ground conditions exhibiting a decrease in strength with depth, for strength varying throughout the fixed length, or for very weak bands intermixed within the deposit at irregular depths. In the latter case, the number of unit anchors is designed to allow for a potential failure of one or two unit anchors while ensuring the remaining (intact) unit anchors still safely sustain the total anchor working load (for an appropriate factor of safety or resistance factor). Furthermore, for the SBMA system, there is no theoretical limit to the total (or overall) fixed length, whereas there is little or no practical increase in load capacity for conventional anchors with fixed lengths greater than about 10 m (33 ft).

In the case of non-homogenous soil conditions throughout the fixed length, each unit fixed length can be designed for the appropriate condition and available strength. If the soil is weaker within the upper portion of the fixed length, then the proximal unit anchors will have longer unit fixed lengths compared to those at greater depth. Regardless of the unit length, equal load is applied to each unit anchor such that each unit anchor is mobilizing the same percentage of the ultimate ground-to-grout bond capacity (or, in other words, each failure would occur simultaneously). However, if the unit anchors are founded in soil conditions exhibiting different creep characteristics, the unit fixed lengths would be designed such that each unit anchor design would comply with the appropriate creep criterion in its particular service condition.

CONSTRUCTION CONSIDERATIONS

The construction and installation of SBMAs follows the general methodologies adopted in most conventional grouted anchor construction (i.e., tendon fabrication, drilling, installation, and grouting). By doubling the loads that could be applied to an SBMA, the overall quantity of anchors required for a particular structure could effectively be reduced by 50%. Such reductions in the quantity of anchors required generate significant savings in project time and costs by reducing the quantity of drilling rig set ups, drilled holes, and stressing operations.

In general, SBMAs use essentially the same overall drilled length as conventional anchors, but the composition is significantly different (i.e., about 50% longer fixed lengths per anchor but only about 67% of the total quantity of SBMAs as compared to conventional anchors). That is, irrespective of the type of anchor - conventional or SBMA, the free length (i.e., unbonded zone) is the same because this length is based on the retained height of the wall and/or the geometry of the unstable soil/rock mass. However, the arrangement and length of the fixed length (i.e., bond zone) for SBMAs is significantly different from conventional anchors (Figure 2), which results in fewer and longer SBMAs compared to more and shorter conventional anchors. Ultimately, because the goal of the SBMA design is to utilize the resistance afforded more efficiently, the overall drilled lengths are effectively similar but the quantity of SBMAs installed is less than for conventional anchors. In addition, there are greater safeguards being utilized with SBMAs such that properly designed and well-constructed, high load SBMAs do not fail (i.e., no remedial

work or specialty contractor-induced delays) even in the weakest of materials because more unit lengths can be added, as appropriate, to subsequent anchors.

The positive implications to project time and costs cannot be over-emphasized. Furthermore, whether for multiple level anchored deep basements, anchors holding down a dock floor, anchored slopes or diaphragm walls, a SBMA's high capacity can reduce the quantity of anchors, which correlates to fewer rows of anchors and/or greater spacing between anchors. Where permanent anchors are required and high capacity SBMAs can reduce the quantity of anchors, prefabricated double corrosion protected tendons offer a major advantage with respect to durability.

SBMA TESTING

Similar to all grouted anchor systems, testing of SBMAs by means of a direct tension test is a mandatory requirement, and applies to temporary, permanent, and removable SBMA systems. As described above, the systems involve the installation of multiple unit anchors into a single borehole, whereby each unit anchor has its own individual tendon, its own unit fixed length of borehole, and is loaded with its own unit stressing jack. The loading of all of the unit anchors is performed simultaneously by using multiple hydraulically synchronized jacks, which ensures that the load in each unit anchor is always identical to the others (Figure 4). That is, each unit anchor has its own hydraulic jack and each jack imparts the same load on each unit anchor; however, ram extensions differ due to different free length of each tendon element.

Under appropriate circumstances, recent developments have allowed a single jack to be employed to stress all of the SBMA tendons without overstressing any of the tendon elements during simultaneous tensile loading (Figure 5). Undoubtedly, this innovation clearly saves a considerable amount time since only one set of data for the load-extension response needs to be recorded.

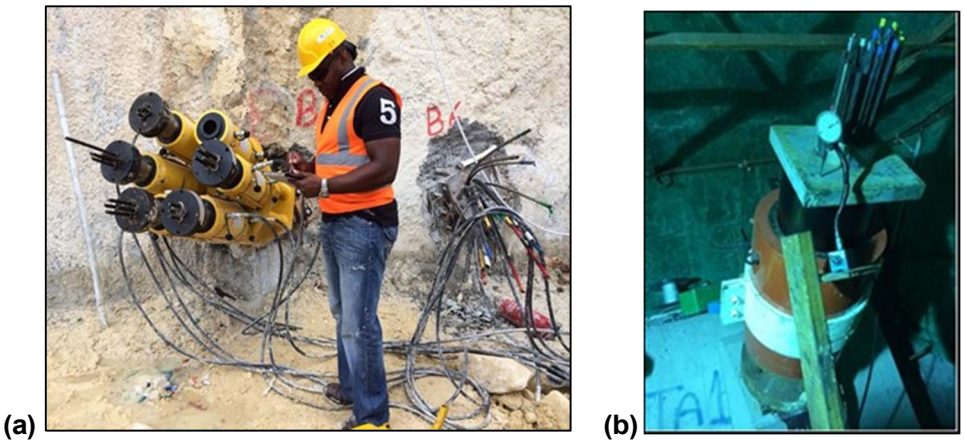


Figure 4. Testing of SBMA anchors: (a) in weak limestone using multiple jacks (Doha metro, Qatar), and (b) a single hollow ram jack simultaneously stresses a 3-unit system (Izmir, Turkey)

CASE HISTORIES

Temporary SBMAs in an Anchored Diaphragm Wall - Boston, Mass., USA

The construction of deep basement structures in Boston Clay demanded the use of innovative techniques to provide temporary support to a diaphragm wall in a notoriously weak material, which had SPT N-values between 2 and 7 blows/0.3 m (blows/ft) (Figure 5a). The use of conventional ground anchors imposed serious project restraints by the quantity of anchors required. Therefore, a proposed alternative solution, which incorporated the use of SBMAs, was considered and subsequently implemented.

In August 2007, a series of field trials were performed using SBMAs in the soft Boston Clay located at the site for the construction of the new for the construction of the MIT Management Building. The objective of this test program was to ascertain the ultimate ground-to-grout bond stresses that could be achieved at the different target anchor depths to confirm the geotechnical parameters that could be used for the design of the production anchors. Various designs for the test anchors were adopted but generally consisted of up to four unit anchors, each with a length of about 3 m (10 ft) and with between 2 and 4 15.2 mm (0.6 in) diameter 'noded' strands per unit anchor. A noded strand is also known as "bird caging," which refers to a process by which the strand wires are locally separated to enhance bond. The nature of the soft ground also necessitated the use of sophisticated secondary post-grouting techniques in the fixed anchor zone in conjunction with a double inflatable packer to maximize the capacity of the unit anchors (Figure 5b).

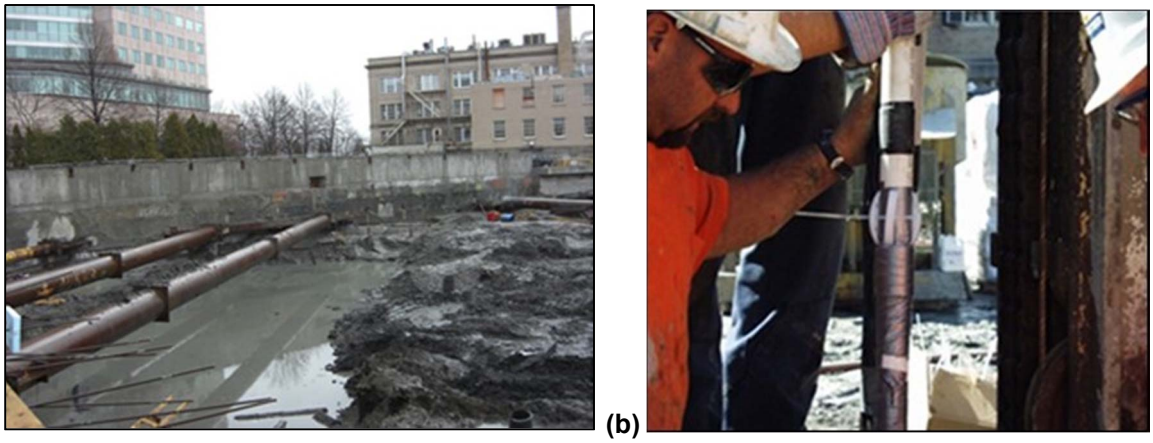


Figure 5. Photographs of (a) the excavation site, and (b) the installation of a post-grouting tube that was used with a double inflatable packer for secondary grouting of the fixed anchor zone

The carefully supervised work successfully demonstrated the SBMAs with three unit anchors could support test loads of up to 1,200 kN (270 kip), which exceeded the capacity, by as much as 50%, achieved by conventional anchor systems. Furthermore, the addition of more unit anchors can achieve a proportional increase in the load that could be supported; that is, the use of six unit anchors would provide double the capacity provided by three unit anchors (i.e., a capacity of at least 2,400 kN (540 kip)).

During the incremental loading of the individual unit anchors, simultaneous plotting and analysis of the load-extension data was performed to facilitate an immediate assessment of the behavior of the fixed anchor and apparent free tendon lengths. The results from this work were then used to optimize the design of the production anchors. The increased loads generated by the SBMAs reduced the quantity of the anchor holes drilled and, correspondingly, the project time required for the construction of the anchors.

Temporary SBMAs in an Anchored Diaphragm Wall – Moscow, Russia

Mothersille et al (2015) reported on the testing program and installation of approximately 3,600 SBMAs to support a diaphragm wall in the highly heterogeneous soil conditions for the pedestrian-oriented, mixed-use Kuntsevo Plaza development in the Kuntsevo district of southwestern Moscow, Russia, which was the first project in Russia to utilize the SBMA technology. The challenging variable geology consisted low strength clays, sands, and sandy silts with lenses of gravel and fluvio-glacial deposits. The depth to the groundwater table ranged from about 3 to 9.5 m (10 to 31 ft), and artesian conditions were encountered deeper in the deposit in the fluvio-glacial and Lower Cretaceous sands. The anchored diaphragm wall structure was about 650 m (2,135 ft) in length along the perimeter, about 800 mm (32 in) in thickness, and was embedded to depths varying from 38 to 45 m (125 to 150 ft).

The specified design working load for each of the anchors was 600 kN (135 kip), which could not be achieved with conventional anchors due to unacceptable creep displacements. To determine the ultimate ground-to-grout bond stresses (i.e., at geotechnical failure), conventional tremie grouted anchors with a single 8 m (26 ft) long bond length, borehole diameters of either 150 or 178 mm (6 or 7 in), were installed vertically to depths between about 18 and 27 m (60 and 90 ft) into the two distinct founding layers. For pre-production or verification testing (i.e., trial anchors), it is common to use vertically installed elements to isolate the bond zone within the layer(s) of interest; moreover, there is no practical opportunity (trial anchors installed prior to the wall) or benefit to installing sub-horizontal anchors. The ultimate test load sustained was about 450 kN (101 kip), at which point the anchor exhibited continuous upward displacement. The back-calculated ground-to-grout bond stresses were approximately 175 kPa (25 psi) in the upper clays and 195 kPa (28 psi) in the lower sand layers.

Given the sensitivity of adjacent understructures and services, an extensive testing program was performed to determine the feasibility of and design parameters for the SBMA technology, to evaluate enhanced anchor construction techniques (i.e. end-of-casing grouting in the granular soils and post-grouting in the cohesive soils), and to observe the performance data of the ground anchors with respect to limiting wall movements. The test results indicated that the maximum working loads ranged from about 580 to 780 kN (130 to 175 kip), which were greater than the maximum design load of 532 kN (120 kip). It is important to note that the ultimate bond stresses that could be achieved are a function of both the technique being utilized and the contractor's construction methodology and quality.

Using the determined anchor capacities, the final design for the anchored structure used six levels (Figures 6 and 7) of three unit temporary SBMAs (Figure 6b) with varying overall length and a working load up to 600 kN (135 kip). On the rare occasion when the installed SBMA did not satisfy the acceptance criterion, additional applications of post-grouting were used, and the anchor retested until the creep criteria was achieved (Figure 7b). The anchoring solution successfully restricted lateral wall deformations to about 7.5 mm (0.3 in) over the maximum excavated depth of about 25 m (82 ft). The use of the SBMA technology and the use of end-of-casing grouting and/or post-grouting resulted in anchor capacities that were more than double those previously achieved in the same ground conditions. Ultimately, the alternative approach and use of the techniques described led to considerable savings to the project by avoiding top-down construction, proposed compensation grouting, and proposed realignment of the existing sewage pipe.

Anchored Diaphragm Wall – Izmir, Turkey

Nearly 1,064 linear meters (3,500 LF) of 800 mm (32 in) thick diaphragm walls in three areas were constructed for the Mahall Bomonti mixed-use development in the Izmir region of Turkey (Mothersille et al, 2018), as denoted by Blocks A, B, and C in Figure 8a. Some 2,600 temporary SBMAs were successfully installed and tested to support the 27,500 sq m (296,010 sq ft) of exposed face of the diaphragm walls, whose excavated depths ranged from 14 to 18.5 m (46 to 61 ft), as shown in Figure 8b.

Anchored diaphragm walls were constructed in highly heterogeneous alluvial soils (i.e., clays, silts, sands, and gravels) with a highly variable strength profile. In the sand and gravel layers, the SPT N-values ranged from 30 to 45 blows/0.3 m (blow/ft) with CPT tip resistance (q_c) values ranging from about 4 to 40 MPa (42 to 418 tsf). In the clay and silt layers, the SPT N-values ranged from 5 to 15 blows/0.3 m (blow/ft) with CPT q_c values ranging from about 0.1 to 4 MPa (1 to 42 tsf). In addition, the depth to the groundwater table was relatively shallow and was located about 2 m (6.6 ft) below the ground surface; artesian conditions were observed around 38 m (125 ft) below ground surface within the gravel layers.

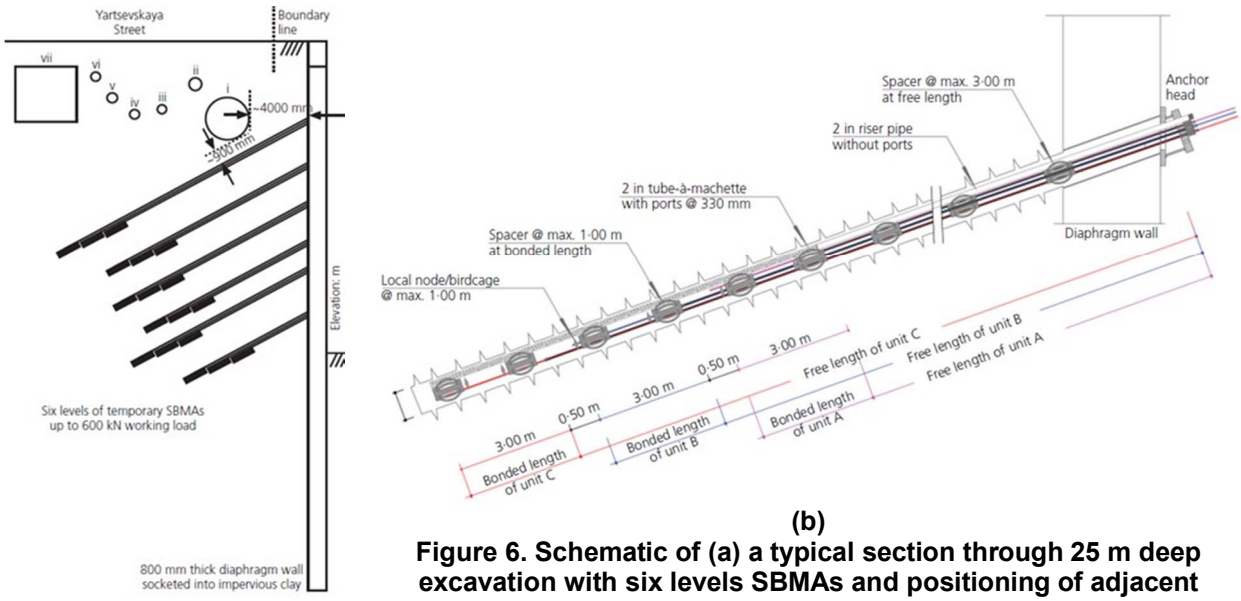


Figure 6. Schematic of (a) a typical section through 25 m deep excavation with six levels SBMAs and positioning of adjacent utilities and structures, and (b) a three unit SBMA

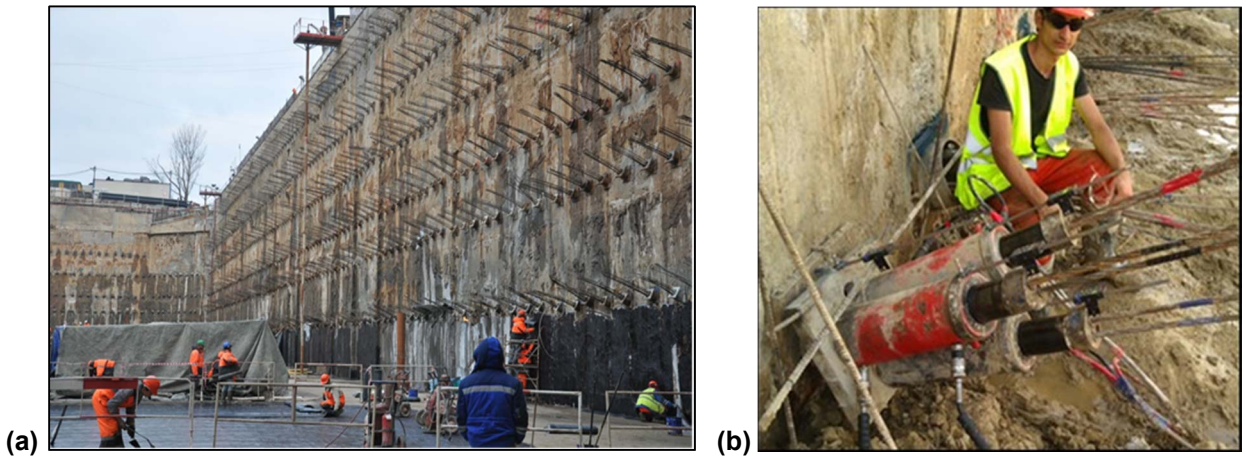


Figure 7. Photographs of (a) the anchored diaphragm wall with six rows of SBMAs and (b) the testing of production SBMAs using synchronized hydraulic jacks (Mothersille et al, 2015)

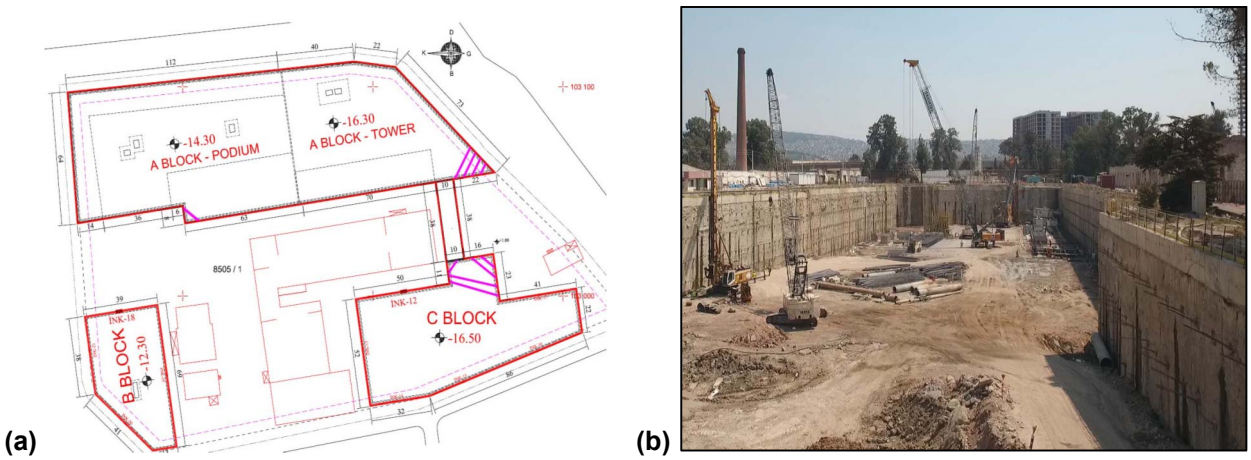


Figure 8. Mahall Bomonti project (Izmir, Turkey): (a) plan view of the three construction blocks and (b) photograph of SBMA anchored diaphragm wall in Block A

A pre-production test program was implemented to verify the assumed anchor capacity of 550 kN (124 kip) could be achieved at the site. Based on the results from several tested single unit anchors and full SBMAs, the anchor working (design) loads were increased to as much as 650 kN (146 kip) and test loads of up to 1,850 kN (416 kip) were demonstrated, which were the highest anchor loads ever achieved in the region. Therefore, the total length of anchors installed at the site for the three diaphragm wall structures was about 55,200 linear meter (181,100 LF), which was a reduction of about 64% from the original design comprising about 153,000 linear meter (502,000 LF) of anchor length. Ultimately, due to the redesign and pre-production anchor testing program, the project realized a savings of up to 60% in construction time and 35% in the total price of the anchoring work.

Permanent SBMAs in Austria

The effective use of the SBMA technology was highlighted on a prestigious project undertaken on the A2 motorway between Graz and Vienna in Austria. The purpose of this remediation project was to replace about 400 previously installed conventional ground anchors, each with a load of about 1500 kN (337 kip), because they had failed due to corrosion of the strands below the anchor head. The originally proposed solutions consisted of installing 400 new conventional ground anchors, one new for one failed anchor. However, SBMA Ltd. proposed an alternative scheme to reduce overall project time and costs by utilizing specialist techniques that were not included in the original specifications. In lieu of installing 400 new conventional ground anchors with a 1,500 kN (337 kip) working load, an alternative approach was proposed and comprised installing and testing 200 SBMAs into the weak rock, each with a working load of about 3,600 kN (810 kip).

Ultimately, the alternative design for this slope stabilization endeavor was accepted, and the final system (Figure 9) consisted of 200 double corrosion protected, permanent SBMAs in accordance with the criteria stipulated in BS 8081:1989 (BSI, 1989). Each SBMA was installed with an overall length of about 82 m (270 ft) and a working load of about 3,800 kN (855 kip). Each SBMA consisted of three unit anchors, which were 6.3 m (21 ft) long, incorporating 6 Dyform strands that were 18 mm (0.7 in) in diameter. In addition, the SBMA system specifically addressed the vulnerable zone with the use of a double plastic strand protection and continuity of corrosion protection below and within the anchor head.



Figure 9. Photograph of permanent SBMAs for slope stabilization (Degendamm, Austria)

Removable Anchors - Corniche, Abu Dhabi

The mixed-use Corniche Towers development in Abu Dhabi, U.A.E., comprised the construction of three new towers, each more than thirty stories in height, to house residential apartments, offices, and retail floors at the podium levels. Below the podium level, there are four levels of common basement to accommodate underground parking. Some 600 temporary ground anchors were used around the main

excavation combined with steel strut pipes, used at the corners and along the short-span corridor, support the diaphragm and secant pile walls that formed the shoring structure for the 20 m (66 ft) deep excavation. Along the Corniche Road side, removable ground anchors with working loads varying from 915 to 1,125 kN (206 to 253 kip) were implemented to avoid conflict with future infrastructural development plans proposed by the municipality (Figure 10). The AnchorTest™ (AnchorTest, 2015) tablet-based software was utilized for the real-time and post-testing analysis and data management of the removable SBMAs that were used for the temporary foundation works.



Figure 10. Photograph of construction site for Corniche Towers development (Abu Dhabi, UAE)

The design of the removable SBMAs was optimized by using the results of a preliminary investigation test program in which vertical test anchors and removable anchors were installed. Removable anchors were incorporated into the test program and subjected to suitability testing and to evaluate their removability. During these test trials, a maximum test load of 1,700 kN (382 kip) was applied to and successfully resisted by the test anchors, and all of the associated data was analyzed real-time with the tablet-based software (Figure 11a). As shown in Figure 11b, the vertically installed removable anchors were tested up to a maximum test load of 1,150 kN (259 kip), which was 1.25 times the required working load, in accordance with requirements of the applicable code provisions of BS8081:1989 (BSI, 1989). As part of the QA/QC protocol requirements, the tablet-based software was used to monitor and analyze real-time and record the routine onsite acceptance testing work before each production anchor was locked-off.

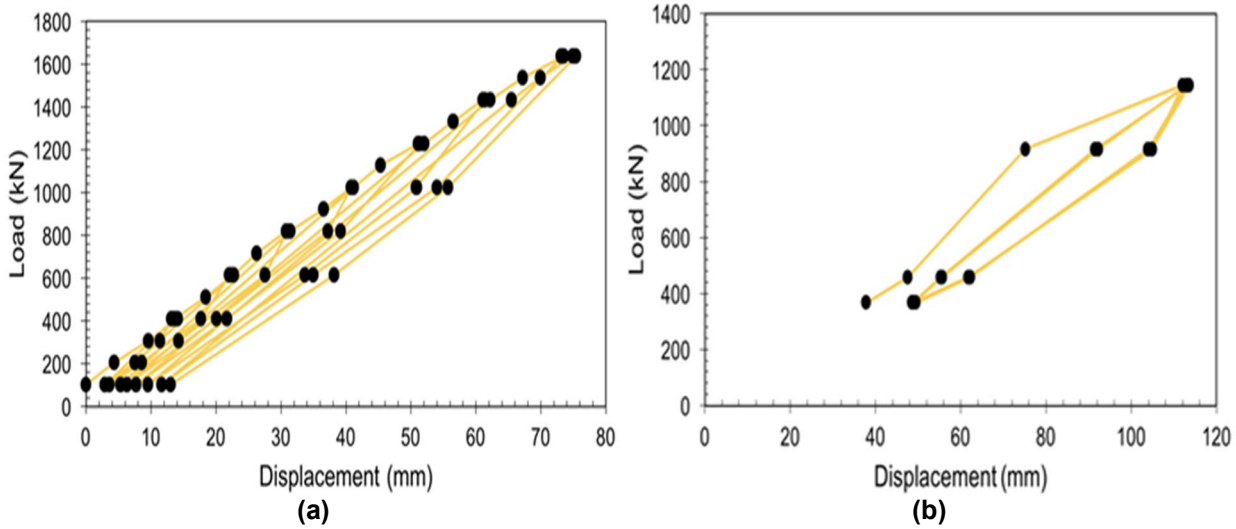


Figure 11. SBMA test results: (a) proving test for anchor A4, and (b) suitability test for removable trial anchor R1 using a single hollow ram stressing jack

CONCLUSION

The relatively high load transfer efficiency of short bond lengths is exploited in the SBMA system which is now in international use. This system will be especially valuable in earth retention systems in urban areas. The introduction of a new anchor system with more than double the working capacity of conventional anchors in soils and weak rocks has provided a supplementary economic benefit in the use of the anchor systems. One of these is the advantage of open inhibited working space for construction within the deep anchored excavations. High load and low load capacity anchor systems now exist which allow the total removal of the steel tendon from the anchor borehole and from the ground. This removal after temporary provision of safe support of the excavation makes the use of anchors more 'environmentally friendly' and more acceptable to adjacent land owners. The use of the tablet-based software platform, AnchorTest^{TM}, for the analysis and management of load/extension data has proved to be an effective tool and has been successfully implemented on SBMA projects worldwide. As observed with increasing frequency throughout the construction industry, tablet-based (real-time) software outperforms and exceeds the capabilities of laptop-based spreadsheets in the field for several reasons, including ease of use, enhanced user interface, user customability, and web-based data management. Select benefits of the tablet-based anchor analysis and data management system include superior user interface (i.e., iPad vs. laptop), more robust for field applications, digitized immediate cloud storage, instant third-party access for assessment and decision making, real-time assessment of anchor behavior against acceptance criteria, and facilitates all major international codes within a single package.

REFERENCES

AnchorTest Ltd. (2015). "AnchorTest for iPad Software," London, U.K. http://www.anchortest.info

Barley, A.D. (1997). "The Single Bore Multiple Anchor System," *Proceedings of the International Conference, Ground Anchorages and Anchored Structures*, Institution of Civil Engineers (ICE), London, U.K., pp. 65-75.

BSI. (1989). BS 8081:1989: British Standard Code of Practice for Ground Anchorages. London, U.K.

BSI. (2015). BS 8081:2015: British Standard Code of Practice for Grouted Anchors. London, U.K.

BSI. (2013). BS EN 1537:2013: Execution of Special Geotechnical Work. Ground Anchors. London, U.K.

Mothersille, D., Düzceer, R., Gökalp, A., and Okumuşoğlu, B. (2015). "Support of 25 m Deep Excavation using Ground Anchors in Russia," *Proceedings of the Institution of Civil Engineers, Geotechnical Engineering*, Vol. 168, pp. 281-295.

Mothersille, D.K.V, and Okumusoglu, B. (2016). "Anchor Testing using Innovative Software on a Tablet." Technical Feature, *Foundation Drilling* Magazine of the ADSC-IAFD, October, pp. 23-35.

Mothersille D., Düzceer R., Gökalp A., and Adatepe, S. (2018). "Design, Construction, and Performance of Single Bore Multiple Anchored Diaphragm Wall in Izmir, Turkey." *Proceedings of the International Conference on Deep Foundations and Ground Improvement Urbanization and Infrastructure Development – Future Challenges*. DFI-EFFC, Rome, June 5-8. pp. 135-148.

Ostermayer H. and Barley A.D. (2003). "Fixed anchor design - Ground Anchors", Geotechnical Engineering Handbook, Vol. 2, Pub Ernst and Sohn, Berlin, Germany, 189–205.

Post Tensioning Institute (PTI). (2014). Recommendations for Prestressed Rock and Soil Anchors. DC351-14. Farmington Hills, MI. 110 pp.

Roads & Traffic Authority (RTA). (2009). "RTA QA Specification R56, Ground Anchors (Schedule of Rates)," 3rd edition. Bridge Engineering Section. Parramatta, New South Wales, Australia.

SLOPE PROTECTION AND SEEPAGE CONTROL FOR DEEP EXCAVATION ADJACENT TO LAKE – CASE STUDY

Raja Rajan. K, Asst. Engg. Manager, CMPC division, EDRC, L&T Chennai. k-raja@lntecc.com
Nagarajan. D, Sr. Engineer, CMPC division, EDRC, L&T Chennai. nagarajan-d@lntecc.com
Vijayakumar. T, Head of Division, CMPC division, EDRC, L&T Chennai. tvk@lntecc.com

ABSTRACT

Greater Hyderabad Municipal Corporation proposed to build Extra dozed bridge across Dhurgam Cheruvu Lake at Madhapur, Hyderabad. The main pylon foundation is at merge point of the downhill and lake. Temporary shore protection bund of 4m height proposed to retain the lake water for constructing the open foundation. HDPE sheet and sand bags were provided on bund to control the seepage. Submersible pumps used to dewater the excavated area. Base of foundation rests on hard rock which is 7m below existing ground level and 11m from top of temporary bund. Deep excavation designed by PLAXIS software with safe slope of 1H: 1V for top 6m soil along with bund and 1H: 3V for weathered rock of 5m depth till excavation level. But during excavation weathered rock encountered at greater depth, because of which slope angle of excavation increased and fouling with foundation. Bund was re-aligned during the process of excavation with many challenges. Steeper slope angles adopted with toe protection. Continuous seepage found along the slope during bund rectification. Paper highlights the difficulties faced during excavation due to change in soil strata and describes the challenges faced in slope protection using conventional methods for safe construction of foundation. Approximately 1070 cum of concrete had been laid successfully for foundation construction by overcoming many challenges.

Keywords: Deep excavation, Dewatering, Foundation construction, PLAXIS, Seepage control, Slope protection.

INTRODUCTION

Greater Hyderabad Municipal Corporation (GHMC) proposed to construct extra dozed bridge across Dhurgam Cheruvu Lake at Madhapur to mitigate the vehicular traffic congestion. This bridge will reduce the distance from Madhapur to Gachibowli by 2 kilometers. Besides easing the traffic, the bridge would add to the iconic image of the city, a modern landmark in an already bustling metropolis. Conceptual figure of Dhurgam Cheruvu Bridge is shown in fig.1. Extra dozed bridge has total length of 426m including back span of 96m on either side. Bridge has 2 pylons each of height 74m in order to suspend the cables, located on the littoral zone of lake.

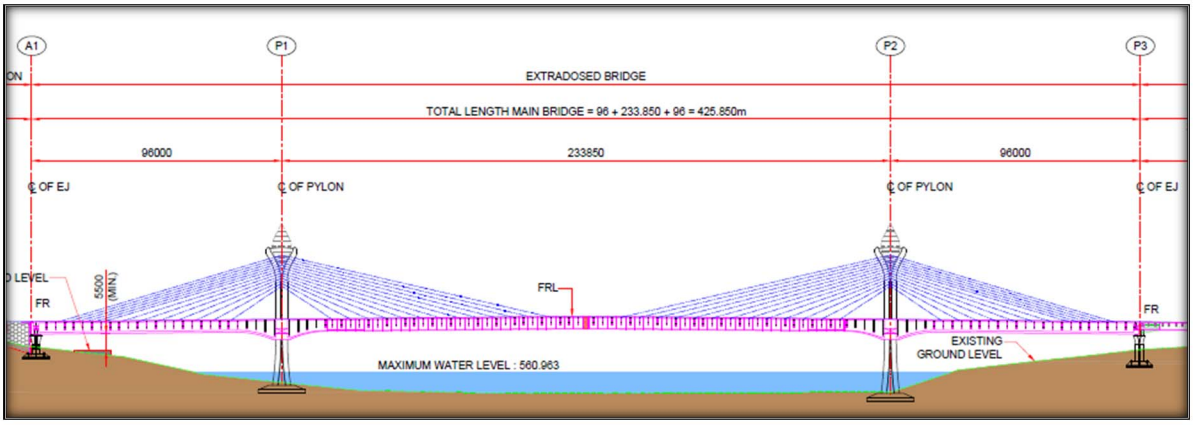


Fig.1 Conceptual figure of Dhurgam Cheruvu Bridge

Sensitivity: Unclassified

© 2018 Deep Foundations Institute

Base of foundation to be rested on hard rock which is 7m below the existing ground level. Location of foundation lies adjacent to lake. Temporary bund of 4m height is required to avoid the lake water intrusion for construction of foundation. Deep excavation with stable slope for 11m along with seepage control been planned for foundation construction with respect to available soil borelogs. But due to difference in soil strata, designed soil slopes couldn't be followed. Change in soil strata encountered only during foundation excavation, that too after constructing the temporary bund.

The author in this paper tries to explain the problems faced during deep excavation and challenges to maintain stable slopes with seepage control measures during bund modification. Though conventional methods adopted for addressing slope stability issues, author willing to emphasis the delay in construction time and cost taken for remedial measures due to change in soil strata as a case study.

GENERALIZED SUB SOIL PROFILE

The Hyderabad district forms part of the upland plateau region called the "Deccan Plateau". As per IS 1893, the site falls under Seismic Zone II, which corresponds to a zone factor (Z) of 0.10. The detailed geotechnical investigation were carried out at proposed pier location to interpret the engineering properties of soil and rock. Boreholes were drilled under each and every pier to encounter the actual geological strata. Subsurface profile generally consists of residual soils underlain by completely weathered rock and then granite bedrock. Ground water is present 1 to 3m below ground level. Since this case history is related to P2 pylon foundation, corresponding sub-soil profile shown in below Fig.2.

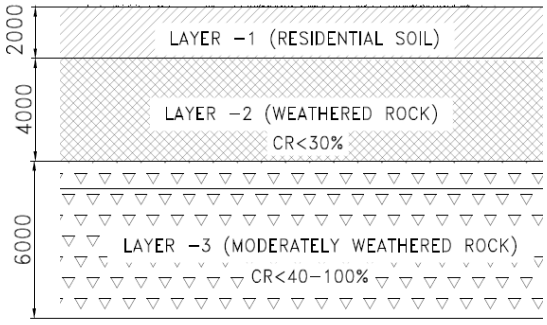


Fig.2 Sub soil profile for P2 pylon location

Description of soil layers at P2 pylon location are given below:
Layer 1: Residual Soil, consisting mostly of clay, was encountered at ground surface. Based on the Standard Penetration Tests (SPT), consistency of the cohesive soil was medium stiff. The lower boundary of this layer was encountered at a depth of 2.0m below ground.

Layer 2: Completely weathered rock bedrock was encountered at ground surface in most boreholes. At some boreholes, this layer was encountered at a depth of 1.0m below ground surface. This layer is formed by the complete in-place disintegration of parent bedrock material, but still partially retains the original rock mass structure. Core recoveries were typically less than 30% while Rock Quality Designations (RQD) were typically nil. The lower boundary of this layer encountered at depths of 1.0m to 4.0m below ground.

Layer 3: Moderately weathered granite bedrock was encountered at depths of 3.0m to 6.0m ground surface in the borehole. The bedrock was moderately weathered to sound. Core Recoveries varied between 40% and 100%, while Rock Quality Designation (RQD) ranged between nil and 100%. Compressive strength of rock cores ranged from 30 MPa to 160 MPa.

Sensitivity: Unclassified

P2 FOUNDATION WITH SLOPE PROTECTION BUND

Two pylons P1 & P2 located on either side of lake for which the foundation located on the littoral zone of the lake. Open foundation proposed by the designer as hard rock encountered at shallow depth. P2 Foundation size is 18m X 17m X 3.5m depth along with a pedestal, founded on moderately weathered rock. Bottom level of foundation is RL 549.272, whereas ground level is RL 556 on the banks of the lake. For placing the foundation approximately 7m excavation is required and 4m bund is required in order to stop the water for dry excavation and foundation works. Figure 3 shows the P2 foundation location along with temporary shore protection.

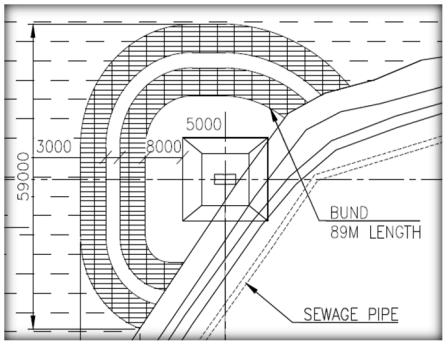
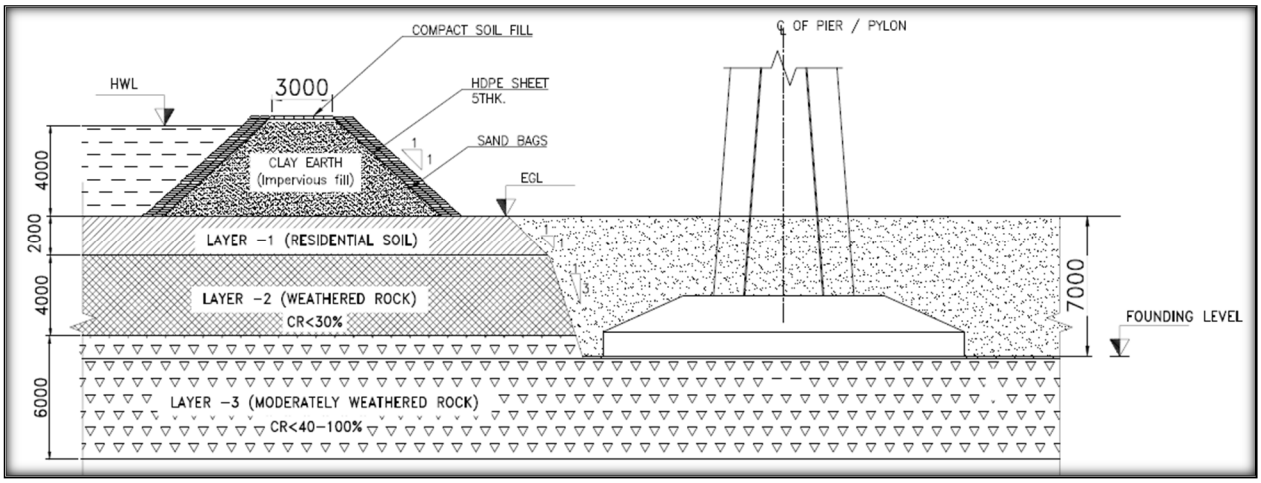


Fig.3 Plan of shore protection bund around P2 pylon foundation

Since pylon P2 is located at downhill, bund is required at water side only. Usage of sheet pile is not possible due to inability of driving sheet piles in weathered / hard rock. Earthen bund found to be more effective to enhance the excavation. Since hard rock encountered at downhill, vertical cut was proposed on one side of the foundation and on other side sloped excavation till depth of soil and after reaching the rock, steeper slopes was planned while designing the shore protection bund. End on dumping method used to construct the bund as per the required layout. Vibratory rollers were used to compact the bund. Seepage of water not only percolates, rather it weakens the stability of the bund. HDPE sheets were proposed on the inward sides of slopes to arrest the seepage of water through bund. Two layers of sand bags been laid on both sides in order to protect the slopes for additional stability. Minimum required bund width provided for vehicular movement during P2 foundation concreting. Figure 4 shows the P2 foundation along with proposed excavation slope.



Sensitivity: Unclassified

Fig.4 Plan & Elevation of shore protection bund

Top of bund taken as RL 561 which is 1m above recorded HWL, whereas proposed foundation RL 549, for foundation construction approximately 7m of excavation is required from existing ground level. Constructed bund was already in place with safe slope of 1H: 1V with height of 4m from ground level with 3m width on top for construction vehicular movement. Excavation has to be performed only below the ground level for 7m for which the safe slope proposed was 1H: 1V for soil strata and 1H: 3V for weathered rock as per borelog data. PLAXIS 2-D used for slope stability analysis shown in figure 5. Both lake side and hill side were modelled and safe slopes were proposed accordingly for excavation.

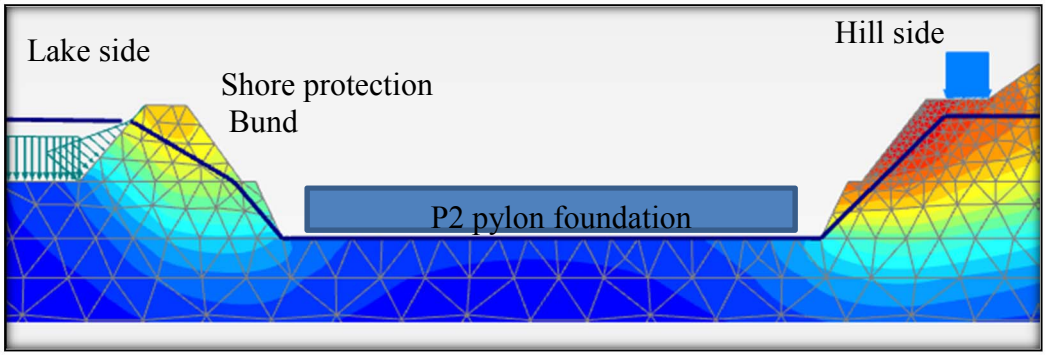


Fig.5 Slope stability Analysis using PLAXIS 2-D for excavation

EXCAVATION WITH SHORE PROTECTION BUND

Bund had been constructed in place and ready for foundation excavation. As per borelog details, top 2m is of residual soil followed by weathered rock on the lake side. But during actual excavation it was encountered that top 4m to 5m is of residual soil, because of which the slope angle increased and bund was protruding inside the foundation area which is clearly shown in fig 6. Earlier as per borelog design proposal was 1H: 1V for soil and 1H: 3V for weathered rock which actually needs only 3.6m distance from edge of excavation. But as per actual site condition due to increase in depth residual soil, 6m edge distance required for excavation slope.

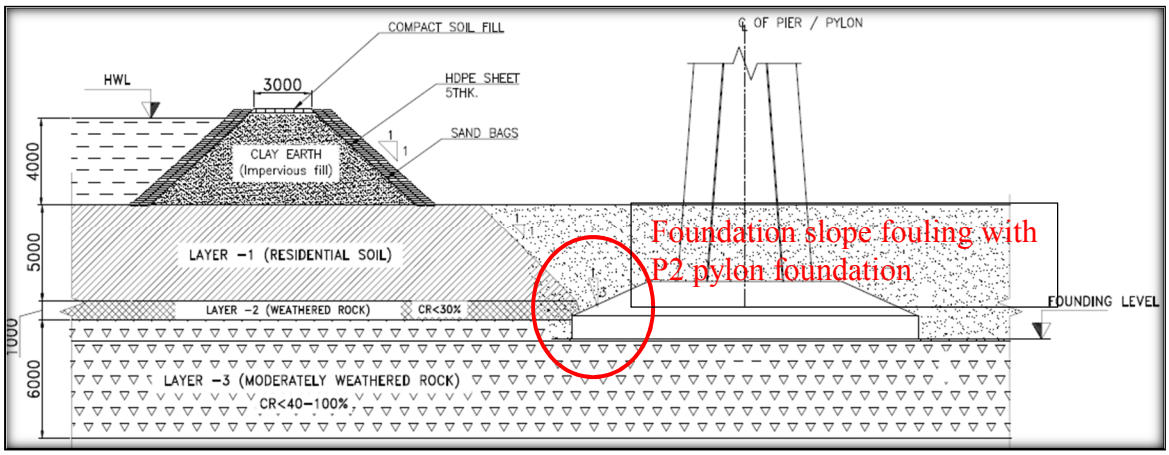


Fig.6 Excavation fouling with P2 pylon foundation

Due to this increase slope, the slope line of soil followed by rock is directly fouling the P2 foundation line. Minimum of 1m to 1.5m is required from the edge of foundation line for workspace such that formwork shutter for foundation shall be placed along with the supporting arrangements. Due to the unexpected soil strata, bund modification is required in order to construct the P2 pylon foundation

Sensitivity: Unclassified

MODIFICATION IN SHORE PROTECTION BUND

It was challenging and herculean task to modify the shore protection bund. With no other way, bund was extended on lake side. Literally the bund was re-aligned and shifted 5m towards lake side. Continuous seepage encountered along the slope of the excavated side shown in Fig7a. As excavation proceeds down water ingress found to be very high, because of which stability of inward slopes of excavated portion also reduced. In order to have minimum workspace from the foundation line, site was forced to execute the steeper slope in soil portion rather than the proposed slope. Sand bags were kept on inward slopes for additional stability. Fig 7b shows the sand bag arrangement on excavated slopes.



Fig-7 a) Excavation in progress **b) Sand bags kept for slope stability**

TOE PROTECTION WALLS

Toe protection walls been provided on one side of bund in order to increase the work area for foundation works. It has been decided to build up 1.2m height of toe protection wall so that 1m work area shall be available more for placing the formwork and supports for foundation works. Precast concrete block used as toe protection walls. Each pedestal size of 0.3m X 0.3m X 2.4m in length approximately weighing to 500 kg. Four number of blocks were placed one and above mount to a height of 1.2m as toe protection walls.



Fig-8 a) Toe protection walls before blasting b) Toe protection wall collapsed after blasting

Sensitivity: Unclassified

As excavation deepens, weathered rock encountered. Rocks present at shallow depth were removed by excavator. Whereas rock at deeper depths were intact and impossible to remove using excavator. So blasting technique used for rock excavation. When blasting happens near the toe protection walls, the pedestals totally collapsed after blasting since there were no interlocking. So immediately blasting was totally avoided near the toe wall and manual drilling took place for excavation. Toe protection walls before and after blasting shown in fig 8. Moreover in order to form bond between the pedestals, steel beams were placed in front of concrete pedestals. Holes were drilled and beams were concreted in front of pedestals @ every 2m such that no more collapse of toe walls. By placing the toe protection walls, slope were made steeper and minimum workplace were provided along the foundation line.

ROCK EXCAVATION

For excavation in rock, controlled blasting technique employed. Weathered rock encountered at a depth 3m to 4m from ground level with very big boulders. Boulders very huge and very compact in ground such that extraction of rock using excavator was impossible. In order to excavate, small holes were drilled in rocks using air compressed driller. Explosive charges were installed in series of holes and then connected to common wire such that blasting takes place simultaneously in all holes. Approximately up to 1m rock shall be broken during controlled blasting. Sufficient precaution had taken during blasting operation.



Fig-9 a) Excavators used for boulders excavation b) Drilling holes in rocks for blasting

After blasting, excavators used to remove the debris and boulders caused by blasting. During blasting, small boulders were lifted nearly 8m from ground level. Safety marshal and representative from client side used to be present during the blasting and also ensured the checklist before blasting.

DEWATERING - OPEN SUMP PUMPING

This is the most common and economical method of dewatering as gravity is the main playing force. Sump was created in the excavated area into which the surrounding water converges and accumulates facilitating easy discharge of water through robust solid handling pumps. Since the bottom of the sump is situated at a level lower than that of the excavation bottom water gets collected in the sump. Main source of water inside the excavated area is the seepage of water through phreatic line. Drains were constructed along the periphery of slope and all drains were connected to sump. Sump size adopted was 1.5 X 1 X 1m for collecting the water. Adding to the seepage, some contribution made by rain during the time of monsoon. Two submersible pumps of 5HP capacity were used to pump out the water.

Sensitivity: Unclassified

P2 FOUNDATION CONCRETING

After reaching the final excavation level, ground has been prepared for laying foundation. Geologist from PMC side checked all four corners of the foundation whether rock strata is uniformly present all over the foundation. Dewatering system was continuously functional till the P2 foundation concreting. PCC was laid and reinforcement tying was taken place for 20 days. Side Shutters were placed with adequate cover to reinforcement. Foundation size was 18m X 17m X 3.5m height and single pour concrete was scheduled. Approximately 1000 cum of concrete was placed continuously with duration of 36 hours by pump concreting method. After the concreting of foundation, pedestal was casted with dowels leading to lower pylon. Remaining area between foundation and bund was backfilled with dry soil.



Fig-10 a) P2 foundation concreting completed b) Staging erected over P2 bund for pier table

REMOVAL OF SHORE PROTECTION BUND

The excavated area been filled till the bund top of +561m RL in order to erect the staging for in-situ pier table concreting. In-situ pier table to be constructed from pylon after that precast segments shall be erected. So bund had been compacted and backfilled in layers such that to take the load of in-situ staging. After the pier table construction, the entire bund shall be removed from the lake. As Eco-friendly measure, the constructed bund shall be totally removed from the lake in order the preserve the eco-system. Long boom excavators shall be used to remove the soil from the bund and put the lake in its natural way.

SUMMARY

Deep Excavation that too adjacent to water body is a very critical activity. Some of the key points to be noted while designing the deep excavation with shore protection bund are as follows

- Retaining system to be carefully chosen depends upon the geological strata, height & material to be retained. As a contractor, retaining system shall be cost effective & requires less time for construction. In this project, since weathered rocks encountered at shallow depths of 1 to 2m from ground level, driving of sheet pile is not possible, so earthen bund is provided as water retaining structure.
- Earthen bund for a height of 5m provided on lake side around the P2 pylon foundation location. PLAXIS software used for analyzing the slope stability with vehicular surcharge. Top of bund was +561m RL with 1m more than the recorded HWL of the lake i.e. +560m RL
- Sand bags were provided for additional stability and in order to stop the erosion of slopes on water side. Approximately 3 to 4m height of water had been retained for which seepage was continuous

Sensitivity: Unclassified

through phreatic line. HDPE sheets were provided on leeward side in order to control the seepage of water.

- As one side of excavation is completely rock, almost vertical cut was made by taking the advantage of intactness of rock. Due to intactness of rock, no water seepage occurred.
- Bund and excavation profile designed and planned as per available borelogs. Weathered rocks anticipated at depth of 1m from ground level whereas residual soil was present till 3m from ground level resulting in more slope width which was fouling the foundation line. Site had to adopt some other technique to steepen the slopes.
- Toe protection walls been provided at the edge in order to increase the work area for foundation work. For toe protection works, already available concrete precast pedestal blocks been used for 1.2m height.
- Rock excavation carried out using blasting techniques. But blasting near the toe protection walls affects the stability of wall and got collapse, which also disturbs the inwards slope. So it was decided to go by manual drilling of rock near the toe protection wall in order to maintain the stability of earthen bund.
- Open sump system been adopted for dewatering. Water ingress through seepage get collected in the drain and connected to sump which was positioned in excavated area. Submersible pumps of 5 HP capacity were used to dewater from excavated area to outside bund.
- After facing many challenges, site could able to successfully cast the foundation, of size 18 X 17 X 3m which accounts to approximately 950 cum of concrete for the pylon foundation of India's longest extra dozed bridge.
- In order to maintain the eco-system, constructed bund shall be totally removed from the lake as an eco-friendly measure.

CONCLUSION

Excavation slopes were planned as per borelog, but in actual site condition proposed slope couldn't be adopted due to change in soil strata. Excavation line was fouling with foundation which ultimately leads to re-alignment of temporary bund along with excavation profile with huge time loss and money. This case study emphasis the significance of sub-soil condition for planning of excavation and also explained the conventional methods like toe protection walls as slope protection measures.

ACKNOWLEDGEMENTS

I would like to convey my thanks to the management for allowing me to present this case study and my regards to my colleagues and site team for their valuable contribution.

REFERENCES

1. Bureau of Indian Standards IS 9759 (1981, reaffirmed 2003): Guidelines for Dewatering during Construction
2. Central Ground Water Board Ministry of Water Resources - Govt. of India, Ground water Brochure Hyderabad
3. Dhurgam Cheruvu Project Hyderabad - Project contract & technical documents
4. Fei Zhang, Aibing Ge, Fei Li, and Gangjung Shen: "Deformation and Stability problems in Large, Deep, Near River Excavation, A Case Study" Electronic Journal of Geotechnical Engineering, 2016 (21.21), pp 6745 – 6753.
5. Koushik Datta and Sudip Nath: "Deep Excavation: An Over view & Case Studies" Indian Geotechnical Journal 2016, IIT Madras, Chennai.
6. PLAXIS 2D – User Manual

Sensitivity: Unclassified

USE OF SOCKETED MICRO PILES FOR EXCAVATION SUPPORT IN HETEROGENEOUS FILL MATERIAL

Shuvranshu K. Rout, Tata Consulting Engineers Limited, Jamshedpur, Jharkhand, India, Phone - 8092472920, Email - skrout@tce.co.in

Manos De, Tata Consulting Engineers Limited, Jamshedpur, Jharkhand, India, Phone - (0657)6696303, Email - mde@tce.co.in

Anup K. Mandal, Tata Consulting Engineers Limited, Jamshedpur, Jharkhand, India, Phone - 9874069837, Email - akmandal@tce.co.in

Biswajit Das, Tata Consulting Engineers Limited, Kolkata, West Bengal, India, Phone - 9874069837, Email - biswajitd@tce.co.in

ABSTRACT

Micro piles are extensively used in various forms with different applications starting from foundation support to landslide mitigation. The present case study highlights a unique experience of socketed micro piles which are subjected to high traffic load and at the same time providing support to shallow excavations. The shallow excavations were required to construct structures like pipe and duct supports / trestles for new power plant inside steel plant premises. Most of the structures were coming in between vicinity of existing building foundation and adjacent plant main road. Open excavation with slope or elaborate excavation support system were not feasible due to space, time and cost constraints. Also, the depth of new foundations could not be reduced in the varying depth of heterogeneous fill material. The heterogeneous fill material comprised of mostly slag, fly ash, concrete debris, broken bricks, loose soils and boulders. The underlying highly weathered mica schist layer or virgin soil layer was most suited for placing the new foundation. Therefore, micro pile option was explored considering availability of small drilling equipment, readily available materials and resources. Steel pipe along with reinforcement rods with cement-sand grout were used for making the micro piles. Wagon driller was used to drill holes for 150mm diameter micro pile. These micro piles were socketed inside the weathered rock layer or grouted slag filled zones. Given the highly variable thickness of heterogeneous fill material above weathered mica schist rock, the lengths of the micro piles above the bond zone were varying significantly. Often these lengths also varied with the depth of highly weathered mica schist rock layer. The field experiences in these conditions are demonstrated with supported reverse design analysis to ascertain the desired safety against uncertainties.

Key Words: Soil Grouting, Open Excavation, Micro Piles

INTRODUCTION

Micro piles have been used as foundation support to resist static and seismic loading in most of the cases all over the world. The application in excavation support has been gaining momentum due to its non-interfaces with surrounding. In addition to that, the construction with simplified equipments has immense benefit on construction schedule and resources in comparison to large diameter piles. The potential benefit of using micro piles to achieve ultimate goal of safe excavation at lesser cost has attracted owner and contractors.

Conventionally open excavation and other support systems are not feasible considering the space and availability of adequate resources. Also, the geotechnical characterization showed variability of filled-up material that had to be supported in order to proceed with vertical excavation. Therefore, micro piles

© 2018 Deep Foundations Institute

were chosen unanimously over other types of protection system considering space-time-cost benefit analysis. The current study attempts to evaluate the adaptability of micro piling in heterogeneous filling material. The presented case study can be improvised in other similar ground condition with existing underground and over ground obstructions without disruption of plant operation and safety.

SITE CONSTRAINTS

The property owner had an ambitious project to install a waste heat recovery type power plant inside its steel plant premises to generate green energy. There were various sizes trestle foundations which required supporting the steam pipe racks to the proposed power plant. Due to space constraint in a century old steel plant, it was planned to make the foundations along the main plant road and parallel to existing other conveyor or pipe trestles.

The new trestles were located just in between spaces of plant main road and existing infrastructures. The property owner had several over ground and underground utility lines going parallel to the road alignment and connected to other existing buildings and utility service stations. The following Bing Earth image shows the tentative location of new trestle foundations along the plant main road at one side and existing buildings / trestles on another side.

To accommodate the new trestle foundation, it was required to excavate just adjacent to existing lightly loaded buildings and trestles of utility lines. The traffic movement on the plant main road couldn't be diverted or stopped temporarily since it caters to material movement for plant operation. The growing concern is about the effect of excavation on the old foundation of existing buildings which are also at shallow depth. The layout for excavation plan had to be optimized under two major constraints; minimal traffic hindrance and no damages to existing buildings and over ground utility lines.



Fig. 1. Proposed Trestle Location (Source from Bing Earth Image)

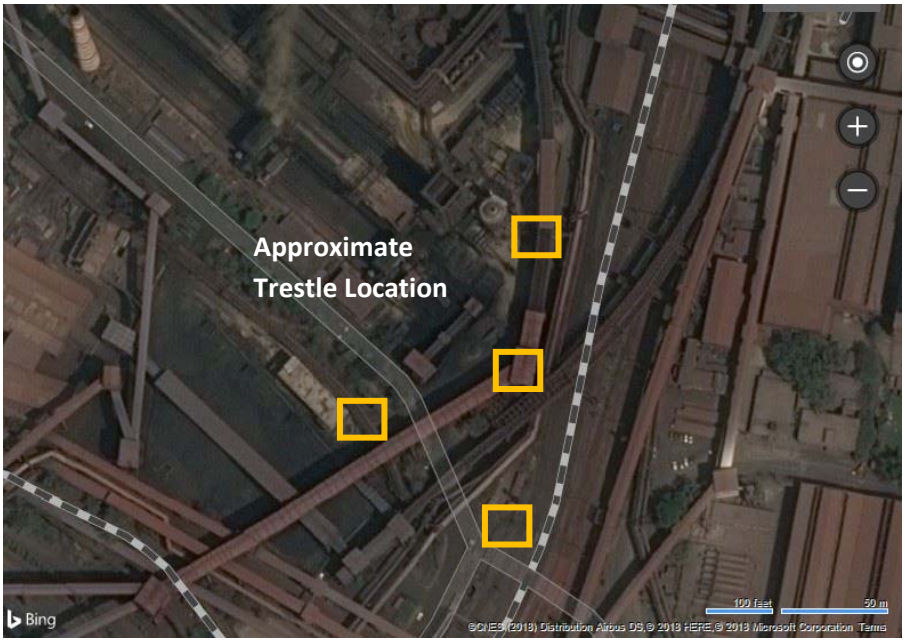


Fig. 2. Proposed Trestle Locations (Source from Bing Earth Image)

SITE CHARACTERIZATION

Preliminary desk study was done with the nearby existing geotechnical reports and old available foundation drawings for existing structures and underground utility lines. Fresh topographical survey was carried out to freeze the trestle layout along the existing plant main road. The geotechnical investigation was planned along with route keeping in mind the existing old trestles foundation, building foundation and underground utility lines.

The site geology of proposed project site comprised fine to medium grained metamorphic rock named Mica-Schist of Dhanjori Group. The schistosity plain was defined by the preferred arrangement of the micaceous minerals. Total 4 nos boreholes were planned for power plant site and 10 boreholes from nearby areas were considered for site characterization. The generalized sub-soil profile are presented below with physical description.

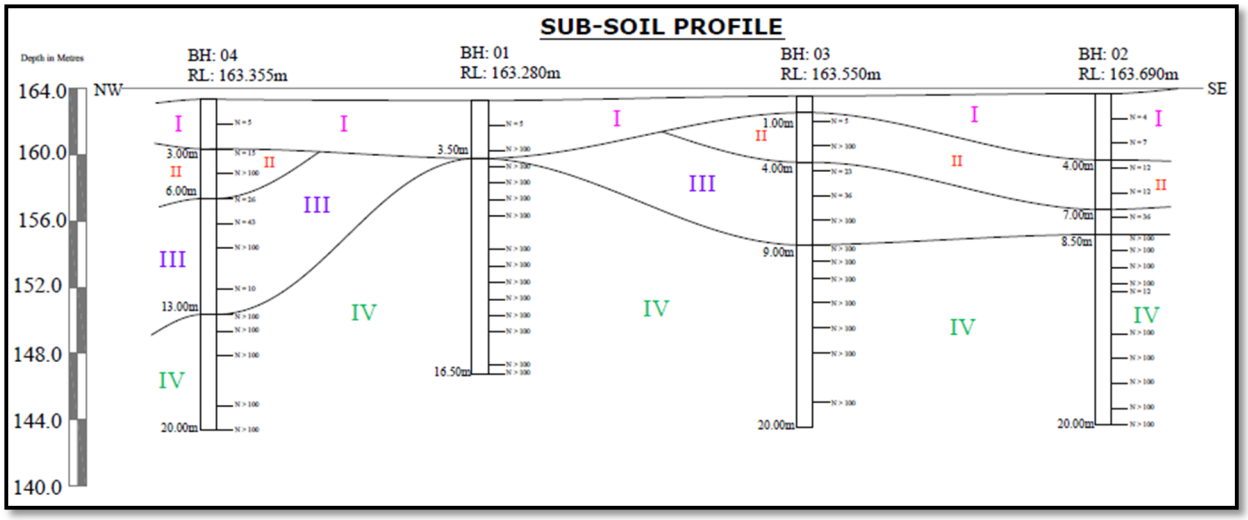


Fig. 3. Sub-soil stratification along the boreholes

Stratum Legend

Stratum-I	Heterogeneous fill materials consisting of brown grey / dark grey, hard slag, coal pieces, cinders, broken concrete, brick pieces , fly ash etc
Stratum-II	Stiff to very stiff, reddish brown to yellowish brown, moorum with clayey silt, micaceous sand, a few quartz pieces etc.
Stratum-III	Completely to highly weathered, bluish grey, micaschist rock with decomposed rock fragments.
Stratum-IV	Moderately to slightly weathered, bluish grey / light greenish grey / yellowish grey, fine grained, micaschist rock with quartz veins.

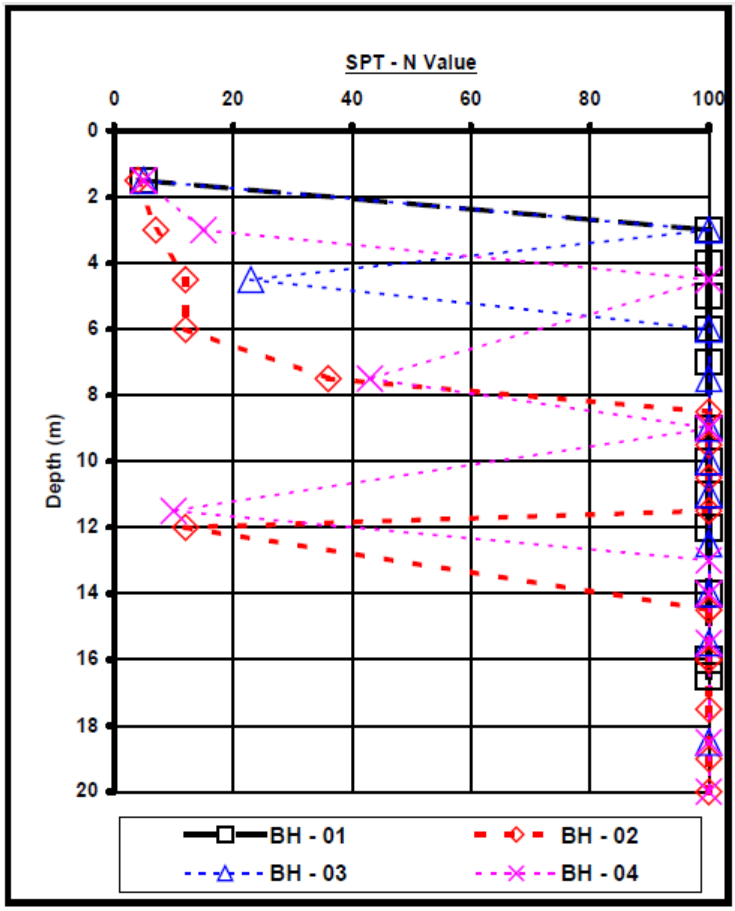


Fig. 4. Summary of SPT N value along the depth

The summary of the geotechnical report is presented herein.
The soil layers encountered at site comprised of upper heterogeneous fill layer of slag, micaceous sand and quartz pieces followed by decomposed mica schist underlain by highly weathered to slightly weathered mica schist rock. Occasionally in some boreholes reddish brown lateritic soil was encountered at upper layers.

Typical SPT N values varied in the range of 4 to 7 for the heterogeneous filled up layer with large voids. The sudden rise of SPT N value to 100 along the top profile exhibited the presence of hard slag and other obstruction like broken concrete pieces etc. The filled up zone was varying from zero to maximum 4m. The next layer was the residual soil from the weathering of underneath decomposed rock with SPT N value varied from 5 to 100. The higher SPT N values were obtained due to localized boulders and

quartz pieces. The depth was varying from zero to maximum 3m. The underneath rock layer was completely weathered to highly weathered micaceous rock. The depth was varying from 1.5m to 7 m with SPT N values greater than 100. The next rock layer was moderately to slightly weathered micaceous rock with quartz veins. The depth was up to end of borehole with core recovery 0-92 % and RQD 0-67 %. The unconfined compressive strength was varying in between 3-64 MPa with water absorption 0.08 to 4.04 %. The recorded standing water level in boreholes was varying from 3.1 to 4.6 m on the project site.

Subsequently laboratory testing program were done on collected samples to generate complete geotechnical reports. However, undisturbed samples could not be extracted from any of the boreholes.
The input design parameters for sub-soil profile for design of excavation support as correlated from field and laboratory test results were shown under Table 1.

Table 1. Geotechnical Parameters for Design

Sub-strata	Description	Unit weight (kN/m^3)	Cohesion (kN/m^2)	Internal Friction Angle (degree)
Stratum-I	Filled up soil	19	0.5	30
Stratum-II	Residual soil	20	10	32
Stratum-III	Highly Weathered rock	22	25	35
Stratum-IV	Slightly Weathered rock	25	50	40

EXCAVATION SCHEME

There was negligible experience and reference available for slope protection in heterogeneous filled up materials which consists of slag, fly ash, bricks, pebbles, broken concretes etc. The nature and extent of filled up material was varying significantly along the proposed alignment of pipe rack foundation. This layer was followed by residual soil formed by weathering of mica schist layer and highly to slightly weathered mica schist rock thereafter. Irregularities to make a generalized layering of strata were not apparent even after geotechnical investigations. The trestles for pipe rack foundation required minimum depth of excavation of 3m to reach at the sound ground and to match with foundation level of nearby buildings. The ground water table was at 4m below the existing ground level and seasonal fluctuation had less impact on the rise of water table.

Feasibility of open excavation was explored for excavation sides where free spaces were available. The cement grouting was planned for filling of voids in loose backfilled soil prior to open excavations. Micro piling was used for critical excavation sides where shallow utility service lines are passing parallel to road and lightly loaded foundations were present.
The next action was to evaluate the construction methodology based the available resources and equipment in this part of country. Since the site was inside a steel plant, scrap circular steel tube sections were sufficiently available. The possibility of use of these sections would bring down the cost and time. The contractor had earlier mobilized wagon drilling equipments for soil nailing work at nearby project site. The percussion drilling machines were capable to drill 125 t0 150 mm drill holes by use of DTH hammer (down the hole). These machines could drill vertically through the heterogeneous fill material even in hard slag and broken concrete pieces.

After finalization of material and equipment for micro piling, detail design analyses were carried out presuming various micro pile lengths and spacing in order to prepare construction drawings and finalization of schedule of quantities. Furthermore, detailed site specific modifications were done time to time during execution to arrive at micro pile embedment length and spacing.

The details for micro piles used for all trestles were summarized below.

Table 2. Summary of Excavation Support Systems

Micro Piles	
Vertical Slope height, m	3-4
Micro Pile length, m	5-6
Micro Pile Diameter, m	0.10
Micro Pile Spacing, m	0.3-0.5
Grade of reinforcement bar	Fe 500
Grade of steel pipe	Fe 250
Drill hole diameter, m	0.15
Grout Compressive Strength, Mpa	25
Cement-sand-aggregate filler material, Mpa	20

DESIGN AND EXECUTION

Design Approach

Guideline by FHWA (Federal Highway Administration) &IS (Indian Standard) codes were used for the analysis of micro piles. Embedded length of micro pile was calculated by traditional lateral earth pressure theory for cantilever pile wall. Stability of slopes was commonly analyzed by established classical limit equilibrium methods of slope stability analysis using in-house design excel sheets and commercial software package (GeoStudio 2007).

Considering the temporary nature excavation and absence of ground water levels, the minimum global 'Factor of Safety (FOS) were targeted in the range of 1.2 to 1.3 for all stages of construction. The typical design aspect of one foundation was presented in this case study paper.

Two criteria were considered in designing of excavation wall stabilization system. First, limit equilibrium method that investigates the equilibrium of the soil mass tending to slide down under the influence of gravity. Second, the finite element method to investigate the stress-deformation behaviors of the continuous micro pile wall under the influence of surrounding loadings.

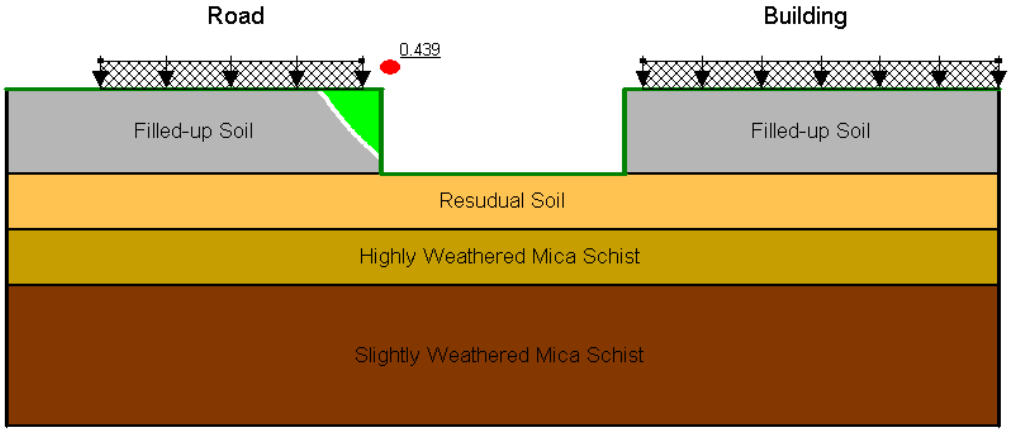


Fig. 5. FOS =0.439 with vertical excavation and no provision of excavation slope protection along road side

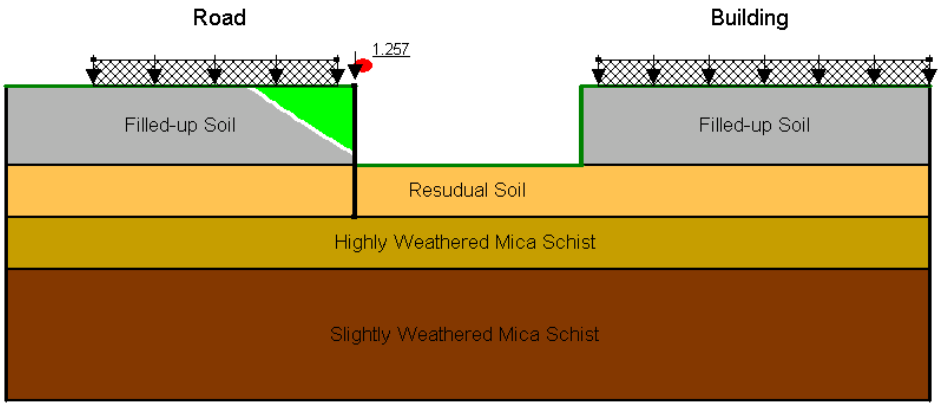


Fig. 6. FOS =1.257 with vertical excavation after installation of micro piles at 300 mm spacing. (Additional precaution were planned to increase FOS by diverting heavily loaded trucks away from the excavation face.)

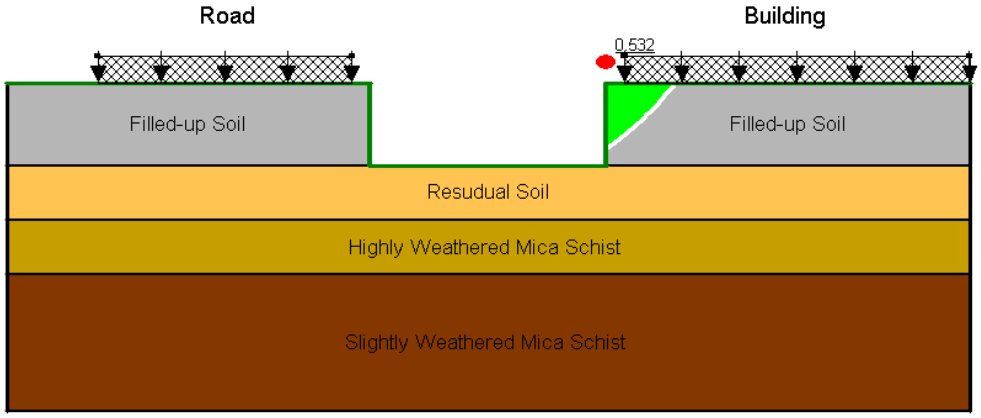


Fig. 7. FOS =0.532 with vertical excavation and no provision of excavation slope protection along building side.

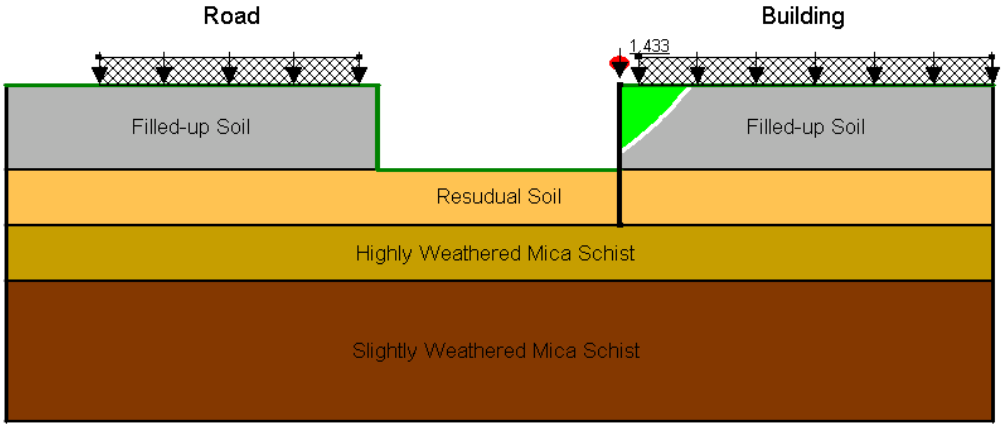


Fig. 8. FOS =1.433 with vertical excavation after installation of 5m length micro pile at 375 mm spacing.

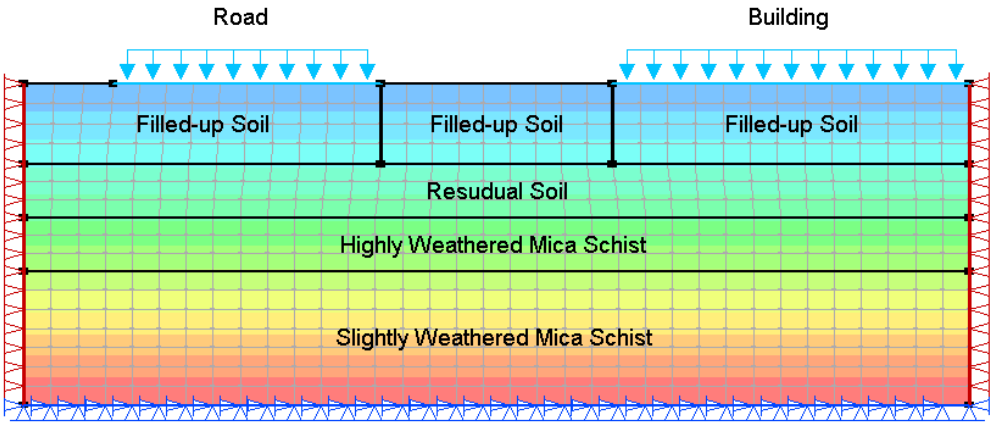


Fig. 9. Initial stress condition before excavation

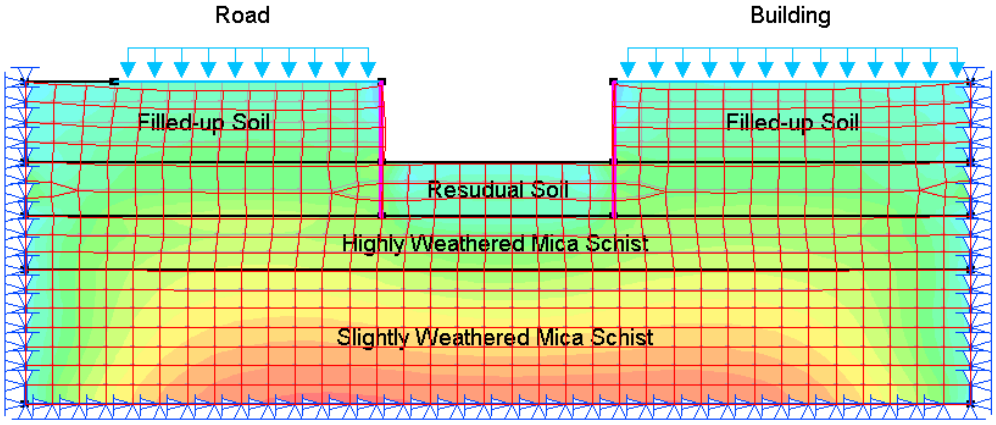


Fig. 10. Final stress condition after excavation with micro pile

Execution Approach

The filled up layer had enormous voids inside which was treated with pressure grouting before installation of micro piling. This had resulted in reducing further collapse of during open excavation and drilling operation. During drilling, it was observed that the filled up strata was varying significantly from one trestle location to other due to varying original ground levels. Therefore, a common embedded length was not fixed for all trestles. Some stretches, slag filled zone was present beyond the foundation bottom level. The embedment of mico piles were done by grouting that layer. Also, the upper slag filled layer was having significant amount of broken concrete pieces which also influenced drilling time through this layer. At some piles casing was introduced at top 1.5m layer due to collapse of drill holes where fly ash layer and mixed soils with high silt content were encountered.

Additional precaution was taken by welding of reinforcement bar to all micro piles in line vertical intervals of 1.0 m after excavation. The drilling time through the filled up strata were recorded to arrive at the field estimation of that layer and finalization of embedment length. However, theoretical correlation could not be established with drilling time due to the nature and variation of material. Occasionally, obstructions like steel scraps were encountered through which drilling were not possible. The spacing was adjusted accordingly as per the excavation plan. To strengthen the local stretch, extra angle steel sections were welded with the other micro piles at different depth along the excavation process. Inclined lateral

supports were provided from excavation side when there was insufficient embedded length and wide spacing. Drilling logs and embedment length with spacing were interpreted simultaneously and their impacts on final excavated faces were analyzed prior to excavation.After completion of drill holes, steel pipes were inserted immediately with a centrally placed 25mm TMT bar. The inside space was grouted with cement-sand-aggregate mixture and outside space between drill hole and steel pipe with cement grout only.

RISK MITIGATION & SITE SAFETY

Special geotechnical instrumentation was eliminated for this work considering the small depth of excavation. However, conventional surveying methods were adopted for monitoring movement of ground and displacement of micro piles. Safety inspectors were engaged for continuous monitoring of traffic movement and excavation work. In addition to that, high resolution cameras were installed at site for 24/7 monitoring of site activity from one control room.

CONCLUSIONS

The grouted micro piles were successfully installed at site inside slag filled zone in a constrained area especially with existing main plant road and old infrastructures. The excavation by introducing micro piles achieved the desired safety of existing structures without minimal hindrance of vehicular movement on plant main road. The following learning from the presented case study can be used in future projects:

- The design and execution of micro pile shall be evaluated on the basis of availability of site resources and equipments.
- The desired FOS for a temporary excavation was achieved with the deflection limit of 5 mm which was validated through field measurements.
- Micro piling could be potential solutions for excavation support where interferences from existing underground and over ground obstructions are exist.
- The reliability and performance of micro pile in uncertain conditions of filled up material would provide confidence in future brown field projects of similar kind.

ACKNOWLEDGMENTS

The authors gratefully recognise Tata Steel Limited, India for giving opportunity to Tata Consulting Engineers to work as "Consultant" in such a complex brown field project. Similarly, the authors would like to thank L & T Limited for their continuous support on site specific inputs throughout the project execution.

REFERENCES

Godavarthi VR, et. al. Contiguous Pile Wall as a Deep Excavation Supporting System. Leonardo Electronic Journal of Practices and Technologies; Issue 19; P. 144-160, 2011.

Micropile Design and Construction Guidelines – Implementation Manual. In: FHWA-SA-97-070, U.S. Department of Transportation, Federal Highway Administration, Washington, D.C.,2000.

Micropile Design and Construction – Reference Manual. In: FHWA-NHI-05-039, National Highway Institute, U.S. Department of Transportation, Federal Highway Administration, Washington, D.C.,2005.

Niroumand H, et. al. Slope Stability and Sheet Pile and Contiguous Bored Pile Walls. Electronic Journal of Geotechnical Engineering; Vol. 17: Bund, HN, 2012.

SITE PHOTOGRAPHS



Fig. 11. Excavation work in progress near existing building and plant main road



Fig. 12. Excavation work in progress near existing trestles and plant main road